Universitat Autònoma de Barcelona

Stereoselective Synthesis of Conformationally Restricted Cyclohexanyl Nucleoside Analogues

Sergio Jurado Moreno

Universitat Autònoma de Barcelona
Facultat de Ciències
Departament de Química

Stereoselective Synthesis of Conformationally Restricted Cyclohexanyl Nucleoside Analogues

Ph.D. Thesis

Ph.D. in Chemistry

Sergio Jurado Moreno

2020

Supervisors:

Dr. Ramon Alibés Arqués

Dr. Félix Busqué Sánchez

Grupo de Síntesis
Orgánica Estereoselectiva

Memoria presentada para aspirar
al grado de Doctor por Sergio Jurado Moreno

Sergio Jurado Moreno

Con el visto bueno de,

Dr. Ramon Alibés Arqués

Dr. Félix Busqué Sánchez

Bellaterra, Julio de 2020

TABLE OF CONTENTS

ABBREVIATION

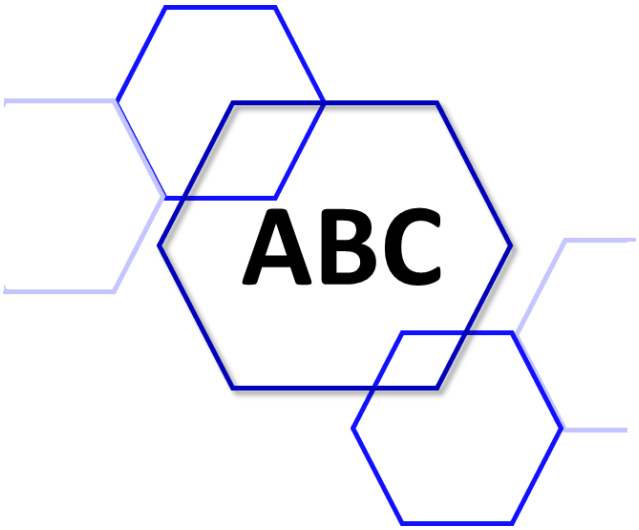

9-BBN	9-borabicyclo[3.3.1]nonane
A	adenine
Ac	acetyl
ACN	acetonitrile
ACV	acyclovir
Ar	aryl
Asc	ascorbate
ATH	asymmetric transfer hydrogenation
atm	atmosphere
ATR	attenuated total reflectance
ax	axial
B	nitrogenous base
Bn	benzyl
bp	boiling point
br	broad (spectral)
brsm	based in recovered starting material
t-Bu	*tert*-butyl
Bz	benzoyl
BzOH	benzoic acid
C	cytosine (base); carbon
ca.	*circa* (approximately)
Calcd.	calculated
CMV	cytomegalovirus
CNAs	carbocyclic nucleoside analogues
conc.	concentration
COSY	correlation spectroscopy
COVID-19	coronavirus disease 2019
m-CPBA	*meta*-chloroperoxybenzoic acid
CSA	camphorsulfonic acid
CTAB	cetyltrimethylammonium bromide
CuAAc	copper-catalyzed azide-alkyne cycloaddition
d	day(s); doublet (spectral)
DBAD	di-*tert*-butyl azodicarboxylate
dC	deoxycytidine
DCG	D-cyclohexenyl-G
de	diastereomeric excess
DEAD	diethyl azodicarboxylate
DEPT	distortionless enhancement by polarisation transfer
DIAD	diisopropyl azodicarboxylate
DIPEA	*N*,*N*-Diisopropylethylamine
DMAP	4-(*N*,*N*-dimethylamino)pyridine
DMF	dimethylformamide
DMSO	dimethyl sulfoxide
DNA	deoxyribonucleic acid
DPPA	diphenylphosphoryl azide
dT	deoxythymidine
E2	bimolecular elimination
EC_{50}	effective concentration in 50% of test subjects
ee	enantiomeric excess
EMA	european medicines agency
eq	equivalent
FDA	food and drug administration

G	guanine
GCV	ganciclovir
h	hour(s)
HBV	hepatitis B virus
HCMV	human cytomegalovirus
HIV	human immunodeficiency virus
HMBC	heteronuclear multiple bond correlation
HRMS	high-resolution mass spectrometry
HSQC	heteronuclear single quantum correlation
HSV	herpes simplex virus
IBA	*o*-iodosobenzoic acid
IBX	*o*-iodoxybenzoic acid
IC_{50}	Inhibitory concentration in 50% of test subjects
Im.	imidazole
IR	infrared
J	coupling constant (spectral)
LCG	L-cyclohexenyl-G
M	molar (moles per liter); mega
m	multiplet (spectral)
MHz	megahertz
min	minutes
m.p.	melting point
MPO	4-methoxypyridine-*N*-oxide
mRNA	messenger ribonucleic acid
Ms	methylsulfonyl (mesyl)
MW	microwave
NAs	nucleoside analogues
NDPK	nucleoside diphosphate kinase
NK	nucleoside kinase
NMPK	nucleoside monophosphate kinase
NMR	nuclear magnetic resonance
n.O.e	nuclear Overhauser effect
NOESY	nuclear Overhauser effect spectroscopy
o.n.	overnight
PG	protecting group
ppm	part(s) per million
PPTS	pyridinium *p*-toluenesulfonate
py	pyridine
q	quartet (spectral)
R_f	retention factor (in chromatography)
RNA	ribonucleic acid
rRNA	ribosomal ribonucleic acid
rt	room temperature
s	singlet (spectral); second(s)
T	thymine
t	triplet (spectral)
TBAC	tetrabutylammonium chloride
TBDPS	*tert*-butyldiphenylsilyl
TBS	*tert*-butyldimethylsilyl
Tf	trifluoromethanesulfonyl (triflyl)
TFA	trifluoroacetic acid

THF	tetrahydrofuran
TiPDS	tetraisopropyldisiloxane-1,3-diyl
TK	thymidine kinase
TLC	thin-layer chromatography
TMSOTf	trimethylsilyl trifluoromethanesulfonate
Tr	triphenylmethyl (trityl)
Ts	*para*-toluenesulfonyl (tosyl)
U	uracil
VZV	varicella-zoster virus
[α]	specific rotation
δ	chemical shift

FORMULA INDEX

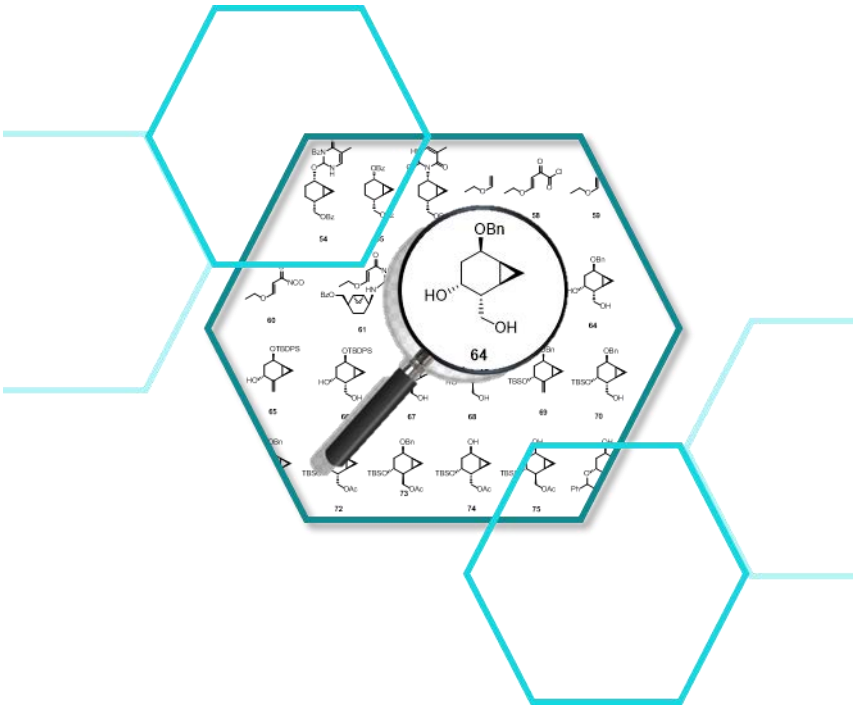

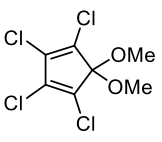

1

2

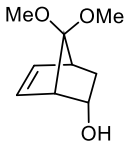

3

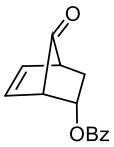

4

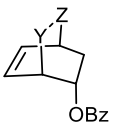

5

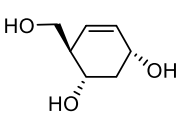

6

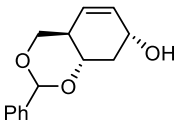

7

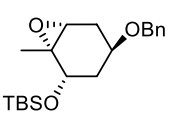

8

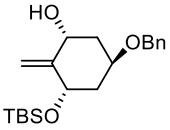

9

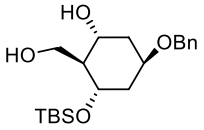

10

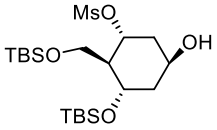

11

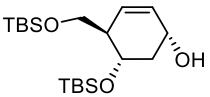

12

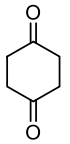

13

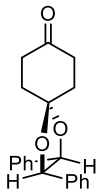

14

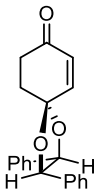

15

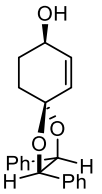

16

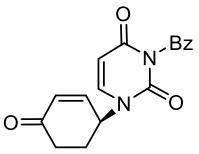

(1'*S*)-**17**

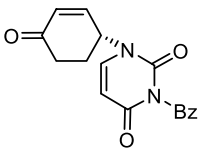

(1'*R*)-**17**

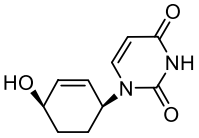

D-(1'*S*,4'*R*)-U-**18**

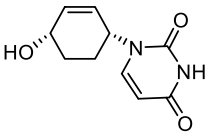

L-(1'*R*,4'*S*)-U-**18**

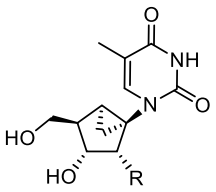

R = H, **19**
R = F, **20**

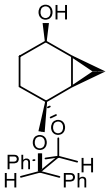

21

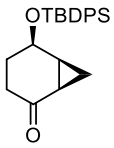

22

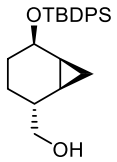

23

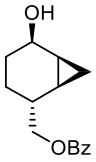

24

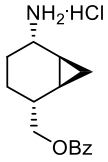

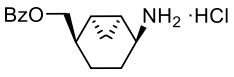

25

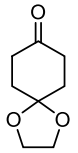

26

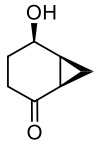

27

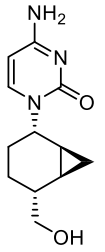

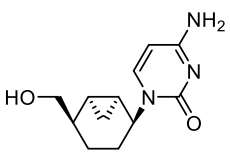

28

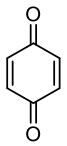

29

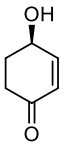

30

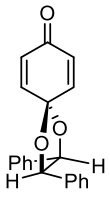

31

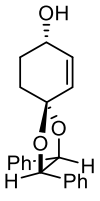

32

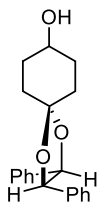

33

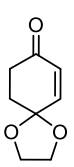

34

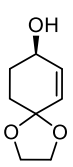

35

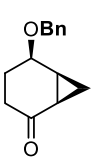

36

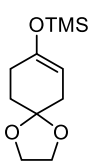

37

38

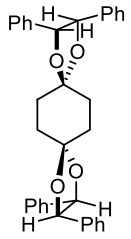

39

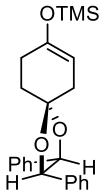

40

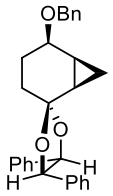

41

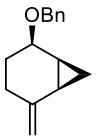

42

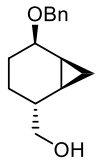

43

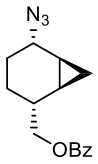

44

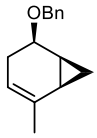

45

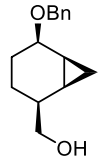

46

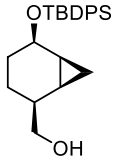

47

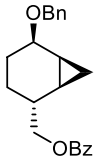

48

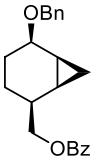

49

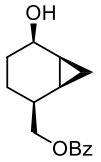

50

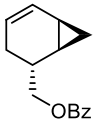

51

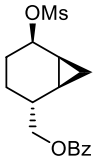

52

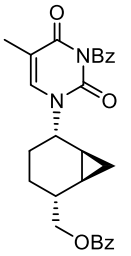

53

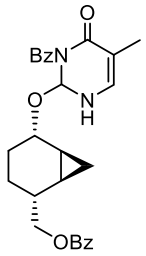

54

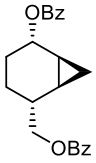

55

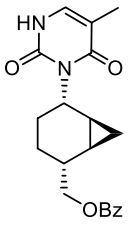

56

57

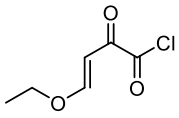

58

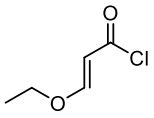

59

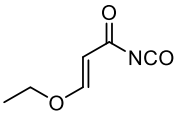

60

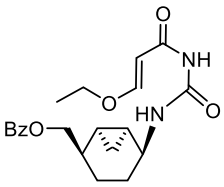

61

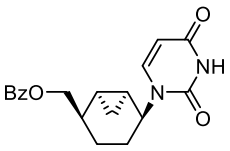

62

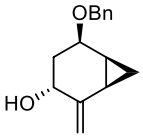

63

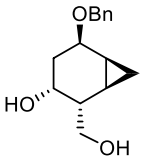

64

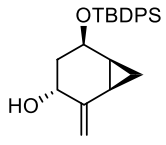

65

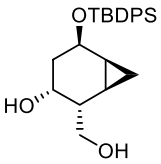

66

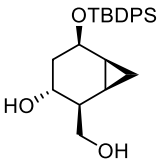

67

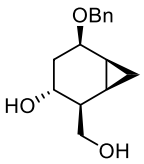

68

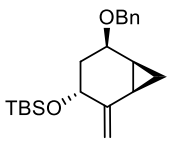

69

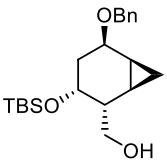

70

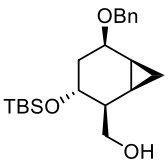

71

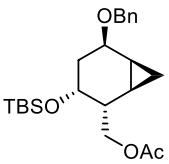

72

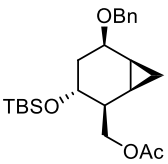

73

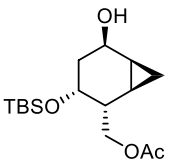

74

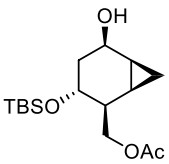

75

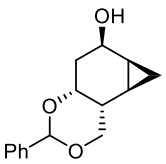

76

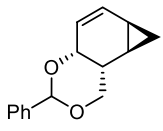

77

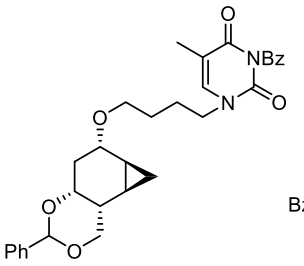

78

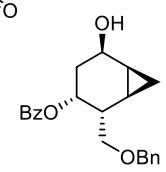

79

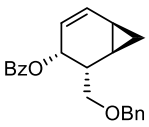

80

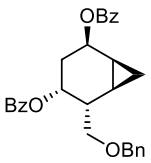

81

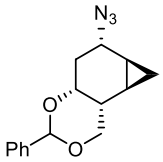

82

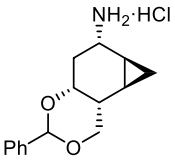

83

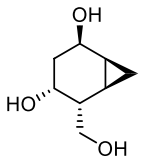

84

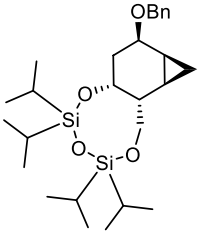

85

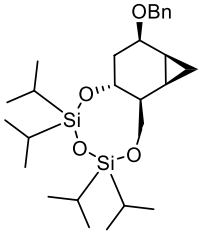

86

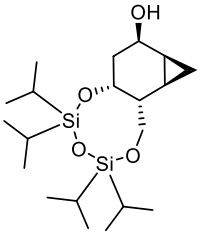

87

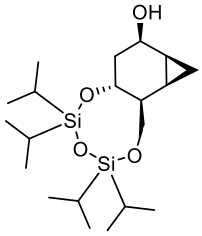

88

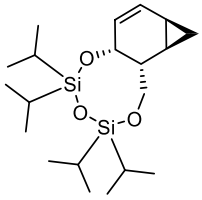

89

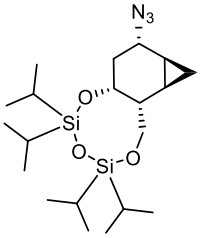

90

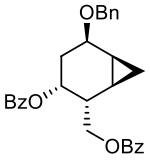

91

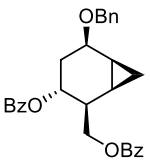

92

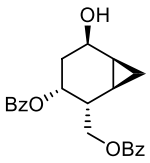

93

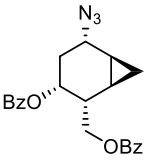

94

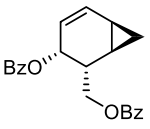

95

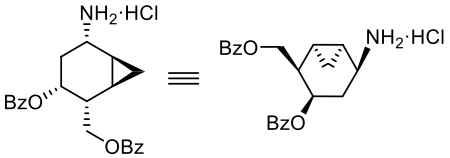

96

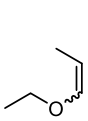

97

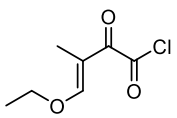

98

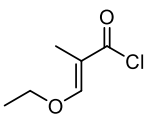

99

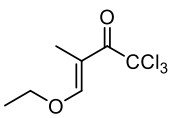

100

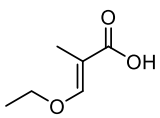

101

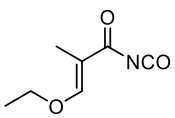

102

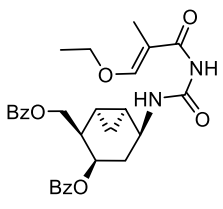

103

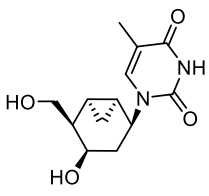

104

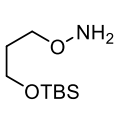

105

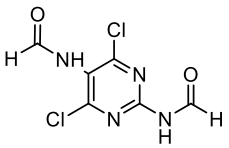

106

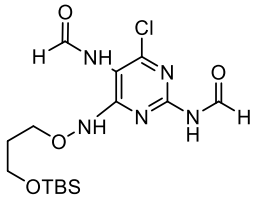

107

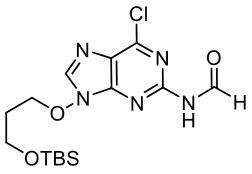

108

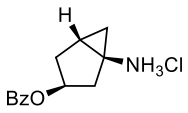

109

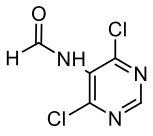

110

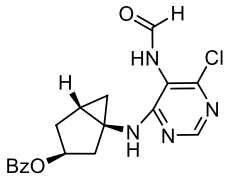

111

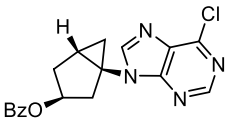

112

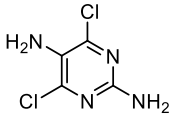

113

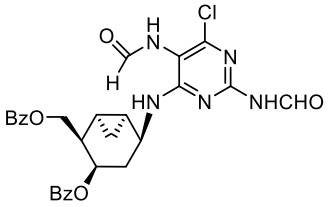

114

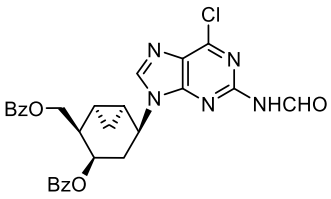

115

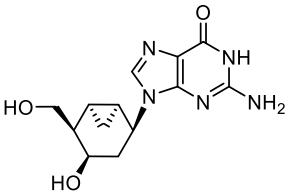

116

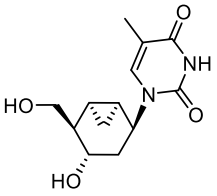

117

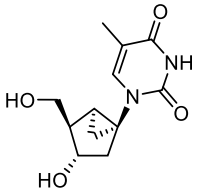

118

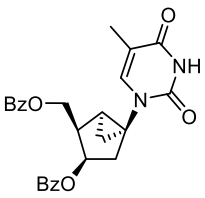

119

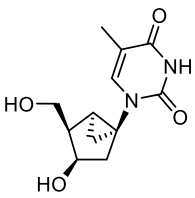

120

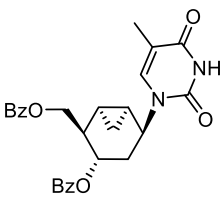

121

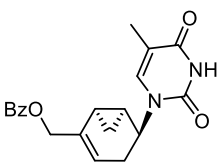

122

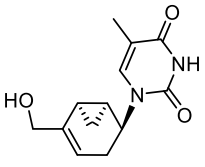

123

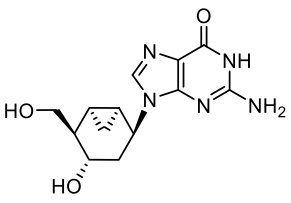

124

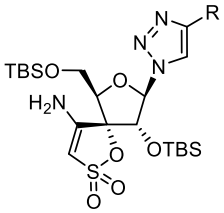

125, R = acyl, alkyl

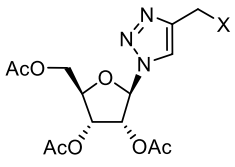

126, X = halogen

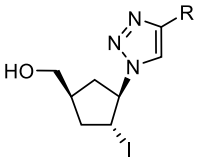

127, R = CO_2Me, $CONH_2$, Ar

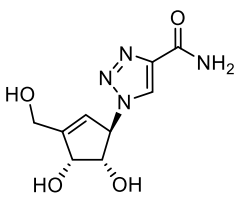

128

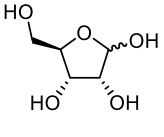

129

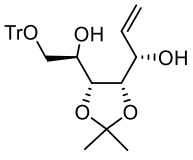

130

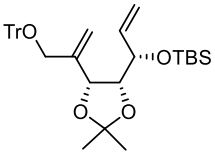

131

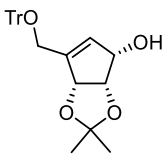

132

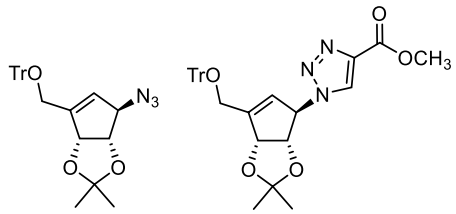

133 **134** **135** **136** **137** **138**

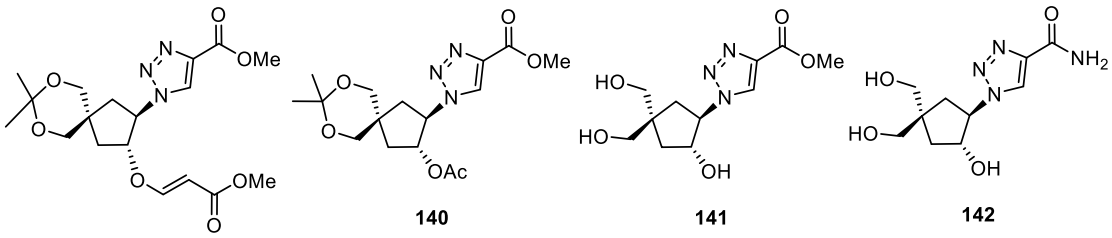

139 **140** **141** **142**

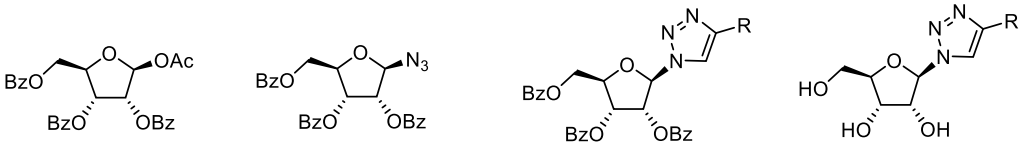

143 **144**

145

R = Ph, CH_2-Ph, $(CH_2)_3CH_3$,OCH_2CH_3

146

R = Ph, CH_2-Ph, $(CH_2)_3CH_3$,OCH_2CH_3

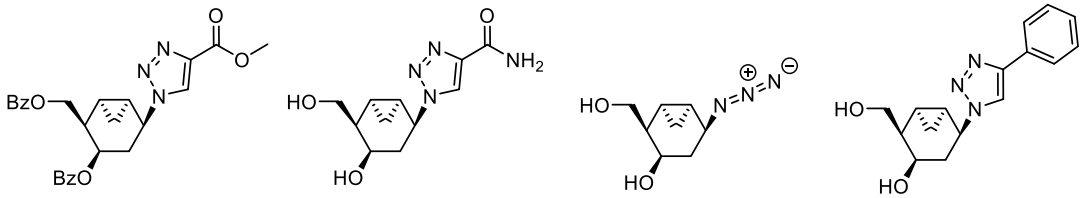

147 **148** **149** **150**

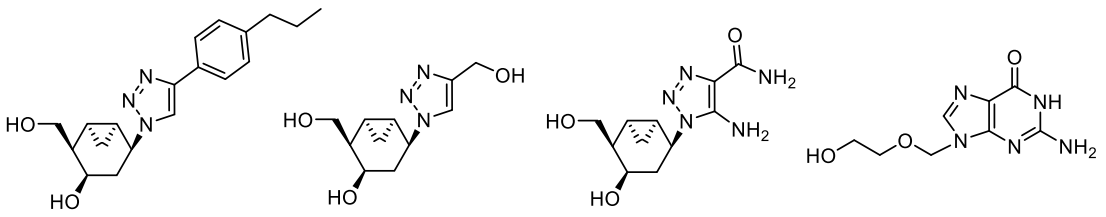

151 **152** **153** **Acyclovir (ACV)**

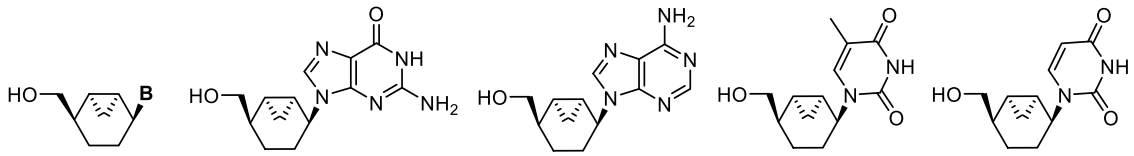

Bicyclo[4.1.0]heptane

BCH **BCH-G** **BCH-A** **BCH-T** **BCH-U**

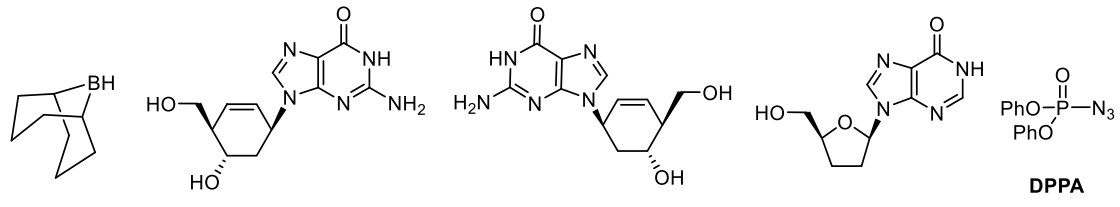

9-BBN **D-Cyclohexenyl-G** **L-Cyclohexenyl-G** **Didanosine (ddI)** **DPPA**

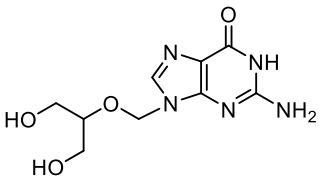

Ganciclovir (GCV)

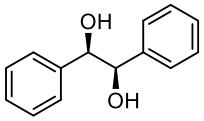

(*R*,*R*)-hydrobenzoin

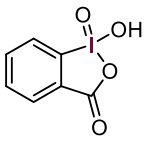

IBX

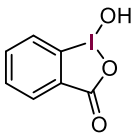

IBA

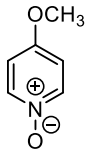

MPO

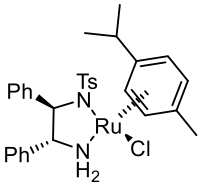

(*R*,*R*)-Noyori-I

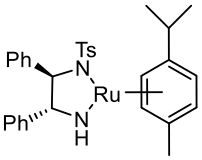

(*R*,*R*)-Noyori-II

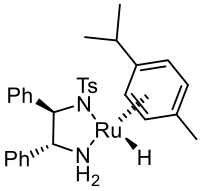

(*R*,*R*)-Noyori-III

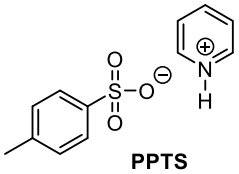

PPTS

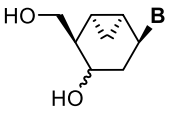

XVI

I. GENERAL INTRODUCTION

Nucleoside analogues as antiviral/anticancer agents.

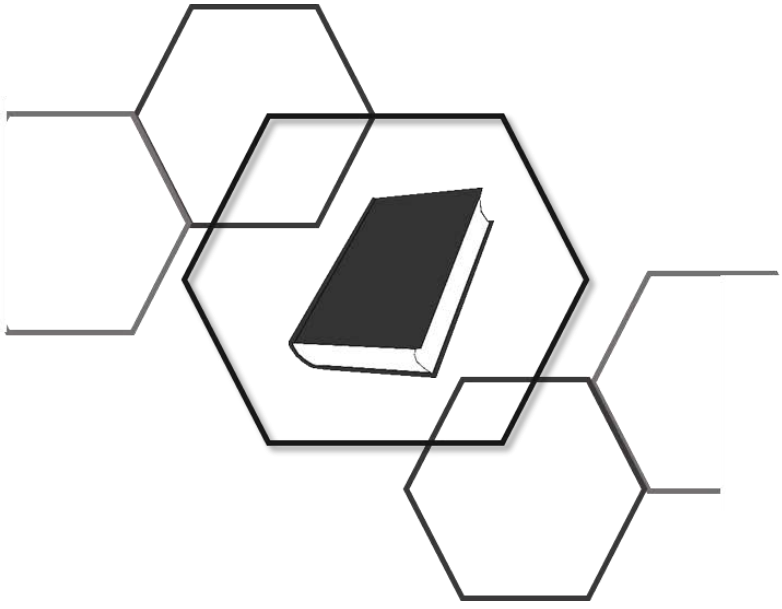

1. NUCLEOSIDE ANALOGUES (NAs)

Natural D-nucleosides and D-nucleotides are endogenous compounds that are involved in several cellular processes such as nucleic acids synthesis (deoxyribonucleic acid (DNA) and ribonucleic acid (RNA)). They also play a central role in the cellular metabolism as carriers of chemical energy in the form of the nucleoside triphosphates such as adenosine triphosphate (ATP). In addition, nucleosides/tides participate in cell signalling (cyclic guanosine monophosphate or cGMP and cyclic adenosine monophosphate or cAMP), and are incorporated into important cofactors of enzymatic reactions (e.g. coenzyme A (CoA), NAD^+ or $NADP^+$ among others).[1]

In terms of their structure, nucleosides can be considered to be constituted by three key subunits: (I) the hydroxymethyl group, which is necessary for the phosphorylation of the molecule by kinases in order to achieve biological activity, (II) a purine or pyrimidine base, which can be adenine (A), guanine (G), thymine (T), cytosine (C) or uracil (U) and participates in the recognition process of the nucleoside through specific hydrogen bonds, and (III) a sugar moiety, which can be either ribose (RNA) or deoxyribose (DNA). The furanose ring in several instances seems to act as a spacer presenting the hydroxymethyl group and the base in the correct orientation[2] (Figure 1). A nucleotide is a compound consisting of a nucleoside whose primary alcohol group ($-CH_2-OH$) has been phosphorylated one, two or three times by specific kinases in the cell.

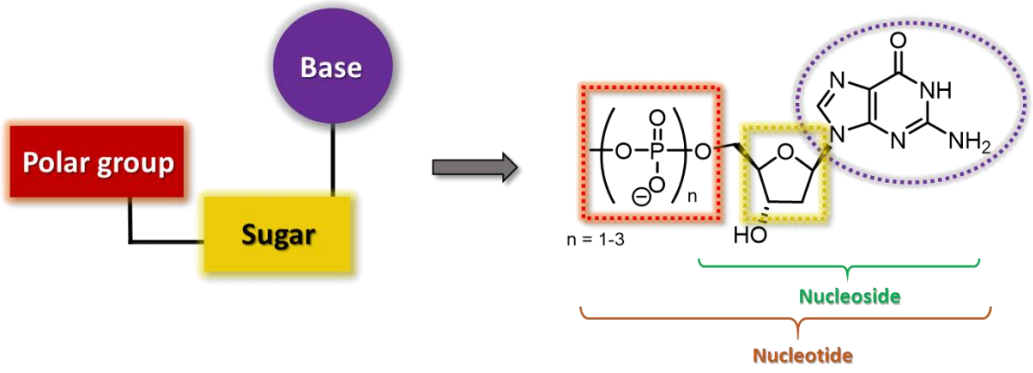

Figure 1. General structure of a nucleoside/tide and structure of a natural guanosine nucleoside.

Their essential role in all aspects of cellular and physiological processes has inspired decades of elegant studies linking the worlds of chemistry and biology, becoming one of the main class of natural products which has had a greater impact on the discovery of therapeutic drugs, particularly as anticancer and antiviral agents as will be seen in following sections.

Nucleoside/tide analogues are synthetic compounds that mimic the structure of a natural nucleoside, so they can be recognized by cellular or viral enzymes, but including modifications on their structure that lead to disruption and/or termination of replication or other biological processes of the corresponding cells or virus.

Different strategies have been employed in the modification of nucleosides to obtain bioactive analogues, altering each of the three previously mentioned subunits. On account of that, a general classification of the nucleoside analogues in different groups based on their structural modifications can be made[2] (Figure 2):

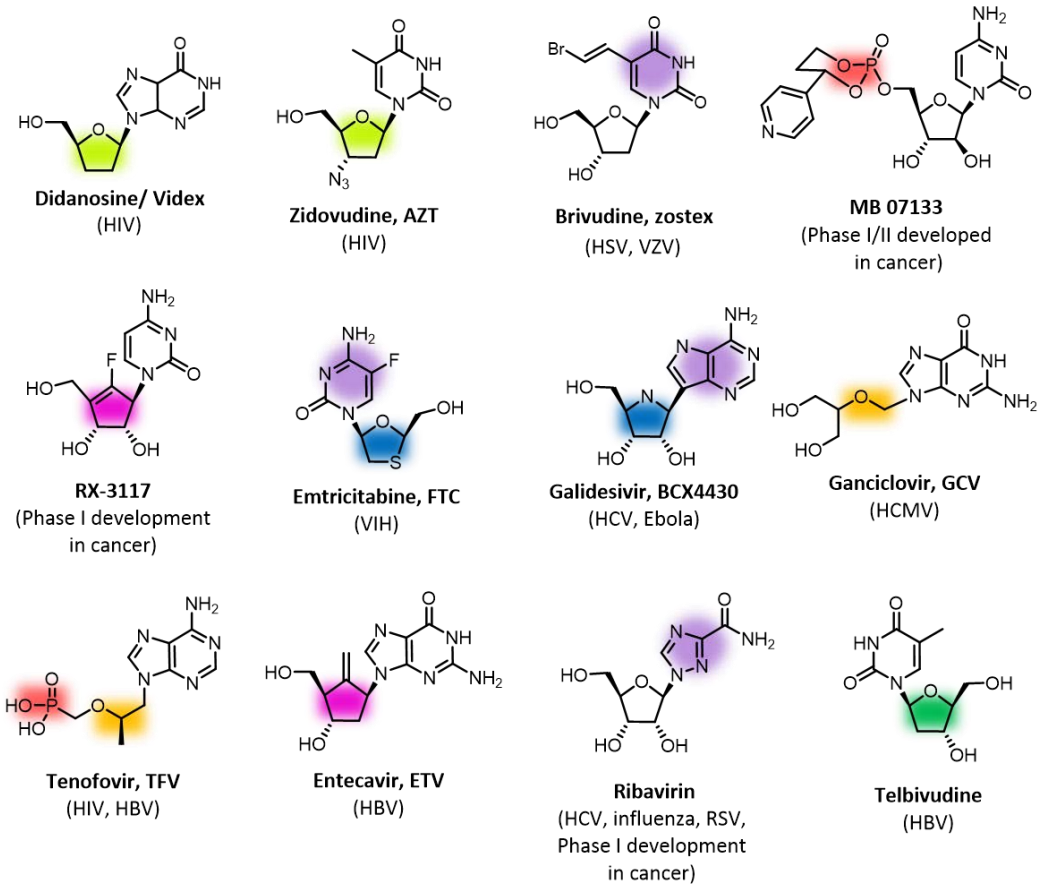

Figure 2. Examples of nucleosides analogues currently used for virus and cancer treatment. The specific virus or cancer phase inhibited by each drug is indicated in parenthesis. Colour is associated to the structural modification and to what type of nucleoside it belongs.

- **2',3'-dideoxynucleosides analogues** lacking hydroxyl groups at the 2' and 3' position (e.g. Didanosine, Zidovudine). (🟢)
- **L-nucleosides analogues** such as Telbivudine. (🔵)
- **Nucleobase modificated analogues** such as Brivudine, Ribavirin, Emtricitabine or Galidesivir. (🟣)
- **Nucleotide analogues**, which include phosphate (or phosphate-like) groups (such as Tenofovir and MB 07133). (🔴)

- **Acyclic nucleosides analogues**, which replace the furanose ring by an acyclic carbon chain (such as Ganciclovir or Tenofovir). (🟠)
- **Carbocyclic analogues**, which contain a carbocycle instead of the furanose ring (Entecavir and RX-3117). (🟣)
- **Heterocyclic-Sugar analogues**, in which the furanose ring contains an additional heteroatom (e.g. Emtricitabine) or the furanose oxygen atom is replaced by a heteroatom such as the azanucleosides (e.g. Galidesivir). (🔵)

Currently, there are more than 30 nucleoside/tide analogues on the market approved to treat viruses, cancers, as well as bacterial and fungal infections, with many more in clinical and preclinical trials.[3-5]

2. NUCLEOSIDE ANALOGUES AS ANTIVIRAL AGENTS

2.1. About virus

Over the course of human civilization, every year, millions of people are infected worldwide by different types of viruses. These viral infections can cause from simple diseases such as common cold (caused by Rhinovirus A, B or C) to serious diseases such as lethal haemorrhagic fever (Ebola virus). There are more than 5.000 different virus species described,[6] some of them that cause main diseases in human around the world are: **HIV** (Human Immunodeficiency Virus), **HBV** (Hepatitis B Virus), **HCV** (Hepatitis C Virus), **HSV** (Herpes Simplex Virus), **HCMV** (Human CytoMegaloVirus), **HPV** (Human Papilloma-Virus), **VZV** (Varicella-Zoster Virus), influenza virus (types A, B, C, D), **HRSV** (Human Respiratory Syncytial Virus) and the recently **SARS-CoV-2** (Severe acute respiratory syndrome coronavirus 2) that causes the coronavirus disease 2019 (**COVID-19**).

Among the mentioned viral diseases, particularly dramatic are those caused by HIV, the agent provoking acquired immunodeficiency syndrome (AIDS), and HSV. In the past 3 decades, HIV has caused a great burden to global wealth and health. According to the *World Health Organization* (WHO), in 2017, 37 million people worldwide were living with HIV, and 950.000 people died because of this pathogen.[7] In the case of herpes disease an estimated 3.7 billion people under age 50 (67% of the population) have herpes simplex virus type 1 infection globally (HSV-1, which causes “cold sores” and genital herpes) and 417 million people aged 15-49 (11%) worldwide

have HSV-2 infection (genital herpes). Currently, there is no cure for none of the HIV and HSV infections, despite some antiviral drugs are effective reducing the synthoms.[8]

All viruses require the biological machinery of the host cell to replicate and spread.[9] This dependence on the cell machinery to survive implies that viruses can be found both inside and outside the cells. The virus particle, also known as a virion, is metabolically inert outside the cells, whereas becomes active inside the cells, specifically within the nucleus where the cell replication enzymes resides.[10] During the replication process, a virus induces a living host cell to synthesise the essential components for the synthesis of new viral particles.

Different strategies of replication are known, depending on the coding capability of the viral genome. For instance, HIV belongs to the retrovirus family, which are RNA-based viruses that take advantage of the enzyme called reverse transcriptase (RT) to transcribe their genetic information into DNA.

The replication cycle of conventional viruses follows similar steps although the details of each step can vary widely. For instance, in the case of HIV, the first step of the virus replication[11,12] consists in the recognition of the virion by binding of a virus-attachment protein to a specific receptor on the host cell membrane (***Attachment***, Figure 3). The virion penetrates the cell by endocytosis or by fusion with the host cell lipid membranes among other processes (***Penetration***). Once inside the cell, the capsid is completely or partially removed to let the genetic material free for its replication (***Uncoating***). Then, reverse transcriptase starts transcribing the viral RNA into DNA (***Reverse Transcription***), which enters the nucleus and is added to the cell genome by the enzyme integrase (***Integration***), allowing the formation of virus mRNAs (***Replication***). The new viral genetic material is then assembled into new virions (***Assembly***). The new virions are delivered from the cell by different ways. Virions without envelope are released by lysis while those with envelope are liberated by emerging from the cell surface and acquiring their outer lipid envelope from the host plasma membrane (***Release***). The new virions formed are then free to infect neighbouring cells and start the process again. Interestingly, the complete viral life cycle generally takes between 6 and 8 hours, and as many as 10.000 virions may be released from an infected cell.[6]

Undeniably, knowing and understanding the virus replication process has been one of the key points in the search for effective antiviral drugs.

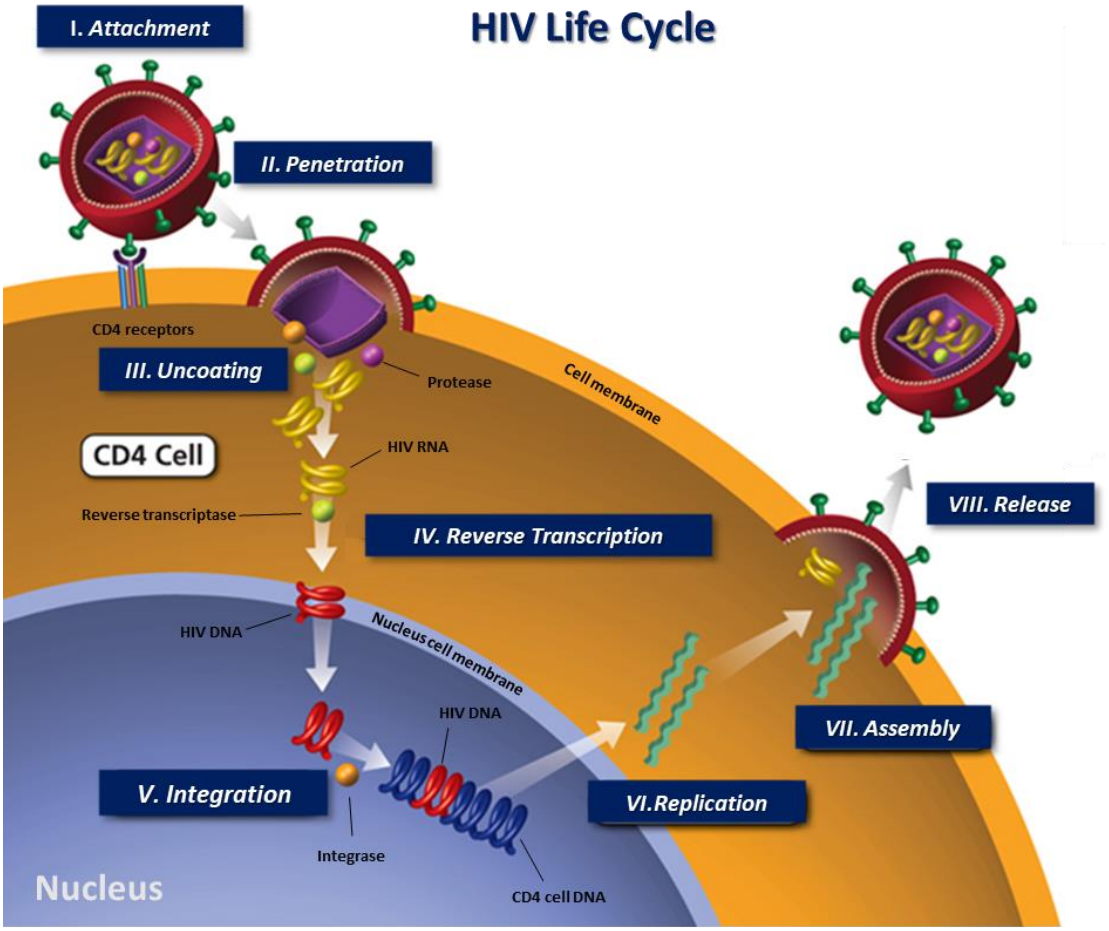

Figure 3. HIV life cycle.[11]

2.2. Antiviral drugs

Viral infections have caused millions of human casualties worldwide, driving the development of antiviral drugs in a pressing need. The aim of an effective antiviral drug is to inhibit the virus replication without causing toxic effects on the host cells.

During the last decades many efforts have been made on the development of novel vaccines against viruses,[13] some of them proving successful (e.g. hepatitis B, smallpox) but, for most of viral diseases no vaccines are available, or are either under development or in different stages of clinical trials (e.g. human papillomavirus, influenza, VZV).

The antiviral drug development began when the first antiviral drug Idoxuridine, a nucleoside analogue, was approved in June 1963 against herpes simplex virus (Figure 4). Since then, many

antiviral drugs have been developed for clinical use to treat millions of humans worldwide. Between June 1963 and April 2016, 90 drugs were formally approved, by the *US Food and Drug Administration* (FDA) and the *European Medicines Agency* (EMA), to treat 9 human infectious diseases.[4]

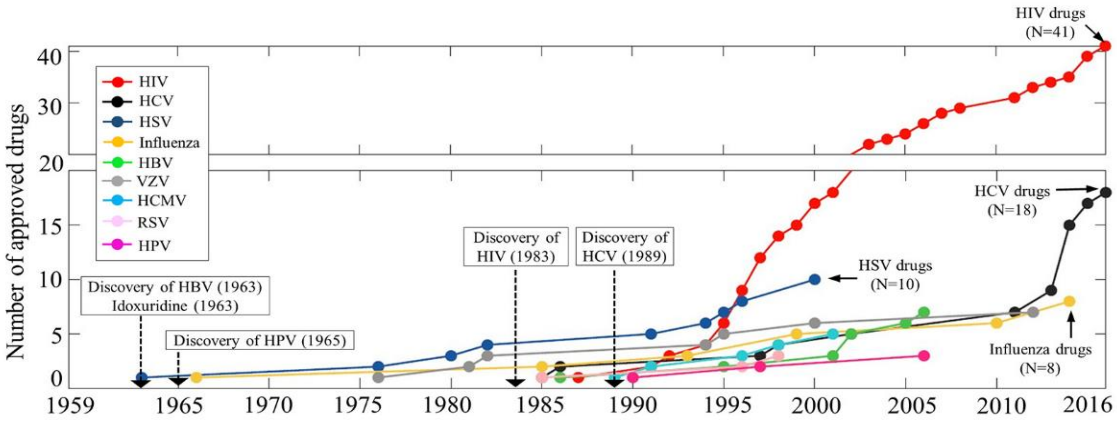

Figure 4. Timeline of approval of drugs against 9 human infectious diseases (HIV, HBV, HCV, HSV, HCMV, HPV, RSV, VZV, and influenza virus). The x axis indicates the period from January 1959 to April 2016, and the y axis shows the total number of approved drugs. For each virus, a coloured line indicates the total number of approved drugs. Moreover, years of discovery of HBV (1963), HPV (1965), HIV (1983), and HCV (1989) are indicated, while the other five viruses were discovered before 1959.[4]

Almost any stage on the replication process of viruses is susceptible to be a target for antiviral compounds. As an example, for HIV, antiviral drugs can be classified in different categories depending on the replication cycle step to which they are aimed to (Figure 5):[4,14,15]

- **Viral entry inhibitors.** This class of drugs including co-receptor inhibitors (CRIs) and fusion inhibitors (FIs) interferes with the binding, fusion and entry of a virion to a host cell (e.g. Maraviroc as a CRI and Enfuvirtide as a FI).

- **Transcriptase inhibitors.** This class of antiretroviral drug includes Nucleoside and Nucleotide Reverse Transcriptase Inhibitors (NRTIs and NtRTIs), and the Non-Nucleoside Reverse Transcriptase Inhibitors (NNRTIs) and are designed to inhibit activity of reverse transcriptase, a viral DNA polymerase that is required for replication of HIV and other retroviruses, avoiding its replication and spread (e.g. Didanosine (NRTI), Tenofovir (NtRTI) and Neviparine (NNRTIs)).

- **Protease inhibitors (PIs).** In this case, the viral replication is prevented by selectively binding to viral proteases and blocking proteolytic cleavage of protein precursors that are necessary to produce infectious viral particles (e.g. Darunavir).

- **Integrase inhibitors (INIs)**. These drugs are designed to block the action of integrase, a viral enzyme that inserts the viral genome into the DNA of the host cell (e.g. Raltegravir).

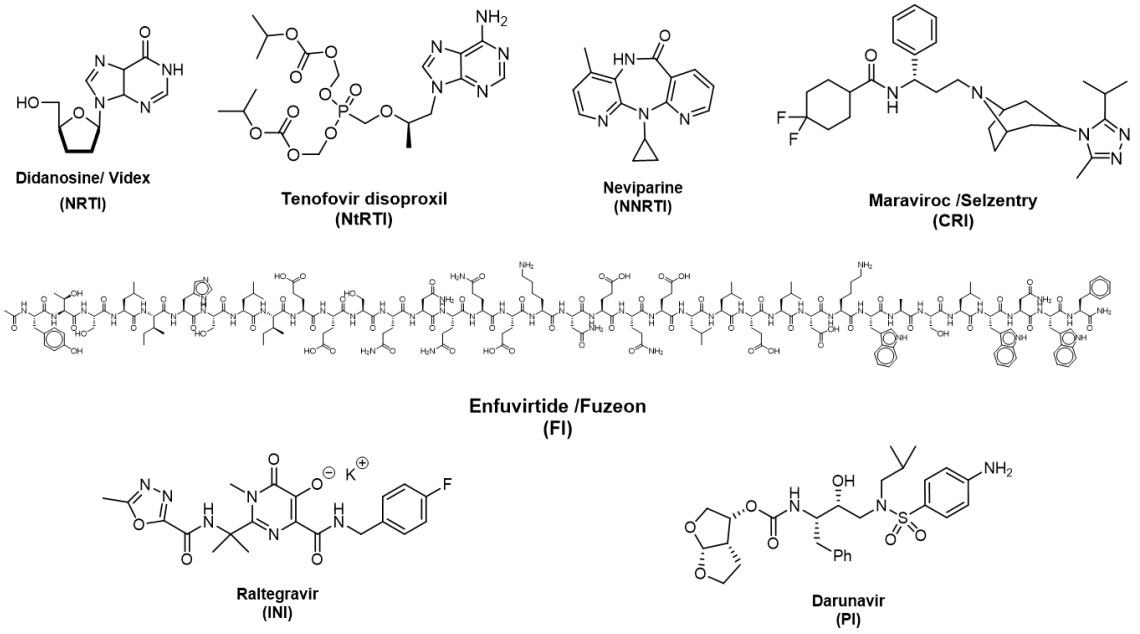

Figure 5. Antiviral drugs currently used for the treatment of HIV. The type of inhibitor to which they belong is indicated in parenthesis.

Nucleoside analogues (NAs) are nowadays the active ingredient of one third of the antiviral drugs approved by the FDA, thus having great importance among the compounds with antiviral activity. [16,17]

2.2.1. Nucleoside analogues in viral treatments

The era of NAs for antiviral drug therapy started with idoxuridine (IDU) and trifluridine (TFT, Figure 6). IDU was first synthesised as a potential anticancer drug by Prusoff[18] in 1959. Furthermore, it was first shown in 1961 to possess activity against herpes simplex virus (HSV) and vaccinia virus.[19] Two years later, Kaufman and Heidelberger also unleashed trifluridine (TFT) for the topical treatment of herpetic keratitis.[20] Nowadays, IDU and TFT are still used in the topical treatment of herpetic eye infections.[21]

After that, a variety of biologically interesting and promising NAs have been discovered, some of which are being used clinically or are undergoing preclinical or clinical development. Two of the major breakthroughs in this field were the synthesis of acyclic Acyclovir (ACV) by Elion and Hitchings[22] in 1978, which was reported to exhibit antiviral activity against herpes simplex virus

(HSV-1, HSV-2) and varicella-zoster virus (VZV),[17] and the discovery of the anti-HIV agent Zidovudine (azidothymidine, AZT) in 1985 which contains an 3'-azide group instead of the 3'-hydroxyl group of the natural nucleoside.[23] Those findings encouraged investigators to search for novel nucleoside analogues with potent antiviral activity (Figure 6).

In the case of the treatment of herpes viruses, the discovery of ACV (commercialized in 1982) quickly prompted the synthesis of other acyclic nucleoside analogues such as Ganciclovir[24] (GCV, 1989), Penciclovir[25] (PCV, 2002) and their prodrugs Valaciclovir[26] (Val-ACV, 1996), Valganciclovir[27] (Val-GCV, 2001) and Famciclovir[28] (FCV, 2007), as well as Brivudine[29] (BVDU, 1979) as a cyclic nucleoside analogue. It is worth noting the acyclic nucleotide analogue Cidofovir[30] ((*S*)-HMPC, 1996), which is stable to hydrolysis due to presence of methylphosphonate group in its structure (Figure 6).

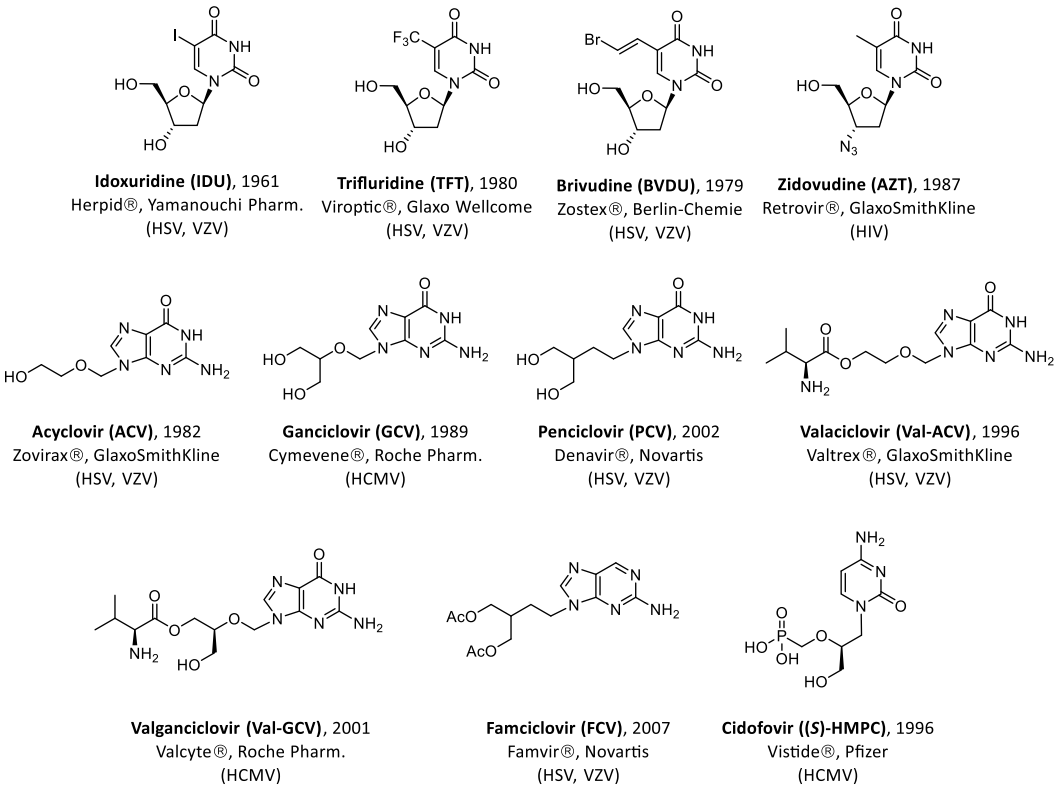

Figure 6. FDA-approved antiviral nucleos(t)ide analogues drugs (first drugs and acyclic compounds): active principal ingredient, approved year by FDA, trade name and manufacturer. The specific virus inhibited by each drug is indicated in parenthesis.[31]

Inspired by the success of zidovudine, a wide range of 2',3'-dideoxynucleosides were synthesised and subsequently approved to treat HIV or HBV infections such as Didanosine[32] (ddI, 1991), Zalcitabine[33] (ddC, 1992) and Stavudine[34] (d4T, 1994) (Figure 7). Moreover, further structural modifications led to the discovery of the antiviral activity of some carbocyclic

nucleoside analogues such as Abacavir[35] (ABC, 1998) which present a carbocycle instead of the furanose ring, and L-nucleosides analogues[36], enantiomers of natural or modified nucleosides, such as Lamivudine[37] (3TC, 1995) and Emtricitabine[38] (FTC, 2003). Also, the acyclic nucleoside phosphonate Tenofovir disoproxil fumarate[39] (TDF, 2008) proved to be active against HIV (Figure 7).

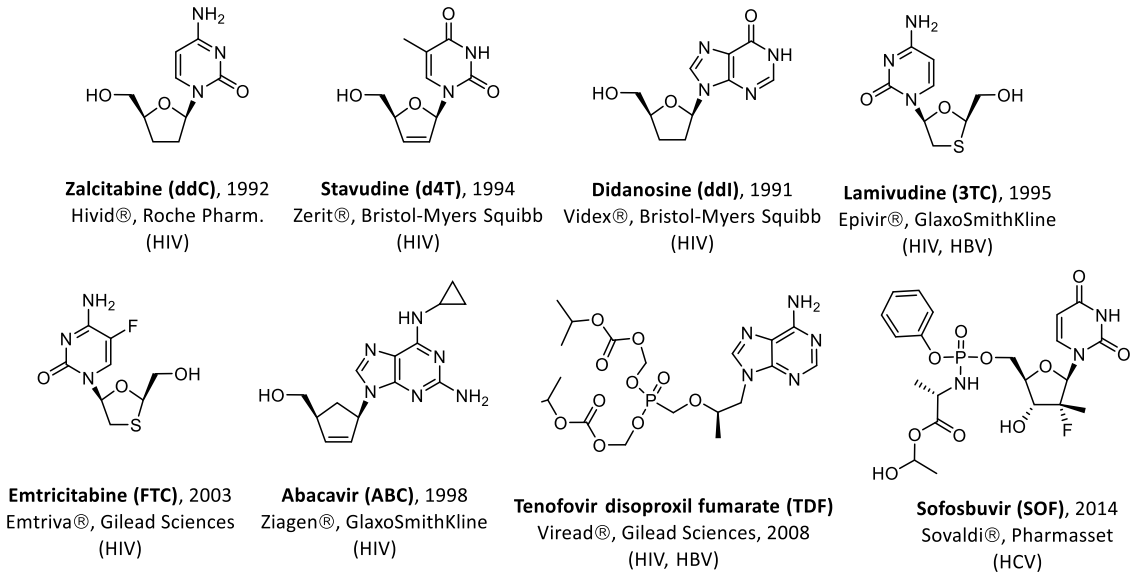

Figure 7. FDA-approved antiviral nucleos(t)ide analogues drugs (cyclic compounds and last approved examples) : active principal ingredient, approved year by FDA, trade name and manufacturer. The specific virus inhibited by each drug is indicated in parenthesis.[31]

Approximately 30 approved nucleoside and nucleotide analogues are used as antiviral agents for several indications.[4] One of the last to be approved have been Sofosbuvir[40] (SOF) for the treatment of hepatitis C viral infections and marketed under the trade name Sovaldi® in 2014[31] (Figure 7). Additionally, several new NAs are in various stages of clinical development to be used as antiviral drugs. These approved antiviral drugs continue to be essential for antiviral treatments against current and emerging viral infections.

Despite these achievements, the development of successful antiviral treatments remains a challenge. The development of newer antiviral agents with improved properties is still necessary. Major efforts are being made in the search for nucleoside analogues that overcome the main deficiencies of the current drugs, such as their side effects, metabolic degradation,[41] toxicity[42] and, more importantly, the emergence of virus drug resistance.[43,44]

An in-depth knowledge of the mechanism of action of currently used compounds can be of great value for the development of novel antiviral nucleoside analogues to face the resistance issue.

Currently used therapeutic nucleoside and nucleotide analogues exploit the same metabolic pathways as endogenous nucleosides or nucleotides, and they also act as antimetabolites. The pharmacokinetics of NAs starts when they get inside the body by intravenously infusion or oral formulation. Once inside the body, the NAs can face a major bottleneck in cellular uptake (Figure 8). The NAs can cross the cell membrane using a carrier proteins (active transport), like nucleoside transporters (NTs),[a] which are involved in the cellular uptake for the majority of agents.[45] There is emerging evidence that the abundance and tissue distribution of nucleoside transport proteins contributes to cellular specificity and sensitivity to nucleoside analogues. Also, NAs can cross by passive diffusion which is limited in regard to cellular uptake, depending on the nucleosides cell concentration gradient and lipophilicity.

Concerning to pharmacodynamics, the main target of antiviral NAs are the polymerases responsible for carrying out the viral nucleic acid replication (reverse transcriptase, DNA polymerase or RNA polymerase), whose substrates are the triphosphorylated nucleosides. Hence, nucleoside analogues are the prodrug forms of the corresponding active compounds and must be converted into their triphosphorylated derivatives after their penetration into the host cell to be bioactive. The triphosphorylated derivatives cannot themselves be used as drugs, since they are unable to cross the cell membranes. The activation process consists of three successive phosphorylation steps catalysed by kinases which may be present in the host cell or encoded by the virus itself. The kinases involved in the activation of nucleosides are the following: nucleoside kinase, nucleoside monophosphate kinase (NMPK) and nucleoside diphosphate kinase (NDPK), which catalyse the addition of the first, second, and third phosphoryl groups at 5' position of nucleoside analogues, respectively (Figure 8).[46,47] The first phosphorylation reaction in the virus-infected cells is often postulated to be the rate-limiting step in the enzymatic activation of the nucleosides; hence, in addition to the final interaction with viral DNA polymerase, phosphorylation of the hydroxyl analogues by viral kinase may be a prerequisite for antiviral activity.[46]

The inhibition of the replication process by nucleoside analogues may be performed in several ways. Mainly, if the NAs lack the 3'-hydroxyl group (such as Didanosine, Figure 8), which is

[a] **Nucleoside transporters (NTs):** are a group of membrane transport proteins which transport nucleoside substrates like adenosine across the membranes of cells and/or vesicles. There are two known types of nucleoside transporters, concentrative nucleoside transporters (CNTs) and equilibrative nucleoside transporters (ENTs).

[b] **Passive Diffusion**: is a facilitated transport that does not directly require chemical energy from ATP hydrolysis in the transport step itself; rather, molecules and ions move down their concentration gradient reflecting its diffusive nature.

essential to add further nucleotides into the DNA growing chain, its incorporation into the primer DNA strand will definitely stop the elongation process. These compounds are therefore known as chain terminators.[48-50] NAs that contain the 3'-hydroxyl group may also interrupt the replication of the viral nucleic acid by different mechanisms, such as causing steric hindrance when some of them have been added into the DNA growing chain as in the case of Idoxuridine or Trifluridine. Moreover, nucleoside analogues may stop the replication of the viral polymerase via competitive inhibition with the native triphosphorylated nucleoside.

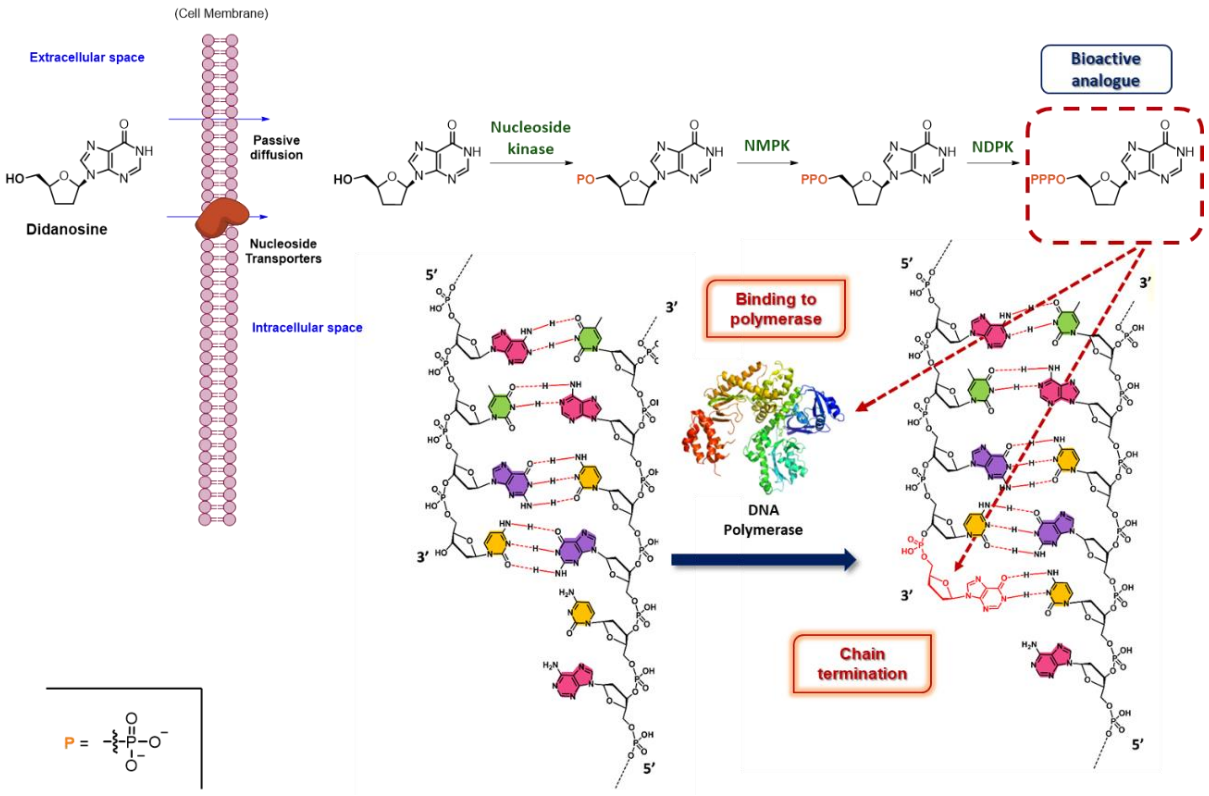

Figure 8. General pharmacokinetics and pharmacodynamics of antiviral 2',3'-dideoxynucleosides.[4]

Nucleoside analogue affinity must be higher for the virus-associated polymerase than for the human one in order to improve its selectivity and therefore reduce its toxicity to the host cells.[47] Remarkably, the low toxicity of some antiviral compounds, such as ACV, is also related to the narrow substrate acceptance of human kinases compared to the viral counterparts.[51] In the case of ACV, the first phosphorylation step is catalysed by the HSV kinase but not by the human kinase thus preventing its activation in non-infected cells.[22]

In conclusion, the search for novel NAs featuring higher selectivity and different resistance profiles than the currently used is still a major cornerstone of today's antiviral research. Therefore, more efficient methods are still in demand for the preparation of NAs.

3. NUCLEOSIDE ANALOGUES AS ANTITUMOR AGENTS

3.1. About Cancer

Cancer, or neoplasm, is a collective term used for a group of diseases that are characterized by the loss of control of the growth, division, and spread of a group of cells, leading to a primary tumor that invades and destroys adjacent tissues. In some cases, it may also spread to other regions of the body through a process known as metastasis, which is the cause of 90% of cancer deaths.[52]

Cancer is normally caused by abnormalities of the genetic material of the affected cells. Tumorigenesis is a multistep process that involves the accumulation of successive mutations in oncogenes and suppressor genes that deregulates the cell cycle.[53] This phenomenon can be linked to several factors, including gender, ethnicity, age of onset, and lifestyle,[54] but cancer can also be caused by cellular transformation linked to viral infection, chemical exposure, or radiation exposure, or the cause can be unknown (spontaneous) in nature.[55,56]

Cancer remains one of the most difficult diseases to treat and is responsible for about 13% of all deaths worldwide, and this incidence is increasing due to the ageing of population in most countries, but especially in the developed ones.[57] According to the Global Cancer Observatory (GCO) in 2018 were diagnosed 18,1 million of new cases of cancer worldwide and it is estimated that the number rises to 29,5 million in 2040.[58] There are more than 200 different types of cancer, but seven particular tumor type: lung, breast, colorectal, prostate, stomach, liver and oesophagus cancer, constitute over half of all new cases diagnosed around the world. In Spain the number of new cases diagnosed was 270.000 in 2018.[59]

A correct cancer diagnosis is essential for adequate and effective treatment because every cancer type requires a specific treatment regimen that encompasses one or more modalities such as surgery, radiotherapy, and chemotherapy. Surgery and radiation therapy, which are, when possible, rather successful regional intervention in order to remove, kill or damage cancer cell in certain area, but chemotherapy can work throughout the whole body, being able to kill cancer cells that have spread (metastasized) to parts of the body far away from the original (primary) tumor. According to that, sometimes surgery and radiation may be a second-tier treatment, with chemotherapy being used first to reduce the tumor burden.[52]

3.2. Chemotherapy

Chemotherapy for the treatment of cancer was introduced into clinic more than sixty years ago. The aim of most cancer chemotherapy drugs used currently is to kill malignant tumor cells by inhibiting some mechanisms implied in cellular division, stopping or slowing their growth. Accordingly, the antitumor compounds developed through this approach are cytostatic or cytotoxic. Most of them affect either deoxyribonucleic acid (DNA) replication or protein synthesis in actively replicating cells affecting its cell-cycle in specific or nonspecific manner.[60]

The side effects of chemotherapy can include fatigue, risk of infection, nausea and vomiting, hair loss, loss of appetite and diarrhea. Advances in supportive care, along with optimization of dose (which almost always involves combinations of drugs) and scheduling have reduced mortality for a number of cancers and have provided the chance for cures. In addition, the effective use of chemotherapy has allowed for not only survival but also improved quality of life in metastatic disease (palliative chemotherapy).[52,54a]

Many efforts to investigate and develop chemotherapeutic approaches are carried out in the field of medicinal chemistry in order to increase effectiveness, selectivity, survivability, and quality of life. More than 150 different drugs have been approved in the period between 1949 and 2018 for different types of cancer.[61] These drugs can be divided into several categories, depending on their origin (natural such as Taxol or Doxorubicin; or synthetic such as Carboplatin or Cyclophosphamide) and the mechanism of action (such as DNA-alkylating agents, tyrosine-kinase inhibitors, microtubule inhibitors or antimetabolite products).[60,62] One of the interesting anticancer drugs are the antimetabolite nucleosides which are a class of prodrug that due to a central role in DNA processes, constitute a productive area for discovering new drugs for the treatment of cancer.

3.2.1. Nucleoside Analogues in cancer treatment

Because natural nucleosides play a central role in DNA processes, its analogues have proven to be an important class of anticancer agents.[63] As it has been explained, these compounds are prodrugs that need to be activated (cell phosphorylation) in order to alter the DNA and RNA by themselves and/or by interfering with various enzymes involved in the nucleic acids synthesis. In the case of NAs in cancer treatment, this interaction leads to the production of cytotoxic effects inducing apoptotic cell death.[64] NAs are used to treat a high percentage of clinical cancers, as a monotherapy or usually in combination with other agents.[60,65]

The history of NAs in cancer therapy started, in the early 1950s, with 6-Mercaptopurine and 6-thioguanine (Figure 9). Elion and Hitchings reported the preparation of 6-Mercaptopurine in 1952[66] which was approved in 1953 for the treatment of childhood acute lymphocytic leukemia, where it is curative and is still the standard of treatment for this disease.[67] Two years later, they also synthesised 6-Thioguanine[68] but, it was not until 1966 that FDA approved it in the use of myelogenous leukemia.

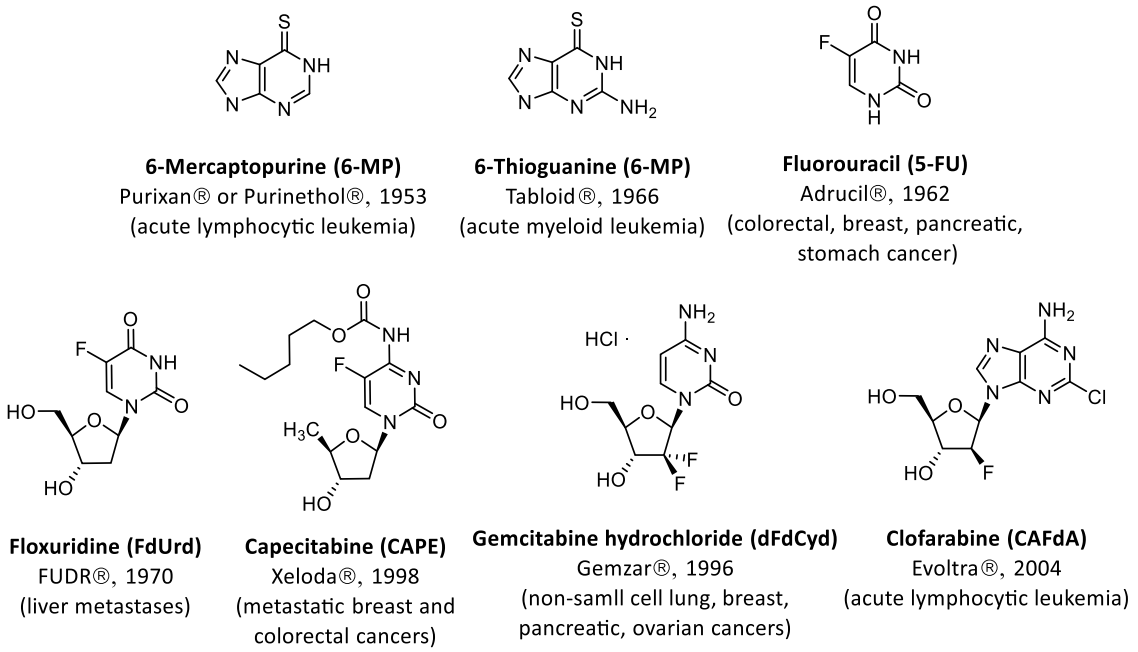

Figure 9. FDA-approved anticancer nucleoside analogues in cancer treatment. Name, FDA-approved year, brand name and the specific cancer inhibited by each drug are indicated.[69,65]

One of the major breakthroughs in the field of NAs was undoubtedly the synthesis of Fluorouracil (5-FU) by Heidelberger and colleagues[70] in 1954, which was FDA approved in 1962 used as a palliative treatment for colorectal, breast, pancreatic and stomach cancers.[71] Because there are several major obstacles for the effective use of 5-FU as a chemotherapeutic agent,[72] other investigators promoted the synthesis of alternative fluoropyrimidines analogues[73] such as Floxuridine[74] (FDA-approved in 1970), in liver metastases treatment, and Capecitabine[75] (1998) against metastatic breast and colorectal cancer. Other fluorinated NAs such as Gemcitabine[76] (1996) and Clofarabine[77] (2004) were also developed. Gemcitabine hydrochloride is used in non-small cell lung, breast, pancreatic and ovarian cancers and Clofarabine is used in acute lymphocytic leukemia treatment (Figure 9).

On the other hand, in the 1960s, Seymour Cohen reported promising cytotoxic effects in cancer cells of a natural cytosine arabinoside: Cytarabine[78] (ara-C, Figure 10). The anticancer agent

rapidly progressed through rodent models and clinical trials to gain FDA approval as a cancer therapy. Thus, Cytarabine was approved in 1969 in some leukemia treatment.[79] Later, inspired by the success of natural aca-C, different analogues as Azacytidine[80] (2004) and Decitabine[81] (2006) were approved both against myelodysplastic syndromes. In the case of purine nucleoside analogues, Cladribine[82] (1992) and Nelarabine[83] (2005) were approved mainly in leukemia treatment among others. A particularly analogue is the Pentostatin[84] (1991) which is used in the treatment of hairy-cell leukemia. It is a potent inhibitor of adenosine deaminase (ADA) and is the only purine or pyrimidine antimetabolite approved by FDA that is active without metabolism[85] (Figure 10).

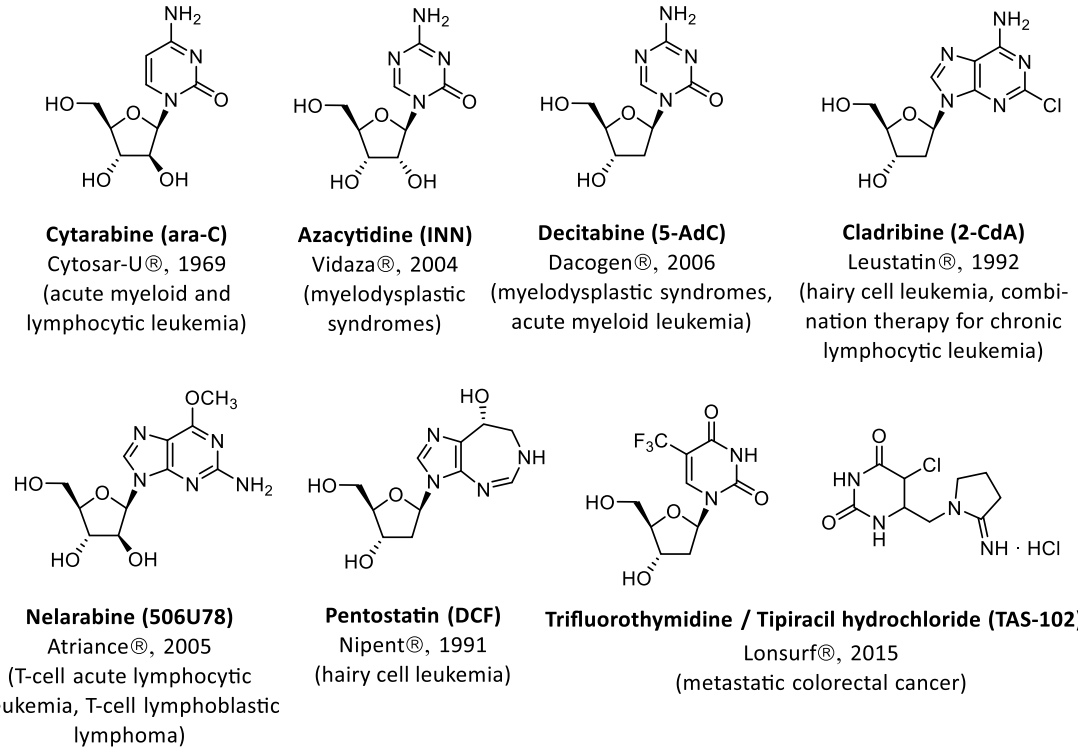

Figure 10. FDA-approved anticancer nucleoside analogues in cancer treatment. Name, FDA-approved year, brand name and the specific cancer inhibited by each drug are indicated.[69,65]

Currently, there are 15 clinical FDA-approved pyrimidine and purine nucleoside analogues.[61] The more recent clinical approved nucleoside analogue anticancer drug was Lonsurf® (TAS-102,[86] combination drug composed by trifluorothymidine and tipiracil hydrochloride, Figure 10) in metastatic colorectal cancer treatment in 2015.

Similar to its utilization as antiviral agents, NAs used in carcinogenic treatments share similar mechanism of action. The anticancer NAs also cross the membrane by active transport (NTs) or passive diffusion (Figure 11). The abundance and tissue distribution of nucleoside transport proteins contributes to cellular specificity and sensitivity to NAs.

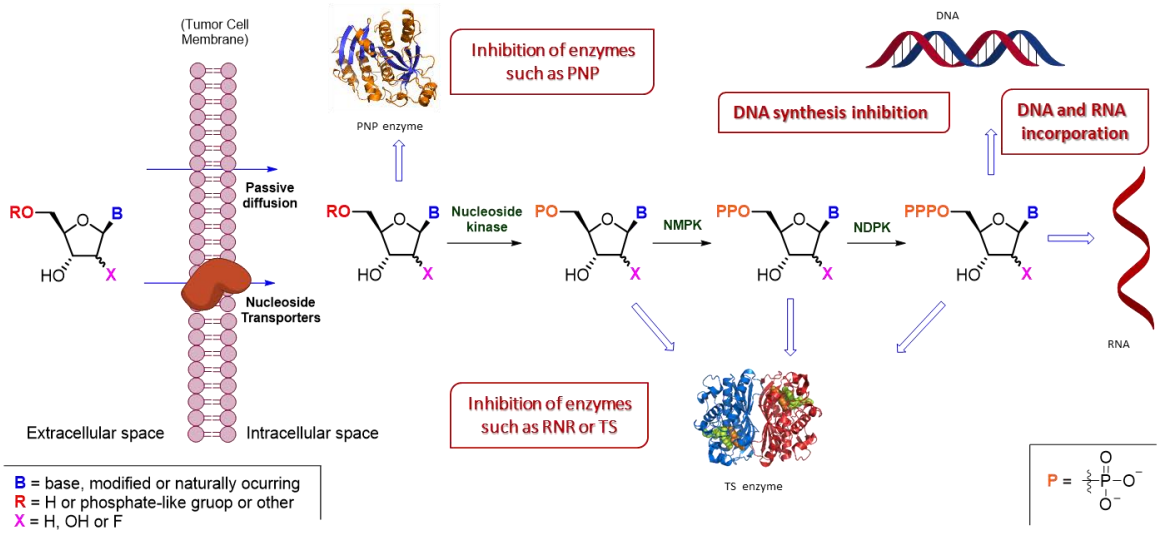

Figure 11. General pharmacokinetics and pharmacodynamics of anticancer NAs.[69]

Regarding to the pharmacodynamics, the NAs must be mono-, di- and tri-phosphoriled by human kinase to be active. In similar way than antiviral treatment, nucleoside-5'-triphosphate analogues are substrates for DNA polymerases and can be incorporated into DNA during replication or DNA excision repair synthesis, which gives rise to stalled replication forks and chain termination (Figure 11). In the case of anticancer treatment, these events activate various DNA damage sensors, which stimulate DNA repair, halt cell progression, and often lead to apoptosis. Moreover, certain nucleoside-5'-triphosphate analogues can be incorporated into RNA, leading to transcriptional termination, and messenger RNA (mRNA) and ribosomal RNA (rRNA) instability. Since most cancer cells replicate their genome more frequently than a majority of normal adult cells, which are quiescent and not actively synthesizing their DNA, this phenomenon allows for a certain degree of cancer cell selectivity.[69,87,88]

Nucleoside and nucleotide (mono-, di-, or triphosphates) derivatives can also inhibit other key cellular enzymes, providing a secondary mode of action that inhibits cell growth or promotes apoptosis. Examples of these enzymes are ribonucleotide reductase (RNR), which removes the 2'-OH group from the ribose sugar in order to generate 2'-deoxyribonucleoside diphosphate or Thymidine Synthase (TS), which can catalyse the conversion of deoxyuridine-5'-monophosphate to thymidine-5'-monophosphate using 5,10-methylenetetrahydrofolate as a methyl source and Purine Nucleoside Phosphorylase (PNP), which is involved in purine metabolism catalysing the reversible phosphorolysis of purine nucleosides (Figure 11).[69]

Greater understanding of the metabolism and mechanisms of action of NAs has created opportunities for improving their antitumor efficacy. Nevertheless, the chemotherapeutic treatment of tumours with NAs is potentially limited by their narrow therapeutic index,[c] due to low anticancer activity and/or severe side effects.[88,89] NAs are cytotoxic molecules and they are not naturally specific to tumour cells, hence they accumulate not only in tumours but also in healthy tissues.[87,90] Another major challenge is intracellular delivery of NAs, because these compounds are hydrophilic and therefore require facilitated transport to cross cellular membranes.[45,91] Furthermore, most NAs have short half-life in the systemic circulation due their rapid enzymatic degradation.[92] As a consequence of all this, high and growing doses have to be given for efficient tumour treatment.

Despite these limitations, the great abundance of molecular targets of NAs in cancer treatments (enzymes and proteins in DNA processes), makes this type of compound worth of investigation.

4. CARBOCYCLIC NUCLEOSIDE ANALOGUES (CNAs)

Among the modifications on the nucleoside skeleton to develop therapeutic agents to control viral and cancer diseases, the replacement of the endocyclic oxygen atom of furanose by a -CH_2- unit generates the so-called carbocyclic nucleoside analogues, CNAs (or carbanucleosides).[93] These analogues have the nucleobase attached at a simple alkyl carbon rather than being part of a hemiaminal ether linkage, increasing not only the general chemical stability of these compounds but also making them metabolically resistant to the action of several enzymes such as pyrimidine and purine nucleoside phosphorylases. Furthermore, the higher lipophilicity of carbocyclic nucleosides compared to the natural counterparts could be beneficial favouring absorption and penetration through the cell membrane.[94,95]

The first CNAs, Aristeromycin[96] (isolated from *Streptomices citricolor* bacteria in 1968) and Neplanocin A[97] (isolated from *Ampullariella regularis* fungus in 1981) (Figure 12), exhibited a potent antitumoral and antibiotic activity. The biological properties of these compounds

[c] The **therapeutic index** (TI) is a quantitative measurement of the relative safety of a drug. It is a comparison of the amount of a therapeutic agent that causes the therapeutic effect to the amount that causes toxicity. TI can be defined as TI = LD_{50}/ED_{50}, lethal dose of a drug for 50% of the population (LD_{50}) divided by the minimum effective dose for 50% of the population (ED_{50}).

triggered a new investigation line in the search of new antiviral and anticancer drugs focused in the synthesis of carbocycle nucleoside analogues.

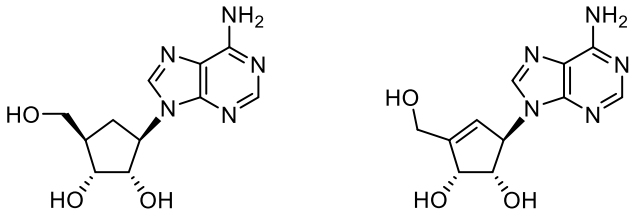

Aristeromycin **Neplanocin A**

Figure 12. Structure of the first CNAs isolated from natural sources.

During the last 30 years, a broad range of CNAs featuring different ring sizes have been synthesised and studied as potential antitumor and antiviral agents.[98-101] The five-membered ring analogues are by far the most extensively studied, although three-, four- and six-membered ring nucleoside analogues have also been prepared.[102-105]

Among the cyclopentyl derivatives (Figure 13), Carbovir (CBV) was prepared for the first time in 1988 and was shown to have an activity similar to AZT against HIV, but it was limited by its pharmacokinetic and toxicological deficiencies.[106,107] Better results were found for Abacavir (ABC), which was approved by the FDA for the HIV treatment in 1998.[108,109] Another successful nucleoside belonging to the five-membered carbocyclic nucleosides is Entecavir (ETV). It was shown to display a potent anti-HBV activity and in 2005 was approved by the FDA for the treatment of chronic HBV.[110] Regarding to antitumoral five-membered ring analogues, the more noteworthy example is the Fluorocyclopentenylcytosine (RX-3117) which was shown to inhibit DNA and RNA synthesis and induce apoptotic cell death of tumor cells. RX-3117 has therapeutic potential in a broad range of cancers, including pancreatic, bladder, colon, and lung cancer.[111] Another example is Pevonedistat (MLN4924) that presents a saturated cyclopentane as main scaffold and a sulphonamide group. MLN4924 blocks the important homeostatic balance between protein synthesis and degradation, which is essential for cell survival, and cell division leading to cell cycle arrest and apoptosis of the cancer cells. It is used in the treatment of large B-cell lymphoma, solid tumours and melanoma.[112]

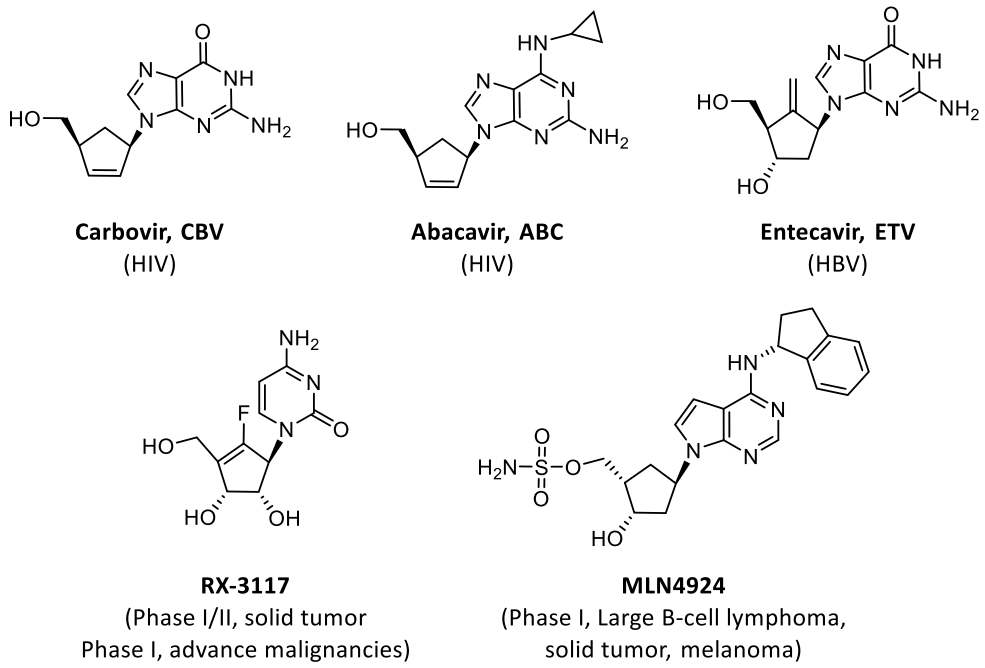

Figure 13. Structure of the FDA-approved five-membered carbocyclic nucleosides. The specific viruses or cancer phase inhibited by each drug are indicated in parenthesis.

With respect to four-membered analogues, Oxetanocin A presents a 4-membered sugar ring which was isolated from a bacteria (*Bacillus megaterium*) and was found to be very active against HIV as well as HSV-1 and HSV-2.[113] Oxetanocin G is the corresponding guanosine derivative which proved effective against HIV[114] (Figure 14). Interestingly, the carbocyclic derivatives of both Oxetanocin A (carba-oxetanocin A)[115] and Oxetanocin G (carba-oxetanocin G; Lobucavir) displayed high antiviral activity against different viruses, including HSV-1, HSV-2, HCMV, and VZV (Figure 14).[116]

Cyclopropyl nucleosides, which introduce extreme rigidity to the sugar scaffold, also exhibited good antiviral activity.[117,118] Zemlicka *et al*. developed the *Z*-isomers of 2-hydroxymethylcyclopropylidenemethyl purines and pyrimidines (Synadenol and Synguanol) that demonstrated potent activity against HCMV (Figure 14).[119] Later, Tsuji and co-workers synthesised a guanine derivative A-5021, which displays high antiviral activity against HSV-1, HSV-2 and VZV (20 times more potent than ACV).[120]

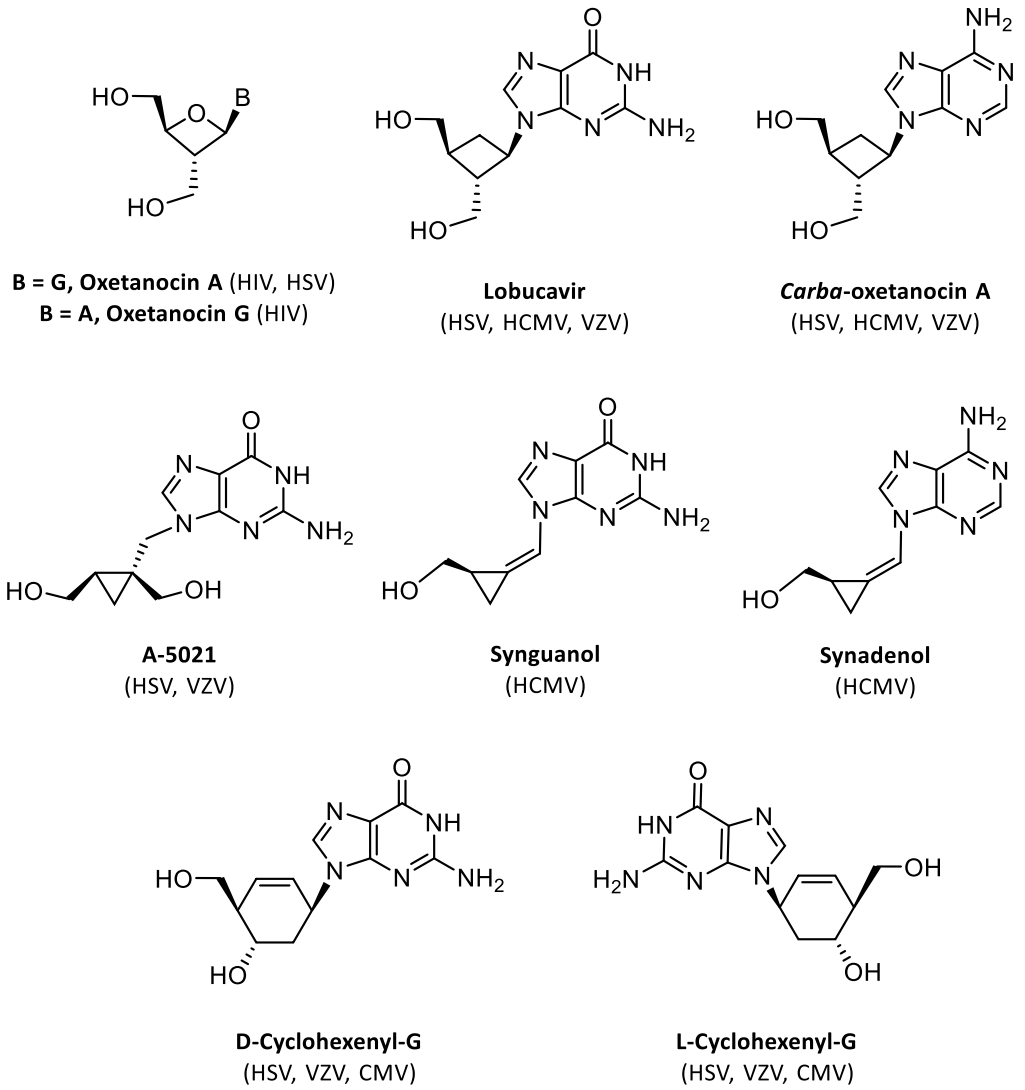

Figure 14. Three-, four- and six-membered carbocyclic nucleoside analogues that display antiviral activity, and the naturally occurring nucleoside analogue Oxetanocin A and G. The specific viruses inhibited by each compound are indicated in parenthesis.

Among analogues presenting six-membered rings, Herdewijn *et al.* proposed, based on conformational studies, that the cyclohexenyl analogues could be considerate bioisosteres of furanose ring. In particular, they demonstrated that both enantiomers of cyclohexenyl G exhibited potent and selective activity against HSV-1, HSV-2, VZV, and HCMV (Figure 14).[121,122] It is the first nucleoside analogue in which both enantiomers show a similar activity, although the D- is slightly more powerful.[121a-b,135]

Considering all these precedents, it can be concluded that the ring size plays an important role in recognition and activity. Therefore, the synthesis of new structures and the development of novel methodologies to extend the structural diversity of this family of molecules are still very active areas of research.

4.1. Cyclohexanyl and cyclohexenyl nucleoside analogues

With regards to CNAs with a six-membered ring, during the 90s, different examples of saturated cyclohexane derivatives were synthesised[123a-e]: monosubstituted compounds with an hydroxymethyl group either at 4' or at 2' position, **I**[123a] and **II**,[123b] respectively; and disubstituted and trisubstituted derivatives such as **III**[123c-d] and **IV**[123e] (Figure 15). The synthesis of most of these compounds were carried out in a racemic form except for compounds **III**, which were obtained in an enantiopure form by means of a racemic resolution. Unfortunately, none of them displayed remarkable antiviral activity.

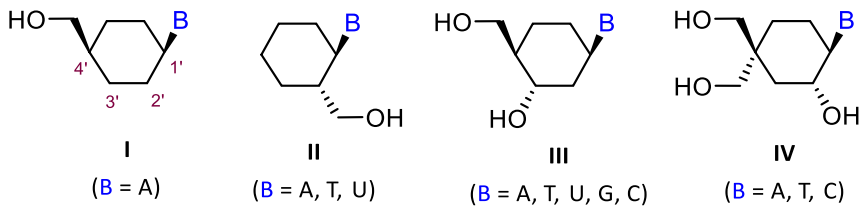

Figure 15. Structures of different cyclohexanyl nucleoside analogues synthesised.

It was postulated that the absence of biological activity could be caused by the inability of cyclohexanyl nucleoside analogues to mimic the conformational behaviour of the furanose ring.[124] Therefore, in order to design novel six-membered ring candidates, a detailed close-up view of the conformational behaviour of furanose nucleosides was required.

The furanose ring of nucleosides features one or two atoms out of the plane. This displacement from planarity is called puckering. If one atom is significantly displaced out of the plane, the conformation is denoted as *envelope* (E) whereas if two atoms are shifted from the plane of the others, the resulting conformation is referred as *twist* (T) (Figure 16).

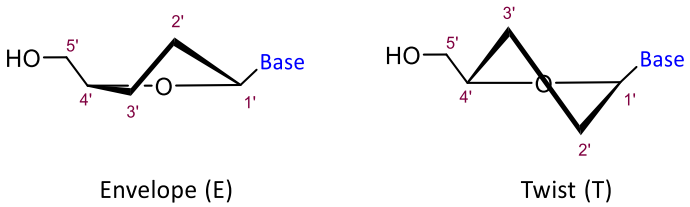

Figure 16. Conformations of the furanose ring.

In the practice, these two limit situations are rarely observed, because conformations do not respond to a perfect twist or envelope, rather there are intermediate forms. Frequently, neither

the four atoms forming a plane in an envelope conformation are coplanar, nor the deviation from the plane of the two atoms in a twist form are exactly the same. For this reason, the maximum of these displacements is defined as *major puckering*, and the least as *minor puckering*. The atoms that are displaced from the plane and are on the same face as C-5' are called *endo* while those that are on the opposite face are called *exo*.

There is an abbreviated conformational nomenclature that describes these conformations,[125] consisting in indicating, the number of the carbon atom that is displaced from the plane as a super- or subscript depending if the atom is *endo* or *exo*, respectively. Moreover, it is written before or after the letter E or T depending on the *major* or *minor puckering*, respectively. Thus, a C3'-endo-C2'exo twist asymmetric conformation, where C3' is more deviated from the plane (*major puckering*) than C2' (*minor puckering*) is abbreviated as $^{3}T_{2}$ (Figure 17). In the case that both atoms show a twist symmetric deviation, the conformation should be labelled as $^{3}_{2}T$. Finally, C3'-exo and C2'-endo envelopes should be represented as $_{3}E$ and ^{2}E, respectively.

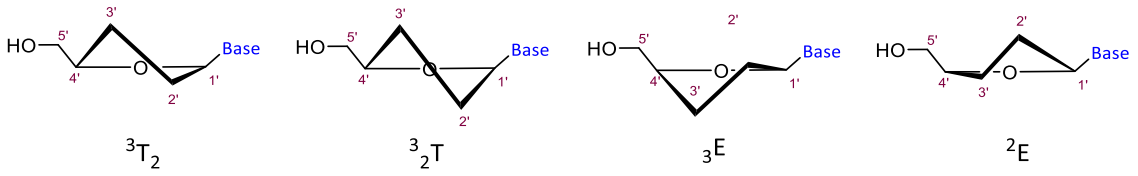

Figure 17. Examples of abbreviated conformational nomenclature of a nucleoside furanose ring.

As previously mentioned, some conformational studies of the cyclohexene ring suggest that cyclohexenyl nucleoside analogues can be considered as bioisostere of furanose nucleosides.[121a-b,122,126] Indeed, the conformational behaviour of the cyclohexene ring is similar to that of the furanose ring due to the presence of two sp^2-hybridized carbon atoms in the cyclohexene ring, which reduce its flexibility,[121a] as shown in Figure 18. A cyclohexene ring mainly exists in the two *half-chair* forms, which interconverts via the symmetrical *boat* form. The energy barrier of interconversion between the two twist conformations of furanose and the two half-chair counterparts in cyclohexene ring are very similar. The half-chair ($^{3}_{2}H$ north and $^{2}_{3}H$ south) conformations of the cyclohexene ring are structurally equivalent to the twist ($^{3}_{2}T$ north and $^{2}_{3}T$ south) forms of the furanose ring.[121a-b]

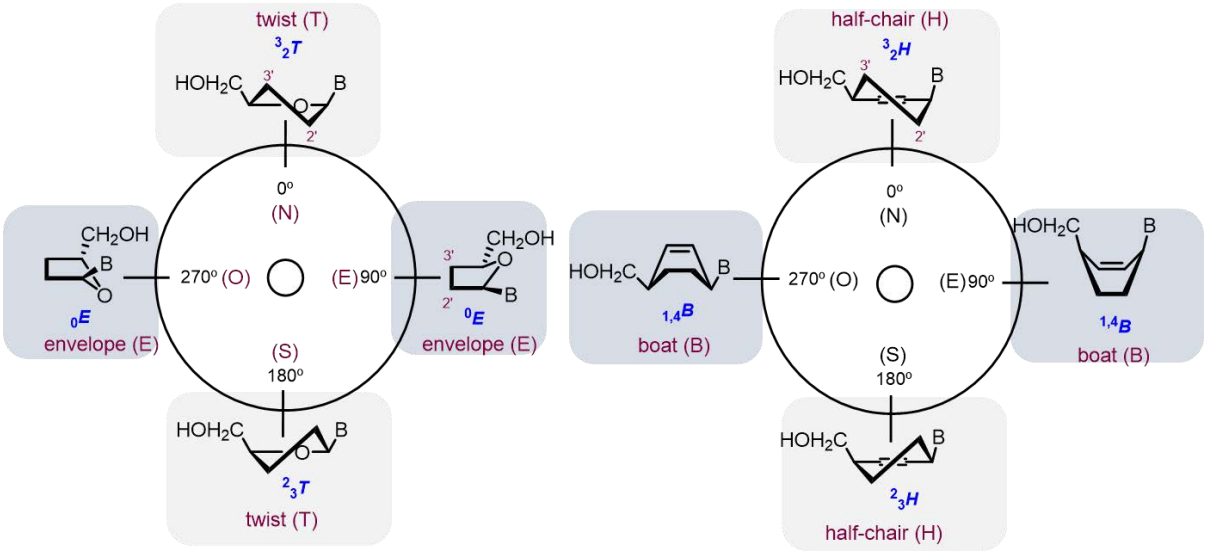

Figure 18. Equivalence between twist (T) and envelope (E) conformations of furanose ring and half-chair (H) and boat (B) of cyclohexene ring in a pseudorotational cycle.

These conformational studies encouraged investigators to keep looking for novel cyclohexenyl nucleosides analogues. To date, six families of cyclohexenyl analogues have been synthesised (Figure 19): i) 4'-hydroxycyclohexenyl nucleosides, **V**;[127a-c] ii) L-4'-hydroxymethylcyclohexenyl nucleosides, **VI**;[128a-c] iii) 4'-hydroxymethyl-3'-hydroxycyclohexenyl nucleosides, **VII**;[121a-b,122,129] iv) 3',4'-dihydroxymethylcyclohexenyl nucleosides, **VIII**;[130] v) *ribo*-cyclohexenyl nucleosides, **IX**[131] and vi) *ara*-cyclohexenyl nucleosides, **X**.[132a,b]

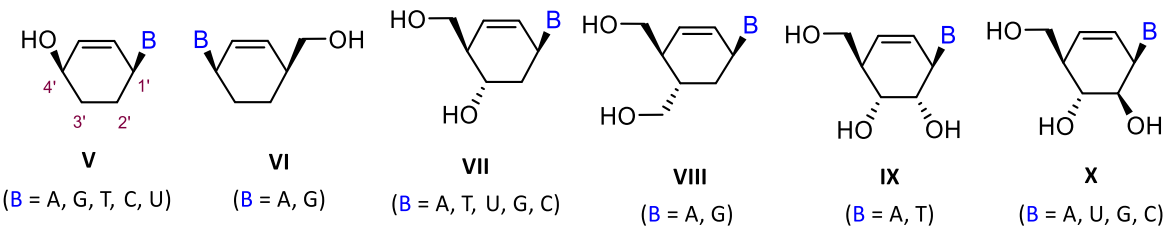

Figure 19. Structures of cyclohexenyl nucleoside analogues.

These enantiopure cyclohexenyl nucleoside analogues (Figure 19) have been synthesised *via* three different strategies:[103] i) through kinetic resolution by enzymatic catalysis[129a] (Scheme 1), ii) starting from chiral pool molecules[121a-b,132a-b] (Scheme 2) and iii) from cyclohexane derivatives (quinones), where chirality is introduced through chiral auxiliaries[133] (Scheme 3). Herein, a brief overview of some reported examples is given.

The first strategy which involves enzymatic kinetic resolution of racemic intermediates was applied to the synthesis of both enantiomers of cyclohexenyl G.[129a] The preparation of the

racemic intermediates (±)-**7** began with a Diels–Alder reaction of commercially available substituted cyclopentadiene, **1** and vinyl acetate, **2** to give the racemic adduct **3** (Scheme 1), which was transformed into intermediate (±)-**7** by ketal hydrolysis, Baeyer–Villiger reaction, lactone reduction and diol protection as the benzylidene acetal.[134] The separation of both enantiomers (±)-**7** was carried out *via* an enzymatic kinetic resolution using *Candida antarctica lipase* B, Novozyme® 435, which only acetylates alcohols with *S* configuration.[129a] Once both enantiomers of **7** were separated, the following steps were the introduction of the base moiety *via* a Mitsunobu reaction and removal of the protecting group to deliver both enantiomers of Cyclohexenyl G, **DCG** and **LCG**, in 11 and 12 steps, respectively, and 1% overall yield in both cases.

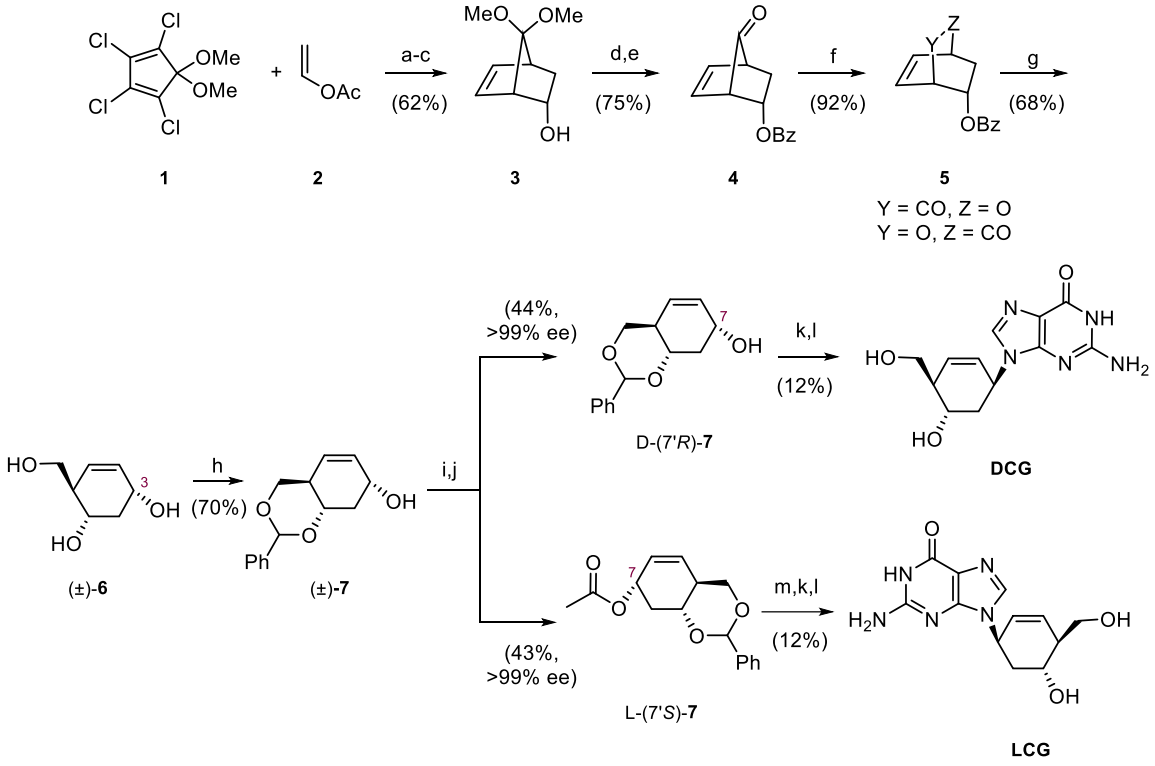

Scheme 1. Synthesis of both enantiomers **DCG** and **LCG** using an enzymatic kinetic resolution. Reagents and conditions: (a) 120 °C, 4 h; (b) MeOH, 5% H_2SO_4, 5 h; (c) Na/Liq NH_3, THF-EtOH, 20 min; (d) BzCl, py; (e) aq AcOH, reflux; (f) *m*-CPBA, CH_2Cl_2(dry), Na_2CO_3, 6 h; (g) $LiAlH_4$, THF(dry), -15 °C; (h) $PhCH(OMe)_2$, dioxane, PTSA; (i) Novozyme® 435, isopropenyl acetate, CH_2Cl_2; (j) recrystallization twice in EtOAc/n-hexane 50%; (k) PPh_3, DEAD, 2-amino-6-cloropurine, dioxane; (l) TFA/H_2O (3:1); (m) NH_3, MeOH.

In another approach, Hederwijn and co-workers reported the enantiopure synthesis of D-Cycohexenyl G using (*R*)-carvone as a chiral pool starting material (Scheme 2).[122] (*R*)-carvone was converted into epoxide **8** in 7 steps and 26% overall yield.[136] The regioselective reductive opening of this epoxide afforded olefin **9** which by the hydroboration with 9-BBN of the exo

double bond led to diol **10**. This compound was further elaborated to obtain allylic alcohol **12** through alcohol **11**. Finally, introduction of the base moiety via Mitsunobu reaction and successive treatment with TFA delivered D-Cyclohexenyl G (**DCG**) in 12 steps and 1.5% overall yield.

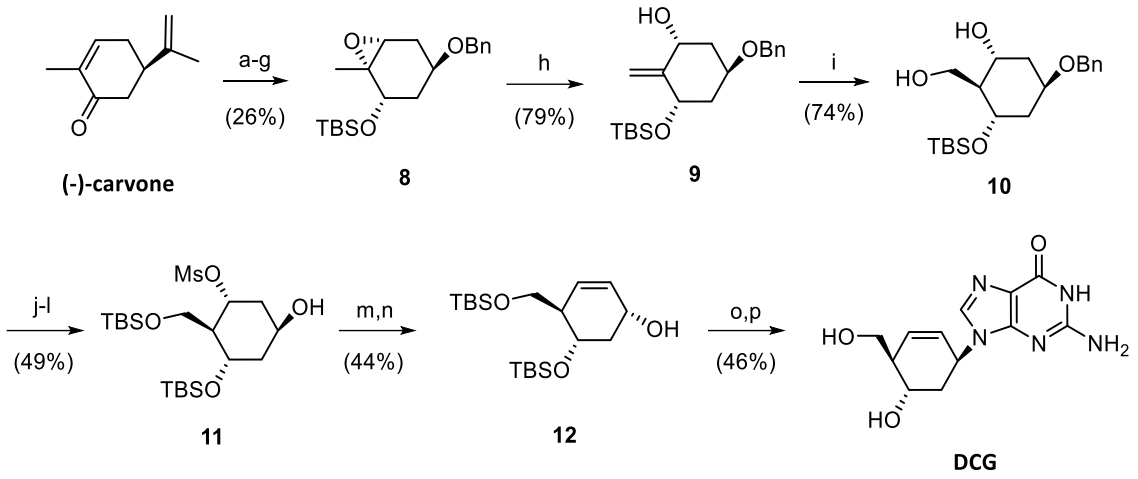

Scheme 2. Synthesis of D-cyclohexenyl G (**DCG**). Reagents and conditions: (a) H_2O_2, NaOH, MeOH; (b) L-Selectride, THF; (c) TBSCl, imidazole, DMF; (d) OsO_4, KIO_4, THF/H_2O; (e) *m*-CPBA, $CHCl_3$, pH = 8; (f) K_2CO_3, MeOH; (g) NaH, BnBr, TBAI, THF; (h) LiTMP, Et_2AlCl, toluene; (i) I) 9-BBN, THF; II) H_2O_2, NaOH, H_2O; (j) TBSCl, imidazole, DMF; (k) MsCl, Et_3N, CH_2Cl_2; (l) Pd-C, $HCOONH_4$, MeOH; (m) MnO_2, CH_2Cl_2; (n) $NaBH_4$, $CeCl_3 \cdot 7H_2O$, MeOH; (o) 2-amino-6-chloropurine, DEAD, PPh_3, 1,4-dioxane; (p) CF_3COOH/H_2O (3:1).

Finally, an enantiodivergent approach towards the synthesis of both D- and L-enantiomers of 4'-hydroxycyclohexenyl nucleosides was developed in our group starting from the commercially available 1,4-cyclohexanedione, **13**.[133] This approach relied on the use of (*R,R*)-hydrobenzoin as chiral auxiliary and catecholborane paired with (S)-2-Me-CBS as stereoselective chiral reducing agent. Thus, 1,4-cyclohexanedione was monoprotected with (*R*,*R*)-hydrobenzoin to give monoketal **14** (Scheme 3). The synthesis continues with the generation of a double bond and the stereoselective reduction of the ketone to give the corresponding allylic alcohol **16** in 66% overall yield. Then, the nucleobase was introduced with either inversion (Mitsunobu methodology) or retention (Pd-catalysed allylic substitution) of the configuration in the chiral centre. Final stereoselective reduction of the carbonyl group delivered the target D- and L-enantiomers of (4'-hydroxycyclohexenyl)uracil nucleosides, D-(1'*S*,4'*R*)-U-**18** and L-(1'*R*,4'*S*)-U-**18** in 31% and 22% overall yield respectively. These compounds were evaluated on MT4 cells for anti-HIV-1 activity against wild-type NL4-3 strain as well as cytotoxicity. Unfortunately, although a weak anti-HIV activity was found, it was not separated from cytotoxicity.

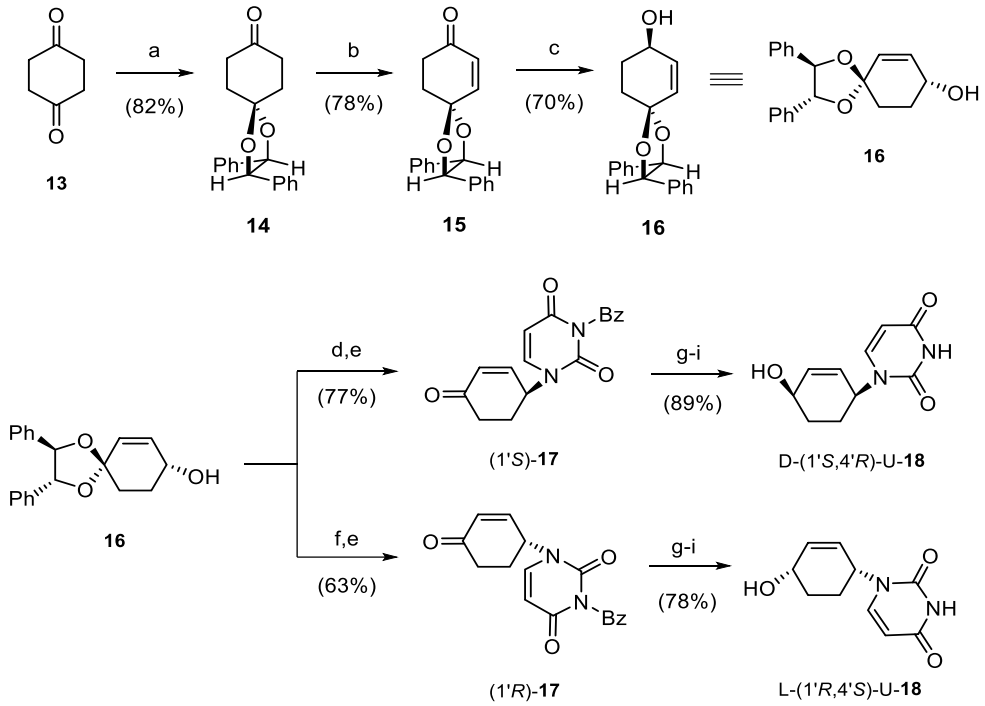

Scheme 3. Synthesis of (4'-hydroxycyclohexenyl)uracil D-(1'*S*,4'*R*)-U-**18** and its enantiomer L-(1'*R*,4'*S*)-U-**18**. Reagents and conditions: (a) (*R*,*R*)-hydrobenzoin, *p*-TsOH, benzene, reflux; (b) I) Br_2, diethyl ether; II) DBU, dioxane, 100 °C; (c) catecholborane, (*S*)-2-Me-CBS, CH_2Cl_2, -78 °C to rt; d) N^3-benzoyluracil, DBAD, Ph_3P, THF; (e) CF_3CO_2H/H_2O (14:1); f) I) $ClCO_2Et$, py, DMAP, CH_2Cl_2; II) N^3-benzoyluracil, $[(\eta^3\text{-}C_3H_5)PdCl]_2$, dppe, DMF; (g) catecholborane, (*S*)-2-Me-CBS for (1'*S*)-**GI11** or (*R*)-2-Me-CBS for (1'*R*)-**GI11**, CH_2Cl_2; (h) *p*-NO_2BzOH, DBAD, Ph_3P, THF; (i) $MeNH_2$, EtOH.

Unfortunately, the major part of the synthesised cyclohexenyl analogues (Figure 19) did not display any significant biological activity.

4.2. Conformationally locked carbocyclic analogues

As aforementioned, during the last decades, many efforts have been made trying to mimic the conformational behaviour of the sugar moiety of natural nucleosides.[137,138] In particular, conformationally locked carbocyclic analogues have been reported to present similar conformations than natural counterparts and some of them showing high antiviral activity.[137-142] Introducing a conformational restriction by means of a fused cyclopropane is a well-known approach to modulate the antiviral activity of a nucleoside.

In this context, the groups of Marquez [137-141,143,144] and Jung[145] have reported new families of conformationally rigid *carba*-nucleoside analogues (Figure 20) built on a bicyclo[3.1.0]hexane template that can lock the cyclopentane ring mimicking the *North* and *South* conformations of the natural furanose ring. All of this compounds showed biological activity such as *N*-**MCT**[146] which display potent antiviral activity against herpes virus (EC_{50} = 0.03 µg/mL for HSV-1 and EC_{50} = 0.09 µg/mL for HSV-2 in human foreskin fibroblasts) or **MRS 2346**[147] which is an anticancer agent, fully activates the human A_3 Adenosine Receptor (AR) with EC_{50} = 1.4 nM in Chinese Hamster Ovary (CHO) cells.[d]

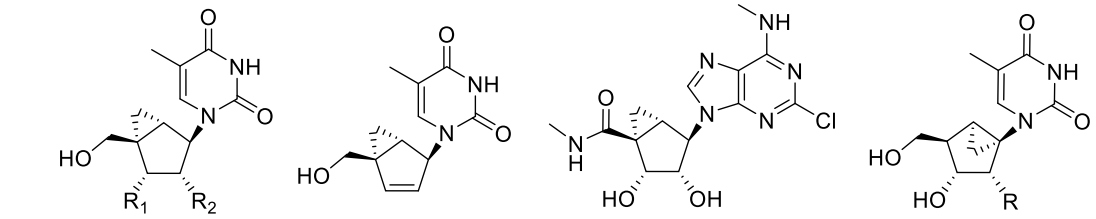

Figure 20. Structures of conformationally locked nucleoside analogues built on a bicyclo[3.1.0]hexane scaffold with biological activity.

The introduction of the cyclopropane ring to the carbocycle unit confers a certain degree of rigidity and since kinases and polymerases prefer different nucleoside conformations,[137] the sugar/carbocyclic moieties should not be completely rigid.

4.3. Last precedents in the research group

Considering the interesting anti-HSV activity of D-Cyclohexenyl G[121,122] and the results previously exposed by the introduction of a fused cyclopropane into the carbocycle unit, a new series of enantiopure bicyclo[4.1.0]heptanyl nucleoside analogues as potential anti-HSV agents were proposed based in our previous work[133] and wherein the double bond was replaced by a fused cyclopropane (structure **BCH**, Figure 21).[148]

[d] Chinese Hamster Ovary (**CHO**) cells are an epithelial cell line derived from the ovary of the Chinese hamster, often used in biological and medical research and commercially in the production of therapeutic proteins. CHO cells are the most commonly used mammalian hosts for industrial production of recombinant protein therapeutics.

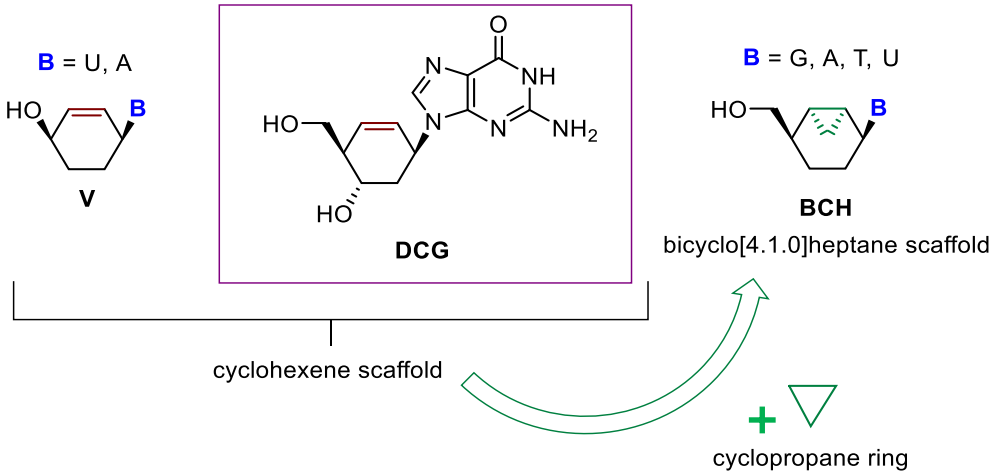

Figure 21. Strategy to convert cyclohexene to bicyclo[4.1.0]heptane scaffold (**BCH**) by replacing the double bond by fused cyclopropane ring.

First it was evaluated whether imposing rigidity with a cyclopropane unit fused to the cyclohexane could affect their binding into the active site of the HSV-1 TK involved in the first phosphorylation step by protein-ligand docking studies.

The docking results were analysed on structural and energetic terms considering binding and catalytic activity. The main criterion used to analyse the docking outcomes was to check that, at least, several low-energy binding modes were consistent with precatalytic orientations and that their corresponding binding energies were similar to those of the reference compounds (dT and ACV, and DCG for pyrimidine and purine analogues, respectively). For example, for **BCH-G** and **DCG** the nucleobase moiety was sandwiched between Met-128 and Tyr-172, and it was stabilized by pairwise hydrogen bond interactions with Gln-125 as well as with the side chain of Arg-176 (Figure 22). The 5'-OH was hydrogen bonded to Arg-163 and Glu-83, which is responsible for deprotonating the alcohol to be phosphorylated. The bicyclic scaffold provides favourable van der Waals interactions with the hydrophobic pocket of HSV-1 TK shaped by the side chain of tryptophan (Trp88), isoleucine (Ile97), and histidine (His-58).

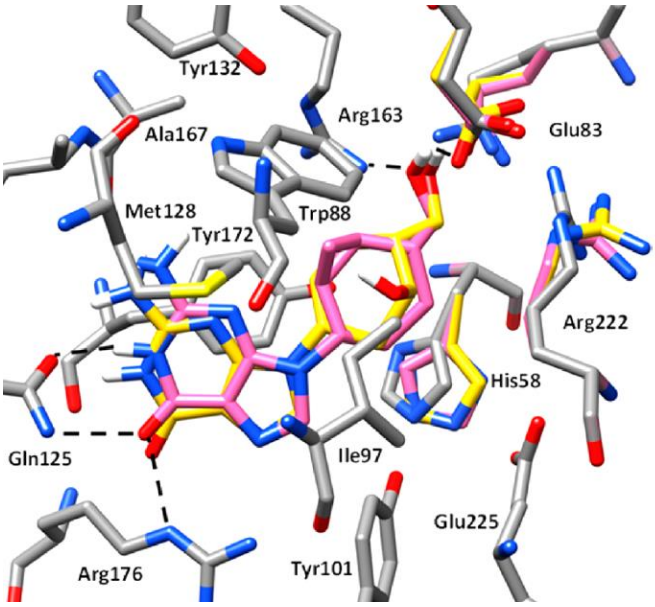

Figure 22. Compound **BCH-G** (pink) superimposed with DCG (yellow) in HSV-1 TK (PDB 2KI5; X-ray residues shown in grey). Hydrogen bonds are depicted as dotted lines. For the sake of clarity, hydrogen atoms are only shown when they are bound to a heteroatom of the ligand.[148]

These results clearly indicated that the replacement of the double bond for a fused cyclopropane ring did not alter the binding mode of the nucleosides in this kinase and, consequently, the synthetic analogues envisaged should be correctly activated at the first phosphorylation step.[148]

Having verified the capability to interact properly with the binding site of the HSV-1 TK, the synthesis of candidates **BCH**-(**G**, **A**, **T** and **U**) was undertaken. Thus, the synthesis started from enantiopure allylic alcohol **16** which was obtained from commercially available 1,4-cyclohexanedione, **13** over 3 steps in 66% yield (Scheme I-4). Bicyclo[4.1.0]heptanyl alcohol **21** was achieved after of a Simmons-Smith reaction in order to introduce the cyclopropane ring into the cyclohexenyl scaffold. Next, ketone **22** was afforded after alcohol protection and carbonyl deprotection and was further transformed into alcohol **23** through Wittig olefination and a hydroboration−oxidation reaction. Alcohol **23** was protected and TBDPS was removed in order to provide the alcohol **24**. Finally, the introduction of the base moiety was accomplished, in all cases, via stepwise construction of the nucleobase from the ammonium chloride derivative **25**, which was afforded from alcohol **24** in 2 steps and 72% yield. The purine derivatives **BCH-G** and **BCH-A** were achieved starting from **25** in 4 steps and 25% and 53% overall yield, respectively. The pyrimidine derivatives **BCH-T** and **BCH-U** were afforded in 3 steps and 13% and 27% overall yield, respectively.

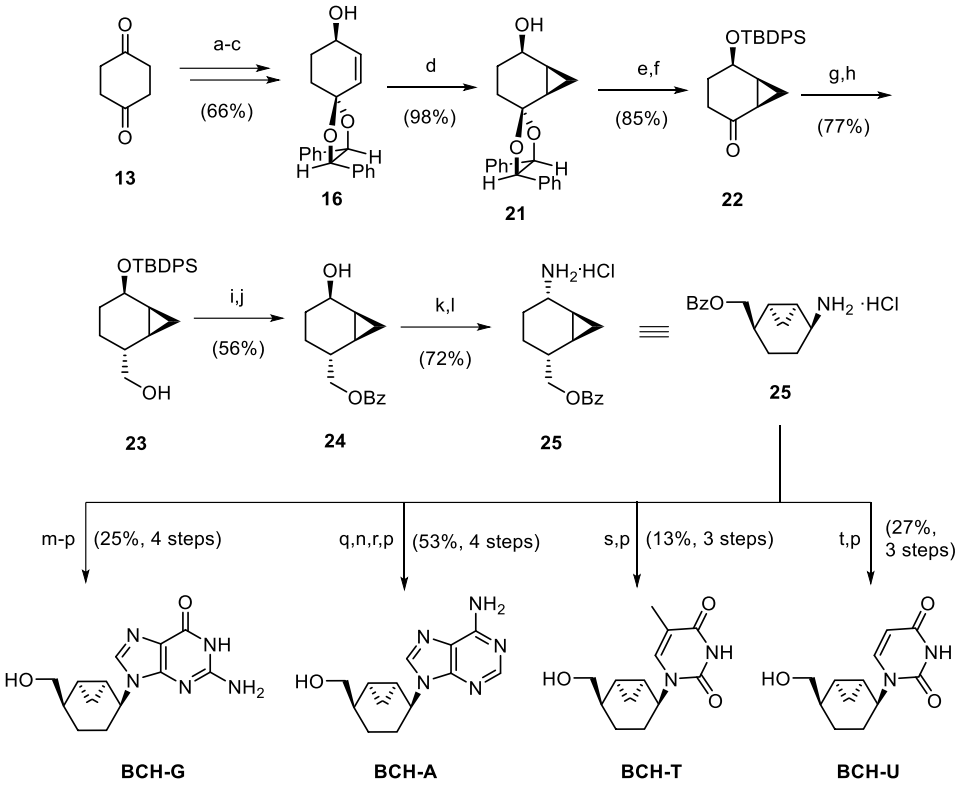

Scheme 4. Synthesis of bicyclo[4.1.0]heptane nucleoside analogues **BCH**-(**G**, **A**, **T**, and **U**). Reagents and conditions: (a) (*R*,*R*)-hydrobenzoin, PPTS, benzene, reflux; (b) I) Et_3N, TMSOTf CH_2Cl_2, -10 °C, II) IBX·MPO, DMSO, rt; (c) (*R*,*R*)-Noyori-I (3%mol), HCO_2Na, CTAB, CH_2Cl_2/ H_2O (1:1), rt, 24 h; (d) $CH_3COOZnCH_2I$, CH_2Cl_2, -10 °C; (e) TBDPSCl, im, CH_2Cl_2, rt, 16 h; (f) $In(OTf)_3$, acetone; (g) Ph_3CH_3I, *t*-BuOK, THF, 0 °C to rt; (h) I) 9-BBN, THF, -10 ° C to rt, 16 h, II) NaOH, H_2O_2; (i) BzCl, Et_3N, CH_2Cl_2; (j) TBAF, THF, rt; (k) $(PhO)_2PON_3$, DBAD, PPh_3, toluene, 0 °C to rt, 16 h; (l) H_2 (2 atm), Pd/C, EtOAc, rt; (m) *N*,*N*'-(4,6-dichloropyrimidine-2,5-diyl)diformamide, DIPEA, dioxane, 100 °C, MW; (n) diethoxymethyl acetate, 120 °C, MW; (o) HCOOH 80%, 100 °C; (p) $MeNH_2$, EtOH, rt, 24 h; (q) *N*-(4,6-dichloropyrimidin-5-yl)formamide, DIPEA, dioxane, reflux; (r) NH_4OH, dioxane, 100 °C, MW; (s) I) ethyl (*E*)-(3-ethoxy-2-methylacryloyl)carbamate, Et_3N, dioxane, 100 °C, II) HCl, 2 M, 90 °C; (t) I) (*E*)-3-ethoxyacryloyl isocyanate, THF, -10 °C to rt, II) H_2SO_4 1 M, MeOH, reflux.

The prepared compounds **BCH**-(**G**, **A**, **T**, and **U**) were subjected to comprehensive screening for antiviral activity. In particular, the compounds were examined for antiherpetic activity (herpes simplex virus-1 (HSV-1; strain KOS), herpes simplex virus-2 (G), and herpes simplex virus-1 (KOS thymidine kinase-deficient acyclovir resistant)) in human embryonic lung (HEL) cell cultures. Unfortunately, none of the compounds showed significant antiviral activity at subtoxic concentrations (~250 µM).[148] The lack of activity indicates that these functionalized NAs might eventually not reach the HSV DNA incorporation step catalysed by the HSV-encoded DNA polymerases and further studies are required to reveal the molecular basis of the antiherpetic inactivity of the test compounds; in particular, some single enzymatic assays with these compounds should be made.

5. REFERENCES

[1] J.D. Rawn, *Bioquimica.* Vol I. McGraw Hill-Interamericana de España, 1989.

[2] Seley-Radtke, K. L.; Yates, M. K. *Antiviral Res.* **2018**, *154*, 66–86.

[3] Jordheim, L. P.; Durantel, D.; Zoulim, F.; Dumontet, C. *Nat. Rev. Drug Discov.* **2013**, *12*, 447–464.

[4] De Clercq, E.; Li, G. *Clin. Microbiol. Rev.* **2016**, *29*, 695–747.

[5] Shelton, J.; Lu, X.; Hollenbaugh, J. A.; Cho, J. H.; Amblard, F.; Schinazi, R. F. *Chem. Rev.* **2016**, *116*, 14379–14455.

[6] Collier, L. H.; Oxford, J. S. *Human Virology*; 3rd ed.; Oxford University Press, 2006.

[7] World Health Organization (WHO). HIV/AIDS. Data and statistics. https://www.who.int/hiv/data/en/ (acceded, 08/02/2020).

[8] World Health Organization (WHO). Herpes simplex virus. https://www.who.int/news-room/fact-sheets/detail/herpes-simplex-virus (acceded, 08/02/2020).

[9] Wagner, K. E.; Hewlett, M. J. *Basic Virology*; 2nd ed.; Blackwell Publishing, 2004.

[10] Cann, A. J. *Principles of molecular virology*; 5th ed.; Academic Press, 2011.

[11] AIDSinfo. The HIV Life Cycle https://aidsinfo.nih.gov/understanding-hiv-aids/fact-sheets/19/73/the-hiv-life-cycle (acceded, 08/02/2020)

[12] HIV life cycle. https://aidsinfo.nih.gov/understanding-hiv-aids/fact-sheets/19/73/the-hiv-life-cycle (acceded 08/02/2020)

[13] (a) Morrison, J.; Plotkin, S. *Viral Vaccines: Fighting Viruses with Vaccines*, Third Edit.; Elsevier, 2016; (b) Arvin, A. M.; Greenberg, H. B. *Virology* **2006**, *344*, 240–249.

[14] De Clercq, E. *Antiviral Res.* **2010**, *85*, 19–24.

[15] De Clercq, E. *Future Virol.* **2008**, *3*, 393–405.

[16] Martin, J. C.; Hitchcock, M. J. M.; De Clercq, E.; Prusoff, W. H. *Antiviral Res.* **2010**, *85*, 34–38.

[17] Razonable, R. R. *Mayo Clin. Proc.* **2011**, *86*, 1009–1026.

[18] Prusoff, W. H. *Biochim. Biophys. Acta.* **1959**, *32*, 295–296.

[19] Herrmann, E.C. *Proc. Soc. Exp. Biol. Med*. **1961**, *107*, 142-145.

[20] Heidelberger, C.; Parsons, D.; Remy, D. C. *J. Am. Chem. Soc.* **1962**, *84*, 3597–3598.

[21] Wilhelmus, K.R. *Cochrane Database of Systematic Reviews* **2015**, 1.

[22] Elion, G. B.; Furman, P. A.; Fyfe, J. A.; De Miranda, P.; Beauchampt, L.; Schaeffert, H. J. *Proc. Natl. Acad. Sci. USA* **1977**, *74*, 5716–5720.

[23] Broder, S. *Antiviral Res.* **2010**, *85*, 1–18.

[24] Smith, K. O.; Galloway, K. S.; Kennell, W. L.; Ogilvie, K. K.; Radatus, B. K. *Antimicrob. Agents Chemother.* **1982**, *22*, 55–61.

[25] Harnden, M. R.; Jarvest, R. L. *Tetrahedron Lett.* **1985**, *26*, 4265–4268.

[26] Colla, L.; De Clercq, E.; Busson, R.; Vanderhaeghe, H. *J. Med. Chem.* **1983**, *697*, 602–604.

[27] Pescovitz, M. D.; Rabkin, J.; Merion, R. M.; Paya, C. V.; Pirsch, J.; Freeman, R. B.; O'Grady, J.; Robinson, C.; To, Z.; Wren, K.; Banken, L.; Buhles, W.; Brown, F. *Antimicrob. Agents Chemother.* **2000**, *44*, 2811–2815.

[28] Gill, K. S.; Wood, M. J. *Clin. Pharmacokinet.* **1996**, *31*, 1–8.

[29] De Clercq, E.; Descamps, J.; De Somer, P.; Barr, P. J.; Jones, A. S.; Walker, R. T. *Proc. Natl. Acad. Sci. USA* **1979**, *76*, 2947–2951.

[30] Snoeck, R.; Sakuma, T.; De Clercq, E.; Rosenberg, I.; Holy, A. *Antimicrob. Agents Chemother.* **1988**, *32*, 1839–1844.

[31] Mahmoud, S.; Hasabelnaby, S.; Hammad, S.; Sakr, T. *J. Adv. Pharm. Res.* **2018**, *2*, 73–88.

[32] Yarchoan, R.; Mitsuya, H.; Thomas, R. V.; Pluda, J. M.; Hartman, N. R.; Perno, C. F.; Marczyk, K. S.; Allain, J. P.; Johns, D. G.; Broder, S. *Science* **1989**, *245*, 412–415.

[33] Mitsuya, H.; Broder, S. *Proc. Natl. Acad. Sci. U.S.A.* **1986**, *83*, 1911–1915.

[34] Lin, T. S.; Schinazi, R. F.; Prusoff, W. H. *Biochem. Pharmacol.* **1987**, *36*, 2713–2718.

[35] Daluge, S. M.; Good, S. S.; Faletto, M. B.; Miller, W. H.; St Clair, M. H.; Boone, L. R.; Tisdale, M.; Parry, N. R.; Reardon, J. E.; Dornsife, R. E.; Averett, D. R.; Krenitsky, T. A. *Antimicrob. Agents Chemother.* **1997**, *41*, 1082–1093.

[36] Gumina, G.; Song, G. Y.; Chu, C. K. *FEMS Microbiol. Lett.* **2001**, *202*, 9–15.

[37] Schinazi, R. F.; Chu, C. K.; Peck, A.; McMillan, A.; Mathis, R.; Cannon, D.; Jeong, L.-S.; Beach, J. W.; Choi, W.-B.; Yeola, S.; Liotta, D. C. *Antimicrob. Agents Chemother.* **1992**, *36*, 672–676..

[38] Schinazi, R. F.; McMillan, A.; Cannon, D.; Mathis, R.; Lloyd, R. M.; Peck, A.; Sommadossi, J.-P.; Clair, M. S.; Wilson, J.; Furman, P. A.; Painter, G.; Choi, W.-B.; Liotta, D. C. *Antimicrob. Agents Chemother.* **1992**, *36*, 2423–2431.

[39] Balzarini, J.; Holy, A.; Jindrich, J.; Naesens, L.; Snoeck, R.; Schols, D.; De Clercq, E. *Antimicrob. Agents Chemother.* **1993**, *37*, 332–338.

[40] Sofia, M. J.; Bao, D.; Chang, W.; Du, J.; Nagarathnam, D.; Rachakonda, S.; Reddy, G. P.; Ross, B. S.; Wang, P.; Zhang, H.; Bansal, S.; Espiritu, C.; Keilman, M.; Lam, A. M.; Micolochick Steuer, H. M.; Niu, C.; Otto, M. J.; Furman, P. A. *J. Med. Chem*. **2010**, *53*, 7202–7218.

[41] Gallant, J. E.; Staszemski, S.; Pozniak, A. L.; DeJesus, E.; Suleiman, J. M. A. H.; Miller, M. D.; Coakley, D. F.; Lu, B.; Toole, J. J.; Cheng, A. K. *J. Am. Med. Assoc.* **2004**, *292*, 191–201.

[42] Calmy, A.; Hirschel, B.; Cooper, D. A.; Carr, A. *Antivir. Ther.* **2009**, *14*, 165–179.

[43] Paredes, R.; Clotet, B. *Antiviral Res.* **2010**, *85*, 245–265.

[44] Kuritzkes, D. R. *Curr. Opin. Virol.* **2011**, *1*, 582–589.

[45] Damaraju, V. L.; Damaraju, S.; Young, J. D.; Baldwin, S. A.; Mackey, J.; Sawyer, M. B.; Cass, C. E. *Oncogene* **2003**, *22,* 7524–7536.

[46] Deville-Bonne, D.; El Amri, C.; Meyer, P.; Chen, Y.; Agrofoglio, L. A.; Janin, J. *Antiviral Res.* **2010**, *86*, 101–120.

[47] Furman, P. A.; Fyfe, J. A.; St. Clair, M. H.; Weinhold, K.; Rideout, J. L.; Freeman, G. A.; Lehrman, S. N.; Bolognesi, D. P.; Broder, S.; Mitsuya, H.; Barry, D. W. *Proc. Natl. Acad. Sci. USA* **1986**, *83*, 8333–8337.

[48] El Safadi, Y.; Vivet-Boudou, V.; Marquet, R. *Appl. Microbiol. Biotechnol.* **2007**, *75*, 723–737.

[49] Arts, E. J.; Wainberg, M. A. *Antimicrob. Agents Chemother.* **1996**, *40*, 527–540.

[50] Elion, G. B. *J. Antimicrob. Chemother.* **1983**, *12*, 9–17.

[51] Prichard, M. N.; Keith, K. A.; Johnson, M. P.; Harden, E. A.; McBrayer, A.; Luo, M.; Qiu, S.; Chattopadhyay, D.; Fan, X.; Torrence, P. F.; Kern, E. R. *Antimicrob. Agents Chemother.* **2007**, *51*, 1795–1803.

[52] Avendaño, C.; Menéndez, J. C. *Medicinal chemistry of anticancer drugs.* 2nd Ed. Elsevier, 2015.

[53] Nelson, S. M., Ferguson, L. R., and Denny, W. A. *Cell & Chromosome* **2004,** 3, 1-26.

[54] (a) Rasool, S.; Kadla, S. A.; Rasool, V.; Ganai, B. A. *Tumor Biol*. **2013**, *34*, 2469−2476; Anand, P.; (b) Kunnumakara, A. B.; Sundaram, C.; Harikumar, K. B.; Tharakan, S. T.; Lai, O. S.; Sung, B.; Aggarwal, B. B. *Pharm. Res.* **2008**, *25*, 2097–2116.

[55] Saeki, N.; Ono, H.; Sakamoto, H.; Yoshida, T. *Cancer Sci*. **2013**, *104*, 1−8.

[56] Yanik, E. L.; Tamburro, K.; Eron, J. J.; Damania, B.; Napravnik, S.; Dittmer, D. P. *Infect. Agents Cancer* **2013**, *8*, 18.

[57] World Health Organization (WHO). Cancer, Key facts. https://www.who.int/news-room/fact-sheets/detail/cancer (acceded, 08/02/2020).

[58] World Health Organization (WHO). Cancer tomorrow. http://gco.iarc.fr/tomorrow/home (acceded, 08/02/2020).

[59] World Health Organization (WHO). Cancer in Spain 2018. http://gco.iarc.fr/today/data/factsheets/populations/724-spain-fact-sheets.pdf (acceded, 08/02/2020

[60] Lash, B. W.; Gilman, P. B. *Principles of Cytotoxic Chemotherapy*, *Chapter 12*, Elsevier Inc., USA, 2013.

[61] Sun, J.; Wei, Q.; Zhou, Y.; Wang, J.; Liu, Q.; Xu, H. *BMC Syst. Biol.* **2017**, *11*, 87.

[62] Fortin, S.; Berube, G. *Expert Opin. Drug Discovery* **2013**, *8*, 1029−1047.

[63] Secrist, J. A. *Nucleic Acids Symp. Ser.* **2005**, *49*, 15–16.

[64] Périgaud, C.; Gosselin, G.; Imbach, J. L. *Nucleos. Nucleot.* **1992**, *11*, 903–945.

[65] Parker, W. B. *Chem Rev.* **2009**, *109*, 2880–2893.

[66] Elion, G. B., Burgi, E.; Hitchings, G. H. *J. Am. Chem. Soc.* **1952**, *74*, 411-414.

[67] Levinsen, M.; Rotevatn, E. O.; Rosthoj, S.; Nersting, J.; Abrahamsson, J.; Appell, M. L.; Bergan, S.; Bechensteen, A. G.; Harila-Saari, A.; Heyman, M.; et al. *Pediatr. Blood Cancer* **2014**, *61*, 797−802.

[68] Elion, G. B.; Hitchings, G. H. *J. Am. Chem. Soc.* **1955***, 77*, 1676-1676.

[69] Shelton, J.; Lu, X.; Hollenbaugh, J. A.; Cho, J. H.; Amblard, F.; Schinazi, R. F. *Chem. Rev.* **2016**, *116*, 14379–14455.

[70] Heidelberger, C.; Chaudhuri, N. K.; Danneberg, P.; Mooren, D.; Griesbach, L.; Duschinsky, R.; Schnitzer, R. J.; Pleven, E.; Scheiner, J. *Nature* **1957**, *179*, 663−666.

[71] Longley, D. B.; Harkin, D. P.; Johnston, P. G. *Nat. Rev. Cancer* **2003**, *3*, 330−338.

[72] (a) Pratt, S.; Shepard, R. L.; Kandasamy, R. A.; Johnston, P. A.; Perry, W., 3rd; Dantzig, A. H. *Mol. Cancer Ther*. **2005**, 4, 855−863; (b) Diasio, R. B.; Harris, B. E. *Clin. Pharmacokinet*. **1989**, 16, 215−237.

[73] Cavaliere, A.; Probst, K. C.; Westwell, A. D.; Slusarczyk, M. *Future Med. Chem.* **2017**, *9*, 1809–1833.

[74] DiMasi, J. A.; Paquette, C. *PharmacoEconomics* **2004**, *22*, 1−14.

[75] Shimma, N.; Umeda, I.; Arasaki, M.; Murasaki, C.; Masubuchi, K.; Kohchi, Y.; Miwa, M.; Ura, M.; Sawada, N.; Tahara, H.; Kuruma, I.; Horii, I.; Ishitsuka, H. *Bioorg. Med. Chem*. **2000**, *8*, 1697−1706.

[76] Hertel, L. W.; Boder, G. B.; Kroin, J. S.; Rinzel, S. M.; Poore, G. A.; Todd, G. C.; Grindey, G. B. *Cancer Res.* **1990**, *50*, 4417−4422.

[77] Lech-Maranda, E.; Korycka, A.; Robak, T. *Mini Rev. Med. Chem.* **2009**, *9*, 805–812.

[78] Cohen, S. S. *Perspect. Biol. Med*. **1963**, 6, 215−227.

[79] Wang, J. J.; Selawry, O. S.; Vietti, T. J.; Bodey, G. P., Sr. *Cancer* **1970**, *25*, 1−6.

[80] Píškala, A.; Šorm, F. *Collect. Czech. Chem. Commun*. **1964**, *29*, 2060−2076.

[81] Winkley, M. W.; Robins, R. K. *J. Org. Chem.* **1970**, *35*, 491−495.

[82] Christensen, L. F.; Broom, A. D.; Robins, M. J.; Bloch, A. *J. Med. Chem*. **1972**, *15*, 735−739.

[83] Krenitsky, T. A.; Koszalka, G. W.; Jones, L. A.; Averett, D. R.; Moorman, A. R. EP Patent 0294114, 1988.

[84] Woo, P. W. K.; Dion, H. W.; Lange, S. M.; Dahl, L. F.; Durham, L. J. *Heterocycl. Chem*. **1974**, *11*, 641−643.

[85] Chen, S. F.; Stoeckler, J. D.; Parks, R. E., Jr. *Biochem. Pharmacol*. **1984**, *33*, 4069−4079.

[86] Ursem, C.; Van Loon, K.; Venook, A. *Cancer J*. **2016**, *22*, 196−198.

[87] Galmarini, C. M.; Mackey, J. R.; Dumontet, C. *Lancet Oncol.* **2002**, *3*, 415–424.

[88] Diab, R.; Degobert, G.; Hamoudeh, M. *Expert Opin. Drug Deliv*. **2007**, *4,* 513-531.

[89] Holohan, C.; Van Schaeybroeck, S.; Longley, D. B.; Johnston, P. G. *Nat. Rev. Cancer* **2013**, *13*, 714−726.

[90] Song, X.; Lorenzi, P. L.; Landowski, C. P.; Vig, B. S.; Hilfinger, J. M.; Amidon, G. L. *Mol. Pharm.* **2005**, *2*, 157–167.

[91] Van Rompay, A. R.; Johansson, M.; Karlsson, A. *Pharmacol. Ther.* **2003**, *100*, 119–139.

[92] Shipley, L. A.; Brown, T. J.; Cornpropst, J. D.; Hamilton, M.; Daniels, W. D.; Culp, H. W. *Drug. Metab. Dispos.* **1992**, *20,* 849 -855.

[93] (a) Marquez, V. S. *Advances in Antiviral Drug Design*, Vol. 2, Elsevier 1996; (b) Marquez, V. E., Lim, M. I. *Med. Res. Rev.*, **1986**, *6*, 1-40

[94] Shealy, Y. F.; Clayton, J. D. *J. Am. Chem. Soc.* **1966**, *88*, 3885–3887.

[95] Shealy, Y. F.; Clayton, J. D. *J. Am. Chem. Soc.* **1969**, *91*, 3075–3083.

[96] Kusaka, T.; Yamamoto, H.; Shibata, M.; Muroi, M.; Kishi, T.; Mizuno, K. *J. Antibiot.* **1968**, *21*, 255-263.

[97] Yaginuma, S.; Muto, N.; Tsujino, M.; Sudate, Y.; Hayashi, M.; Otani, M. *J. Antibiot.* **1981**, *34*, 359–366.

[98] Seley-Radtke, K. L.; Yates, M. K. *Antiviral Res.* **2018**, *154*, 66–86.

[99] Ichikawa, E.; Kato, K. Review. *Curr. Med. Chem.* **2012**, *8*, 385–423.

[100] Schneller, S. *Curr. Top. Med. Chem.* **2005**, *2*, 1087-1092.

[101] Zhu, X. F. *Nucleo., Nucleot. Nucl.* **2000**, *19*, 651–690.

[102] Mulamoottil, V. A.; Nayak, A.; Jeong, L. S. *Asian J. Org. Chem.* **2014**, *3*, 748–761.

[103] Boutureira, O.; Isabel Matheu, M.; Díaz, Y.; Castillón, S. *Chem. Soc. Rev.* **2013**, *42*, 5056–5072.

[104] Burger, A. *J. Med. Chem.* **2005**, *6*, 829–829.

[105] Marquez, V. S.; Lim, M. *Carbocyclic Nucleosides*, **1986**, *6*, 1-40.

[106] Vince, R.; Hua, M.; Brownell, J.; Daluge, S.; Lee, F.; Shannon, W. M.; Lavelle, G. C.; Qualls, J.; Weislow, O. S.; Kiser, R.; Canonico, P. G.; Schultz, R. H.; Narayanan, V. L.; Mayo, J. G.; Shoemaker, R. H.; Boyd, M. R. *Biochem. Biophys. Res. Commun*. **1988**, *156*, 1046–1053.

[107] Carter, S. G.; Kessler, J. A.; Rankin, C. D. *Antimicrob. Agents Chemother.* **1990**, *34*, 1297-1300.

[108] Daluge, S. M.; Good, S. S.; Faletto, M. B.; Miller, W. H.; Clair, M. H. S. T.; Boone, L. R.; Tisdale, M.; Parry, N. R.; Reardon, J. E.; Dornsife, R. E.; Averett, D. R.; Krenitsky, T. A. *Antimicrob. Agents Chemother*. **1997**, *41*, 1082–1093.

[109] Crimmins, M. T.; King, B. W. *J. Org. Chem.* **1996**, *61*, 4192–4193.

[110] Zoulim, F. *J. Clin. Virol.* **2006**, *36*, 8–12.

[111] Peters, G. J.; Smid, K.; Vecchi, L.; Kathmann, I.; Sarkisjan, D.; Honeywell, R. J.; Losekoot, N.; Ohne, O.; Orbach, A.; Blaugrund, E.; L. S. Jeong, Y. B. Lee, C. Ahn, D. J. Kim. *Invest. New Drugs* **2013**, *31*, 1444−1457.

[112] Soucy, T. A.; Smith, P. G.; Milhollen, M. A.; Berger, A. J.; Gavin, J. M.; Adhikari, S.; Brownell, J. E.; Burke, K. E.; Cardin, D. P.; Critchley, S. *Nature* **2009**, *458*, 732−736.

[113] Shimada, N.; Hasegawa, S.; Harada, T.; Tomisawa, T.; Fujii, A.; Takita, T. *J. Antibiot*. **1986**, *39*, 1623-1625.

[114] Hoshino, H.; Shimizu, N.; Shimada, N.; Takita, T.; Takeuchi, T. *J. Antibiot.* **1987**, *40*, 1077–1078.

[115] Honjo, M.; Maruyama, T.; Sato, Y.; Horii, T. *Chem. Pharm. Bull.* **1989**, *37*, 1413–1415.

[116] Norbeck, D. W.; Kern, E.; Hayashi, S.; Rosenbrook, W.; Sham, H.; Herrin, T.; Plattner, J. J.; Erickson, J.; Clement, J.; Swanson, R.; Shipkowitz, N.; Hardy, D.; Marsh, K.; Arnett, G.; Shannon, W.; Broder, S.; Mitsuya, H. *J. Med. Chem.* **1990**, *33*, 1281–1285.

[117] Sekiyama, T.; Hatsuya, S.; Tanaka, Y.; Uchiyama, M.; Ono, N.; Iwayama, S.; Oikawa, M.; Suzuki, K.; Okunishi, M.; Tsuji, T. *J. Med. Chem.* **1998**, *41*, 1284–1298.

[118] Ashton, W. T.; Canning Meurer, L.; Cantone, C. L.; Kirk Field, A.; Hannah, J.; Karkas, J. D.; Liou, R.; Patel, G. F.; Perry, H. C.; Wagner, A. F. *J. Med. Chem.* **1988**, *31*, 2304–2315.

[119] Qiu, Y. L.; Ksebati, M. B.; Ptak, R. G.; Fan, B. Y.; Breitenbach, J. M.; Lin, J. S.; Cheng, Y. C.; Kern, E. R.; Drach, J. C.; Zemlicka, J. *J. Med. Chem.* **1998**, *41*, 10–23.

[120] Onishi, T., Matsuzawa, T., Nishi, S., & Tsuji, T. *Tetrahedron Lett.* **1999**, *40*, 8845-8847.

[121] (a) Herdewijn, P; De Clercq, E. *Bioorg. Med. Chem. Lett.* **2001**, *11*, 1591-1597; (b) Wang, J.; Froeyen, M.; Hendrix, C.; Andrei, G.; Snoeck, R.; De Clercq, E.; Herdewijn, P. *J. Med. Chem.* **2000**, *43*, 736–745.

[122] Wang, J.; Herdewijn, P. *J. Org. Chem.* **1999**, *64*, 7820–7827.

[123] (a) Schaeffer, H. J.; Odin, E. *J. Pharm. Sci.* **2006**, *54*, 421–424; (b) Viña, D.; Santana, L.; Uriarte, E. *Nucleos. Nucleot.* **2001**, *20*, 1363–1365; (c) Maurinsh, Y.; Rosemeyer, H.; Esnouf, R.; Medvedovici, A.; Wang, J.; Ceulemans, G.; Lescrinier, E.; Hendrix, C.; Busson, R.; Sandra, P.; Seela, F.; Van Aerschot, A.; Herdewijn, P. *Chem. Eur. J.* **1999**, *5*, 2139–2150; (d) Maurinsh, Y.; Schraml, J.; De Winter, H.; Blaton, N.; Peeters, O.; Lescrinier, E.; Rozenski, J.; Van Aerschot, A.; De Clercq, E.; Busson, R. *J. Org. Chem.* **1997**, *62*, 2861–2871; (e) Mikhailov, S. N.; Blaton, N.; Rozenski, J.; Balzarini, J.; De Clercq, E.; Hederwijn, P. *Nucleos. Nucleot.* **1996**, *15*, 869–878.

[124] Neidle, S. *Principles of nucleic acid structure*, Academic Press: Amsterdam, 2008.

[125] Sundaralingam, M. *J. Am. Chem. Soc*. **1971**, *93*, 6644-6647 and references cited therein.

[126] Wang, J.; Froeyen, M.; Herdewijn, P. *Adv. Antivir. Drug Des.* **2004**, *4*, 119–145.

[127] (a) Perez-Perez, M.-J.; Rozenski, J.; Busson, R.; Herdewijn, P. *J. Org. Chem.* **1995**, *60*, 1531–1537; (b) Arango, J. H.; Geer, A.; Rodríguez, J.; Young, P. E.; Scheiner, P. *Nucleo. Nucleot.* **1993**, *12*, 773–784; (c) Ramesh, K.; Wolfe, M. S.; Lee, Y.; Vander Velde, D.; Borchardt, R. T. *J. Org. Chem.* **1992**, *57*, 5861–5868

[128] (a) Olivo, H. F.; Yu, J. *J. Chem. Soc. Perkin Trans. 1* **1998**, *3*, 391–392; (b) Konkel, M. J.; Vince, R. *Tetrahedron* **1996**, *52*, 799–808; (c) Katagiri, N.; Ito, Y.; Shiraishi, T.; Maruyama, T.; Sato, Y.; Kaneko, C. *Nucleos. Nucleot.* **1996**, *15*, 631–647.

[129] (a) Gu, P.; Griebel, C.; Van Aerschot, A.; Rozenski, J.; Busson, R.; Gais, H.-J.; Herdewijn, P. *Tetrahedron* **2004**, *60*, 2111–2123; (b) Wang, J.; Morral, J.; Hendrix, C.; Herdewijn, P. *J. Org. Chem.* **2001**, *66*, 8478–8482.

[130] Rosenquist, A.; Kvarnström, I.; Classon, B.; Samuelsson, B. *J. Org. Chem.* **1996**, *61*, 6282–6288.

[131] Vijgen, S.; Nauwelaerts, K.; Wang, J.; Van Aerschot, A.; Lagoja, I.; Herdewijn, P. *J. Org. Chem.* **2005**, *70*, 4591–4597.

[132] (a) Horváth, A.; Ruttens, B.; Herdewijn, P. *Tetrahedron Lett.* **2007**, *48*, 3621–3623; (b) Wang, J.; Viña, D.; Busson, R.; Herdewijn, P. *J. Org. Chem.* **2003**, *68*, 4499–4505.

[133] Ferrer, E.; Alibés, R.; Busqué, F.; Figueredo, M.; Font, J.; De March, P. *J. Org. Chem.* **2009**, *74*, 2425–2432.

[134] Varada, M.; Kotikam, V.; Kumar, V. A. *Tetrahedron* **2011**, *67*, 5744–5749.

[135] Herdewijn, P. *Antiviral Res.* **2006**, 71, 317-321.

[136] Wang, J.; Busson, R.; Blaton, N.; Rozenski, J.; Herdewijn, P. J. *Org. Chem*. **1998**, *63*, 3051-3058.

[137] Marquez, V. E.; Ben-kasus, T.; Barchi, J. J.; Green, K. M.; Nicklaus, M. C.; Agbaria, R. *J. Am. Chem. Soc.* **2004**, *126*, 543–549.

[138] Marquez, V. E.; Choi, Y.; Comin, M. J.; Russ, P.; George, C.; Huleihel, M.; Ben-Kasus, T.; Agbaria, R. *J. Am. Chem. Soc.* **2005**, *127*, 15145–15150.

[139] Marquez, V. E.; Comin, M. J. *Núcleos. Nucleot.* **2007**, *26*, 585–588.

[140] Moon, H. R.; Ford, H.; Marquez, V. E. *Org. Lett.* **2000**, *2*, 3793–3796.

[141] Moon, H. R.; Kim, H. O.; Chun, M. W.; Jeong, L. S.; Marquez, V. E. *J. Org. Chem.* **1999**, *64*, 4733–4741.

[142] Zhu, X.-F. *Nucleos. Nucleot.* **2000**, *19*, 651–690.

[143] Joshi, B. V; Moon, H. R.; Fettinger, J. C.; Marquez, V. E.; Jacobson, K. A. *J. Org. Chem.* **2005**, *70*, 439–447.

[144] Comin, M. J.; Vu, B. C.; Boyer, P. L.; Liao, C.; Hughes, S. H.; Marquez, V. E. *ChemMedChem* **2008**, *3*, 1129–1134.

[145] Jung, M. E., Dwight, T. A., Vigant, F., Østergaard, M. E., Swayze, E. E., & Seth, P. P. *Angew. Chem.* **2004**, 126, 10051-10055.

[146] Marquez, V. E.; Siddiqui, M. A.; Ezzitouni, A.; Russ, P.; Wang, J.; Wagner, R. W.; Matteucci, M. D. *J. Med. Chem.* **1996**, *39*, 3739–3747.

[147] a) Joshi, B. V; Moon, H. R.; Fettinger, J. C.; Marquez, V. E.; Jacobson, K. A. *J. Org. Chem.* **2005**, *70*, 439–447; b) Gao, Z. G.; Kim, S.-K.; Biadatti, T.; Chen, W.; Lee, K.; Barak, D.; Kim, S. G.; Johnson, C. R.; Jacobson, K. A. *J. Med. Chem.* **2002**, *45*, 4471-4484.

[148] Domínguez-Pérez, B., Ferrer, E., Figueredo, M., Maréchal, J. D., Balzarini, J., Alibés, R., Busqué, F. *J. Org. Chem.* **2015**, *80*, 9495-9505.

II. OBJECTIVES

OBJECTIVES

Considering the background about NAs and, in particular, conformationally locked CNAs, and their use in antiviral therapies, the present work is aimed towards the enantioselective synthesis of novel nucleoside analogues built on a bicyclo[4.1.0]heptane scaffold and their evaluation as antiviral agents. Consequently, we have focused on four main objectives:

➢ OBJECTIVE 1. Synthesis of key ketone intermediate

The first objective is to stablish a reliable synthetic procedure for the multigram scale preparation of the bicyclo[4.1.0]heptane scaffold **XI** which is the starting material for the synthesis of novel nucleoside analogues. Two synthetic pathways, previously used in our research group, will be optimized in order to determine the more efficient and reproducible route to prepare **XI**.

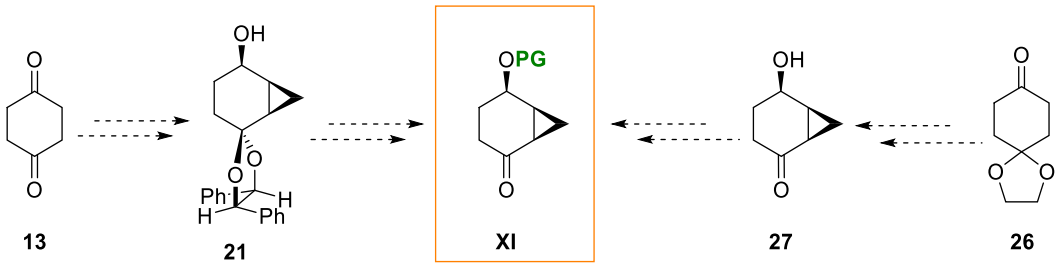

Scheme O-1. Planned synthetic strategies towards the preparation of ketone **XI.**

➢ OBJECTIVE 2. Cytosine nucleoside analogue 28

The 5'-hydroxymethylbicyclo[4.1.0]heptane analogues **BCH**-(**A**, **G**, **T** and **U**) NAs, previously synthesised in the research group, did not show significant antiviral activity. However, some enzymatic assays of these compounds were still pending. Moreover, in order to complete the 5'-hydroxymethylbicyclo[4.1.0]heptanyl family, the cytosine analogue **28** has to be synthesised and its activity evaluated. Thus, the second objective of the present thesis involves the preparation of **28** which will be synthesised following a known synthetic approach starting from ketone **XI** which will be converted to the key intermediate ammonium compound **25** through alcohol **24** (Scheme O-2). The desired cytosine compound **28** will be obtained from **25** by a

stepwise construction of the nucleobase. Compound **28** will be screened for antiviral activity along with enzymatic assays.

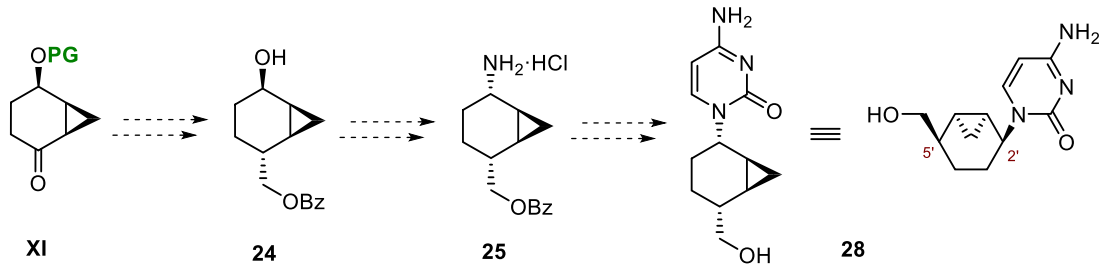

Scheme O-2. Planned synthetic strategy towards the cytosine analogue **28**.

➢ OBJECTIVE 3. Synthesis of 5'-hydroxymethyl-4'-hydroxybicyclo[4.1.0]heptane nucleoside analogues with natural nucleobases

The third objective is devoted to the enantiopure synthesis of the novel 5'-hydroxymethyl-4'-hydroxybicyclo[4.1.0]heptane nucleoside analogues **XIV** (Scheme O-3) based on D-cyclohexenyl G. In this case, we plan to develop a synthetic sequence to reach ammonium compound **XIII** through azide **XII**. From **XIII**, different natural nucleobases (pyrimidine and purine bases) will be stepwise constructed.

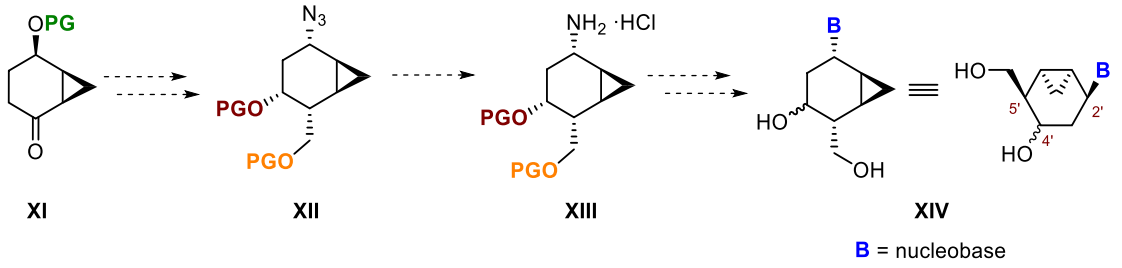

Scheme O-3. Planned synthetic strategy towards the synthesis of 5'-hydroxymethyl-4'-hydroxybicyclo[4.1.0]heptane nucleoside analogues.

All these newly synthesised 5'-hydroxymethyl-4'-hydroxybicyclo[4.1.0]heptanyl nucleoside analogues **XIV** will be screened for antiviral activity against different viruses such as HSV, HIV or Zika virus and also its cellular cytotoxicity will be evaluated.

➢ OBJECTIVE 4. Synthesis of new 5'-hydroxymethyl-4'-hydroxybicyclo[4.1.0]heptane nucleoside analogues with 1,2,3-triazolo-nucleobases

In order to explore the possible effect in the antiviral activity of introducing more structural diversity in the bicyclo[4.1.0]heptane scaffold, a new 5'-hydroxymethyl-4'-hydroxybicyclo[4.1.0]heptane nucleoside analogues with an 1,2,3-triazole moiety as a nucleobase will be constructed from common azide **XII** (Scheme O-4).

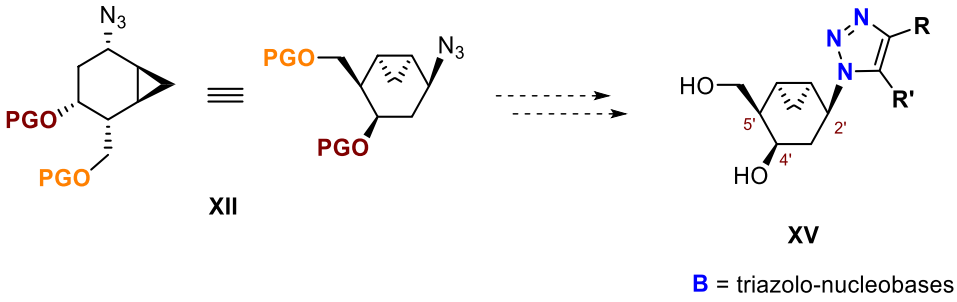

Scheme O-4. Planned synthetic strategy towards the synthesis of 5'-hydroxymethyl-4'-hydroxybicyclo[4.1.0]heptane nucleoside analogues.

All these newly synthesised 1,2,3-triazolo-carbanucleoside analogues **XV** also will be screened for antiviral activity against different viruses and its cellular cytotoxicity evaluated.

III. Results and discussion

CHAPTER I: Synthesis of pivotal intermediate bicyclo[4.1.0]heptane, **36**.

CHAPTER II: Synthesis of cytosine 5'-hydroxymethyl-bicyclo[4.1.0]heptanyl NA, **28**.

CHAPTER III: Synthesis of 5'-hydroxymethyl-4'-hydroxybicyclo[4.1.0]heptan-2'-yl NAs based on cyclohexanyl G.

CHAPTER IV: Synthesis of new substituted 1,2,3-triazolo-carbanucleoside analogues.

III. CHAPTER I

Synthesis of pivotal intermediate

bicyclo[4.1.0]heptane, **36**

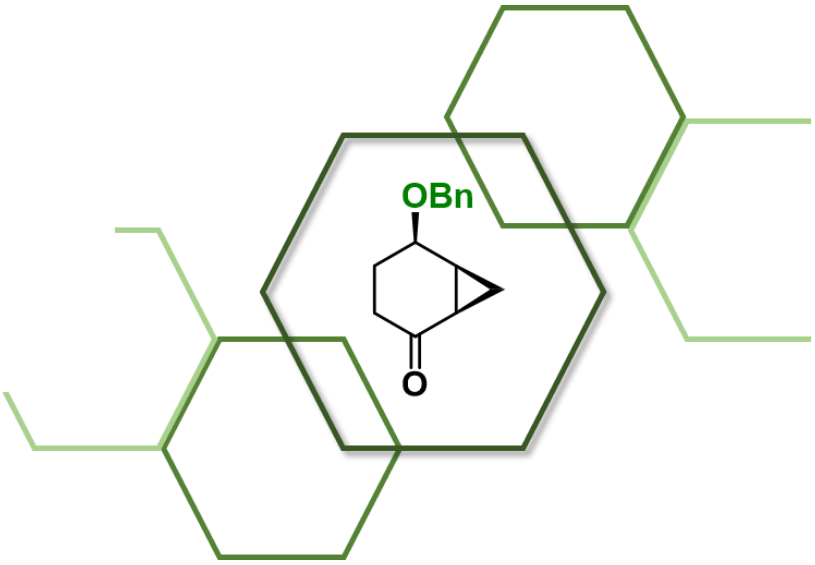

1. INTRODUCTION

Over the past few years, our research group has been involved in the enantioselective synthesis of bioactive products containing a cyclohexene unit in their structure.[1a-f] The enantiopure allylic alcohol **16** (Scheme I-1) has been used as a building block in the synthesis of several of these bioactive compounds such as the natural alkaloid Allosecurinine[1c] or (*R*)-(–)-Sporochnol A which is a defensive agent against herbivores.[1b] Allylic alcohol **16** is also a precursor of 4-hydroxy-2-cyclohexenone, **30**, which has been used by different research groups in the synthesis of other bioactive compounds, such as the bacterial DNA primase inhibitor (+)-Sch 642305[2] or the anti-cholesterol agent ML-236A.[3] In our group, **16** was prepared by two different methodologies using as starting material either *p*-benzoquinone, **29**, or 1,4-cyclohexanedione, **13** (Scheme I-1).

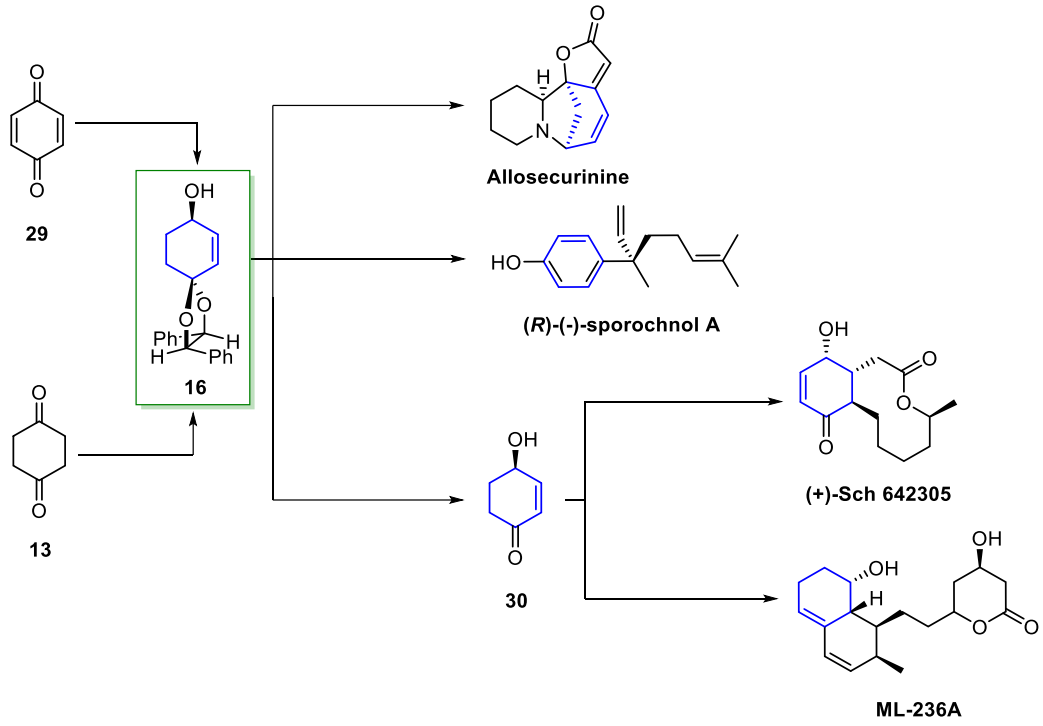

Scheme I-1. Allylic alcohol **16** as a building block in the synthesis of several bioactive compounds.

1.1. Precedents in the research group

The first synthesis of enantiopure allylic alcohol **16** was performed in our research group from *p*-benzoquinone **29** in 3 steps and 21% overall yield (Scheme I-2, red).[1a] The synthetic approach started with a selective ketalization with (*R,R*)-hydrobenzoin, as a chiral auxiliary, to afford monoketal **31** in 84% yield. Then, partial hydrogenation using Wilkinson's catalyst ($RhCl(PPh_3)_3$) led to enone **15** albeit in low yield (38%), and reduction using $NaBH_4$ delivered a 4:1 mixture of

allylic alcohols **16** and **32**, which was enriched with the desired alcohol **16** (67% yield) after several recrystallizations. This synthesis presented some disadvantages in its scale-up: first, the low yield in the hydrogenation step and the high price of the Wilkinson's catalyst; and second, the poor diastereoselectivity achieved in the carbonyl reduction, requiring few recrystallizations to purify allylic alcohol **16**.

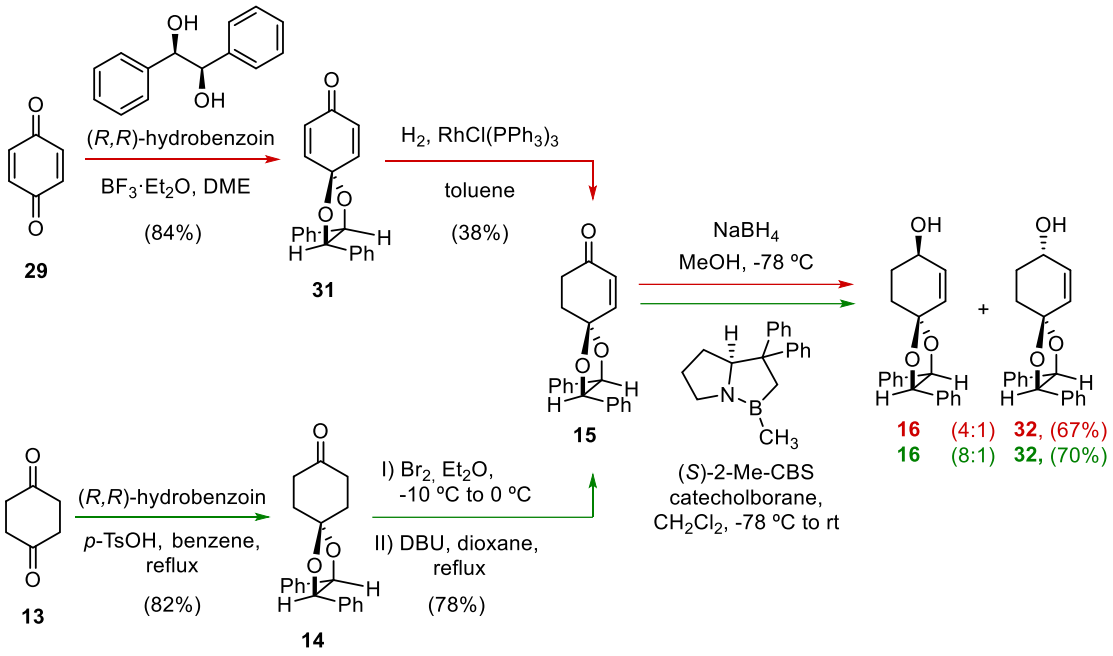

Scheme I-2. Synthesis of allylic alcohol **16** previously developed in our research group.[1a,4]

With the aim of overcoming these problems, a more practical preparation of **16** was set up in 3 steps and 45% overall yield (Scheme I-2, green).[4] This synthetic strategy started with the monoprotection of commercially available 1,4-cyclohexanedione **13** using the (*R,R*)-hydrobenzoin, providing ketone **14** in 82% yield. Then, sequential α-bromination of ketone **14** with Br_2 and dehydrobromination using DBU in 1,4-dioxane at the reflux temperature furnished enone **15** in 78% yield. Finally, reduction of the carbonyl group of enone was carried out following the Corey-Bakshi-Shibata reduction,[5,6] delivering an 8:1 mixture of allylic alcohols **16** and **32**.

This synthetic strategy was later improved, affording allylic alcohol **16** in 3 steps and 81% overall yield (Scheme I-3).[7] The yield of the selective ketalization was slightly enhanced by using pyridinium *p*-toluenesulfonate (PPTS) instead of *p*-TsOH, leading to monoketal **14** in 88% yield. Then, the monodehydrogenation of ketone **15** was achieved following Nicolaou's methodology,[8,9] by treatment with Et_3N and TMSOTf in anhydrous CH_2Cl_2 at -10 ºC and

subsequent oxidation using an IBX·MPO complex in DMSO at rt, delivering enone **15** in 96% yield. Finally, reduction of the carbonyl group was carried out following an asymmetric transfer hydrogenation (ATH) using a chiral ruthenium catalyst (Noyori catalyst),[10,11] leading to a 24:1:2.4 mixture of allylic alcohols **16** and **32** and saturated alcohol **33**, respectively, in good yield (82%).

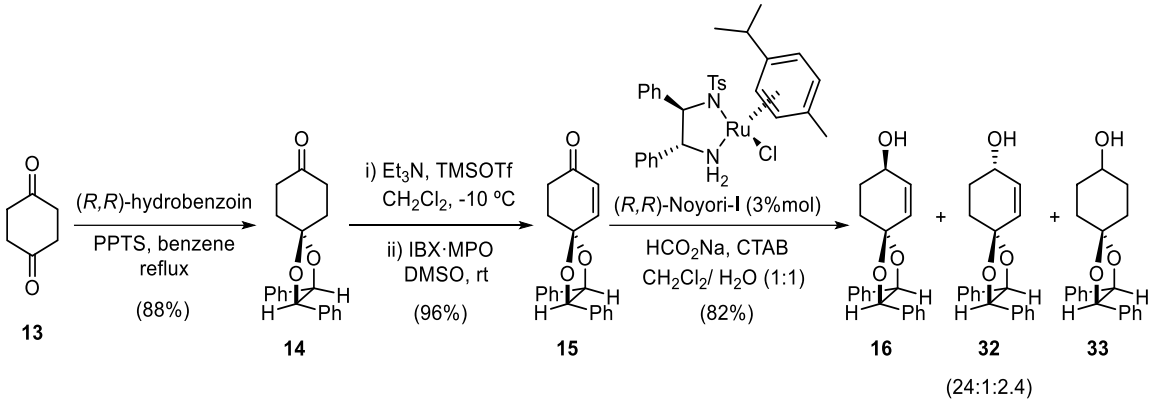

Scheme I-3. Most recent synthetic pathway to prepare allylic alcohol **16**.[7]

As previously seen in the general introduction, from allylic alcohol **16**, our group designed a new strategy directed to the synthesis of enantiopure carbocyclic nucleoside analogues built in a bicyclo[4.1.0]heptane scaffold (type **BCH**, Scheme I-4).[7] Although the synthesis of these compounds was carried out in good yields, one of the biggest challenges, in this synthesis, was/is the preparation of ketone **22** which required a cyclopropanation reaction, alcohol protection and removal of the ketal. This last step was more problematic that it was expected, since in some reaction conditions the ketal hydrolysis was accompanied of alcohol deprotection. Finally, it was found that the reaction could be successfully done under mild neutral conditions *via* a transacetalization with acetone and indium(III) trifluoromethanesulfonate, In(OTf$_3$) as a catalyst. However, the reaction presented two main drawbacks, a lack of reproducibility and the price of the catalyst when it was scaled-up.

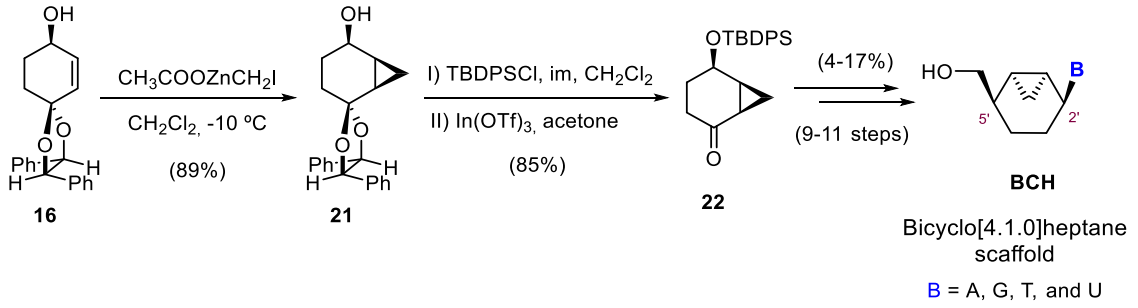

Scheme I-4. Synthesis of 5'-hydroxymethylbicyclo[4.1.0]heptane nucleoside analogues **BCH** from **16**.[7]

In parallel, a different synthetic approach towards intermediate **22** was evaluated from commercially available monoketal **26** (Scheme I-5).[12] This synthesis started with the monodehydrogenation of the monoketal **26** followed by an asymmetric reduction using chiral Noyori's catalyst, to deliver allylic alcohol **35** in 79% yield (92% ee determined by CHPLC). Next, the cyclopropanation reaction was performed to afford directly the ketone **27** since ketal was removed in the reaction conditions. Finally, after protection of alcohol as a *tert*-butyldiphenylsilyl ether, ketone **22** was obtained in 15% overall yield over the 4 steps. This low yield was attributed to the high volatility of **27** intermediate.

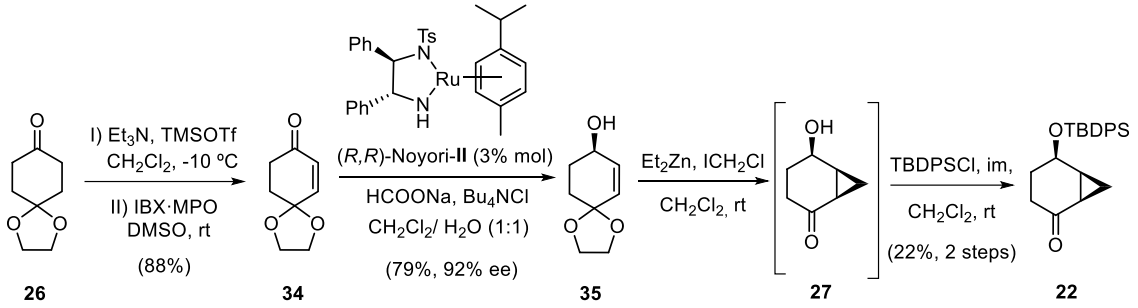

Scheme I-5. Synthesis of ketone **22** in the absence of the chiral auxiliary.[12]

Due to the importance of ketone **22** as a pivotal intermediate for the preparation of new conformationally restricted bicyclo[4.1.0]heptane NAs, it was decided to prepare it in large scale adopting the previous synthetic strategies (Schemes I-(3-5)) but performing some synthetic modifications in order to obtain it in a robust and reproducible way. For that proposal, since TBDPS as protecting group gave problems in the hydrolysis step, it was decided to use another protecting group that could resist the hydrolysis conditions. In that sense, the benzyl group was envisaged to be a good option due to its stability in front of acid conditions and its easy deprotection (Scheme I-6). Pivotal ketone **36** will be used in posterior chapters for the synthesis of new carbocycle nucleoside analogues with bicyclo[4.1.0]heptanyl scaffold.

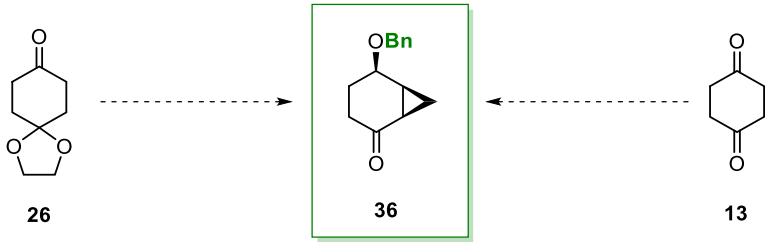

Scheme I-6. Preparation of ketone **36** by two different pathways from **26** and **13**.

2. SYNTHESIS OF PIVOTAL KEY INTERMEDIATE 36

2.1. Synthetic strategy

In this chapter, it is described the synthesis of the key intermediate **36** following the two previous explained approaches (Scheme I-(3-5)). It was decided to start with the synthetic *pathway A* since it has fewer steps than *pathway B* (Scheme I-7). In this route, **36** will be synthesised from commercially available 1,4-cyclohexanedione monoethylene acetal **26** which will be dehydrogenated and stereoselective reduced to the corresponding allylic alcohol **35**. Then, the formation of the cyclopropane will lead to alcohol **27**, which will be converted into **36** after alcohol protection. Similarly, this intermediate **36** will be obtained by the synthetic *pathway B*, following the same reactions that in the previous *pathway A*, but starting from commercially available 1,4-cyclohexanedione **13** and protecting one of the carbonyl groups using (*R*,*R*)-hydrobenzoin (**14**).

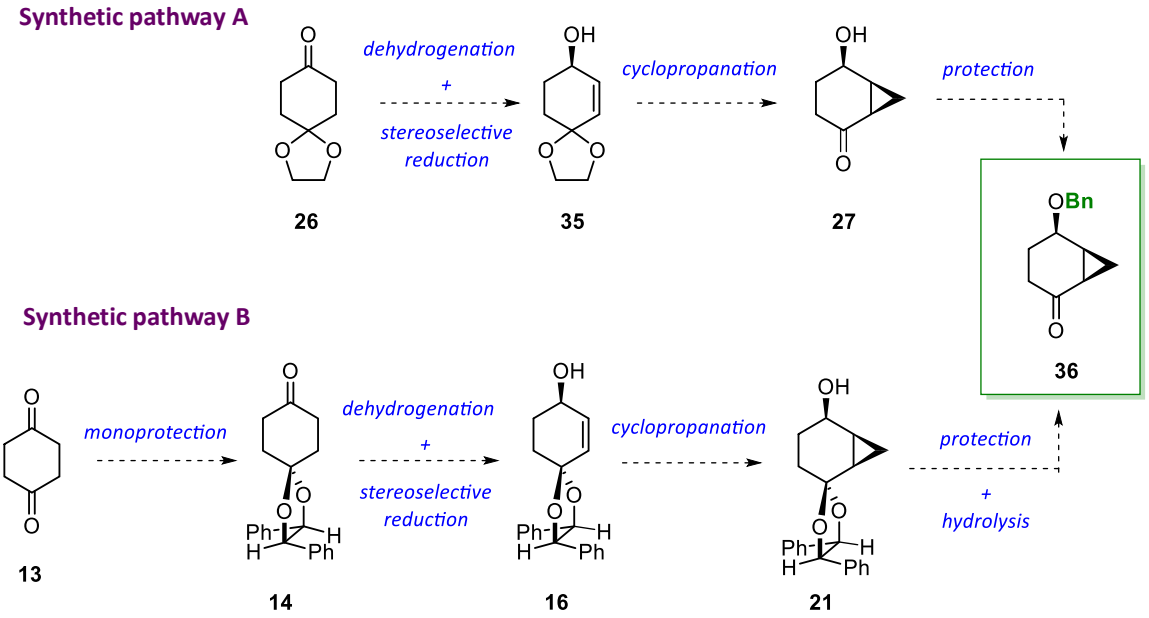

Scheme I-7. Foreseen synthetic pathways to prepare key intermediate **36**.

2.2. Synthetic pathway A. Synthesis of 36 with ethylene acetal as protecting group

In this pathway, the synthesis of **36** started from achiral 1,4-cyclohexanedione monoethylene acetal **26** which was mono-dehydrogenated following Nicolaou's methodology.[8,9] This

methodology, allows to prepare α,β-unsaturated ketones and aldehydes in mild conditions from silyl enol ethers by using hypervalent iodine species. In particular, the use of IBX (*o*-iodoxybenzoic acid) in complex with 4-methoxypyridine-*N*-oxide (MPO) in DMSO allows to oxidize silyl enol ethers to the corresponding α,β-unsaturated carbonyl compounds at room temperature.

IBX is commercially available but was easily prepared in large scale following a protocol developed by Santagostino *et al.*,[13] which involves oxidation of *o*-iodobenzoic acid with Oxone® (oxidizing agent with composition $2KHSO_5 \cdot KHSO_4 \cdot K_2SO_4$) in water at 70 °C for 1.5 h. (Scheme I-8). IBX is an unstable compound that must be stored at low temperatures (2-8 °C), since at room temperature it slowly decomposes to IBA (*o*-iodosobenzoic acid).[14]

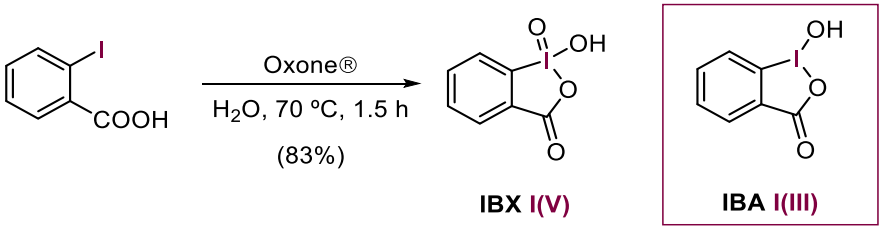

Scheme I-8. Preparation of IBX by Santagostino *et al*.[13] and structure of IBA.

Thus, treatment of monoketal **26** with Et_3N and TMSOTf in anhydrous CH_2Cl_2 at -10 °C leading to the corresponding silyl enol ether **37**, which was then oxidised with IBX·MPO complex to furnish enone **34** in 88% yield (Scheme I-9). It should be noted that IBX must be pure in order to avoid the possible hydrolysis of the ketal that would eventually lead to hydroquinone.

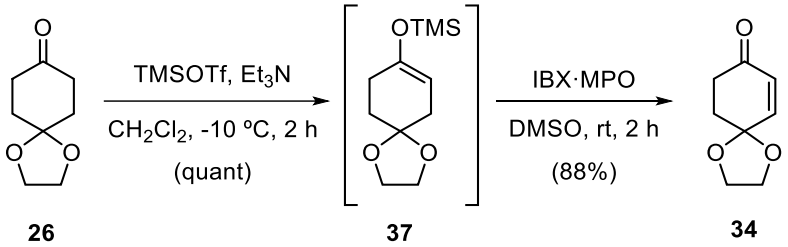

Scheme I-9. Mono-dehydrogenation of monoketal **26** following Nicolaou's methodology.

The next step consists in the reduction of the carbonyl group of enone **34** which was undertaken by means of an asymmetric transfer hydrogenation (ATH). In 1997, Noyori and co-workers reported a new methodology for ATH reactions using chiral ruthenium catalysts and H-donor.[15] The ruthenium catalyst features a chiral tosylated diamine and a *p*-cymene (η^6) ring as ligands

(Scheme I-10).This methodology was extensively studied on different functionalised ketones, aldehydes, such as aromatic or α,β-unsaturated ketones,[11,16] because of its operational simplicity and high selectivity.

The postulated mechanism for this asymmetric reduction involves a previous reaction of the (*R,R*)-Noyori-**I** with a base to generate the active catalyst (*R,R*)-Noyori-**II** which is an amido Ru-complex with a 16-electron square-planar geometry (Scheme I-10).[17,18] Then, the amido Ru-complex dehydrogenates the hydrogen donor (DH_2) to produce an amine-hydrido Ru-complex, (*R,R*)-Noyori-**III** (18-electrons), as a single diastereomer. The resulting amine-hydric Ru-complex "transfer" hydrogens, reducing the ketone to afford the corresponding alcohol. The six membered cyclic transition structure is schematically visualized in the possible transition state. The enantiomeric bias in the ketone reduction could result from steric and electronic differentiation of the two carbonyl faces.[15]

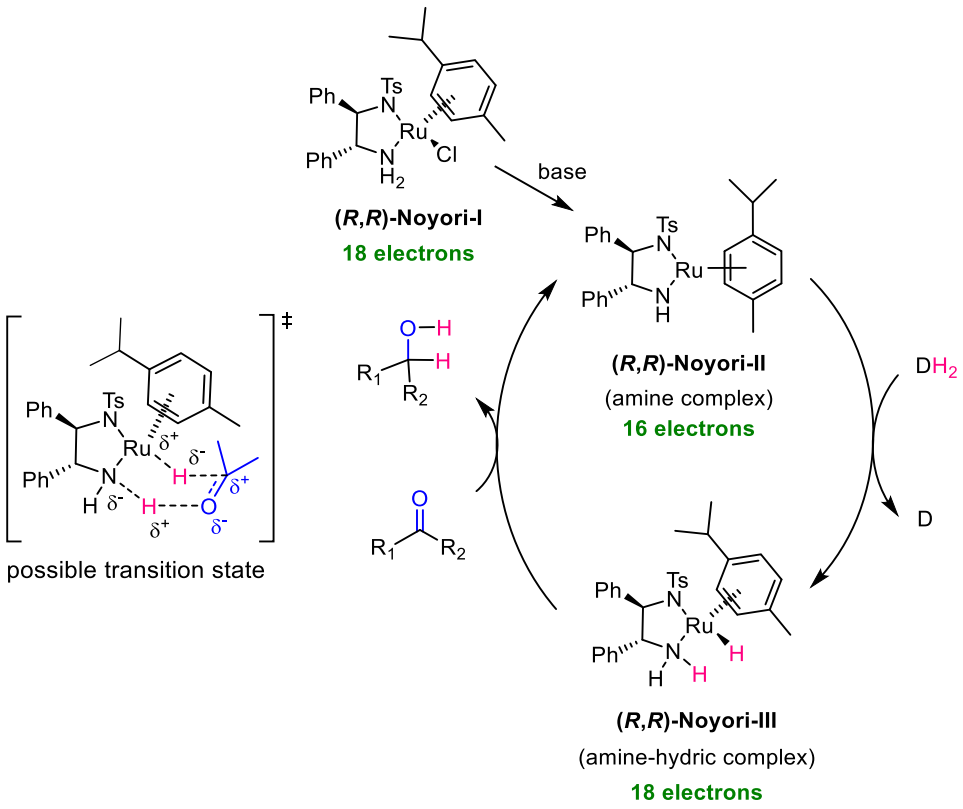

Scheme I-10. Postulated mechanism of the Asymmetric Transfer Hydrogenation (ATH).

Thus, the asymmetric reduction of enone **34** was carried in a biphasic media (CH_2Cl_2/H_2O, 1:1), using (*R,R*)-Noyori-**I**, as catalyst, tetrabutylammonium chloride (TBAC) as a phase-transfer agent and sodium formate (HCO_2Na) as hydrogen source (it decomposes into H_2 and CO_2 under the catalytic conditions). Under these experimental conditions, allylic alcohol **35** was obtained along

with its totally hydrogenated derivative **38** in a 6:1 ratio and 67% yield considering the starting material recovered (Scheme I-11). The poor conversion achieved was attributed to the degradation of the catalyst.

Baldwin *et al.*[19] reported a procedure to prepare the active catalyst (*R*,*R*)-Noyori-**II** by treatment of $[RuCl_2(p\text{-cymene})]_2$ with (*R,R*)-TsDPEN in the presence of KOH. Taking this into account, the commercially catalyst (*R*,*R*)-Noyori-**I** (18 electrons) was activated by treatment with stoichiometric KOH in CH_2Cl_2 and subsequent addition of water, delivering the active complex (*R*,*R*)-Noyori-**II** (16 electrons) in quantitative yield.

When the ATH reaction was repeated using the active catalyst (*R,R*)-Noyori-**II** and adding it in portions, the yield was improved affording allylic alcohol **35** and the totally hydrogenated derivative **38** in a 6:1 ratio in 59% combined yield (Scheme I-11). Considering the recovered starting material **34** the yield increases up to 80%. The mixture of alcohols **35** and **38** was possible to separate after several flash column chromatographies.

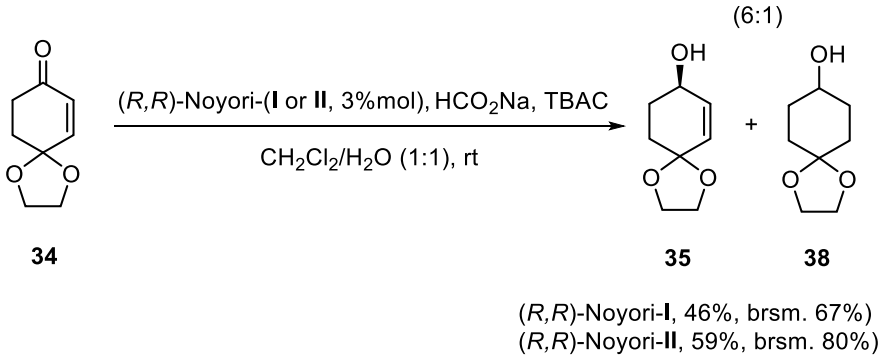

Scheme I-11. Asymmetric reduction of enone **34** using chiral ruthenium catalyst.

Finally, the last steps involve the introduction of a cyclopropane ring by a cyclopropanation reaction and the protection of alcohol as a benzyl protecting group.

The cyclopropanation reaction was previously attempted in our group using Shi's carbenoid ($CF_3COOZnCH_2I$).[20] During the reaction process the ketal group was removed affording keto alcohol **27**, which is a highly volatile compound, leading to a low yield in the reaction (Scheme I-12). Nevertheless, when the reaction of the cyclopropanation was carried out by Furukawa's procedure[21] using Et_2Zn and ICH_2Cl in CH_2Cl_2 at rt, the ketone **27** was obtained in 59% yield. It is worth mentioning that this yield was not reproducible due to the volatility of 4-hydroxy-2-cyclohexenone, **27**.

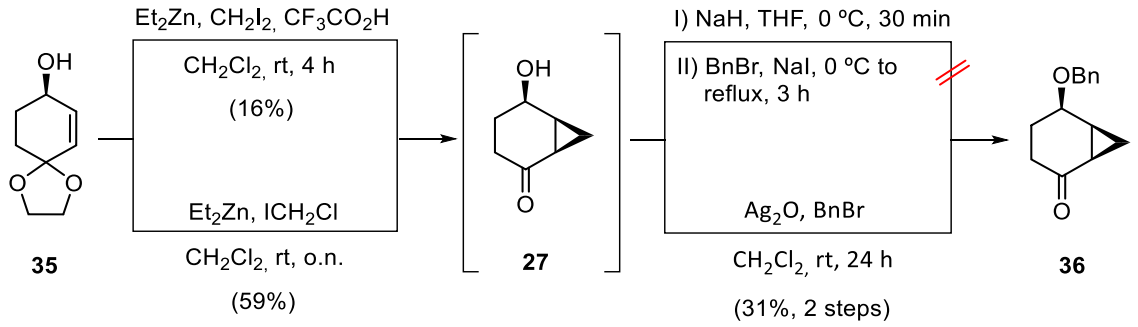

Scheme I-12. Cyclopropanation by Furukawa's procedure and subsequent protection of alcohol as a benzyl protecting group.

The *cis* relationship between the cyclopropane and the hydroxyl of **27** was determined by means of 2D-NOESY experiment which display cross peaks between H-7endo and H-4ax (Figure I-1) indicating that the hydroxyl group directs the attack of the reagent *via* zinc chelation.

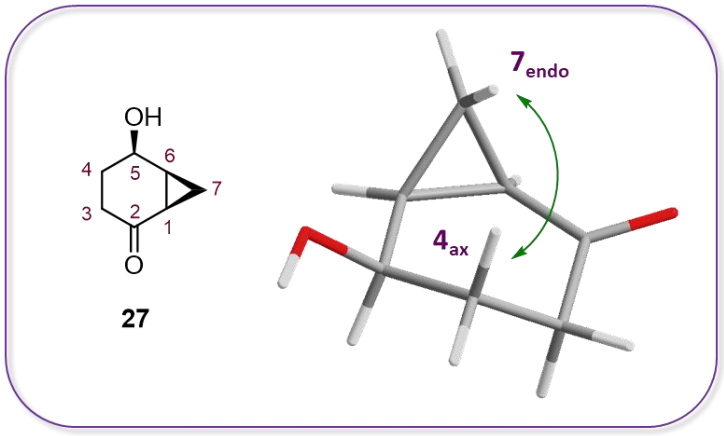

Figure I-1. Cross peaks in 2D-NOESY experiment of ketone alcohol **27**.

Due to the low yield of ketone alcohol **27**, the next protection step was performed immediately after the cyclopropanation reaction without further purification (Scheme I-12). In the first attempt to protect the alcohol of **27** as a benzyl ether, using sodium hydride at 0 °C and then, treated with benzyl bromide only decomposition products were obtained.

After some experimentation, it was found that when the reaction was performed in mild conditions using silver oxide (Ag_2O) and benzyl bromide at rt for 24 h, ketone **36** was obtained in 31% overall yield over the 2 steps after flash column purification (Scheme I-12).

The formation of the ketone **36** was confirmed by ^{1}H-NMR spectrum with the presence of the aromatic and benzylic signals, as well as the presence of a new peak at 208 ppm in the ^{13}C-NMR spectrum corresponding to carbonyl group (Figure I-2).

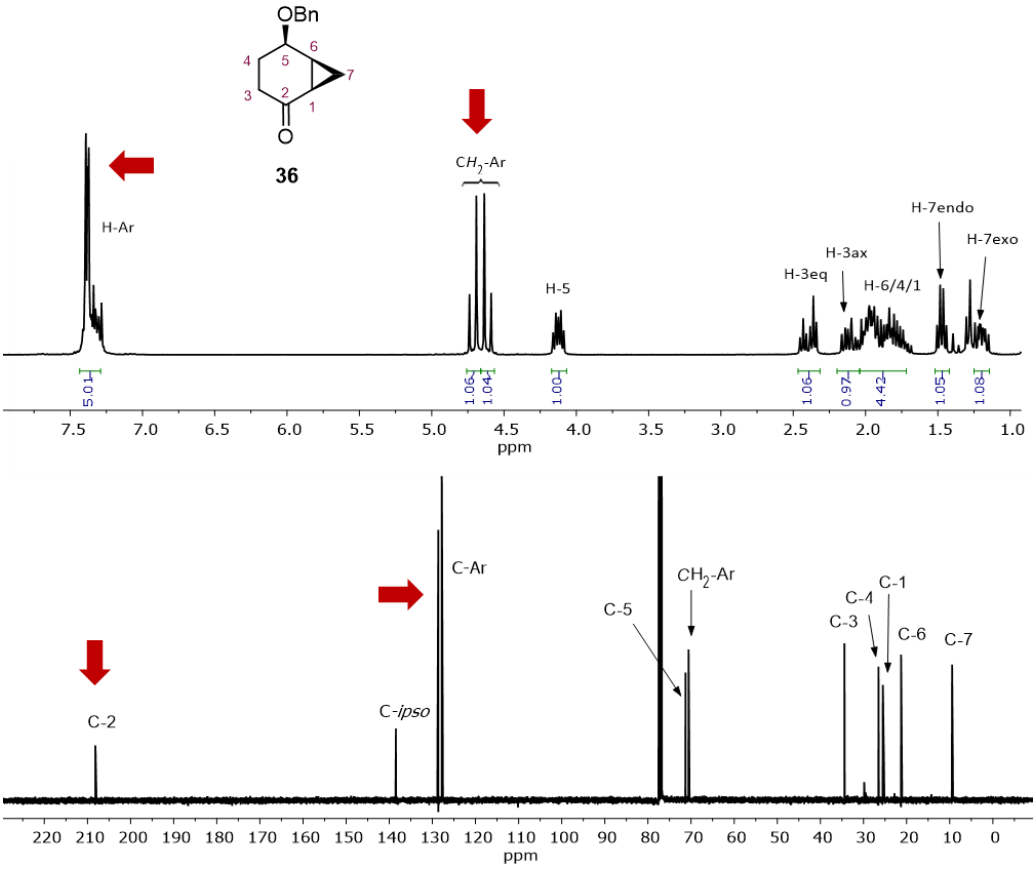

Figure I-2. ^{1}H-NMR (400 MHz, $CDCl_3$) and ^{13}C-NMR (400 MHz, $CDCl_3$) of ketone **36**.

By this synthetic *pathway A*, compound **36** has been enantiopure synthesised in 13% overall yield from commercially available **26**, in 4 steps.

2.3. Synthetic pathway B. Synthesis of 36 with (*R*,*R*)-hydrobenzoin as protecting group

The synthesis of **36** was also carried out following *pathway B* which follows a similar synthetic strategy than *pathway A*. The first step consists of a selective ketalization of one of carbonyl groups of commercially available 1,4-cyclohexanedione **13** using (*R,R*)-hydrobenzoin. Thus, the treatment of **13** with hydrobenzoin in benzene at reflux temperature in the presence of pyridinium *p*-toluenesulfonate (PPTS) as catalyst using a Dean-Stark apparatus gave a 2:1 mixture of monoketal **14** and bisketal **39**, which were straightforward separated by flash column chromatography, in 68% and 32% yield, respectively (Scheme I-13). Due to the hazard of benzene, the solvent was changed by toluene but, unfortunately, the product was achieved in much lower yield.

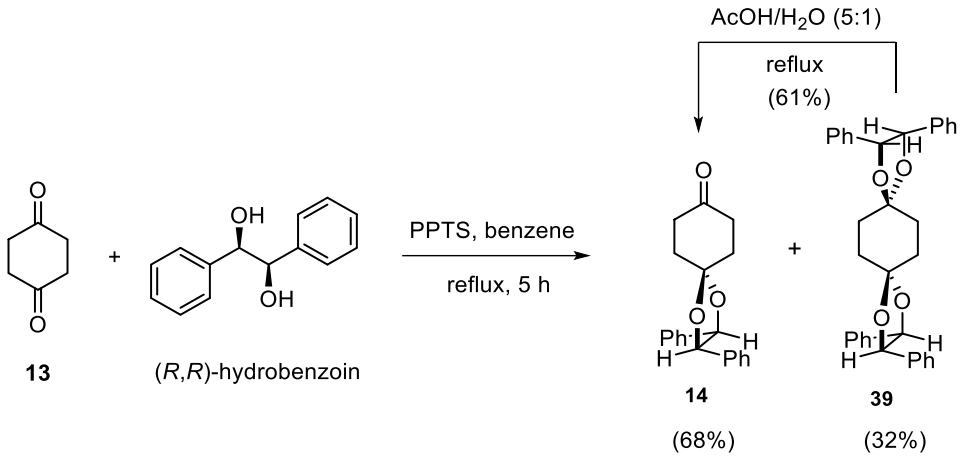

Scheme I-13. Selective monoketalization and monohydrolysis reaction for the formation of **14**.

Monohydrolysis of **39** by treatment with a mixture of AcOH/H_2O (5:1) at reflux temperature furnished an additional amount of **14** (Scheme I-13). Therefore, the overall yield of **14** was 88%.

The second step involves the mono-dehydrogenation of monoketal **14** following the already mentioned Nicolaou's methodology.[8,9] Thus, the treatment of monoketal **14** with Et_3N in dry CH_2Cl_2 at -10 °C and subsequent dropwise addition of TMSOTf led to the silyl enol ether **40** in quantitative way, which was then oxidized with the IBX·MPO complex to provide enone **15** in 98% overall yield (Scheme I-14). It is worth highlighting that, as in the previously case, IBX must be pure of other iodine species. For example, the presence of IBA leads to a detrimental effect in the reaction rate and appearance of precipitate during the reaction.[9]

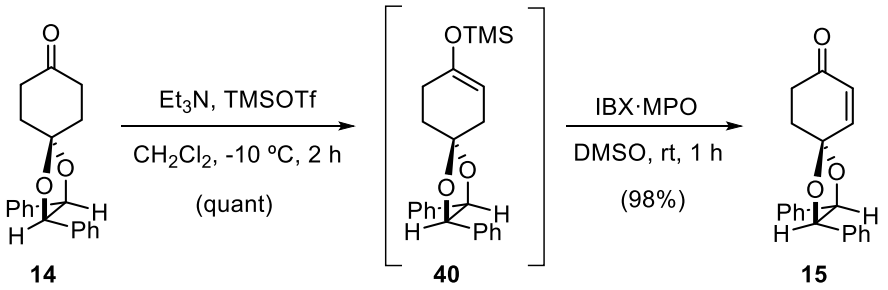

Scheme I-14. Preparation of enone **15**.

The following step consists on the reduction of the carbonyl group of enone **15** which was undertaken by means of an asymmetric transfer hydrogenation (ATH) using the previously described Noyori catalyst.[15] Thus, the treatment of **15** with (*R*,*R*)-Noyori-**I** in a biphasic media (CH_2Cl_2/H_2O, 1:1) in presence of CTAB, as a transfer agent, and HCO_2Na at rt for 24 h, provided an inseparable mixture of allylic alcohol **16**, and saturated alcohol **33** in a 10:1 ratio (determined

by ^{1}H-NMR) and 82% yield (Scheme I-15). Remarkably, for optimal results, the Noyori catalyst had to be added in different portions along the reaction time (*ca.* 1% mol/hour).

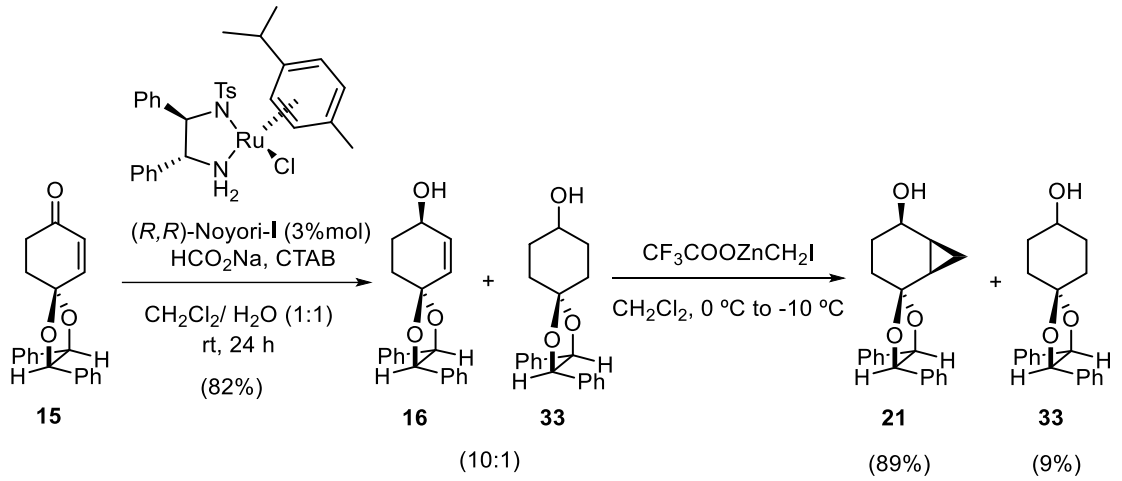

Scheme I-15. Asymmetric transfer hydrogenation of enone **15** using chiral ruthenium catalyst.

The last step is the cyclopropanation reaction of allylic alcohol **16** to generate the bicyclo[4.1.0]heptane scaffold. As it has been seen in the previous section, the cyclopropanation of **16** was already studied in our group using different methodologies and conditions.[12] The best results were achieved by using the Shi's carbenoid ($CF_3COOZnCH_2I$).[20] Thus, the mixture of alcohols **16** and **33** was treated with $CF_3COOZnCH_2I$ (generated *in situ* from Et_2Zn, CH_2I_2 and CF_3COOH) in CH_2Cl_2 at -10 °C in anhydrous conditions providing alcohol **21** in 89% yield and alcohol **33** in 9% yield (Scheme I-15).

The formation of the cyclopropane was observed in the ^{1}H-NMR spectrum by the disappearance of the olefinic proton signals along with the presence of two new peaks at 0.96 and 0.83 ppm, corresponding to the diastereotopic H-7 protons (H-7endo and H-7exo, respectively) of the cyclopropane. Additionally, a new signal at 4.4 ppm in the ^{13}C-NMR, corresponding to C-7 carbon, also confirms the formation of the cyclopropane ring.

As in the previous section, the *cis* stereochemistry between the alcohol and the cyclopropane moieties was determined earlier in our group by means of 2D-NOESY experiment.[12]

At this point it was decided to investigate if saturated alcohol **33** could be transformed back into unsaturated ketone **15**.

In 2000, Nicolau and co-workers reported a general method for mild, swift, and highly efficient conversion of saturated alcohols to α,β-unsaturated carbonyl compounds.[22] This reaction

involves an oxidation reaction using IBX at elevated temperatures (65-85 °C) to give unsaturated carbonyl compounds in one pot. Many examples of this reaction have been reported in the literature (Scheme I-16).[22,23]

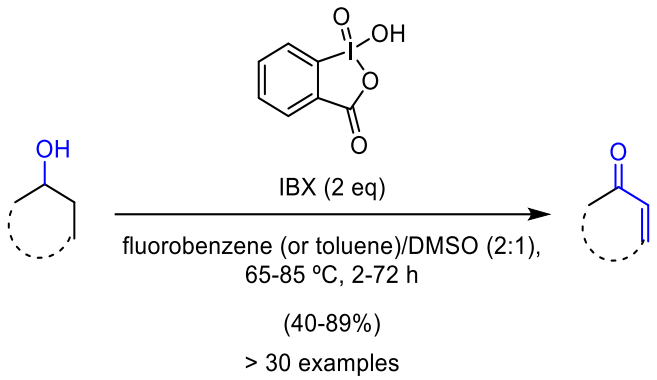

Scheme I-16. General method for conversion of saturated alcohol to α,β-unsaturated carbonyl compounds.[22]

The IBX oxidizes the alcohol to an α,β-unsaturated carbonyl by two oxidation steps. In the first step, initially the alcohol reacts with one equivalent of IBX in a fast pre-equilibrium, which can be formally considered as ligand exchange (hydroxyl-alkyloxy) on the iodine atom (Scheme I-17). The product **XVI** then, disproportionates to the carbonyl derivative and the IBA (*o*-iodosobenzoic acid). Afterwards, keto-enolate reacts with other equivalent of IBX providing structure **XVII**. This step is the key step in the mechanism. Finally, intermediate **XVII** evolved to the α,β-unsaturated carbonyl compound and IBA. Therefore, from a saturated alcohol, an unsaturated ketone can be obtained with 2 equivalents of IBX. By merely adjusting the stoichiometry of IBX, temperature, and reaction time employed, the reaction could be easily programmed to provide different degrees of oxidation, for instance, a dienone derivative can be obtained using an excess of IBX.[22]

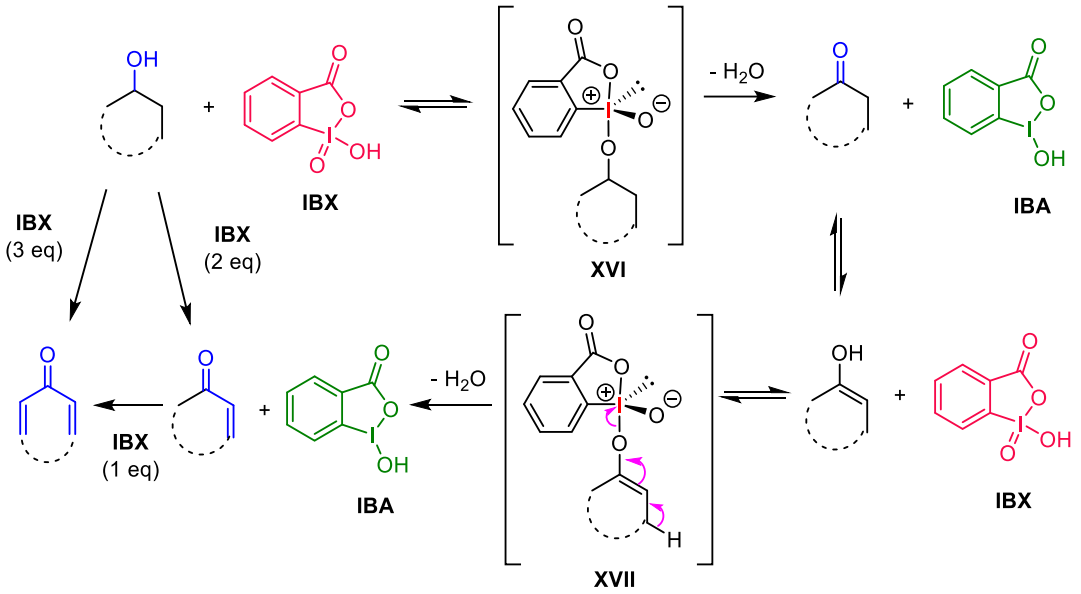

Scheme I-17. General proposed mechanism for the IBX-induced synthesis of α,β-unsaturated systems from alcohols and ketones.

Taking this result into account, the saturated alcohol **33** was treated with 2.5 equivalents of IBX in toluene/DMSO (2:1) media at 65 °C for 4 h. Under these conditions, enone **15** was obtained in 86% yield (Scheme I-18) and could be used again in our synthetic pathway.

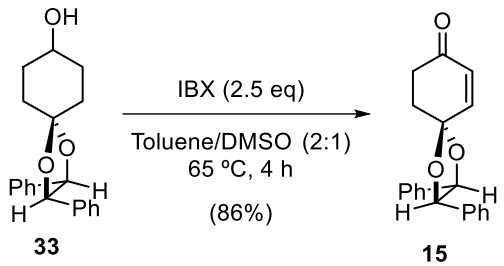

Scheme I-18. α,β-Unsaturated ketone **15** obtained by oxidation reaction using IBX.

The last steps to obtain key ketone **36** are the protection of alcohol as a benzyl ether and removal of the ketal protecting group. In the event, alcohol **21** was firstly treated with sodium hydride at 0 °C in order to generate the corresponding alkoxide, which was then treated with benzyl bromide in presence of a catalyst amount of NaI to afford the benzyl ether, **41** in 85% yield (Scheme I-19).

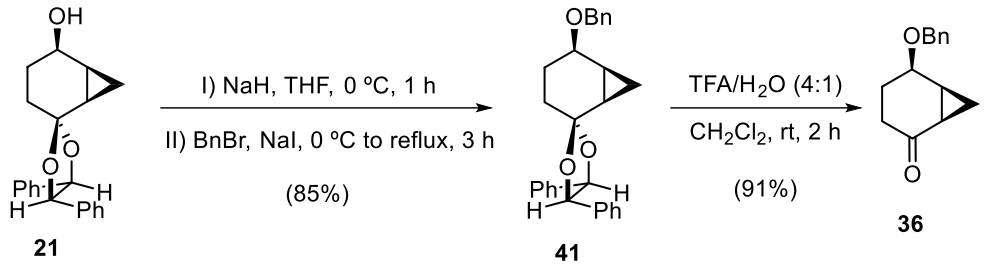

Scheme I-19. Protection of alcohol **21** as a benzyl ether and posterior hydrolysis in acidic conditions led to ketone **36**.

Removal of the ketal group in **41** was performed in acidic conditions (4:1 mixture of TFA/H_2O in CH_2Cl_2) at rt for 2 h to afford ketone **36** in 91% yield (Scheme I-19).

Therefore, enantiopure **36** was synthesised in 49% overall yield from **13**, on a multigram scale following a robust and reproducible 6-steps synthesis. From this intermediate **36**, different conformationally restricted 5'-hydroxymethyl- and 5'-hydroxymethyl-4'-hydroxybicyclo[4.1.0]heptane nucleoside analogues (structures **BCH** and **XVI**, respectively) will be prepared on this Ph.D thesis (Scheme I-20).

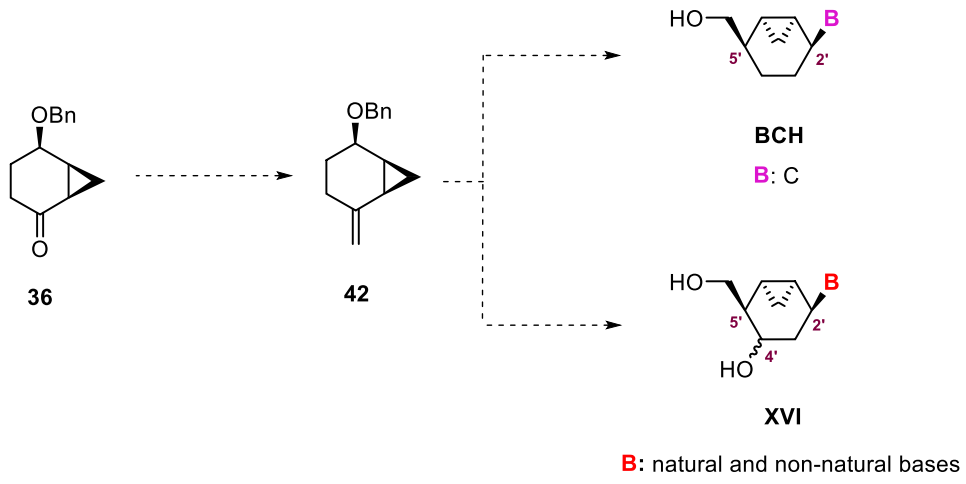

Scheme I-20. Synthetic route towards conformationally restricted nucleoside analogues **BCH** and **XIV**.

3. CHAPTER I OUTLINE

In summary, two synthetic strategies developed in our research group have been optimized (Scheme I-21), to prepare key ketone **36**. Synthetic *pathway B* is the most robust, reproducible and efficient 6-steps approach to prepare **36** on a multigram scale in 6 synthetic steps and 49% overall yield.

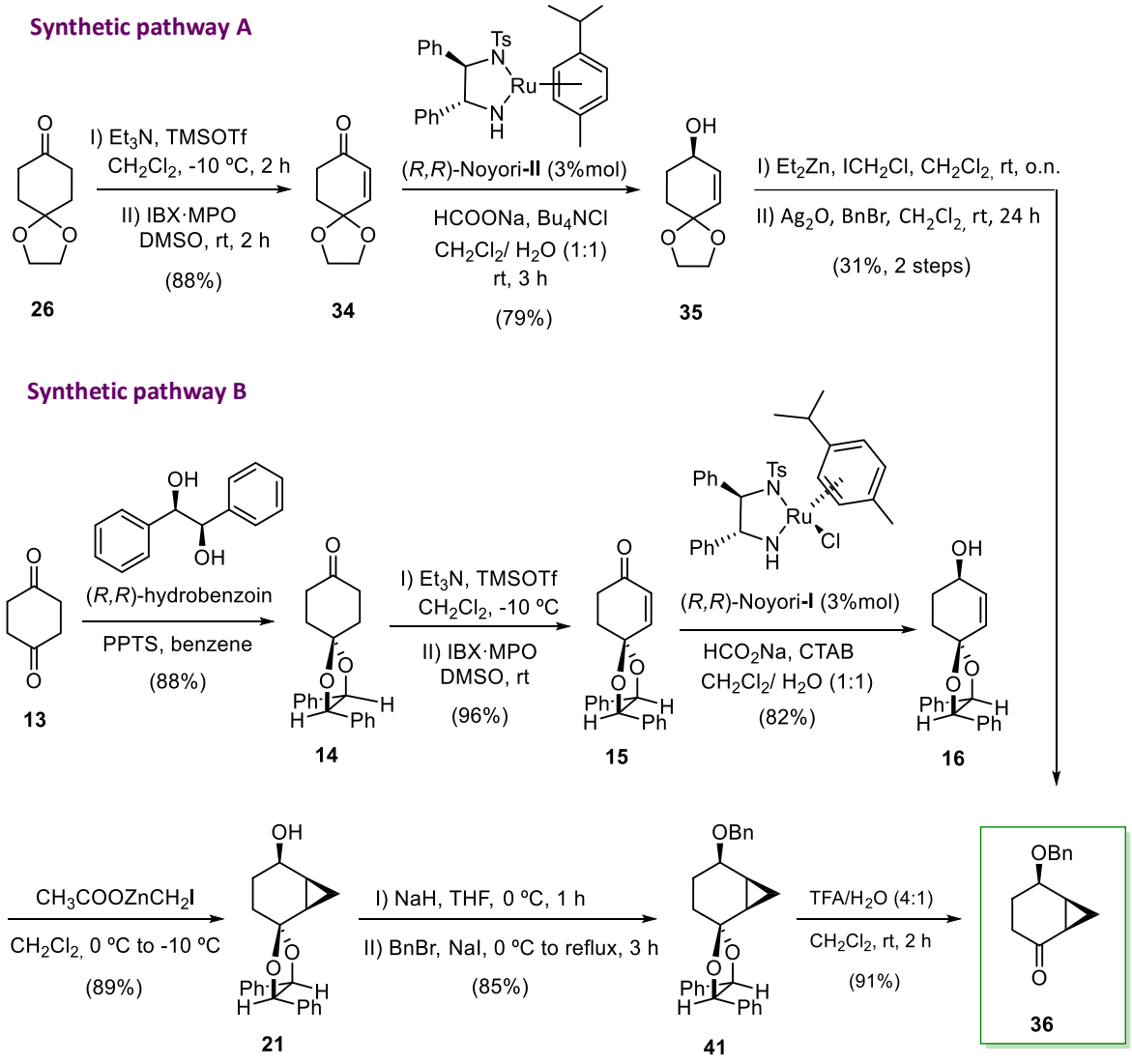

Scheme I-21. Synthetic pathways (A and B) to prepare ketone **36**.

4. REFERENCES

[1] (a) de March, P.; Escoda, M.; Figueredo, M.; Font, J.; García-García, E.; Rodríguez, S. *Tetrahedron: Asymmetry* **2000**, *11*, 4473−4483; (b) Alibés, R.; Busqué, F.; Bardaji, G. G.; de March, P.; Figueredo, M.; Font, J. *Tetrahedron: Asymmetry* **2006**, *17*, 2632−2636; (c) Bardaji, G. G.; Cantó, M.; Alibés, R.; Bayón, P.; Busqué, F.; de March, P.; Figueredo, M.; Font, J. *J. Org. Chem.* **2008**, *73*, 7657−7662; (d) Toribio, G.; Marjanet, G.; Alibés, R.; de March, P.; Font, J.; Bayón, P.; Figueredo, M. *Eur. J. Org. Chem.* **2011**, *2011*, 1534−1543; (e) Fresneda, M. A.; Alibés, R.; Font, J.; Bayón, P.; Figueredo, M. *J. Org. Chem.* **2012**, *77*, 5030−5035; (f) Fresneda, M. A.; Alibés, R.; Font, J.; Bayón, P.; Figueredo, M. *Org. Biomol. Chem.* **2013**, *11*, 6562−6568.

[2] (a) García-Fortanet, J.; Carda, M.; Marco, J. A. *Tetrahedron* **2007**, *63*, 12131–12137; (b) Wilson, E. M.; Trauner, D. *Org. Lett.* **2007**, *9*, 1327–1329.

[3] Danishefsky, S. J.; Simoneau, B. *J. Am. Chem. Soc.* **1989**, *111*, 2599–2604.

[4] Ferrer, E.; Alibés, R.; Busqué, F.; Figueredo, M.; Font, J.; de March, P. *J. Org. Chem.* **2009**, *74*, 2425–2432.

[5] Corey, E. J.; Bakshi, R. K.; Shibata, S. *J. Am. Chem. Soc.* **1987**, *109*, 5551–5553.

[6] Corey, E. J.; Helal, C. J. *Angew. Chem. Int. Ed.* **1998**, *37*, 1986–2012.

[7] Domínguez-Pérez, B., Ferrer, E., Figueredo, M., Maréchal, J. D., Balzarini, J., Alibés, R., Busqué, F. *J. Org. Chem*. **2015**, *80*, 9495-9505.

[8] Nicolaou, K. C.; Gray, D. L. F.; Montagnon, T.; Harrison, S. T. *Angew. Chem. Int. Ed.* **2002**, *41*, 996–1000.

[9] Nicolaou, K. C.; Montagnon, T.; Baran, P. S. *Angew. Chem. Int. Ed.* **2002**, *41*, 993–996.

[10] Gladiali, S.; Alberico, E. *Chem. Soc. Rev.* **2006**, *35*, 226–236.

[11] Noyori, R.; Hashiguchi, S. *Acc. Chem. Res.* **1997**, *30*, 97–102.

[12] Beatriz-Dominguez, B. Doctoral Thesis, Universitat Autònoma de Barcelona, 2015.

[13] Frigerio, M.; Santagostino, M.; Sputore, S. *J. Org. Chem.* **1999**, *64*, 4537–4538.

[14] Fuchs, P. L. *Catalytic oxidation reagents*. vol. 14, Wiley, West Sussex, U.K. 2013.

[15] Hashiguchi, S.; Fujii, A.; Takehara, J.; Ikariya, T.; Noyori, R. *J. Am. Chem. Soc.* **1995**, *117*, 7562–7563.

[16] Noyori, R.; Ohkuma, T. *Angew. Chem. Int. Ed.* **2001**, *40*, 40–73.

[17] Ikariya, T.; Blacker, A. J. *Acc. Chem. Res.* **2007**, *40*, 1300–1308.

[18] Dub, P. A.; Ikariya, T. *J. Am. Chem. Soc.* **2013**, *135*, 2604–2619.

[19] Kirkham, J. E. D.; Courtney, T. D. L.; Lee, V.; Baldwin, J. E. *Tetrahedron* **2005**, *61*, 7219–7232.

[20] Yang, Z.; Lorenz, J. C.; Shi, Y. *Tetrahedron Lett.* **1998**, *39*, 8621–8624.

[21] Furukawa, J.; Kawabata, R. *Tetrahedron Lett.* **1966**, 3353–3354.

[22] Nicolaou, K. C., Zhong, Y. L., & Baran, P. S. *J. Am. Chem. Soc.* **2000**, *122*, 7596-7597.

[23] Wirth, T. *Angew. Chem. Int. Ed.* **2001**, *40*, 2812-2814 and references cited therein.

.

III. CHAPTER II

Synthesis of cytosine 5'-hydroxymethyl-bicyclo[4.1.0]heptanyl nucleoside analogue, **28**

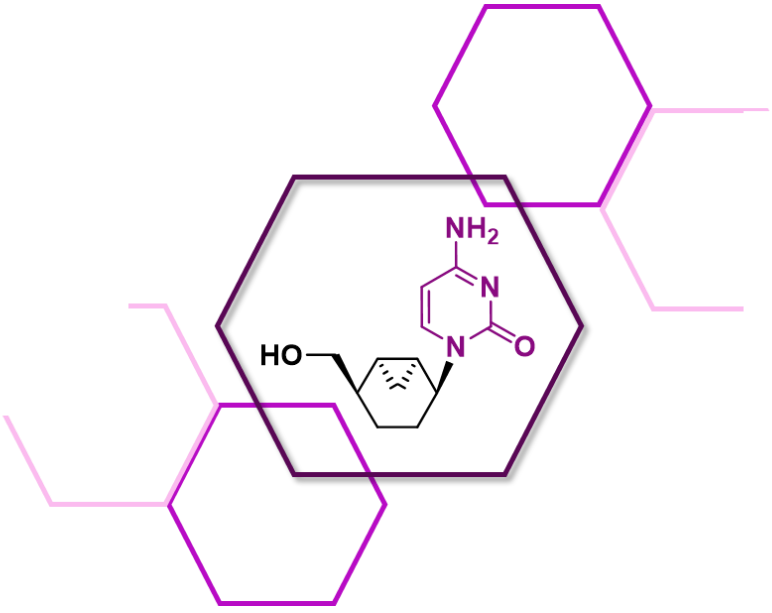

1. INTRODUCTION

As previously mentioned (section 4.3 of introduction) protein–ligand docking studies carried out in our research group for 5'-hydroxymethylbicyclo[4.1.0]heptanyl NAs (**BCH**-(**A**, **G**, **T** and **U**), Figure II-1) for the first phosphorylation step by the herpes simplex virus thymidine kinase (HSV-TK) suggested that these synthetic analogues should be correctly activated.[1]

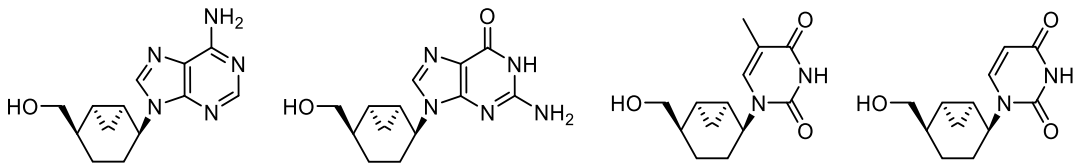

Figure II-1. 5'-hydroxymethylbicyclo[4.1.0]heptanyl analogues **BCH**-(**A**, **G**, **T** and **U**) synthesised in our group.

However, despite this theoretical validation these CNAs were inactive at ~250 μM against herpes simplex virus 1 (HSV-1) in cell culture. The lack of activity may arise by poor affinity of the 5'-triphosphate metabolites to the virus-encoded DNA polymerase and/or by low affinity for HSV encoded thymidine kinase activated enzyme to convert the compounds to their 5'-monophosphate metabolites. In this chapter, with the aim of shedding light on this last point the HSV-1 TK activity of these compounds will be presented. Moreover, in order to complete the 5'-hydroxymethylbicyclo[4.1.0]heptanyl family, the cytosine analogue will be synthesised and its activity evaluated.

2. SYNTHESIS OF CYTOSINE DERIVATIVE 28

2.1. Synthetic strategy

The synthesis of cytosine 5'-hydroxymethylbicyclo[4.1.0]heptanyl nucleoside analogue will be performed from intermediate **36** previously synthesised in the previous chapter, following the synthetic sequence developed by Dr. Domínguez-Pérez[1] (section 4.3 of introduction) but using a different protecting group for the reasons already exposed. Thus, the synthesis would start from ketone **36**, which after an olefination and hydroboration-oxidation would provide alcohol **43** (Scheme II-1). Subsequent protection and deprotection steps would provide alcohol **24**, which

would be converted into the ammonium chloride **25** by a substitution reaction with azide and subsequence reduction. Finally, the desired cytosine analogue would be obtained by a stepwise construction of the nucleobase followed by a deprotection step.

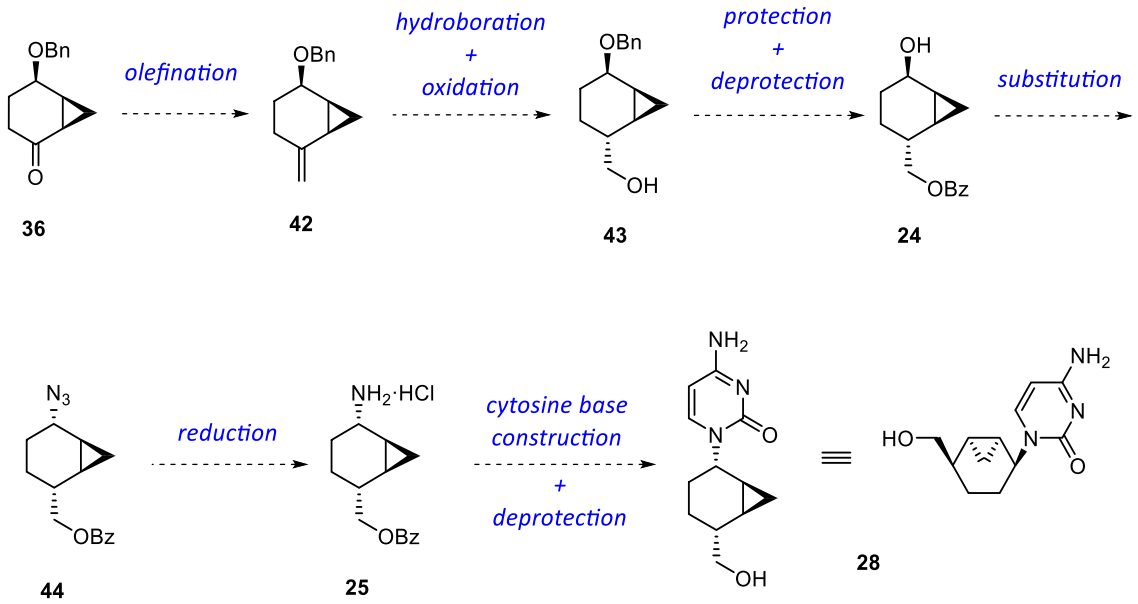

Scheme II-1. Synthetic pathway foreseen to prepare cytosine nucleoside analogue.

2.2. Synthesis of alcohol 24

2.2.1. Preparation of hydroxymethyl intermediate 43

The synthesis of alcohol **43** started with the olefination of ketone **36** *via* a Wittig reaction. Thus, the treatment of ketone **36** with freshly prepared ylide, generated from methyltriphenylphosphonium iodide (Ph_3PCH_3I) and *t*-BuOK in anhydrous THF, furnished olefin **42** in 88% yield after purification by flash column chromatography (Scheme II-2).

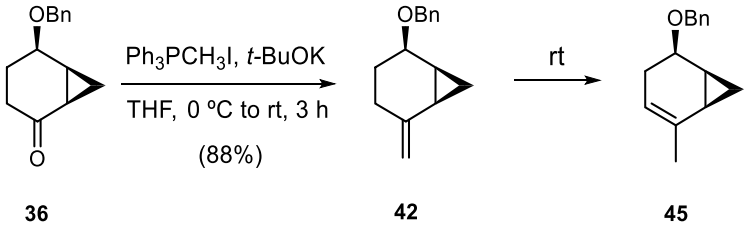

Scheme II-2. Wittig reaction on ketone **36** to provide terminal alkene **42** and its isomerization to **45**.

The formation of alkene **42** can be confirmed in the ^{1}H-NMR spectrum by the presence of two singlet signals at δ 4.86 and 4.76, corresponding to protons H-1' (Figure II-2) as well as the disappearance of the carbonyl group C-2 signal of **36** at 208.2 ppm in the ^{13}C-NMR spectrum. Nevertheless, exocyclic alkene **42** is unstable and rapidly isomerises to the more stable endocyclic regioisomer **45** (Scheme II-2). The isomerization can be observed in the ^{1}H-NMR spectrum (in purple) by the formation of a new singlet at 1.82 ppm and a doublet at 5.01 ppm, corresponding to the methyl group generated and the new olefinic proton H-3, respectively (Figure II-2).

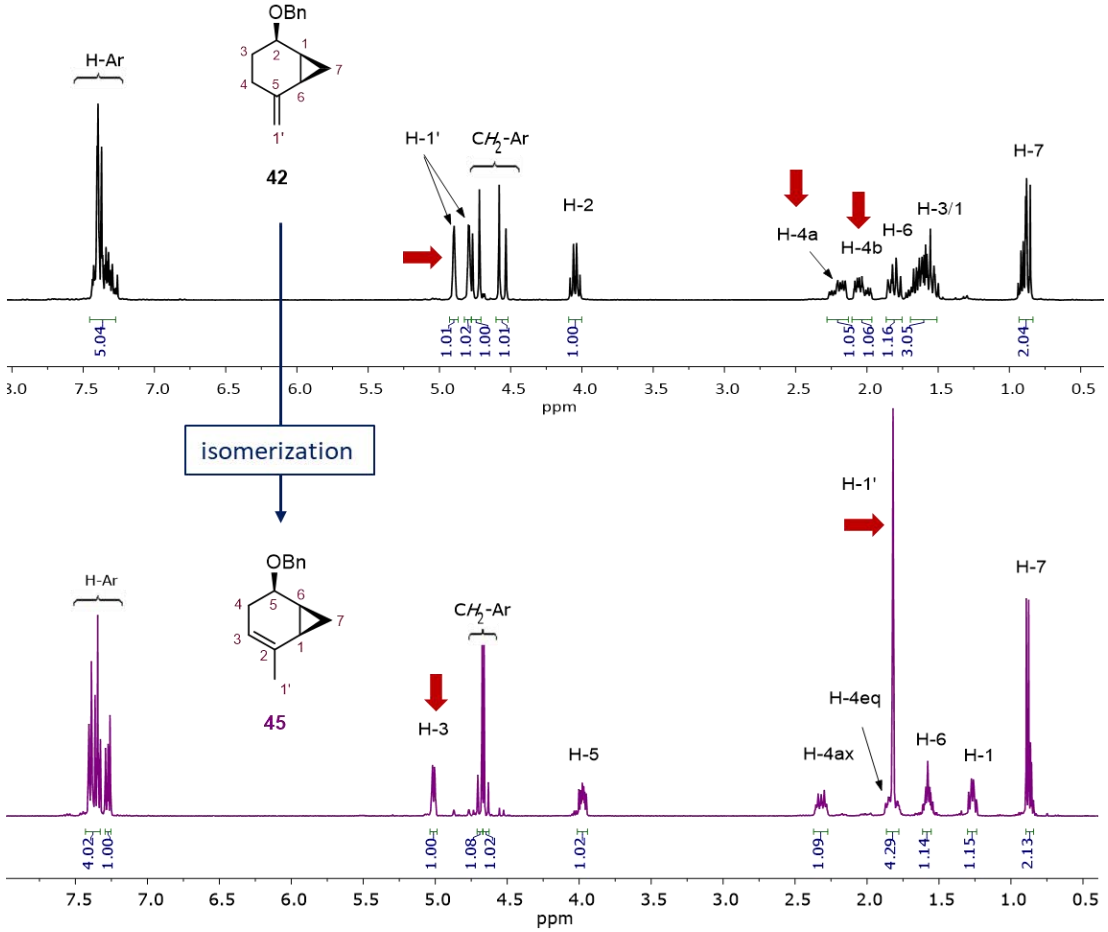

Figure II-2. ^{1}H-NMR (400 MHz, $CDCl_3$) spectra of **42** and **45**.

In order to avoid the isomerization process, the following hydroboration was carried out immediately after the Wittig reaction without further purification of the olefin intermediate. Thus, alkene **42** was treated with 9-borabicyclo[3.3.1]nonane (9-BBN) in anhydrous THF at -10 ºC, followed by the addition of NaOH (3 M) and H_2O_2 (30% in water), to furnish a chromatographically inseparable 2:1 mixture of diastereomers **43** and **46** in 95% combined yield

over the three steps (Scheme II-3). After several purifications by flash column chromatography, a pure fraction of the main product was obtained.

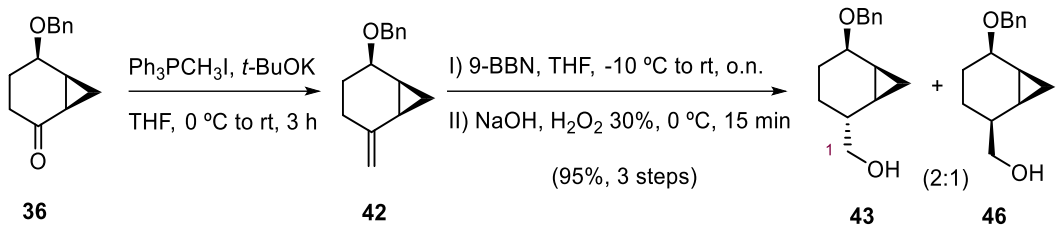

Scheme II-3. Preparation of diastereoisomeric alcohols **43** and **46** by sequential Wittig and hydroboration-oxidation reactions.

The success of the reaction was confirmed in the ^{1}H-NMR spectrum with the presence of a new peak at 3.57 ppm corresponding to the H-1 of the hydroxymethyl group as well as at 67.98 ppm in the ^{13}C-NMR spectrum. The relative configuration of C-2', of the main product, has been determined with the aid of a 2D-NOESY experiment (Figure II-3) which shows cross peaks between H-7'endo and H-2'. Therefore, alcohol **43** is the major product being the absolute configuration (1'*S*,2'*R*,5'*R*,6'*S*).

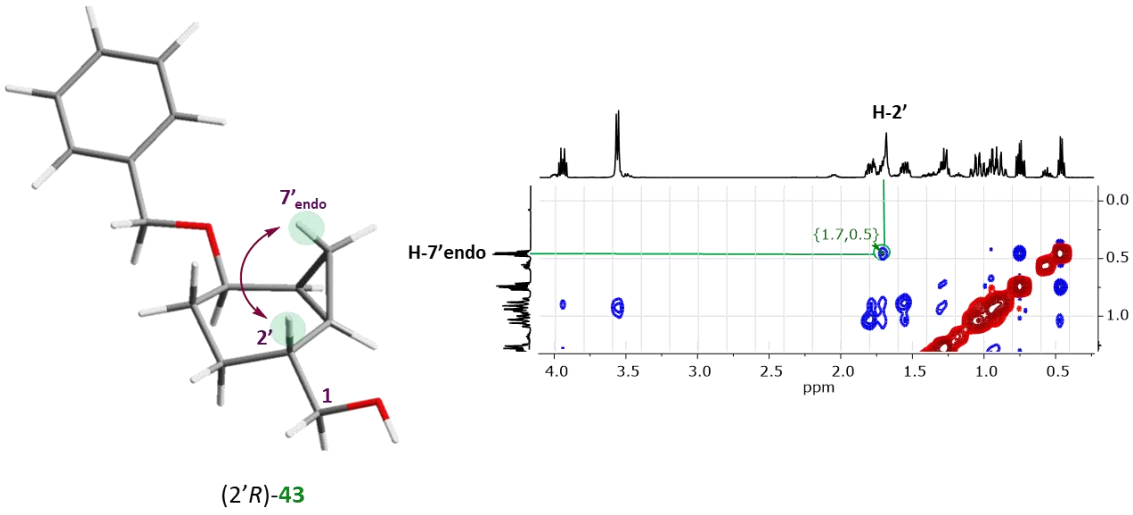

Figure II-3. Cross peaks between H-2' and H-7'endo in the 2D-NOESY spectrum (400 MHz, $CDCl_3$) of **43**.

In the hydroboration reaction there are two possible approaches of the borane (9-BBN) to the diastereotopic faces[2] of the alkene **42**: by the ***re*** face, in which 9-BBN approaches the alkene through its less hindered face, and by the ***si*** face, in which the approach is through the face bearing the cyclopropane (Figure II-4). The 2D-NOESY experiment shows that the addition of the borane took place preferentially by the ***si*** face leading mainly to the isomer **43** with the

hydroxymethyl substituent located in *trans* respect to the cyclopropane and the benzyloxy. Although the ***re*** face is more accessible, the four-centre transition state toward the all *cis*-substituted derivative is more unfavoured due to steric repulsion between the new alkylborane and the cyclopropane.

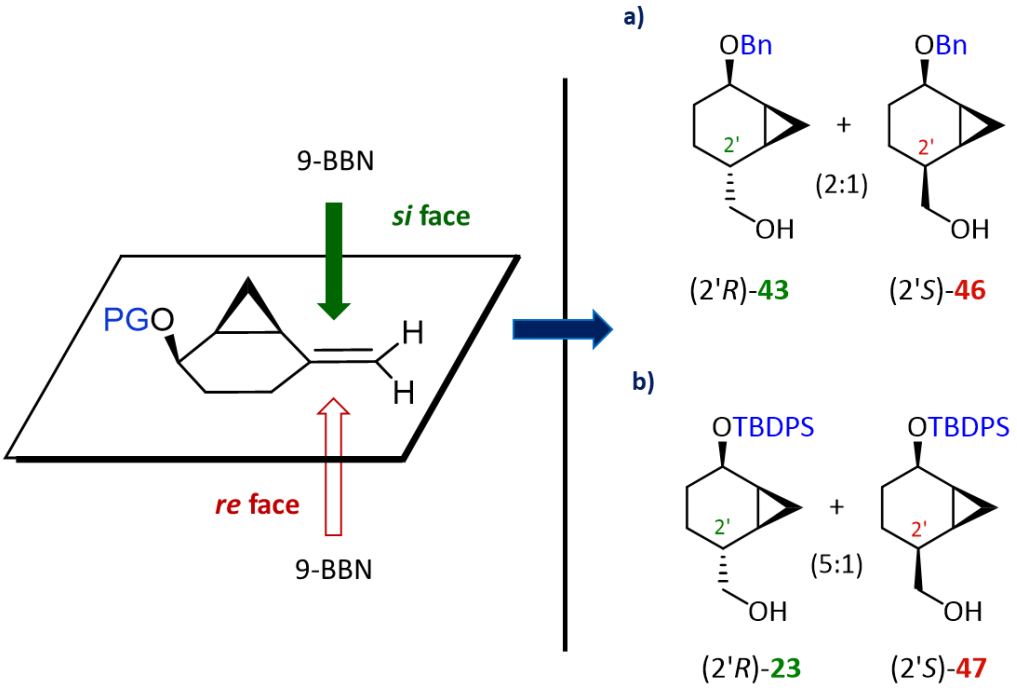

Figure II-4. *si*/*re* approaches of 9-BBN to the diastereotopic faces to the alkene. Comparative ratio obtained using benzyl (a) or TBDPS (b) protecting group.

Previously in our group, when the same reaction was performed using TBDPS as the protecting group, a 5:1 ratio was obtained from the two diastereoisomers (Figure-II-4). The lowest stereoselectivity achieved in the compound bearing a benzyl protecting group could be explained considering that the four-centre transition state toward the all-*cis*-substituted derivative is less unfavoured than the one coming from the compound bearing TDBPS which is a more voluminous protecting group.

2.2.2. Preparation of alcohol 24

The next transformation planned was the orthogonal protection of the hydroxyl group of the mixture of **43** and **46** as a benzoate followed by the removal of the benzyl protecting group. Thus, treatment of the (2:1) diastereomeric mixture of alcohols **43** and **46** with trimethylamine and benzoyl chloride in CH_2Cl_2 provided a mixture of derivatives **48** and **49** in quantitative yield (Scheme II-4). This protected mixture was used in the next steps without further purification.

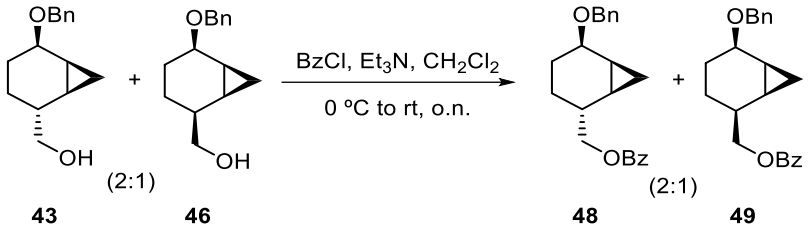

Scheme II-4. Protection of alcohols **43** and **46** as the corresponding benzoyl esters.

Subsequent cleavage of the benzyl group was accomplished by hydrogenation under hydrogen at 2 atm of pressure in the presence of Pd/C (10%) in EtOH at rt, affording, after purification by flash column chromatography, the desired alcohol **24** in 62% yield and its diastereomer **50** in 29% yield in the 2 steps, (Scheme II-5).

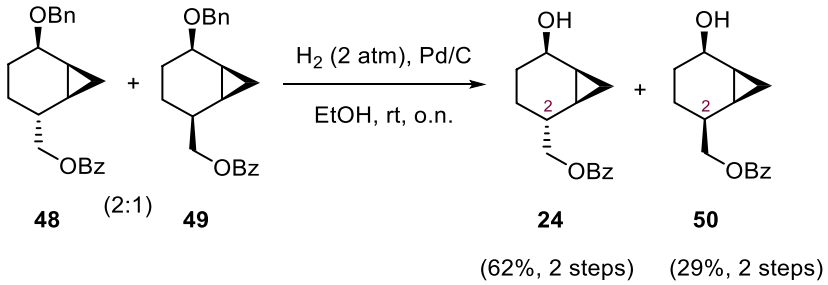

Scheme II-5. Removal of the benzyl protecting group by hydrogenation.

The formation of diastereoisomeric alcohols **24** and **50** was confirmed by the ^{1}H-NMR and ^{13}C-NMR spectra in base to the new aromatic signals corresponding to the two benzoyl protecting groups, as well as, the disappearance of signals corresponding to the benzyl ether. The spectroscopy differences between the two diasteromers can be observed in the ^{1}H-NMR spectra, where H-2' appear as a multiplet at 2.05 ppm for **24** derivative and as a dq at 2.36 ppm for **50**.

2.3. Precedents in the research group for the introduction of the base moiety

In general, there are two fundamental approaches to introduce a nucleobase: coupling of the nucleobase with an appropriately functionalised carbocyclic ring or through stepwise construction of the nucleobase from an amine substituent present on the carbocycle.[3] Direct coupling of the nucleobase is the most widely used procedure and can be accomplished by

several methods, such as the Mitsunobu reaction or converting the alcohol into a good leaving group followed by a nucleophilic substitution.

In our group, the introduction of the nucleobase was first attempted by a coupling methodology from alcohol **24**.[4] Direct coupling was tried by the nucleophilic substitution of the corresponding activated alcohol as a mesylate. However, the formation of the mesylate **52** was not achieved due to a competitive elimination reaction (Scheme II-6). All the attempts to avoid the formation of elimination product **51** met with failure.

A second approach consisted of the direct introduction of the nucleobase via Mitsunobu reaction.[5] In this case, *N*3 protected thymine was used as base in order to optimise the reaction. Unfortunately, after trying several reaction conditions (DBAD, DIAD, THF, toluene, ACN or different temperature), the thymine derivative **53** was only obtained in 6% yield along with many other by-products (Scheme II-6).

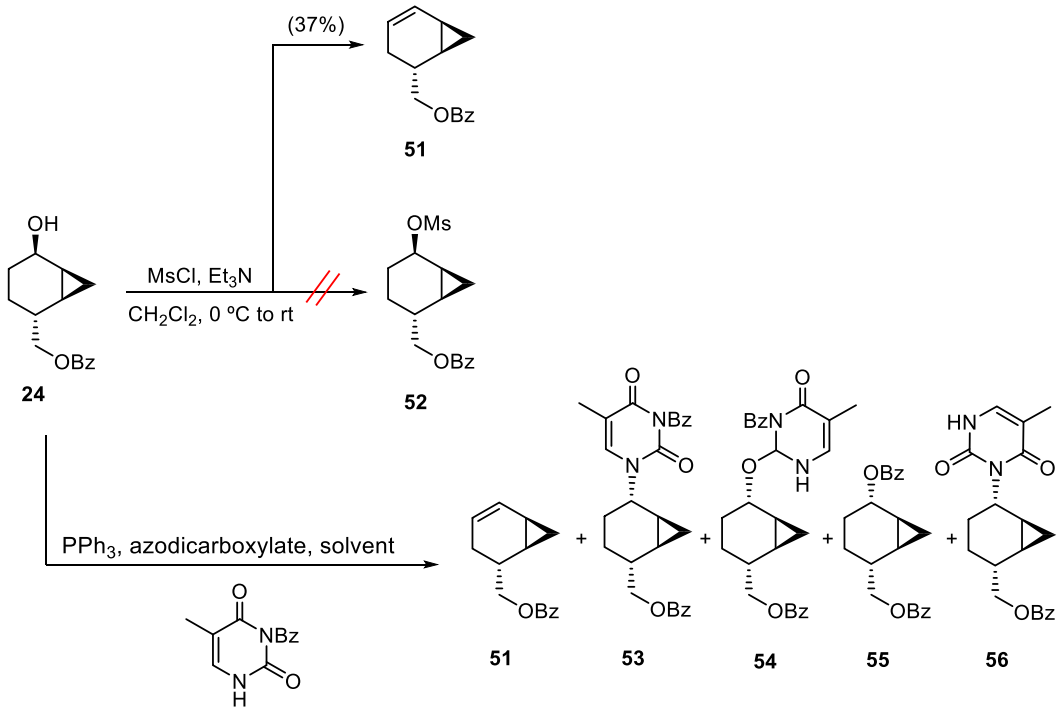

Scheme II-6. All failed attempters for direct coupling of the nucleobase in alcohol **24**.[4]

Since all the attempts to directly couple the nucleobase to the cyclohexane moiety met with failure, it was decided to introduce it *via* a stepwise construction from an ammonium chloride derivative (see next section).

2.4. Synthesis of ammonium chloride 25

The corresponding amine **25** required for the nucleobase construction was synthesised starting from alcohol **24** through the azide **44**.

The azide **44** was envisaged to be prepared by the methodology reported by Bose[6] which consists of a Mitsunobu reaction using diphenylphosphoryl azide (DPPA), an azodicarboxyate derivative, and triphenylphosphine. The mechanism of this Mitsunobu reaction for the formation of azide is showed in Scheme II-7.[6] The reaction starts with the nucleophilic attack of triphenylphosphine to the azodicarboxylate **XVIII** to form the betaine **XIX** which reacts with DPPA delivering intermediate **XX** and an azide anion. Then, an alkoxyphosphonium salt **XXIII** is generated after the addition of one equivalent of alcohol (**XXI**) by a proton transfer (P.T.) process. Finally, the alkoxyphosphonium salt **XXIII** undergoes a substitution reaction to give azide **XXIV** with inversion of configuration and triphenylphosphine oxide.

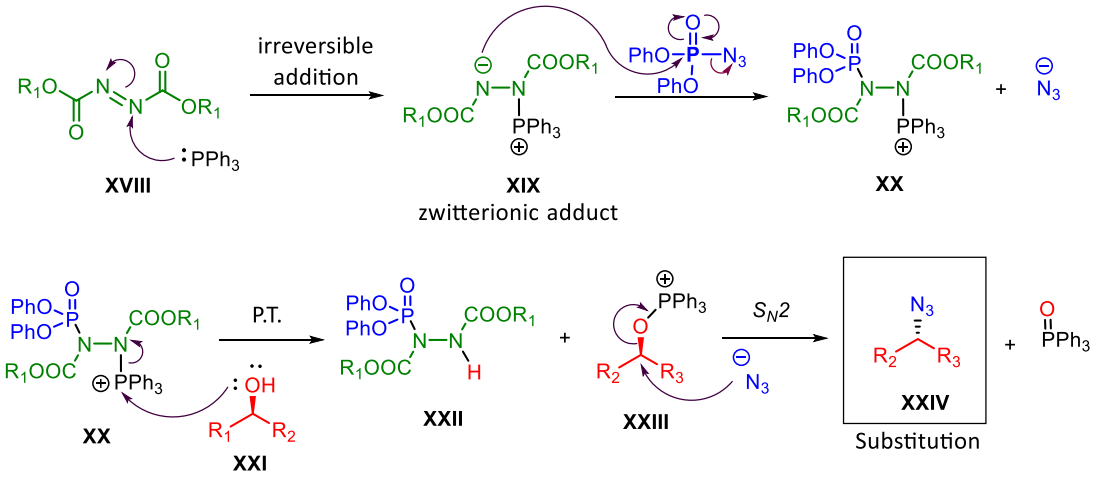

Scheme II-7. General mechanism of Mitsunobu reaction using DPPA for azide formation.[6]

Thus, the alcohol **24** was treated with DPPA in presence of di-*tert*-butylazodicarboxylate (DBAD) and triphenylphosphine in toluene from 0 °C to rt leading to azide **44** in 84% yield (Scheme II-8).

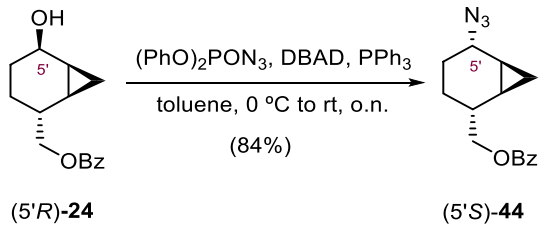

Scheme II-8. Formation of azide **44** *via* Mitsunobu reaction.

The formation of azide **44** was confirmed by the ^{13}C-NMR spectrum, in which the signal of C-5' appeared upfield shifted (57.0 ppm) compared to the alcohol **24** (68.0 ppm). The assignment of C-5' as *S* configuration could be established by the presence of cross peaks between H-7'endo and H-5' in the 2D-NOESY spectrum (Figure II-5), thus being the absolute configuration of **44** (1'*R*,2'*R*,5'S,6'*S*).

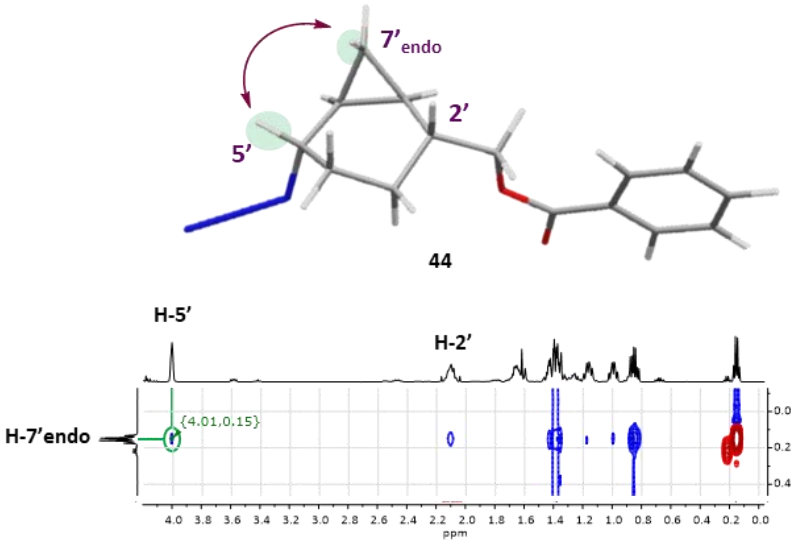

Figure II-5. Cross peaks between H-5' and H-7'endo in the 2D-NOESY spectrum (400 MHz, $CDCl_3$) of **44**.

Finally, the generation of the required key amine was achieved by a catalytic hydrogenation under hydrogen at 2 atm of pressure in the presence of Pd/C (10%) in EtOAc at rt. This amine was transformed to the more stable ammonium chloride salt **25** by treatment with a solution of HCl 2 M in diethyl ether in an almost quantitative yield (Scheme II-9).

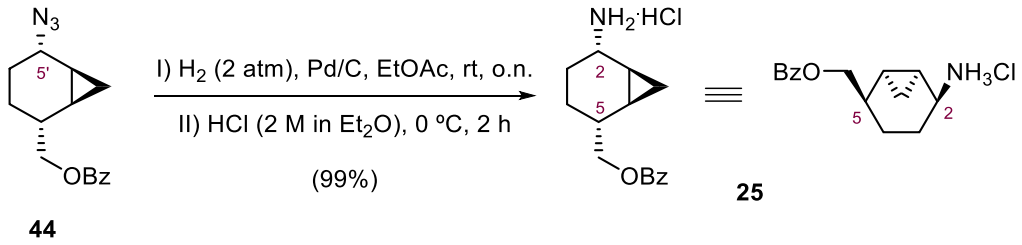

Scheme II-9. Reduction of azide **44** to **25** by hydrogenation and posterior acid treatment.

The formation of ammonium chloride salt **25** was confirmed by ^{1}H-NMR with the presence of a new signal at 8.69 ppm corresponding to the ammonium group (-NH_3^+) and the displacement of the proton H-2 which appeared upfield shifted (3.84 ppm) compared to the H-5' of azide **44** (4.01 ppm).

2.5. Synthesis of cytosine nucleoside analogue 28

The better way to obtain cytosine nucleosides is through the amination of the corresponding uridine derivatives.[7,8] Therefore, the synthetic strategy to prepare our desired cytosine nucleoside analogue consists of the stepwise construction of the uracil base from ammonium chloride derivative **25** and then, the ammonolysis of the C4-carbonyl group of uridine nucleobase.

The first methodology to construct pyrimidine bases stepwise was reported by Shaw and Warrener in 1958.[9] This procedure was based on a two-step reaction consisting of the addition of an amine (**XXV**) to an isocyanate followed by a cyclization of the formed acryloyl urea **XXVII** (Scheme II-10).

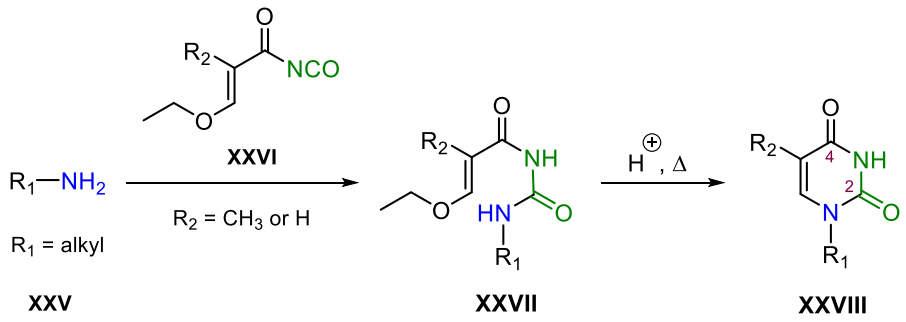

Scheme II-10. Stepwise construction of the pyrimidine bases.[9]

Isocyanate **XXVI** (R_2 = H, 3-ethoxy-2-propenoyl isocyanate) can be prepared by different routes. In 1993, Tietze[10] and co-workers published a procedure to obtain isocyanates by nucleophilic addition of vinyl ethers to oxalyl chloride to afford the chloride derivative (-COCl) which was then converted into isocyanate derivative (-CONCO) using the AgOCN salt (Scheme II-11). Isocyanates are very moisture-sensitive and reactive compounds and thus they are generally generated *in situ* for the construction of the nucleobase.

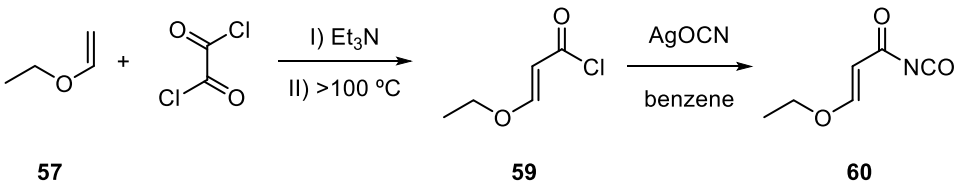

Scheme II-11. Tietze's methodology to synthesize isocyanate **60**.[10]

It was decided to prepare, first, the chloride derivative **59** in one pot following Tietze's procedure.[10] Hence, nucleophilic addition of ethyl vinyl ether **57** to oxalyl chloride at rt afforded the α-keto acid chloride **58**, which was decarbonylated upon vacuum distillation to give acryloyl chloride **59** in 53% yield (Scheme II-12).

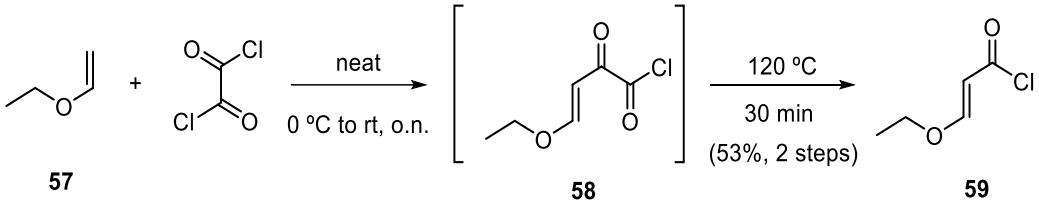

Scheme II-12. Preparation of acryloyl chloride **59** by Tietze's procedure.

Afterwards, the formation of the uracil ring was performed following a methodology described by Garcia-Mera and co-workers.[11] Thus, treatment of acryloyl chloride **59** with silver cyanate (AgOCN) in dry benzene at the reflux temperature for 3 h led to the corresponding isocyanate **60.** Given the instability of the isocyanate, it was directly added as a solution in benzene, to a reaction mixture of amine **25** and Et_3N in dry DMF at -20 °C. Finally, the resulting acryloyl urea **61** was cyclized in acidic conditions (H_2SO_4 1 M in MeOH) to afford the desired uracil compound **62** in 46% yield from **25** (Scheme II-13).

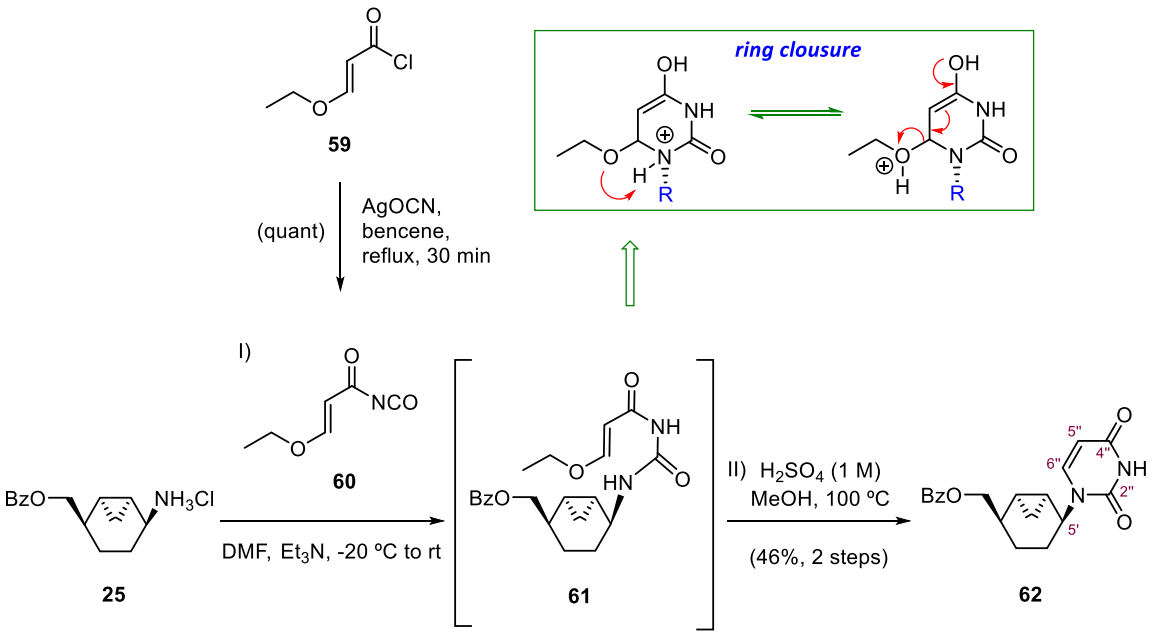

Scheme II-13. Stepwise construction of uracil nucleobase from ammonium chloride **25**.

The presence of uracil base in **62** could be easily confirmed in the ^{1}H-NMR and ^{13}C-NMR spectra. In the former, two new doublets appear at 5.46 ppm and 7.96 ppm ($J_{5'',6''}$ = 8.0 Hz), corresponding to H-5'' and H-6'', respectively; and, in the latter, new carbon peaks appears at δ 152.7 and 166.3 corresponding to C-2'' and C-4'', respectively. In addition, the displacement of H-5' to higher chemical shifts (from δ 3.84 in **25** to 4.83 in **62**) confirms the attachment of the uracil base in the bicyclo scaffold.

With **62** in hands, we targeted the transformation of uridine derivative into cytosine *via* an ammonolysis at C4-carbonyl group of uracil nucleobase[8] (Scheme II-14).

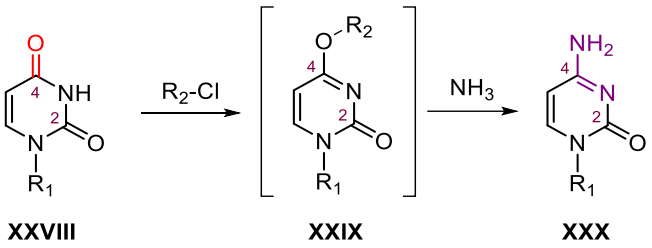

Scheme II-14. General transformation of uracil into cytosine by amination.

Among the number of amination methods reported, reactions with $POCl_3$/triazoles,[12] 4-chlorophenyl phosphorodichloridate/1,2,4-triazole,[13] and 2,4,6-triisopropylsulfonyl chloride (TPS-Cl),[14] followed by ammonolysis with ammonia (NH_3), are currently the best protocols. In 2004, Komatsu and co-workers[8] described an efficient amination method to prepare cytidines using *p*-toluenesulfonyl chloride (TsCl) as an alternative inexpensive and industrially available reagent for activating the C4-carbonyl group of uridines (Scheme II-15).

When TsCl is used, nucleophilic NH_3 competes with the attack at C4 of **XXXI** to deliver **XXX** (*path B*, Scheme II-15) and with the attack of sulfonyl group of **XXXI** that reverts to the starting **XXVIII** (*path A*). A transient substitution of TsO group with tertiary amines (such as *N*-methylpiperidine) avoids the *path A*. *N*-methylpiperidine replaces the TsO group, and a quaternary ammonium salt **XXXII** is produced (*path C*). Even if *path C* competed with *path D*, a presumable product **XXXIII** is likely to convert **XXVIII** to **XXXI** without consuming the reagents.[15] Ammonolysis by nucleophilic NH_3 occurred at the C4-position of **XXXII** giving **XXX** in high yield.

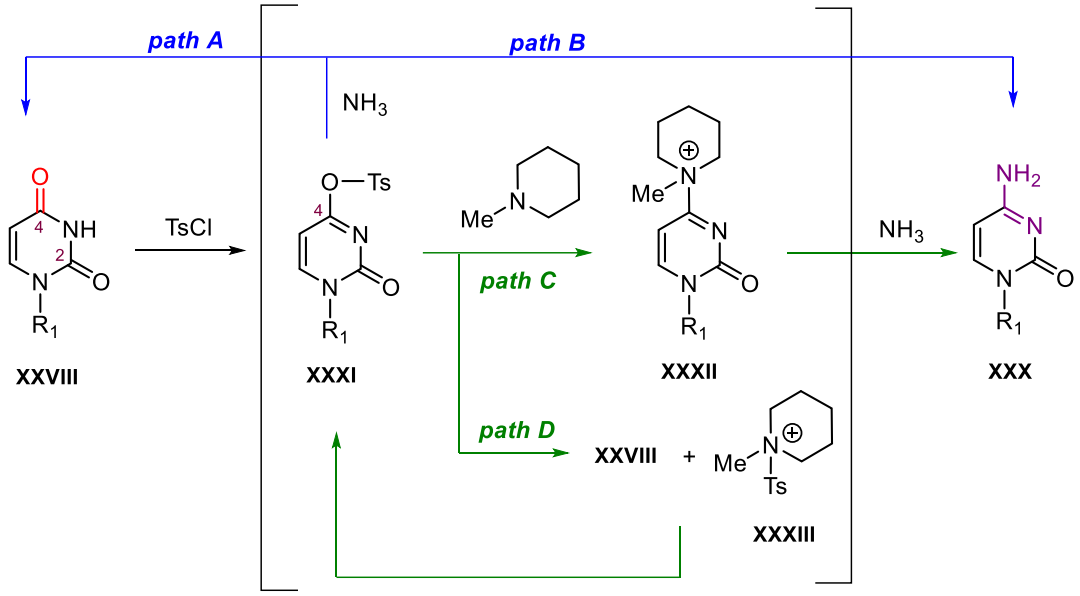

Scheme II-15. Proposed mechanism of ammonolysis at the C^4 –position of uridine derivative using TsCl and 1-methylpiperidine.[8]

Taking into account all these results, a one pot amination of **62** was performed in the presence of TsCl, Et_3N and *N*-methylpiperidine at 0 °C, followed by ammonolysis with 30% NH_4OH solution in water. Finally, removal of the benzoyl protecting group was performed by CH_3NH_2 (33% in EtOH), to give, after purification by flash column chromatography, the desired cytosine nucleoside analogue **28** in 29% overall yield (Scheme II-16).

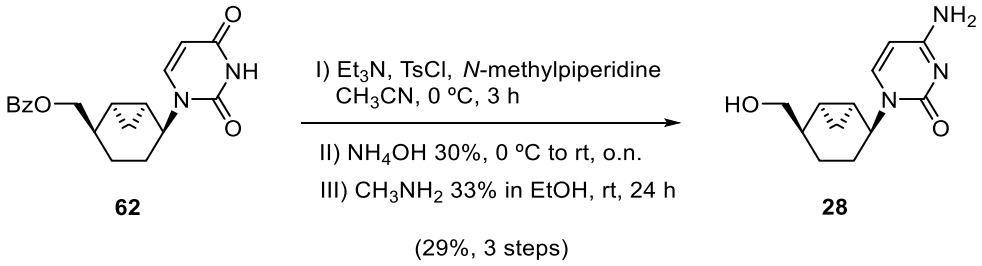

Scheme II-16. Transformation of uridine **62** to cytosine nucleoside analogue **28.**

The formation of cytidine nucleoside analogue **28** was confirmed by the displacement of C-4 and C-2 signals to higher chemical shifts (from 166.3 and 152.7 ppm in **62** to 167.3 and 159.0 ppm in **28**, respectively) in the ^{13}C-NMR spectrum, as well as, by the disappearance of the peaks corresponding to benzoyl group in the ^{1}H-NMR and ^{13}C-NMR spectra (Figure II-6).

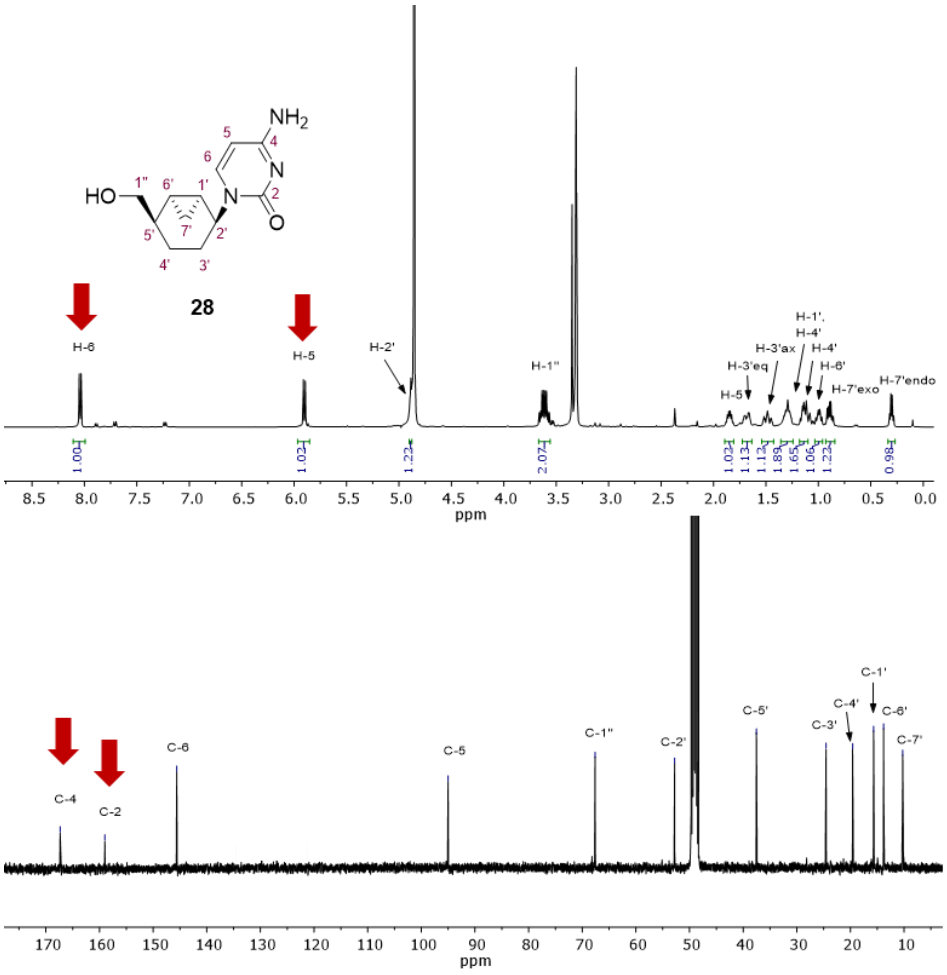

Figure II-6. ^{1}H-NMR (400 MHz, MeOH-d_4) and ^{13}C-NMR (100 MHz, MeOH-d_4) of cytosine analogue **28**.

3. EVALUATION OF THE ANTIVIRAL ACTIVITY

The antiviral activity of the synthesised cytosine nucleoside analogue **28** has been evaluated at the group leaded by Prof. Jan Balzarini at the *Rega Institute for Medical Research, Katholieke Universiteit Leuven*. Cytidine analogue **28** has been tested for the cytotoxicity and antiviral activity against different viruses (Table II-(1-4)).

Table II-1. Cytotoxicity and antiviral activity in HeLa (cervical cancer) cell cultures.

Compound	Conc. Unit	Cytotoxixity CC_{50}[a]	Antiviral EC_{50}[b]		
			Vesicular stomatitis virus	Coxsackie virus B4	Respiratory syncytial vius
28	µM	>100	>100	>100	>100
DS-10,000	µg/ml	>100	0.08	2.5	0.01
Ribavirin	µM	>250	149	117	6.7

[a] 50% Cytotoxic concentration, as determined by measuring the cell viability with the colorimetric formazan-based MTS assay.
[b] 50% Effective concentration, or concentration producing 50% inhibition of virus-induced cytopathic effect, as determined by measuring the cell viability with the colorimetric formazan-based MTS assay.

Table II-2. Cytotoxicity and antiviral activity in Vero cell (kidney epithelial cells from African green monkey) cultures.

Compound	Conc. Unit	Cytotoxixity CC_{50}[a]	Antiviral EC_{50}[b]					
			Reovirus-1	Sindbis virus	Coxsackie virus B4	Punta Toro virus	Yellow Fever virus	Zika virus
28	µM	>100	>100	>100	>100	>100	>100	>100
Ds-10,000	µg/ml	>100	>100	45	8.9	100	0.6	3.4
Mycophenolic acid	µM	>100	1.8	0.8	100	20	1.1	0.2

[a] 50% Cytotoxic concentration, as determined by measuring the cell viability with the colorimetric formazan-based MTS assay.
[b] 50% Effective concentration, or concentration producing 50% inhibition of virus-induced cytopathic effect, as determined by measuring the cell viability with the colorimetric formazan-based MTS assay.

Table II-3. Cytotoxicity and antiviral activity in HEL (Human Erythroleukemia) cell cultures.

Compound	Conc. Unit	Cytotoxixity CC_{50}[a]	Antiviral EC_{50}[b]				
			Herpes simplex virus-1 (KOS)	Herpes simplex virus-2 (G)	Vaccinia virus	Adeno virus-2	Human Coronavirus (229E)
28	µM	>100	>100	>100	>100	>100	>100
Brivudin	µM	>250	0.04	112	29	-	-
Cidofovir	µM	>250	2.0	1.4	14	5.8	-
Acyclovir	µM	>250	0.4	0.4	>250	-	-
Ganciclovir	µM	>100	0.02	0.05	>100	-	-
Zalcitabine	µM	-	-	-	-	7.2	-
Alovudine	µM	-	-	-	-	5.8	-
UDA	µg/ml	-	-	-	-	-	8.9

[a] 50% Cytotoxic concentration, as determined by measuring the cell viability with the colorimetric formazan-based MTS assay.
[b] 50% Effective concentration, or concentration producing 50% inhibition of virus-induced cytopathic effect, as determined by measuring the cell viability with the colorimetric formazan-based MTS assay.

Table II-4. Cytotoxicity and antiviral activity in MDCK (Madin-Darby Canine Kidney) cell cultures.

Compound	Conc. Unit	Cytotoxixity CC_{50}[a]	Antiviral EC_{50}[b]		
			Influenza A/H1N1 A/Ned/378/05	Influenza A/H3N2 A/HK/7/87	Influenza B B/Ned/537/05
28	µM	>100	>100	>100	>100
Zanamivir	µM	>100	0.02	0.03	0.03
Ribavirin	µM	>100	6.1	4.0	1.5
Amantadine	µM	>100	4.1	0.3	>100
Rimantadine	µM	>200	1.6	0.01	>200

[a] 50% Cytotoxic concentration, as determined by measuring the cell viability with the colorimetric formazan-based MTS assay.
[b] 50% Effective concentration, or concentration producing 50% inhibition of virus-induced cytopathic effect, as determined by measuring the cell viability with the colorimetric formazan-based MTS assay.

Unfortunately, cytosine nucleoside analogue **28** was inactive at concentrations up to 100 µM against different virus. This result is not surprising considering the results obtained for the other 5'-hydroxymethylbicyclo[4.1.0]heptanyl analogues compounds.

4. EVALUATION OF THE ENZYMATIC ACTIVITY IN HSV-TK

As it has been previously mentioned, among the factors that may explain the lack of significant activity against herpes virus of the 5'-hydroxymethylbicyclo[4.1.0]heptanyl NAs could be a low affinity or substrate activity for the viral-encoded or cellular nucleoside kinases. In order to evaluate this last point, the cellular HSV-1 and VZV thymidine kinases (TKs) affinity of the synthesised compounds (**BCH**-(**A**, **G**, **T**, **U**) and **28**) were tested (Table II-5).

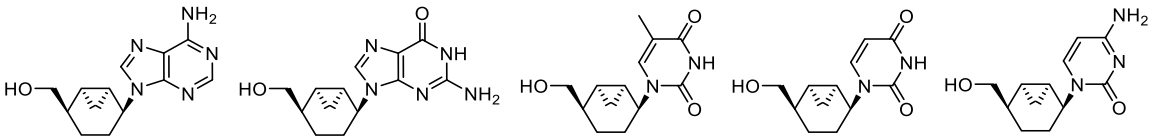

BCH-A BCH-G BCH-T BCH-U 28

Compound	Conc. Unit	EC_{50}[a]			
		Human TK-1	Human TK-2	HSV-1 TK	VZV TK
BCH-A	µg/ml	>200	>200	>200	>200
BCH-G	µg/ml	>200	>200	52 ± 28	>200
BCH-T	µg/ml	>200	93 ± 7	1.6 ± 0.1	10.5
BCH-U	µg/ml	>200	>200	150 ± 15	>200
28	µg/ml	>100	>100	>100	>100

[a]50% effective concentration.

Table II-5. Evaluation of kinase activity.

From these results, it can be observed that compounds **BCH-T** and in less extension **BCH-G** were nicely recognised by herpes simplex virus-TK (EC_{50} = 1.6 ± 0.1 µg/mL and 52 ± 28 µg/mL, respectively) in agreement with our modelling studies. Moreover, the **BCH-T** analogue was tested for substrate activity by HPLC and it was found to be a substrate with a nice conversion at the mono phosphate metabolite. Regarding **28**, it did not display affinity in HSV-1 TK. It was expected that this cytosine analogue would show affinity, since the natural nucleoside (2-deoxycytidine, 2-dC) is known to be recognised by several kinases but apparently it was not the case. However, it should be noted that the test of the **28** was performed in the presence of dT as natural competing substrate, and thus, to be more accurate, the test should be done in the presence of dC as natural competing substrate. Interestingly, none of the analogues showed significant affinity to human cellular kinases. Therefore, since some of the synthesised analogues are recognised by the virus-encoded kinase, the lack of antiherpetic activity could be attributed to a low affinity of the 5'-triphosphate metabolites to the virus-encoded DNA polymerase.

5. CHAPTER II OUTLINE

In summary, the synthesis of cytosine carbocyclic analogue **28** built on a bicyclo[4.1.0]heptane scaffold has been developed (Scheme II-17). The introduction of the base moiety was accomplished, *via* stepwise construction of the nucleobase from the ammonium chloride derivative **25**. Transformation of the uridine derivative **62** into the cytosine one *via* ammonolysis at C4-carbonyl group was carried out obtaining, finally, the nucleoside analogue **28** in 12 steps from **36** and 7% overall yield.

The nucleoside compound **28** has been evaluated against several viruses. Unfortunately, it showed no significant activity against any virus and cytotoxicity. In addition, the affinity of the 5'-hydroxymethylbicyclo[4.1.0]heptanyl NAs for HSV-1 TK and VZV TK was evaluated. The compound **BCH-T** display an interesting great affinity for HSV-TK (EC_{50} = 1.6 ± 0.1 µg/mL) which was consistent with our computational model performed for the first stage of the phosphorylation process.

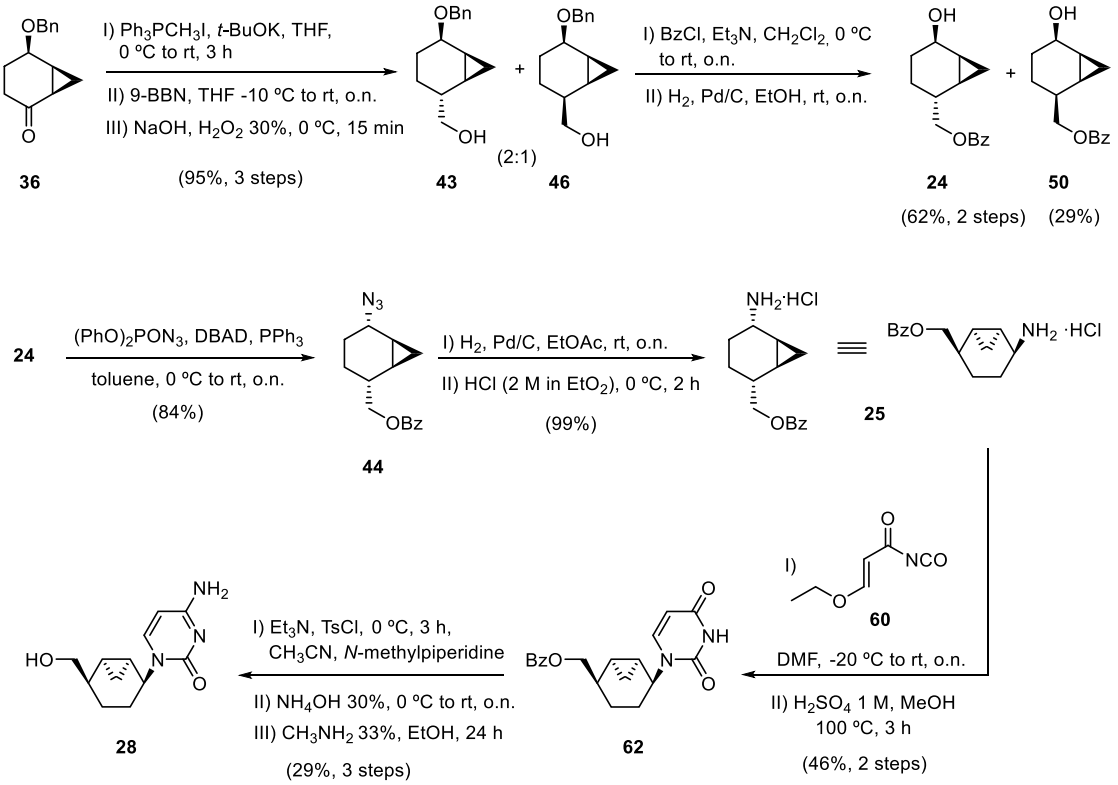

Scheme II-17. Synthesis of cytosine bicyclo[4.1.0]heptane nucleoside analogue **28** from ketone **36**.

6. REFERENCES

[1] Domínguez-Pérez, B., Ferrer, E., Figueredo, M., Maréchal, J. D., Balzarini, J., Alibés, R., Busqué, F. *J. Org. Chem*. **2015**, *80*, 9495-9505.

[2] (a) Brown, H. C., Jadhav, P. K. Asymmetric hydroboration. *Asymmetric Synth.* **1983**, *2*, 1-43; (b) Brown, H. C., Rao, B. C. S. *J. Am. Chem. Soc.* **1956**, *78*, 5694-5695.

[3] Crimmins, M. T. *Tetrahedron* **1998**, *54*, 9229–9272.

[4] Beatriz-Dominguez, B. Doctoral Thesis, Universitat Autònoma de Barcelona, 2015.

[5] (a) Swamy, K. C. K.; Kumar, N. N. B.; Balaraman, E.; Kumar, K. V. P. P. *Chem. Rev.* **2009**, *109*, 2551–2651; (b) Jenny, T. F.; Previsani, N.; Benner, S. A. *Tetrahedron Lett.* **1991**, *32*, 7029–7032.

[6] Lal, B.; Pramanik, B. N.; Manhas, M. S.; Bose, A. K. *Tetrahedron Lett.* **1977**, *18*, 1977−1980.

[7] Huryn, D. M., Okabe, M. *Chem. Rev.* **1992**, *92*, 1745-1768.

[8] Komatsu, H., Morizane, K., Kohno, T., Tanikawa, H. *Org. Process Res. Dev.* **2004**, *8*, 564-567.

[9] (a) Shaw, G.; Warrener, R. N. *J. Chem. Soc.* **1958**, 157–161; (b) Shaw, G.; Warrener, R. N. *J. Chem. Soc.* **1958**, 153–156.

[10] Tietze, L. F.; Schneider, C.; Pretor, M. *Synthesis* **1993**, 1079–1080.

[11] Fernández, F.; García-Mera, X.; Morales, M.; Rodríguez-Borges, J. E. *Synthesis* **2001**, *2*, 239–242.

[12] (a) Matsuda, A.; Obi, K.; Miyasaka, T. *Chem. Pharm. Bull.* **1985**, *33*, 2575-2578; b) Hodge, R. P.; Brush, C. K.; Harris, C. M.; Harris, T. M *J. Org. Chem.* **1991**, *56*, 1553-1564.

[13] Sung, W. L. J. *Org. Chem*. **1982**, *47*, 3623-3628.

[14] (a) Awano, H.; Shuto, S.; Miyashita, T.; Ashida, N.; Machida, H.; Kira, T.; Shigeta, S.; Matsuda, A. *Arch. Pharm. Pharm. Med. Chem.* **1996**, *329*, 66-72; (b) Matsuda, A.; Yasuoka, J.; Sasaki, T.; Ueda, T. *J. Med. Chem*. **1991**, *34*, 999-1002; (c) Sekine, M. *J. Org. Chem.* **1989**, *54*, 2321-2326; (d) Reese, C. B.; Ubasawa, A. *Tetrahedron Lett*. **1980**, *21*, 2265-2268.

[15] Yoshida, Y.; Sakakura, Y.; Aso, N.; Okada, S.; Tanabe, Y. *Tetrahedron* **1999**, *55*, 2183-2192.

III. CHAPTER III

Synthesis of 5’-hydroxymethyl-4’-hydroxybicyclo[4.1.0]heptan-2’-yl nucleoside analogues based on Cyclohexanyl G

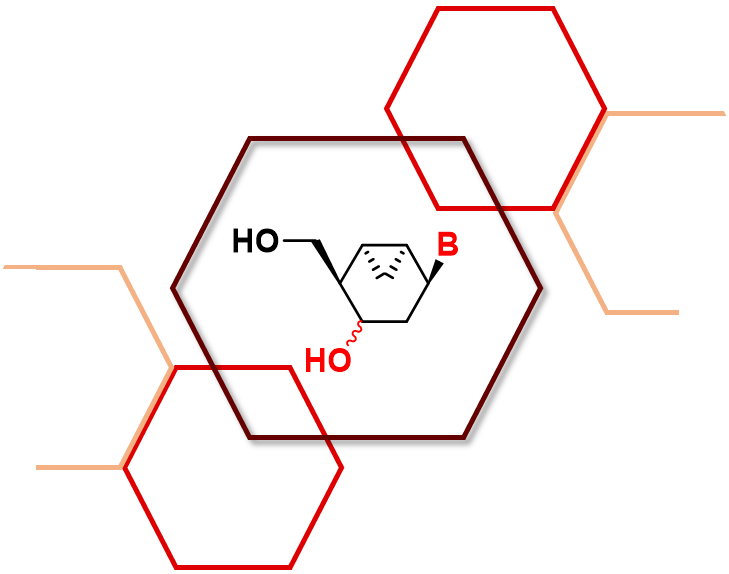

1. INTRODUCTION

1.1. About Cyclohexenyl G

As it has been mentioned in the *Introduction*, different conformational studies on the cyclohexene moiety of cyclohexenyl NAs suggested that these compounds could be considered as bioisosteres of natural furanose nucleosides.[1-3] These studies prompted investigators to synthesise different families of cyclohexenyl analogues, but unfortunately, the most part of these compounds did not display significant biological activity.[4a-j]

However, in 1999 Herdewijn and co-workers reported the enantioselective synthesis of both enantiomers of cyclohexenyl G (4'-hydroxymethyl-3'-hydroxycyclohexenyl guanine (Figure III-1),[5] which showed potent and selective antiviral activity against HSV-1, HSV-2, VZV, HCMV and HBV).[2] For instance, D-cyclohexenyl G (**DCG**) has an IC_{50} = 0.002 μg/mL and L-cyclohexenyl G (**LCG**) has and IC_{50} = 0.003 μg/mL for HSV-1 (KOS) while the IC_{50} for HSV-2 (G) are 0.05 and 0.07 μg/mL, respectively. D- and L-cyclohexenyl G are the first example of two enantiomeric nucleosides that show similar activity and toxicity profile, although the D- is slightly more powerful.[1,2,6] Their anti-herpes virus activity is comparable to other analogues that are on clinical use such as Acyclovir (ACV, Zovirax® 1982) and Ganciclovir (GCV, Cymevene® 1989).[2]

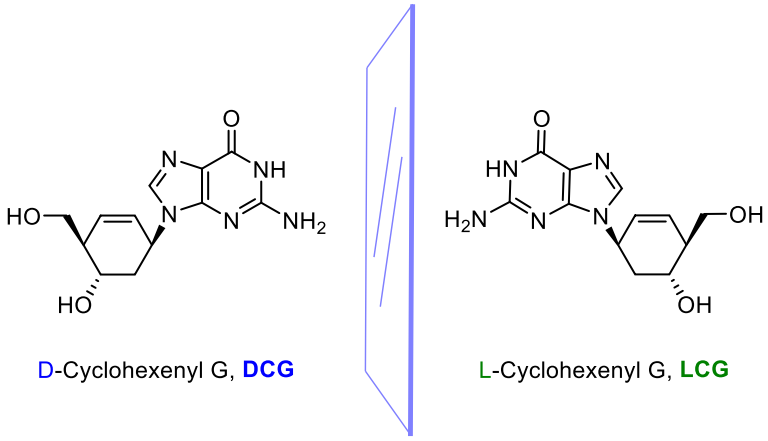

Figure III-1. Structure of D- and L-cyclohexenyl G.

This great biological activity was related to the cyclohexenyl ring conformational behaviour.[2] In general, the conformation of nucleosides is determined by competitive steric and stereoelectronic effects. In the case of cyclohexene nucleosides their conformation is controlled by steric effects as well as by the $\pi \rightarrow \sigma^*_{C1'\text{-}N}$ interaction between the C5'-C6' double bond and the heterocyclic aglycon,[2] that is similar to the anomeric effect in furanose nucleosides and can

be explained as an overlap between the antibonding C1'-N and the orbitals of the π bond (Figure III-2).

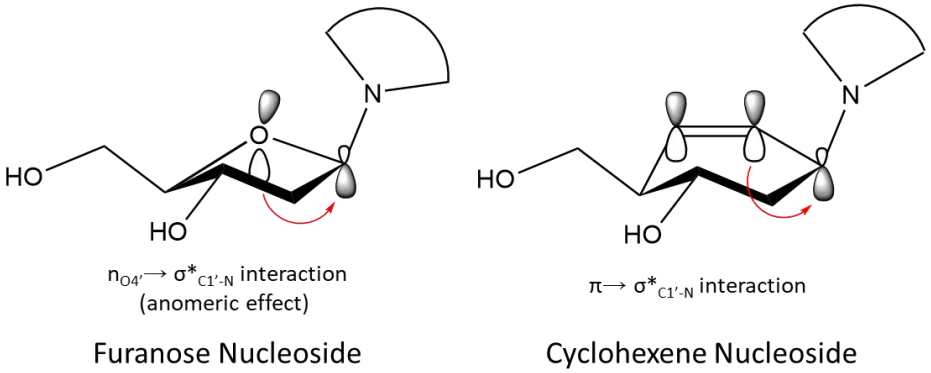

Figure III-2. Comparison of anomeric effect in furanose nucleosides with $\pi \rightarrow \sigma^*_{C1'-N}$ effect in cyclohexene nucleosides**.**

Structural analysis demonstrated that these cyclohexenyl nucleosides have a flexible conformation. In solution, there is an equilibrium between the most stable $^3H_2$ conformation, due to the $\pi \rightarrow \sigma^*_{C1'-N}$ interaction, and the $^2H_3$ conformation (Figure III-3).[1,2] This easy equilibrium allows cyclohexenyl G to adapt their conformations easily to different enzymatic requirements of the virus kinases. This flexibility is an important conformational feature explaining the potent antiviral activity of these cyclohexenyl nucleosides. This effect was confirmed by different NMR experiments suggesting that the half-chair conformation with the base in a pseudo-axial position ($^3H_2$) is preferred in solution.[5]

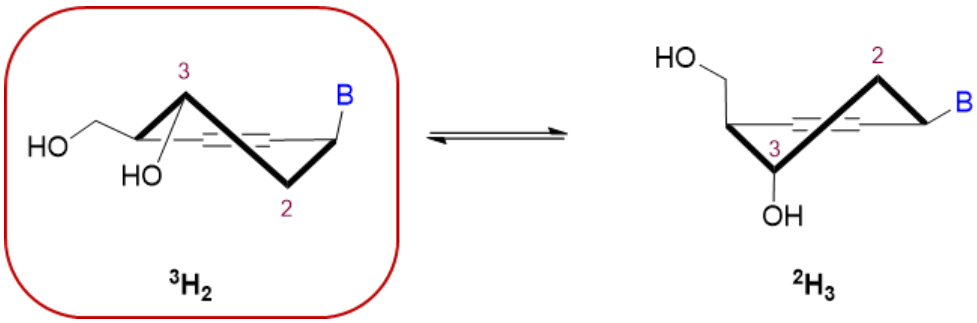

Figure III-3. Comparison of $^3H_2$ and $^2H_3$ conformational equilibrium of cyclohexene nucleoside where $^3H_2$ conformer is favoured.

As it has been explained, Dr. Beatriz Domínguez in her doctoral thesis[7] performed *in silico* molecular studies focused in cyclohexanyl nucleoside analogues built on a bicyclo[4.1.0]heptane scaffold. In this study, the molecular modelling was also carried out in 5'-hydroxymethyl-4'-hydroxybicyclo[4.1.0]heptane NAs, **XIV** (B = T or G) on the active site of the HSV-1 thymidine

kinase to evaluate if these compounds could interact properly with the binding site in the phosphorylation step (Figure III-4).

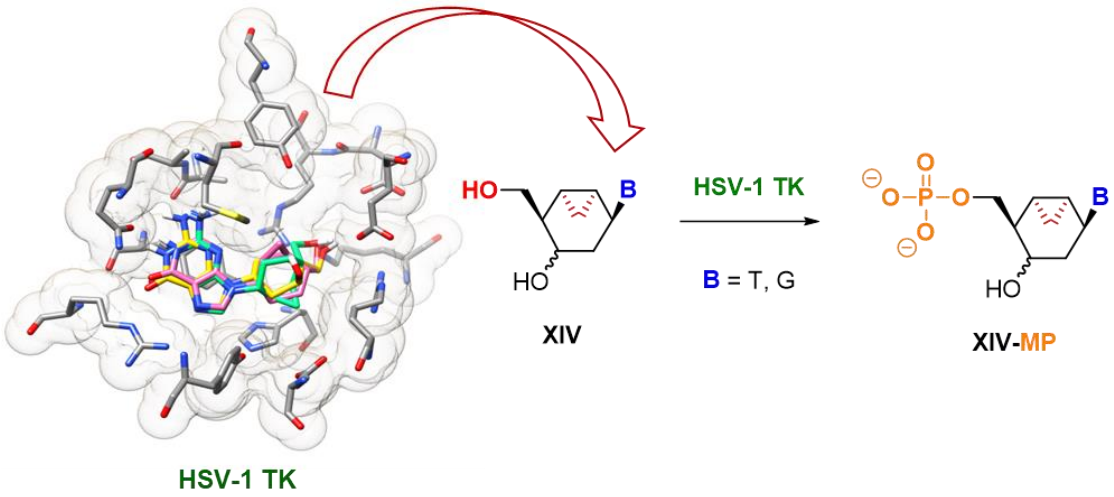

Figure III-4. Protein–ligand docking calculations in NAs with structure **XIV** on HSV-1 TK for the first phosphorylation step and the structure of the benchmarks used in this study.

This computational study suggested that the replacement of double bond by fused cyclopropane ring does not alter the binding mode of the nucleosides in this kinase and, as a consequence, the 5'-hydroxymethyl-4'-hydroxybicyclo[4.1.0]heptanyl nucleoside analogues, **XIV** (B = T, G) envisaged could be correctly activated at the first phosphorylation step.[7] In this chapter, it is described the preparation of a novel family of cyclohexanyl NAs with structure **XIV** and its biological evaluation against different virus.

2. SYNTHESIS OF 5'-HYDROXYMETHYL-4'-HYDROXYBICYCLO[4.1.0]HEPTANE NAs

2.1. Synthetic strategy

The synthetic pathway to reach the new targeted enantiopure 5'-hydroxymethyl-4'-hydroxybicyclo[4.1.0]heptane NAs, **XIV**, is planned to be carried out based on a similar synthetic plan that was developed in our group by Dr. Ferrer in its Ph.D thesis.[8] The synthesis would start from the previous synthesised olefin intermediate **42**, obtained by olefination from the key ketone **36** (Scheme III-1). Allylic oxidation should provide the allylic alcohol **63** which, after stereoselective hydroboration-oxidation reaction would lead to diol **64**. The diol protection and posterior benzyl deprotection will afford alcohol **XXXIV**. As in *Chapter II*, considering our research group precedents, nucleobase stepwise construction will be carried out in order to obtain the targeted different nucleoside analogues based in structure **XIV**.

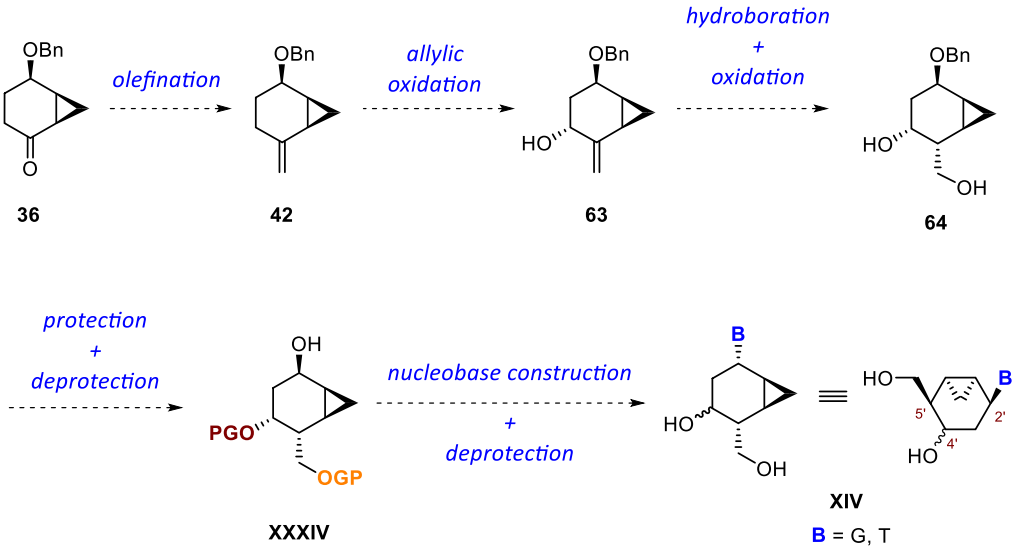

Scheme III-1. Synthetic pathway foreseen to prepare nucleoside analogues with structure **XIV**.

2.2. Synthesis of alcohol allylic 63

As it has been explained in *Chapter II*, olefination of ketone **36** was accomplished by Wittig reaction using freshly prepared ylide generated from methyltriphenylphosphonium iodide (Ph_3PCH_3I) and *t*-BuOK, providing the corresponding terminal olefin **42** (Scheme III-2). This exocyclic olefin isomerized at rt to the endocyclic olefin product (see *Chapter II*, section 2.2.1, Scheme II-2). In order to avoid the isomerization process, the allylic oxidation was carried out

immediately after the Wittig reaction without further purification, using the methodology developed by Sharpless and co-workers[9,10] using catalytic selenium dioxide (SeO_2) and *tert*-butyl hydroperoxide as a stoichiometric co-oxidant agent.

Therefore, the freshly prepared exocyclic alkene **42** was treated with catalytic selenium dioxide (SeO_2) and stoichiometric *tert*-butyl hydroperoxide (*t*-BuOOH, 70% in water) for 20 minutes, furnishing the corresponding allylic alcohol **63** as a single diastereoisomer in 79% yield from ketone **36** (Scheme III-2).

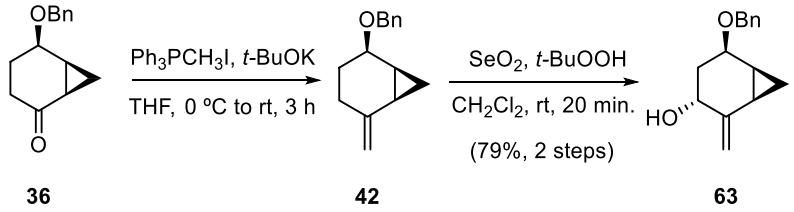

Scheme III-2. Olefination by Wittig reaction and posterior allylic oxidation to synthesise **63**.

The excellent diastereoselectivity produced by this oxidation reaction can be explained considering the postulated reaction mechanism (Scheme III-3). It consists of two consecutive pericyclic reactions: an ene reaction and a [2,3]-sigmatropic rearrangement where the latter takes place through the *anti* face with respect the cyclopropane, which present less steric hindrance than the *syn* face.[11]

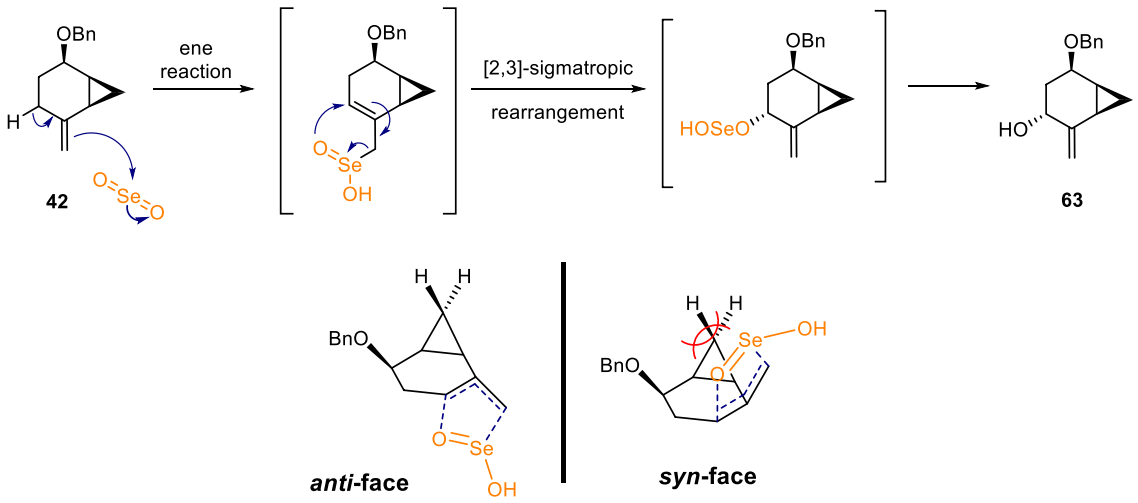

Scheme III-3. Postulated mechanism of the allylic oxidation of **42** and proposed transition state of the [2,3]-sigmatropic rearrangement leading to **63**.

The presence of a new peak at 4.22 ppm in the ^{1}H-NMR spectrum (Figure III-5), corresponding to H-3, as well as at 67.6 ppm in the ^{13}C-NMR confirms the formation of the allylic alcohol **63**. Further, a broad peak at 3388 cm^{-1} is observed in the IR spectrum corresponding to alcohol H-O stretching.

The configuration of the new stereogenic centre created was determined by a 2D-NOESY spectrum (Figure III-5), where cross peak between the H-3 proton and the methylene proton H-7endo of the cyclopropane ring can be observed, revealing the *cis* relationship between H-3 proton and the cyclopropane. Therefore, the absolute configuration of **63** is (1*R*,3*R*,5*R*,6*S*).

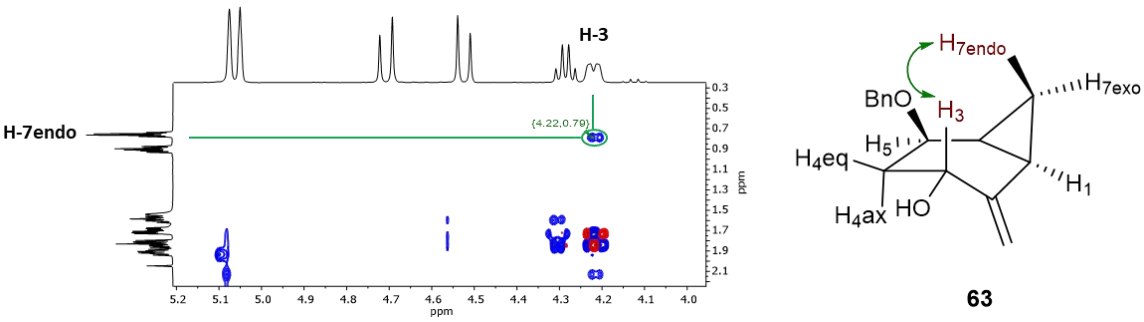

Figure III-5. Cross peak between H-3 and H-7endo in the 2D-NOESY spectrum (400 MHz, $CDCl_3$) of **63**.

2.3. Generation of the hydroxymethyl group *via* hydroboration-oxidation reaction

The next step of our synthetic plan was the anti-markovnikov hydration of the olefinic present in **63** by a hydroboration-oxidation procedure.

Previously in our group, this reaction was carried in a similar compound **65** bearing a TBDPS as a protecting group.[8] In a first attempt, the hydroboration-oxidation of allylic alcohol **65** was carried out using BH_3·THF as a reagent from 0 °C to rt, followed by usual oxidation step affording an inseparable 4:1 mixture of diols **66** and **67** in moderate yield (Table III-1, entry 1). However, when the reaction was performed using 9-BBN from 0 °C to rt, only single diastereoisomer **66** was obtained in good yield (entry 2).

This excellent stereoselectivity can be explained considering that the borane reagent (9-BBN) readily reacts with the hydroxyl group before the addition to the olefinic unit, and the produced borate acts as a steric fence favouring the addition of the second borane reagent by the opposite face.[12c] Thus, in these cases, more than two equivalents of a borane reagent have been

employed. The borate intermediate ultimately hydrolyses to the original alcohol in the basic oxidation step.[12a-e]

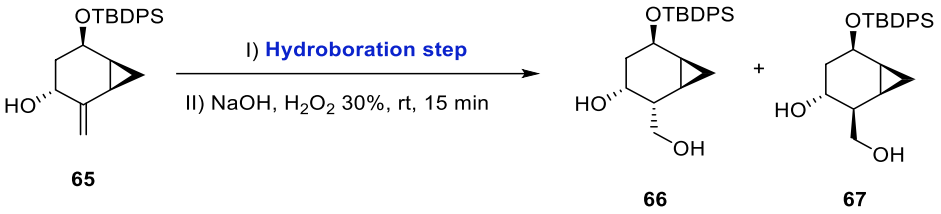

65 66 67

Exp.	Borane reagent	Temperature	Time	Yield	66 : 67
1	BH_3·THF	0 °C to rt	3 h	70%	4:1
2	9-BBN·THF	0 °C to rt	16 h	92%	only **66**

Table III-1. Previously results obtained in the hydroboration-oxidation reaction in our research group.[8]

2.3.1. Approach A. Hydroboration-oxidation reaction with non-protected alcohol

Taking into account the above results, the hydroboration-oxidation reaction with our new olefin **63** was first attempt using 9-BBN. In this case, treatment of **63** with 9-BBN (from 0 °C to rt) and subsequent oxidation step, afforded a 20:1 mixture of diols **64** and **68** in 92% yield (entry 1). The same result was observed when the temperature was changed from 0 °C to -10 °C (entry 2).

63 64 68

Exp.[a]	Borane reagent[b]	Temperature	Time	Yield	Ratio[C] (**64** : **68**)
1	9-BBN·THF	0 °C to rt	16 h	90%	20:1
2	9-BBN·THF	-10 °C to rt	16 h	92%	20:1
2	BH_3·THF	-10 °C to rt	4 h	91%	5:1

[a]All the reaction was carried out with dry THF; [b]2.5 eq of borane derivative was added; [c]Ratios were determined by ^{1}H-NMR.

Table III-2. Hydroboration-oxidation procedure on **63**. Fist hydroboration step conditions and final yield and ratio of the diols mixture.

Although the process proceeded with high selectivity, it was lower than that observed using TBDPS as protecting group. Moreover, the reaction was also performed using BH_3·THF from -10 °C to rt. In this case the stereoselectivity was also decreased delivering a 5:1 mixture of diols **64** and **68** in 91% yield (Table III-2, entry 3).

As it has been explained, the use of 9-BBN offers a strong steric hindrance hindering the entry of a second equivalent of borane for this face (*si* face) and, therefore, favouring the attack on the *re* face (Figure III-6), so obtaining **64** as a major product.[12c]

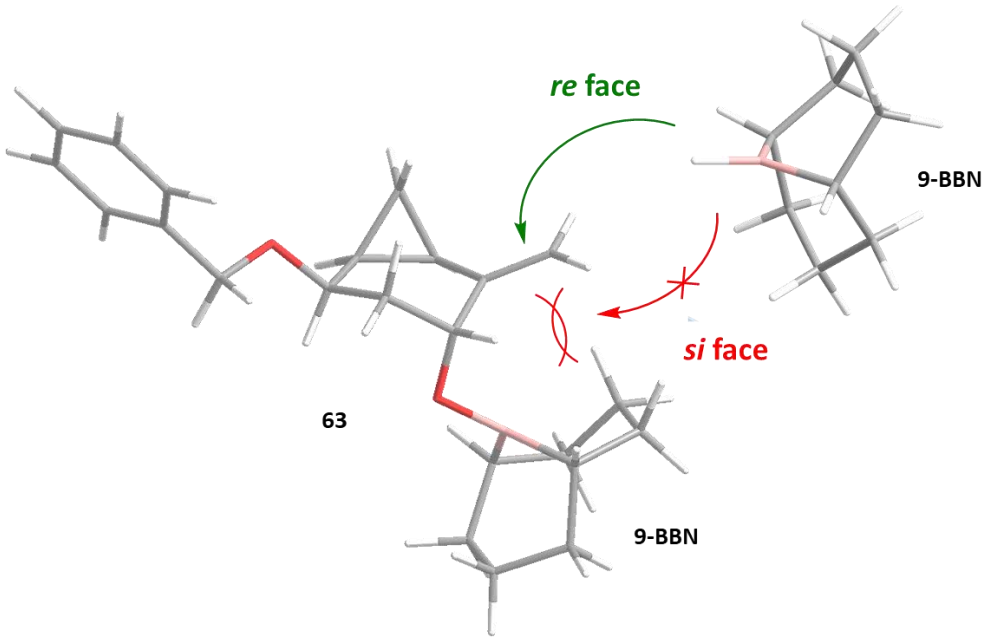

Figure III-6. Plausible approximation of second equivalent of 9-BBN by more accessible β face onto borate in the hydroboration reaction.

The mixture of diols **64** and **68** was very difficult to be separated by flash column chromatography, but it was possible to obtain a pure fraction of **64**. The presence of the hydroxymethyl group in **64** was observed in ^{1}H-NMR spectrum with a new signal as multiplet at 3.91 – 3.81 ppm corresponding to the two protons H-1' of hydroxymethyl group, as well as, in the ^{13}C-NMR spectrum with a signal at 65.2 ppm.

The configuration of the new stereogenic centre created was determined by a 2D-NOESY spectrum (Figure III-7), where cross-peaks between the H-2, H-7endo and H-4ax protons can be observed, revealing the *cis* relationship between these three protons. This fact confirms the favoured attack of second equivalent of 9-BBN by *re* face. Thus, the absolute configuration of **64** is (1*R*,2*R*,3*R*,5*R*,6*S*).

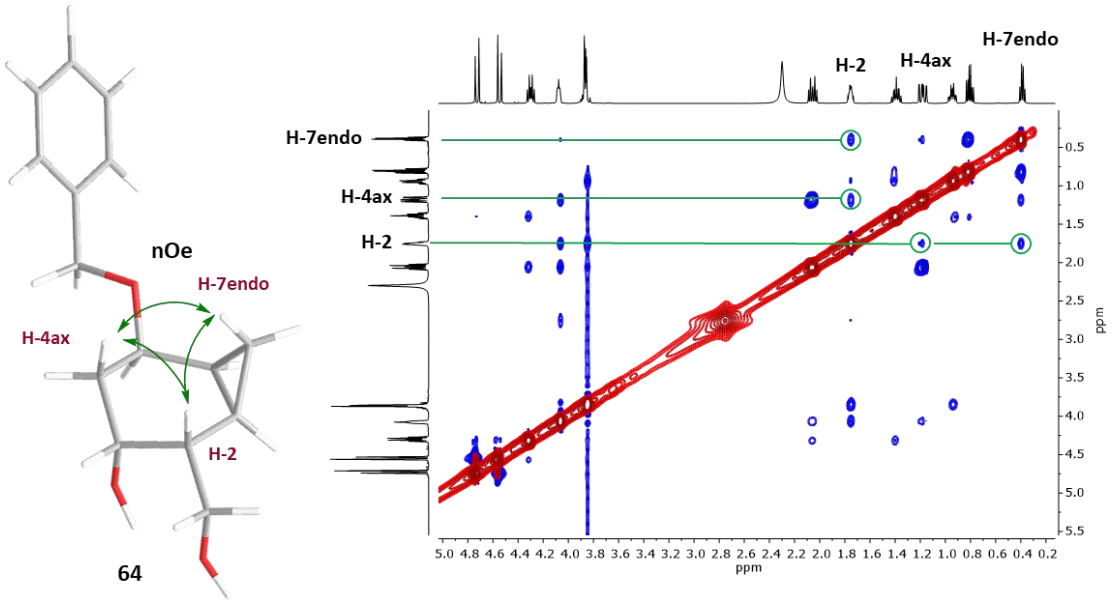

Figure III-7. Cross-peaks between H-2, H-4ax and H-7'endo in the 2D-NOESY spectrum (400 MHz, $CDCl_3$) of **64**.

2.3.2. Approach B. Hydroboration-oxidation reaction with protected alcohol.

Although the hydroboration reaction took place with good stereoselectivity, it was decided to explore whether the presence of an additional protecting group in the hydroxyl group could affect this selectivity. With this aim, *tert*-butildimethylsilyl (TBS) protecting group was chosen in order to hinder the approach of the borane. Accordingly, allylic alcohol **63** was protected using *tert*-butyldimethylsilyl chloride in the presence of imidazole at rt, affording the silyl ether **69** in good yield (Scheme III-4).

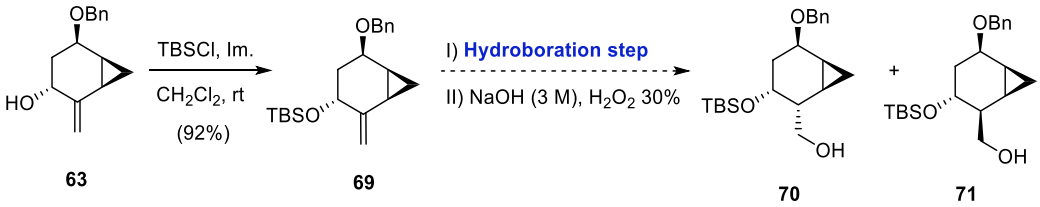

Scheme III-4. Protection of allylic alcohol **63** and subsequence hydroboration-oxidation reaction.

Then, olefin **69** was submitted to the hydroboration-oxidation process. The first experiment was performed using 9-BBN·THF (from -10 °C to rt) for 16 h (entry 1, Table III-3). Unfortunately, after the oxidation step, only a mixture of starting material **69**, accompanied by unidentified by-products was observed in the ^{1}H-NMR. The next experiment increasing the temperature, from

-10 °C to the reflux temperature (entry 2), led to an unidentified mixture of decomposition products.

Table III-3. Attempts and results using different conditions in the first hydroboration step.

Exp.[a]	Borane reagent[b]	Temperature	time	Results
1	9-BBN·THF	-10 °C to rt	16 h	**69** + by-products
2	9-BBN·THF	-10 °C to reflux	16 h	decomposed
3	BH_3·THF	-10 °C to rt	3 h	**70** + **71** (91%, 3:1[c])

[a]All the reaction was carried out with dry THF; [b]1.5 eq of borane derivative; [c]Ratios were determined by ^{1}H-NMR.

By changing to a less sterically hindered borane, BH_3·THF (entry 3), the reaction proceeded smoothly to afford after oxidative workup, a 3:1 mixture of alcohols **70** and **71** in 91% combined yield over the two steps. The mixture of alcohols **70** and **71** was very difficult to be separated by flash column chromatography, but it was possible to obtain a pure fraction of **70.**

The success of the reaction was confirmed by ^{1}H-NMR spectrum with the presence of new peaks at 3.78-3.71 and 1.78 ppm corresponding to the two proton H-1 of the hydroxymethyl group and H-2', respectively, as well as its signals at 65.4 and 42.2 ppm in the ^{13}C-NMR. Through 2D-NOESY, it was determined that the main alcohol obtained was alcohol **70**, denoting that mostly the attack of the borane occurs by the opposite face of the protecting group (*re* face) (Figure III-8).

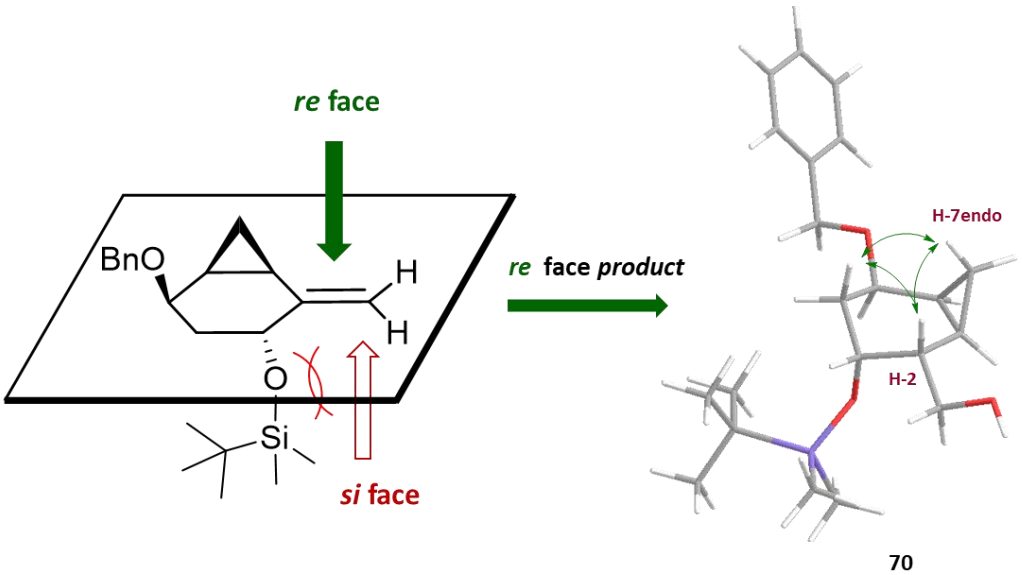

Figure III-8. Approaches of BH_3·THF to the diastereotopic faces of the alkene **69** and cross peaks in 2D-NOESY experiments of alcohol **70**.

In order to separate the diastereomeric mixture of **70** and **71** it was necessary to protect the hydroxyl group to the corresponding acetate form and removing the benzyl ether protecting group through hydrogenation providing after purification by flash column chromatography the diastereoisomeric alcohols **74** and **75** in 68% and 21% yield, respectively over the 2 steps (Scheme III-5).

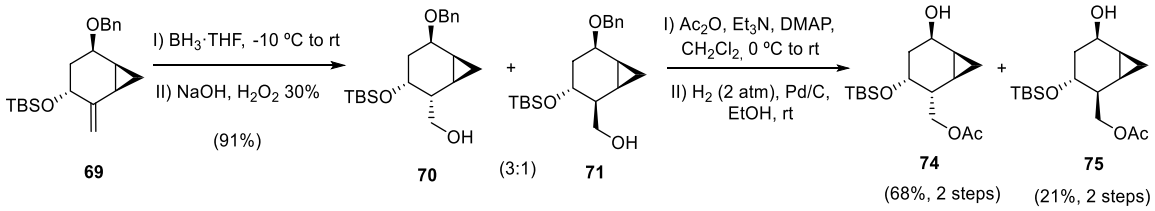

Scheme III-5. Hydroboration-oxidation reaction providing an inseparable diastereomeric mixture 3:1 of alcohols **70** and **71** and subsequence transformation into the separable derivatives **74** and **75**.

Due to the low selectivity produced in the hydroboration-oxidation with the protected alcohol, it was decided to follow the synthesis from the 20:1 mixture of **64** and **68** (*Approach A*).

2.4. Precedents in the research group for the introduction of the base moiety

In a previous work in our research group, Dr. Éric Ferrer during his PhD thesis,[8] studied the direct coupling of a nucleobase *via* a Mitsunobu reaction into the bicyclic scaffold **66** (Scheme III-6).

In a first attempt, the diol **66** was initially protected as a benzylidene acetal and the silyl ether was removed to provide the alcohol **76** in 87% yield. Then, the Mitsunobu reaction of **76** with the *N*3-benzoylthymine was attempted under different reaction conditions such as the use of different azodicarboxylate derivatives (DIAD, DBAD and DCAD) or solvents. Unfortunately, the desired substitution product was not obtained. In most cases, the elimination product **77** was obtained. In addition, it should be noted that in different tests, a product presenting a chain (derived from THF) between the base and the carbocyclic skeleton, **78** was isolated (Scheme III-6).

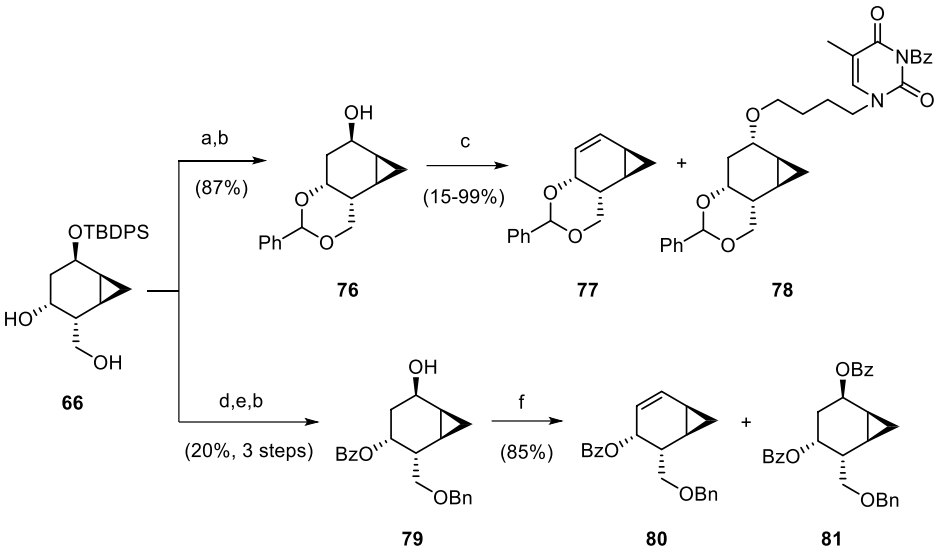

Scheme III-6. Different attempts of the direct coupling of a nucleobase *via* a Mitsunobu reaction.[8] Reagents: (a) $PhCH(OMe)_2$, CH_2Cl_2, rt; (b) TBAF, THF, reflux; (c) *N*3-benzoylthymine, DIAD/DBAD/DCAD, PPh_3, THF, -10 °C to rt; (d) I)Bu_2SnO, MeOH, reflux; II) BnBr, TBAI, toluene, reflux; (e) BzCl, py, DMAP, CH_2Cl_2, rt; (f) *N*3-benzoylthymine, DCAD, PPh_3, THF, -10 °C to rt.

In a second attempt, the diol **66** was protected in a non-cyclic manner. First, the hydroxymethyl was regioselective benzylated using a tin oxide (Bu_2SnO) intermediate and then, the remaining secondary alcohol was benzoylated. Alcohol **79** was obtained after removing the silyl protecting group in 20% overall yield over the 3 steps. Next, the treatment of **79** with *N*3-benzoylthymine, DCAD and PPh_3 in THF did not lead to the desired thymine derivative, but to the elimination product **80** along with compound **81**, where the hydroxyl group was protected in the form of benzoate (Scheme III-6).

In summary, all our efforts to directly introduce the nucleobase from **76** and **79** intermediates *via* Mitsunobu methodology met with failure. Therefore, it was decided to introduce the different nucleobases step by step from an amino derivative as in *Chapter II*.

2.5. Synthesis of ammonium salt 96

The synthesis of the ammonium salt would start from diol **64** (as a 20:1 mixture of **64** and **68**) that will be transform into the alcohol **XXXIV** after protection and deprotection reaction. This compound **XXXIV** will be converted to azide *via* Mitsunobu reaction (Scheme III-7), followed by reduction and treatment with acid conditions to provided key ammonium chloride intermediate **XXXVI**, from which the different nucleobases would be constructed in a stepwise manner.

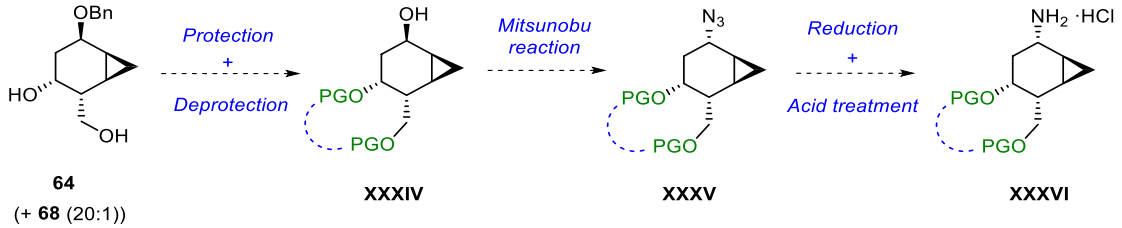

Scheme III-7. Synthetic strategy towards key ammonium chloride **XXXVI**.

2.5.1. Approach A. Benzylidene acetal as the 3,1'-diol protecting group

First, it was decided to protect simultaneously the diol functionality using a cyclic acetal group which was previously used in our group for similar molecules. Due to instability of benzylidene acetal to hydrogenation, the envisaged sequence (Scheme III-8) involves formation of the azide **82** which will be transformed into ammonium salt **83** through a Staudinger reaction.

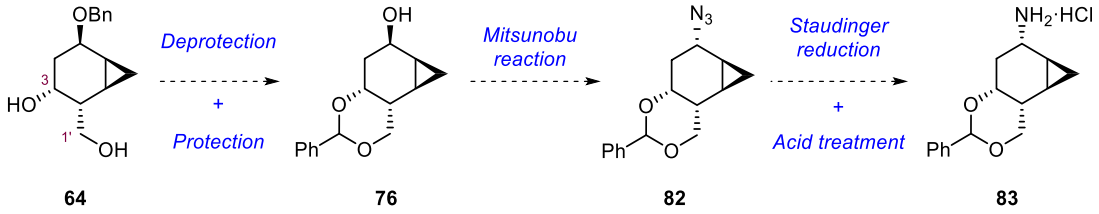

Scheme III-8. Synthetic strategy towards ammonium chloride **83**.

2.5.1.1. Synthesis of the benzylidene acetal intermediate 76.

Cleavage of the benzyl ether protecting group of the 20:1 diastereomeric mixture of **64** and **68** by hydrogenation under Pd/C provided a mixture of the corresponding triols in almost quantitative yield as a white solid. Then, this mixture (20:1) was re-crystallized by vapor diffusion using MeOH/Et_2O at rt to afford pure **84** as colourless crystals in 82% yield (Scheme III-9).

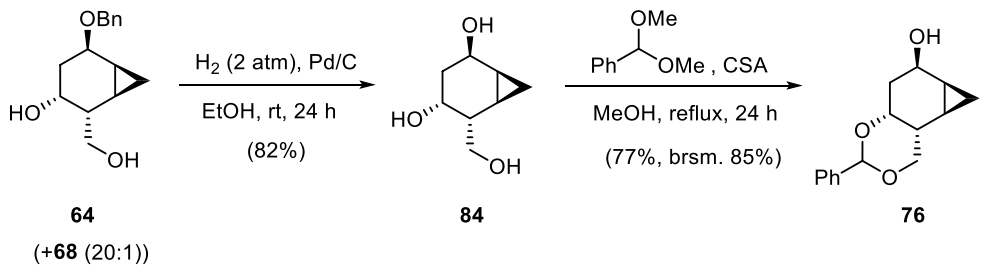

Scheme III-9. Deprotection of benzyl ether and protection as benzylidene acetal.

To our delight, **84** provided adequate crystals for X-ray analysis. Single crystal X-ray diffraction was performed by Dr. Ángel Álvarez at the *Servei Difracció Raigs X* of *Universitat Autónoma de Barcelona* (Figure III-9) The crystal structure obtained of **84** confirmed the relative stereochemistry of the molecule where the absolute configuration is (1*S*,2*R*,4*R*,5*R*,6*R*).

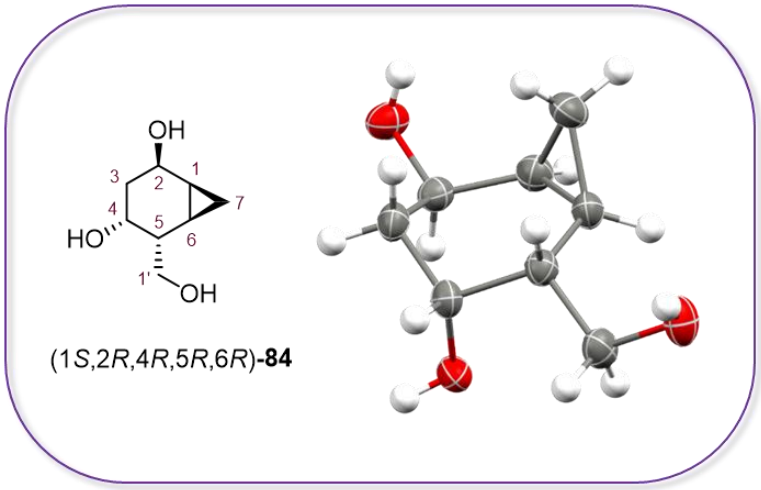

Figure III-9. Crystal structure of **84** (thermal ellipsoids at 50% probability level).

Treatment of **84** with benzaldehyde dimethyl acetal in presence of camphorsulfonic acid at the reflux temperature provided the desired benzylidene acetal **76** in 77% yield (brsm 85%, Scheme III-9). The formation of **76** was observed by ^{1}H-NMR spectrum with the presence of a new singlet peak at 5.42 ppm corresponding to the benzyl proton H-3', as well as, the new aromatic signals corresponding to the benzylidene acetal.

2.5.1.2. Attempt to prepare azide 82.

Next the substitution of alcohol by azide using Mitsunobu reaction was undertaken. The same Bose conditions[13] previously employed in *Chapter II* were used. Unfortunately, when **76** was treated with DPPA in the presence of di-*tert*-butylazodicarboxylate (DBAD) and PPh_3 in toluene, an elimination reaction took place, giving rise to olefin **77** instead of the substitution product **82**. (Scheme III-10).

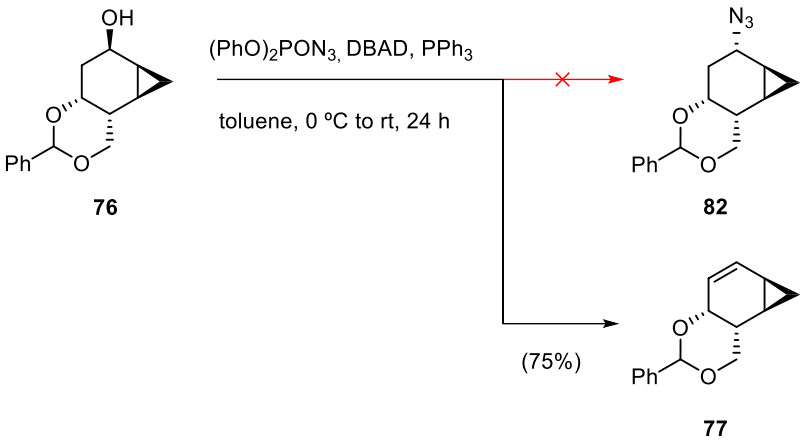

Scheme III-10. Attempt of synthesis of azide **82** by a Mitsunobu reaction.

These results could be justified due to the rigidity of the system, imparted by the fusion of two six-membered rings, where the elimination reaction seems to be more favoured than the substitution. Consequently, it was decided to select another protective group that would give less rigidity into the system.

2.5.2. Approach B. Tetraisopropyldisiloxane-1,3-diyl protecting group

An alternative cyclic protecting group is the tetraisopropyldisiloxane-1,3-diyl (TiPDS)[14] which was introduced by Markiewicz in 1979 for the simultaneous protection of two hydroxyls in ribonucleosides.[14b-c] Compared with benzylidene acetal, the tetraisopropyldisiloxane-1,3-diyl could offer less rigidity to the bicyclo[4.1.0]heptane system, since an eight-membered ring is formed.

2.5.2.1. Synthesis of tetraisopropyldisiloxane-1,3-diyl alcohol 87

Thus, a 20:1 mixture of **64** and its (2*S*)-diastereoisomer **68** was dissolved in DMF and treated with 1,3-dichloro-1,1,3,3-tetraisopropyldisiloxane and imidazole[14a] providing a chromatographic inseparable mixture of **85** and its (9b*S*)-diastereoisomer **86** in good yield. This 20:1 diastereomeric mixture was hydrogenated, in order to remove the benzyl ether, delivering a chromatography separable mixture of alcohols **87** and **88** in 87% and 3% yield, respectively (Scheme III-11).

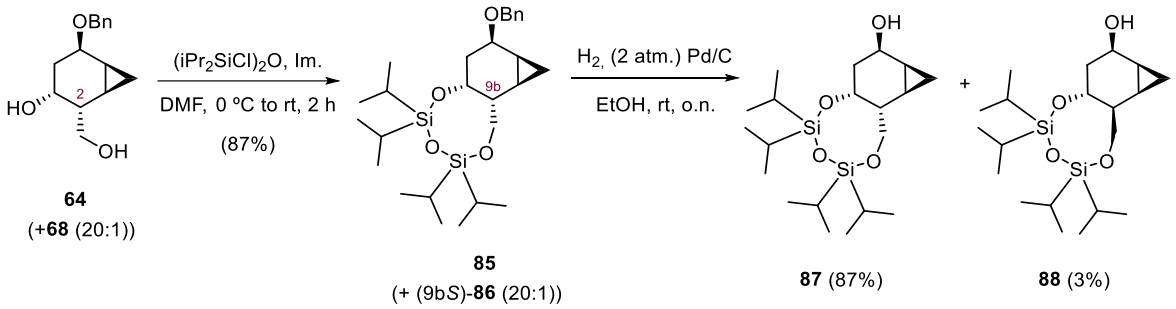

Scheme III-11. Synthesis of alcohol **87** protected with tetraisopropyldisiloxane and its diastereomer **88**.

The structure of alcohol **87** was confirmed by ^{1}H-NMR spectrum which displays a multiplet at 1.12 – 0.96 ppm corresponding to the aliphatic protons of the isopropyl groups, and also by the disappearance of the aromatics signals corresponding to the benzyl protecting group.

2.5.2.2. Attempt to prepare azide 90

With alcohol **87** in hands, attention was focused on the azide introduction employing the Mitsunobu reaction. The reaction was monitored by TLC which revealed that after 48 h, there was still a considerable amount of starting material. Although one additional equivalent of DPPA was added, no further reaction evolution was observed by TLC after 72 h. Purification of the crude by flash column chromatography afforded an inseparable mixture of elimination and substitution products identified by ^{1}H-NMR along with starting material (*c.a.* 50%.) (Scheme III-12).

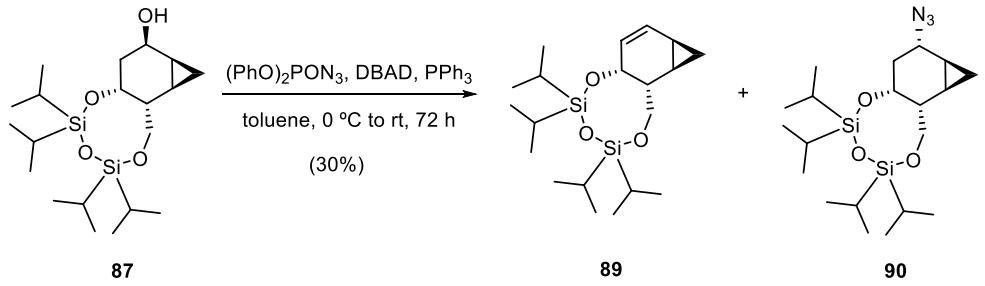

Scheme III-12. Mitsunobu reaction to introduce azide moiety.

From these results and the previously exposed in *section 2.5.2*, it can be concluded that the use of a cyclic protecting group either decreases the reactivity or favours the formation of elimination product. Therefore, it was decided to change the protecting group of the diol to a non-cyclic one to favour the substitution product.

2.5.3. Approach C. Benzoyl protecting group

2.5.3.1. Synthesis of the 1,3'-dibenzoyl alcohol 93

The diol **64** was foreseen to be protected as a dibenzoyl derivative. Thus, the 20:1 diastereomeric mixture of diols **64** and **68** was treated with an excess of benzoyl chloride using pyridine as a solvent at the reflux temperature. Purification by flash column chromatography, furnished a separable mixture of diastereoisomers **91** and **92** in 92% and 5% yield, respectively (Scheme III-13). Subsequent removal of the benzyl protecting group in **91** by hydrogenation under palladium catalyst, delivered alcohol **93** in quantitative yield.

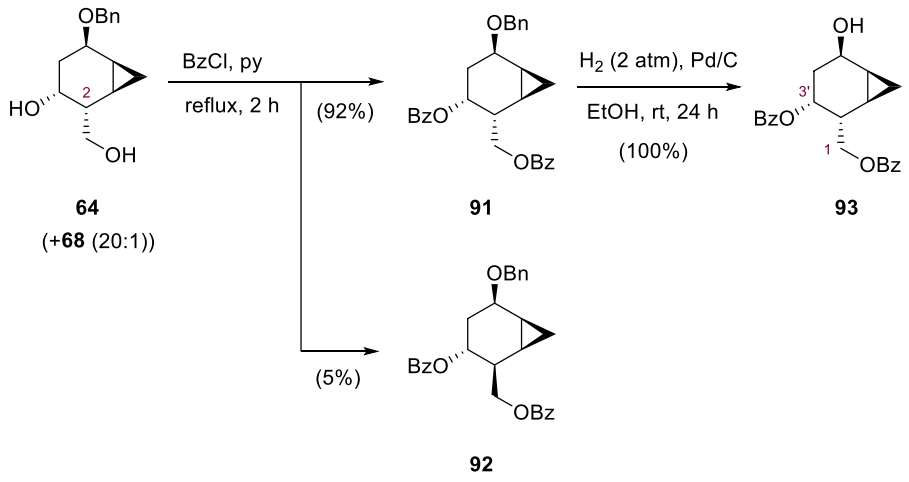

Scheme III-13. Synthesis of 1,3'-dibenzoyl derivative **93**.

The formation of alcohol **93** was confirmed by ^{1}H-NMR and ^{13}C-NMR spectra on the base of the new aromatic signals corresponding of the two benzoyl protecting groups, as well as by the disappearance of signals corresponding to the benzyl ether protecting group.

2.5.3.2. Synthesis of the azide product 94 and its corresponding ammonium chloride 96

Finally, alcohol **93** was converted to the desired azide **94** in 64% yield following the previously used Mitsunobu conditions[14] using DPPA in presence of DBAD and triphenylphosphine (Scheme III-14). As a by-product, the elimination product **95** was also formed in 9% yield. Therefore, increasing the conformational flexibility on the bicyclo[4.1.0]heptane favored the nucleophilic substitution. Moreover, it should be noted that in order to minimize the elimination reaction, it

is important to carry out the reaction at low temperatures (-10 °C) and let it evolve very slowly at rt overnight.

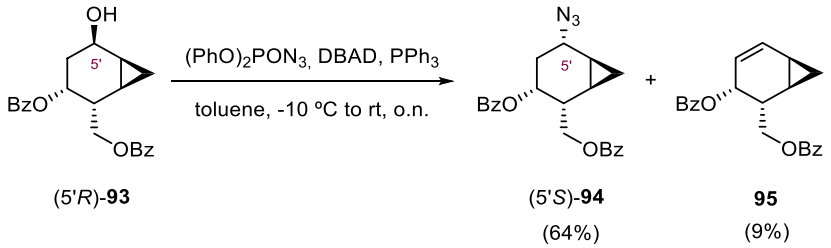

(5'*R*)-**93** (5'*S*)-**94** (64%) **95** (9%)

Scheme III-14. Formation of azide **94** with C-5' configuration inversion via Mitsunobu type reaction.

The substitution of alcohol group by azide was confirmed by ^{1}H- and ^{13}C-NMR spectra where the signals corresponding to H-5' and C-5' appear at lower chemical shifts (from δ 4.50 and 63.88 in **93** to 4.02 and 55.2 in **94**, respectively) (Figure III-10). Also, the IR spectrum shows strong absorption at 2109 cm^{-1} corresponding to the N=N=N stretching of azide.

In the ^{1}H-NMR spectrum of alcohol **93**, H-5' appears as a doublet of triplets (dt) showing a large coupling constant with the axial proton H-4'ax ($J_{4'ax,5'}$ = 11.2 Hz) and two smaller ones with the equatorial protons H-4'eq and H-6' ($J_{5',4'eq}$ = $J_{5',6'}$ = 6.1 Hz) which means that H-5' is in pseudo-axial position. (Figure III-10, a). However, in **94**, the H-5' proton signal appears as a triplet of doublets (td) with two coupling constants with H-4'ax and H-4'eq ($J_{5',4'ax}$ = $J_{5'4'eq}$ = 5.1 Hz) and a smaller one with H-6' ($J_{5',6'}$ = 1.5 Hz) consistent with a pseudo-equatorial position for H-5' (Figure III-10, b).

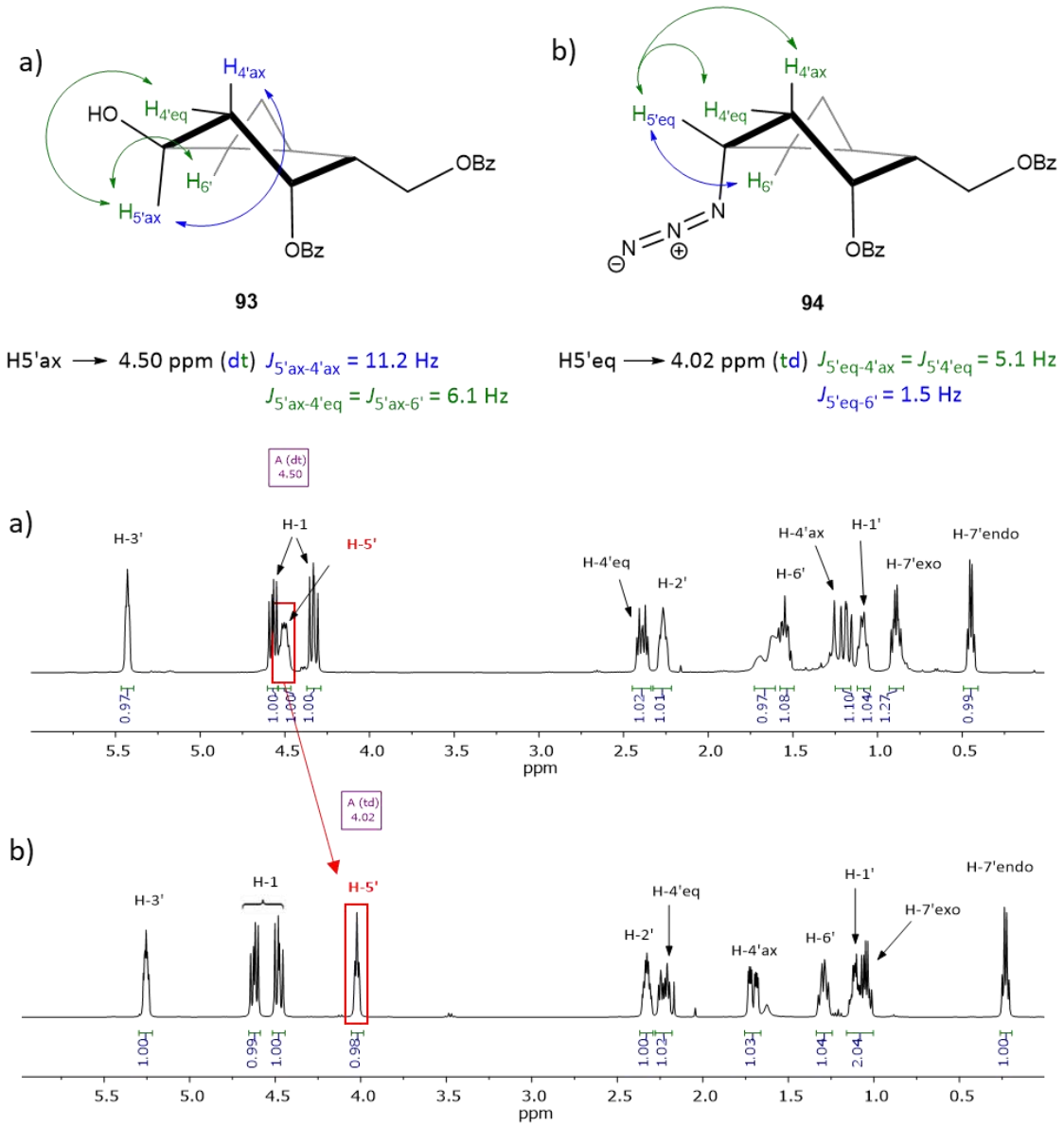

Figure III-10. a) Structure and ^{1}H-NMR (400 MHz, $CDCl_3$) spectrum of alcohol **93**; b) structure and ^{1}H-NMR (400 MHz, $CDCl_3$) spectrum of azide **94.**

This inversion of the configuration was further confirmed by a 2D-NOESY experiment (Figure III-11, a). The spectrum shows a strong cross peak signals between H-5' and H-7'endo and H-4'ax; and between H-5' and H-2' and H-3' protons. This was also consistent with the X-ray diffraction structure of **94** (Figure III-11, b). Accordingly, it was confirmed that the absolute configuration of **94** was (1'*R*,2'*R*,3'*R*,5'*S*,6'*S*).

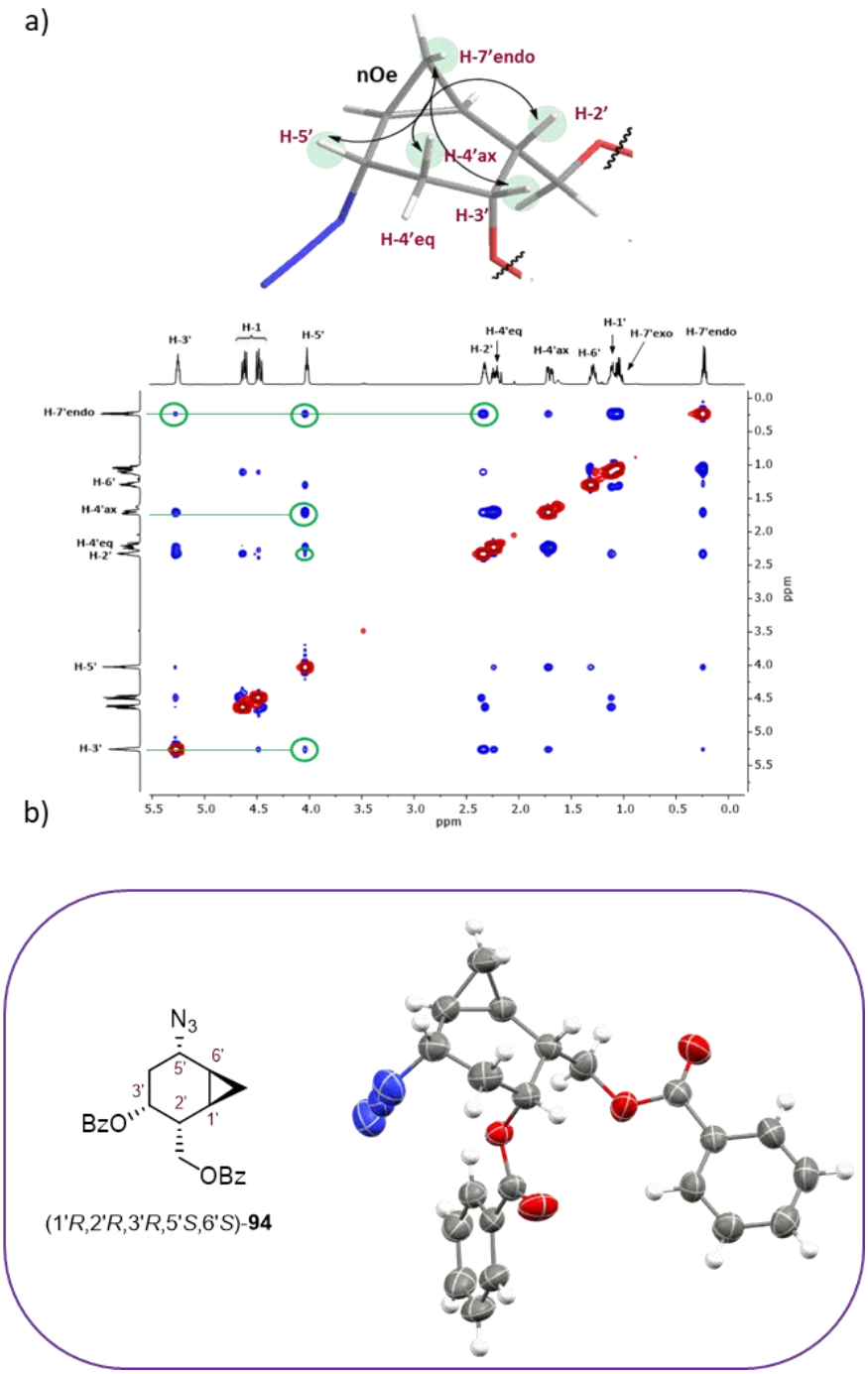

Figure III-11. a) Main n.O.e on **94** and the corresponding 2D-NOESY spectrum (400 MHz, $CDCl_3$); b) crystal structure of **94** (thermal ellipsoids at 50% probability level).

Finally, the key amine was achieved quantitatively from **94** by a catalytic hydrogenation under 2 atm of pressure in the presence of Pd/C (10%). This amine was then transformed into the corresponding ammonium chloride salt **96** by treatment with a solution of HCl 2 M in diethyl ether at 0 °C (Scheme III-15).

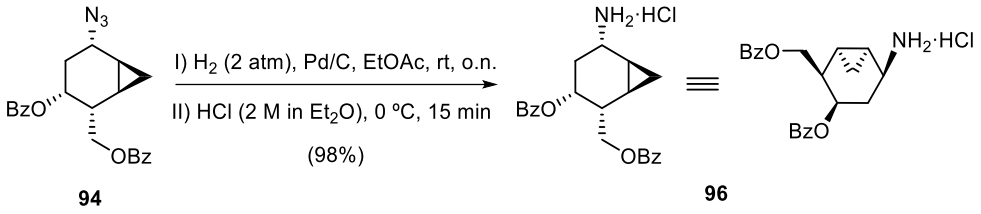

94 **96**

Scheme III-15. Reduction of azide **94** by hydrogenation and conversion to the ammonium salt.

2.6 Synthesis of pyrimidine nucleoside analogues

As it has been explained in *Chapter II*, the procedure described by Shaw and Warrener[15] for the stepwise construction of pyrimidine base consists in a two-step reaction: the addition of an amine to an isocyanate followed by an acidic cyclization of the formed acryloyl urea (Scheme III-16).

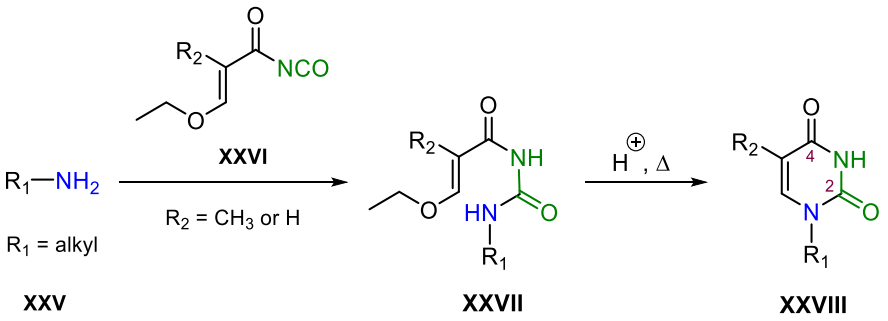

Scheme III-16. Methodology to construct pyrimidine bases stepwise.

2.6.1. Synthesis of thymine nucleoside analogue 104

First, isocyanate **XXVI** (R_2 = CH_3, 3-ethoxy-2-methylacryloyl isocyanate) was envisaged to be prepared from the chloride derivative (-COCl) following the same methodology as in *Chapter II*. However, the change in the substituent (from R_2 = -H to R_2 = -CH_3) which involved the preparation of the acyl chloride **99** using Tietze's procedure[16] met with failure. The treatment of **97** with oxalyl chloride, followed by a thermal decarbonylation and purification by vacuum distillation did not achieve the expected acyl chloride **99** but only decomposition products (Scheme III-17). Therefore, another synthetic methodology was needed to prepare **99**.

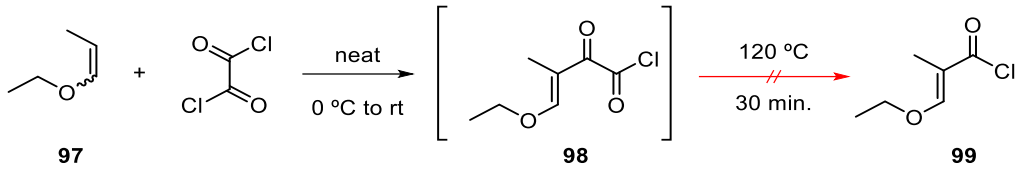

Scheme III-17. Preparation of 2-methyl acyl chloride **99** by Tietze's procedure.

The acyl chloride **99** could be prepared from its acid derivative, which has been reported to be synthesised by a number of methods.[15b,17] In our hands, the Hojo's methodology resulted to be the most efficient.[18] Thus, the reaction of ethyl 1-propenyl ether (2:1, cis/trans mixture) **97** with trichloroacetyl chloride (Cl_3COCl) in pyridine gave the trichloro intermediate **100**. Hydrolysis of **100** under controlled conditions using KOH, water, and tetrabutylammonium hydrogen sulphate in toluene at 90 °C afforded acid **101** as a solid in 64% overall yield for the 2 steps (Scheme III-18). Finally, the acid **101** was treated with oxalyl chloride using DMF as catalyst in benzene and purified by vacuum distillation providing acyl chloride **99** in 80% yield.[19]

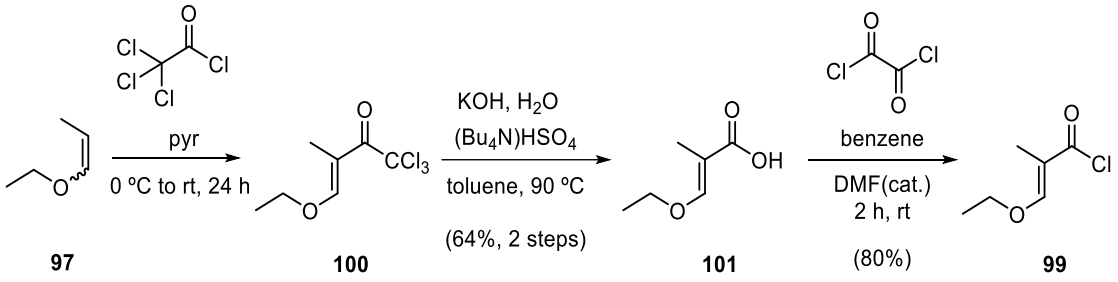

Scheme III-18. Preparation of acyl chloride **99** from ethyl 1-propenyl ether.

Next, the formation of the thymidine ring was performed following a procedure described by Jung and co-workers.[20] Thus, treatment of acyl chloride **99** with anhydrous silver cyanate (AgOCN) in dry toluene at the reflux temperature for 1.5 h led to the corresponding isocyanate **102** (Scheme III-19), which was used without further purification for the construction of the base moiety, due to the expected instability of this intermediate.

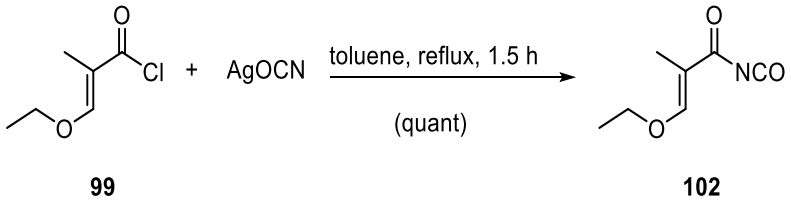

Scheme III-19. Synthesis of acyl isocyanate **102**.

The isocyanate in toluene was directly added to a solution of amine **96** and Et_3N in dry CH_2Cl_2 at -78 °C giving the urea intermediate **103** which then, was heated at the reflux temperature in acidic ethanol in order to produce the ring closure (Scheme III-20). Finally, the hydroxy groups were deprotected using a methylamine solution in ethanol to afford the desired thymine nucleoside analogue **104** in 79% overall yield from **96.**

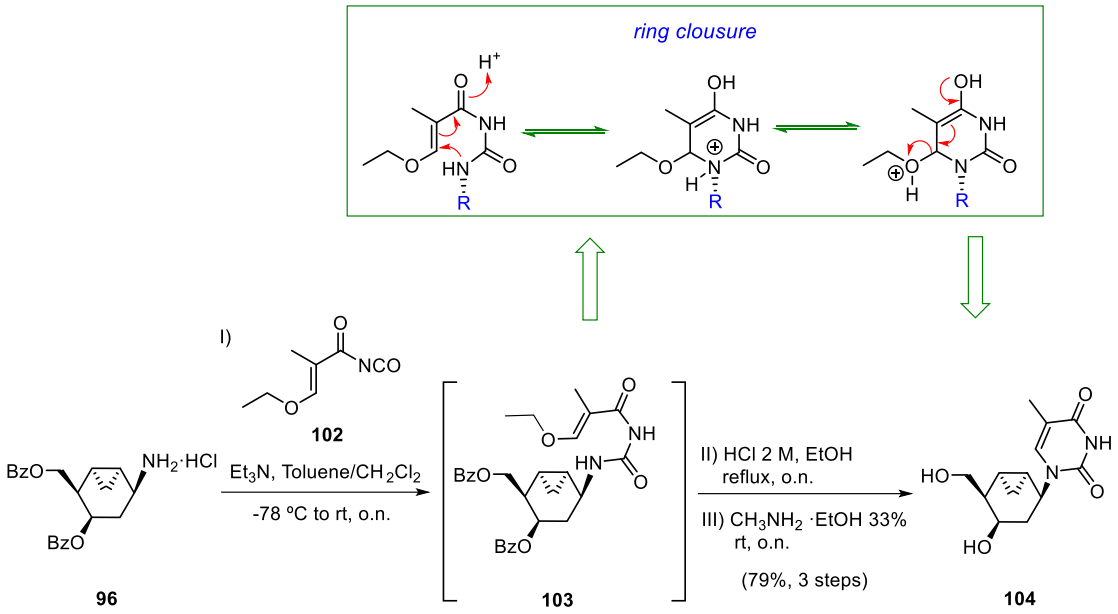

Scheme III-20. Synthesis of thymine analogue **104** from **96** using freshly prepared acyl isocyanate **102**.

The successfully construction of the thymine nucleobase on substrate **96** was established by the appearance of extra signals on the ^{1}H-NMR and ^{13}C-NMR spectra. Thus, the proton spectrum features four additional protons at 7.82 and 1.89 ppm as quartet and doublet ($J_{6,CH3}$= 1.1 Hz) corresponding to H-6 and methyl group, respectively (Figure III-12), while the carbon spectrum shows additional signals at 166.7-110.2 ppm corresponding to the thymine sp^2 carbons. The deprotection of alcohols groups was confirmed with the disappearance of the signals corresponding to two benzoyl groups observed in the ^{1}H- and ^{13}C-NMR, as well as, the upfield displacement of H-4' and H-1'' (from δ 5.43 and 4.60 in **96** to 3.89-3.80 in **104**, respectively). Also, the IR spectrum shows two strong absorptions at 1700 and 1660 cm^{-1} corresponding to the C=O groups of the nucleobase.

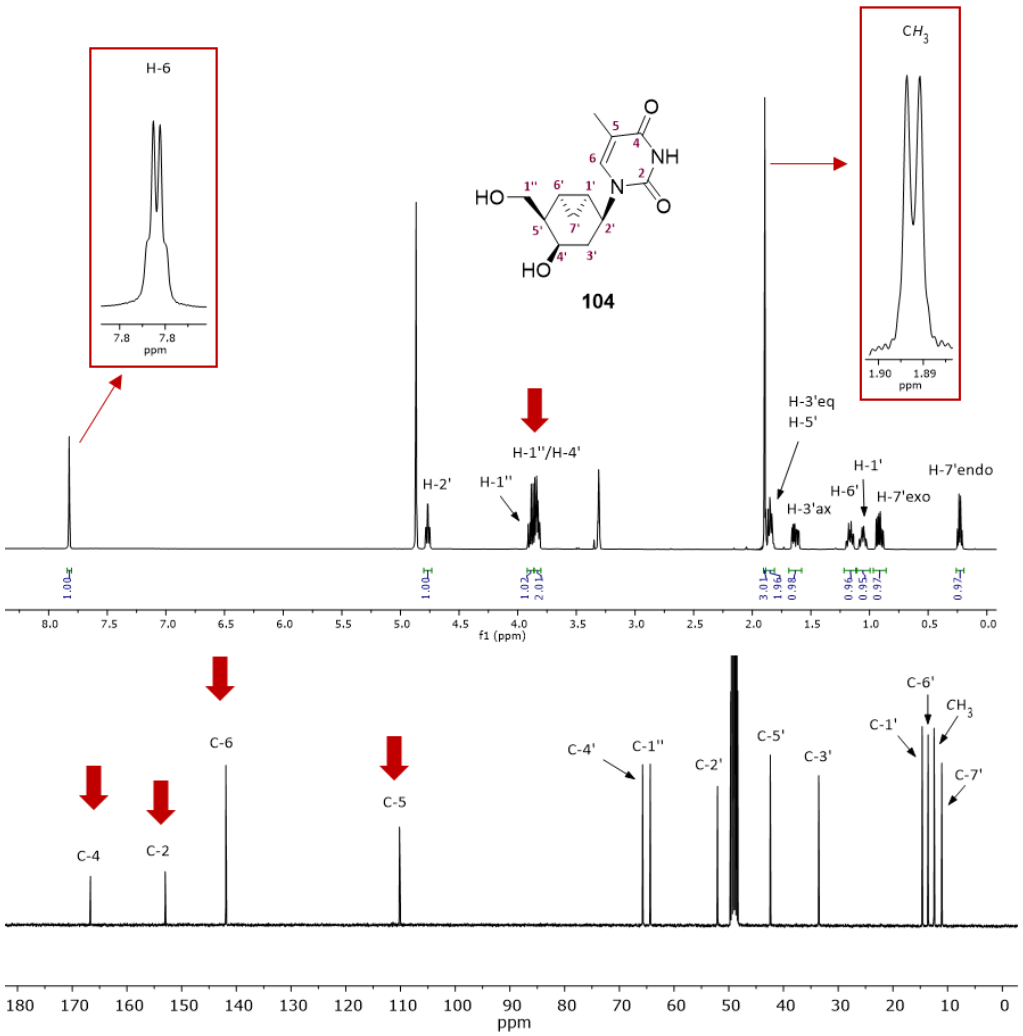

Figure III-12. ^{1}H-NMR (400 MHz, MeOH-d_4) and ^{13}C-NMR (101 MHz, MeOH-d_4) of analogue **104**.

In the ^{1}H-NMR spectrum (Figure III-13) H-2' resonates at δ 4.77 ppm and appears as a triplet of doublets (td) with a medium coupling constants ($J_{2',3'ax}$ = $J_{2',3'eq}$ = 6.3 Hz) and a smaller one ($J_{2',1'}$ = 1.5 Hz); while H-3'ax displays a doublet of doublet of doublets (ddd) at 1.63 ppm with a large germinal coupling constant, $J_{3ax',3'eq}$ = 14.2 Hz, other smaller coupling constant, $J_{3ax',2'}$ = 6.1 Hz and a smaller one $J_{3'ax,4'}$ = 2.9 Hz. These data suggested that the main conformation is $^{4}H_3$ where the thymine base and the hydroxyl group (-OH) are located in a pseudo-axial position, while the hydroxymethyl group (-CH_2OH) is in a pseudo-equatorial orientation.

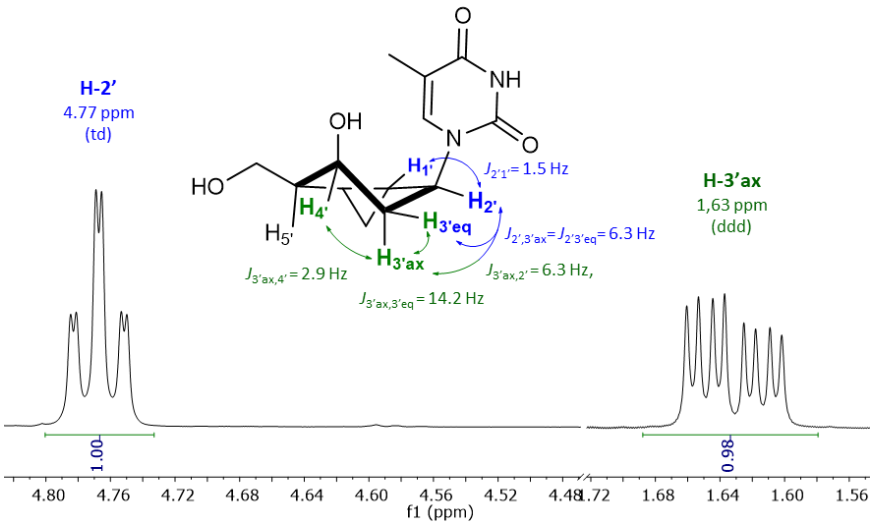

Figure III-13. Coupling constants of the H-2' and H-3'ax protons of **104** (400 MHz, MeOH-d_4).

That NMR analysis was consistent with an X-ray diffraction structure of **104** which was crystallized by vapor diffusion using a mixture of MeOH and Et_2O. The crystal structure obtained of **104** confirmed the relative stereochemistry of the molecule and that the compound is settled in a $^4H_3$ conformation (Figure III-14).

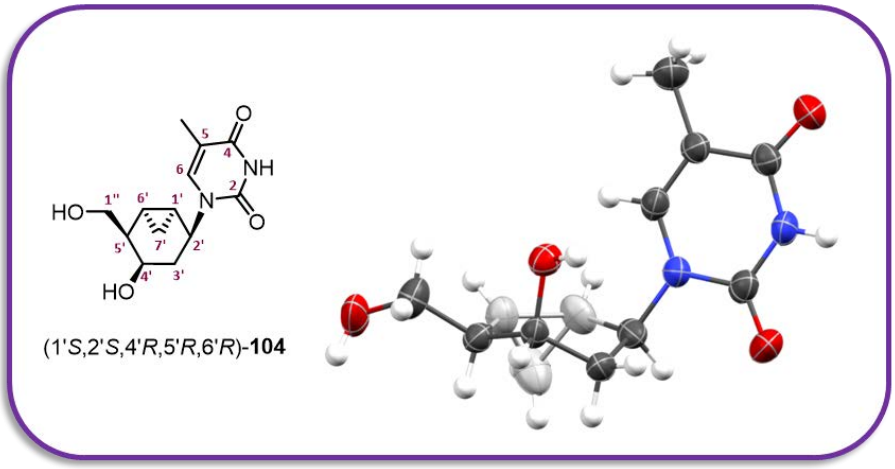

Figure III-14. Crystal structure (thermal ellipsoids at 50% probability level) of **104**.

2.7. Synthesis of purine nucleoside analogues.

In 1990, Harnden and co-workers described a new methodology to construct purine bases.[21] This methodology, that is one of the most used, consists of a nucleophilic aromatic substitution on the *N,N'*-(4,6-dichloropyrimidine-2,5-diyl)diformamide **106** by the amino group of the alkoxyamine **105** in presence of *N,N*-diisopropylethylamine (*i*-Pr_2NEt, DIPEA), followed by a reaction with diethoxymethyl acetate to allow the closure of the ring, giving the corresponding chloropurine derivative **108** (Scheme III-21). This procedure has been used for the synthesis of several nucleoside analogues.[22a-c]

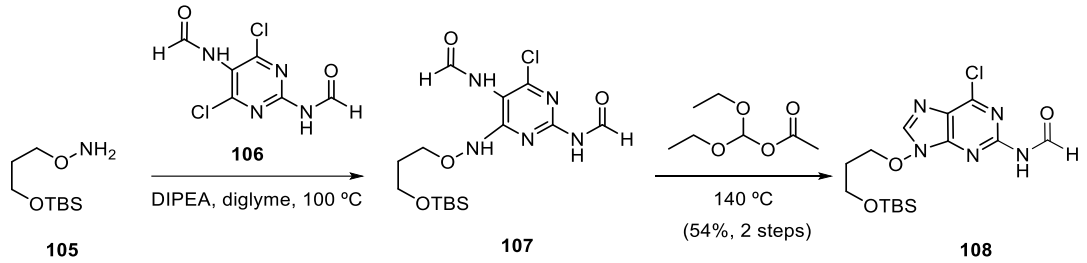

Scheme III-21. Construction of purine ring reported by Harnden and co-workers.[21]

Next, in 2010 Marquez and co-workers improved the effectiveness of the Harden's methodology for the stepwise construction of the purine ring by using microwave (MW) irradiation (Scheme III-22).[23] For example, the chloropurine derivative **112** was prepared in 81% yield by treatment of the ammonium chloride **109** with formamidopyrimidine **110** and DIPEA and a further cyclization using diethoxymethyl acetate, both under microwave irradiation.

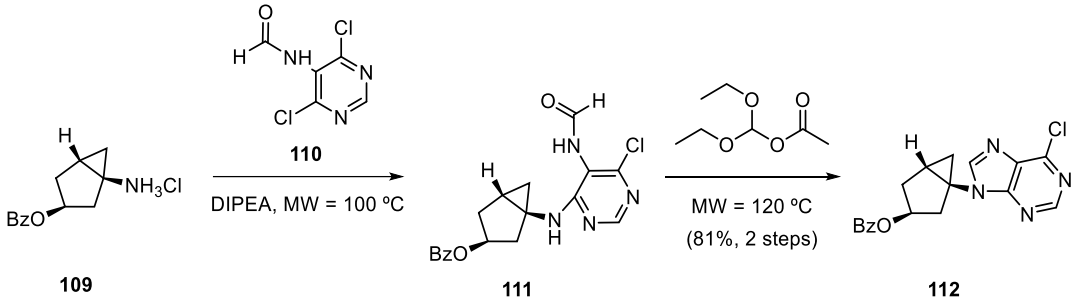

Scheme III-22. Construction of the purine ring using MW irradiation reported by Marquez *et al.*[23]

Taking this into account, the two-step construction of the purine ring in our compound was attempted under microwave irradiation.

2.7.1. Synthesis of purine nucleoside analogues assisted by MW.

2.7.1.1. Microwave heating in organic synthesis

Using microwave irradiation in synthesis to accelerate chemical transformations has attracted much attention in recent years.[24a-f] Microwaves are a type of electromagnetic radiation with wavelengths comprised between 1 mm and 1 m, located between infrared radiation (IR) and radio waves. Importantly, the energy of the microwave photon in this frequency region is too low to break chemical bonds, preventing microwaves to induce chemical reactions, in contrast to ultraviolet and visible radiations. Accordingly, the usefulness of microwaves in organic synthesis is related to the efficient heating of materials by microwave radiations.

MW dielectric heating depends on the ability of a specific material (e.g. solvent or reagent) to absorb microwave energy and convert it into heat. This ability is, in its turn, strongly related to the dielectric properties of each particular material, and it is determined by the so-called loss factor/loss tangent (tan δ). This loss factor is expressed as the quotient tan δ = ε''/ε', where ε'' is the dielectric loss, which quantifies the efficiency with which the absorbed energy is converted into heat, and ε' is the dielectric constant, representing the ability of molecules to store electrical potential energy under the influence of an electric field. The larger the dielectric loss tangent (tan δ), the more efficiently the solvent converts MW energy into heat. The tan δ values for common solvents are presented in Table III-4.[24f,25]

Table III-4. Boiling point and dielectric loss tangent for some common organic solvents (2.45 GHz, 20 °C).

Solvent	b.p. (°C)	tan δ	Solvent	b.p. (°C)	tan δ
Ethylene glycol	198	1.350	Chloroform	61	0.091
Ethanol	78	0.941	Acetonitrile	82	0.062
DMSO	189	0.825	Acetone	56	0.054
Methanol	65	0.659	THF	66	0.047
Acetic Acid	118	0.174	Dichloromethane	40	0.042
DMF	152	0.161	Toluene	111	0.040
Water	100	0.123	Hexane	68	0.020

Undoubtedly, one of the main advantages of microwave irradiation over conventional heating systems is the achievement of dramatically reduced reaction times. While the external heat sources usually used in organic synthesis depend on thermal conductivity of the various

materials that must be penetrated, microwave radiation passes through the walls of the reaction vessels and heats only the molecules (solvents, reagents, catalysts), producing an efficient internal heating. Thus, microwave irradiation raises the temperature of the whole volume simultaneously, producing a fast and homogeneous heating, whereas when using an oil bath, the reaction mixture in contact with the vessel wall is heated first (Figure III-15).[4c] Consequently, the heating profiles attained by microwave irradiation are very difficult to reproduce by standard thermal heating. Moreover, the monitoring mechanisms for temperature and pressure in modern microwave reactors allow for an excellent control of reaction parameters.

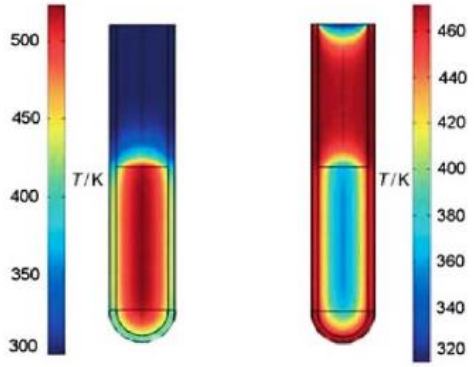

Figure III-15. The temperature profile after 60 sec as affected by microwave irradiation (left) compared to treatment in an oil bath (right). Microwave irradiation raises the temperature of the whole reaction volume simultaneously, whereas in the oil heated tube, the reaction mixture in contact with the vessel wall is heated first.[24c]

2.7.1.2. Synthesis of guanine nucleoside analogue, 116 under MW.

In order to form the guanine base, first, the dichloropyrimidine precursor **106** was synthesised following a procedure described by Harnden *et al.*[21] Accordingly, commercially available 2,5-diamino-4,6-dichloropyrimidine, **113**, was formylated by means of a mixture of formic acid and acetic anhydride, to afford compound **106** (Scheme III-23). The formylation was confirmed by ^{1}H-NMR spectrum showing a singlet and a doublet at 8.32 and 9.23 ppm ($J_{CHO,NH}$ = 9.4 Hz), respectively, corresponding to the formamide protons.

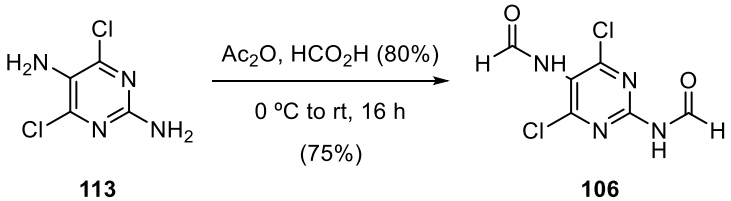

113 **106**

Scheme III-23. Preparation of **106** by formylation described by Harnden *et al.*

Next, the two-step construction of the guanine ring following the previous methodology described by Marquez[23] under MW irradiation was attempted. Thus, ammonium chloride **96** was treated with diformamidopyrimidine **106** and DIPEA in 1,4-dioxane at 100 °C by MW irradiation for 40 min and then, the corresponding intermediate **114**, was allowed to react in the presence of diethoxymethyl acetate at 140 °C for 120 min (Scheme III-24). In both steps the starting material was totally consumed but no defined spots were present on TLC. After purification by flash column chromatography, only decomposition products were observed by ^{1}H-NMR.

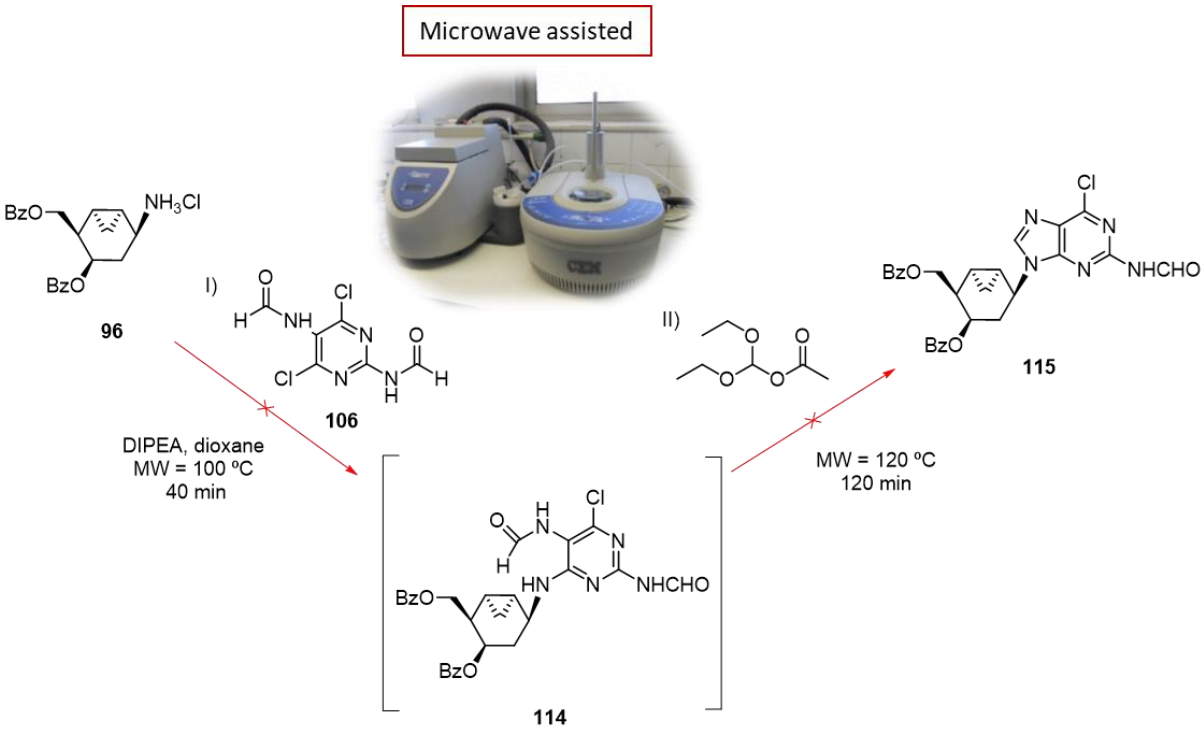

Scheme III-24. Attempt of guanine ring formation using MW irradiation.

All different attempts to construct the purine ring under MW irradiation by changing the temperature, reaction time or the irradiation power met with failure, leading to decomposition products.

2.7.2. Synthesis of purine nucleoside analogues using classical methodology

In view of these results, the formation of chloropurine ring was undertaken using the classical conditions previous described by Harnden and co-workers[21] with some modifications inspired by Marquez *et al.*[26] Thus, **96** was coupled with the diformyl derivative **106** in presence of DIPEA in dry dioxane at rt overnight, and then, heating at the reflux temperature for 30 min to render

intermediate **114** (Scheme III-25). Next, the ring closure of imidazole ring in **114** was performed by heating in the presence of diethoxymethyl acetate at 140 °C for 24 h to give, successfully, the 6-chloropurine **115** in 76% overall yield.

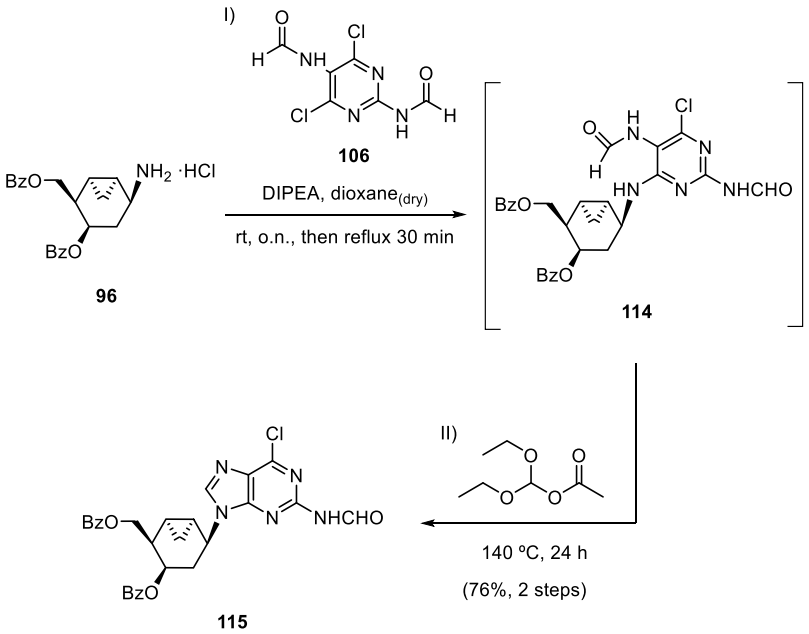

Scheme III-25. Formation of chloropurine ring using classical methodology.

The nucleobase formation was corroborated by the ^{1}H-NMR spectrum where a new singlet at 8.12 ppm corresponding to H-8'', as well as, two doublets (both with $J_{CHO,NH}$ = 10.3 Hz) at 8.94 and 9.55 ppm corresponding to –N*H*– and –*CH*O formamide appeared (Figure III-16).

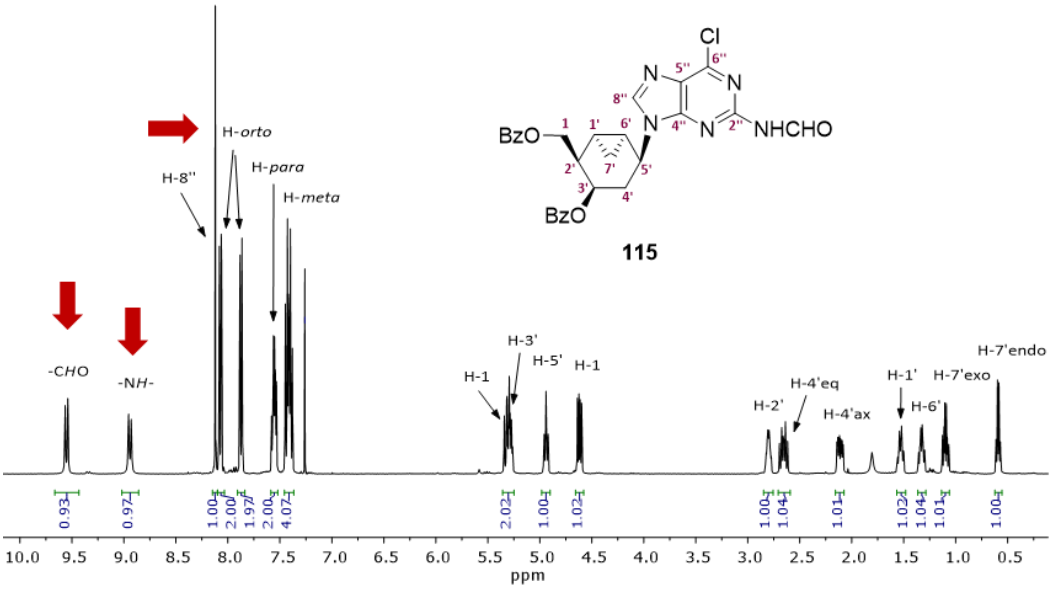

Figure III-16. ^{1}H-NMR (400 MHz, $CDCl_3$) of intermediate **115**.

In addition, to ensure the purine base formation, an HMBC experiment was registered. The spectrum revealed correlation between H-5' of the bicyclo[4.1.0]heptane fragment and the two carbons C-8'' and C-4'' of the purine ring, thus confirming the 6-chloropurine ring formation (Figure III-17).

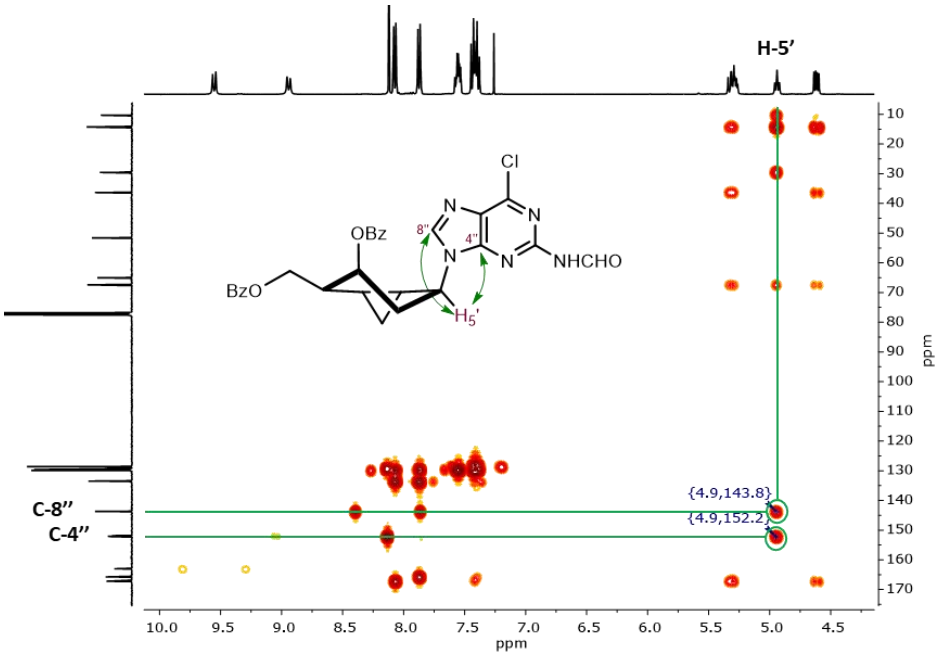

Figure III-17. HMBC spectrum (400 MHz, $CDCl_3$) of intermediate **115**.

Hydrolysis of **115** with 80% formic acid at the reflux temperature followed by exposure to ammonia solution (7 M in methanol) at rt for 3 days provided the guanine ring formation and also removal of the benzoyl protecting groups, to give the carbocycle nucleoside analogue **116** in 2 steps and 57% overall yield (Scheme III-26). The low yield was attributed to the difficult isolation of the desired product from the reaction mixture.

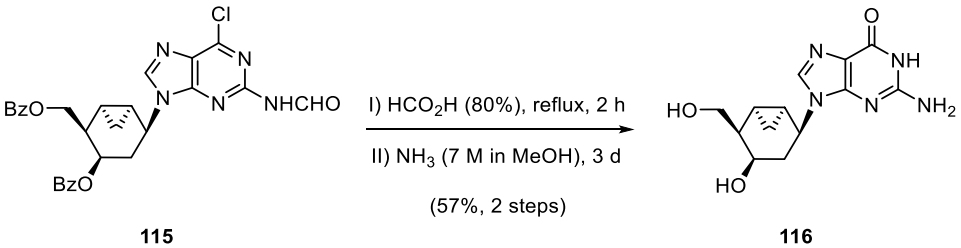

115 **116**

Scheme III-26. Hydrolysis of **115** to provide nucleoside analogue **116**.

The formation of the guanine nucleoside **116** was confirmed by the disappearance of the peaks corresponding to the benzoyl and –CHO groups in the ^{1}H- and ^{13}C-NMR spectra as well as by the

displacement of C-6 signal in the ^{13}C-NMR spectrum to higher chemical shifts (from 152.1 ppm in **115** to 158.0 ppm in **116**).

2.8. Epimerization of 104, synthesis of nucleoside analogues 117 and 123

As it has been explained in the introduction, cyclohexenyl G displays high antiviral activity against herpes virus comparable with other analogues of clinical use.[2] For this reason, it was decided to epimerize the C-4' centre of the thymine analogue **104** in order to obtain a compound with similar relative stereochemistry than D-cyclohexenyl G (Scheme III-27).

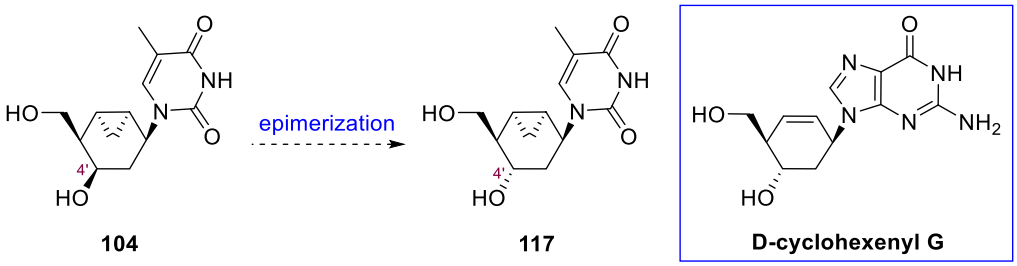

Scheme III-27. General scheme of epimerization of C-4'and the D-cyclohexenyl G structure.

In the literature, there are many examples to epimerize cyclic secondary alcohols.[27] One of these methodologies consists of the use of the Mitsunobu reaction where the alcohol group is replaced by an ester group with inversion of the configuration (S_N2) followed by a saponification step. Marquez and co-corkers used this strategy to epimerize the C-3' centre in several bicyclo[3.1.0]hexane systems,[28] employing standard Mitsunobu conditions with benzoic acid as nucleophile, on carbathymidine (3'*S*)-**118** (Scheme III-28). The reaction proceeded with inversion of configuration at C-3' to give the corresponding dibenzoate ester **119** which was hydrolysed to the corresponding epimeric diol (3'*R*)-**120** in 72% overall yield.

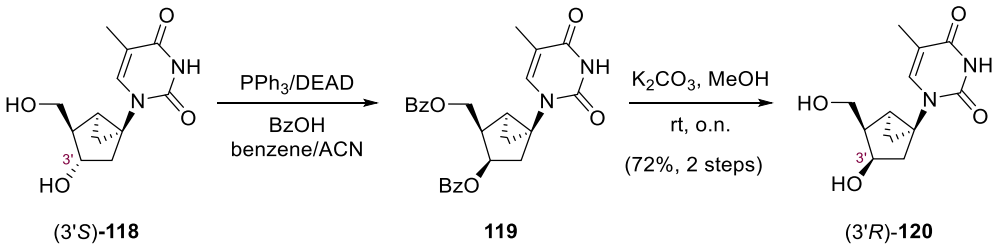

Scheme III-28. Epimerization of C-3' via Mitsunobu reaction and its posterior saponification.

2.8.1 Epimerization of C-4'of Thymidine and guanine nucleoside analogues

Taking into account the results described by Marquez and co-workers, the epimerization at the C-4'centre of thymine **104** was attempted using the same reaction conditions. Thus, nucleoside analogue **104** was treated with PPh_3, diethyl azodicarboxylate (DEAD) and benzoic acid from 0 °C to rt, giving a 2:1 chromatographically inseparable mixture of dibenzoate substitution product **121** and the elimination product **122** (Scheme III-29), according to the ^{1}H-NMR spectrum. At this point, alcohol deprotection using ammonium solution in methanol gave a mixture of deprotected compounds that was separated by column chromatography to deliver **117** and **123** in 37% and 18% overall yield, respectively.

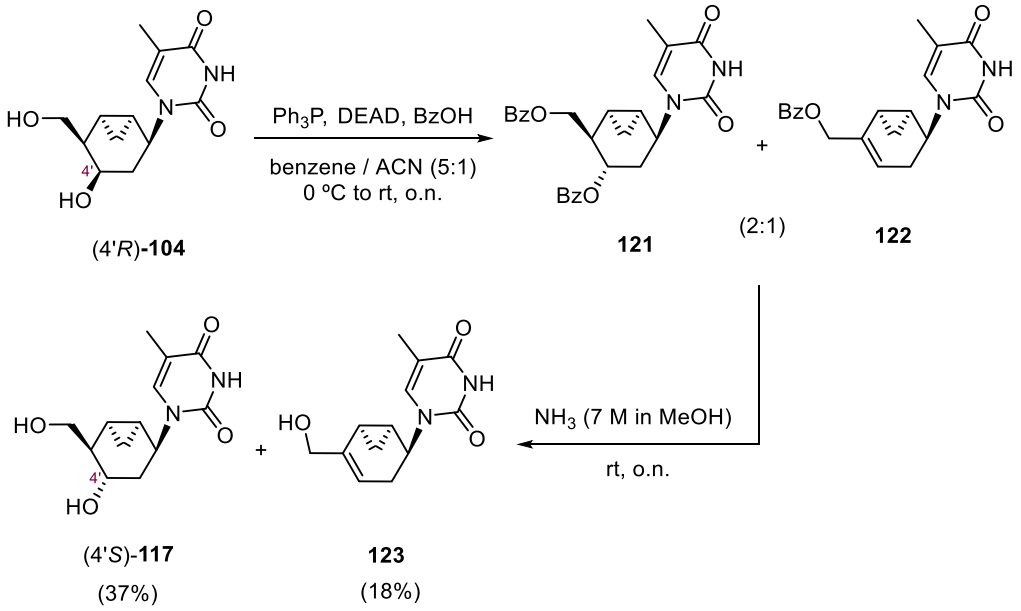

Scheme III-29. Epimerization at C-4'centre of thymine **104** by Mitsunobu reaction.

The formation of the substitution product **117** was confirmed by ^{1}H-NMR and ^{13}C-NMR observing similar signals than the **104** analogue. The spectroscopic differences between the two thymine C4'-epimers, **104** and **117**, can be observed in the ^{1}H-NMR spectrum (Figure III-18), especially in the H-4' proton that appears overlapped with the protons H-1'' as a multiplet signal at 3.86-3.80 ppm in the **104** epimer (in red) while for the **117** derivative (in black) appears as doublet of doublet of doublets (ddd) at 3.61 ppm. In addition, the proton H-2' is also displaced from 4.77 ppm in **104** to 5.00 ppm in **117** with the same multiplicity (td).

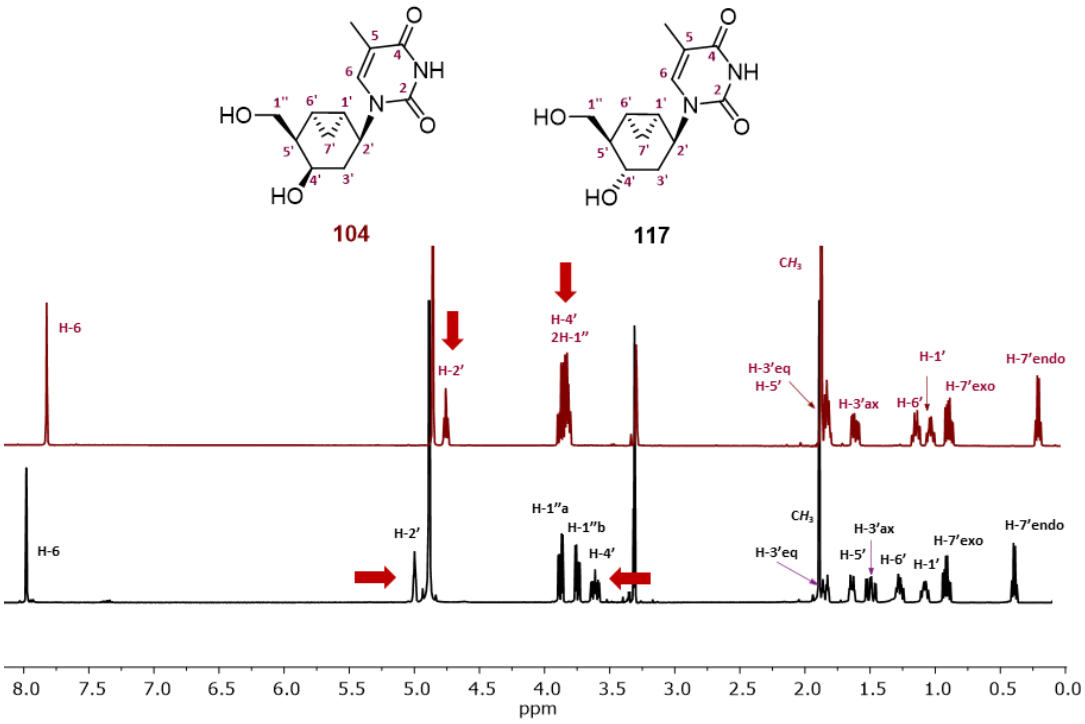

Figure III-18. Comparison of ^{1}H-NMR (400 MHz, MeOH-d_4) spectra of **104** (red) and **117** (black).

The inversion of the configuration on C-4' of **117** was determined by ^{1}H-NMR and 2D-NOESY experiment. Thus, in the ^{1}H-NMR, the attention was fixed on the values of the coupling constants of the protons H-4' and H-2' (Figure III-19). On one hand, the proton H-4 'appears at 3.61 ppm with a ddd multiplicity displaying two large coupling constants (12.2 Hz and 9.1 Hz) with H-3'ax and H-5', respectively; and a small one (3.8 Hz) with H-3'eq, which determines a pseudo-equatorial position of the hydroxymethyl (C5'-CH_2OH) and hydroxyl (C4'-OH) groups. On the other hand, the proton H-2', which appears at 5.00 ppm as a triplet of doublet (td), has a small coupling constant (3.8 Hz) with the two H-3' protons and another small one with H-1' (1.2 Hz), establishing a pseudo-axial disposition for the thymine base ($^{4}H_3$ conformation).

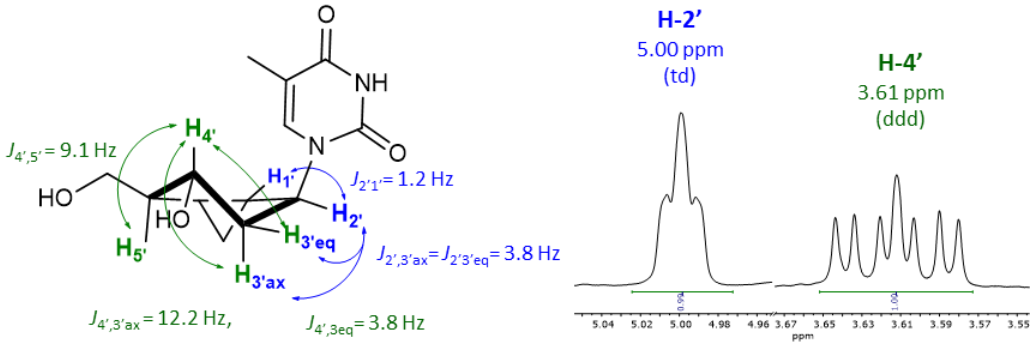

Figure III-19. Coupling constants of the protons H-4 'and H-2' of **117**.

Additionally, the 2D-NOESY spectrum (Figure III-20) shows a strong cross peak signal between the H-4' proton of the bicyclo system and H-6 of the thymine base. This 2D-NOESY was consistent with the previous coupling constant values. Thus, the only possible stereochemistry is a 2,4-*trans* relation between the thymine and the C4'-OH group, confirming the C-4' inversion. Accordingly, the absolute configuration of **117** is (1'*S*,2'*S*,4'*S*,5'*R*,6'*R*).

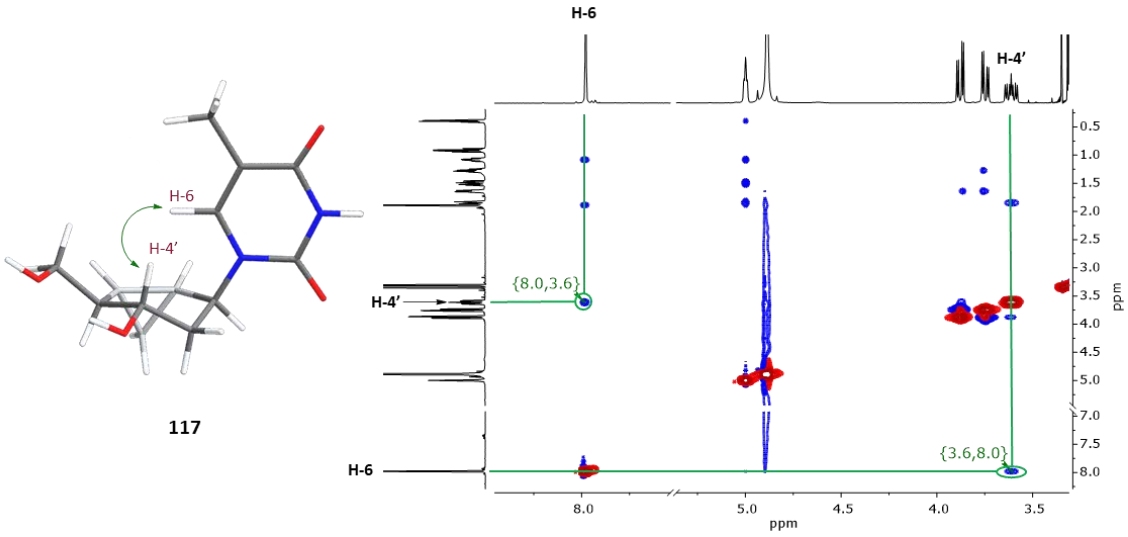

Figure III-20. 2D-NOESY (400 MHz, MeOH-d_4) spectrum of **117**.

The formation of olefin **123** can be explained considering the rigidity of the bicyclo[4.1.0]heptane system, that allows an axial location of the alkoxyphosphonium group (-$OPPh_3^+$) and axial proton H-5' in an antiperiplanar disposition (Figure III-21) in the corresponding intermediate of the reaction, facilitating the 1,2-elimination *via* E2 and obtaining the expected Zaitsev's product **123**.

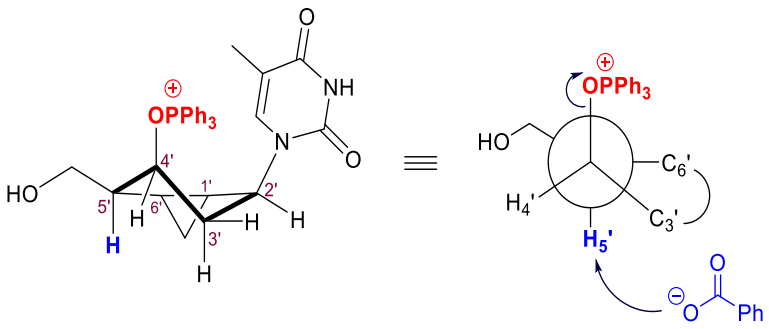

Figure III-21. Antiperiplanar disposition of alkoxyphosphonium group and H-5' proton**.**

The formation of the double bond in **123** product was confirmed by ^{1}H- and ^{13}C-NMR spectroscopy, where the olefinic proton H-4' appeared at 5.37 ppm and at 114.2 ppm, respectively; as well as the disappearance of the proton H-5' and the emergence of C-5' to higher chemical shift at 143.0 ppm.

2.8.2 Attempt of C-4' epimerization of 116.

Taking into account the success in the thymine analogue epimerization, attention was next focused on the epimerization of the C'-4 of **116** using the same conditions in order to obtain similar structure than D-cyclohexenyl G.

Thus, nucleoside analogue **116** was treated with PPh_3, diethyl azodicarboxylate (DEAD) and benzoic acid from 0 °C to rt in 5:1 benzene/ACN mixture (Scheme III-30). However, after 72 h, the analysis by TLC of the reaction mixture showed only presence of starting material. This could be explained due to the low solubility of the guanine product **116** in the 5:1 mixture of benzene/ACN.

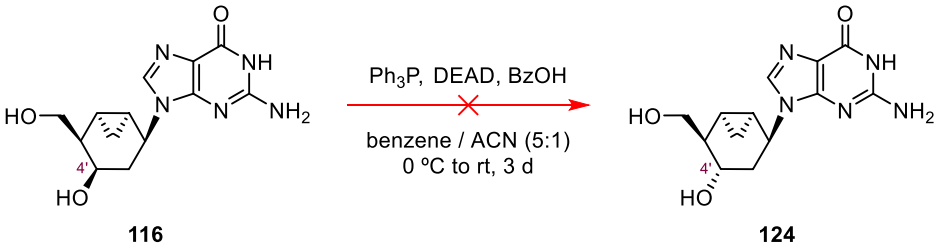

116 **124**

Scheme III-30. Attempt of C-4' epimerization via Mitsunobu of **116**.

Other conditions should be tested in order to obtain **116**, such as, changing the solvent mixture to more polar ones or protecting both the amine of the guanine moiety and the hydroxymethyl group to improve solubility. Unfortunately, due to a lack of product quantity and time, it was not possible to test these reaction conditions to carry out the epimerization process.

3. EVALUATION OF CYTOTOXICITY AND THE ANTIVIRAL ACTIVITY

The antiviral activity of the different analogues synthesised in this chapter have been evaluated against several viruses at the group headed by Prof. Christophe Pannecouque at the *Rega Institute for Medical Research, Katholieke Universiteit Leuven*. Nucleosides analogues **104**, **116**, **117** and **123**, as well as, the compounds **84** and **94** (Figure III-22), have been tested for the cytotoxicity and antiviral activity against different viruses, such as HSV-1 (KOS), HSV-2 (G) in human erythroleukemia (HEL) cell cultures, among others (Tables III-5-9).

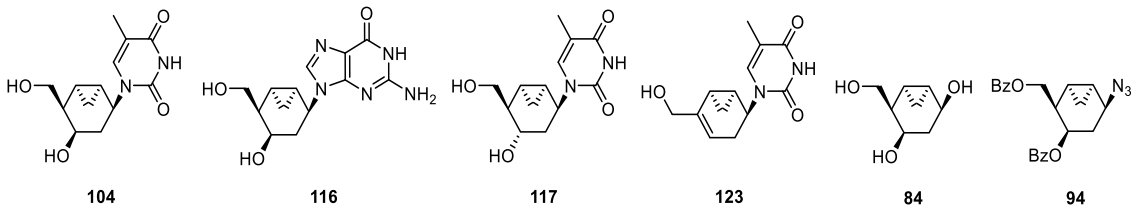

Figure III-22. Synthesised prodrug candidates evaluated against different virus.

Table III-5. Cytotoxicity and antiviral activity in HEL (Human Erythroleukemia) cell cultures.

Compound	Conc. Unit	Cytotoxicity CC_{50}[a]	Antiviral EC_{50}[b]				
			Herpes simplex virus-1 (KOS)	Herpes simplex virus-2 (G)	Vaccinia virus	Adeno virus-2	Human Coronavirus (229E)
104	µg/mL	>50	>50	>50	>50	>50	>50
116	µg/mL	>50	>50	>50	>50	>50	>50
117	µg/mL	>50	>50	>50	>50	>50	>50
123	µg/mL	>50	>50	>50	>50	>50	>50
94	µg/mL	>50	>50	>50	>50	>50	>50
84	µg/mL	>50	>50	>50	>50	>50	>50
Brivudin	µM	>250	0.2	22.1	12.6	-	-
Cidofovir	µM	>250	39.3	7.5	8.7	9.9	-
Acyclovir	µM	>250	1.9	0.5	>250	-	-
Ganciclovir	µM	>100	0.4	0.09	>100	-	-
Zalcitabine	µM	-	-	-	-	12.0	-
Alovudine	µM	-	-	-	-	0.4	-
UDA	µg/mL	-	-	-	-	-	1.2

[a] 50% Cytotoxic concentration, as determined by measuring the cell viability with the colorimetric formazan-based MTS assay.
[b] 50% Effective concentration, or concentration producing 50% inhibition of virus-induced cytopathic effect, as determined by measuring the cell viability with the colorimetric formazan-based MTS assay.

Table III-6. Cytotoxicity and antiviral activity in HEp-2 (Human Epidermoid carcicoma) cell cultures.

Compound	Conc. Unit	Cytotoxixity CC_{50}[a]	Antiviral EC_{50}[b]		
			Vesicular stomatitis virus	Coxsackie virus B4	Respiratory syncytial vius
104	µg/mL	>50	>50	>50	>50
116	µg/mL	>50	>50	>50	>50
117	µg/mL	>50	>50	>50	>50
123	µg/mL	>50	>50	>50	>50
94	µg/mL	>50	>50	>50	>50
84	µg/mL	>50	>50	>50	>50
DS-10,000	µg/mL	>100	0.08	2.5	0.01
Ribavirin	µM	>250	149	117	6.7

[a] 50% Cytotoxic concentration, as determined by measuring the cell viability with the colorimetric formazan-based MTS assay.
[b] 50% Effective concentration, or concentration producing 50% inhibition of virus-induced cytopathic effect, as determined by measuring the cell viability with the colorimetric formazan-based MTS assay.

Table III-7. Cytotoxicity and antiviral activity in Vero cell (kidney epithelial cells from African green monkey) cultures.

Compound	Conc. Unit	Cytotoxixity CC_{50}[a]	Antiviral EC_{50}[b]					
			Reo-virus-1	Sindbis virus	Coxsackie virus B4	Punta Toro virus	Yellow Fever virus	Zika virus
104	µg/mL	>50	>50	>50	>50	>50	>50	>50
116	µg/mL	>50	>50	>50	>50	>50	>50	>50
117	µg/mL	>50	>50	>50	>50	>50	>50	>50
123	µg/mL	>50	>50	>50	>50	>50	>50	>50
94	µg/mL	>50	>50	>50	>50	>50	>50	>50
84	µg/mL	>50	>50	>50	>50	>50	>50	>50
Ds-10,000	µg/mL	>100	>100	14.9	3.8	1.3	6.9	3.4
Mycophenolic acid	µM	>100	7.1	3.6	>100	>100	2.6	0.2

[a] 50% Cytotoxic concentration, as determined by measuring the cell viability with the colorimetric formazan-based MTS assay.
[b] 50% Effective concentration, or concentration producing 50% inhibition of virus-induced cytopathic effect, as determined by measuring the cell viability with the colorimetric formazan-based MTS assay.

Table III-8. Cytotoxicity and antiviral activity in MDCK (Madin-Darby Canine Kidney) cell cultures.

Compound	Conc. Unit	Cytotoxixity CC_{50}[a]	Antiviral EC_{50}[b]		
			Influenza A/H1N1 A/Ned/378/05	Influenza A/H3N2 A/HK/7/87	Influenza B B/Ned/537/05
104	µg/mL	>50	>50	>50	>50
116	µg/mL	>50	>50	>50	>50
117	µg/mL	>50	>50	>50	>50
123	µg/mL	18.6	>50	>50	>50
94	µg/mL	>50	>50	>50	>50
84	µg/mL	>50	>50	>50	>50
Zanamivir	µM	>100	0.9	4.9	1.4
Ribavirin	µM	>100	7.4	6.4	9.3
Rimantadine	µM	>200	88.8	0.06	>200

[a] 50% Cytotoxic concentration, as determined by measuring the cell viability with the colorimetric formazan-based MTS assay.
[b] 50% Effective concentration, or concentration producing 50% inhibition of virus-induced cytopathic effect, as determined by measuring the cell viability with the colorimetric formazan-based MTS assay.

Table III-9. Cytotoxicity and antiviral activity in MT-4 cell cultures (human lymphocytic cell line).

Compound	Conc. Unit	Cytotoxixity CC_{50}[a]	Antiviral EC_{50}[b]	
			Human immunodeficiency virus (III_B)	Human immunodeficiency virus (ROD)
104	µg/mL	99.07	>99.07	>99.07
116	µg/mL	>125	>125	>125
117	µg/mL	>125	>125	>125
123	µg/mL	109.2	>109.2	>109.2
94	µg/mL	70.4	>70.4	>70.4
84	µg/mL	>125	>125	>125
Neviparine	µg/mL	>4	0.075	>4
Zidovudine	µg/mL	>2	0.002	0.002
Lamivudine	µg/mL	>20	0.58	2.27
Didanosine	µg/mL	>50	17.95	19.40

[a] 50% Cytotoxic concentration, as determined by measuring the cell viability with the colorimetric formazan-based MTS assay.
[b] 50% Effective concentration, or concentration producing 50% inhibition of virus-induced cytopathic effect, as determined by measuring the cell viability with the colorimetric formazan-based MTS assay.

Overall, all compounds but **123** (in MDK cell cultures, Table III-8) and **104** (in MT-4 cell cultures, Table III-9) have not shown cytotoxicity. The fact that **123** and **104** display those effects suggest that this new series of compounds are able to pass through the cellular membranes.

Unfortunately, this new family of compounds does not fulfil its major objective since none of them exhibit significant antiviral activity at subtoxic concentrations (~50 µg/mL).

Plausible causes for the low antiviral activity include the lack of sufficient affinity or substrate activity for virus-encoded or cellular nucleoside kinases as the activating enzymes, lack of substrate activity for one of the cellular nucleotide kinases to further convert the compounds to their 5'-triphosphate metabolites, and/or lack of sufficient substrate activity of the 5'-triphosphate metabolites against the virus-encoded DNA polymerases. In any way, further studies are required to reveal the molecular basis of the antiviral inactivity of the test compounds.

4. CHAPTER III OUTLINE

A synthetic strategy for the preparation of 4'-hydroxymethyl-3'-hydroxybicyclo[4.1.0]heptanyl nucleoside analogues starting from the ketone **36** has been developed (Scheme III-31). Thymine and guanine nucleosides **104** and **116** have been obtained following a synthetic sequence of 11 and 12 steps and 36% and 20% yield from **36**, respectively.

The thymine epimer **117** and the thymine alkene **123** have been synthesised in 13 steps and 13% and 6% overall yield, respectively.

Finally, the nucleoside compounds **104**, **116**, **117** and **123,** as well as the molecules **84** and **94** have been evaluated against several viruses. Unfortunately, none of them showed significant antiviral activity.

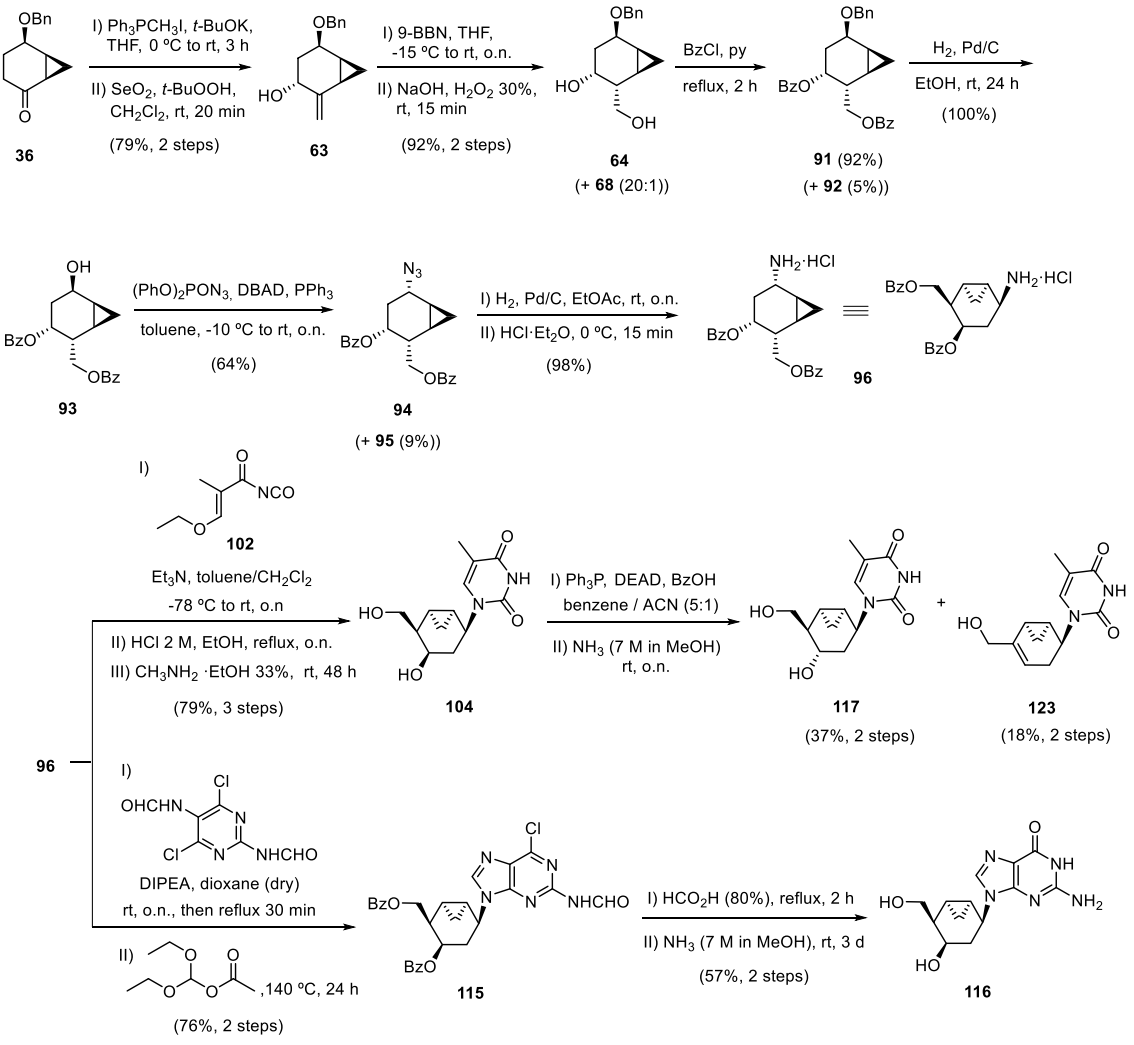

Scheme III-31. Chapter III summary.

5. REFERENCES

[1] Herdewijn, P; De Clercq, E. *Bioorg. Med. Chem. Lett.* **2001**, *11*, 1591-1597.

[2] Wang, J.; Froeyen, M.; Hendrix, C.; Andrei, G.; Snoeck, R.; De Clercq, E.; Herdewijn, P. *J. Med. Chem.* **2000**, *43*, 736–745.

[3] Wang, J.; Froeyen, M.; Herdewijn, P. *Adv. Antivir. Drug Des.* **2004**, *4*, 119–145.

[4] (a) Horváth, A.; Ruttens, B.; Herdewijn, P. *Tetrahedron Lett.* **2007**, *48*, 3621–3623; (b) Vijgen, S.; Nauwelaerts, K.; Wang, J.; Van Aerschot, A.; Lagoja, I.; Herdewijn, P. *J. Org. Chem.* **2005**, *70*, 4591–4597; (c) Wang, J.; Viña, D.; Busson, R.; Herdewijn, P. *J. Org. Chem.* **2003**, *68*, 4499–4505; (d) Olivo, H. F.; Yu, J. *J. Chem. Soc. Perkin Trans. 1* **1998**, *3*, 391–392; (e) Rosenquist, A.; Kvarnström, I.; Classon, B.; Samuelsson, B. *J. Org. Chem.* **1996**, *61*, 6282–6288; (f) Konkel, M. J.; Vince, R. *Tetrahedron* **1996**, *52*, 799–808; (g) Katagiri, N.; Ito, Y.; Shiraishi, T.; Maruyama, T.; Sato, Y.; Kaneko, C. *Nucleos. Nucleot.* **1996**, *15*, 631–647; (h) Perez-Perez, M.-J.; Rozenski, J.; Busson, R.; Herdewijn, P. *J. Org. Chem.* **1995**, *60*, 1531–1537; (i) Arango, J. H.; Geer, A.; Rodríguez, J.; Young, P. E.; Scheiner, P. *Nucleos Nucleot* **1993**, *12*, 773–784; (j) Ramesh, K.; Wolfe, M. S.; Lee, Y.; Vander Velde, D.; Borchardt, R. T. *J. Org. Chem.* **1992**, *57*, 5861–5868.

[5] Wang, J.; Herdewijn, P. *J. Org. Chem.* **1999**, *64*, 7820–7827.

[6] Herdewijn, P. *Antiviral Res.* **2006**, 71, 317-321.

[7] Beatriz-Dominguez, B. Doctoral Thesis, Universitat Autònoma de Barcelona, 2015.

[8] Ferrer, E. Doctoral Thesis, Universitat Autònoma de Barcelona, 2010.

[9] Umbreit, M. A.; Sharpless, K. B. *J. Am. Chem. Soc*. **1977**, *99*, 5526-5529.

[10] Barrero, A. F.; Oltra, J.E.; Cuerva, J.M.; Rosales, A. *J. Org. Chem*. **2002**, *67*, 2566-2571.

[11] Ra, C. S., Park, G. *Tetrahedron Lett.* **2003** *44*, 1099-1102.

[12] (a) Tashenov, Y., Daniels, M., Robeyns, K., Van Meervelt, L., Dehaen, W., Suleimen, Y., & Szakonyi, Z. *Molecules* **2018**, *23*, 771; (b) Alvarez-Manzaneda, E. J., Chahboun, R., Barranco Pérez, I., Cabrera, E., Alvarez, E., & Alvarez-Manzaneda, R. *Org. Lett*. **2005**, *7*, 1477-1480; (c) Sugimura, T., Nishida, F., Tei, T., Morisawa, A., Tai, A., & Okuyama, T. *ChemComm.* **2001**, *21*, 2180-2181; (d) Klement, I., Knochel, P. *Synlett*. **1996**, *10*, 1004-1006; (e) Lütjens, H., Knochel, P. *Tetrahedron: Asymmetry* **1994**, *5*, 1161-

1162; (f) Reusch, W., Hwang, C.-S. *Heterocycles* **1987**, *25*, 589-600; g) Birtwistle, D. H., Brown, J. M., Foxton, M. W. *Tetrahedron Lett*. **1986**, *27*, 4367-4370.

[13] Lal, B.; Pramanik, B. N.; Manhas, M. S.; Bose, A. K. *Tetrahedron Lett.* **1977**, 1977–1980.

[14] a) Johnsson, R. *Carbohydr. Res*. **2012**, *353*, 92-95; b) Markiewicz, W. T.J. *Chem. Soc.* **1979**, 24–25; c) Markiewicz, W. T.J. *Chem. Soc.* **1979**, 178–194.

[15] a) Shaw, G.; Warrener, R. N. *J. Chem. Soc.* **1958**, 157–161; b) Shaw, G.; Warrener, R. N. *J. Chem. Soc.* **1958**, 153–156.

[16] Tietze, L. F.; Schneider, C.; Pretor, M. *Synthesis* **1993**, 1079–1080.

[17] Bowman, N. B ; Rexford, D. R. *J. Org. Chem.* **1954**, *19*, 1219-1224.

[18] Hojo, M.; Masuda, R.; Sakagushi, S.; Takagawa, M. *Synthesis-Stuttgart*. **1986**, *12*, 1016-1017.

[19] Hjelmgaard, T., Tanner, D. *Org. Biomol. Chem.* **2006**, *4*, 1796-1805.

[20] Jung, M. E., Dwight, T. A., Vigant, F., Østergaard, M. E., Swayze, E. E., Seth, P. P. *Angew. Chem. Int. Ed.* **2014**, *126*, 10051-10055.

[21] Harnden, M. R.; Wyatt, P. G.; Boyd, M. R.; Sutton, D. *J. Med. Chem.* **1990**, *33*, 187–196.

[22] (a) Hinton, S.; Riddick, A.; Serbessa, T. *Tetrahedron Lett.* **2012**, *53*, 1753–1755; (b) Helguera, A. M.; Rodríguez-Borges, J. E.; Caamaño, O.; García-Mera, X.; González, M. P.; Cordeiro, M. N. D. S. *Mol. Inform.* **2010**, *29*, 213–231; (c) Wang, P.; Agrofoglio, L. A.; Newton, M. G.; Chu, C. K. *J. Org. Chem.* **1999**, *64*, 4173–4178.

[23] Saneyoshi, H.; Deschamps, J. R.; Marquez, V. E. *J. Org. Chem.* **2010**, *75*, 7659–7669.

[24] (a) Baig, R. B. N.; Varma, R. S. *Chem. Soc. Rev.* **2012**, *41*, 1559–1584; (b) Kappe, C. O. *Chem. Soc. Rev.* **2008**, *37*, 1127–1139; (c) Kappe, C. O. *Angew. Chem. Int. Ed.* **2004**, *43*, 6250–6284; (d) Lidström, P.; Tierney, J.; Wathey, B.; Westman, J. *Tetrahedron* **2001**, *57*, 9225–9283; (e) Kappe, C. O.; Dallinger, D.; Murphree, S. *Practical microwave synthesis for organic chemists*; Wiley-VCH, 2009. (f) Kappe, C. O.; Stadler, A.; Dallinger, D. *Microwaves in organic and medicinal chemistry*; Wiley-VCH, 2012.

[25] Gabriel, C.; Gabriel, S.; Grant, E. H.; Halstead, B. S. J.; Mingos, D. M. P. *Chem. Soc. Rev.* **1998**, *27*, 213–223.

[26] Ezzitouni A., Marquez, V. E. *J. Chem. Soc., Perkin Trans. 1*, **1997**, *7*, 1073-1078.

[27] (a) Frihed, T. G., Pedersen, C. M., Bols, M. *Eur. J. Org. Chem.* **2014**, *2014*, 7924-7939; (b) Persky, R., & Albeck, A. *J. Org. Chem*. **2000**, *65*, 3775-3780; c) Hughes, D. L. *Org. Prep. Proced. Int.* **1996**, *28*, 127-164.

[28] Marquez, V. E., Ezzitouni, A., Russ, P., Siddiqui, M. A., Ford, H., Feldman, R. J., Mitsuya, H., George, C., Barchi, J. J. *J. Am. Chem. Soc.* **1998**, 120, 2780-2789.

III. CHAPTER IV

Synthesis of new substituted 1,2,3-triazolo-carbanucleoside analogues

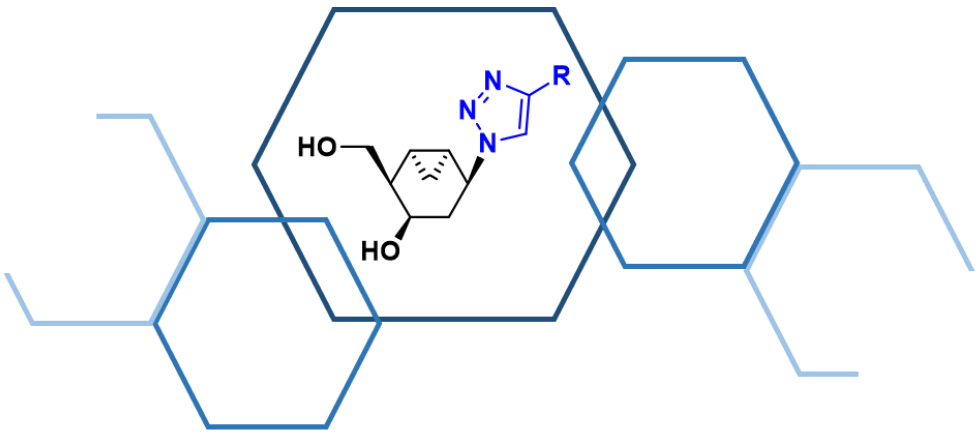

1. INTRODUCTION

As it has been mentioned, the structure of natural nucleosides has been the object of numerous chemical modifications in the search for new therapeutic entities. The nucleobase has been one of the main targets of these modifications, either removing or adding atoms to the rings themselves, or changing positions of the atoms. These types of changes have served to create many new classes of nucleoside analogues over the years.[1] A common modification is based on removing or relocating nitrogen atoms from the nucleobase (Figure IV-1). For example, removal of a nitrogen from the purine or pyrimidine ring system (referred to as a "deaza" analogues) could be utilized to explore the effect of hydrogen bonding interactions in enzyme binding sites (such as 3-deaza-deoxyguanine[2] or 7-deazaadenosine[3]); the addition of a nitrogen to the nucleobase (referred to as "aza" analogues) can introduce new hydrogen bonding donors or acceptors (such as 5-azacytidine[4] or 5-aza-2'-deoxycytidine[5]) and finally nitrogens can also be repositioned in the ring introducing alternative hydrogen bond donors or acceptors which can interact with new areas of the enzyme binding site (such as 8-aza-7-deazapurine[6]).

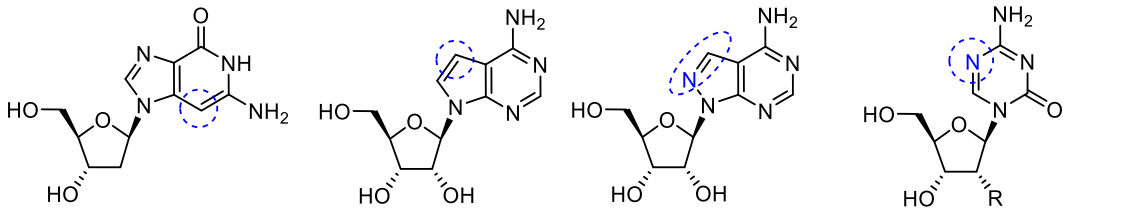

Figure IV-1. Examples of "deaza" and "aza" modifications on the heterobase scaffold where a nitrogen is removed or added from either the purine or pyrimidine ring, respectively.

Different "deaza" or "aza" nucleoside analogues have been synthesised in the last decades in order to find new antiviral candidates.[1] Other strategy in modificated nucleobase consists on substituting the purine or pyrimidine base by an imidazole or triazole ring. From this strategy, in the early 1970s raised up Ribavirin (Virazole®, Figure IV-2) described by Sidwell *et al.*[7] that displays a broad antiviral spectrum in clinical use for the treatment of RSV infections, lassa fever, hepatitis (A, B, and C), measles and mumps. It was FDA-approved 15 years ago for the combination treatment of hepatitis C virus.[8] In addition, Ribavirin is currently being evaluated to treat the new appeared COVID-19 (coronavirus disease 2019) and related human coronavirus

diseases.[9] Also it is evaluated to treat many cancers such as malignant solid tumors or in combination therapy for head and neck cancer.[10] The structure of this nucleoside analogue consists on a β-D-ribose ring attached to a 1,2,4-triazole derivative replacing the natural base.

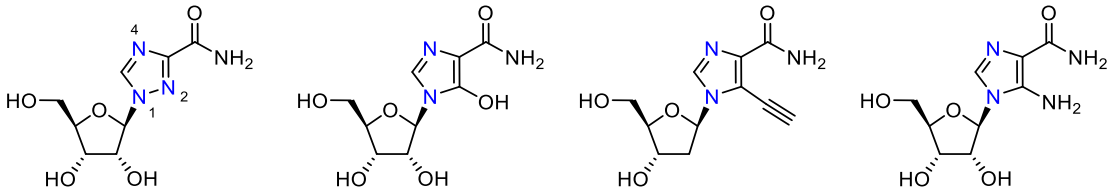

Ribavirin
Virazole®, 1971
(antiviral and anticancer agent)

Brenedin
(immunosuppressive agent)

EICAR
(antiviral agent)

Acadesine
(anticancer agent)

Figure IV-2. Selected NAs with imidazole or triazole bases owning remarkable biological activities.

Other NAs bearing 5-membered heterocyclic bases, such as imidazoles and triazoles, have displayed interesting biological properties;[11] for instance, Brenedin (Mizoribine®, Figure IV-2) is currently in clinical use as an immunosuppressor for the treatment of patients with transplants[12a], EICAR causes depletion of purine nucleotides resulting in a broad spectrum of activity against RNA and DNA viruses and tumour cell proliferation[12b] and Acadesine (AICA-Ribonucleotide (AICAR)), is currently in a phase I/II study for myelodysplastic syndromes and acute myelogenous leukemia.[10]

In this context, a several number of 1,2,3-triazolo-nucleoside analogues have shown a great potential as antiviral, anticancer or antibacterial agents,[13,14] such as compounds **125**[15] and **126**[16] (Figure IV-3) exhibiting interesting antiviral and cytostatic activities, respectively.

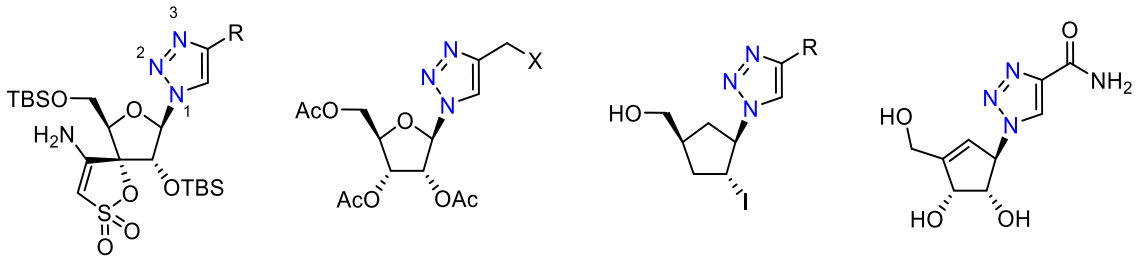

125, R = acyl, alkyl

126, X = halogen

127, R = CO_2Me, $CONH_2$, Ar

128

Figure IV-3. Recently reported 1,2,3-triazolyl carbanucleosides with antiviral activities.

More recently, compound (±)-**127** (R = 2-C_6H_4OMe) exhibited specific inhibitory potential against TK^+VZV (EC_{50} = 11 μM)[13a] and **128** showed potent antiviral activity against vaccinia virus (EC_{50} = 0.4 μM), but moderate activity against cowpox virus (EC_{50} = 39 μM) and Severe Acute Respiratory Syndrome CoronaVirus (SARSCoV) (EC_{50} = 47 μM). [17]

In 2006, the 1,2,3-triazolo-carbanucleoside analogue **128** was synthesised by Chu *et al.* in enantiomerically pure form (Scheme IV-1).[17] The sequence started from D-ribose (**129**), which was converted in the single diastereomeric diol **130** after two steps of selective protection of alcohols and posterior alkylation by vinylmagnesium bromide. To incorporate another double bond for RCM reaction, protection of allylic alcohol was followed by oxidation and Wittig reaction of free secondary alcohol giving the corresponding diene **131**. Then, through a RCM reaction, diene **131** was transformed into cyclopentene **132**. The 1,2,3-triazole derivative **134** was synthesised by cycloaddition reaction catalysed with copper between methyl propiolate and the azide derivative **133**, prepared from alcohol **132**. The ester **134** was converted to the amide in saturated methanolic ammonia, which was treated in acid media to afford the 1,4-disubstituted-1,2,3-triazolocarbocyclic nucleoside **128** in 44% overall yield over 13 steps.

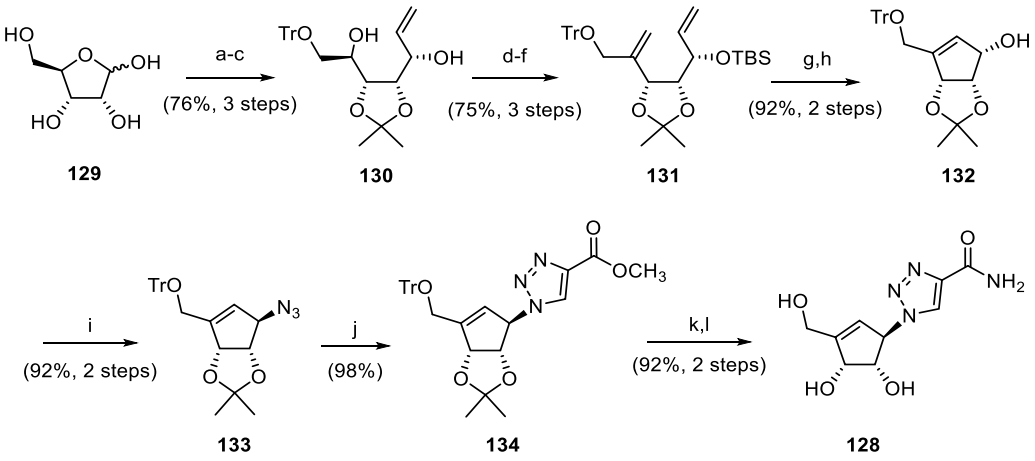

Scheme IV-1. Synthesis of 1,2,3-triazolo-carbanucleoside analogue **128**.[17] Reagents and conditions: (a) 2,2-dimethoxypropane, $TsOH·H_2O$, acetone, 0 °C to rt, 1 h; (b) TrCl, Et_3N, DMAP, DMF, rt, 48 h; (c) vinylmagnesium bromide, THF, -78 °C to rt, 12 h; (d) TBDMSCl, imidazole, CH_2Cl_2-DMF (10:1 v/v), 0 °C to rt, 24 h; (e) $(COCl)_2$, Et_3N, CH_2Cl_2, -60 °C; (f) Ph_3PCH_3Br, *n*-BuLi, THF, 0 °C to rt, 12 h; (g) TBAF, THF, rt, 6 h; (h) second-generation Grubbs catalyst, CH_2Cl_2, rt, 24 h; (i) I) MsCl, Et_3N, CH_2Cl_2, 0 °C, 2 h; II) NaN_3, DMF, 80 °C, 24 h; (j) methyl propiolate, CuI, Et_3N, THF, rt, 12 h; (k) NH_3, MeOH, rt, 24 h; (l) 1.0 M HCl in ether, MeOH, 0 °C, 4 h.

The classic way to construct 1,2,3-triazole ring is by a 1,3-dipolar cycloaddition reaction between an azide and an alkyne. The 1,3-dipole (azide) reacts with a dipolarophile (alkyne) via a concerted mechanism to form a five-membered heterocycle (1,2,3-triazole).[18,19] This reaction is also known as Huisgen cycloaddition in honour of the seminal works of Professor Rolf Huisgen, and usually gives poor regioselectivity which leads two possible regioisomers: the 1,4-disubstituted and 1,5-disubstituted regioisomers. The thermally induced 1,3-dipolar azide–alkyne cycloaddition, in general, results in an approximately 1:1 mixture of 1,4- and 1,5-triazole isomers. These reactions require elevated temperatures because alkynes are poor 1,3-dipolar acceptors (Scheme IV-2).[20]

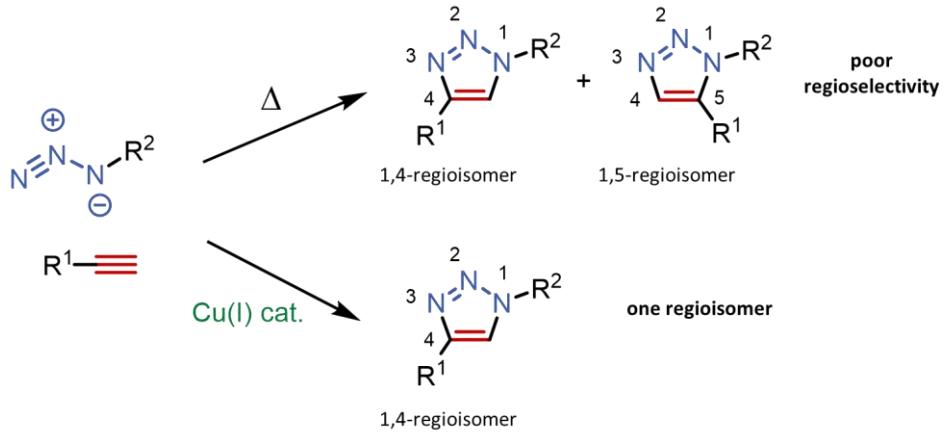

Scheme IV-2. Cu-catalysed versus thermal 1,3-Dipolar Cycloaddition of azides and alkynes

A modification of the Huisgen reaction was independently discovered, in 2002 by Meldal *et al.*[21] in Denmark and Sharpless *et al.*[22] in USA, consisting in the use of substoichiometric amounts of a copper(I) salt to produce a significant increase in the reaction rate, which allows these reactions to be performed at rt and in very short reaction times. In addition, 1,4-substituted triazoles are obtained regioselectively (Scheme IV-2). While this copper(I)-catalyzed variant gives rise to a triazole from a terminal alkyne and an azide, formally it is not a concerted 1,3-dipolar cycloaddition and thus should not be termed as a Huisgen cycloaddition. This reaction is better termed as Copper(I)-catalyzed Azide-Alkyne Cycloaddition (CuAAC) which constitutes a powerful synthetic tool and is one of the most productive fields in modern organic chemistry.[23] The CuAAc is an example of a "click reaction" and often is referred with this name.

Despite the apparent simplicity and widespread use of the reaction, its mechanism has emerged as particularly complex, which was a matter of debate, prompting a range of experimental and theoretical studies. A general, simplified mechanism of CuAAC under aprotic conditions is postulated to include Cu-bound alkynyl and triazolide intermediates, but the nuclearity of the

copper ([Cu]) intermediates was uncertain.[24,25] Recently, computational studies,[26] kinetics studies,[27] isotopic copper labeling,[28] mass spectroscopy,[29] and isolation of presumed copper intermediates[30] suggested the intermediacy of di-copper species in catalytic mechanism. In this context a generally accepted mechanism of CuAAc has been described supported by these studies[28,30b,31] (Scheme IV-3):

The postulated mechanism starts when the copper(I) species forms a π complex with the triple bond of a terminal alkyne (**I**). In the presence of a base, the terminal hydrogen, being the most acidic, is deprotonated first to give a Cu acetylide intermediate (**II**). The reaction is assisted by the copper, which, when coordinated with the acetylide lowers the pKa of the alkyne C-H by up to 9.8 units thus, under certain conditions, the reaction may be carried out even in the absence of a base. Studies have shown that the reaction is second order with respect to copper. It has been suggested that the transition state involves two copper atoms. One copper atom is bonded to the acetylide while the other Cu atom serves to activate the azide. The metal centre coordinates with the electrons on the nitrogen atom (**III**). The azide and the acetylide are not coordinated to the same Cu atom in this case. The ligands employed are labile and are weakly coordinating. The azide displaces one ligand to generate a copper-azide-acetylide complex (**IV**). At this point cyclization takes place (**V**) followed by protonation (**VI**), being the source of proton the hydrogen which was pulled off from the terminal acetylene by the base. The product is formed by dissociation and the catalyst ligand complex is regenerated for further reaction cycles.

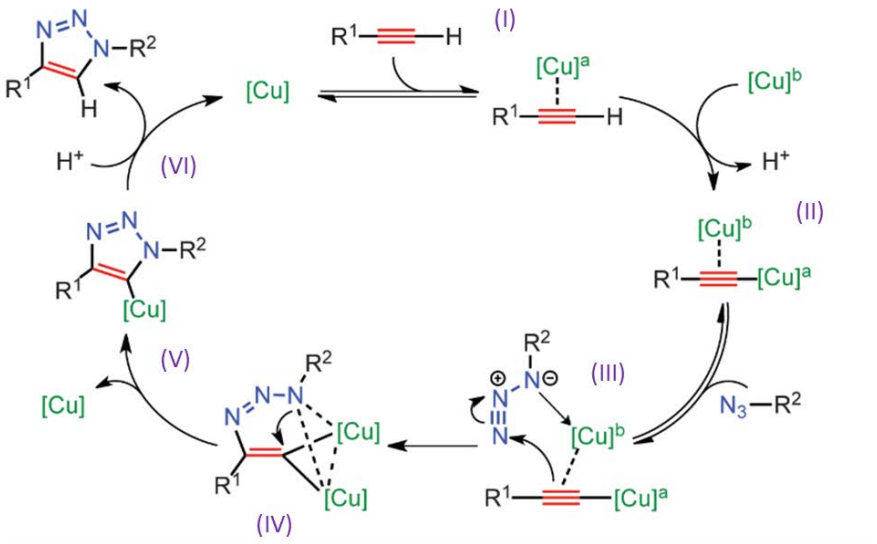

Scheme IV-3. Generally postulated mechanism of CuAAC.[28]

With regards to nucleoside analogues synthesis, different copper(I) sources have been used as catalyst. Copper(I) can be used directly as copper(I) iodide, CuI,[13a,32] (such as in the synthesis of **128**[17], Scheme IV-1) which is widely used in this type of synthesis. Often, due to the known instability of numerous copper(I) species, the active species can be generated *in situ* from a copper(II) salt (usually copper sulphate pentahydrate, $CuSO_4 \cdot 5H_2O$) and a reducing agent (most often sodium ascorbate, NaAsc);[33,34] or using the mixture of metallic copper (Cu^0) and copper(II) salt ($CuSO_4 \cdot 5H_2O$), which *in situ* comproportionate to form Cu(I).[34,35] This last option is particularly attractive, as copper metal and sulfate copper are inexpensive and also the reducing agent ascorbate and its oxidation products, which are sometimes not tolerated by the substrate, are avoided.

In 2009, Broggi *et al.* described the synthesis of (±)-1,2,3-triazolo-3'-deoxy-4'-hydroxymethyl carbanucleosides *via* 'click' cycloaddition using the mixture of $CuSO_4$/NaAsc as copper(I) source.[34] The synthetic strategy for the preparation amido-triazole (±)-**142** is depicted in Scheme IV-4. Cyclopentene **137** was obtained *via* malonic synthesis from **135** and **136** followed by a reduction and alcohol protection. The azido-carbocycle (±)-**138** was achieved after epoxidation and nucleophilic ring opening using sodium azide. First attempts of cycloaddition between azide (±)-**138** and methyl propiolate using the mixture of $CuSO_4$/NaAsc afforded the 4-methyl carboxylate triazole (±)-**139** in which a Michael addition of the 2'-hydroxyl on a second molecule of alkyne also occurred. These results will be latter considered when synthetizing our new analogues. To overcome this reactivity, the alcohol in position 2' of **138** was protected as an acetate prior to the cycloaddition. In this way, the CuAAc was carried out using the same condition than before obtaining the desired 1,4-disubstituted-1,2,3-triazole (±)-**141.** Subsequent deprotection and aminolysis afforded the amido-triazole (±)-**142** in 20% overall yield. Unfortunately, (±)-**142** did not inhibit production of vaccinia virus or cowpox virus in vero cells.

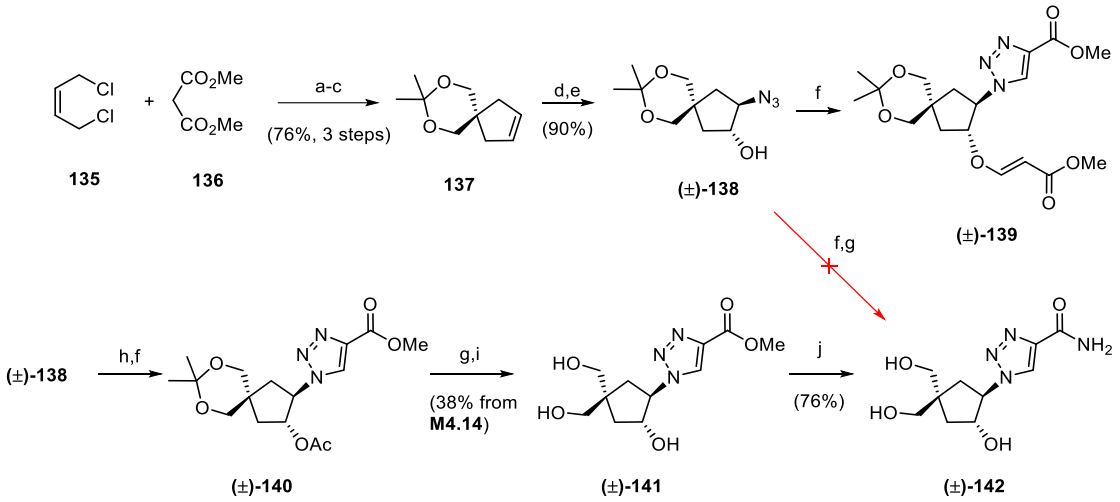

Scheme IV-4. Synthesis of 1,2,3-triazolo-carbanucleoside analogue (±)-**M4.18** using the mixture of $CuSO_4$/NaAsc as copper(I) source.[34] Reagents and conditions: (a) LiH, DMF, rt, 3 d; (b) $LiAlH_4$, Et_2O, 0 °C, 1 h; (c) 2-methoxypropene, PTSA, DMF, 0 °C to rt, 16 h; (d) *m*-CPBA, CH_2Cl_2, 0 °C to rt, 4 d; (e) NaN_3, MeOH/H_2O (8:2), reflux, 3 days; (f) methyl propiolate, $CuSO_4{\cdot}5H_2O$ (5 mol %), NaAsc (10 mol %), H_2O/EtOH (1:1), rt, 16 h; (g) 80% AcOH in H_2O, rt, 16 h; (h) Ac_2O, pyridine, rt, o.n.; (i) 0.1 N NaOMe in MeOH, rt, o.n.; (j) NH_3/MeOH, rt, 24 h.

Alternatively, in 2008, Pradere and co-workers reported another synthesis of 1,2,3-triazolo-nucleoside analogues using a the mixture of $Cu^0_{(powder)}/CuSO_4$ as a Cu(I) source.[35b] The synthesis of various protected 1,4-disubstituted-1,2,3-triazolyl-nucleoside analogues was performed regioselectively using the mixture $Cu^0/CuSO_4$ as catalyst precursor from azide **144** (Scheme IV-5). The desired new compounds **145a–d** were obtained in yields ranging from 63 to 93%. This system has the advantage that the products can be obtained from the reaction mixture by simple extraction. Finally, the deacylation was carried out using a solution of ammonia in methanol and led quantitatively to the final 1,4-disubstituted-1,2,3- triazolo-nucleosides (**146a–d**). None of these compounds showed activity against viral strains tested or cytotoxicity.

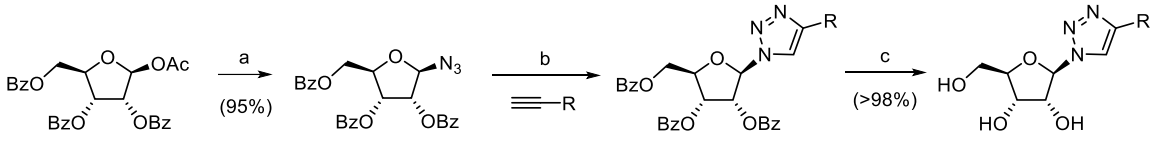

R = Ph, (86%), **a**
R = CH_2-Ph, (93%), **b**
R = $(CH_2)_3CH_3$, (89%), **c**
R = OCH_2CH_3 (63%), **d**

R = Ph, **a**
R = CH_2-Ph, **b**
R = $(CH_2)_3CH_3$, **c**
R = OCH_2CH_3, **d**

Scheme IV-5. Synthesis of 1,4-disubstituted-1,2,3-triazolo-nucleosides (**146a–d**) using $Cu^0/CuSO_4$ mixture.[35b] Reagents and conditions: (a) $TMSN_3$, $SnCl_4$(cat), CH_2Cl_2, 12 h; (b) $Cu^0/CuSO_4{\cdot}5H_2O$ (20:1), *t*-BuOH/H_2O (1:1), o.n., rt; (c) NH_3/MeOH.

Taking these results into account, our strategy to synthesize the 1,4-disubstituted-1,2,3-triazolo-analogues involves the construction of the 1,2,3-triazole ring *via* Copper(I)-catalyzed Azide-Alkyne cycloaddition (CuAAc) between previously synthesised azide **94** (*Chapter III*) and different alkynes (Scheme IV-6).

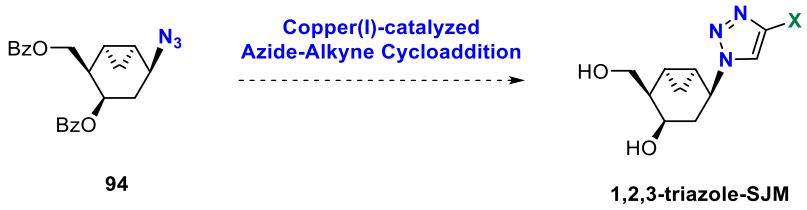

94 **1,2,3-triazole-SJM**

Scheme IV-6. Proposed synthetic strategy for the preparation of targeted compounds.

2. SYNTHESIS OF 4-SUBSTITUTED-1,2,3-TRIAZOLE ANALOGUES *VIA* CuAAc

2.1 Synthesis of 4-carboxamide ribavirin analogue

The synthesis of 1,2,3-triazole-4-carboxamide derivative will be carried out *via* CuAAc using the standard conditions described by Broggi and co-workers[34] (Scheme IV.4). The combination of $CuSO_4 \cdot 5H_2O$/NaAsc as Cu(I) catalyst will be used in the formation of triazole ring, where the ascorbate (Asc^-) reduces Cu^{2+} producing Cu^+ ions.

Thus, azide **94** was treated with methyl propiolate in the presence of $CuSO_4 \cdot 5H_2O$ (10 mol %) and NaAsc (20 mol %) in a (2:1) mixture EtOH/H_2O overnight. Unfortunately, the reaction did not work and practically all starting material was recovered, probably due to the low solubility of **94** in the EtOH/H_2O mixture. The same result was obtained when the alcohol and its ratio was changed by MeOH or *t*-BuOH (Scheme IV-7).

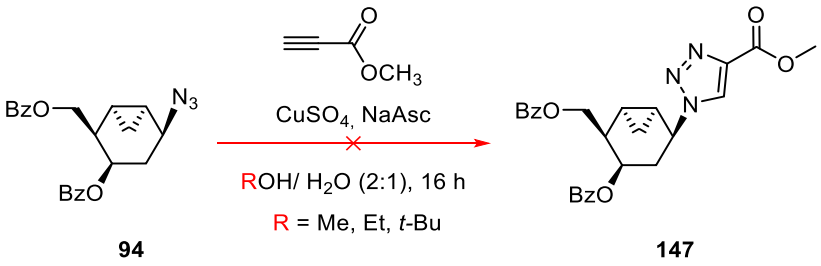

Scheme IV-7. Attempt to prepare the triazole ring using different alcohols/water media.

The possibility of deprotecting the alcohols of **94** in order to increase the solubility in the reaction conditions was precluded to avoid the Michael addition (Scheme IV-4) previously described by Broggi *et al*.[34] Next, it was decided to use other water miscible solvents in which the protected azide **94** was more soluble such as acetonitrile. Thus, in the same reaction conditions described above but using ACN/H_2O (2:1) media it was possible to build the 1,2,3-triazole ring in our bicyclo[4.1.0]heptane scaffold. The 4-methyl carboxylate triazole **147** was obtained in 79% yield (Scheme IV-8).

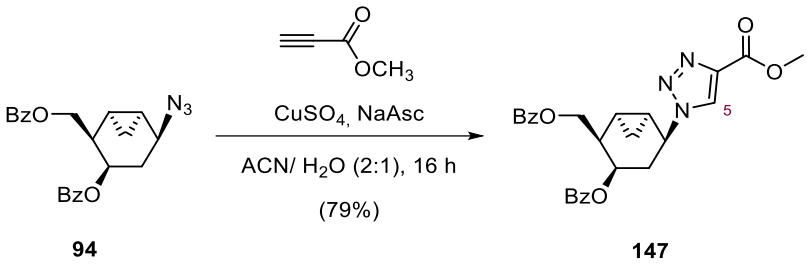

Scheme IV-8. Synthesis of 4-methyl carboxylate triazole **147** in ACN/water media.

The formation of the triazole ring on substrate **94** was established by the appearance of additional signals on the ^{1}H and ^{13}C spectra. Thus, the proton spectrum features new singlet signals at 8.28 and 3.77 ppm corresponding to the H-5 of triazole ring and the three protons of the ester group ($-CH_3$), respectively, while the carbon spectrum shows additional signals at 126.8 and 139.4 ppm (corresponding to two triazole sp^2 carbons) as well as by new peaks at 160.8 and 52.0 ppm corresponding to the ester group.

The regioselectivity of the cycloaddition reaction under this conditions was confirmed using ^{1}H-^{13}C long-range NMR experiments (HMBC) which shows a cross-peak between the H-2' of the bicyclo[4.1.0]heptane moiety and C-5 of the 1*H*-triazole H-5, confirming the formation of the 1,4-regioisomer (Figure IV-4).

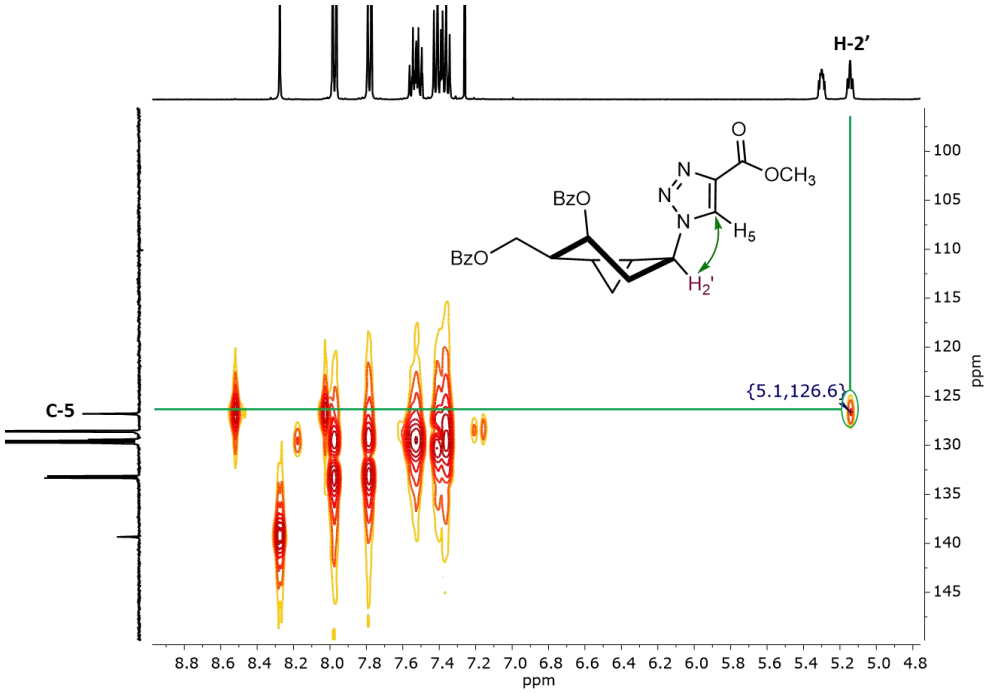

Figure IV-4. HMBC correlation spectrum (400 MHz, $CDCl_3$) of 1,2,3-triazole **147**.

Finally, with the aim of obtaining the 4-carboxamide compound, protected methyl carboxylate adduct **147** was treated with an ammonia solution in methanol (Scheme IV-9). In these conditions the desired deprotected 1,2,3-triazole-4-carboxamide **148** was afforded in 92% yield. Thus, compound **148** was obtained in 2 steps in 73% overall yield from **94**.

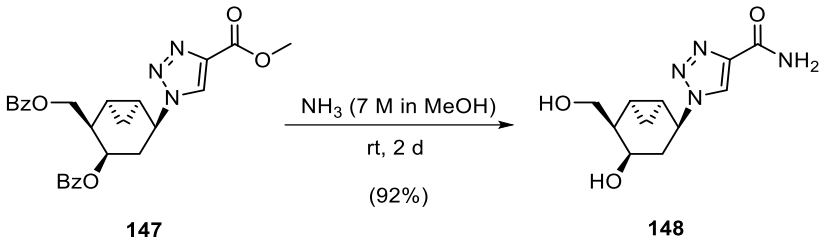

Scheme IV-9. Aminolysis of **147** affording nucleoside analogue **148**.

The formation of the 1,2,3-triazole-4-carboxamide nucleoside analogue **148** was confirmed by the disappearance of the peaks corresponding to the methyl carboxylate ester and the two benzoyl groups in the ^{1}H-NMR and ^{13}C-NMR spectra as well as by the displacement of H-4' and the two diastereotopic H-1'' signals to lower chemical shifts (from 5.30 and 4.72-4.54 ppm in **147** to 3.96 and 3.86-3.81 ppm in **148**, respectively) (Figure IV-5).

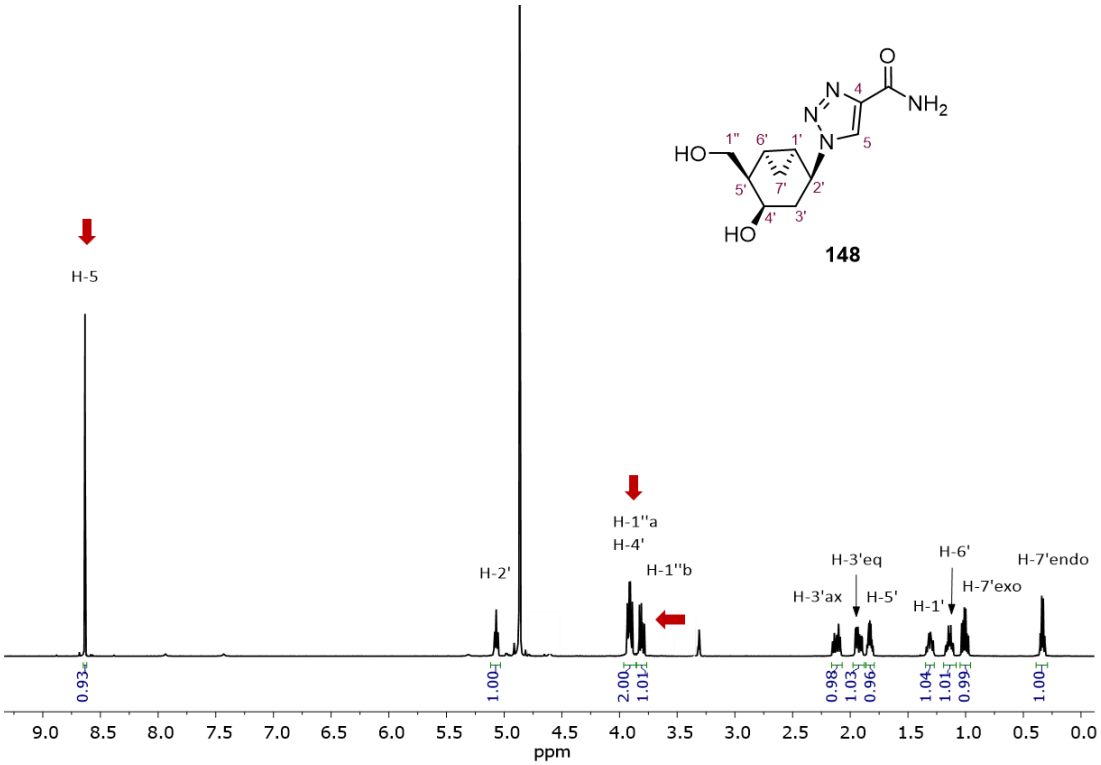

Figure IV-5. ^{1}H-NMR spectrum (400 MHz, MeOH-d_4) of **148**.

2.2 Synthesis of different 4-substituted triazoles.

With the objective to broaden the family of nucleoside analogues bearing triazole rings, the synthesis of different 4-substituted triazole compounds were set out using our starting azide **94** and different alkynes via CuAAc.

Since the selected alkynes to prepare the new triazole rings cannot act as Michael acceptors giving rise to the Michael adduct,[34] it was decided to remove the benzoyl protecting groups of **94** avoiding the previously referred solubility problems.

Accordingly, reaction of azide **94** with ammonia solution in methanol for 3 days at rt afforded deprotected azide **149** in 85% yield (Scheme IV-10). Removal of the benzoyl groups was confirmed by disappearance of the aromatic signals in the ^{1}H-NMR and ^{13}C-NMR spectra.

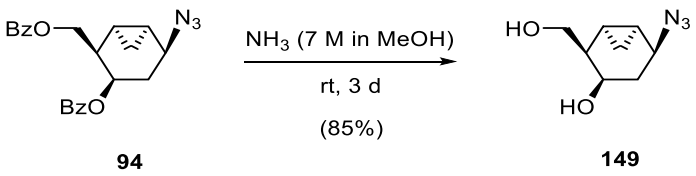

94 **149**

Scheme IV-10. Deprotection of **94** using ammonia solution to give **149**.

In the previous preparation of triazole ring in **147**, long reaction times (16 hours) were required with a moderate yield. Although the overall yield of the final product **148** was good, it was decided to explore other CuAAc approaches as reported by Sharpless *et al.*[36] using $Cu^{0}/CuSO_4$ mixture as Cu(I) source.

As it has been mentioned, the mixture of copper (Cu^{0})/copper sulfate ($Cu(II)SO_4$) comproportionate to form Cu(I) generating *in situ* the catalyst in the CuAA cycloaddition reaction.[37] Different experiments showed that this comproportionation reaction occurs on the surface of the copper particles, rather than *via* Cu^{0} atoms or Cu(I)/Cu(II) ions that are leached into the reaction mixture.[38]

In addition, Broggi and co-workers described[34,35a] that using $Cu^{0}/CuSO_4$ mixture under microwave (MW) irradiation, the reaction times could be further shortened to only few minutes without formation of by-products.

Taking these results into account, it was decided to prepare the new triazole nucleoside analogues from **149** under Broggi conditions[34] using copper powder (Cu^0, 80 mol %), a solution 1 M of copper(II) sulfate in water ($CuSO_4 \cdot 5H_2O$, 20 mol %) in *t*-BuOH/H_2O (1:1) media under MW irradiation at 125 °C. The use of this methodology in the reaction of azide **149** with different terminal alkynes produced the 4-substituted-1,2,3-triazole carbanucleosides **150**, **151** and **152**, entry 1-3, respectively (Table IV-1).

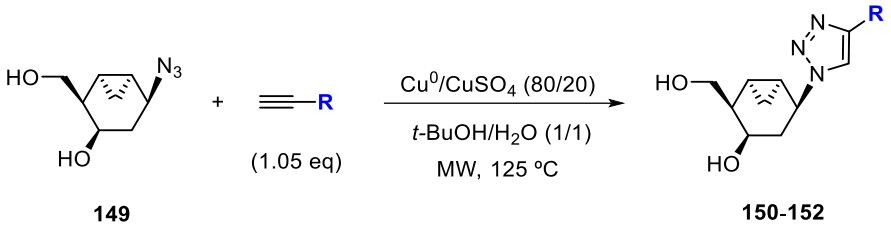

149 **150-152**

Exp.	R	Triazole	Time	Yield (%)
1	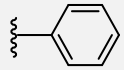	**150**	2 min	97
2	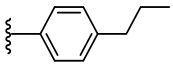	**151**	10 min	94
3		**152**	<1 min	80

Table IV-1. Microwave assisted cycloaddition of unprotected azido derivative **149**.

In the three cases, complete conversion of **149** into the desired triazoles were obtained in short reaction times with no observable formation of by-products. As expected, electron-poor alkyne (propargyl alcohol, entry 3) was more reactive than electron-rich alkynes (aryl alkyne, entries 1 and 2). The cycloaddition reaction afforded 4-aryl compounds, **150** and **151** in less than 10 min in high yields (97-94%, respectively) and the compound with electron-withdrawing substituent, **152**, was obtained in less than one minute in 80% yield.

The success of the reactions was mainly confirmed by the presence of H-5^{II} corresponding to the triazole ring in the proton spectra for **150**, **151** and **152** (8.52, 10.03 and 8.14 ppm, respectively). In addition, for the 4-aryl compounds new aromatic signals are observed, and also, alkyl signals (4.18, 3.22 and 2.53 ppm) in the case of **151**. For compound **152** a new signal at 4.68 ppm corresponding to the triazole-hydroxymethyl group appears as a broad singlet.

Analogously to compound **148**, the regioselectivity of the reaction was confirmed by HMBC experiments. The HMBC spectra, for the three compounds, show cross-peaks between H-5 of the bicyclo[4.1.0]heptane moiety with C-5^{II} of the triazole ring, confirming the formation of the 1,4-regioisomers (Figure IV-6).

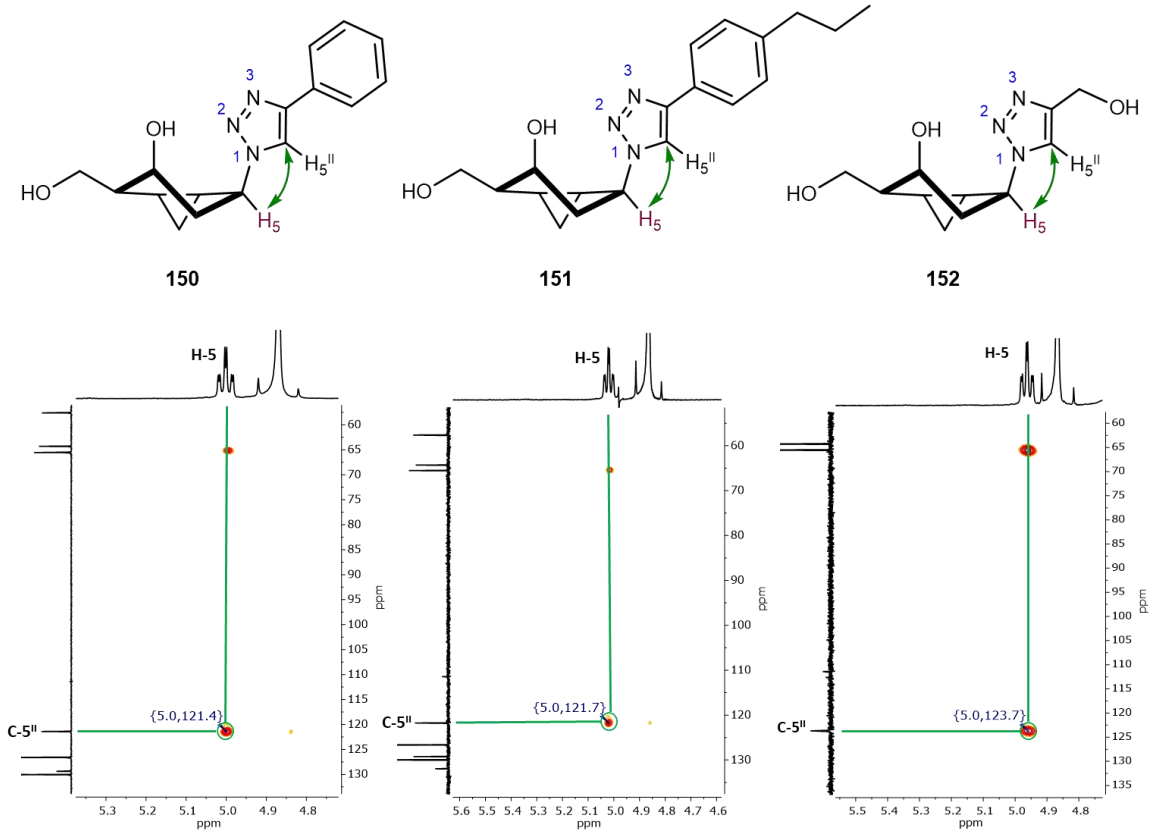

Figure IV-6. Cross peak between H-5 and C-5^{II} in HMBC spectra (400 MHz, MeOH-d_4) of **150**, **151** and **152**.

3. SYNTHESIS OF 4,5-DISUBSTITUTED-1,2,3-TRIAZOLE ANALOGUE

So far, only the synthesis of 1,4-disubstituted triazole analogues have been described. In order to explore more structural diversity, this section is focused in the synthesis of 1,4,5-trisubstituted-triazolo carbanucleoside analogues.

As seen in the introduction to this chapter, many examples of 4,5-imidazole nucleoside analogues have been reported as active biological molecules (Figure IV-2). Among them, Acadesine (AICAR, 5-aminoimidazole-4-carboxamide-1-β-D-ribofuranoside) is currently being

evaluated in Phase I/II for myelodysplastic syndromes and acute myelogenous leukemia.[10] Taking these results into account, it was decided to study the formation of 5-amino-1,2,3-triazole-4-carboxamide moiety into compound **94**.

To achieve the synthesis of the 5-amino-4-carboxamide-1,2,3-triazolo carbanucleoside **153**, a reported cycloaddition reaction between an azide and the 2-cyanoacetamide was selected.[39] Thus, azide **94** was treated with 2-cyanoacetamide in the presence of K_2CO_3 in DMSO at 50 °C. Due to the basic conditions, deprotected 1,4,5-trisubstituted, **153** was achieved in moderate yield (Scheme IV-11).

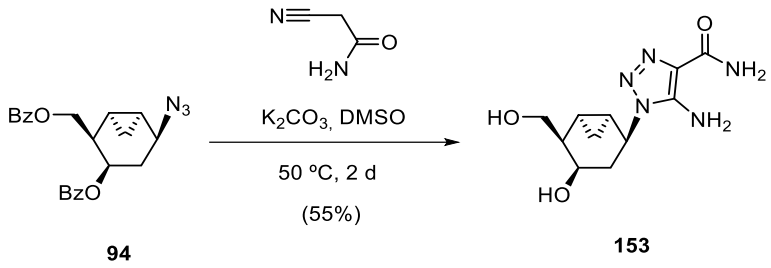

Scheme IV-11. Cycloaddition between azide **94** and 2-cyanoacetamide in basic conditions obtaining **153**.

In 1982, Chretien and Gross[40] proposed a mechanism for the cycloaddition between an azide and 2-cyanoacetamide in basic conditions. In presence of base, 2-cyanoacetamide is deprotonated obtaining the acetamido anion, **XXXVIII** (Scheme IV-12). This anion attacks azide (**XXXVII**) forming intermediate **XXXIX**. This latter undergoes ring closure into amide **XL** which is finally protonated in **XLI** yielding 5-amino-4-carboxamidetriazole ring.

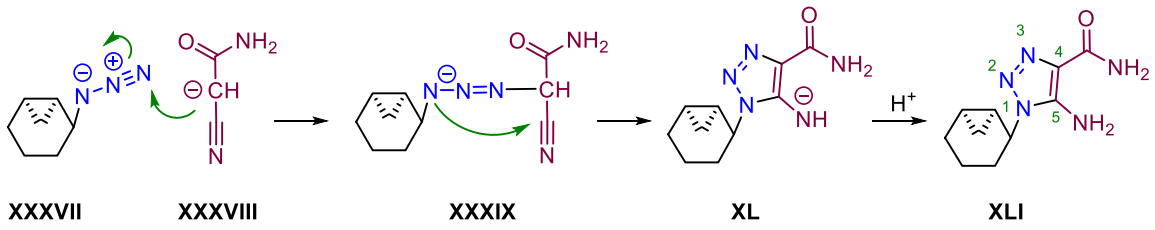

Scheme IV-12. Proposed mechanism of cycloaddition between an azide and 2-cyanoacetamide in basic conditions.[40]

The formation of the product was confirmed by proton and carbon (Figure IV-8) NMR spectra where new carbon signals corresponding to C-4, C-5 and *C*=O of the triazole ring (123.3, 146.0 and 167.1 ppm, respectively) appear and, in addition, aromatic signals corresponding to benzoyl groups are no longer observed.

Also, the IR spectrum shows strong absorptions at 3308 and 3173 cm^{-1} corresponding to -NH_2 groups and 1662, 1633, 1560 and 1517 cm^{-1} corresponding to -C(O)NH_2 and -NH_2 groups of the triazole ring.

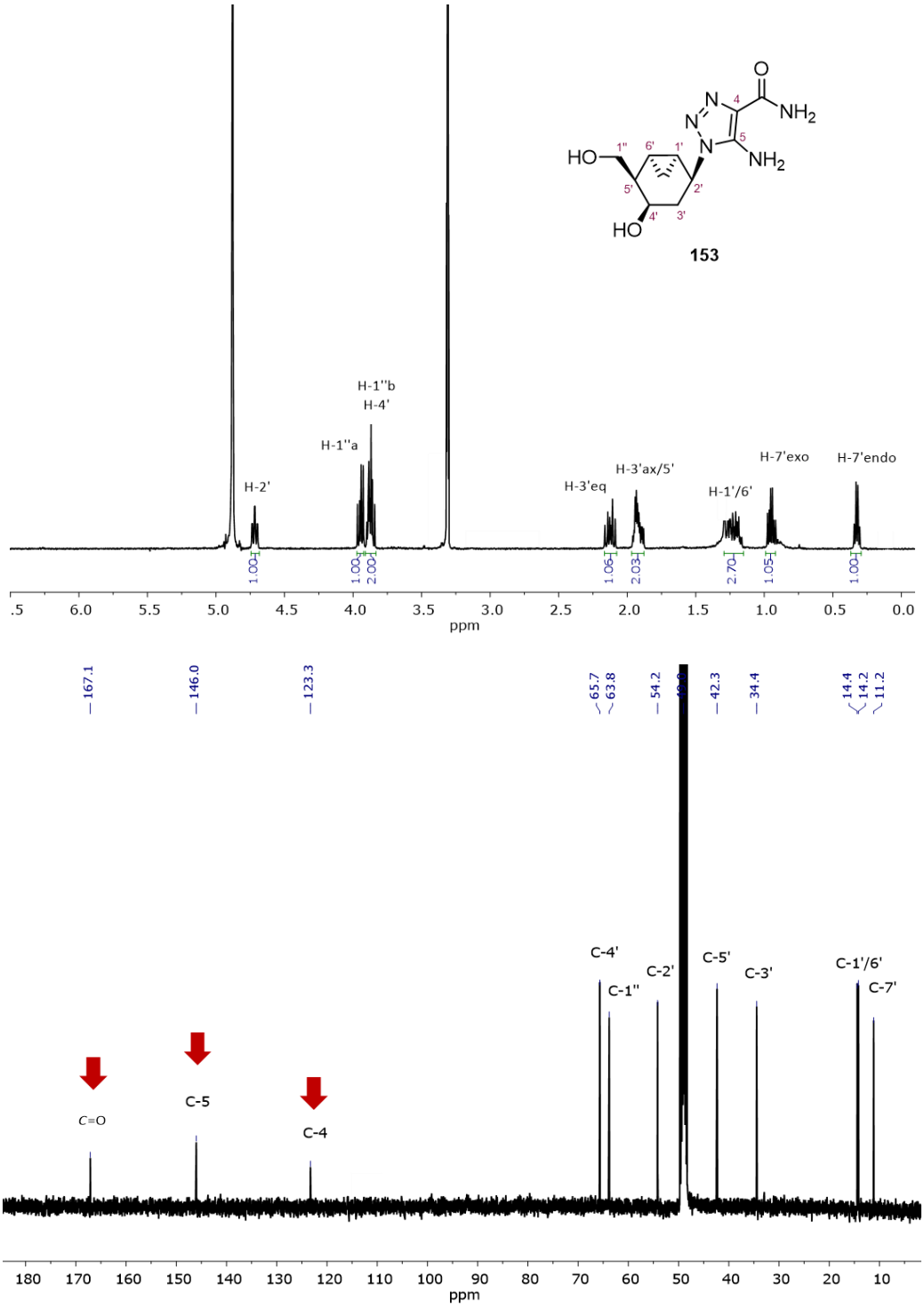

Figure IV-8. ^{1}H-NMR and ^{13}C-NMR spectra (400 MHz, MeOH-d_4) of **153**.

The regioselectivity of the formed 1,2,3-triazolo product **153** was confirmed by NMR using HMBC which shows cross peaking between H-2’ of bicyclo[4.1.0]heptane moiety with C-5 of the triazole ring confirming 5-amino-1-bicyclo[4.1.0]hept-2’-yl]-1,2,3-triazole-4-carboxamide structure (Figure IV-9).

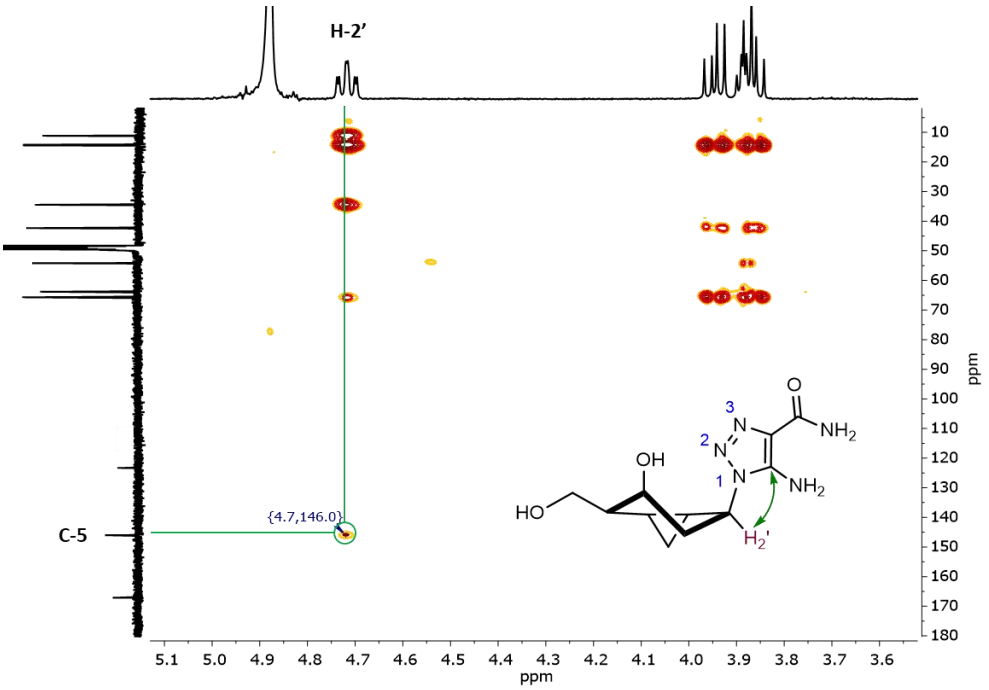

Figure IV-9. HMBC spectrum (400 MHz, MeOH-d_4) of **153**.

4. EVALUATION OF THE ANTIVIRAL ACTIVITY

The new triazolo carbanucleosides synthesised in this chapter **148**, **153**, **151**, **150** and **152**, as well as the molecules **149** and **147** (Figure IV-10) have been tested for the cytotoxicity and antiviral activity against several viruses at the group headed by Prof. Pannecouque at *Katholieke Universiteit Leuven*. The results are summarized in Tables IV-(2-6).

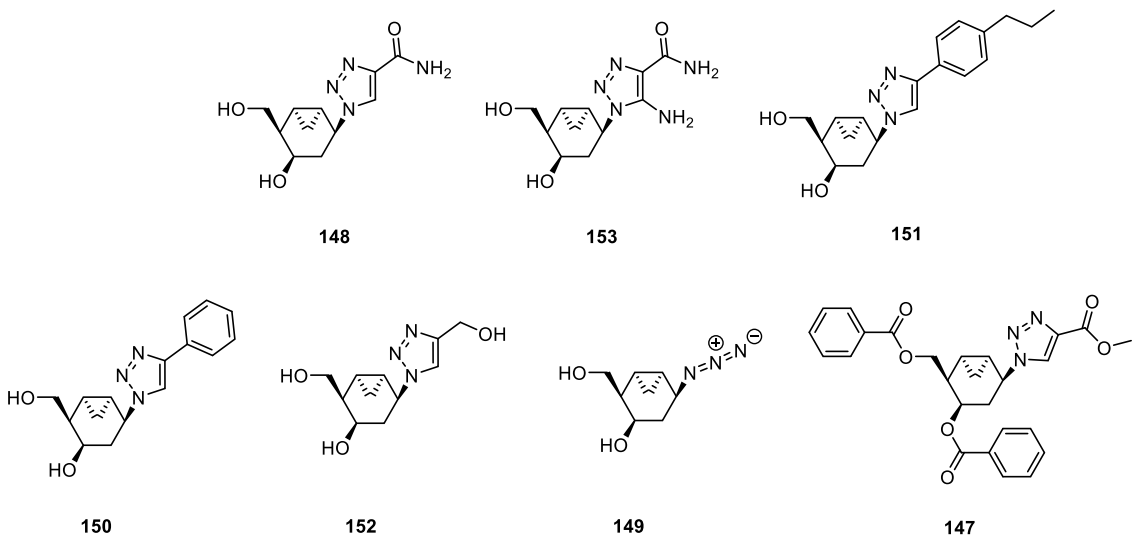

Figure IV-10. Synthesised prodrug candidates evaluated against different virus.

Table IV-2. Cytotoxicity and antiviral activity in HEp-2 (Human Epidermoid carcicoma) cell cultures.

Compound	Conc. Unit	Cytotoxixity CC_{50}[a]	Antiviral EC_{50}[b]		
			Vesicular stomatitis virus	Coxsackie virus B4	Respiratory syncytial vius
148	µg/mL	>50	>50	>50	>50
153	µg/mL	>50	>50	>50	>50
151	µg/mL	17.8	>50	>50	>50
150	µg/mL	>50	>50	>50	>50
152	µg/mL	>50	>50	>50	>50
149	µg/mL	>50	>50	>50	>50
147	µg/mL	15.5	>50	>50	>50
DS-10,000	µg/mL	>100	0.08	2.5	0.01
Ribavirin	µM	>250	149	117	6.7

[a] 50% Cytotoxic concentration, as determined by measuring the cell viability with the colorimetric formazan-based MTS assay.
[b] 50% Effective concentration, or concentration producing 50% inhibition of virus-induced cytopathic effect, as determined by measuring the cell viability with the colorimetric formazan-based MTS assay.

Table IV-3. Cytotoxicity and antiviral activity in HEL (Human Erythroleukemia) cell cultures.

Compound	Conc. Unit	Cytotoxicity CC_{50}[a]	Antiviral EC_{50}[b]				
			Herpes simplex virus-1 (KOS)	Herpes simplex virus-2 (G)	Vaccinia virus	Adeno virus-2	Human Coronavirus (229E)
148	µg/mL	>50	>50	>50	>50	>50	>50
153	µg/mL	>50	>50	>50	>50	>50	>50
151	µg/mL	>50	>50	>50	>50	>50	>50
150	µg/mL	>50	>50	>50	>50	>50	>50
152	µg/mL	>50	>50	>50	>50	>50	>50
149	µg/mL	>50	>50	>50	>50	>50	>50
147	µg/mL	>50	>50	>50	>50	>50	>50
Brivudin	µM	>250	0.2	22.1	12.6	-	-
Cidofovir	µM	>250	39.3	7.5	8.7	9.9	-
Acyclovir	µM	>250	1.9	0.5	>250	-	-
Ganciclovir	µM	>100	0.4	0.09	>100	-	-
Zalcitabine	µM	-	-	-	-	12.0	-
Alovudine	µM	-	-	-	-	0.4	-
UDA	µg/mL	-	-	-	-	-	1.2

[a] 50% Cytotoxic concentration, as determined by measuring the cell viability with the colorimetric formazan-based MTS assay.
[b] 50% Effective concentration, or concentration producing 50% inhibition of virus-induced cytopathic effect, as determined by measuring the cell viability with the colorimetric formazan-based MTS assay.

Table IV-4. Cytotoxicity and antiviral activity in Vero cell (kidney epithelial cells from African green monkey) cultures.

Compound	Conc. Unit	Cytotoxicity CC_{50}[a]	Antiviral EC_{50}[b]					
			Reo-virus-1	Sindbis virus	Coxsackie virus B4	Punta Toro virus	Yellow Fever virus	Zika virus
148	µg/mL	>50	>50	>50	>50	>50	>50	>50
153	µg/mL	>50	>50	>50	>50	>50	>50	>50
151	µg/mL	>50	>50	>50	**13.5**	>50	>50	>50
	µg/mL	78.8	>100	>100	**9.4**	>100	>100	>100
150	µg/mL	>50	>50	>50	>50	>50	>50	>50
152	µg/mL	>50	>50	>50	>50	>50	>50	>50
149	µg/mL	>50	>50	>50	>50	>50	>50	>50
147	µg/mL	>50	>50	>50	>50	>50	>50	>50
DS-10,000	µg/mL	>100	>100	14.9	3.8	1.3	6.9	3.4
Mycophenolic acid	µM	>100	7.1	3.6	>100	>100	2.6	0.2

[a] 50% Cytotoxic concentration, as determined by measuring the cell viability with the colorimetric formazan-based MTS assay.
[b] 50% Effective concentration, or concentration producing 50% inhibition of virus-induced cytopathic effect, as determined by measuring the cell viability with the colorimetric formazan-based MTS assay.

Table IV-5. Cytotoxicity and antiviral activity in MDCK (Madin-Darby Canine Kidney) cell cultures.

Compound	Conc. Unit	Cytotoxicity CC_{50}[a]	Antiviral EC_{50}[b]		
			Influenza A/H1N1 A/Ned/378/05	Influenza A/H3N2 A/HK/7/87	Influenza B B/Ned/537/05
148	µg/mL	>50	>50	>50	>50
153	µg/mL	>50	>50	>50	>50
151	µg/mL	10.6	>50	>50	>50
150	µg/mL	20.4	>50	>50	>50
152	µg/mL	>50	>50	>50	>50
149	µg/mL	>50	>50	>50	>50
147	µg/mL	16.1	>50	>50	>50
Zanamivir	µM	>100	0.9	4.9	1.4
Ribavirin	µM	>100	7.4	6.4	9.3
Rimantadine	µM	>200	88.8	0.06	>200

[a] 50% Cytotoxic concentration, as determined by measuring the cell viability with the colorimetric formazan-based MTS assay.
[b] 50% Effective concentration, or concentration producing 50% inhibition of virus-induced cytopathic effect, as determined by measuring the cell viability with the colorimetric formazan-based MTS assay.

Table IV-6. Cytotoxicity and antiviral activity in MT-4 cell cultures (human lymphocytic cell line).

Compound	Conc. Unit	Cytotoxixity CC_{50}[a]	Antiviral EC_{50}[b]	
			Human immunodeficiency virus (III_B)	Human immunodeficiency virus (ROD)
148	µg/mL	>125	>125	>125
153	µg/mL	>125	>125	>125
151[c]	µg/mL	9.36	>9.36	>9.36
150	µg/mL	96.22	>96.22	>96.22
152	µg/mL	≥115.82	>115.82	>115.82
149	µg/mL	≥99.04	>99.04	>99.04
147	µg/mL	64.03	>64.03	>64.03
Neviparine	µg/mL	>4	0.075	>4
Zidovudine	µg/mL	>2	0.002	0.002
Lamivudine	µg/mL	>20	0.58	2.27
Didanosine	µg/mL	>50	17.95	19.40

[a] 50% Cytotoxic concentration, as determined by measuring the cell viability with the colorimetric formazan-based MTS assay.
[b] 50% Effective concentration, or concentration producing 50% inhibition of virus-induced cytopathic effect, as determined by measuring the cell viability with the colorimetric formazan-based MTS assay.
[C] Crystallization observed at 125 µg/mL.

In general terms, most of these tested compounds do not show significant antiviral activity at subtoxic concentrations (~50 µg/mL). The only activity observed is the inhibition of Coxsackie virus B4 by the aromatic alkyl compound **151** in vero cells (EC_{50} = 13.5-9.4 µg/mL, Table IV-4).

Coxsackie virus is a virus that belongs to a family of *Picornaviridae* and the genus *Enterovirus*. These viruses recognize receptors expressed in various types of cells and tissues, and cause a wide range of diseases such as human heart diseases (myocarditis or pericarditis),[41] the *Hand, foot, and mouth* disease in children under the age of 10[42] or aseptic meningitis.[43] In particular, Coxsackie B4 virus has a cell tropism for natural killer cells and pancreatic islet cells. Infection can lead to beta-cell (type of cell that synthesize and secrete insulin and amylin) apoptosis which increases the risk of insulitis (diabetes mellitus type-1).[44]

Comparing the results of the antiviral activity against coxsackie virus B4 of **151** and **150** it can be assumed that the propyl chain present in compound **151** is a key factor. Therefore, modification of this alkyl chain, either changing the length or introducing functionality (Figure IV-11, structure **XLII**) could lead to analogues with potential activity.

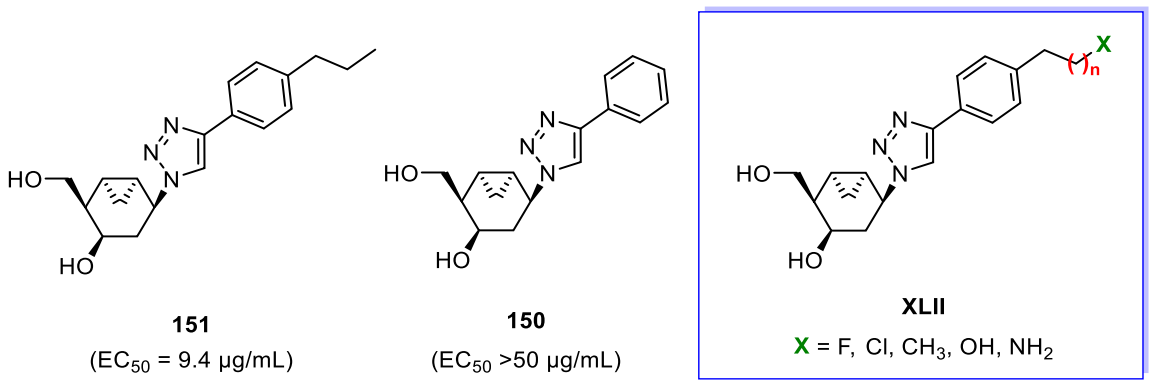

Figure IV-11. Antiviral activity of **151** and **150** against coxsackie B4 virus and proposed alkyl chain modification in order to improve the antiviral activity.

In terms of cytotoxicity, these compounds present more cytotoxicity than the above synthesised NAs, in particular, **150**, **151** and **147** are the most cytotoxic so far (for example the Table IV-5). Considering this feature, these compounds could be potential agents against some cancers, although more specific tests should be performed.

5. CHAPTER IV OUTLINE

In this chapter, four 4-substituted-1,2,3-triazolo-carbanucleosides **148**, **152**, **150** and **151** have been synthesised from azide **94** *via* CuAAc in 2 steps and 73%, 71%, 83% and 80% overall yield, respectively (Scheme IV-13). In order to explore more structural diversity, the 4,5-substituted-1,2,3-triazolo-carbanucleoside **153** has also been prepared in one step from **94** in 55% yield.

These five 1,2,3-triazolo-carbanucleosides **148**, **152**, **150**, **151**, **153** and the molecules **149** and **147** have been evaluated against several viruses. Unfortunately, most of them did not show significant activity. Only compound **151** showed activity against Coxsackie B4 virus (EC_{50} = 13.5-9.4 µg/mL).

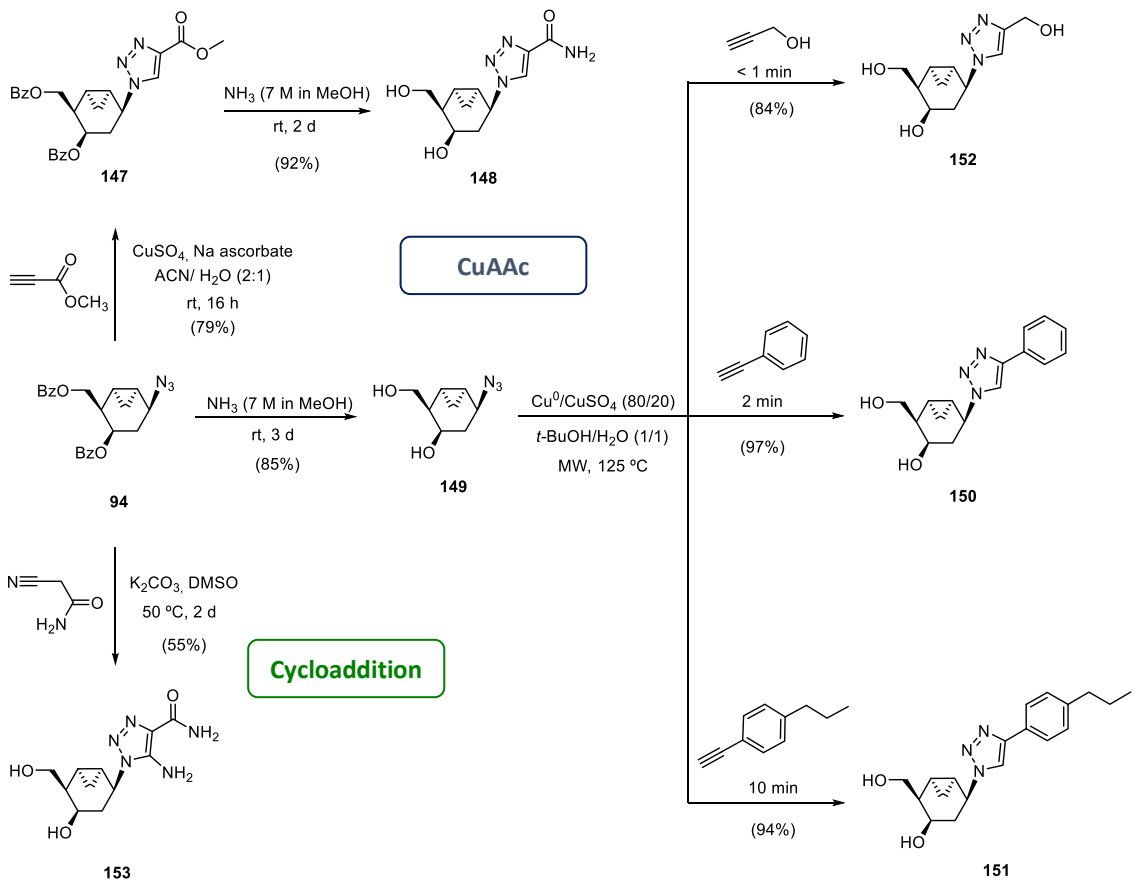

Scheme IV-13. Chapter IV summary.

6. REFERENCES

[1] Seley-Radtke, K. L.; Yates, M. K. *Antiviral Res.* **2018**, *154*, 66–86.

[2] Liu, M. C.; Luo, M. Z.; Mozdziesz, D. E.; Lin, T. S.; Dutschman, G. E.: Gullen, E. A.; Sartorelli, A. C. *Nucleos. Nucleot. Nucl.* **2001**, *20*, 1975-2000.

[3] Olsen, D.B.; Eldrup, A.B.; Bartholomew, L.; Bhat, B.; Bosserman, M.R.; Ceccacci, A.; Colwell, L.F.; Fay, J.F.; Flores, O.A.; Getty, K.L.; Grobler, J.A.; LaFemina, R.L.; Markel, E.J.; Migliaccio, G.; Prhavc, M.; Stahlhut, M.W.; Tomassini, J. E.; MacCoss, M.; Hazuda, D.J.; Carroll, S.S. *Antimicrob. Agents Chemother*. **2004**, *48*, 3944–3953.

[4] Píškala, A.; Šorm, F. *Collect. Czech. Chem. Commun*. **1964**, 29, 2060−2076.

[5] Winkley, M. W.; Robins, R. K. *J. Org. Chem.* **1970**, 35, 491−495.

[6] Petrie, C. R.; Cottam, H. B.; McKernan, P. A.; Robins, R. K.; Revankar, G. R. *J. Med. Chem.* **1985**, *28*, 1010–1016.

[7] Sidwell, R. W.; Huffman, J. H.; Khare, G. P.; Allen, L. B.; Witkowski, J. T.; Robins, R. K. *Science* **1972**, *177*, 1971–1973.

[8] James, J. S. *AIDS Treatment News* **1998**, 297, 7.

[9] Liu, C.; Zhou, Q.; Li, Y.; Garner, L. V.; Watkins, S. P.; Carter, L. J.; Smoot, J.; Gregg, A. C.; Daniels, A. D.; Jervey, S.; Albaiu, D. *ACS Cent. Sci.* **2020**, *6*, 315-331.

[10] Shelton, J.; Lu, X.; Hollenbaugh, J. A.; Cho, J. H.; Amblard, F.; Schinazi, R. F. *Chem. Rev.* **2016**, *116*, 14379–14455.

[11] (a) Srivastava, P. C.; Ivanovics, G. A.; Rousseau, R. J.; Robins, R. K.. *J. Org. Chem.* **1975**, *40*, 2920–2924; (b) Witkowski, J. T.; Robins, R. K.; Sidwell, R. W.; Simon, L. N. *J. Med. Chem.* **1972**, *15*, 1150–1154; (c) Bergstrom, D. E., Zhang, P., Zhou, J. *J. Chem. Soc., Perkin Trans. 1* **1994,** *20*, 3029-3034; (d) Pochet, S., Dugué, L., Meier, A., Marlière, P. *Bioorg. Med. Chem. Lett.* **1995**, *5*, 1679-1684.

[12] (a) Humble, R. W.; Middleton, D. F.; Banoub, J;, Ewing, D. F;, Boa, A. N.; Mackenzie, G. Tetrahedron letters **2011**, *52*, 6223-6227; (b) de Clercq, E.; Cools, M.; Balzarini, J.; Snoeck, R.; Andrei, G.; Hosoya, M.; Matsuda, A. *Antimicrob. Agents Chemother.* **1991**, *35*, 679-684.

[13] See for instance: (a) Pérez-Castro, I.; Caamaño, O.; Fernández, F.; García, M. D.; López, C.; de Clercq, E. *Org. Biomol. Chem.* **2007**, *5*, 3805–3813; (b) Mingdong, C.; Shijie, L.; Guanqpu, Y.; Shiyan, Y.; Xuaoli,

D. *Heterocycl. Commun.* **2000**, *6*, 421-426; (c) Manfredini, S.; Vicentini, C. B.; Manfrini, M.; Bianchi, N.; Rutigliano, A.; Mistiachi C.; Gambari, R. *Bioorg. Med. Chem*. **2000**, *8*, 2343-2346.

[14] Nájera, C.; Sansano, J. M. *Org. Biomol. Chem.* **2009**, *7*, 4567–4581.

[15] (a) Velazquez, S.; Alvarez, R.; Perez, C.; Gago, F.; De Clercq, E.; Balzarini, J.; Camarasa, M. J. *Antiviral Chemistry and Chemotherapy* **1998**, *9*, 481-489; (b) Alvarez, R.; Velazquez, S.; San-Felix, A.; Aquaro, S.; de Clercq, E.; Perno, C. F.; Camarasa, M. J. *J. Med. Chem*. **1994**, *37*, 4185-4194.

[16] Alonso, R.; Camarasa, M. J.; Alonso, G.; de las Heras, F. G. *Eur. J. Med. Chem*., **1980**, 15, 105-109.

[17] Cho, J. H.; Bernard, D. L.; Sidwell, R. W.; Kern, E. R.; Chu, C. K. *J. Med. Chem.* **2006**, *49,* 1140–1148.

[18] Huisgen, R., *Angew. Chem. Int. Ed.* **1963**, *75*, 565-598.

[19] Huisgen, R. *Angew. Chem., Int. Ed*. **1963**, *2*, 633– 696.

[20] (a) 1,3-Dipolar Cycloaddition Chemistry, Vols. 1 y 2 (Ed.: A. Padwa), Wiley Interscience, New York, 1984; (b) The Chemistry of Heterocyclic Compounds, Vol. 59: Synthetic Applications of 1,3-Dipolar Cycloaddition Chemistry Toward Heterocycles and Natural Products, (Eds.: A. Padwa, W. H. Pearson), John Wiley & Sons, Nueva York, 2002.

[21] Tornøe, C. W.; Christensen, C.; Meldal, M. *J. Org. Chem*. **2002**, *67*, 3057–3064.

[22] Rostovtsev, V. V.; Green, L. G.;. Fokin, V. V.; Sharpless, K. B. *Angew. Chem. Int. Ed*. **2002**, *41*, 2596–2599.

[23] (a) Singh, M. S.; Chowdhury, S.; Koley, S. *Tetrahedron* **2016**, *72*, 5257-5283; (b) Thirumurugan, P.; Matosiuk, D.; Jozwiak, K. *Chem. Rev.* **2013**, *11*, 4905-4979; (c) Hein, C. D.; Liu, X. M.; Wang, D. *Pharm. Res.* **2008**, *25*, 2216-2230.

[24] Hein, J. E.; Fokin, V. V. *Chem. Soc. Rev.* **2010**, *39*, 1302-1315.

[25] Berg, R.; Straub, B.; Beilstein, F. *J. Org. Chem*. **2013**, *9*, 2715-2750.

[26] (a) Özkılıç, Y., Tüzün, N. S. *Organometallics* **2016**, *35*, 2589-2599; (b) Kalvet, I.; Tammiku-Taul, J.; Mäeorg, U.; Tämm, K.; Burk, P.; Sikk, L. *ChemCatChem* **2016**, *8*, 1804-1808; (c) Cantillo, D.; Ávalos, M.; Babiano, R.; Cintas, P.; Jiménez, J. L.; Palacios, J. C. *Org. Biomol. Chem*. **2011**, *9*, 2952-2958.

[27] a) Rodionov, V. O.; Presolski, S. I.; Díaz Díaz, D.; Fokin, V. V.; Finn, M. G. *J. Am. Chem. Soc.* **2007**, *129*, 12705-12712; b) Kuang, G.-C.; Guha, P. M.; Brotherton, W. S.; Simmons, J. T.; Stankee, L. A.; Nguyen, B. T.; Clark, R. J.; Zhu, L. *J. Am. Chem. Soc*. **2011**, *133*, 13984-14001; c) Berg, R.; Straub, J.; Schreiner, E.; Mader, S.; Rominger, F.; Straub, B. F. *Adv. Synth. Catal*. **2012**, *354*, 3445-3450.

[28] Worrell, B. T.; Malik, J. A.; Fokin, V. V. *Science* **2013**, *340*, 457-460.

[29] (a) Iacobucci, C.; Lebon, A.; De Angelis, F.; Memboeuf, A. *Chem. Eur. J*. **2016**, *22*, 18690-18694; (b) Iacobucci, C., Reale, S., Gal, J. F., De Angelis, F. *Angew. Chem. Int. Ed.*, **2015**, *54*, 3065-3068.

[30] (a) Jin, L.; Romero, E. A.; Melaimi, M.; Bertrand, G. *J. Am. Chem. Soc*. **2015**, *137*, 15696-15698; (b) Jin, L., Tolentino, D. R., Melaimi, M., Bertrand, G. *Sci. Adv*. **2015**, *1*, e1500304.

[31] Makarem, A., Berg, R., Rominger, F., & Straub, B. F. *Angew. Chem. Int. Ed.* **2015***, 54*, 7431-7435.

[32] a) Kiss, L., Forro, E., Fulop, F. *Lett. Org. Chem.* **2011**, *8*, 220-228; b) Kiss, L., Forró, E., Sillanpää, R., Fülöp, F. *Tetrahedron* **2010**, *66*, 3599-3607; c) Guezguez, R., Bougrin, K., El Akri, K., Benhida, R. *Tetrahedron Lett.* **2006**, *47*, 4807-4811; d) El Akri, K., Bougrin, K., Balzarini, J., Faraj, A., Benhida, R. *Bioorg. Med. Chem. Lett.* **2007**, *17*, 6656-6659.

[33] a) Bag, S. S., Talukdar, S., Matsumoto, K., & Kundu, R. *J. Org. Chem.* **2013**, *78*, 2278-291; b) Richters, T., Krug, O., Kösters, J., Hepp, A., Müller, J. *Chem. Eur. J*. **2014**, *20*, 7811-7818; c) Liu, Y.; Peng, Y.; Lu, J.; Wang, J.; Ma, H.; Song, C.; Liu, B.; Qiao, Y.; Yu, W.; Wu, J. *Eur. J. Med. Chem.* **2018**, *143*, 137–149.

[34] Broggi, J.; Joubert, N.; Díez-González, S.; Berteina-Raboin, S.; Zevaco, T.; Nolan, S. P.; Agrofoglio, L. A. *Tetrahedron* **2009**, *65*, 1162–1170.

[35] (a) Broggi, J.; Kumamoto, H.; Berteina-Raboin, S.; Nolan, S. P.; Agrofoglio, L. A. *Eur. J. Org. Chem.* **2009**, *12*, 1880–1888; (b) Pradere, U., Roy, V., McBrayer, T. R., Schinazi, R. F., Agrofoglio, L. A. *Tetrahedron* **2008**, *64*, 9044-9051.

[36] Kolb, H. C.; Finn, M. G.; Sharpless, K. B. *Angew. Chem. Int. Ed.* **2001**, *40*, 2004–2021.

[37] a) Quader, S.; Boyd, S. E.; Jenkins, I. D.; Houston, T. A. *J. Org. Chem.* **2007**, *72*, 1962–1979; b) Zhan, W.-H.; Barnhill, H. N.; Sivakumar, K.; Tian, H.; Wang, Q. *Tetrahedron Lett.* **2005**, *46*, 1691–1695; c) Appukkuttan, P.; Dehaen, W.; Fokin, V. V.; Van der Eycken, E. *Org. Lett*. **2004**, *6*, 4223–4225; d) Deiters, A.; Cropp, T. A.; Mukerji, M.; Chin, J. W.; Anderson, J. C.; Schultz, P. G. *J. Am. Chem. Soc.* **2003**, *125*, 11782–11783; e) Lee, L. V.; Mitchell, M. L.; Huang, S.-J.; Fokin, V. V.; Sharpless, K. B.; Wong, C.-H. *J. Am. Chem. Soc*. **2003**, *125*, 9588– 9589.

[38] Durán Pachón, L.; Van Maarseveen, J. H.; Rothenberg, R. *Adv. Synth. Catal*. **2005**, *347*, 811–815.

[39] (a) Saito, Y.; Escuret, V.; Durantel, D.; Zoulim, F.; Schinazi, R. F.; Agrofoglio, L. A. *Bioorg. Med. Chem.* **2003**, *11*, 3633-3639; (b) Ewing, D. F.; Goethals, G.; Mackenzie, G.; Martin, P.; Ronco, G.; Vanbaelinghem, L.; Villa, P. *J. Carbohydr. Chem*. **1999**, *18*, 441–450; (c) Ewing D. F.; Goethals, G.; Mackenzie, G.; Martin, P.; Ronco G.; Vanbaelinghem, L.; Villa P. *Carbohydr. Res*. **1999**, 190–196.

[40] Chretien, F.; Gross, B. *Tetrahedron* **1982**, *38*, 103-112.

[41] Baboonian, C.; Davies, M. J;, Booth, J. C.; McKenna, W. J. *Springer, Berlin, Heidelberg* **1997**, 31-52.

[42] Repass, G. L.; Palmer, W. C.; Stancampiano, F. F. *Cleve*. *Clin*. *J. Med*. **2014**, *81*, 537-543.

[43] Frisk, G.; Diderholm, H. *J. Infect.* **1997**, *34*, 205-210.

[44] Dotta, F.; Censini, S.; van Halteren, A. G.; Marselli, L.; Masini, M.; Dionisi, S.; Elliott, J. F. *Proc. Natl. Acad. Sci. U.S.A* **2007**, *104*, 5115-5120.

IV. SUMMARY

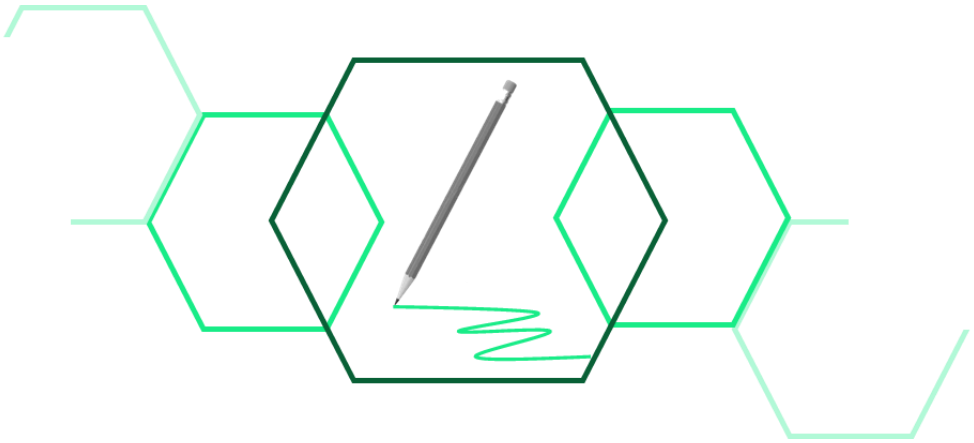

SUMMARY

I) Two synthetic strategies developed in our research group have been optimized (Scheme S-1), to prepare the key ketone **36**. Synthetic pathway B is the most robust, reproducible and efficient 6-steps approach to prepare **36** on a multigram scale in 49% overall yield.

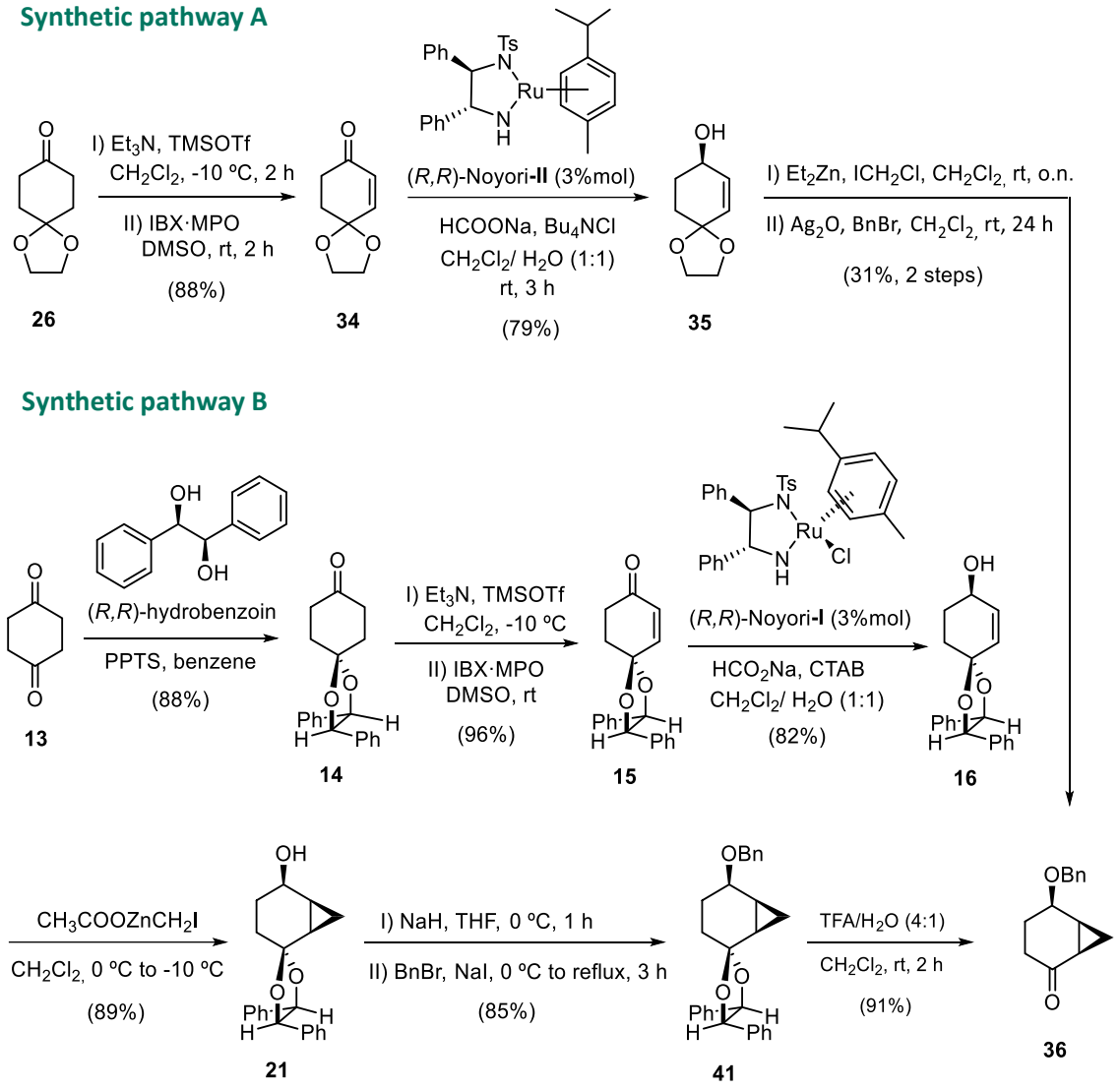

Scheme S-1. Optimization of synthetic pathways (A and B) to prepare key intermediate **36**.

Ketone **36** has been used as starting material for the preparation of conformationally restricted bicyclo[4.1.0]heptane nucleoside analogues.

II) In order to complete the biological studies of the 5'-hydroxybicyclo[4.1.0]heptane NAs previously prepared in our research group, the cytosine analogue **28** has been synthesised in 7% overall yield in 11 steps from ketone **36**. The cytosine analogue **28** has been evaluated against several viruses, but, unfortunately, it did not show significant activity or cytotoxicity.

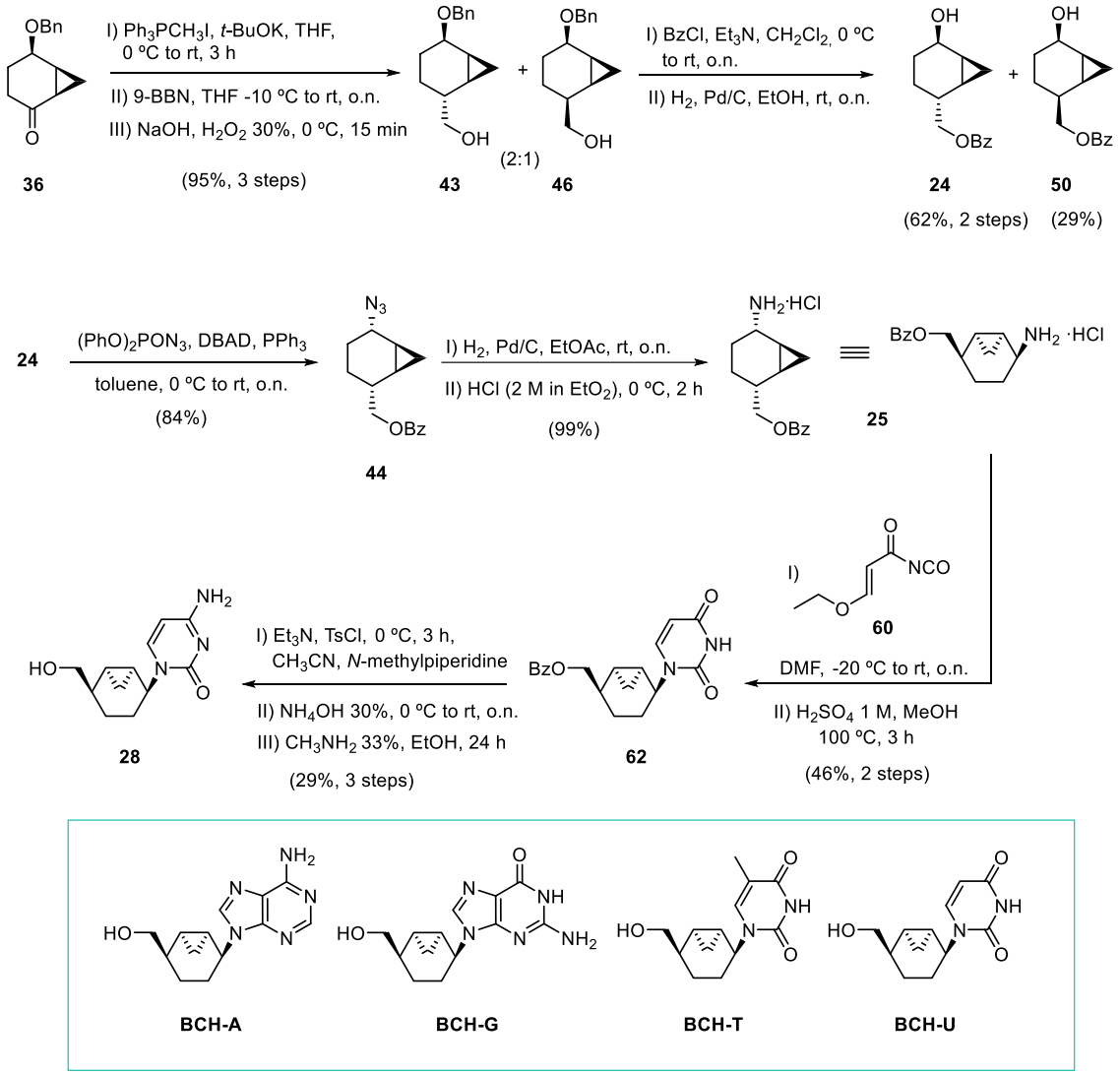

Scheme S-2. Synthesis of cytosine 5'-hydroxybicyclo[4.1.0]heptane nucleoside analogue **28**.

Finally, the cellular HSV-1 and VZV TKs affinity of the cytosine analogue **28** and previously synthesised 5'-hydroxybicyclo[4.1.0]heptane NAs (**BCH**-(**A**, **G**, **T**, **U**) were evaluated. Compound **BCH-T** had an interesting great affinity for HSV-TK (EC_{50} = 1.6 ± 0.1 µg/mL) which was consistent with our computational model performed for the first stage of phosphorylation.

III) A novel family of 5'-hydroxymethyl-4'-hydroxybicyclo[4.1.0]heptan-2'-yl NAs based on D-cyclohexenyl G has been synthesised from ketone **36** (Scheme S-3). Thymine and guanine nucleosides analogues **104** and **116** have been obtained in 11 and 12 steps and 36% and 20% overall yield, respectively. The thymine epimer **117** and the thymine alkene **123** have been synthesised in 13 steps and 13% and 6% overall yield, respectively. These four NAs have been screened for antiviral activity, although none of them showed significant activity.

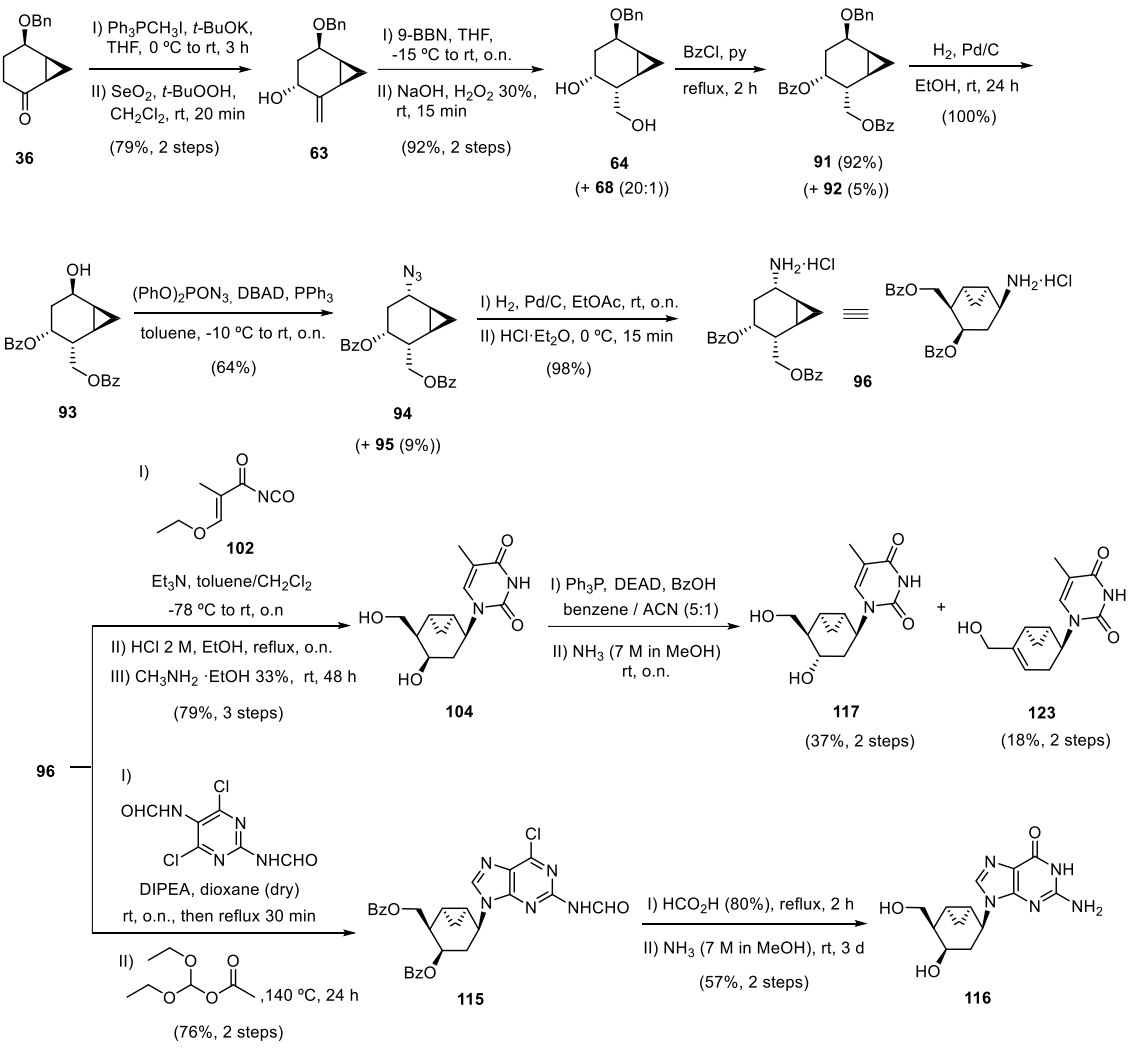

Scheme S-3. Enantiopure synthesis of thymine and guanine 5'-hydroxymethyl-4'-hydroxybicyclo[4.1.0]heptan-2'-yl NAs.

IV) A new family of 1,2,3-triazolo-carbanucleosides has been synthesised from azide **94** (Scheme S-4). This approach has allowed the preparation of the four 4-substituted-1,2,3-triazolo-carbanucleosides **148**, **152**, **150** and **151** *via* CuAAc in 2 steps and 73%, 71%, 83% and 80% overall yield, respectively. Also, the 4,5-substituted-1,2,3-triazolo-carbanucleoside **153** has been

synthesised in one step *via* cycloaddition and 55% yield. The biological activity of these analogues against several viruses has been evaluated, although only **151** showed a considerable activity against Coxsackie B4 virus (EC_{50} = 13.5-9.4 µg/mL).

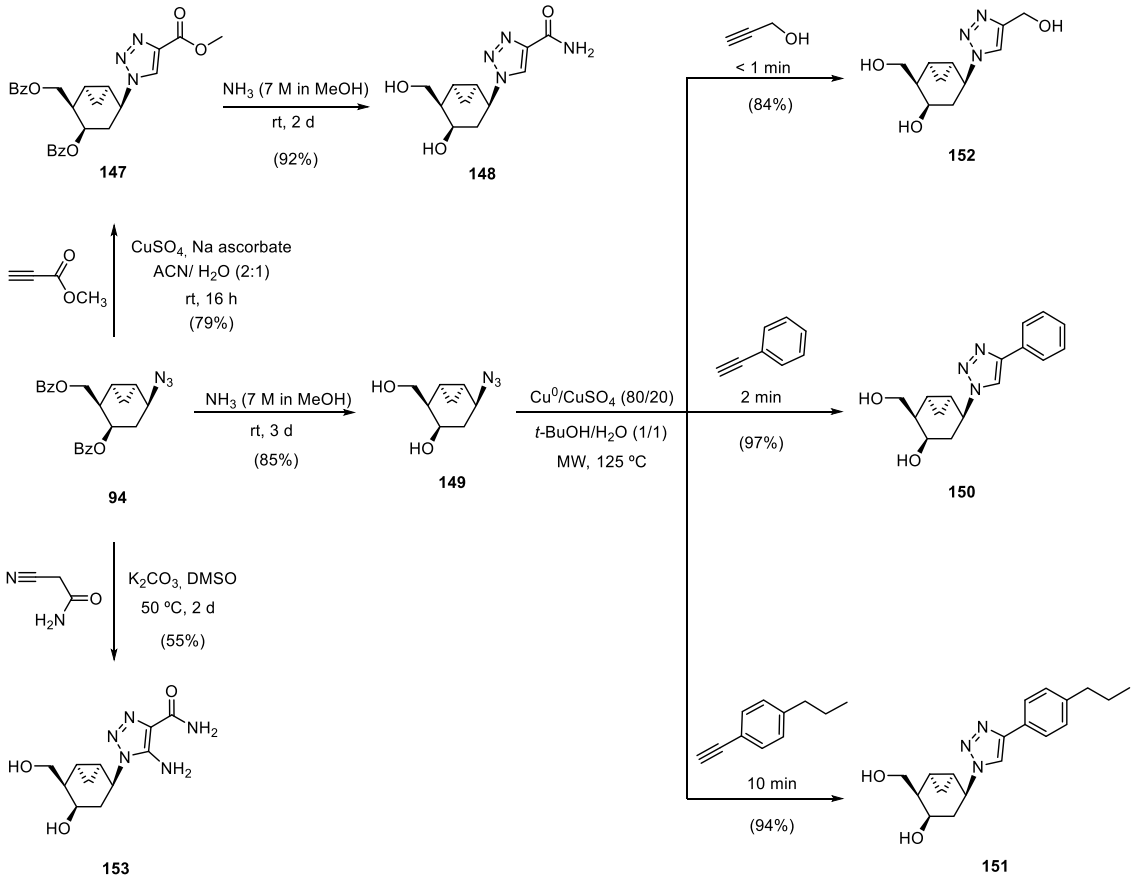

Scheme S-4. Synthesis of new substituted triazolo-carbanucleosides compounds from azide **94.**

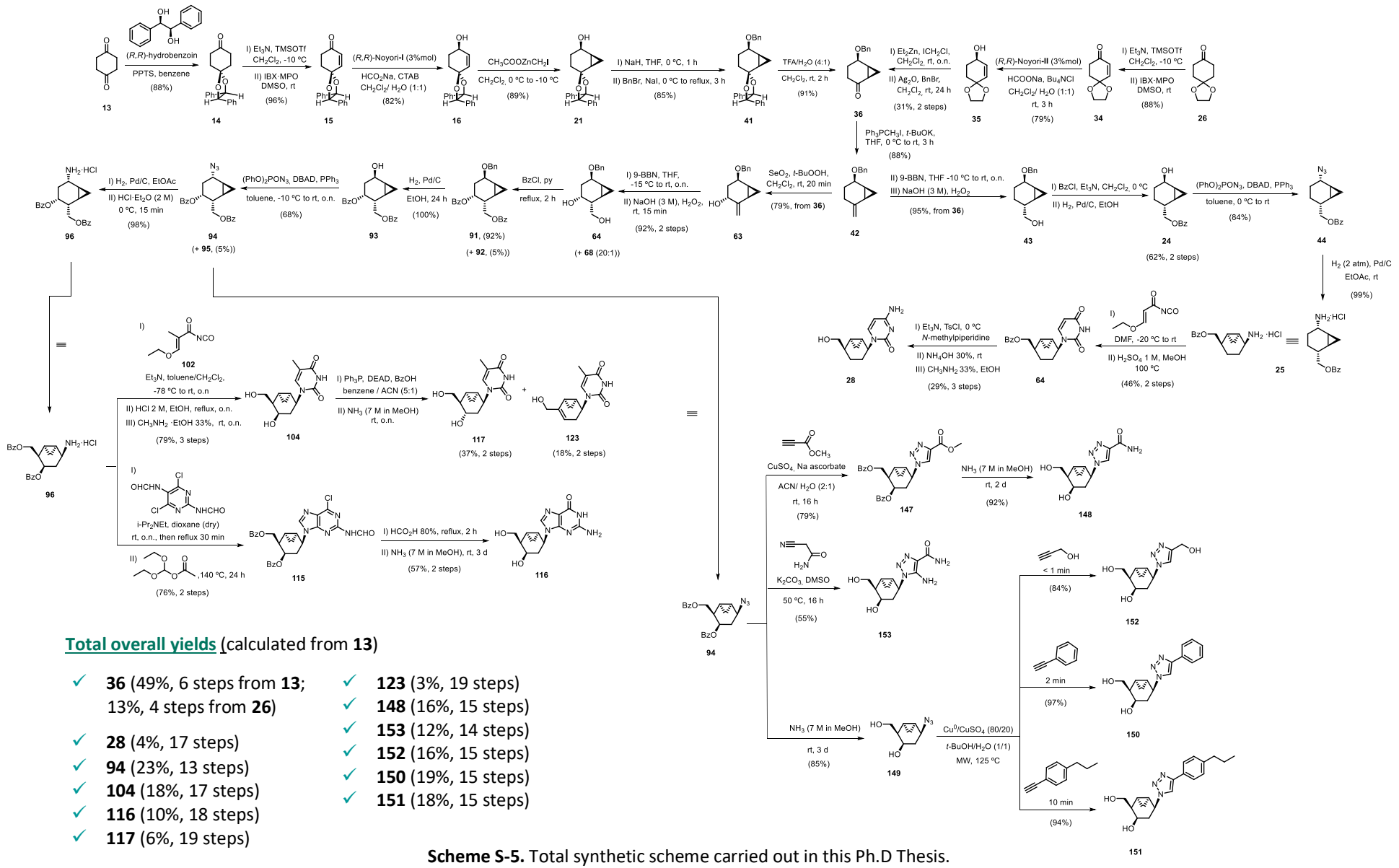

Total overall yields (calculated from **13**)

- ✓ **36** (49%, 6 steps from **13**; 13%, 4 steps from **26**)
- ✓ **28** (4%, 17 steps)
- ✓ **94** (23%, 13 steps)
- ✓ **104** (18%, 17 steps)
- ✓ **116** (10%, 18 steps)
- ✓ **117** (6%, 19 steps)
- ✓ **123** (3%, 19 steps)
- ✓ **148** (16%, 15 steps)
- ✓ **153** (12%, 14 steps)
- ✓ **152** (16%, 15 steps)
- ✓ **150** (19%, 15 steps)
- ✓ **151** (18%, 15 steps)

Scheme S-5. Total synthetic scheme carried out in this Ph.D Thesis.

V. EXPERIMENTAL SECTION

1. GENERAL PROCEDURES

Reagents and solvents

All commercially available reagents were used as received. Solvents were dried by distillation over the appropriate drying agents: CH_2Cl_2 (CaH_2), THF (Na^0), ACN (CaH_2), toluene (Na^0), benzene (Na^0), dioxane (molecular sieve 0.4 nm). When required, reactions were performed avoiding moisture by standard procedures and under nitrogen or argon atmosphere.

Chromatography (TLC and FCC)

All the reactions were monitored by analytical thin-layer chromatography (TLC) using silica gel 60 F254 pre-coated aluminium plates (0.25 mm thickness). Compounds were visualized using an UV lamp at 254 nm and/or using a $KMnO_4$/KOH aqueous solution or Vanillin solution. Flash column chromatography (FCC) was performed using silica gel (230-400 mesh).

Spectroscopy

Nuclear magnetic resonance spectra (NMR) were registered at the *Servei de Ressonància Magnètica Nuclear* of the *Universitat Autònoma de Barcelona*. ^{1}H-NMR spectra were recorded on Bruker DPX250 (250 MHz), Bruker DPX360 (360 MHz) and Bruker AR430 (400 MHz) spectrometers. Proton chemical shifts (δ) are reported in ppm ($CDCl_3$, 7.26 ppm, MeOH-d_4, 3.31 ppm and DMSO-d_6, 2.50 ppm). ^{13}C-NMR spectra were recorded with complete proton decoupling on Bruker DPX250 (62.5 MHz) and Bruker AR430 (100.6 MHz) spectrometers. Carbon chemical shifts are reported in ppm ($CDCl_3$, 77.16 ppm, MeOH-d_4, 49.00 ppm and DMSO-d_6, 39.52 ppm). NMR signals were assigned with the help of COSY, dept135, HSQC, HMBC and NOESY experiments. All spectra were measured at 298 K.

The abbreviations used to describe signal multiplicities are: s (singlet), d (doublet), t (triplet), q (quartet), quint (quintet), sext (sextet), dd (doublet of doublets), ddd (doublet of doublet of doublets), dddd (doublet of doublet of doublet of doublets), ddt (doublet of doublet of triplets), dtd (doublet of triplet of doublets), dt (doublet of triplets), dq (doublet of quartets), td (triplet of doublets), m (multiplet), b (broad signal) and *J* to indicate coupling constants.

Infrared spectra (IR) were recorded on a Bruker Tensor 27 Spectrophotometer equipped with a Golden Gate Single Refraction Diamond ATR (Attenuated Total Reflectance) accessory at *Servei d'Anàlisi Química* of the *Universitat Autònoma de Barcelona*. Peaks are reported in cm^{-1}.

Single crystal X-ray diffraction were recorded on three-circle SMART APEX single crystal diffractometer from Bruker provided with a CCD APEX area detector, molybdenum anode X-ray tube and *Krioflex* low-temperature device which allows measurements from T_{room} to T = -180 °C. X-ray crystal structures was performed by Dr. Ángel Álvarez from the *Servei Difracció Raigs X* of *Universitat Autónoma de Barcelona*.

Mass Spectrometry

High resolution mass spectra (HRMS) were recorded at the *Servei d'Anàlisi Química* of the *Universitat Autònoma de Barcelona* in a Bruker micrOTOFQ spectrometer using ESIMS (QTOF) or at *Parque Científico Tecnológico* of the *Universidad de Burgos* in a Micromass AutoSpec using EI-HR.

Optical Rotatory Power

Specific optical rotations ($[\alpha]_D^{20}$) were measured at 20 ± 2 °C and 589.6 nm using a AUTOPOL I automatic polarimeter of RUDOLPH RESEARCH ANALYTICAL and using a 0.1 dm long cuvette at *Servei d'Anàlisi Química (SAQ)* in the *Universitat Autònoma de Barcelona*

Melting Points (MP)

Melting points were determined using a Koffler-Reichert apparatus and were not corrected.

Microwave (MW)

The present work was carried out with a CEM Discover® microwave instrument (Figure ES-1, a), which allowed us to set the following parameters: temperature, reaction time, power, maximum pressure and PowerMAX™.

Temperature stands for the set temperature that will be maintained during the reaction time. Power corresponds to the maximum power at which the sample will be irradiated, albeit the power may change in the course of the reaction. PowerMAX™ is a technology that allows introducing more energy in the reaction (by increasing the power) while maintaining the temperature, by simultaneous cooling of the reaction with compressed gas on the outside of the reaction vessel. In all the experiments performed in the present thesis, power was set at 250 W, maximum pressure at 250 psi and the PowerMAX™ option was always enabled.

All the reactions were conducted in 10 mL glass vessels sealed with a septum (Figure ES-1, b). Temperature was measured with an infrared sensor placed under the reaction vessel. All experiments were performed using a stirring option whereby the contents of the vessel were stirred by means of a rotating magnetic plate located below the floor of the microwave cavity and a Telfon-coated magnetic stir bar in the vessel.

a) b)

Figure ES-1. a) CEM Discover® microwave instrument used in this thesis work; b) 10 mL glass reaction vessel, sealed with a click septum and equipped with stirring bar.

In this work some of the compounds prepared were already described in the literature. Therefore, only the physical and/or spectroscopic data necessary for their identification are presented.

2. EXPERIMENTAL DESCRIPTION

2.1. CHATER I. Synthesis of key pivotal intermediate 36.

2.1.1. Synthetic pathway A.

2.1.1.1 Synthesis of *o*-Iodoxybenzoic acid, IBX.

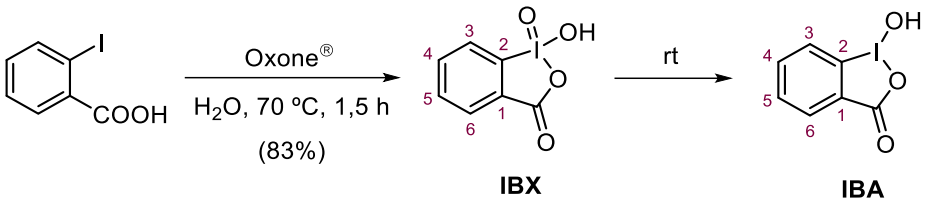

2-Iodobenzoic acid (15.05 g, 59.47 mmol) was added to a solution of Oxone® (2 $KHSO_5$ – $KHSO_4$ – K_2SO_4 , 73.05 g, 118.82 mmol) in deionized water (300 mL) and the reaction mixture was warmed to 70-73 °C over 30 min and was mechanically stirred at this temperature for 1,5 h. After that time, the suspension was cooled to 0 °C and stirred slowly for a further 1 h. The mixture was then filtered, and the solid was washed with cooled water (3 x 100 mL) and acetone (2 x 50 mL) to furnish a white crystalline solid identified as *o*-iodoxybenzoic acid, **IBX** (13.82 g, 48.08 mmol, 83% yield) as a white solid. Mother and washing liquors were oxidizing and acid. They were treated with solid N_2SO_3 and neutralized with NaOH (1 M) before disposal.

IBX must be stored in a dark bottle at 2-8 °C in order to avoid the disproportionation to *o*-iodosobenzoic acid, **IBA** at room temperature.

Spectroscopic data of **IBX**

^{1}H-NMR (250 MHz, DMSO-d_6): δ 8.15 (d, $J_{3,4}$ = 7.9 Hz, 1H, H-3), 8.04 (m, 2H, H-4, H-6), 7.84 (t, $J_{5,4}$ = $J_{5,6}$ = 7.4 Hz, 1H, H-5).

^{13}C-NMR (101 MHz, DMSO-d_6) δ: 167.6 (*C*OO), 146.6 (C-1), 133.5 (C-3), 133.0 (C-4), 131.4 (C-2), 130.1 (C-6), 125.0 (C-5).

Spectroscopic data of **IBA**

^{1}H-NMR (250 MHz, DMSO-d_6): δ 8.04 – 7.92 (m, 2H, H-4, H-6), 7.84 (d, $J_{3,4}$ = 7.6 Hz, 1H, H-3), 7.70 (t, $J_{5,4}$ = $J_{5,6}$ = 7.3, 1H, H-5).

^{13}C-NMR (101 MHz, DMSO-d_6) δ 167.7 (*C*OO), 134.5 (C-3), 131.5 (C-1), 131.1 (C-4), 130.4 (C-6), 126.3 (C-5), 120.4 (C-2).

2.1.1.2 Synthesis of 1,4-dioxaspiro[4.5]dec-6-en-8-one, 34.

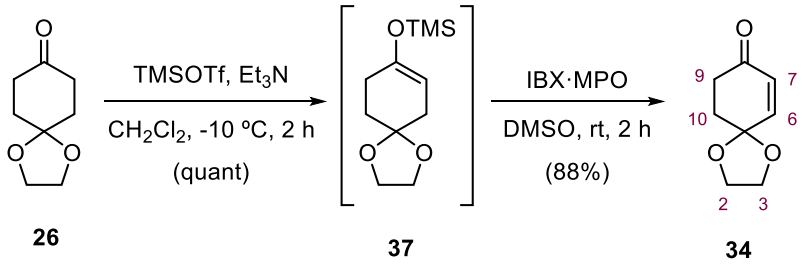

26 **37** **34**

To a stirred solution of monoketal **26** (3.00 g, 18.7 mmol) and Et_3N (5.20 mL, 37.3 mmol) in dry CH_2Cl_2 (130 mL) at -10 °C, under nitrogen atmosphere, was added dropwise TMSOTf (4.20 mL, 23.2 mmol) and the reaction mixture was stirred for 2 h and then concentrated under reduced pressure to obtain crude **221**, which was used in the next step without further purification.

Then, a solution of the crude **221** in DMSO (50 mL) was poured onto a solution of **IBX** (10.4 g, 37.3 mmol) and MPO (4.82 mg, 37.3 mmol) in DMSO (35 mL), that had been previously stirred during 1 h until becoming a clearly solution. After 2 h of stirring at room temperature, CH_2Cl_2 (150 mL) and a saturated aqueous $NaHCO_3$ solution (150 mL) were added. The two phases were separated and the aqueous layer was extracted with CH_2Cl_2 (2 x 100 mL). The organic phase was concentrated under reduced pressure and washed with a solution of HCl 5% (100 mL) and brine (2 x 100 mL), dried (Na_2SO_4) , concentrated under vacuum to provide enone **34** (2.52 g, 16.4 mmol, 88% yield) as a yellow oil.

Spectroscopic data of **34**

^{1}H-NMR (250 MHz, $CDCl_3$): δ 6.60 (d, $J_{6,7}$ = 10.2 Hz, 1H, H-6), 5.99 (d, $J_{7,6}$ = 10.2 Hz, 1H, H-7), 4.11 – 3.98 (m, 4H, H-2, H-3), 2.62 (t, $J_{9,10}$ = 6.5 Hz, 2H, H-9), 2.19 (t, $J_{10,9}$ = 6.6 Hz, 2H, H-10).

^{13}C-NMR (90 MHz, $CDCl_3$): δ 198.8 (*C*=O), 146.5 (C-6), 130.6 (C-7), 104.0 (C-5), 65.2 (C-2, C-3), 35.4/ 33.0 (C-9, C-10).

R_f of **37** (hexane-EtOAc 4:1) = 0.43 ($KMnO_4$).

R_f of **34** (hexane-EtOAc 4:1) = 0.18 ($KMnO_4$).

2.1.1.3. Activation of the (*R*,*R*)-Noyori-I catalyst and subsequent synthesis of (*8R*)-1,4-dioxaspiro[4.5]dec-6-en-8-ol, 35.

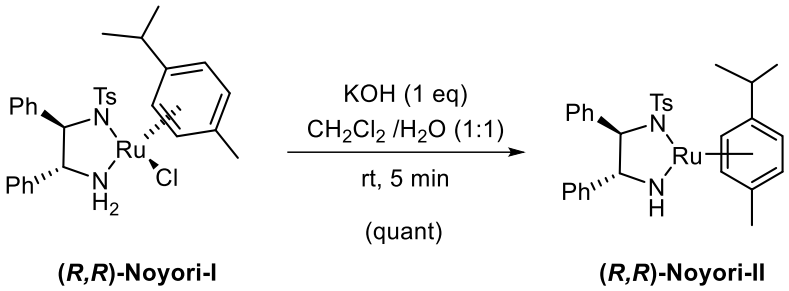

(*R*,*R*)-Noyori-I **(*R*,*R*)-Noyori-II**

To a solution of commercially RuCl(*p*-cymene)[(*R*,*R*)-Ts-DPEN] catalyst ((*R*,*R*)-Noyori-**I**, 13 mg, 0.02 mmol) in CH_2Cl_2 (1 mL), 0.02 M aqueous solution of KOH (1 mL, 0.02 mmol) was added at rt. The mixture was vigorously stirred for 5 min (the solution turned from brown to purple) and then, the solution was directly used for the next reduction reaction.

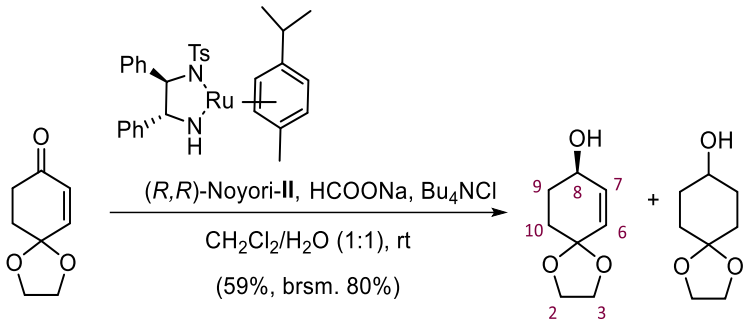

34 **35** **38**

To a stirred solution of enone **34** (104 mg, 0.68 mmol) in a biphasic media of CH_2Cl_2 (2.3 mL) and water (2.3 mL), tetrabutylammonium chloride (57 mg, 0.20 mmol), sodium formate (139 mg, 2.04 mmol) and the freshly prepared (*R,R*)-Noyori-**II** catalyst solution (2 mL, 0.02 mmol) were sequentially added at room temperature. The reaction mixture was allowed to stir for 3 h, when TLC analysis (diethyl ether 100%) shows totally consumption of the starting material. Then, the phases were separated and the aqueous layer was extracted with more CH_2Cl_2 (2 x 2 mL) and the organic layers were concentrated under reduced pressure affording a yellow oil, which was purified by column chromatography (SiO_2, Et_2O 100%) to furnish allylic alcohol (*R*)-**35** and the totally hydrogenated derivative **38** in a 6:1 ratio (63 mg, 0.40 mmol, 59% yield) as a yellow oil. Considering the recovered starting material **34** (26 mg, 0.17 mmol) the yield arises until 80%.

Spectroscopic and physical data of **35**

^{1}H-NMR (250 MHz, $CDCl_3$): δ 5.94 (ddd, $J_{7,6}$ = 10.1 Hz, $J_{7,8}$ = 2.8 Hz, $J_{7,9}$ = 1.1 Hz, 1H, H-7), 5.61 (dt, $J_{6,7}$ = 10.1 Hz, $J_{6,8}$ = $J_{6,10}$ = 1.5 Hz, 1H, H-6), 4.29 – 4.12 (m, 1H, H-8), 4.05 – 3.85 (m, 4H, H-2, H-3), 2.17 – 2.02 (m, 1H, H-9), 2.00 – 1.89 (m, 1H, H-9), 1.85 – 1.65 (m, 2H, H-10).

^{13}C-NMR (90 MHz, $CDCl_3$) δ: 135.3 (C-7), 129.0 (C-6), 105.2 (C-5), 66.0 (C-8), 64.8/ 64.6 (C-2, C-3), 31.1/ 30.7 (C-9, C-10).

R_f (Et_2O 100%) = 0.20 ($KMnO_4$).

$[\alpha]_D^{20}$= +39.0 (*c* 1.2, $CHCl_3$).

2.1.1.4. (1*R*,5*R*,6*S*)-5-(benzyloxy)bicyclo[4.1.0]heptan-2-one, 36.

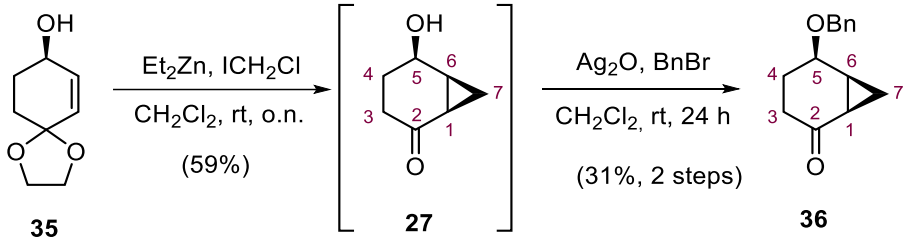

To a stirred solution of allylic alcohol **35** (314 mg, 2.01 mmol) in anhydrous CH_2Cl_2 (10 mL) was added Et_2Zn (4 mL, 4.02 mmol, 1 M in hexane) at 0 °C and the mixture was stirred 5 min at this temperature. At this time, a solution of ICH_2Cl (600 µL, 8.30 mmol) in CH_2Cl_2 (3 mL) was added dropwise via syringe at 0 °C, and the mixture was stirred overnight allowing it to warm to room temperature. Then, a saturated aqueous $NaHCO_3$ solution (10 mL) was added, and the aqueous layer was extracted with CH_2Cl_2 (3 x 10 mL). The organic layer was dried (Na_2SO_4), concentrated under reduced pressure (with vacuum controller) and purified by flash column chromatography (SiO_2, hexane-EtO_2, 4:1) furnishing ketone **27** (149 mg, 1.19 mmol, 59% yield) as a colourless oil. Due to the volatility of **27**, the crude was used without further purification to the next step.

To a solution of crude of the hydroxyacetone **27** in CH_2Cl_2 (4 mL) was added Ag_2O (560 mg, 2.41 mmol) and benzyl bromide (340 µL, 2.81 mmol). The mixture was stirred at room temperature for 24 h at room temperature, filtered through Celite® pad, and concentrated *in vacuo*. The crude was purified by flash column chromatography (SiO_2, hexane-EtOAc, 6:1) to furnish **36** (135 mg, 0.623 mmol, 31% yield) as a pale oil.

Spectroscopic and physical data of **27**

^{1}H-NMR (400 MHz, $CDCl_3$) δ: 4.42 (dddd, $J_{5,4ax}$ = 10.1 Hz, $J_{5,4eq/6}$ = 5.2 Hz, $J_{5,4eq/6}$ = 4.1 Hz, $J_{5,3ax}$ = 0.6 Hz, 1H, H-5), 2.37 (ddd, J_{gem}= 18.3 Hz, $J_{3eq,4ax}$ = 5.5 Hz, $J_{3eq,4eq}$ = 3.6 Hz, 1H, H-3eq), 2.15 (dddd, J_{gem} = 18.4 Hz, $J_{3ax,4ax}$ = 12.1 Hz, $J_{3ax,4eq}$ = 6.6 Hz, $J_{3ax,5}$ = 0.8 Hz, 1H, H-3ax), 1.98 – 1.83 (m, 3H, H-1, H-6, H-4eq), 1.63 (dddd, J_{gem} = 13.8 Hz, $J_{4ax,3ax}$ = 12.1 Hz, $J_{4ax,5}$ = 10.3 Hz, $J_{4ax,3eq}$ = 5.6 Hz, 1H, H-4ax), 1.44 (q, J_{gem} = $J_{7endo,1}$ = $J_{7endo,6}$ = 5.3 Hz, 1H, H-7endo), 1.14 (ddd, $J_{7exo,1/6}$ = 9.8 Hz, $J_{7exo,1/6}$ = 7.7 Hz, J_{gem} = 5.4 Hz, 1H, H-7exo).

^{13}C-NMR (100 MHz, $CDCl_3$) δ: 207.5 (C-2), 65.3 (C-5), 34.8 (C-3), 26.8 (C-1), 26.7 (C-4), 23.3 (C-6), 8.0 (C-7).

COSY, **HSQC**, **DEPT-135** and **NOESY** experiments have been recorded.

IR (ATR): 3359, 2919, 2850, 1659, 1345, 1066, 1041 cm^{-1}.

HRMS (ESI+): Calcd. for $[C_7H_{10}O_2+Na]^+$: 149.0573, Found: 149.0576.

$[\alpha]_D^{20}$= +78.5 (*c* 0.65, $CHCl_3$).

Spectroscopic and physical data of **36**

^{1}H-NMR (400 MHz, $CDCl_3$): δ 7.39 – 7.34 (m, 4H, H-Ar), 7.32 – 7.28 (m, 1H, H-Ar), 4.73 (d, J_{gem} = 11.9 Hz, 1H, CH_2-Ph), 4.64 (d, J_{gem} = 11.9 Hz, 1H, CH_2-Ph), 4.15 (dt, $J_{5,4ax}$ = 9.3 Hz, $J_{5,4eq}$ = $J_{5,6}$ = 4.9 Hz, 1H, H-5), 2.42 (dt, J_{gem} = 17.7 Hz, $J_{3eq,4}$ = 5.5 Hz, 1H, H-3eq), 2.12 (ddd, J_{gem} = 17.7 Hz, $J_{3ax,4x}$ = 10.7 Hz, $J_{3ax,4eq}$ = 6.5 Hz, 1H, H-3ax), 2.05 – 1.93 (m, 2H, H-4), 1.88 – 1.71 (m, 2H, H-1, H-6), 1.50 (q, J_{gem} = $J_{7endo,6}$ = $J_{7endo,1}$ = 5.4 Hz, 1H, H-7endo), 1.24 (td, $J_{7exo,6}$ = $J_{7exo,1}$ = 9.1 Hz, J_{gem} = 5.4 Hz, 1H, H-7exo).

^{13}C-NMR (100 MHz, $CDCl_3$): δ 208.2 (C-2), 138.5 (C-Ar), 128.6/ 128.2/ 127.9/ 127.8 (C-Ar), 71.3 (C-5), 70.6 (CH_2-Ph), 34.4 (C-3), 26.5 (C-4), 25.5 (C-1), 21.3 (C-6), 9.5 (C-7).

IR (ATR): ν 3028, 2857, 1692 ($C=O_{st}$), 1342, 1075, 1028, 881, 631 cm^{-1}.

HRMS (ESI+): Calcd. for $[C_{14}H_{16}O_2+H]^+$: 217.1229, Found: 217.1231.

R_f (hexane-EtOAc, 2:1) = 0.39; ($CHCl_3$ 100%) = 0.22 ($KMnO_4$).

$[\alpha]_D^{20}$= +62.6 (*c* 1.45, $CHCl_3$).

2.1.2. Synthetic pathway B.

2.1.2.1. Synthesis of (2*R*,3*R*)-2,3-diphenyl-1,4-dioxaspiro[4.5]decan-8-one, 14.

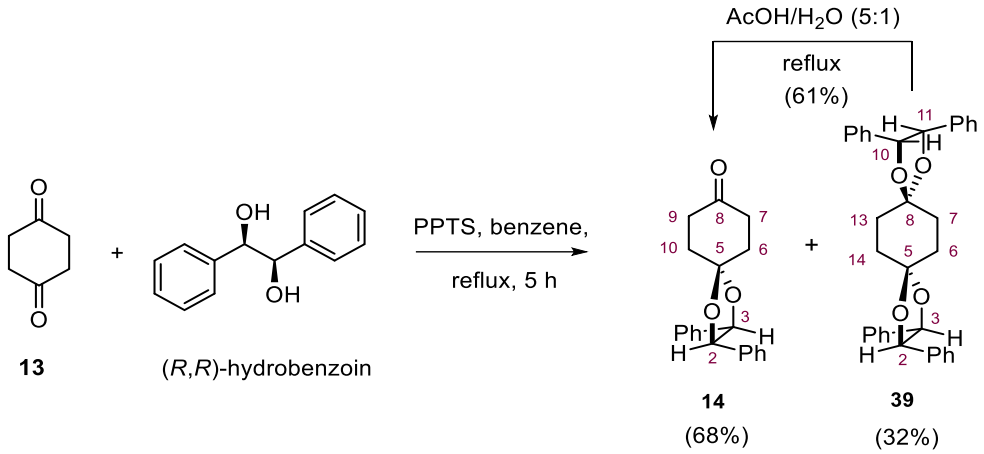

A mixture of 1,4-cyclohexanedione, **13**, (17.6 g, 157 mmol), (*R*,*R*)-hydrobenzoin (16.4 g, 76.5 mmol) and PPTS (1.92 g, 7.66 mmol) was dissolved in benzene (300 mL). Then, a Dean-Stark apparatus was coupled and the reaction mixture was stirred at reflux temperature for 5 h. The reaction mixture was cooled to room temperature and concentrated under vacuum, and the resulting oil was purified by flash column chromatography (SiO_2, gradient of hexane-EtOAc, 10:1→8:1→5:1) to provide the monoketal **14** (16.1 g, 52.2 mmol, 68% yield) and the corresponding bisketal **39** (6.18 g, 12.3 mmol, 32% yield) both as white solids.

The bisketal **39** can be partially nonhydrolyzed by dissolving it in a 5:1 mixture of acetic acid/water, and allowing it to stir at reflux temperature until TLC analysis (hexane-EtOAc, 4:1) shows totally consumption of bisketal product (4-6 h). Same work-up and purification as above, afforded an extra amount of the monoketal **14** (2.31 g, 7.49 mmol, 61% yield). Thus, the monoketal **14** was obtained in 88% overall yield.

Spectroscopic and physical data of **14**

^{1}H-NMR (250 MHz, $CDCl_3$): δ 7.38 – 7.28 (m, 6H, H-Ar), 7.28 – 7.18 (m, 4H, H-Ar), 4.87 (s, 2H, H-2, H-3), 2.69 (t, $J_{7/9,6/10}$ = 7.0 Hz, 4H, H-7, H-9), 2.39 – 2.27 (m, 4H, H-6, H-10).

^{13}C-NMR (100 MHz, $CDCl_3$): δ 210.2 (C-8), 136.2/ 128.6/ 126.8 (C-Ar), 107.9 (C-5), 85.6 (C-2, C-3), 38.2 (C-7, C-9), 35.4 (C-6, C-10).

R_f (hexane-EtOAc, 8:1) = 0.25 ($KMnO_4$).

Spectroscopic and physical data of **39**

^{1}H-NMR (250 MHz, $CDCl_3$): δ 7.42 – 7.25 (m, 12H, H-Ar), 7.32 – 7.21 (m, 8H, H-Ar), 4.82 (s, 4H, H-2, H-3, H10, H-11), 2.29 (s, 8H, H-6, H-7, H-13, H-14).

^{13}C-NMR (100 MHz, $CDCl_3$): δ 137.1/ 128.5/ 128.4/ 126.8 (C-Ar), 109.2 (C-5, C-8), 85.4 (C-2, C-3, C-13, C-14), 33.8 (C-6, C-7, C-9, C-10).

R_f (hexane-EtOAc, 4:1) = 0.42 ($KMnO_4$).

2.1.2.2. Synthesis of (2*R*,3*R*)-2,3-diphenyl-1,4-dioxaspiro[4.5]decan-6-ene-8-one, 15.

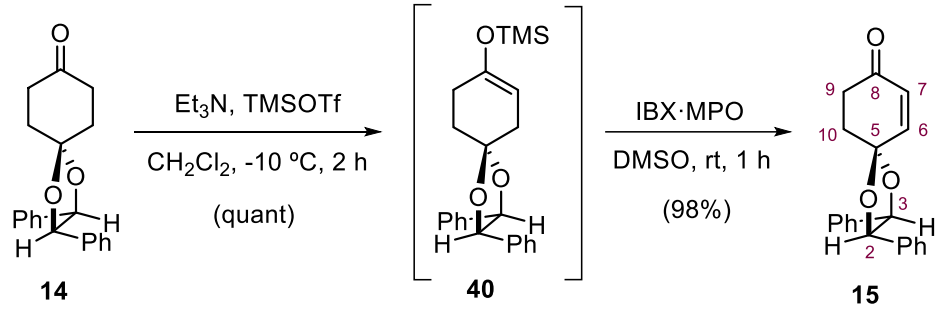

To a stirred solution of monoketal **14** (9.64 g, 31.3 mmol) in anhydrous CH_2Cl_2 (200 mL) at -10 °C, under nitrogen atmosphere, Et_3N (no dry) (6.50 mL, 46.6 mmol) was added dropwise and was stirred 15 min. Then, TMSOTf (8.48 mL, 46.92 mmol) was slowly added dropwise and the reaction mixture was stirred until TLC analysis (hexane-EtOAc, 5:1) shows totally consumption of the starting material (2 h).

Then, a solution of **IBX** (13.60 g, 48.5 mmol) and MPO (5.91 g, 47.2 mmol) in DMSO (200 mL) was stirred during 1 h until becoming a clearly yellow solution and then, poured onto the reaction mixture. After 1 h of stirring at room temperature, a saturated aqueous $Na_2S_2O_5$ and $NaHCO_3$ solution (150 mL) was added and stirred for 30 min. After that time, diethyl ether (100 mL) was added, and the aqueous layer was extracted with more diethyl ether (2 x 100 mL). The organic phase was finally washed with saturated aqueous NaCl solution (100 mL) and then, it was dried (Na_2SO_4) and concentrated under vacuum to provide enone **15** (9.36 g, 30.5 mmol, 98% yield) as a pale yellow oil which can be used without purification in the next step.

Spectroscopic and physical data of **15**

^{1}H-NMR (250 MHz, $CDCl_3$): δ 7.40 – 7.25 (m, 6H, H-Ar), 7.25 – 7.10 (m, 4H, H-Ar), 6.93 (ddd, $J_{6,7}$ = 10.2 Hz, $J_{6,10}$ = 1.4 Hz, $J_{6,10}$ = 0.5 Hz, 1H, H-6), 6.13 (dd, $J_{7,6}$ = 10.2 Hz, $J_{7,9}$ = 0.8 Hz, 1H, H-7), 4.88 (d, $J_{3,2}$ = 8.5 Hz, 1H, H-3), 4.80 (d, $J_{2,3}$ = 8.5 Hz, 1H, H-2), 2.81 (ddt, J = 16.8 Hz, J'=9.3 Hz, J'' = 6.4 Hz, 1H, H-9/H-10), 2.68 (dt, J = 16.8 Hz, J' = J'' =5.5 Hz, 1H, H-9/H-10), 2.60-2.40 (m, 2H, H-9, H-10).

^{13}C-NMR (62.5 MHz, $CDCl_3$): δ 198.6 (C-8), 146.8 (C-6), 135.7/ 135.5 (C-Ar), 130.9 (C-7), 128.8/ 128.8/ 128.7/ 126.7 (C-Ar), 104.6 (C-5), 85.9/ 85.4 (C-2, C-3), 35.3/ 34.1 (C-9, C-10).

R_f of **40** (hexane-EtOAc, 5:1) = 0.69 ($KMnO_4$).

R_f of **15** (hexane-EtOAc, 5:1) = 0.20 ($KMnO_4$).

2.1.2.3. Synthesis of (2*R*,3*R*,8*R*)-2,3-diphenyl-1,4-dioxaspiro[4.5]decan-6-ene-8-ol, 16.

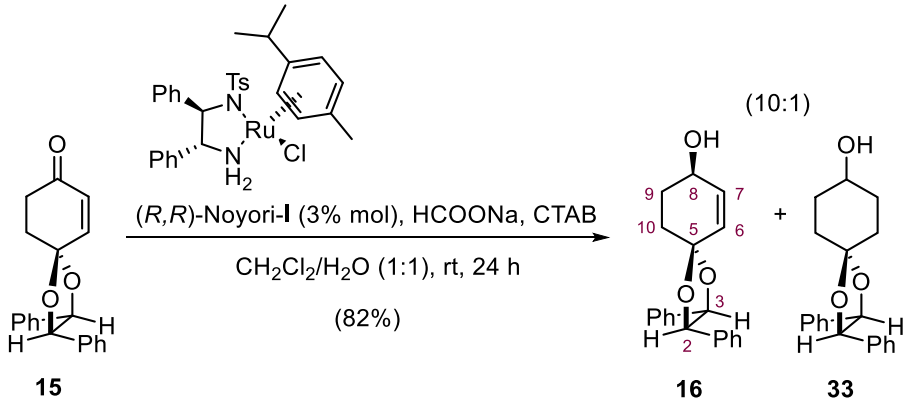

To a stirring solution of enone **15** (9.14 g, 29.82 mmol) in a biphasic media of CH_2Cl_2 (52 mL) and water (52 mL), hexadecyltrimethylammonium bromide (CTAB, 3.27 g, 8.97 mmol), sodium formate (3.09 g, 45.43 mmol) and, finally, (*R,R*)-Noyori-**I** catalyst (569 mg, 0.89 mmol) were sequentially added in solid portion at room temperature. The reaction mixture was allowed to stir for 24 h at rt. When TLC analysis (hexane-EtOAc, 1:1) shows totally consumption of the starting material. Then, the phases were separated and the organic phase was filtered through a short pad of Celite®. The volatiles were removed under reduced pressure affording a yellow oil, which was further purified by flash column chromatography (SiO_2, hexane-EtOAc, 5:1) to furnish an inseparable mixture of allylic alcohol **16** saturated alcohol **33** in a 10:1 ratio (7.54 g, 24.45 mmol, 82% yield), as a white solid.

Spectroscopic and physical data of **16**

^{1}H-NMR (400 MHz, $CDCl_3$): δ 7.36 – 7.26 (m, 6H, H-Ar), 7.26 – 7.17 (m, 4H, H-Ar), 6.05 (ddd, $J_{7,6}$ = 10.1 Hz, $J_{7,8}$ = 2.3 Hz, $J_{7,9}$ = 1.2 Hz, 1H, H-7), 5.92 (dt, $J_{6,7}$ = 10.1 Hz, $J_{6,8}$ = $J_{6,10}$ = 1.8 Hz, 1H, H-6), 4.79 (d, $J_{3,2}$ = 8.5 Hz, 1H, H-3), 4.69 (d, $J_{2,3}$ = 8.5 Hz, 1H, H-2), 4.29 (ddt, $J_{8,9ax}$ = 9.0 Hz, $J_{8,9eq}$ = 4.3 Hz, $J_{8,7}$ = $J_{8,6}$ = 2.0 Hz, 1H, H-8), 2.29 – 2.18 (m, 2H, H-9, H-10), 2.11 – 2.01 (m, 1H, H-9/H-10), 1.93 – 1.80 (m, 1H, H-9/H-10).

^{13}C-NMR (100 MHz, $CDCl_3$): δ 136.4/ 136.3 (C-Ar), 135.8 (C-7), 129.7 (C-6), 128.6/ 128.6/ 128.5/ 127.0/ 126.8 (C-Ar), 105.9 (C-5), 85.6/ 85.2 (C-2, C-3), 66.8 (C-8), 32.9 (C-10), 31.2 (C-9).

R_f of **16** + **33** (10:1) (hexane-EtOAc, 1:1) = 0.38 ($KMnO_4$).

2.1.2.4. Synthesis of (1*R*,4'*R*,5*R*,5'*R*,6*S*)-4',5'-diphenylspiro[bicyclo[4.1.0]heptane-2,2'-[1,3]dioxolan]-5-ol, 21.

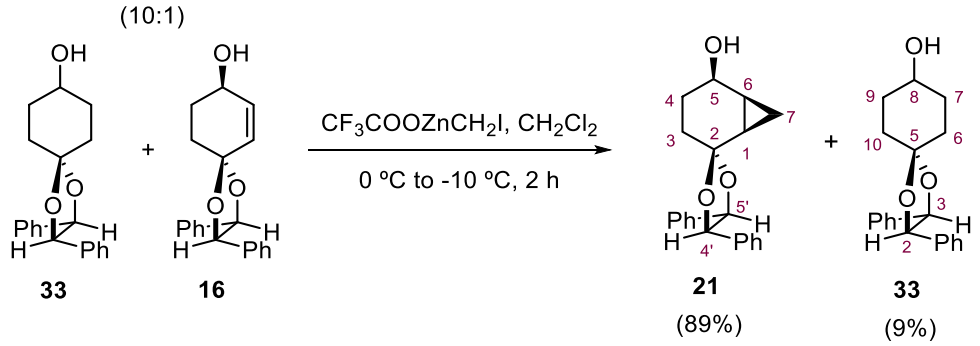

An ice-cooled solution of Et_2Zn (4.50 mL, 4.50 mmol, 1.0 M in hexanes) in dry CH_2Cl_2 (33 mL) was stirred for 15 min under nitrogen atmosphere. Trifluoroacetic acid (350 µL, 4.54 mmol) was added dropwise to the mixture and, after stirring for another 20 min, diiodomethane (370 µL, 4.54 mmol) was added dropwise and stirred for further 20 min. After that time, a solution of alcohol **16** (700 mg, 2.27 mmol) in dry CH_2Cl_2 (15 mL) was introduced at -10 °C. The resulting mixture was stirred for 2 h, then quenched by the addition of saturated aqueous Na_2EDTA solution (40 mL) and extracted with CH_2Cl_2 (2 x 30 mL). The organic layers were dried (Na_2SO_4), concentrated under reduced pressure and purified by flash column chromatography (SiO_2, gradient of hexane-EtOAc, 8:1 → 4:1) to provide tricycle alcohol **21** (651 mg, 2.02 mmol, 89% yield) as a white solid and saturated cyclohexanol **33** (63 mg, 0.204 mmol, 9% yield) as a white solid.

Spectroscopic and physical data of **21**

^{1}H-NMR (400 MHz, $CDCl_3$): δ 7.37 – 7.28 (m, 8H, H-Ar), 7.23 – 7.19 (m, 2H, H-Ar), 4.83 (d, $J_{5',4'}$ = 9.0 Hz, 1H, H-5'), 4.70 (d, $J_{4',5'}$ = 9.0 Hz, 1H, H-4'), 4.35 (q, $J_{5,4ax} = J_{5,4eq} = J_{5,6}$ = 5.5 Hz, 1H, H-5), 1.94 – 1.81 (m, 3H, 2H-3, H-4eq), 1.70 – 1.55 (m, 2H, H-1, H-6), 1.56 –1.41 (m, 1H, H-4ax), 0.96 (q, $J_{7endo,1} = J_{7endo,6} = J_{gem}$ = 5.7 Hz, 1H, H-7endo), 0.83 (td, $J_{7exo,1} = J_{7exo,6}$ = 9.4 Hz, J_{gem} = 5.7 Hz, 1H, H-7exo).

^{13}C-NMR (100 MHz, $CDCl_3$): δ 136.9/ 136.6 (C-Ar), 128.5/ 128.5/ 128.4 (C-Ar), 127.0/ 126.7 (C-Ar), 108.7 (C-2), 85.5/ 85.2 (C-4',C-5'), 65.4 (C-5), 31.8 (C-3), 27.5 (C-4), 23.4 (C-1), 19.4 (C-6), 4.2 (C-7).

R_f (hexane-EtOAc, 1:1) = 0.32 (vanillin, red spot).

Spectroscopic and physical data of **33**

^{1}H-NMR (250 MHz, $CDCl_3$): δ 7.40 – 7.10 (m, 10H, H-Ar), 4.75 (d, J_{gem} = 8.6 Hz, 1H, H-2), 4.71 (d, J_{gem} = 8.6 Hz, 1H, H-3), 3.87 (br s, 1H, H-8), 2.25 – 1.70 (m, 9H, H-9, H-10, OH).

^{13}C-NMR (62.5 MHz, $CDCl_3$): δ 136.8 (C-Ar), 128.4/ 128.3/ 126.7/ 126.7(C-Ar), 109.1 (C-5), 85.2 (C-2,C-3), 68.1 (C-8), 33.1/32.9 (C-6,C-10), 32.0/31.8 (C-7,C-9).

R_f (hexane-EtOAc, 1:1) = 0.41 (vanillin, blue spot).

2.1.2.5. Synthesis of (2*R*,3*R*)-2,3-diphenyl-1,4-dioxaspiro[4.5]decan-6-ene-8-one, 15 from saturated alcohol 33.

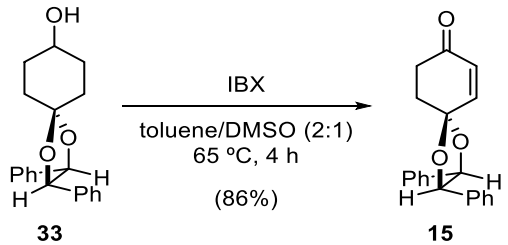

To a solution of saturated alcohol **33** (1.00 g, 3.22 mmol) in a mixture of toluene/DMSO (2:1, 32 mL) was added solid **IBX** (2.08 g, 7.41 mmol, 2.5 eq) in a one portion-wise. The solution was heated to 65 °C and the reaction was monitored by NMR (4 hours). Then, a saturated aqueous $Na_2S_2O_5$ and $NaHCO_3$ solution (50 mL) was added and stirred for 30 min. After that time, Et_2O (50 mL) was added, and the aqueous layer was extracted with more Et_2O (2 x 40 mL). The organic layers were washed with water (30 mL) and brine (30 mL) and then it was dried (Na_2SO_4),

concentrated under reduced pressure and purified by flash column chromatography (SiO_2, hexane-EtOAc, 6:1) to furnish **15** (848 mg, 2.76 mmol, 86% yield) as a pale oil.

Spectroscopic and physical data of **15**

(See **2.1.2.2** section).

2.1.2.6. Synthesis of (1R,4'R,5R,5'R,6S)-5-(benzyloxy)-4',5'-diphenylspiro[bicyclo[4.1.0]-heptane-2,2'-[1,3]dioxolane], 41.

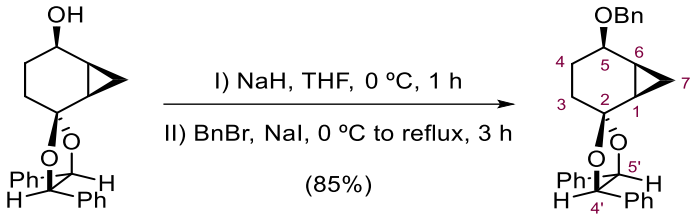

An ice-cooled solution of alcohol **21** (3.02 g, 9.37 mmol) in anhydrous THF (90 mL), NaH (1.27 g, 31.8 mmol) was added in one portion and the mixture stirred for 1 h at 0 °C. At this time, benzyl bromide (1.3 mL, 11.24 mmol) and sodium iodide (1.73 g, 11.5 mmol) were added at 0 °C and then, the mixture was stirred at the reflux temperature for 3 h. After that time, water (60 mL) was carefully added at room temperature and stirred for 15 min. Then, EtOAc (30 mL) was added, and the aqueous layer was extracted with more EtOAc (2 x 30 mL). The organic layers were dried (Na_2SO_4), concentrated under reduced pressure and purified by flash column chromatography (SiO_2, hexane-EtOAc, 6:1) to furnish **41** (3.29 g, 7.96 mmol, 85% yield) as a pale oil.

Spectroscopic and physical data of **41**

^{1}H-NMR (400 MHz, $CDCl_3$): δ 7.46 (m, 3H, H-Ar), 7.43 – 7.34 (m, 8H, H-Ar), 7.32 – 7.28 (m, 4H, H-Ar), 4.94 (d, $J_{5',4'}$ = 8.4 Hz, 1H, H-5'), 4.86 – 4.75 (m, 2H, H-4', CH_2-Ph), 4.59 (d, J_{gem} = 11.8 Hz, 1H, CH_2-Ph) 4.15 (q, $J_{5,6}$ = $J_{5,4}$ = 5.0 Hz, 1H, H-5), 1.99 – 1.80 (m, 4H, H-4, H-3), 1.72 – 1.58 (m, 2H, H-6, H-1), 1.12 (q, J_{gem} = $J_{7endo,1}$ = $J_{7endo,6}$ = 5.7 Hz, 1H, H-7endo), 1.03 (td, $J_{7exo,6}$ = $J_{7exo,1}$ = 9.1 Hz, J_{gem} = 5.7 Hz, 1H, H-7exo).

^{13}C-NMR (100 MHz, $CDCl_3$): δ 139.1 (C-Ar), 137.1/ 136.9 (C-Ar), 128.5/ 128.5/ 128.4/ 128.3/ 127.8/ 127.5/ 126.9/ 126.7 (C-Ar), 109.8 (C-2), 85.6/ 85.3 (C-4',C-5'), 70.7 (C-5), 69.6 (*C*H_2-Ph), 30.2 (C-3), 26.6 (C-4), 22.4 (C-1), 16.5 (C-6), 5.5 (C-7).

IR (ATR): v 3063, 2850, 2524, 2108, 1729, 1495, 1453, 1060, 697 cm^{-1}.

HRMS (ESI+): Calcd. for $[C_{28}H_{28}O_3+H]^+$: 413.2117, Found: 413.2119.

R_f (hexane-EtOAc, 1:1) = 0.68 ($KMnO_4$).

$[\alpha]_D^{20}$= +45.6 (*c* 1.03, $CHCl_3$).

2.1.2.7. Synthesis of (1*R*,5*R*,6*S*)-5-(benzyloxy)bicyclo[4.1.0]heptan-2-one, 36.

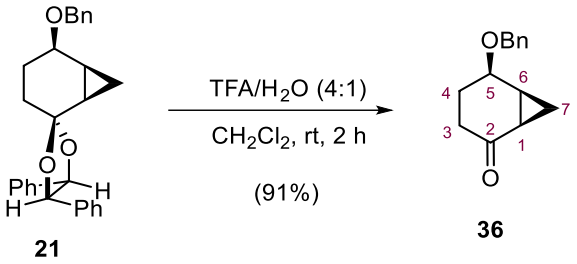

To a stirred solution of ketal **41** (743 mg, 1.81 mmol) in CH_2Cl_2 (18 mL) a 4:1 mixture of TFA (420 µL, 5.43 mmol)/H_2O (100 µL) were added at room temperature. The reaction mixture was allowed to stir for 2 h, until a TLC analysis (hexane-EtOAc, 2:1) showed a total consumption of the starting material. Then, additional CH_2Cl_2 (10 mL) was added, washed with saturated aqueous $NaHCO_3$ solution (20 mL) and extracted with more CH_2Cl_2 (2 x 10 mL). The organic layers were dried (Na_2SO_4), concentrated under reduced pressure and purified by flash column chromatography (SiO_2, $CHCl_3$ 100%) to provide **36** (232 mg, 1.07 mmol, 91% yield) as gold oil.

Spectroscopic and physical data of **36**

(See **2.1.1.4** section).

2.2. CHAPTER II. Synthesis of cytosine 4'-hydroxymehtylbicyclo[4.1.0]-heptane nucleoside analogue, 28.

2.2.1. Synthesis of (1*S*,2*R*,6*R*)-2-(benzyloxy)-5-methylenebicyclo[4.1.0]heptane, 42 and its isomer (1*R*,5*R*,6*S*)-5-(benzyloxy)-2-methylbicyclo[4.1.0]hept-2-ene. From 42, synthesis of [(1*S*',2*R*',5*R*',6*S*')-5'-(benzyloxy)bicyclo[4.1.0]hept-2'-yl]methanol, 43 and its (2'*S*)-diastereoisomer 46.

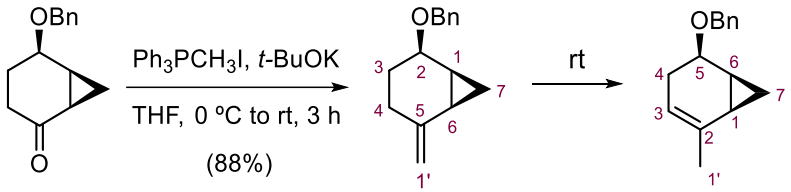

36 **42** **45**

To a stirring solution of Ph_3PCH_3I (1.452 g, 3.59 mmol) in anhydrous THF (4 mL) at 0 ºC, *t*-BuOK (402 mg, 3.58 mmol) was added, under nitrogen atmosphere, and the resulting yellow mixture was allowed to react for 1 h. At this time, a solution of ketone **36** (155 mg, 0.71 mmol) in dry THF (1 mL) was added and the mixture was allowed to warm rt and stirred for 3 h. Then, diethyl ether (10 mL) was added and the crude filtered through a short pad of silica and Celite®, using more diethyl ether as eluent. The volatiles were removed under vacuum to obtain an orange oil as a crude which was purified by flash column chromatography (SiO_2, hexane-EtOAc, 5:1) to furnish alkene **42** (134 g, 0.63 mmol, 88%) as a colourless oil.

Due to its instability and its rapidly isomerisation to the more stable endocyclic regioisomer **45** at rt, the crude can be used for the next step without further purification.

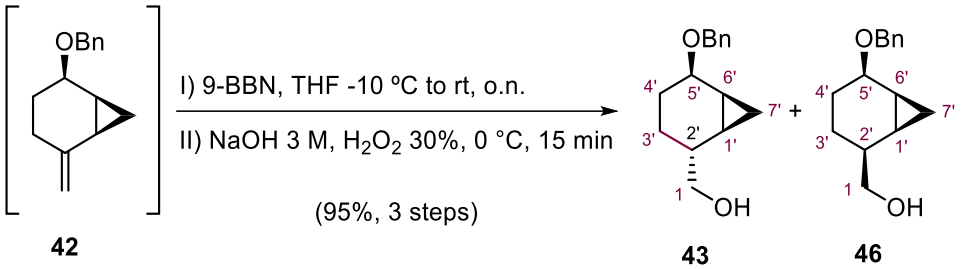

42 **43** **46**

(2:1)

The crude (or purified) alkene **42** was rapidly dissolved in anhydrous THF (7 mL) and 9-BBN (4.30 mL, 2.15 mmol, 0.5 M in THF) was added at -10 °C. The mixture was allowed to warm to room

temperature and stirred overnight. Then, water (1.2 mL), NaOH (1.5 mL, 3 M in water) and H_2O_2 (1.4 mL, 30% in water) were added at 0 °C. After stirring for 15 min, the mixture was diluted with brine (15 mL) and CH_2Cl_2 (15 mL) and the aqueous phase was extracted with more CH_2Cl_2 (2 x 10 mL). The organic layers were dried (Na_2SO_4), concentrated under reduced pressure and purified by column chromatography (SiO_2, gradient hexane-EtOAc, 5:1 → 2:1) to provide a chromatographically inseparable mixture of alcohols **43** and **46** (158 mg, 0.68 mmol, 95% overall yield from **36**, 83% overall yield for the hydroboration-oxidation steps) in a *ca.* 2:1 diastereomeric ratio as a colourless oil.

Spectroscopic and physical data of **42**

^{1}H-NMR (400 MHz, $CDCl_3$): δ 7.46 – 7.25 (m, 5H, H-Ar), 4.90 (br s, 1H, H-1'), 4.79 (br s, 1H, H-1'), 4.74 (d, J_{gem} = 11.9 Hz, 1H, CH_2-Ph), 4.56 (d, J_{gem} = 11.9 Hz, 1H, CH_2-Ph), 4.05 (q, $J_{2,3ax} = J_{2,3eq} = J_{2,1}$ = 5.9 Hz, 1H, H-2), 2.21 (dddt, J_{gem} = 14.9 Hz, $J_{4ax,3ax}$ = 8.5 Hz, $J_{4ax,3eq}$ = 4.4 Hz, $J_{4ax,1'}$ = 1.4 Hz, 1H, H-4ax), 2.03 (dddt, J_{gem} = 14.9 Hz, $J_{4eq,3ax}$ = 7.2 Hz, $J_{4eq,3eq}$ = 4.3 Hz, $J_{4eq,1'}$ = 1.4 Hz, 1H, H-4eq), 1.88 – 1.75 (m, 1H, H-6), 1.71 – 1.50 (m, 3H, H-1, H-3), 0.94 – 0.84 (m, 2H, H-7).

^{13}C-NMR (100 MHz, $CDCl_3$): δ 146.3 (C-5), 139.1 (C-*ipso*), 128.4 / 127.7 / 127.5 (C-Ar), 108.1 (C-1'), 72.0 (C-2), 69.7 (CH_2-Ph), 28.8 (C-4), 27.7 (C-3), 19.9 (C-1), 17.0 (C-6), 8.7 (C-7).

COSY, **HSQC** and **DEPT-135** experiments have been recorded.

IR (ATR): ν 3070, 2930, 1471, 1427, 1106, 806, 741 cm^{-1}.

HRMS (ESI+): Calcd. for $[C_{15}H_{18}O+H]^+$: 215.1436, Found: 215.1465.

R_f (hexane-EtOAc, 2:1) = 0.75 (vanillin, blue spot).

Spectroscopic and physical data of **45**

^{1}H-NMR (400 MHz, $CDCl_3$): δ 7.42 – 7.36 (m, 3H, H-Ar), 7.35 – 7.25 (m, 2H, H-Ar), 5.01 (dq, $J_{3,4eq}$ = 5.3 Hz, $J_{3,4ax} = J_{3,1'}$ = 1.6 Hz, 1H, H-3), 4.69 (d, J_{gem} = 12.0 Hz, 1H, CH_2-Ph), 4.65 (d, J_{gem} = 12.0 Hz, 1H, CH_2-Ph), 3.98 (ddd, $J_{5,4ax}$ = 9.1 Hz, $J_{5,4eq}$ = 6.8 Hz, $J_{5,6}$ = 4.1 Hz, 1H, H-5), 2.32 (ddd, J_{gem} = 15.3 Hz, $J_{4eq,5}$ = 6.8 Hz, $J_{4eq,3}$ = 5.2 Hz, 1H, H-4eq), 1.89 – 1.75 (m, 4H, H-1', H-4ax) 1.64 – 1.51 (m, 1H, H-6), 1.30 – 1.23 (m, 1H, H-1), 0.90 – 0.85 (m, 2H, H-7).

^{13}C-NMR (101 MHz, $CDCl_3$): δ 139.6 (C-*ipso*), 136.7 (C-2), 128.8/ 128.2/ 127.9 (C-Ar), 114.3 (C-3), 73.4 (C-5), 70.6 (CH_2-Ph), 28.0 (C-4), 23.5 (C-1'), 18.0/ 17.8 (C-1, C-6), 10.1 (C-7).

COSY, **HSQC** and **DEPT-135** experiments have been recorded.

IR (ATR): ν 3064, 2910, 2852, 1667, 1452, 1070, 734, 697 cm^{-1}.

HRMS (ESI+): Calcd. for $[C_{15}H_{18}O+H]^+$: 215.1436, Found: 215.1434.

R_f (hexane-EtOAc, 2:1) = 0.75 (vanillin).

Spectroscopic and physical data of a (*ca*. 5:1) mixture of **43** and **46**

^{1}H-NMR (400 MHz, $CDCl_3$) (*ca.* 84% *trans*-isomer **43**): δ 7.40 – 7.31 (m, 4H, H-Ar), 7.30 – 7.24 (m, 1H, H-Ar), 4.71 (d, J_{gem} = 12.0 Hz, 1H, C*H*$_2$-Ph), 4.59 (d, J_{gem} = 12.0 Hz, 1H, C*H*$_2$-Ph), 3.95 (dt, $J_{5',4'ax}$ = 10.0 Hz, $J_{5',4'eq}$ = $J_{5',6'}$ = 5.7 Hz, 1H, H-5'), 3.57 (d, $J_{1,2'}$ = 6.6 Hz, 2H, H-1), 1.79 (dtd, J_{gem} = 13.3 Hz, $J_{4'eq,5'}$ = $J_{4'eq,3'ax}$ = 5.7 Hz, $J_{4'eq,3'eq}$ = 2.4 Hz, 1H, H-4'eq), 1.70 (dddd, $J_{2',3'ax}$ = 8.5 Hz, $J_{2',1}$ = 6.6 Hz, $J_{2',3'eq}$ = 5.4 Hz, $J_{2',1'}$ = 1.9 Hz, 1H, H-2'), 1.55 (dtd, J_{gem} = 13.2 Hz, $J_{3'eq,4'ax}$ = $J_{3'eq,2'}$ = 5.4 Hz, $J_{3'eq,4'eq}$ = 2.4 Hz, 1H, H-3'eq), 1.29 – 1.26 (m, 1H, H-6'), 1.04 (tdd, J_{gem} = $J_{4'ax,3'ax}$ = 13.3 Hz, $J_{4'ax,5'}$ = 10.0 Hz, $J_{4'ax,3'eq}$ = 5.4 Hz, 1H, H-4'ax), 0.99 – 0.83 (m, 2H, H-1', H-3'ax), 0.74 (td, $J_{7'exo,6'}$ = $J_{7'exo,1'}$ = 8.8 Hz, J_{gem} = 5.4 Hz, 1H, H-7'exo), 0.46 (q, J_{gem} = $J_{7'endo,6'}$ = $J_{7'endo,1'}$ = 5.4 Hz, 1H, H-7'endo).

^{1}H-NMR (400 MHz, $CDCl_3$) (*ca.* 16% *cis*-isomer **46**, observable signals): δ 7.40 – 7.31 (m, 4H, H-Ar), 7.30 – 7.24 (m, 1H, H-Ar), 4.72 (d, J_{gem} = 11.8 Hz, 1H, C*H*$_2$-Ph), 4.47 (d, J_{gem} = 11.8 Hz, 1H, C*H*$_2$-Ph), 4.01 (ddd, $J_{5',4'ax}$ = 7.0 Hz, $J_{5',4'eq}$ = 5.1 Hz, $J_{5',6'}$ = 3.4 Hz, 1H, H-5'), 3.57 (m, 1H, H-1a), 3.49 (dd, J_{gem} = 10.5 Hz, $J_{1b,2'}$ = 6.6 Hz, 1H, H-1b), 2.05 (dddd, $J_{2',3'ax}$ = 12.3 Hz, $J_{2',1a}$ = 10.2 Hz, $J_{2',1b}$ = 6.6 Hz, $J_{2',1'}$ = 5.4 Hz, 1H, H-2'), 1.66 – 1.57(m, 1H, H-4'a), 1.44 – 1.33 (m, 2H, H-3'a, H-4'b), 1.18 (tt, $J_{1',6'}$ = $J_{1',7'exo}$ = 8.5 Hz, $J_{1',7'endo}$ = $J_{1',2'}$ = 5.4 Hz, 1H, H-1'), 1.02 – 0.98 (m, 1H, H-3'b), 0.75 (m, 1H, H-6'), 0.60 – 0.51 (m, 2H, H-7').

^{13}C-NMR (101 MHz, CDCl3) (*ca.* 84% *trans*-isomer **43**): δ 139.25 (C-*ipso*), 128.43 (C-*meta*), 127.82 (C-*para*), 127.49 (C-*orto*), 74.44 (C-5'), 69.62 (*C*H$_2$-Ph), 67.98 (C-1), 38.10 (C-2'), 25.31 (C-4'), 25.23 (C-3'), 15.90 (C-1'), 14.88 (C-6'), 8.21 (C-7').

^{13}C-NMR (100 MHz, CDCl3) (*ca.* 16% **46**, observable signals): δ 139.22 (C-*ipso*), 128.43 (C-*meta*), 127.80 (C-*para*), 127.44 (C-*orto*), 70.87 (C-5'), 69.57 (*C*H$_2$-Ph) 67.78 (C-1), 35.64 (C-2'), 28.43 (C-4'), 18.93 (C-3'), 14.19 (C-1'), 13.37 (C-6'), 1.98 (C-7').

COSY, **DEPT-135**, **HSQC**, and **NOESY** experiments have been recorded.

HRMS (ESI+): Calcd. for $[C_{15}H_{20}O_2+H]^+$: 233.1542, Found: 233.1537.

R$_f$ (hexane-EtOAc, 2:1) = 0.20 (vanillin).

2.2.2. Synthesis of [(1'*S*,2'*R*,5'*R*,6'*S*)-5'-hydroxybicyclo[4.1.0]hept-2'-yl]methyl benzoate, 24 and its (2'*S*)-diastereoisomer, 50.

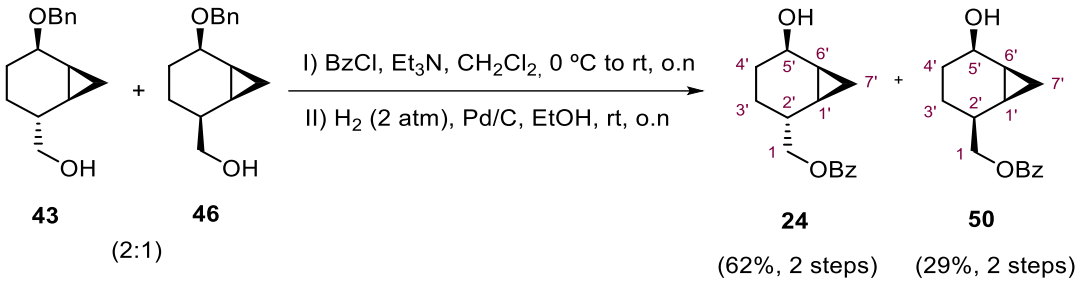

To a stirred solution of **43** and **46** (2:1, 158 mg, 0.68 mmol) in dry CH_2Cl_2 (7 mL) at 0 °C, anhydrous Et_3N (100 µL, 0.71 mmol) and benzoyl chloride (91 µL, 0.78 mmol) were sequentially added under argon atmosphere. The mixture was subsequently allowed to attain room temperature overnight. Then, the solution was treated with HCl 10% solution (7 mL) and CH_2Cl_2 (7 mL), the two phases were separated and the aqueous phase was extracted with CH_2Cl_2 (3 x 7 mL). The organic layers were washed with brine (30 mL), dried (Na_2SO_4) and concentrated under reduced pressure to obtain a colourless oil, which was directly used for the next step without further purification.

Then, the crude was dissolved in EtOH (7 mL) and was hydrogenated in the presence of Pd/C (23 mg, 10% wt.) at 2 atm overnight. The mixture was filtered through a short pad of Celite® and washing it with more EtOH. The solvent was evaporated under reduced pressure and purified by flash column chromatography (SiO_2, hexanes-EtOAc, 10:1 → 5:1) to afford a separable alcohols **24** (104 mg, 0.42 mmol, 62% yield) as a colourless syrup and **50** (49 mg, 0.20 mmol, 29% yield) as a colourless syrup.

Spectroscopic and physical data of **24**

^{1}H-NMR (400 MHz, $CDCl_3$): δ 8.05 (d, $J_{orto,meta}$ = 7.6 Hz, 2H, H-*orto*), 7.61 – 7.51 (m, 1H, H-*para*), 7.44 (t, $J_{meta,orto} = J_{meta,para}$ = 7.6 Hz, 2H, H-*meta*), 4.28 (dd, $J_{1,2'}$ = 6.8 Hz, $J_{1,1'}$ = 2.0 Hz, 2H, H-1), 4.20 (dt, $J_{5',4'ax}$ = 9.5 Hz, $J_{5',4'eq} = J_{5',6'}$ = 5.7 Hz, 1H, H-5'), 2.0 (dddd, $J_{2',3'ax}$ = 13.8 Hz, $J_{2',1}$ = 6.8 Hz, $J_{2',3'eq}$ = 4.4 Hz, $J_{2',1'}$ = 1.9 Hz, 1H, H-2'), 1.86 – 1.72 (m, 1H, H-4'), 1.70 – 1.61 (m, 2H, H-3'), 1.33 (tt, $J_{6',7'endo} = J_{6',7'exo}$ = 8.8 Hz, $J_{6',5'} = J_{6',1'}$ = 5.7 Hz, 1H, H-6'), 1.13 – 0.87 (m, 2H, H-1', H-4'), 0.71 (td, $J_{7'exo,1'} = J_{7'exo,6'}$ = 8.8 Hz, J_{gem} = 4.9 Hz, 1H, H-7'exo), 0.40 (q, $J_{7'endo,1'} = J_{7'endo,6'} = J_{gem}$ = 5.3 Hz, 1H, H-7'endo).

^{13}C-NMR (100 MHz, $CDCl_3$): δ 166.8 (*C*=O), 133.1 (C-*para*), 130.4 (C-*ipso*), 129.7 (C-*orto*), 128.5 (C-*meta*), 69.4 (C-1), 68.0 (C-5'), 34.5 (C-2'), 28.0 (C-4'), 26.0 (C-3'), 18.1 (C-6'), 16.2 (C-1'),.6 (C-7').

COSY, **HSQC**, **HMBC**, **DEPT-135** and **NOESY** experiments have been recorded.

IR (ATR): v 3366, 3066, 3003, 2937, 2869, 1715, 1269, 1110, 1026, 708 cm^{-1}.

HRMS (ESI+): Calcd. for $[C_{15}H_{18}O_3]^+$: 246.1256, Found: 246.1258.

R_f (hexane-EtOAc, 2:1) = 0.26 (vanillin).

$[\alpha]_D^{20}$= +44.9 (*c* 0.88, $CHCl_3$).

Spectroscopic and physical data of **50**

^{1}H-NMR (400 MHz, $CDCl_3$): δ 8.05 (d, $J_{orto,meta}$ = 7.2 Hz, 2H, H-*orto*), 7.56 (t, $J_{para,meta}$ = 7.4 Hz, 1H, H-*para*), 7.44 (t, $J_{meta,orto} = J_{meta,para}$ = 7.6 Hz, 2H, H-*meta*), 4.34 (dt, $J_{5',4'ax}$ = 7.3 Hz, $J_{5',4'eq} = J_{5',6'}$ = 4.7 Hz, 1H, H-5'), 4.29 (dd, J_{gem} = 10.7 Hz, $J_{1a,2'}$ = 6.9 Hz, 1H, H-1a), 4.18 (dd, J_{gem} = 10.7 Hz, $J_{1b,2'}$ = 7.3 Hz, 1H, H-1b), 2.36 (dq, $J_{2',3'ax}$ = 12.6 Hz, $J_{2',1a} = J_{2',1b} = J_{2',3'eq}$ = 6.7 Hz, 1H, H-2'), 1.51 – 1.37 (m, 4H, H-6', 2H-4', H-3'), 1.27 (tt, $J_{1',2'} = J_{1',7'exo}$ = 8.5 Hz, $J_{1',7'endo} = J_{1',6'}$ = 5.7 Hz, 1H, H-1'), 1.23 – 1.13 (m, 1H, H-3'), 0.57 (q, $J_{gem} = J_{7'endo,6'} = J_{7'endo,1'}$ = 5.3 Hz, 1H, H-7'endo), 0.46 (td, $J_{7'exo,1'} = J_{7'exo,6'}$ = 8.9 Hz, J_{gem} = 5.1 Hz, 1H, H-7'exo).

^{13}C-NMR (100 MHz, $CDCl_3$): δ 166.8 (*C*=O), 133.0 (C-*para*), 130.6 (C-*ipso*), 129.7 (C-*orto*), 128.5 (C-*meta*), 68.9 (C-1), 64.7 (C-5'), 31.7 (C-2'), 29.9 (C-4'), 19.4 (C-3'), 17.1 (C-1'), 14.7 (C-6'), 1.7 (C-7').

COSY, **HSQC**, **HMBC**, **DEPT-135** and **NOESY** experiments have been recorded.

IR (ATR): v 3410, 3069, 3009, 2938, 1715, 1273, 1114, 712, 630 cm^{-1}.

HRMS (ESI+): Calcd. for $[C_{15}H_{18}O_3]^+$: 246.1256 Found: 246.1252.

R_f (hexane-EtOAc, 2:1) = 0.29 (vanillin).

$[\alpha]_D^{20}$= -7.2 (*c* 1.03, $CHCl_3$).

2.2.3. Synthesis of [(1'*R*,2'*R*,5'*S*,6'*S*)-5'-azidobicyclo[4.1.0]hept-2'-yl]methyl benzoate, 44.

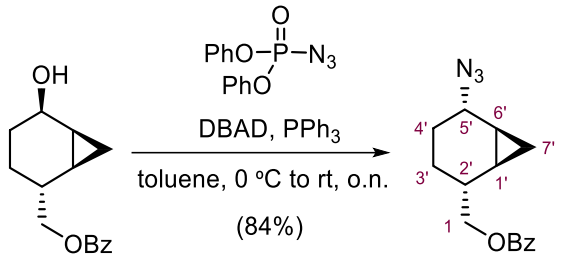

24 **44**

To a stirred solution of Ph_3P (170 mg, 0.65 mmol) in dry toluene (4.5 mL), DBAD (150 mg, 0.65 mmol) was slowly added under argon atmosphere and the mixture was stirred for 45 min at 0 ºC. After 15 min, a white suspension appeared. Then, diphenylphosphoryl azide (DPPA, 100 µL, 0.45 mmol) and a solution of **24** (105 mg, 0.43 mmol) in dry toluene (1 mL) were sequentially added. The mixture was allowed to warm to room temperature and stirred overnight. Then, the solvent was removed and the crude was purified by column chromatography (SiO_2, hexane-EtOAc, 20:1 to 15:1) to obtain azide **44** (97 mg, 0.36 mmol, 84% yield) as a yellowish syrup.

Spectroscopic and physical data of **44**

^{1}H-NMR (400 MHz, $CDCl_3$): δ 8.07 (d, $J_{orto,meta}$ = 7.0 Hz, 2H, H-*orto*), 7.56 (t, $J_{para,meta}$ = 7.5 Hz, 1H, H-*para*), 7.45 (t, $J_{meta,orto} = J_{meta,para}$ = 7.9 Hz, 2H, H-*meta*), 4.32 (d, $J_{1,2'}$ = 6.8 Hz, 2H, H-1), 4.01 (br s, 1H, H-5'), 2.19 – 2.00 (m, 1H, H-2'), 1.70 – 1.58 (m, 1H, H-4'), 1.45 – 1.31 (m, 3H, 2H-3', H-4'), 1.21 – 1.12 (m, 1H, H-6'), 0.99 (ddd, $J_{1',7'exo}$ = 9.3 Hz, $J_{1',7'endo}$ = 5.3 Hz, $J_{1',6'}$ = 1.3 Hz, 1H, H-1'), 0.85 (td, $J_{7'exo,1'} = J_{7'exo,6'}$ = 9.3 Hz, J_{gem} = 5.2 Hz, 1H, H-7'exo), 0.15 (q, $J_{gem} = J_{7'endo,1'} = J_{7'endo,6'}$ = 5.4 Hz, 1H, H-7'endo).

^{13}C-NMR (100 MHz, $CDCl_3$): δ 166.8 (*C*=O), 133.1 (C-*para*), 130.5 (C-*ipso*), 129.7 (C-*orto*), 128.5 (C-*meta*), 69.4 (C-1), 57.0 (C-5'), 34.0 (C-2'), 24.5 (C-4'), 20.2 (C-3'), 14.7 (C-6'), 12.6 (C-1'), 9.9 (C-7').

COSY, NOESY, HSQC, **HMBC** and **DEPT-135** and experiments have been recorded.

IR (ATR): ν 2925, 2089 (N_3), 1716 (*C*=O), 1270, 1110 cm^{-1}.

HRMS (ESI+): Calcd. For $[C_{13}H_{17}N_3O_2]^+$: 271.1321, Found: 271.1324.

R_f (hexane-EtOAc, 2:1) = 0.63 (vanillin, blue stop).

$[\alpha]_D^{20}$= -36.2 (*c* 1.01, $CHCl_3$).

2.2.4. Synthesis of (1*S*,2*S*,5*R*,6*R*)-5-[(benzoyloxy)methyl)]bicyclo[4.1.0]heptan-2-amonium chloride, 25.

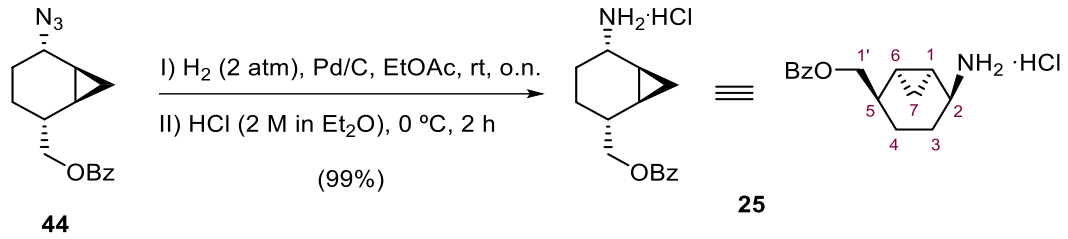

44 **25**

A stirred solution of azide **44** (97 mg, 0.36 mmol) in EtOAc (2 mL) at room temperature, was hydrogenated in the presence of Pd/C (15 mg, 10% wt.) at 2 atm for 24 h. Then, the mixture was filtered through a short pad of Celite® and washed with more EtOAc. The solvent was evaporated under reduced pressure and the crude was treated with 2 M HCl · Et_2O (2 mL, 4 mmol) at 0 °C, stirred for 2 h and filtered to furnish the ammonium salt **25** (101 mg, 0.36 mmol, 99% yield) as a brown solid.

Spectroscopic and physical data of **25**

^{1}H-NMR (400 MHz, $CDCl_3$): δ 8.69 (s, 3H, NH_3^+), 8.08 – 7.97 (m, 2H, H-Ar), 7.56 – 7.50 (m, 1H, H-Ar), 7.44 – 7.36 (m, 2H, H-Ar), 4.45 (d, $J_{1',5}$ = 7.7 Hz, 2H, H-1'), 3.84 (br s, 1H, H-2), 2.15 – 1.89 (m, 2H, H-5, H-4), 1.60 – 1.46 (m, 3H, H-3, H-4), 1.31 – 1.22 (m, 1H, H-1), 1.12 – 1.02 (m, 1H, H-6), 0.91 (td, $J_{7exo,1}$ = $J_{7exo,6}$ = 9.1 Hz, J_{gem} = 5.1 Hz, 1H, H-7exo), 0.19 (q, J_{gem} = $J_{7endo,1}$ = $J_{7endo,6}$ = 5.5 Hz, 1H, H-7endo).

^{13}C-NMR (100 MHz, $CDCl_3$): δ 166.6 (*C*=O), 133.1 (C-*para*), 130.4 (C-*ipso*), 129.7 (C-*orto*), 128.5 (C-*meta*), 69.0 (C-1'), 47.1 (C-2), 33.9 (C-5), 23.2 (C-4), 19.4 (C-3), 14.0 (C-6), 12.5 (C-1), 10.4 (C-7).

COSY, **HSQC**, **HMBC** and **DEPT-135** experiments have been recorded.

IR (ATR): v 3404 (NH_3^+), 2929, 1712, 1273, 1113, 713 cm^{-1}.

HRMS (ESI+): Calcd. for $[C_{15}H_{18}NO_2]^+$: 244.1338, Found: 244.1335.

m.p.: 130-132 °C (from EtO_2).

[α]$_D^{20}$= +14.6 (*c* 1.03, $CHCl_3$).

2.2.5. Synthesis of (2*E*)-3-ethoxyacryloyl chloride, 59.

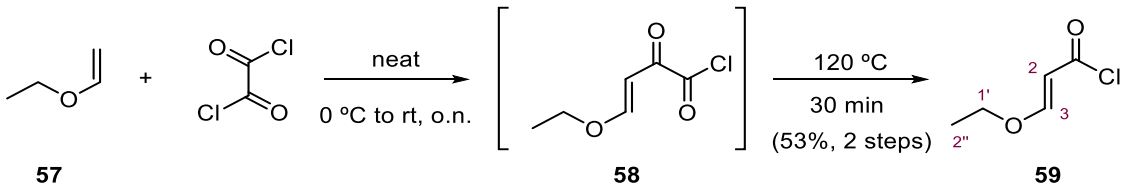

57 **58** **59**

Vinyl ether (5.75 mL, 60 mmol) **57** was added dropwise to oxalyl chloride (7.60 mL, 90 mmol) at 0 °C. The reaction mixture was maintained for 2 hours at 0 °C and then warmed to room temperature overnight. Excess oxalyl chloride was distilled off and the black residue was heated at 120 °C for 30 min. Then, the residue was purified by vacuum distillation, using a short Vigreux column, to obtain (2*E*)-3-ethoxyacryloyl chloride, **59** (4.30 g, 31.97 mmol, 53% yield) as a colourless liquid.

Spectroscopic and physical data of **59**

^{1}H-NMR (250 MHz, $CDCl_3$): δ 7.74 (d, $J_{3,2}$ = 12.1 Hz, 1H, H-3), 5.46 (d, $J_{2,3}$ = 12.1 Hz, 1H, H-2), 4.02 (q, $J_{1',2'}$ = 7.1 Hz, 2H, H-1'), 1.34 (t, $J_{2',3'}$ = 7.1 Hz, 3H, H-2').

Bp: 84-86 °C/ 30 mbar.

2.2.6. Synthesis of (E)-3-ethoxyacryloyl isocyanate, 60 and subsequent synthesis of [(1'*R*,2'*R*,5'*S*,6'*S*)-5'-(2'',4''-dioxo-3'',4''-dihydropyrimidin-1''(2*H*)-yl] bicyclo[4.1.0]heptan-2'-yl)methyl benzoate, 62.

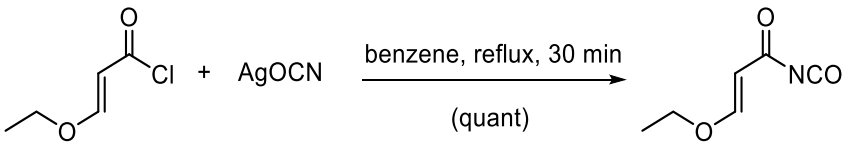

59 **60**

Silver cyanate (90 mg, 0.60 mmol), previously dried over phosphorus pentoxide at 80 ºC for 3 h, in dry benzene (2 mL) was heated to reflux for 30 min and a solution of (2*E*)-3-ethoxyacryloyl chloride, **59** (45 mg, 0.31 mmol) in dry benzene (0.8 mL) was then added dropwise. The mixture was stirred for 30 min before allowing the solid to settle out. The supernatant, which is a solution of the isocyanate **60**, was then decanted and used directly in the next reaction.

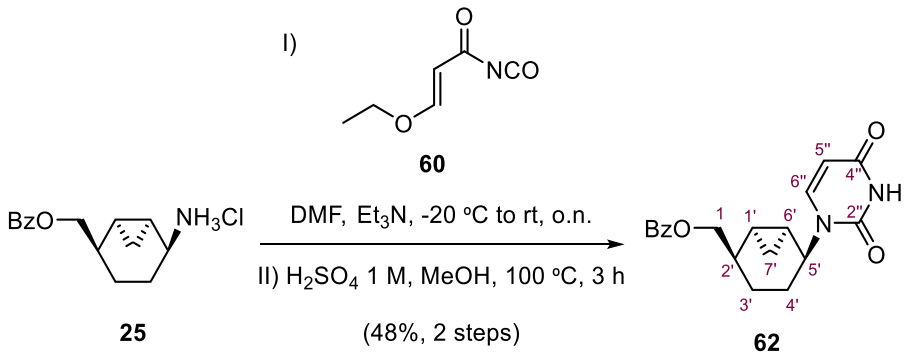

The ammonium chloride **25** (43 mg, 0.153 mmol) was dissolved in dry DMF (1.8 mL) and Et_3N (22 µL, 0.157 mmol) was added. The mixture was cooled to -20 °C and the supernatant was added slowly enough to avoid an increase on the temperature, and the reaction mixture was stirred overnight at rt. The solvent was evaporated *in vacuo*, and then water (2 mL) was added and the residue was extracted with EtOAc (2 x 2 mL), washed with brine (2 mL), dried (Na_2SO_4), filtered, and evaporated under reduce pressure. The residue was dissolved in MeOH (0.40 mL), H_2SO_4 (1 M, 0.62 mL) was added and the mixture was heated to reflux for 3 h. Then, the mixture was concentrated under reduce pressure and purified by flash column chromatography (SiO_2, CH_2Cl_2 100% to CH_2Cl_2-MeOH, 20:1) to provide **62** (25 mg, 0.073 mmol, 48% yield) as a yellowish solid.

Spectroscopic and physical data of **62**

^{1}H-NMR (400 MHz, MeOH-d_4): δ 8.05 (d, $J_{orto,meta}$ = 7.6 Hz, 2H, H-*orto*), 7.96 (d, $J_{6'',5''}$ = 8.0 Hz, 1H, H-6''), 7.64 (d, $J_{para,meta}$ = 7.6 Hz, 1H, H-*para*), 7.52 (t, $J_{meta,orto} = J_{meta,para}$ = 7.6 Hz, 2H, H-*meta*), 5.46 (d, $J_{5'',6''}$ = 8.0 Hz, 1H, H-5''), 4.83 (dt, $J_{5',4'ax}$ = 4.3 Hz, $J_{5',4eq} = J_{5',6'}$ = 2.3 Hz, 1H, H-5'), 4.45 (d, $J_{1,2'}$ = 6.0 Hz, 2H, H-1), 2.21 (dq, $J_{2',3'ax}$ = 11.9 Hz, $J_{2',3'eq} = J_{2'1}$ = 6.0 Hz, 1H, H-2'), 1.78 – 1.68 (m, 1H, H-4'eq), 1.54 (tt, $J_{gem} = J_{4'ax,3'ax}$ = 14.7 Hz, $J_{4'ax,5'} = J_{4'ax,3'eq}$ = 4.3 Hz, 1H, H-4'ax), 1.49 – 1.40 (m, 1H, H-3'), 1.32 – 1.21 (m, 2H, H-3', H-6'), 1.12 – 1.04 (m, 1H, H-1'), 0.97 (td, $J_{7exo,1} = J_{7exo,6}$ = 9.4 Hz, J_{gem} = 5.0 Hz, 1H, H-7'exo), 0.39 (q, $J_{gem} = J_{7endo,1} = J_{7endo,6}$ = 5.3 Hz, 1H, H-7'endo).

^{13}C-NMR (101 MHz, MeOH-d_4): δ 168.1 (*C*=O), 166.3 (C-4''), 152.7 (C-2''), 145.1 (C-6''), 134.4 (C-*para*), 131.5 (C-*ipso*), 130.5 (C-*orto*), 129.7 (C-*meta*), 101.6 (C-5''), 69.9 (C-1), 52.5 (C-5'), 34.7 (C-2'), 24.5 (C-4'), 20.1 (C-3'), 15.3 (C-6'), 13.7 (C-1'), 10.4 (C-7').

COSY and **DEPT-135** experiments have been recorded.

HRMS (ESI+): Calcd. for $[C_{19}H_{20}N_2O_4+Na]^+$: 363.1321, Found: 363.1312.

R_f (CH_2Cl_2-MeOH, 15:2) = 0.57 (vanillin, pale orange spot).

2.2.7. Synthesis of 4-amino-1-[(1'*S*,2'*S*,5'*R*,6'*R*)-5'-(hydroxymethyl)bicyclo[4.1.0]hept-2'-yl]pyrimidin-2(1*H*)-one, 28.

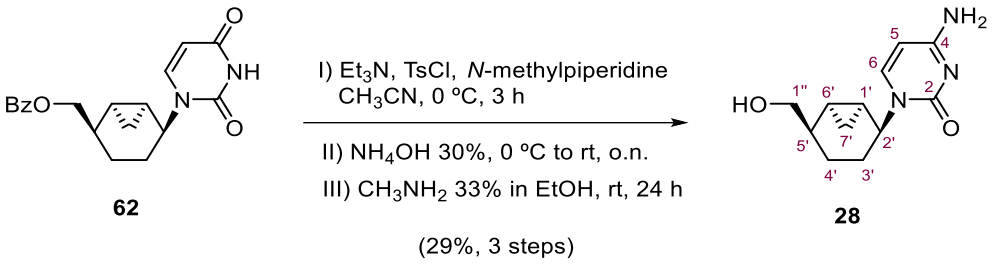

A solution of TsCl (31mg, 0.16 mmol) in dry CH_3CN (104 µL) was added to a mixture of **62** (27 mg, 0.08 mmol), Et_3N (22 µL, 0.16 mmol), and *N*-methylpiperidine (12 µL, 0.1 mmol) in dry CH_3CN (135 µL) at 0 °C, and the reaction mixture was stirred for 3 h. Then, 30% NH_4OH was added at 0 °C, and the reaction solution was stirred at rt overnight. The mixture was diluted with water (1 mL) and EtOAc (1 mL) and the aqueous phase was extracted with more CH_2Cl_2 (2 x 1 mL). The organic layers were dried (Na_2SO_4), concentrated under reduced pressure and purified by flash column chromatography (SiO_2, CH_2Cl_2-EtOAc, 10:2 → CH_2Cl_2-MeOH 15:1) to provide the protected cytosine analogue as a yellowish oil which was dissolved in a 33% solution of methylamine in EtOH (17 mL) and stirred 24 h. Then, the mixture was concentrated under reduce pressure and purified by column chromatography (SiO_2, CH_2Cl_2-MeOH, 20:1) to provide cytosine nucleoside analogue **28** (5.45 mg, 23 µmol, 29% yield) as a yellowish solid.

Spectroscopic and physical data of **28**

^{1}H-NMR (400 MHz, MeOH-d_4): δ 8.04 (d, $J_{6,5}$ = 7.4 Hz, 1H, H-6), 5.90 (d, $J_{5,6}$ = 7.4 Hz, 1H, H-5), 4.91 – 4.87 (m, 1H, H-2') 3.64 (dd, J_{gem} = 10.7 Hz, $J_{1''a,5'}$ = 5.9 Hz, 1H, H-1''a), 3.59 (dd, J_{gem} = 10.7 Hz, $J_{1''a,5'}$ = 5.9 Hz, 1H, H-1''b), 1.85 (dq, $J_{5',4'ax}$ = 11.4 Hz, $J_{5'4'eq}$ = $J_{5',1''a}$ = $J_{5',1''b}$ = 5.9 Hz, 1H, H-5'), 1.68 (dt, J_{gem} = 13.7 Hz, $J_{3'eq,4'ax}$ = $J_{3'eq,5'}$ = 4.4 Hz, 1H, H-3'eq), 1.48 (tt, J_{gem} = $J_{3'ax,4'ax}$ = 13.7 Hz, $J_{3'ax,\ 4'eq}$ = $J_{3'ax,5'}$ = 3.6 Hz, 1H, H-3'ax), 1.34 – 1.26 (m, 2H, H-1', H-4'a), 1.19 – 1.07 (m, 1H, H-4'b), 1.00 (td, $J_{6',7'exo}$ = $J_{6',1'}$ = 9.4 Hz, $J_{6',7'endo}$ = 5.2 Hz, 1H, H-6'), 0.89 (td, $J_{7exo,1}$ = $J_{7exo,6}$ = 9.4, J_{gem} = 5.2 Hz, 1H, H-7'exo), 0.30 (q, J_{gem} = $J_{7endo,1}$ = $J_{7endo,6}$ = 5.2 Hz, 1H, H-7'endo).

^{13}C-NMR (100 MHz, MeOH-d_4): δ 167.3 (C-4), 159.0 (C-2), 145.6 (C-6), 95.0 (C-5), 67.6 (C-1''), 52.8 (C-2'), 37.5 (C-5'), 24.6 (C-3'), 19.6 (C-4'), 15.7 (C-1'), 13.81 (C-6'), 10.26 (C-7').

HRMS (ESI+): Calcd. for $[C_{12}H_{17}N_3O_2+H]^+$: 236.1399, Found: 236.1394.

R_f (CH_2Cl_2-MeOH, 10:3) = 0.39 (vanillin).

2.3. CHAPTER III. Synthesis of 4'-hydroxymehtyl-3'-hydroxybicyclo[4.1.0]-heptane NAs

2.3.1. Synthesis of (1*S*,2*R*,6*R*)-2-(benzyloxy)-5-methylidenebicyclo[4.1.0]heptane, 42 and (1*R*,3*R*,5*R*,6*S*)-5-(benzyloxy)-2-methylidenebicyclo[4.1.0]heptan-3-ol, 63.

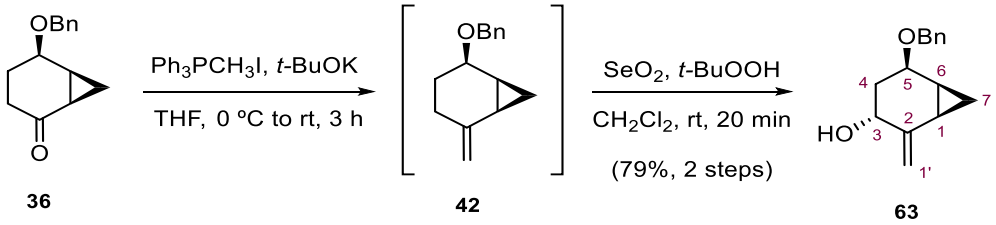

36 **42** **63**

To a stirring solution of Ph_3PCH_3I (11.82 g, 29.2 mmol) in anhydrous THF (30 mL) at 0 °C, *t*-BuOK (3.31 g, 29.5 mmol) was added, under nitrogen atmosphere, and the resulting yellow mixture was allowed to react for 1 h. At this time, a solution of ketone **36** (1.27 g, 5.8 mmol) in anhydrous THF (10 mL) was added and the mixture was stirred for 3 h. Then, diethyl ether (30 mL) was added and the crude filtered through a pad of silica and Celite®, using more diethyl ether (100 mL) as eluent. The volatiles were removed under vacuum to obtain an orange oil, which was directly used for the next step without further purification.

In order to avoid isomerization, crude alkene **42** was rapidly dissolved in CH_2Cl_2 (75 mL) and SeO_2 (128 mg, 1.16 mmol) and *t*-BuOOH (440 µL, 6.38 mmol, 70% in water) were sequentially added at room temperature. After stirring for 20 min, water (50 mL) was added and aqueous phase was extracted with more CH_2Cl_2 (2 x 30 mL). Finally, the organic layers were dried with anhydrous Na_2SO_4, concentrated under reduced pressure and purified by flash column chromatography (SiO_2, hexane-EtOAc, 5:1) to provide allylic alcohol **63** (1.05 g, 4.55 mmol, 79 % overall yield from **36**) as a brown oil.

Spectroscopic and physical data of **42**

(See **2.1.8** section).

Spectroscopic and physical data of **63**

^{1}H-NMR (400 MHz, $CDCl_3$): δ 7.39 – 7.32 (m, 4H, H-Ar), 7.30 – 7.27 (m, 1H, H-Ar), 5.06 (d, J_{gem} = 10.0 Hz, 2H, H-1'), 4.71 (d, J_{gem} = 11.8 Hz, 1H, C*H*$_2$-Ph), 4.52 (d, J_{gem} = 11.8 Hz, 1H, C*H*$_2$-Ph), 4.29 (q, $J_{5,6} = J_{5,4eq} = J_{5,4ax}$ = 6.0 Hz, 1H, H-5), 4.22 (dd, $J_{3,4ax}$ = 8.3 Hz, $J_{3,4eq}$ = 3.2 Hz, 1H, H-3), 1.87 (ddd, $J_{1,7exo}$ = 9.3 Hz, $J_{1,6}$ = 7.8 Hz, $J_{1,7endo}$ = 5.0 Hz, 1H, H-1), 1.77 (ddd, J_{gem} = 13.5 Hz, $J_{4ax,3}$ = 8.3 Hz, $J_{4ax,5}$

= 6.0 Hz, 1H, H-4ax), 1.70 (ddd, J_{gem} = 13.5 Hz, $J_{4eq,5}$ = 6.0 Hz, $J_{4eq,3}$ = 3.2 Hz, 1H, H-4eq), 1.57 (m, 1H, H-6), 0.90 (td, $J_{7exo,6} = J_{7exo,1}$ = 9.3 Hz, J_{gem} = 5.0 Hz, 1H, H-7exo), 0.76 (q, $J_{gem} = J_{7endo,6} = J_{7endo,1}$ = 5.0 Hz, 1H, H-7endo).

^{13}C-NMR (100 MHz, $CDCl_3$): δ 148.6 (C-2), 138.8 (C-*ipso*), 128.4 (C-Ar), 127.7 (C-Ar), 127.5 (C-Ar), 109.2 (C-1'), 70.8 (C-5), 69.8 (*C*H_2-Ph), 67.6 (C-3), 37.0 (C-4), 19.9 (C-1), 16.4 (C-6), 9.0 (C-7).

NOESY experiment has been recorded.

IR (ATR): ν 3399, 3065, 2857, 1640, 1454, 1200, 1066, 824, 698 cm^{-1}.

HRMS (ESI+): calcd. for $[C_{15}H_{18}O_2+H]^+$: 231.1385, found: 231.1375.

R_f (hexane-EtOAc, 2:1) = 0.35 (vanillin, red spot).

$[\alpha]_D^{20}$= +43 (*c* 1.1, $CHCl_3$).

2.3.6. Synthesis of (1*R*,2*R*,3*R*,5*R*,6*S*)-5-(benzyloxy)-2-(hydroxymethyl)bicyclo[4.1.0]heptan-3-ol, 64 and its (2*S*)-diastereoisomer, 68.

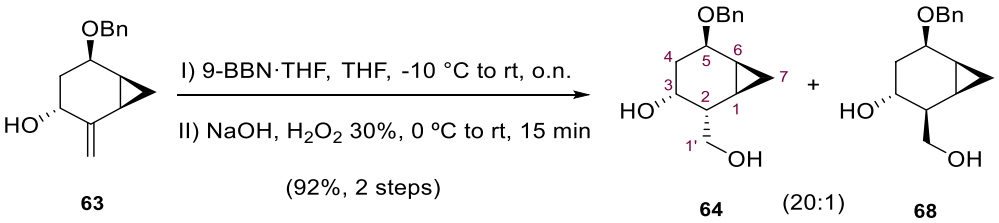

63 **64** (20:1) **68**

To a stirred solution of allylic alcohol **63** (1.750 g, 7.60 mmol) in anhydrous THF (80 mL), 9-borabicyclo[3.3.1]nonane solution (9-BBN, 38 mL, 37.99 mmol, 0.5 M in THF) was added at -10 ºC. The mixture was allowed to slowly warm to rt and stirred overnight. Then, water (18 mL), NaOH (35 mL, 3 M in water) and H_2O_2 (35 mL, 30% in water) were added at 0 ºC. After stirring for 15 min at rt, the mixture was diluted with brine (150 mL) and CH_2Cl_2 (150 mL) and the aqueous phase was extracted with CH_2Cl_2 (2 x 100 mL). The organic layers were dried (Na_2SO_4), concentrated under reduced pressure and purified by flash column chromatography (SiO_2, CH_2Cl_2 100% to CH_2Cl_2-MeOH 20:1 to 10:1) to provide a chromatographically inseparable mixture of alcohols **64** and **68** (1.724 g, 6.94 mmol, 92% overall yield, 2 steps) in a *ca.* 20:1 diastereomeric ratio as a white solid. It was possible to obtain a pure fraction of **64** for its characterization.

Spectroscopic and physical data of **64**

^{1}H-NMR (400 MHz, $CDCl_3$): δ 7.39 – 7.30 (m, 4H, H-Ar), 7.29 – 7.24 (m, 1H, H-Ar), 4.73 (d, J_{gem} = 11.8 Hz, 1H, C*H*$_2$-Ph), 4.55 (d, J_{gem} = 11.8 Hz, 1H, C*H*$_2$-Ph), 4.30 (dt, $J_{5,4ax}$ = 9.5 Hz, $J_{5,4eq} = J_{5,6}$ = 6.1 Hz, 1H, H-5), 4.08 (ddd, $J_{3,4eq}$ = 5.8 Hz, $J_{3,2}$ = 3.5 Hz, $J_{3,4ax}$ = 1.8 Hz, 1H, H-3), 3.91 – 3.80 (m, 2H, H-

1'), 2.30 (s, 2H, 2OH), 2.06 (dt, J_{gem} = 13.8 Hz, $J_{4eq,5}$ = $J_{4eq,3}$ = 6.1 Hz, 1H, H-4eq), 1.76 (tt, $J_{2,1'}$ = 6.2 Hz, $J_{2,1}$ = $J_{2,3}$ = 2.8 Hz, 1H, H-2), 1.39 (tt, $J_{6,7exo}$ = $J_{6,1}$ = 8.8 Hz, $J_{6,7endo}$ = $J_{6,5}$ = 5.9 Hz, 1H, H-6), 1.18 (ddd, J_{gem} = 13.8 Hz, $J_{4ax,5}$ = 9.5 Hz, $J_{4x,3}$ = 1.8 Hz, 1H, H-4ax), 0.93 (tdd, $J_{1,7exo}$ = $J_{1,6}$ = 8.8 Hz, $J_{1,7endo}$ = 5.5 Hz, $J_{1,2}$ = 2.8 Hz, 1H, H-1), 0.81 (td, $J_{7exo,6}$ = $J_{7exo,1}$ = 8.8 Hz, J_{gem} = 4.9 Hz, 1H, H-7exo), 0.39 (q, J_{gem} = $J_{7endo,6}$ = $J_{7endo,1}$ = 5.5 Hz, 1H, H-7endo).

^{13}C-NMR (101 MHz, $CDCl_3$): δ 139.0 (C-*ipso*), 128.5 / 127.9 / 127.6 (C-Ar), 70.7 (C-5), 69.9 (CH2-Ph), 69.0 (C-3), 65.2 (C-1'), 41.2 (C-2), 33.0 (C-4), 13.8 (C-6), 13.0 (C-1), 8.6 (C-7).

COSY, **NOESY**, **HSQC** and **DEPT-135** experiments have been recorded.

IR (ATR): v 3350 (OH), 2872, 2365, 1497, 1454, 1068, 739, 699, 632 cm^{-1}.

HRMS (ESI+): calcd. for $[C_{15}H_{20}O_3+H]^+$: 249.1491; found: 249.1466.

m.p.: 73-75 °C (from Et_2O).

R_f (CH_2Cl_2-MeOH, 10:1) = 0.41; (hexane-EtOAc, 1:1) = 0.1 (vanillin, brown spot);

$[\alpha]_D^{20}$= +104 (*c* 1.0, $CHCl_3$)

2.3.2. Synthesis of {[(1*R*,3*R*,5*R*,6*S*)-5-(benzyloxy)-2-methylenebicyclo[4.1.0]heptan-3-yl]oxy}(*tert*-butyl)dimethylsilane , 69.

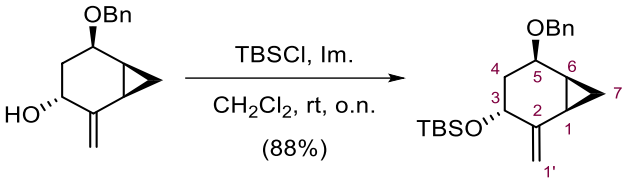

63 **69**

To a stirred solution of allylic alcohol **63** (1.39 g, 6.02 mmol) in CH_2Cl_2 (60 mL), imidazole (492 mg, 7.22 mmol) and *tert*-butyldimethylsilyl chloride (TBSCl, 1.09 g, 7.22 mmol) were added at rt and the mixture was stirred overnight. Water (50 ml) was added, and aqueous phase was extracted with more CH_2Cl_2 (2 x 40 mL). The organic layer was washed with brine (40 ml) and then, dried with Na_2SO_4 and concentrated *in vacuo*. The crude material was purified by flash column chromatography (SiO_2, hexane-EtOAc, 6:1) affording the silyl derivative **69** (1.82 g, 5.29 mmol, 88% yield) as a colourless syrup.

Spectroscopic and physical data of **69**

^{1}H-NMR (400 MHz, $CDCl_3$): δ 7.43 – 7.34 (m, 4H, H-Ar), 7.34 – 7.26 (m, 1H, H-Ar), 5.10 – 4.98 (m, 2H, H-1'), 4.74 (d, J_{gem} = 12.1 Hz, 1H, CH_2-Ph), 4.54 (d, J_{gem} = 12.1 Hz, 1H, CH_2-Ph), 4.29 – 4.20 (m,

2H, H-5, H-3), 1.93 (td, $J_{1,7exo} = J_{1,6} = 8.4$ Hz, $J_{1,7endo} = 5.5$ Hz, 1H, H-1), 1.81 – 1.72 (m, 2H, H-4), 1.55 (dddd, $J_{6,7exo} = 9.0$ Hz, $J_{6,1} = 8.4$ Hz, $J_{6,5} = 6.7$ Hz, $J_{6,7endo} = 5.4$ Hz, 1H, H-6), 0.94 (s, 9H, C(CH_3)$_3$), 0.89 (td, $J_{7exo,1} = J_{7exo,6} = 9.0$ Hz, $J_{gem} = 5.0$ Hz, 1H, H-7exo), 0.79 (q, $J_{gem} = J_{7exo,1} = J_{7exo,6} = 5.4$ Hz, 1H, H-7endo), 0.11 (s, 6H, 2CH_3).

^{13}C-NMR (101 MHz, $CDCl_3$): δ 148.7 (C-2), 139.2 (C-Ar), 128.4 (C-Ar), 127.4 (C-Ar), 127.3 (C-Ar), 107.9 (C-1'), 71.31 (C-5/C-3), 69.7 (*C*H$_2$-Ph), 67.8 (C-3/C-5), 39.6 (C-4), 26.0 (C(*C*H$_3$)$_3$), 20.7 (C-1), 18.4 (*C*(CH$_3$)$_3$), 16.6 (C-6), 9.2 (C-7), -4.7 (Si*C*H$_3$), -4.8 (Si*C*H$_3$).

COSY, **HSQC**, and **DEPT-135** experiments have been recorded.

HRMS (ESI+): calcd. for $[C_{21}H_{32}O_2Si+Na]^+$: 367.2069, found: 367.2066.

R_f (hexane-EtOAc, 2:1) = 0.75 (vanillin, red spot).

$[\alpha]_D^{20}$= +45 (*c* 1.3, $CHCl_3$).

2.3.3. Synthesis of ((1'*R*,2'*R*,3'*R*,5'*R*,6'*S*)-5'-(benzyloxy)-3'-{[*tert*-butyldimethylsilyl]oxy}-bicyclo[4.1.0]heptan-2'-yl)methanol, 70 and its (2'*S*)-diastereoisomer, 71 .

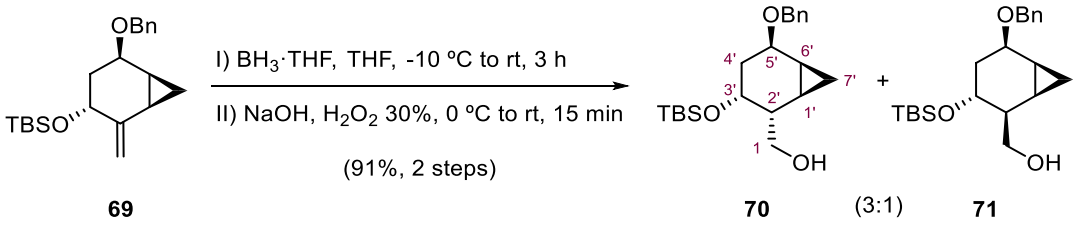

69 **70** (3:1) **71**

To a stirred solution of silyl derivative **69** (1.80 g, 5.21 mmol) in anhydrous THF (95 mL), a borane tetrahydrofuran complex solution (BH_3·THF, 7.82 mL, 7.82 mmol, 1 M in THF) was added at -10 °C. The mixture was allowed to slowly warm to rt and stirred for 3 h. Then, water (8 mL), NaOH (23 mL, 3 M in water) and H_2O_2 (19 mL, 30% in water) were added at 0 °C. After stirring for 15 min at rt, the mixture was treated with brine (200 mL) and CH_2Cl_2 (300 mL) and the aqueous phase was extracted with more CH_2Cl_2 (2 x 200 mL). The organic layers were dried (Na_2SO_4), concentrated under reduced pressure and purified by flash column chromatography (SiO_2, hexane-EtOAc, 6:1 ⟶ 4:1) to provide a chromatographically inseparable mixture of alcohols **70** and **71** (1.71 g, 4.73 mmol, 91% overall yield, 2 steps) in a *ca.* 3:1 diastereomeric ratio as a colourless oil. It was possible to obtain a pure fraction of **70** for its characterization after several purification by flash column chromatography.

Spectroscopic and physical data of **70**

^{1}H-NMR (400 MHz, $CDCl_3$): δ 7.38 – 7.30 (m, 4H, H-Ar), 7.29 – 7.24 (m, 1H, H-Ar), 4.72 (d, J_{gem} = 12.1 Hz, 1H, CH_2-Ph), 4.54 (d, J_{gem} = 12.1 Hz, 1H, CH_2-Ph), 4.22 (dt, $J_{5',4'ax}$ = 9.0 Hz, $J_{5',4'eq}$ = $J_{5',6'}$ = 6.0 Hz, 1H, H-5'), 4.02 (ddd, $J_{3',4'eq}$ = 6.5 Hz, $J_{3',2'}$ = 4.4 Hz, $J_{3',4'ax}$ = 1.8 Hz, 1H, H-3'), 3.78 (dd, J_{gem} = 10.7 Hz, $J_{1a,2'}$ = 7.3 Hz, 1H, H-1a), 3.71 (dd, J_{gem} = 10.7 Hz, $J_{1b,2'}$ = 4.6 Hz, 1H, H-1b), 2.65 (br s, 1H, OH), 1.93 (ddd, J_{gem} = 13.4 Hz, $J_{4'eq,3'}$ = 6.5 Hz, $J_{4'eq,5'}$ = 6.0 Hz, 1H, H-4'eq), 1.78 (dtd, $J_{2',1a}$ = 7.3 Hz, $J_{2',1b}$ = $J_{2',3'}$ = 4.4 Hz, $J_{2',1'}$ = 2.2 Hz, 1H, H-2'), 1.34 (tt, $J_{6',7'exo}$ = $J_{6',1'}$ = 8.8 Hz, $J_{6',7'endo}$ = $J_{6',5'}$ = 5.8 Hz, 1H, H-6'), 1.18 (ddd, J_{gem} = 13.4 Hz, $J_{4'ax,5'}$ = 9.0 Hz, $J_{4'ax,3'}$ = 1.9 Hz, 1H, H-4'ax), 1.04 – 0.92 (m, 1H, H-1'), 0.86 (s, 9H, C(CH_3)$_3$), 0.75 (td, $J_{7'exo,6'}$ = $J_{7'exo,1'}$ = 8.8 Hz, J_{gem} = 5.0 Hz, 1H, H-7'exo), 0.37 (q, J_{gem} = $J_{7'endo,6'}$ = $J_{7'endo,1'}$ = 5.5 Hz, 1H, H-7'endo), 0.07 (s, 3H, CH_3), 0.04 (s, 3H, CH_3).

^{13}C-NMR (101 MHz, $CDCl_3$): δ 139.2 (C-Ar), 128.4 (C-Ar), 127.7 (C-Ar), 127.5 (C-Ar), 70.8 (C-5'), 70.1 (C-3'), 69.7 (*C*H_2-Ph), 65.4 (C-1), 42.2 (C-2'), 33.3 (C-4'), 25.9 (C(*C*H_3)$_3$), 18.1 (*C*(CH$_3$)$_3$), 13.7 (C-6'), 13.6 (C-1'), 8.0 (C-7'), -4.4 (Si*C*H_3), -5.1 (Si*C*H_3).

COSY, **NOESY**, **HSQC**, and **DEPT-135** experiments have been recorded.

HRMS (ESI+): calcd. for $[C_{21}H_{34}O_3Si+Na]^+$: 385.2175, found: 385.2175.

R_f (hexane-EtOAc, 1:1) = 0.57 (vanillin, brown spot).

2.3.4. Synthesis of [(1'*R*,2'*R*,3'*R*,5'*R*,6'*S*)-5'-(benzyloxy)-3'-{(tert-butyldimethylsilyl)oxy}bicyclo[4.1.0]heptan-2'-yl]methyl acetate , 72 and its (2'*S*)-diastereoisomer, 73.

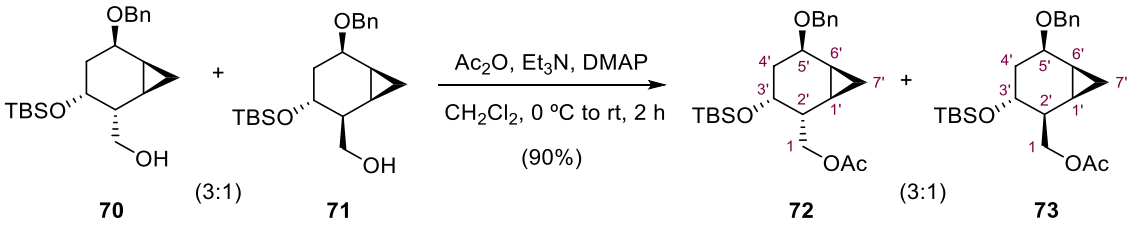

70 (3:1) **71** **72** (3:1) **73**

To a solution of diastereomeric mixture (3:1) of alcohols **70** and **71** (1.71 g, 4.72 mmol) in dry CH_2Cl_2 (47 mL) at 0 °C were added successively Ac_2O (500 µL, 5.29 mmol), DMAP (174 mg, 1.42 mmol) and Et_3N (1 mL, 7.17 mmol). The resulting mixture was allowed to warm to rt and stirred for 2 h. After this time, the reaction was quenched with saturated aqueous $NaHCO_3$ solution (40 mL). Then, the layers were separated and the aqueous one was extracted with CH_2Cl_2 (3 x 20 mL). The organic fractions were combined, dried over anhydrous Na_2SO_4 and concentrated under reduced pressure. The crude product was purified by flash column chromatography (SiO_2, hexane-EtOAc, 10:1 → 5:1 → 1:1) to furnish a chromatographically inseparable mixture of **72** and **73** (1.73 g, 4.27 mmol, 90% yield) in a *ca.* 3:1 diastereomeric ratio as a colourless oil. It was

possible to obtain a pure fraction of **72** and **73** for its characterization after several purification by flash column chromatography.

Spectroscopic and physical data of **72**

^{1}H-NMR (400 MHz, $CDCl_3$): δ 7.41 – 7.32 (m, 4H, H-Ar), 7.30 – 7.25 (m, 1H, H-Ar), 4.74 (dd, J_{gem} = 12.1 Hz, 1H, CH_2-Ph), 4.57 (d, J_{gem} = 12.1 Hz, 1H, CH_2-Ph), 4.27 (dt, $J_{5',4'ax}$ = 10.3 Hz, $J_{5',4'eq}$ = $J_{5',6'}$ = 6.0 Hz, 1H, H-5'), 4.19 (dd, J_{gem} = 10.5 Hz, $J_{1a,2'}$ = 6.8 Hz, 1H, H-1a), 4.07 (dd, J_{gem} = 10.5 Hz, $J_{1b,2'}$ = 8.8 Hz, 1H, 1b), 3.96 (ddd, $J_{3',4'eq}$ = 6.0 Hz, $J_{3',2'}$ = 3.1 Hz, $J_{3',4'ax}$ = 1.4 Hz, 1H, H-3'), 2.06 (s, 3H, CH_3CO), 1.99 (dt, J_{gem} = 13.1 Hz, $J_{4'eq,5'}$ = $J_{4'eq,3'}$ = 6.0 Hz, 1H, H-4'eq), 1.79 (ddt, $J_{2',1b}$ = 8.8 Hz, $J_{2',1a}$ = 6.8 Hz, $J_{2',3'}$ = $J_{2',1'}$ = 3.1 Hz, 1H, H-2'), 1.37 (tt, $J_{1',7'exo}$ = $J_{6',1'}$ = 8.8 Hz, $J_{6',5'}$ = $J_{6',7'endo}$ = 5.9 Hz, 1H, H-6'), 1.06 (ddd, J_{gem} = 13.1 Hz, $J_{4'ax,5'}$ = 10.3 Hz, $J_{4'ax,3'}$ = 1.4 Hz, 1H, H-4'ax), 0.85 (s, 9H, C(CH_3)$_3$), 0.80 (td, $J_{7'exo,6'}$ = $J_{7'exo,1'}$ = 8.8 Hz, J_{gem} = 5.2 Hz, 1H, H-7'exo), 0.76 (tdd, $J_{1',7'exo}$ = $J_{1',6'}$ = 8.8 Hz, $J_{1',7'endo}$ = 5.4 Hz, $J_{1',2'}$ = 3.1 Hz, 1H, H-1'), 0.36 (q, J_{gem} = $J_{7'endo,6'}$ = $J_{7'endo,1'}$ = 5.2 Hz, 1H, H-7'endo), 0.02 (s, 3H, SiCH_3), 0.02 (s, 3H, SiCH_3).

^{13}C-NMR (101 MHz, $CDCl_3$): δ 171.0 (*C*=O), 139.1 (C-Ar), 128.4 (C-Ar), 127.8 (C-Ar), 127.5 (C-Ar), 70.5 (C-5'), 69.8 (*C*H_2-Ph), 67.0 (C-3'), 65.8 (C-1), 40.4 (C-2'), 33.1 (C-4'), 25.8 (C(*C*H_3)$_3$), 21.1 (*C*H_3CO), 18.1 (*C*(CH$_3$)$_3$), 13.8 (C-6'), 12.9 (C-1'), 8.9 (C-7'), -4.4 (Si*C*H$_3$), -5.2 (Si*C*H$_3$).

COSY, **NOESY**, **HSQC**, and **DEPT-135** experiments have been recorded.

HRMS (ESI+): calcd. for $[C_{23}H_{36}O_4Si+H]^+$: 405.2461, found: 405.2446.

R_f (hexane-EtOAc, 4:1) = 0.49 (vanillin, brown spot).

Spectroscopic and physical data of **73**

^{1}H-NMR (400 MHz, $CDCl_3$): δ 7.37 – 7.30 (m, 4H, H-Ar), 7.30 – 7.24 (m, 1H, H-Ar), 4.69 (d, J_{gem} = 12.1 Hz, 1H, CH_2-Ph), 4.48 (d, J_{gem} = 12.1 Hz, 1H, CH_2-Ph), 4.26 – 4.16 (m, 2H, H-5', H-1a), 4.07 (dd, J_{gem} = 10.8 Hz, $J_{1b,2'}$ = 6.7 Hz, 1H, H-1b), 3.64 (ddd, $J_{3',2'}$ = 8.8 Hz, $J_{3',4'ax}$ = 7.0 Hz, $J_{3',4'eq}$ = 3.2 Hz, 1H, H-3'), 2.12 – 2.04 (m, 4H, CH_3CO, H-2'), 1.69 – 1.52 (m, 2H, H-4'), 1.36 – 1.18 (m, 2H, H-1',H-6'), 0.87 (s, 9H, C(CH_3)$_3$), 0.57 – 0.47 (m, 2H, H-7'), 0.04 (s, 6H, 2SiCH_3).

^{13}C-NMR (101 MHz, $CDCl_3$): δ 171.3(*C*=O), 139.3/ 128.4/ 127.5/ 127.4 (C-Ar), 71.6 (C-5'), 69.7 (*C*H_2-Ph), 65.9 (C-3'), 65.7 (C-1), 40.7 (C-2'), 37.0 (C-4'), 25.9 (C(*C*H_3)$_3$), 21.1 (*C*H_3CO), 18.1 (*C*(CH$_3$)$_3$), 15.6 (C-6'), 13.2 (C-1'), 3.4 (C-7'), -4.3 (Si*C*H$_3$), -4.8 (Si*C*H$_3$).

COSY, **HSQC**, and **DEPT-135** experiments have been recorded.

HRMS (ESI+): calcd. for $[C_{23}H_{36}O_4Si+H]^+$: 405.2461, found: 405.2481.

R_f (hexane-EtOAc, 4:1) = 0.53 (vanillin, brown spot).

2.3.5. Synthesis of [(1'*R*,2'*R*,3'*R*,5'*R*,6'*S*)-3'-{(*tert*-butyldimethylsilyl)oxy}-5'-hydroxy-bicyclo[4.1.0]heptan-2'-yl]methyl acetate, 74 and its (2'*S*)-diastereoisomer, 75.

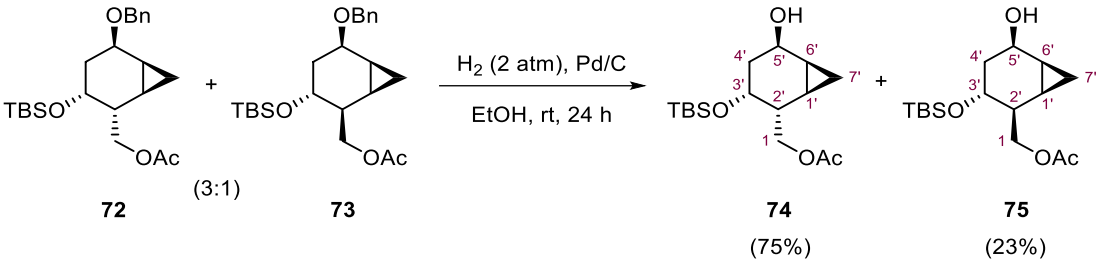

To a solution of diastereomeric mixture (3:1) of **72** and **73** (1.73 g, 4.28 mmol) in EtOH (43 mL) was added Pd/C (190 mg, 10% wt.) follow by H_2 (2 atm) in a hydrogenation reactor. The reaction was stirred at room temperature for 24 h. Then, the mixture was filtered through a short pad of Celite® and rinsed with EtOH. The solvent was evaporated under reduced pressure and the crude was purified by flash column chromatography (SiO_2, hexane-EtOAc, 10:1→ 8:1→ 4:1→ 1:1) to afford a separable alcohols **74** (1.01 g, 3.21 mmol, 75% yield) and **75** (308 mg, 0.99 mmol, 23% yield) both, as a clear oils.

Spectroscopic and physical data of **74**

^{1}H-NMR (400 MHz, $CDCl_3$): δ 4.46 (dt, $J_{5',4'ax}$ = 10.6 Hz, $J_{5',4'eq} = J_{5',6'}$ = 6.1 Hz, 1H, H-5'), 4.14 (dd, J_{gem} = 10.5 Hz, $J_{1a,2'}$ = 6.8 Hz, 1H, H-1a), 4.00 (dd, J_{gem} = 10.5 Hz, $J_{1b,2'}$ = 8.9 Hz, 1H, H-1b), 3.91 (br t, *J*= 3.9 Hz, 1H, H-3'), 2.01 (s, 3H, C*H*$_3$CO), 2.03 – 1.85 (m, 1H, H-4'a), 1.79 – 1.61 (m, 1H, H-2'), 1.41 – 1.25 (m, 1H, H-6'), 0.95 – 0.86 (m, 1H, H-1'), 0.85 (s, 9H, C(C*H*$_3$)$_3$), 0.75 – 0.65 (m, 2H, H), 0.19 (q, $J_{gem} = J_{7'endo,1'} = J_{7'endo,6'}$ = 4.8 Hz, 1H, H-7'endo), 0.04 (s, 3H, SiC*H*$_3$), -0.02 (s, 3H, SiC*H*$_3$).

^{13}C-NMR (101 MHz, $CDCl_3$): δ 171.1(*C*=O), 67.3 (C-3'), 65.8 (C-1), 64.0 (C-5'), 40.2 (C-2'), 35.5 (C-4'), 25.8(C(*C*H$_3$)$_3$), 21.0 (*C*H$_3$CO), 18.1 (*C*(CH$_3$)$_3$), 17.2 (C-6'), 13.1 (C-1') , 8.3 (C-7'), -4.4 (Si*C*H$_3$), -5.3 (Si*C*H$_3$).

COSY, **HSQC**, and **DEPT-135** experiments have been recorded.

HRMS (ESI+): calcd. for $[C_{16}H_{30}O_4Si+H]^+$: 315.1992, found: 315.1992.

R_f (hexane-EtOAc, 2:1) = 0.37 (vanillin, grey spot).

$[\alpha]_D^{20}$= +12 (*c* 1.3, $CHCl_3$).

Spectroscopic and physical data of **75**

^{1}H-NMR (400 MHz, $CDCl_3$): δ 4.46 (td, $J_{5',4'eq} = J_{5',6'}$ = 6.6 Hz, $J_{5',4'ax}$ = 5.3 Hz, 1H, H-5'), 4.01 (d, $J_{1,2'}$ = 6.5 Hz, 2H, H-1), 3.61 (ddd, $J_{3',4'ax}$ = 7.9 Hz, $J_{3',2'}$ = 5.4 Hz, $J_{3',4'eq}$ = 2.5 Hz, 1H, H-3'), 2.09 – 2.01 (m,

1H, H-2'), 2.00 (s, 3H, CH_3CO), 1.57 (ddd, J_{gem} = 13.4 Hz, $J_{4'ax,3'}$ = 7.9 Hz, $J_{4'ax,5'}$ = 5.3 Hz, 1H, H-4'ax), 1.40 – 1.25 (m, 2H, H-4'eq, H-6'), 1.20 (td, $J_{1',7'exo}$ = $J_{1',6'}$ = 9.4 Hz, $J_{1',7'endo}$ = 4.7 Hz, 1H, H-1'), 0.82 (s, 9H, C(CH_3)$_3$), 0.40 – 0.33 (m, 2H, H-7'), -0.01 (s, 3H, SiCH_3), -0.02 (s, 3H, SiCH_3).

^{13}C-NMR (101 MHz, $CDCl_3$): δ 171.2 (*C*=O), 66.4 (C-3'), 65.4 (C-1), 64.5 (C-5'), 39.3 (C-2'), 37.3 (C-4'), 25.8 (C(*C*H$_3$)$_3$), 21.0 (*C*H$_3$CO), 18.0 (*C*(CH$_3$)$_3$), 16.3 (C-6'), 14.8 (C-1'), 2.3 (C-7'), -4.5 (Si*C*H$_3$), -5.0 (Si*C*H$_3$).

COSY, **NOESY**, **HSQC**, and **DEPT-135** experiments have been recorded.

HRMS (ESI+): calcd. for $[C_{16}H_{30}O_4Si+H]^+$: 315.1992, found: 315.1983.

R_f (hexane-EtOAc, 2:1) = 0.30 (vanillin, grey spot).

$[\alpha]_D^{20}$= +106 (*c* 1.3, $CHCl_3$).

2.3.7. Synthesis of (1*S*,2*R*,4*R*,5*R*,6*R*)-5-(hydroxymethyl)bicyclo[4.1.0]heptane-2,4-diol, 84.

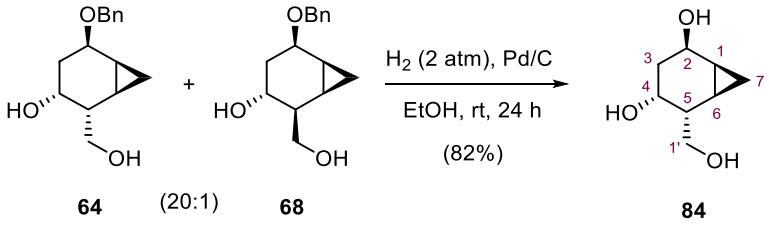

64 (20:1) **68** **84**

To a solution of 20:1 mixture of diols **64** and **68** (101 mg, 0.40 mmol) in EtOH (4 ml) was added a catalytic Pd/C (10 mg, 10% wt.) follow by H_2 (2 atm), and the reaction was stirred at rt for 24 h. Then, the mixture was filtered through a short pad of Celite® dragged with more EtOH. The solvent was evaporated under reduced pressure to give alcohol **84** (63 mg, 0.39 mmol, 95% yield) as a white solid.

Alcohol **84** was re-crystallized by vapor diffusion using MeOH/EtO_2 mixture at rt affording 52 mg (0.33 mmol, 82% yield) of **84** as colourless crystals. X-Ray diffraction structure of **84** was recorded.

Spectroscopic and physical data of **84**

^{1}H-NMR (400 MHz, $CDCl_3$): δ 4.47 (dt, $J_{2,3ax}$ = 10.8 Hz, $J_{2,1}$ = $J_{2,3eq}$ = 5.8 Hz, 1H, H-2), 3.93 (br t, $J_{4,3eq}$ = $J_{4,3eq}$ = 4.3 Hz, 1H, H-4), 3.72 (dd, J_{gem} = 10.6 Hz, $J_{1'a,5}$ = 7.0 Hz, 1H, H-1'a), 3.65 (dd, J_{gem} = 10.6 Hz, $J_{1'b,5}$ = 7.0 Hz, 1H, H-1'b), 1.95 (dt, J_{gem} = 13.3 Hz, $J_{3eq,2}$ = $J_{3eq,4}$ = 5.8 Hz, 1H, H-3eq), 1.58 (tt, $J_{5,1'a}$ = $J_{5,1'b}$ = 7.0 Hz, $J_{5,6}$ = $J_{5,4}$ = 3.0 Hz, 1H, H-5), 1.28 (tt, $J_{1,7exo}$ = $J_{1,6}$ = 8.8 Hz, $J_{1,7endo}$ = $J_{1,4}$ = 5.8 Hz,

1H, H-1), 1.00 (ddd, J_{gem} = 13.3 Hz, $J_{3ax,2}$ = 10.8 Hz, $J_{3ax,4}$ = 1.6 Hz, 1H, H-3ax), 0.83 (tdd, $J_{6,7exo}$ = $J_{6,1}$ = 8.8 Hz, $J_{6,7endo}$ = 5.3 Hz, $J_{6,5}$ = 2.4 Hz, 1H, H-6), 0.73 (td, $J_{7exo,1}$ = $J_{7exo,6}$ = 8.8 Hz, J_{gem} = 4.9 Hz, 1H, H-7exo), 0.27 (q, J_{gem} = $J_{7endo,6}$ = $J_{7endo,1}$ = 5.3 Hz, 1H, H-7endo).

^{13}C-NMR (101 MHz, $CDCl_3$): δ 68.4 (C-4), 65.0 (C-1'), 64.7 (C-2), 43.9 (C-5), 36.0 (C-3), 17.9 (C-1), 14.0 (C-6), 9.6 (C-7).

NOESY, **HSQC** and **DEPT-135** experiments have been recorded.

IR (ATR): ν 3324, 3239, 3019, 2925, 1405, 1250, 1040, 906 cm^{-1}.

HRMS (ESI-): calcd. For $[C_8H_{14}O_3+HCOO]^-$: 203.0919, found: 203.0919.

m.p.: 166-167 °C (from MeOH-Et_2O).

$[\alpha]_D^{20}$= -52 (*c* 1.3, $CHCl_3$).

2.3.8. Synthesis of (1*R*,2*R*,3*R*,3'*S*,5*R*,6*S*)-3'-phenyloctahydrocyclopropa[f][1,3]benzodioxin-5-ol, 76.

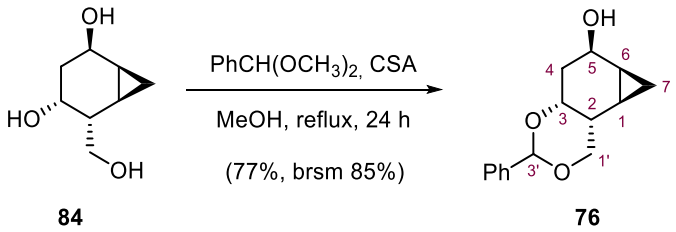

84 **76**

To a solution of triol **84** (131 mg, 0.83 mmol) in MeOH (8 mL), benzaldehyde dimethyl acetal (750 µL, 4.97 mmol) and camphorsulfonic acid (CSA, 20 mg, 0.083 mmol) was added and the mixture was stirred at reflux for 24 h. Upon cooling to rt, the reaction mixture was neutralised with Na_2CO_3, filtered and concentrated *in vacuo*. The crude was purified by flash column chromatography (hexane-EtOAc, 5:1→ 2:1) to afford the tricyclic compound **76** as a white solid (158 mg, 0.64 mmol, 77% yield) and starting material **84** (12 mg, 0.076 mmol, 9%).

Spectroscopic and physical data of **76**

^{1}H-NMR (360 MHz, $CDCl_3$): δ 7.48 (dd, *J* = 8 Hz, *J*= 2.1 Hz, 2H, H-Ar), 7.36 (m, 3H, H-Ar), 5.42 (s, 1H, H-3'), 4.61 (dt, $J_{5,4ax}$ = 11.5 Hz, $J_{5,4eq}$ = $J_{5,6}$ = 6.1 Hz, 1H, H-5), 4.23 (dd, J_{gem} = 11.4 Hz, $J_{1',2}$ = 1.5 Hz, 1H, H-1'), 4.10 (dd, J_{gem} = 11.4 Hz, $J_{1',2}$ = 3.0 Hz, 1H, H-1'), 4.00 (br, 1H, H-3), 2.16 (dt, J_{gem} = 13.6 Hz, $J_{4eq,3}$ = $J_{4eq,5}$ = 6.1 Hz, 1H, H-4eq), 1.49 (m, 2H, H-2, H-6), 1.23 (tddd, $J_{1,6}$ = $J_{1,7exo}$ = 8.6 Hz, $J_{1,7endo}$ = 5.3 Hz, $J_{1,2}$ = 1.7 Hz, $J_{1,3}$ = 1.3 Hz, 1H, H-1), 1.04 (ddd, J_{gem} = 13.4 Hz, $J_{4ax,5}$ = 11.5 Hz, $J_{4ax,3}$ =

1.7 Hz, 1H, H-4ax), 0.77 (td, $J_{7exo,1} = J_{7exo,6}$ = 8.9 Hz, J_{gem} = 5.1 Hz, 1H, H-7exo), 0.27 (q, $J_{gem} = J_{7endo,6} = J_{7endo,1}$ = 5.4 Hz, 1H, H-7endo).

^{13}C-NMR (90 MHz, $CDCl_3$): δ 138.8 (C-Ar), 129.0 (C-Ar), 128.4 (C-Ar), 126.3 (C-Ar), 101.2 (C-3'), 74.7 (C-3), 72.3 (C-1'), 63.8 (C-5), 34.0 (C-2), 33.6 (C-4), 17.9 (C-6), 15.9 (C-1), 8.1 (C-7.)

R_f (hexane-EtOAc, 2:1) = 0.53 (vanillin).

2.3.9. Synthesis of (6a*R*,8*R*,8a*S*,9a*R*,9b*R*)-3,3,5,5-tetraisopropyloctahydrocyclopropa-[3,4]benzo[1,2-*f*][1,3,5,2,4]trioxadisilocin-8-ol, 87 and its (9b*S*)-diastereoisomer, 88.

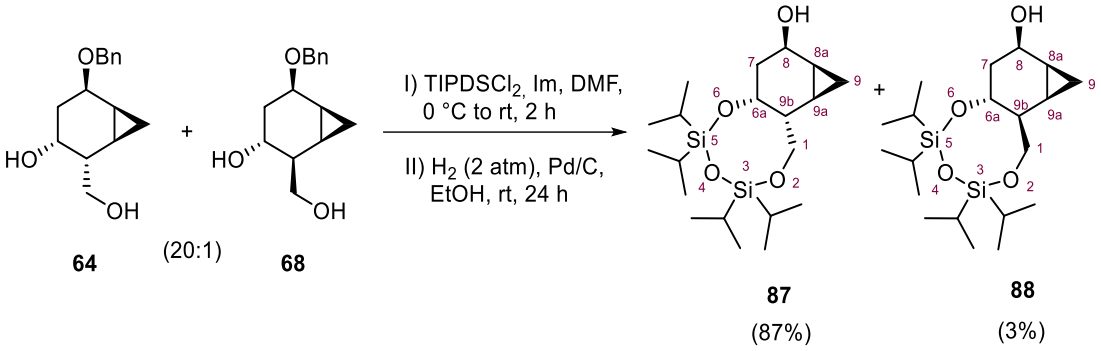

To stirred 20:1 mixture of diols **64** and **68** (100 mg, 0.40 mmol) and imidazole (192 mg, 2.8 mmol) in dry DMF (2.6 mL), 1,3-dichloro-1,1,3,3-tetraisopropyldisiloxane ($TIPDSCl_2$, 135 µL, 0.42 mmol) was added dropwise at 0 °C under nitrogen atmosphere. The mixture was stirred at room temperature for 2 h, quenched with water (2 mL), and extracted with EtOAc (3 x 3 mL). The combined organic layers were washed with brine (4 mL), followed by water (4 mL), and dried over Na_2SO_4. The solvent was removed under reduced pressure, and the residue was purified by flash column chromatography (SiO_2, hexane-EtOAc, 2:1) to give a mixture of inseparable protected alcohols (170 mg, 0.35 mmol, 86% yield) as a colourless oil, which was used directly for the next step.

These oil of mixture of products was dissolved in EtOH (3.5 ml) and was added Pd/C (17 mg, 10% wt.) follow by H_2 (2 atm). The reaction was stirred at rt for 24 h. Then, the mixture was filtered through a short pad of Celite® and rinsed with more EtOH. The solvent was evaporated under reduced pressure and the residue was purified by flash column chromatography (SiO_2, hexane-EtOAc, 10:1) to give the alcohol **87** (140 mg, 0.35 mmol, 87% yield) and its diastereoisomer **88** (5 mg, 0.012 mmol, 3% yield), both as colourless syrups.

Spectroscopic and physical data of **87**

^{1}H-NMR (360 MHz, $CDCl_3$): δ 4.53 (dt, $J_{8,7ax}$ = 11.5 Hz, $J_{8,7eq}$ = $J_{8,8a}$ = 5.9 Hz, 1H, H-8), 4.12 (br t, J= 4.1 Hz, 1H, H-6a), 3.78 (dd, J_{gem} = 10.4, $J_{1,9b}$ = 5.4 Hz, 1H, H-1a), 3.76 – 3.64 (m, 1H, H-1b), 2.07 (dt, J_{gem} = 13.1 Hz, $J_{7eq,8}$ = $J_{7eq,6a}$ = 5.6 Hz, 1H, H-7eq), 1.63 (ddt, $J_{9b,1}$ = 11.1 Hz, $J_{9b,1}$ = 5.4, $J_{9b,9a}$ = $J_{9b,6a}$ = 2.7 Hz, 1H, H-9b), 1.33 (ddd, J_{gem} = 13.1 Hz, $J_{7ax,8}$ = 11.5 Hz, $J_{7ax,6a}$ = 5.9, 1H, H-7ax), 1.36 – 1.30 (m, 1H, H-8a), 1.09 – 0.87 (m, 28H, 2Si[C*H*(CH_3)$_2$]$_2$), 0.67 (td, $J_{9exo,8a}$ = $J_{9exo,9a}$ = 8.7 Hz, J_{gem} = 5.3 Hz, 1H, H-9exo), 0.42 (tdd, $J_{9a,9exo}$ = $J_{9a,8a}$ = 8.7 Hz, $J_{9a,9endo}$ = 5.3 Hz, $J_{9a,9b}$ = 2.3 Hz, 1H, H-9a), 0.20 (q, J_{gem} = $J_{9endo,8a}$ = $J_{9endo,9a}$ = 5.3 Hz, 1H, H-9endo).

HRMS (ESI+): calcd. for [$C_{20}H_{40}O_4Si_2$+Na]$^+$: 423.2363, found: 423.2365.

R_f (hexane-EtOAc, 4:1) = 0.26 (vanillin)

Spectroscopic and physical data of **88**

^{1}H-NMR (360 MHz, $CDCl_3$): δ 4.53 (t, $J_{8,7ax}$ = $J_{8,7eq}$ = 6.4 Hz, 1H, H-8), 4.25 (dd, J_{gem} = 11.2 Hz, $J_{1a,9b}$ = 3.1 Hz, 1H, H-1a), 3.89 – 3.73 (m, 2H, H-1b, H-6a), 1.80 (m, 1H, H-9b), 1.72 – 1.53 (m, 2H, H-7,), 1.41 – 1.28 (m, 1H, H-8a), 1.13 – 0.92 (m, 28H, 2Si[C*H*(CH_3)$_2$]$_2$), 0.92 – 0.76 (m, 2H, H-9a, H-9endo), 0.56 (td, $J_{9exo,8a}$ = $J_{9exo,9a}$ = 9.1 Hz, J_{gem} = 5.2 Hz, 1H, H-9exo).

HRMS (ESI+): Calcd. for [$C_{20}H_{40}O_4Si_2$+Na]$^+$: 423.2363, found: 423.2331

R_f (hexane-EtOAc, 4:1) = 0.29 (vanillin).

2.3.10. Synthesis of [(1'*R*,2'*R*,3'*R*,5'*R*,6'*S*)-3'-(benzoyloxy)-5'-(benzyloxy)bicyclo[4.1.0]hept-2'-yl]methyl benzoate, 91 and its (2'S)-diastereoisomer, 92.

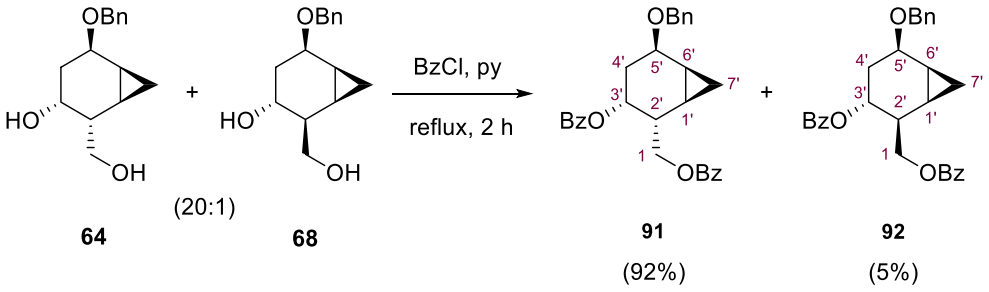

The 20:1 mixture of diols **64** and **68** (1.079 g, 4.35 mmol) was dissolved in dry pyridine (70 mL) and treated with benzoyl chloride (1.76 mL, 15.15 mmol) which was added dropwise at rt. The solution was heated to reflux for 2 h, until TLC analysis (hexane-EtOAc, 1:1) showed a total consumption of the starting material and the monoprotected compound. Then, the solution was

cooled to 70 °C and quenched with MeOH (6 mL). After 30 min, the solvent was removed under reduced pressure and the residue was partitioned between EtOAc (100 mL) and water (100 mL). The organic layer was washed with 1 M HCl (2 × 70 mL) and aqueous saturated $NaHCO_3$ solution (2 × 70 mL) and dried with Na_2SO_4. The filtrate was concentrated under reduced pressure and the residue was purified by flash column chromatography (SiO_2, hexane-EtOAc, 10:1 → 8:1→ 5:1) to afford alcohol **91** (1.826 g, 4.00 mmol, 92% yield) as a clear oil and **92** (98 mg, 0.218 mmol, 5% yield) also as a clear oil.

Spectroscopic and physical data of **91**

^{1}H-NMR (400 MHz, $CDCl_3$): δ 8.06 – 7.98 (m, 4H, H-Ar), 7.63 – 7.53 (m, 2H, H-Ar), 7.45 (m, 4H, H-Ar), 7.40 – 7.24 (m, 5H, H-Ar), 5.50 – 5.44 (m, 1H, H-3'), 4.74 (d, J_{gem} = 11.5 Hz, 1H, CH_2-Ph), 4.63 – 4.52 (m, 2H, CH_2-Ph, H-1), 4.37 (dd, J_{gem} = 10.8 Hz, $J_{1,2'}$ = 8.3 Hz, 1H, H-1), 4.29 (dt, $J_{5',4'ax}$ = 10.0 Hz, $J_{5',4'eq} = J_{5',6'}$ = 6.0 Hz, 1H, H-5'), 2.46 (dt, J_{gem} = 14.1 Hz, $J_{4'eq,5'} = J_{4'eq,3'}$ = 6.0 Hz, 1H, H-4'eq), 2.34 (ddd, $J_{2',1}$ = 8.3 Hz, $J_{2',1}$ = 6.3 Hz, $J_{2',3'}$ = 3.3 Hz, 1H, H-2'), 1.56 (tt, $J_{6',1'} = J_{6',7'exo}$ = 8.7 Hz, $J_{6',7'endo} = J_{6',5'}$ = 5.8 Hz, 1H, H-6'), 1.35 (ddd, J_{gem} = 14.1 Hz, $J_{4'ax,5'}$ = 10.1 Hz, $J_{4'ax,3'}$ = 1.7 Hz, 1H, H-4'ax), 1.11 (tdd, $J_{1',7'exo} = J_{1',6'}$ = 8.7 Hz, $J_{1',7'endo}$ = 5.5 Hz, $J_{1',2'}$ = 2.4 Hz, 1H, H-1'), 0.97 (td, $J_{7'exo,1'} = J_{7'exo,6'}$ = 8.7 Hz, J_{gem} = 5.1 Hz, 1H, H-7'exo), 0.59 (q, $J_{gem} = J_{7'endo,1'} = J_{7'endo,6'}$ = 5.5 Hz, 1H, H-7'endo).

^{13}C-NMR (101 MHz, $CDCl_3$): δ 166.6 (*C*=O), 165.8 (*C*=O), 138.8 / 133.1 / 130.3 / 130.1 / 129.74 / 129.67 / 128.6 / 128.50 / 128.48 / 127.9 / 127.6 (C-Ar), 70.7 (C-5'), 70.22 (C-3'), 70.17 (*C*H_2-Ph), 65.2 (C-1), 38.7 (C-2'), 30.0 (C-4'), 14.3 (C-6'), 13.5 (C-1'), 9.1 (C-7').

COSY, **NOESY**, **HSQC**, and **DEPT-135** experiments have been recorded.

IR (ATR): ν 3066, 3017, 1714, 1602, 1585, 1451, 1268, 1215, 747, 708 cm^{-1}.

HRMS (ESI+): Calcd. For $[C_{29}H_{28}O_5+H]^+$: 457.2015, Found: 457.2015.

R_f (hexane-EtOAc, 1:1) = 0.65; (hexane-EtOAc, 5:1) = 0.25 (vanillin, brown spot).

$[\alpha]_D^{20}$= +16.9 (*c* 2.13, $CHCl_3$)

Spectroscopic and physical data of **92**

^{1}H-NMR (400 MHz, $CDCl_3$): δ 8.10 – 8.00 (m, 4H, H-Ar), 7.61 – 7.52 (m, 2H, H-Ar), 7.47 – 7.36 (m, 8H, H-Ar), 7.35 – 7.29 (m, 1H, H-Ar), 5.24 (ddd, $J_{3',2'}$ = 10.2 Hz, $J_{3',4'eq}$ = 7.7 Hz, $J_{3',4'ax}$ = 3.1 Hz, 1H, H-3'), 4.76 (d, J_{gem} = 11.9 Hz, 1H, CH_2-Ph), 4.58 (d, J_{gem} = 11.9 Hz, 1H, CH_2-Ph), 4.50 (dd, J_{gem} = 11.1 Hz, $J_{1,2'}$ = 6.3 Hz, 1H, H-1), 4.45 (dd, J_{gem} = 11.1 Hz, $J_{1,2'}$ = 6.5 Hz, 1H, H-1), 4.33 (dt, $J_{5',4'ax}$ = 7.3 Hz, $J_{5',4'eq} = J_{5',6'}$ = 5.3 Hz, 1H, H-5'), 2.73 – 2.66 (m, 1H, H-2'), 1.98 (ddd, J_{gem} = 13.6 Hz, $J_{4'ax,5'}$ = 7.3 Hz, $J_{4'ax,3'}$ = 3.1 Hz, 1H, H-4'ax), 1.88 (ddd, J_{gem} = 13.6 Hz, $J_{4'eq,3'}$ = 7.7 Hz, $J_{4'eq,5'}$ = 5.3 Hz, 1H, H-4'eq),

1.53 – 1.46 (m, 2H, H-1', H-6'), 0.79 (q, $J_{gem} = J_{7'endo,1'} = J_{7'endo,6'}$ = 5.6 Hz, 1H, H-7'endo), 0.72 (td, $J_{7'exo,6'} = J_{7'exo,1'}$ = 9.0 Hz, J_{gem} = 5.4 Hz, 1H, H-7'exo).

^{13}C-NMR (101 MHz, $CDCl_3$): δ 166.6 (*C*=O), 165.8 (*C*=O), 138.7 / 133.0 / 132.9 / 130.4 / 130.2 / 129.7 / 128.4 / 128.4 / 127.7 / 127.5 (C-Ar), 70.7 (C-5'), 69.7 (C-3'), 69.6 (CH_2-Ph), 66.1 (C-1), 37.7 (C-2'), 33.4 (C-4'), 15.5 (C-6'), 13.4 (C-1'), 3.5 (C-7').

COSY, **NOESY**, **HSQC** and **DEPT-135** experiments have been recorded.

IR (ATR): ν 3065, 3017, 1716, 1605, 1585, 1453, 1272, 1211, 747, 708 cm^{-1}.

HRMS (ESI+): Calcd. For $[C_{29}H_{28}O_5+Na]^+$: 479.1834, Found: 479.1832.

R_f (hexane-EtOAc, 1:1) = 0.65; (hexanes-EtOAc 5:1) = 0.31 (vanillin, brown spot).

$[\alpha]_D^{20}$= +5.42 (*c* 1.55, $CHCl_3$).

2.3.11. Synthesis of [(1'*R*,2'*R*,3'*R*,5'*R*,6'*S*)-3'-(benzoyloxy)-5'-hydroxybicyclo[4.1.0]hept-2'-yl]methyl benzoate, 93.

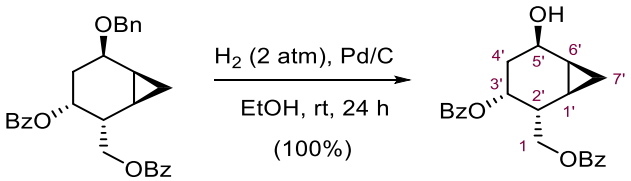

91 **93**

To a solution of **91** (1.872 g, 4.10 mmol) in EtOH (41 ml), Pd/C (190 mg, 10% wt.) was added follow by H_2 (2 atm), and the reaction was stirred at rt for 24 h. Then, the mixture was filtered through a short pad of Celite® and rinsed with EtOH. The solvent was evaporated under reduced pressure to give the alcohol **93** (1.501 g, 4.08 mmol, 100% yield) as a colourless syrup.

Spectroscopic and physical data of **93**

^{1}H-NMR (400 MHz, $CDCl_3$): δ 8.03 – 7.98 (m, 4H, H-*orto*), 7.60 – 7.49 (m, 2H, H-*para*), 7.47 – 7.37 (m, 4H, H-*meta*), 5.43 (br t, $J_{3',4'ax} = J_{3',4'eq} = J_{3',2'}$ = 4.3 Hz, 1H, H-3'), 4.57 (dd, J_{gem} = 10.8 Hz, $J_{1,2'}$ = 6.7 Hz, 1H, H-1), 4.50 (dt, $J_{5',4'ax}$ = 11.2 Hz, $J_{5',4'eq} = J_{5',6'}$ = 5.8 Hz, 1H, H-5'), 4.33 (dd, J_{gem} = 10.8 Hz, $J_{1,2'}$ = 8.8 Hz, 1H, H-1), 2.39 (dt, J_{gem} = 12.4 Hz, $J_{4'eq,5'} = J_{4'eq,3'}$ = 5.8 Hz, 1H, H-4'eq), 2.26 (ddt, $J_{2',1}$ = 8.9 Hz, $J_{2',1}$ = 6.7 Hz, $J_{2',3'} = J_{2'1'}$ = 4.5 Hz, 1H, H-2'), 1.63 (s, 1H, OH), 1.58 – 1.52 (m, 1H, H-6'), 1.28 – 1.14 (m, 1H, H-4'ax), 1.08 (tt, $J_{1',7'exo} = J_{1',6'}$ = 8.5 Hz, $J_{1',7'endo} = J_{1',2'}$ = 4.5 Hz, 1H, H-1'), 0.89 (td, $J_{7'exo,1'} = J_{7'exo,6'}$ = 8.5 Hz, J_{gem} = 5.4 Hz, 1H, H-7'exo), 0.45 (q, $J_{gem} = J_{7'endo,6'} = J_{7'endo,1'}$ = 5.4 Hz, 1H, H-7'endo).

^{13}C-NMR (101 MHz, $CDCl_3$): δ 166.5 (*C*=O), 165.8 (*C*=O), 133.2 (C-*para*), 133.1 (C-*para*), 130.2 (C-*ipso*), 130.0 (C-*ipso*), 129.7 (C-*orto*), 129.6 (C-*orto*), 128.6 (C-*meta*), 128.5 (C-*meta*), 70.4 (C-3'), 65.2 (C-1), 63.9 (C-5'), 38.5 (C-2'), 32.4 (C-4'), 17.4 (C-6'), 13.5 (C-1'), 8.6 (C-7').

COSY, **HSQC**, and **DEPT-135** experiments have been recorded.

IR (ATR): v 3489, 3005, 2953, 2338, 1713, 1601, 1450, 1265, 1108, 708 cm^{-1}.

HRMS (ESI+): Calcd. For $[C_{22}H_{22}O_5+Na]^+$: 389.1365, Found: 389.1363.

R_f (hexane-EtOAc, 1:1) = 0.28 (vanillin, garnet spot).

$[\alpha]_D^{20}$= -25.0 (*c* 1.45, $CHCl_3$)

2.3.12. Synthesis of [(1'*R*,2'*R*,3'*R*,5'*S*,6'*S*)-5'-azido-3'-(benzoyloxy)bicyclo[4.1.0]hept-2-yl]methyl benzoate, 94 and [(1'*R*,2'*R*,3'*R*,6'*R*)-3'-(benzoyloxy)bicyclo[4.1.0]hept-4'-en-2'-yl]methyl benzoate, 95.

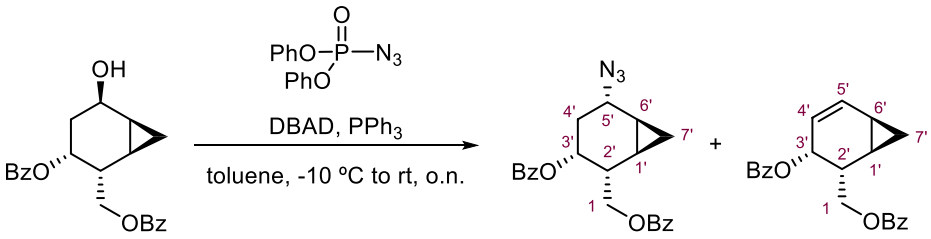

93 **94** (64%) **95** (9%)

To a stirred solution of Ph_3P (1.25 g, 4.76 mmol) in dry toluene (35 mL), DBAD (1.10 g, 4.76 mmol) was slowly added under argon atmosphere and the mixture was stirred for 45 min at 0 °C (after 15 min, a white suspension appeared). Then, diphenylphosphoryl azide (DPPA, 720 µL, 3.33 mmol) and a solution of **93** (1.161 g, 3.17 mmol) in dry toluene (15 mL) were sequentially added at -10 °C. The mixture was allowed to slowly warm to room temperature and stirred overnight. Then, the solvent was removed and the crude was purified by flash column chromatography (SiO_2, hexane-EtOAc, 30:1 → 20:1 → 15:1) to provide azide **94** (794 mg, 2.03 mmol, 64% yield) as a white solid and the elimination product **95** (98 mg, 0.28 mmol, 9% yield) as a colourless syrup.

Azide **94** was re-crystallized by vapor diffusion using MeOH/EtO_2 mixture at room temperature yielding colourless crystals adequated for X-Ray diffraction analysis.

Spectroscopic and physical data of **94**

^{1}H-NMR (400 MHz, $CDCl_3$): δ 8.08 (d, $J_{orto,meta}$ = 7.5 Hz, 2H, H-*orto*), 8.00 (d, $J_{orto,meta}$ = 7.5 Hz, 2H, H-*orto*), 7.58 – 7.52 (m, 2H, H-*para*), 7.42 (m, 4H, H-*meta*), 5.25 (ddd, $J_{3',4'eq}$ = 6.5 Hz, $J_{3',2'}$ = 4.1 Hz, $J_{3',4ax}$= 2.8 Hz, 1H, H-3'), 4.62 (dd, J_{gem} = 10.9 Hz, $J_{1,2'}$ = 7.2 Hz, 1H, H-1), 4.48 (dd, J_{gem} = 10.9 Hz, $J_{1,2'}$ = 7.2 Hz, 1H, H-1), 4.02 (td, $J_{5',4ax}$ = $J_{5',4eq}$ = 5.4 Hz, $J_{5',6'}$ = 1.5 Hz, 1H, H-5'), 2.33 (tt, $J_{2',1}$ = 7.2 Hz, $J_{2',3'}$ = $J_{2'1'}$ = 3.4 Hz, 1H, H-2'), 2.23 (dt, J_{gem} = 15.0, $J_{4'eq,5'}$ = $J_{4'eq,3'}$ = 5.4 Hz, 1H, H-4'eq), 1.71 (ddd, J_{gem} = 15.0 Hz, $J_{4'ax,5'}$ = 5.4 Hz, $J_{4'ax,3'}$ = 2.8 Hz, 1H, H-4'ax), 1.30 (td, $J_{6',7'exo}$ = $J_{6',1'}$ = 9.0 Hz, $J_{6',7'endo}$ = 5.3 Hz, 1H, H-6'), 1.12 (td, $J_{1',7'exo}$ = $J_{1',6'}$ = 9.0 Hz, $J_{1',7'endo}$ = 5.3 Hz, 1H, H-1'), 1.04 (td, $J_{7'endo,6}$ = $J_{7'endo,1}$ = 9.0 Hz, J_{gem} = 5.1 Hz, 1H, H-7'exo), 0.23 (q, J_{gem} = $J_{7'endo,6'}$ = $J_{7'endo,1'}$ = 5.3 Hz, 1H, H-7'endo).

^{13}C-NMR (101 MHz, $CDCl_3$): δ 166.6 (*C*=O), 166.2 (*C*=O), 133.2 (2C, C-*para*), 130.3 (C-*ipso*), 130.0 (C-*ipso*), 129.8 (C-*orto*), 129.7 (C-*orto*), 128.52 (C-*meta*), 128.50 (C-*meta*), 66.6 (C-3'), 65.2 (C-1), 55.2 (C-5'), 38.3 (C-2'), 29.2 (C-4'), 14.1 (C-6'), 11.3 (C-1'), 11.0 (C-7').

COSY, **NOESY**, **HSQC**, and **DEPT-135** experiments have been recorded.

IR (ATR): ν 2922, 2109 (N=N=N), 1709 (C=O), 1599, 1449, 1267, 1248 cm^{-1}.

HRMS (ESI+): Calcd. For $[C_{22}H_{21}N_3O_4+H]^+$: 392.1610, Found: 392.1607.

m.p.: 109-108 °C (from MeOH-Et_2O).

R_f (hexane-EtOAc, 3:1) = 0.31 (vanillin, orange spot)

$[\alpha]_D^{20}$= -73.9 (*c* 0.98, $CHCl_3$).

Spectroscopic and physical data of **95**

^{1}H-NMR (400 MHz, $CDCl_3$): δ 8.06 – 8.01 (m, 2H, H-*orto*), 7.94 – 7.87 (m, 2H, H-*orto*), 7.53 – 7.44 (m, 2H, H-*para*), 7.40 – 7.29 (m, 4H, H-*meta*), 6.27 (ddd, $J_{5',4'}$ = 10.1 Hz, $J_{5',6'}$ = 4.7 Hz, $J_{5',3'}$ = 2.4 Hz, 1H, H-5'), 5.51 (dt, $J_{3',2'}$ = 6.8 Hz, $J_{3',4'}$ = $J_{3',5'}$ = 2.4 Hz, 1H, H-3'), 5.47 (dd, $J_{4',5'}$ = 10.2 Hz, $J_{4',3'}$ = 2.0 Hz, 1H, H-4'), 4.57 (dd, J_{gem} = 11.0 Hz, $J_{1a,2'}$ = 5.7 Hz, 1H, H-1a), 4.31 (dd, J_{gem} = 11.0 Hz, $J_{1b,2'}$ = 7.0 Hz, 1H, H-1b), 3.10 (qd, $J_{2',3'}$ = $J_{2'1a}$ = $J_{2',1b}$ = 6.7 Hz, $J_{2',1'}$ = 2.5 Hz, 1H, H-2'), 1.49 (tdd, $J_{1',7'exo}$ = $J_{1',6'}$ = 8.5 Hz, $J_{1',7'endo}$ = 5.7 Hz, $J_{1',2'}$ = 2.5 Hz, 1H, H-1'), 1.42 (tt, $J_{6',7'exo}$ = $J_{6',1'}$ = 8.5 Hz, $J_{6',7'endo}$ = $J_{6',5'}$ = 4.7 Hz, 1H, H-6'), 1.03 (td, $J_{7'exo,6'}$ = $J_{7'exo,1'}$ = 8.5 Hz, J_{gem} = 4.7 Hz, 1H, H-7'exo), 0.68 (dt, $J_{7'endo,1'}$ = 5.7 Hz, J_{gem} = $J_{7'endo,6'}$ = 4.7 Hz, 1H, H-7'endo).

^{13}C-NMR (101 MHz, $CDCl_3$): δ 166.8 (*C*=O), 166.0 (*C*=O), 133.2 (C-*para*), 132.9 (C-*para*), 132.3 (C-5'), 130.2 (C-*ipso*), 130.2 (C-*ipso*), 129.8 (C-*orto*), 129.6 (C-*orto*), 128.5 (C-*meta*), 128.3 (C-*meta*), 122.1 (C-4'), 68.3 (C-3'), 65.7 (C-1), 33.0 (C-2'), 13.7 (C-1'), 13.2 (C-7'), 9.7 (C-6').

COSY, **NOESY**, **HSQC**, and **DEPT-135** experiments have been recorded.

IR (ATR): ν 3063, 2922, 1712, 1601, 1265, 1109, 1025, 707 cm^{-1}.

HRMS (ESI+): Calcd. For $[C_{22}H_{20}O_4+Na]^+$: 371.1254, Found: 371.1247.

R_f (hexane-EtOAc, 3:1) = 0.44 (vanillin, blue spot).

2.3.13. [(1'R,2'R,3'R,5'S,6'S)-5'-amino-3'-(benzoyloxy)bicyclo[4.1.0]hept-2'-yl]methyl benzoate hydrochloride, 96.

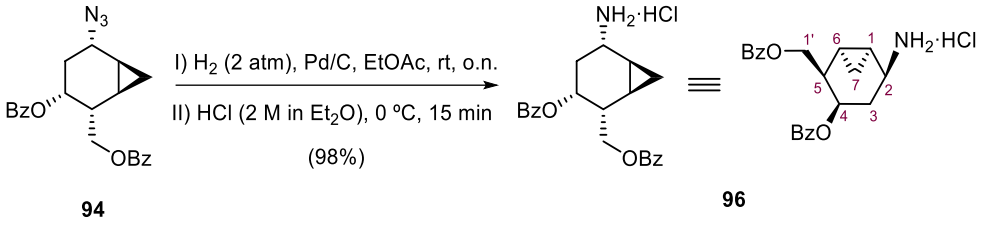

94 **96**

A stirred solution of azide **94** (615 mg, 1.57 mmol) in EtOAc (16 ml) was hydrogenated in the presence of Pd/C (61.5 mg, 10% wt.) at 2 atm for 24 h at rt. Then, the mixture was filtered through a short pad of Celite® and rinsed with more EtOAc. The solvent was evaporated under reduced pressure and the crude was treated with 2 M HCl·Et_2O (1 mL, 2 mmol) at 0 °C and stirred for 15 min. The suspension was filtered obtaining a white solid identified as the ammonium salt **96** (618 mg, 1.54 mmol, 98% yield).

Spectroscopic and physical data of **96**

^{1}H-NMR (400 MHz, MeOH-d_4): δ 8.05 (d, $J_{orto,meta}$ = 7.4 Hz, 2H, H-*orto*), 7.92 (d, $J_{orto,meta}$ = 7.8 Hz, 2H, H-*orto*), 7.65 – 7.52 (m, 2H, H-*para*), 7.50 – 7.36 (m, 4H, H-*meta*), 5.43 (dt, $J_{3',4'ax}$ = 6.3 Hz, $J_{3',4'eq}$ = $J_{3',2'}$ = 4.3 Hz, 1H, H-3'), 4.63 – 4.56 (m, 2H, H-1), 3.61 (br t, $J_{5',4'eq}$ = $J_{5'4'ax}$ = 6.4 Hz, 1H, H-5'), 2.49 (tt, $J_{2',1}$ = 7.7 Hz, $J_{2',3'}$ = $J_{2',1'}$ = 4.0 Hz, 1H, H-2'), 2.19 (dt, J_{gem} = 14.7 Hz, $J_{4'eq,3'}$ = $J_{4'eq,5}$ = 4.9 Hz, 1H, H-4'eq), 1.99 (dt, J_{gem} = 14.7 Hz, $J_{4'ax,3'}$ = $J_{4'ax,5'}$ = 6.3 Hz, 1H, H-4'ax), 1.33 – 1.19 (m, 2H, H-1',H-6'), 1.11 (td, $J_{7'endo,6}$ = $J_{7'endo,1}$ = 8.9 Hz, J_{gem} = 5.4 Hz, 1H, H-7'exo), 0.52 (q, J_{gem} = $J_{7'endo,6'}$ = $J_{7'endo,1'}$ = 5.4 Hz, 1H, H-7'endo).

^{13}C-NMR (101 MHz, MeOH-d_4): δ 167.7 (*C*=O), 167.2 (*C*=O), 134.6 (C-*para*), 134.3 (C-*para*), 131.1 (C-*ipso*), 131.0 (C-*ipso*), 130.7 (C-*orto*), 130.5 (C-*orto*), 129.7 (C-*meta*), 129.5 (C-*meta*), 69.0 (C-3'), 65.9 (C-1), 47.6 (C-5'), 38.3 (C-2'), 30.6 (C-4'), 13.9 (C-6'), 12.3 (C-1'), 11.3 (C-7').

COSY, **HSQC**, and **DEPT-135** experiments have been recorded.

IR (ATR): v 3048, 2922, 1714, 1615, 1514, 1269, 1099, 708 cm^{-1}.

HRMS (ESI+): Calcd. for $[C_{22}H_{24}NO_4]^+$: 366.1705, Found: 366.1703.

m.p.: >210-215°C (decomposes) (from Et_2O).

$[\alpha]_D^{20}$ = -33.5 (*c* 0.82 , $CHCl_3$).

2.3.14. Synthesis of (E)-3-ethoxy-2-methylacrylic acid, 101.

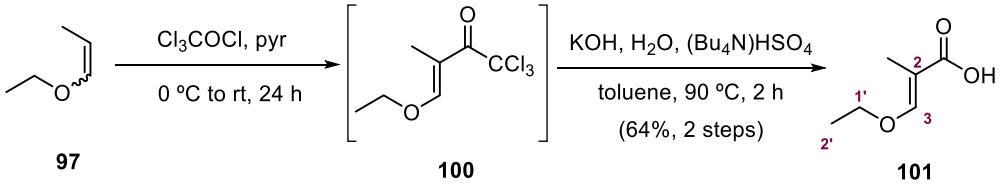

97 100 101

A mixture of **97** (*cis*/*trans* 2:1, 6.40 mL, 58.1 mmol) and pyridine (4.70 mL, 58.1 mmol) was added to a cooled solution of trichloroacetyl chloride (7.90 mL, 70.38 mmol) in $CHCl_3$ (29 mL) at such a rate to keep the reaction temperature between 0-3 °C. After the addition, the reaction was allowed to warm to rt and stirred for 16 h. Water (30 mL) was then added cautiously and the mixture was stirred for 5 min. The layers were separated and the aqueous phase was extracted with $CHCl_3$ (2 x 25 mL). The combined organic phases were washed with 0.1 M HCl (80 mL), 0.1 M KOH (80 mL) and brine (80 mL), dried (Na_2SO_4), filtered, and evaporated *in vacuo* in order to obtain a yellow oil identified as **100**, which was used in the next step without further purification. Water (1.7 mL) was added to an ice-cooled mixture of **100**, toluene (28 mL) and KOH (2.245 g, 40.09 mmol), followed by tetrabutylammonium hydrogen sulphate (5.207 g, 15.34 mmol) and then the mixture was heated to 90 °C for 2 h. Then, the reaction was cooled at rt extracted with water (25 mL) and 0.5 M solution of KOH (10 mL). The aqueous layers were washed with toluene (25 mL), combined and acidified with 5 M HCl solution (10 mL). The suspension was extracted with EtOAc (4 x 40 mL) and the combined extracts were washed with brine (50 mL). The organic layer was stirred with activated charcoal (Norit®, 3 g), filtered through Celite® and evaporated to afford the methylacrylic acid **101** (4.810 g, 36.96 mmol, 64% yield) as a pale-yellow solid.

Spectroscopic data of **101**

^{1}H-NMR (360 MHz, $CDCl_3$): δ 7.48 (q, $J_{3,CH3}$ = 1.3 Hz, 1H, H-3), 4.07 (q, $J_{1',2'}$ = 7.1 Hz, 1H, H-1'), 1.73 (d, $J_{CH3,3}$ = 1.3 Hz, 3H, CH_3), 1.33 (t, $J_{2',1'}$ = 7.1 Hz, 3H, H-1').

2.3.15. Synthesis of (E)-3-ethoxy-2-methylacryloyl chloride, 99.

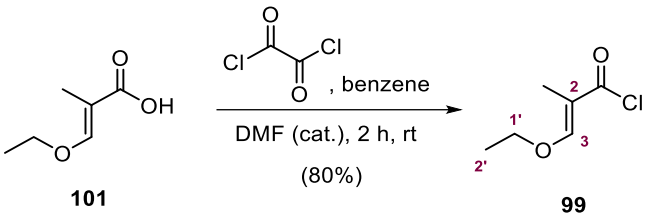

Oxalyl chloride (1.2 mL, 13.56 mmol) was added dropwise to a solution of **101** (1.471 g, 11.30 mmol) and DMF (10 drops) in dry benzene (8 mL) at rt under N_2 atmosphere. The mixture was stirred for 2 h and then was concentrated under reduce pressure. Distillation *in vacuo* gave **99** (1.343 g, 9.04 mmol, 80% yield) as a colourless oil.

Spectroscopic and physical data of **99**

^{1}H-NMR (360 MHz, $CDCl_3$): δ 7.75 (s, 1H, H-3), 4.19 (q, $J_{1',2'}$ = 7.1 Hz, 2H, H-1'), 1.76 (s, 3H, CH_3), 1.36 (t, $J_{2',1'}$ = 7.1 Hz, 3H, H-2'').

b.p.: 90-95°C/ 16 mbar.

2.3.16. Synthesis of (E)-3-ethoxy-2-methylacryloyl isocyanate, 102 and subsequent synthesis of 1-((1'*S*,2'*S*,4'*R*,5'*R*,6'*R*)-4'-hydroxy-5'-(hydroxymethyl) bicyclo[4.1.0]heptan-2'-yl)-5-methylpyri-midine-2,4(1*H*,3*H*)-dione, 104.

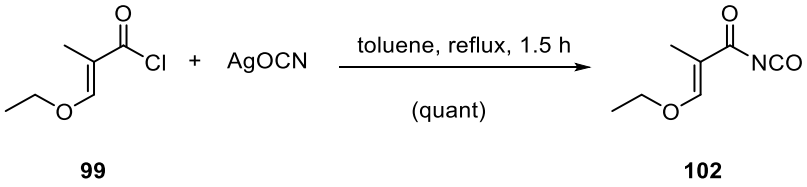

To a suspension of silver cyanate (235 mg, 1.57 mmol), previously dried over phosphorus pentoxide at 80 °C for 3 h, in dry toluene (3 mL), a solution of acid chloride **99** (196 mg, 1.32 mmol) was added dropwise in dry toluene (0.8 mL). The heterogeneous mixture was refluxed under an argon atmosphere for 1.5 h before allowing to cool to rt. The precipitate was allowed to settle and the supernatant was transferred via cannula to a dry Schlenk flask. The precipitate was further washed with a small quantity of dry CH_2Cl_2 (1 mL) and also transferred to the same flask.

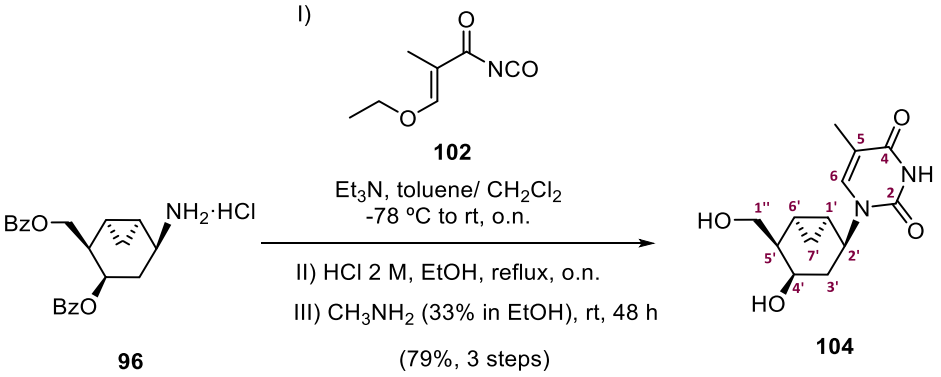

The freshly isocyanate solution was cooled to -78 °C and a solution of the amine **96** (175 mg, 0.44 mmol) with Et_3N (65 µL, 0.47 mmol) in dry CH_2Cl_2 (1.5 mL) was added dropwise over 3 min. The solution was allowed to warm slowly to rt and stirred overnight (16 h). The intermediate has an R_f value of 0.13 by thin layer chromatography (hexane-EtOAc, 4:1). EtOH (3 mL) was added and the reaction mixture was concentrated *in vacuo*. To the crude residue was added EtOH (4 mL) and 2 M HCl (1.25 mL, 2.5 mmol). The reaction mixture was refluxed overnight (20 h), then, was cooled to rt and the solution was concentrated *in vacuo* (the residual water was azeotroped with toluene). The residue was dissolved in a 33% solution of methylamine in EtOH (50 mL) in a sealed flask and stirred 48 h at rt. Then, the mixture was concentrated under reduce pressure, and purified by flash column chromatography (SiO_2, gradient of CH_2Cl_2-MeOH, 20:1 → 15:1) to provide nucleoside analogue **104** (92 mg, 0.36 mmol, 79% overall yield) as a white solid.

Thymine compound **104** was crystallized by vapor diffusion using MeOH-EtO_2 mixture at low temperature giving colourless crystals suitable for X-Ray diffraction analysis.

Spectroscopic and physical data of **104**

^{1}H-NMR (400 MHz, MeOH-d_4): δ 7.82 (q, $J_{6,CH3}$ = 1.1 Hz, 1H, H-6), 4.77 (td, $J_{2',3'ax}$ = $J_{2',3'eq}$ = 6.3, $J_{2',1'}$ = 1.5 Hz, 1H, H-2'), 3.89 (dd, J_{gem} = 10.7 Hz, $J_{1''a,5'}$ = 6.4 Hz, 1H, H-1''), 3.86 – 3.80 (m, 2H, H-4', H-1''), 1.89 (d, $J_{CH3,6}$ = 1.1 Hz, 3H, CH_3), 1.87-1.82 (m, 2H, H-3'eq, H-5'), 1.63 (ddd, J_{gem} = 14.2 Hz, $J_{3'ax,2'}$ = 6.3 Hz, $J_{3'ax,4'}$ = 2.9 Hz, 1H, H-3'ax), 1.17 (tdd, $J_{6',7'exo}$ = $J_{6',1'}$ = 8.5 Hz, $J_{6',7'endo}$ = 5.5 Hz, $J_{6'5'}$ = 2.6 Hz, 1H, H-6'), 1.06 (tdd, $J_{1',7'exo}$ = $J_{1'6'}$ = 8.5 Hz, $J_{1'7'endo}$ = 6.2 Hz, $J_{1'2'}$ = 1.5 Hz, 1H, H-1'), 0.91 (td, $J_{7'exo,6'}$ = $J_{7'exo,1'}$ = 8.5 Hz, J_{gem} = 5.3 Hz, 1H, H-7'exo), 0.23 (q, J_{gem} = $J_{7'endo,1'}$ = $J_{7'endo,6'}$ = 5.3 Hz, 1H, H-7'endo).

^{13}C-NMR (101 MHz, MeOH-d_4): δ 166.7 (C-2), 153.0 (C-4), 141.9 (C-6), 110.2 (C-5), 65.7 (C-4'), 64.4 (C-1''), 52.1 (C-2'), 42.4 (C-5'), 33.6 (C-3'), 14.5 (C-1'), 13.6 (C-6'), 12.5 (CH_3), 11.1 (C-7').

COSY, **NOESY**, **HSQC**, **HMBC**, and **DEPT-135** experiments were recorded.

IR (ATR): ν 3483, 3270, 3019, 2885, 2360, 1700 (C=O), 1660 (C=O), 1269, 1002, 847 cm^{-1}.

HRMS (ESI+): calcd. for $[C_{13}H_{18}N_2O_4+H]^+$: 267.1345, found: 267.1344.

m.p.: 189-191 °C (MeOH/ Et_2O).

R_f (CH_2Cl_2-MeOH 1:1) = 0.26 (vanillin, blue/grey spot)

$[\alpha]_D^{20}$= +63.8 (*c* 0.47 , MeOH).

2.3.17. Synthesis of (4,6-dichloropyrimidine-2,5-diyl)diformamide, 106.

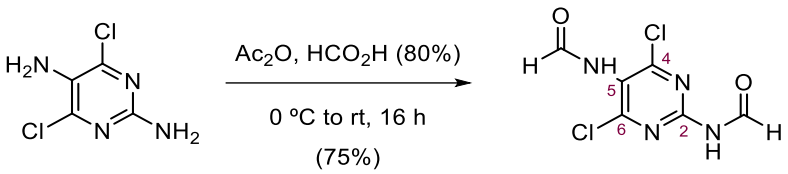

113 **106**

Acetic anhydride (3 mL) was added dropwise to a solution of **113** (1.00 g, 5.6 mmol) in formic acid 99% (10 mL) at 0 °C. After 15 min, the solution was allowed to warm to rt and was stirred for further 16 h. The solvent was then removed and the residue co-evaporated twice with toluene. The yellow residue was purified by flash column chromatography (SiO_2, hexane-acetone, 3:2) to afford **106** (985 mg, 4.19 mmol, 75%) as a yellowish solid.

Spectroscopic data of **106**

^{1}H-NMR (360 MHz, DMSO-d_6): δ 11.54 (d, $J_{CHO,NH}$ = 9.4 Hz, 1H, N*H*), 10.28 (s, 1H, N*H*), 9.22 (d, $J_{CHO,NH}$ = 9.4 Hz, 1H, C*H*O), 8.32 (s, 1H, C*H*O).

R_f (hexane-EtOAc, 1:1 + 3 drops EtN_3 / 10 mL of eluent) = 0.16 (vanillin, yellow spot).

2.3.18. Synthesis of ((1'*R*,2'*R*,3'*R*,5'*S*,6'*S*)-3'-(benzoyloxy)-5'-[6''-chloro-2''-(formylamino)-9''*H*-purin-9''-yl]bicyclo[4.1.0]hept-2'-yl)methyl benzoate, 115.

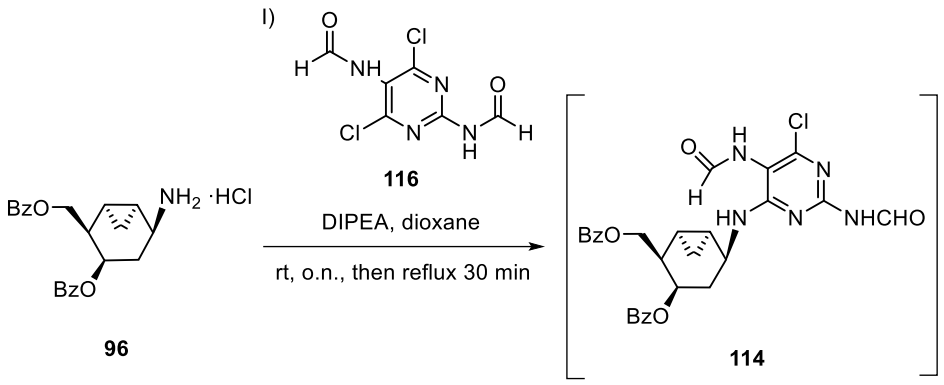

A solution of ammonium **96** (100 mg, 0.25 mmol), 4,6-dichloro-2,5-diformamidopyrimidine **106** (64 mg, 0.25 mmol) and *N,N*-diisopropylethylamine (DIPEA, 175 µL, 1.0 mmol) in dry 1,4-dioxane (5 mL) was stirred under argon atmosphere at room temperature for 12 h and then, refluxed for 30 min. The solvent was evaporated to dryness under reduced pressure and the residue was dissolved in EtOAc (7 mL), washed with water (5 mL), brine (5 mL), dried (Na_2SO_4), filtered, and evaporated *in vacuo*.

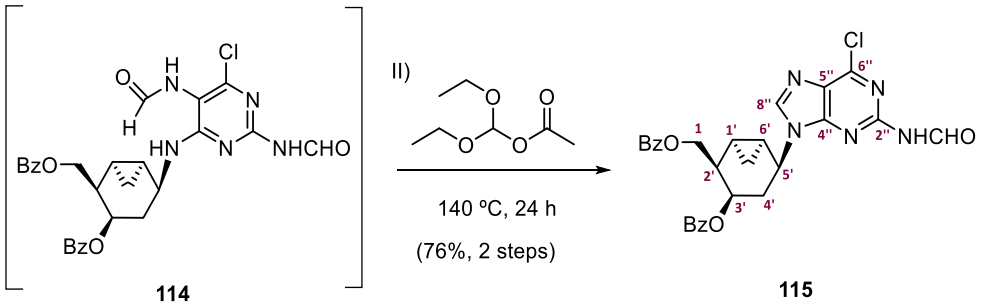

The crude **114** was then dissolved in diethoxymethyl acetate (5 mL) and was stirred at 140 °C under argon for 24 h. The mixture was cooled to room temperature and treated with MeOH (4 mL) and concentrated aqueous ammonia (0.5 mL) while stirring was continued. The solvent was evaporated to dryness and the residue was dissolved in EtOAc (30 mL) and extracted with water (3 × 15 mL) until neutral pH of the washings was obtained. The organic layer was dried (Na_2SO_4), filtered and evaporated to dryness. The resultant yellow solid was purified by flash column chromatography (SiO_2, hexane–EtOAc, 5:1 → 1:1) to give compound **115** (103 mg, 0.19 mmol, 76% overall yield) as a yellowish solid.

Spectroscopic and physical data of **115**

^{1}H-NMR (400 MHz, MeOH-d_4): δ 9.55 (d, $J_{CHO,NH}$ = 10.3 Hz, 1H, C*H*O), 8.94 (d, $J_{NH,CHO}$ = 10.3 Hz, 1H, N*H*), 8.12 (s, 1H, H-8''), 8.10 – 8.05 (m, 2H, H-*orto*), 7.90 – 7.84 (m, 2H, H-*orto*), 7.60 – 7.52 (m, 2H, H-*para*), 7.48 – 7.34 (m, 4H, H-*meta*), 5.35 – 5.25 (m, 2H, H-1a, H-3'), 4.94 (ddd, $J_{5',4'ax}$ = 8.2 Hz, $J_{5',4'eq}$ = 6.7 Hz, $J_{5',6'}$ = 1.6 Hz, 1H, H-5'), 4.62 (dd, J_{gem} = 10.7 Hz, $J_{1b,2'}$ = 5.5 Hz, 1H, H-1b), 2.80 (dtd, $J_{2',3'}$ = 8.3 Hz, $J_{2',1b}$ = $J_{2',1a}$ = 5.5 Hz, $J_{2',1'}$ = 2.4 Hz, 1H, H-2'), 2.66 (dt, J_{gem} = 13.9 Hz, $J_{4'ax,5'}$ = $J_{4'ax,3'}$ = 8.2 Hz, 1H, H-4'ax), 2.11 (ddd, J_{gem} = 13.9 Hz, $J_{4'eq,5'}$ = 6.7 Hz, $J_{4'eq,3'}$ = 3.5 Hz, 1H, H-4'eq), 1.53 (tdd, $J_{1',7'exo}$ = $J_{1',6'}$ = 8.5 Hz, $J_{1',7'endo}$ = 5.7 Hz, $J_{1',2'}$ = 2.4 Hz, 1H, H-1'), 1.33 (tdd, $J_{6',7'exo}$ = $J_{6',1'}$ = 8.5 Hz, $J_{6',7'endo}$ = 5.7 Hz, $J_{6',5'}$ = 1.6 Hz, 1H, H-6'), 1.10 (td, $J_{7'exo,6'}$ = $J_{7'exo,1'}$ = 8.5 Hz, J_{gem} = 5.8 Hz, 1H, H-7'exo), 0.59 (q, J_{gem} = $J_{7'endo,6'}$ = $J_{7'endo,1'}$ = 5.7 Hz, 1H, H-7'endo).

^{13}C-NMR (101 MHz, MeOH-d_4): δ 167.2 (*C*=O), 165.7 (*C*=O), 163.0 (*C*HO), 152.2 / 152.0 / 151.8 (C-4'', C-2'', C-6''), 143.7 (C-8), 133.7 (C-*para*), 133.5 (C-*para*), 129.9 (C-*orto*), 129.7 (C-*ipso*), 129.5 (C-*orto*), 129.4 (C-*ipso*), 129.3 (C-5''), 128.6 (C-*meta*), 128.6 (C-*meta*), 67.4 (C-3'), 65.0 (C-1), 51.6 (C-5'), 36.3 (C-2'), 29.5 (C-4'), 14.3 (C-1'), 14.2 (C-6'), 10.3 (C-7').

COSY, **NOESY**, **HSQC**, **HMBC**, and **DEPT-135** experiments have been recorded.

IR (ATR): ν 3276, 2922, 2360, 1700, 1601, 1574, 1266, 1110, 749, 709 cm^{-1}.

HRMS (ESI+): calcd. for $[C_{28}H_{24}ClN_5O_5+H]^+$: 546.1544, found: 546.1546.

R_f of **114** (EtOAc, 100%) = 0.46 (vanillin, brown spot); **R_f** of **115** (hexane-EtOAc, 1:1) = 0.11 (vanillin, red spot).

$[\alpha]_D^{20}$ = +12.7 (*c* 0.79, $CHCl_3$).

2.3.19. Synthesis of 2-amino-9-[(1'*S*,2'*S*,4'*R*,5'*S*,6'*S*)-4'-hydroxy-5'-(hydroxymethyl) bicyclo[4.1.0]hept-2'-yl]-1,9-dihydro-6*H*-purin-6-one, 116.

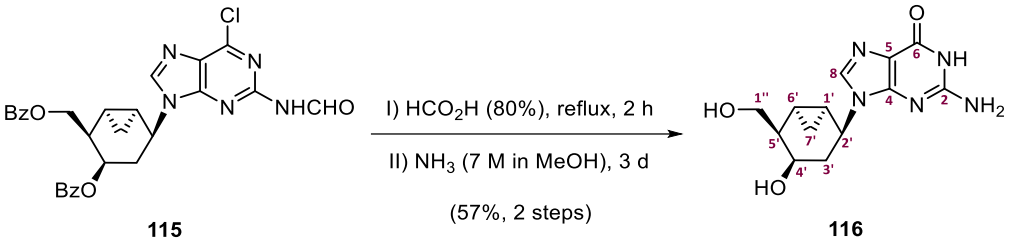

115 **116**

A solution of **115** (100 mg, 0.18 mmol) in 80% HCO_2H (4.5 mL) was stirred at reflux for 2 h. The solution was cooled and the solvent was evaporated under reduced pressure. The residue was dissolved in a NH_3 solution in MeOH (7 M, 20 mL) and stirred at rt for 3 d. Then, the mixture was concentrated under reduce pressure and purified by flash short column chromatography (SiO_2,

CH_2Cl_2-MeOH, 10:1 → 5:1 → 1:1) to provide guanine compound **116** (30 mg, 0.10 mmol, 57% yield) as a pale white solid.

Spectroscopic and physical data of **116**

^{1}H-NMR (400 MHz, MeOH-d_4): δ 7.99 (s, 1H, H-8), 4.73 (td, $J_{2',3'ax} = J_{2',3'eq} = 6.5$ Hz, $J_{2',1'} = 1.6$ Hz, 1H, H-2'), 3.94 (dd, $J_{gem} = 10.7$ Hz, $J_{1''a,5'} = 6.5$ Hz, 1H, H-1''a), 3.91 – 3.83 (m, 2H, H-1''b, H-4'), 2.06 (dt, $J_{gem} = 14.1$ Hz, $J_{3'ax,2'} = J_{3'ax,4'} = 6.5$ Hz, 1H, H-3'ax), 1.87 (tdd, $J_{5',1''a} = J_{5',1''b} = 6.7$ Hz, $J_{5',3'ax} = 6.5$ Hz, $J_{5',3'eq} = 3.0$ Hz, 1H, H-5'), 1.76 (ddd, $J_{gem} = 14.1$ Hz, $J_{3'eq,2'} = 6.5$ Hz, $J_{3'eq,4'} = 3.0$ Hz, 1H, H-3'eq), 1.31 – 1.13 (m, 2H, H-1', H-6'), 0.96 (td, $J_{7'exo,1'} = J_{7'exo,6'} = 9.2$ Hz, $J_{gem} = 5.0$ Hz, 1H, H-7'exo), 0.28 (q, $J_{gem} = J_{7'endo,1'} = J_{7'endo,6'} = 5.4$ Hz, 1H, H-7'endo).

^{13}C-NMR (101 MHz, MeOH-d_4): δ 158.0 (C-6), 153.6 (C-2), 151.3 (C-4), 138.1 (C-8), 115.9 (C-5), 64.4 (C-4'), 63.0 (C-1''), 49.2 (C-2'), 41.4 (C-5'), 33.3 (C-3'), 14.0 (C-1'), 12.2 (C-6'), 10.1 (C-7').

COSY, **NOESY**, **HSQC**, **HMBC**, and **DEPT-135** experiments have been recorded.

HRMS (ESI+): calcd. for $[C_{13}H_{17}N_5O_3+H]^+$: 292.1410, found: 292.1410.

R_f (CH_2Cl_2-MeOH, 15:1) = 0.09 (vanillin, grey spot).

2.3.20. Synthesis of 1-[(1'*S*,2'*S*,4'*S*,5'*R*,6'*R*)-4'-hydroxy-5'-(hydroxymethyl)bicyclo[4.1.0]hept-2'-yl]-5-methylpyrimidine-2,4(1*H*,3*H*)-dione, 117 and 1-[(1'*S*,2'*S*,6'*R*)-5'-(hydroxymethyl)-bicyclo[4.1.0]hept-4'-en-2'-yl]-5-methylpyrimidine-2,4(1*H*,3*H*)-dione, 123.

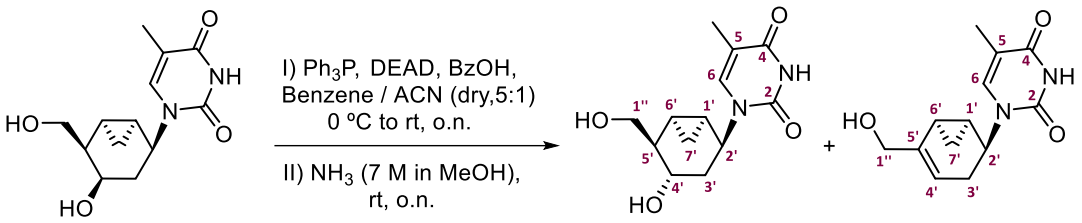

104 → **117** (37%) + **123** (18%)

A solution of compound **104** (30 mg, 0.11 mmol), triphenylphosphine (118 mg, 0.45 mmol), and benzoic acid (55 mg, 0.45 mmol) in a mixture of dry benzene/acetonitrile (5:1, 2.5 mL) was stirred at 0 °C under Ar atmosphere. Diethyl azodicarboxylate (DEAD, 71 µL, 0.45 mmol) was added dropwise during the course of 1 min, the ice bath was removed, and stirring was continued at rt for 12 h. The solvent was evaporated to dryness and the residue was purified by flash chromatography (SiO_2, CH_2Cl_2-MeOH, 20:1) to provide a white solid still contaminated with Ph_3P. The solid was dissolved in a solution of NH in $MeOH_3$ (7 M, 2 mL) in a sealed flask and

stirred for 48 h at rt. Then, the mixture was concentrated under reduce pressure and purified by flash column chromatography (SiO_2, slow gradient of CH_2Cl_2-MeOH, 40:1 → 30:1 → 20:1 → 15:1 →10:1) to provide substitution product **117** (11 mg, 4.1 µmol, 37% overall yield) as a white solid and the elimination product **123** (5 mg, 2.0 µmol, 18% overall yield) as a white solid.

Spectroscopic and physical data of **117**

^{1}H-NMR (400 MHz, MeOH-d_4): δ 7.98 (q, $J_{6,CH3}$ = 1.2 Hz, 1H, H-6), 5.00 (td, $J_{2',3'ax}$ = $J_{2'3'eq}$ = 3.8 Hz, $J_{2'1'}$ = 1.2 Hz, 1H, H-2'), 3.88 (dd, J_{gem} = 10.6 Hz, $J_{1''a,5'}$ = 3.5 Hz, 1H, H-1''a), 3.75 (dd, J_{gem} = 10.6 Hz, $J_{1''b,5'}$ = 3.5 Hz, 1H, H-1''b), 3.61 (ddd, $J_{4',3'ax}$ = 12.2 Hz, $J_{4',5'}$ = 9.1 Hz, $J_{4',3eq}$ = 3.8 Hz, 1H, H-4'), 1.89 (d, $J_{CH3,6}$ = 1.2 Hz, 3H, CH_3), 1.85 (dt, J_{gem} = 14.2 Hz, $J_{3'eq,2'}$ = $J_{3'eq,4'}$ = 3.8 Hz, 1H, H-3'eq), 1.64 (dtd, $J_{5',4'}$ = 9.1 Hz, $J_{5',1''a}$ = $J_{5',1''b}$ = 3.5 Hz, $J_{5',6'}$ = 1.3 Hz, 1H, H-5'), 1.49 (ddd, J_{gem} = 14.2 Hz, $J_{3'ax,4'}$ = 12.2 Hz, $J_{3'ax,2'}$ = 3.8 Hz, 1H, H-3'ax), 1.27 (dddd, $J_{6',7'exo}$ = 9.3 Hz, $J_{6',1'}$ = 7.7 Hz, $J_{6',7'endo}$ = 5.3 Hz, $J_{6',5'}$ = 1.3 Hz, 1H, H-6'), 1.08 (dddd, $J_{1',7'exo}$ = 9.3 Hz, $J_{1',6'}$ = 7.7 Hz, $J_{1',7'endo}$ = 5.3 Hz, $J_{1',2'}$ = 1.2 Hz, 1H, H-1'), 0.91 (td, $J_{7'exo,6'}$ = $J_{7'exo,1'}$ = 9.3 Hz, J_{gem} = 5.3 Hz, 1H, H-7'exo), 0.39 (q, J_{gem} = $J_{7'endo,1'}$ = $J_{7'endo,6'}$ = 5.3 Hz, 1H, H-7'endo).

^{13}C-NMR (101 MHz, MeOH-d_4): δ 166.6 (C-2), 153.0 (C-4), 141.2 (C-6), 110.1 (C-5), 64.1 (C-4'), 63.0 (C-1''), 53.7 (C-2'), 46.1 (C-5'), 33.3 (C-3'), 15.3 (C-1'), 14.9 (C-6'), 12.4 (CH_3), 10.4 (C-7').

COSY, **NOESY**, **HSQC**, **HMBC**, and **DEPT-135** experiments have been recorded.

HRMS (ESI+): calcd. for $[C_{13}H_{18}N_2O_4+Na]^+$: 289.1164, found: 289.1164.

R_f (CH_2Cl_2-MeOH, 15:1) = 0.15 (vanillin, blue/grey spot).

Spectroscopic and Physical data of **123**

^{1}H-NMR (400 MHz, MeOH-d_4): δ 7.54 (q, $J_{6,CH3}$ = 1.1 Hz, 1H, H-6), 5.37 (m, 1H, H-4'), 5.12 (dt, $J_{2',3'ax}$ = 6.6 Hz, $J_{2',3'eq}$ = $J_{2',1'}$ = 2.1 Hz, 1H, H-2'), 4.17 (m, 1H, H-1''a), 4.16 – 4.07 (m, 1H, H-1''b), 2.28 (ddd, J_{gem} = 18.2 Hz, $J_{3'ax,2'}$ = 6.9 Hz, $J_{3'ax,4'}$ = 2.4 Hz, 1H, H-3'ax), 2.18 (ddd, J_{gem} = 18.2 Hz, $J_{3'eq,4'}$ = 5.5 Hz, $J_{3'eq,2'}$ = 2.1 Hz, 1H, H-3'eq), 1.84 (d, $J_{CH3,6}$ = 1.2 Hz, 3H, CH_3), 1.72 (td, $J_{6',7exo}$ = $J_{6',1'}$ = 8.7 Hz, $J_{6',7'endo}$ = 4.8 Hz, 1H, H-6'), 1.50 (tdd, $J_{1',7exo}$ = $J_{1',6'}$ = 8.7 Hz, $J_{1',7'endo}$ = 4.8 Hz, $J_{1',2'}$= 2.1 Hz, 1H, H-1'), 1.17 (td, $J_{7'exo,6'}$ = $J_{7'exo,1'}$ = 8.7 Hz, J_{gem} = 4.8 Hz, 1H, H-7'exo), 0.86 (q, J_{gem} = $J_{7'endo,6'}$ = $J_{7'endo,1'}$ = 4.8 Hz, 1H, H-7'endo).

^{13}C-NMR (101 MHz, MeOH-d_4): δ 166.4 (C-4), 153.0 (C-2), 143.0 (C-5'), 140.6 (C-6), 114.2 (C-4'), 110.4 (C-5), 66.5 (C-1''), 47.6 (C-2'), 27.3 (C-3'), 18.5 (C-1'), 12.9 (C-6'), 12.6 (CH_3), 11.3 (C-7').

COSY, **NOESY**, **HSQC**, **HMBC** and **DEPT-135** experiments have been recorded.

HRMS (ESI+): calcd. for $[C_{13}H_{16}N_2O_3+Na]^+$: 271.1059, found: 271.1035.

R_f (CH_2Cl_2-MeOH, 15:1) = 0.36 (vanillin, blue/grey spot).

2.4. CHAPTER IV. Synthesis of new 1,2,3-triazolo-carbanucleosides compounds.

2.4.1. Synthesis of methyl 1-{(1'*S*,2'*S*,4'*R*,5'*R*,6'*R*)-4'-(benzoyloxy)-5'-[(benzoyloxy)methyl]-bicyclo[4.1.0]hept-2'-yl}-1*H*-1,2,3-triazole-4-carboxylate, 147.

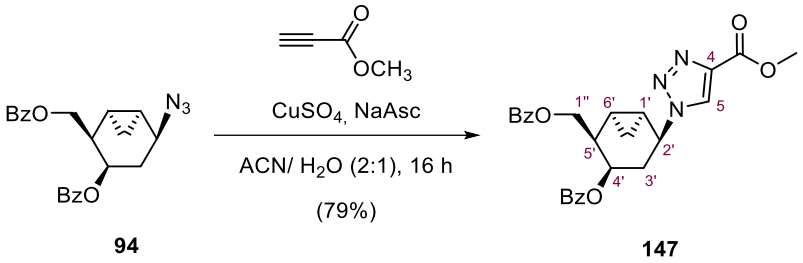

94 **147**

The benzyl protected azido alcohol **94** (200 mg, 0.511 mmol) was suspended in a 2:1 mixture of acetonitrile and water (8 mL) and then, methyl propiolate (70 µL, 0.767 mmol) was added. A solution 1 M of sodium ascorbate in water (205 µL, 0.205 mmol, 40 mol%) was added follow by a 1 M of $CuSO_4 \cdot 5H_2O$ in water (102 µL, 0.10 mmol, 20 mol%). The round-bottom flask was wrapped with aluminium foil and the reaction mixture was stirred 16 h at rt. Then, the mixture was filtered through a short pad of Celite® and washed with EtOAc. The solvent was evaporated under reduced pressure and purified by flash column chromatography (SiO_2, hexane-EtOAc, 4:1 → 1:1) to afford triazole compound **147** 192 mg, 0.40 mmol, 79% yield) as a white solid.

Spectroscopic and physical data of **147**

^{1}H-NMR (400 MHz, $CDCl_3$): δ 8.28 (s, 1H, H-5), 7.98 (dd, $J_{orto,meta}$ = 8.4 Hz, $J_{orto,para}$ = 1.3 Hz, 2H, H-*orto*), 7.78 (dd, $J_{orto,meta}$ = 8.4 Hz, $J_{orto,para}$ = 1.3 Hz, 2H, H-*orto*), 7.58 – 7.48 (m, 2H, H-*para*), 7.46 – 7.33 (m, 4H, H-*meta*), 5.30 (ddd, $J_{4',3'ax}$ = 5.8 Hz, $J_{4',5'}$ = 4.4 Hz, $J_{4',3'eq}$ = 2.9 Hz, 1H, H-4'), 5.14 (ddd, $J_{2',3'eq}$ = 6.2 Hz, $J_{2',3'ax}$ = 4.8, $J_{2',1'}$ = 1.6 Hz, 1H, H-2'), 4.72 (dd, J_{gem} = 10.9 Hz, $J_{1''a,5'}$ = 7.3 Hz, 1H, H-1''a), 4.54 (dd, J_{gem} = 10.9 Hz, $J_{1''b,5'}$ = 8.1 Hz, 1H, H-1''b), 3.77 (s, 3H, OC*H*$_3$), 2.78 (ddd, J_{gem} = 15.3 Hz, $J_{3'ax,4'}$ = 5.8 Hz, $J_{3'ax,2'}$ = 4.8 Hz, 1H, H-3'ax), 2.49 (tdd, $J_{5',1''a}$ = $J_{5',1''b}$ = 7.3 Hz, $J_{5',4'}$ = 4.4 Hz, $J_{5',6'}$ = 2.8 Hz, 1H, H-5'), 2.08 (ddd, J_{gem} = 15.3 Hz, $J_{3'eq,2'}$ = 6.2 Hz, $J_{3'eq,4'}$ = 2.9 Hz, 1H, H-3'eq), 1.67 – 1.60 (m, 1H, H-1'), 1.35 (tdd, $J_{6',7'exo}$ = $J_{6',1'}$ = 9.3 Hz, $J_{6',7'endo}$ = 5.5 Hz, $J_{6',5'}$ = 2.8 Hz, 1H, H-6'), 1.23 (td, $J_{7'exo,6'}$ = $J_{7'exo,1'}$ = 9.3 Hz, J_{gem} = 5.5 Hz, 1H, H-7'exo), 0.50 (q, J_{gem} = $J_{7'endo,6'}$ = $J_{7'endo,1'}$ = 5.5 Hz, 1H, H-7'endo).

^{13}C-NMR (100 MHz, $CDCl_3$): δ 166.5 (*C*=O), 165.5 (*C*=O), 160.8 (*C*(O)OCH$_3$), 139.3 (C-4), 133.3 (C-*para*), 133.1 (C-*para*), 129.8 (C-*ipso*), 129.7 (C-*orto*), 129.5 (C-*orto*), 129.4 (C-*ipso*), 128.6 (C-*meta*), 128.5 (C-*meta*), 126.8 (C-5), 66.5 (C-4'), 64.8 (C-1''), 54.8 (C-2'), 52.0 (O*C*H$_3$), 38.0 (C-5'), 30.7 (C-3'), 14.1 (C-1'), 11.4 (C-7'), 11.2 (C-6').

COSY,**HSQC**, **HMBC** and **DEPT-135** experiments have been recorded.

IR (ATR): ν 3007, 2164, 2111, 1712, 1601, 1265, 1175, 752, 710 cm^{-1}.

HRMS (ESI+): calcd. for $[C_{26}H_{25}N_3O_6+H]^+$: 476.1822, found: 476.1821.

R_f (hexane-EtOAc, 1:1) = 0.27 (vanillin, purple spot).

$[\alpha]_D^{20}$= -115 (*c* 0.40, $CHCl_3$).

2.4.2. Synthesis of 1-[(1'*S*,2'*S*,4'*R*,5'*R*,6'*R*)-4'-hydroxy-5'-(hydroxymethyl)bicyclo[4.1.0]hept-2'-yl]-1*H*-1,2,3-triazole-4-carboxamide, 148.

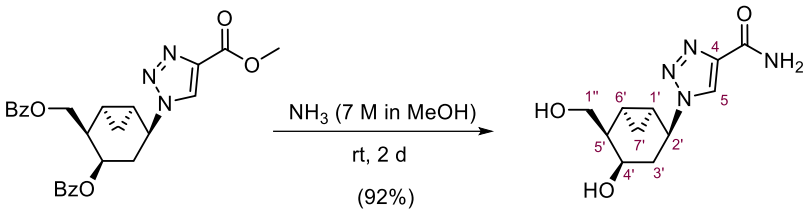

147 **148**

The ester-triazole **147** (130 mg, 0.27 mmol) was dissolved in a solution of NH_3 in MeOH (7 M, 6 mL) in a sealed flask and was stirred for 2 d at rt. Then, the mixture was concentrated under reduced pressure and purified by flash column chromatography (SiO_2, CH_2Cl_2-MeOH, 20:1 → 15:1 → 10:1) to provide a deprotected carboxamide compound **148** (61 mg, 0.24 mmol, 92% yield) as a white solid.

Spectroscopic and physical data of **148**

^{1}H-NMR (400 MHz, MeOH-d_4): δ 8.63 (s, 1H, H-5), 5.07 (ddd, $J_{2',3'eq}$ = 6.1 Hz, $J_{2',3'ax}$ = 5.5 Hz, $J_{2',1'}$ = 1.6 Hz, 1H, H-2'), 3.96 – 3.86 (m, 2H, H-4', H-1''a), 3.81 (dd, J_{gem} = 10.7 Hz, $J_{1''b,5'}$ = 6.7 Hz, 1H, H-1''b), 2.12 (ddd, J_{gem} = 14.5 Hz, $J_{3'ax,4'}$ = 6.3 Hz, $J_{3'ax,2'}$ = 5.5 Hz, 1H, H-3'ax), 1.93 (ddd, J_{gem} = 14.5 Hz, $J_{3'eq,2'}$ = 6.1 Hz, $J_{3'eq,4'}$ = 3.0 Hz, 1H, H-3'eq), 1.83 (tt, $J_{5',1''a}$ = $J_{5',1''b}$ = 6.7 Hz, $J_{5',4'}$ = $J_{5',6'}$ = 3.5 Hz, 1H, H-5'), 1.36 – 1.26 (m, 1H, H-1'), 1.14 (tdd, $J_{6',7'exo}$ = $J_{6',1'}$ = 8.9 Hz, $J_{6',7'endo}$ = 5.4 Hz, $J_{6',5'}$ = 3.5 Hz, 1H, H-6'), 1.01 (td, $J_{7'exo,6'}$ = $J_{7'exo,1'}$ = 8.9 Hz, J_{gem} = 5.4 Hz, 1H, H-7'exo), 0.33 (q, J_{gem} = $J_{7'endo,6'}$ = $J_{7'endo,1'}$ = 5.4 Hz, 1H, H-7'endo).

^{13}C-NMR (101 MHz, MeOH-d_4): δ 165.0 (*C*(O)NH_2), 143.1 (C-4), 127.4 (C-5), 65.1 (C-4'), 64.4 (C-1''), 57.2 (C-2'), 43.1 (C-5'), 35.1 (C-3'), 15.4 (C-1'), 12.8 (C-6'), 11.5 (C-7').

COSY, **DEPT-135**, **HSQC** and **HMBC** experiments have been recorded.

IR (ATR): ν 3339, 3195, 2886, 1661, 1603, 1289, 1046, 855, 721 cm^{-1}.

HRMS (ESI+): calcd. for $[C_{11}H_{16}N_4O_3+Na]^+$: 275.1120, found: 275.1121.

R_f (hexane-EtOAc, 1:1) = 0.15 (vanillin, pinkish spot).

2.4.3. Synthesis of (1*R*,2*R*,3*R*,5*S*,6*S*)-5-azido-2-(hydroxymethyl)bicyclo[4.1.0]heptan-3-ol, 149.

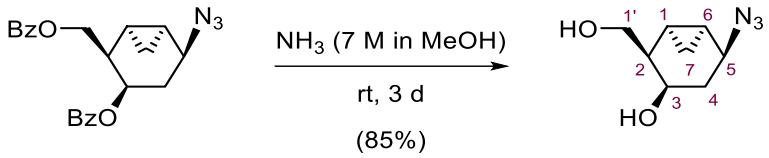

94 **149**

The protected azido compound **94** (320 mg, 0.82 mmol) was dissolved in a solution of NH_3 solution in MeOH (7 M, 50 mL) in a sealed flask and was stirred for 3 d at rt. Then, the mixture was concentrated under reduced pressure and purified by flash column chromatography (SiO_2, CH_2Cl_2-MeOH, 30:1 → 20:1 → 10:1) to provide a deprotected azide compound **149** (128 mg, 0.70 mmol, 85% yield) as a white solid.

Spectroscopic and physical data of **149**

^{1}H-NMR (400 MHz, MeOH-d_4): δ 3.90 – 3.76 (m, 3H, H-3, H-5, H-1'a), 3.68 (dd, J_{gem} = 10.6 Hz, $J_{1'b,2}$ = 7.1 Hz, 1H, H-1'b), 1.82 – 1.67 (m, 2H, H-4ax, H-2), 1.62 (ddd, J_{gem} = 14.3 Hz, $J_{4eq,5}$ = 5.8 Hz, $J_{4eq,3}$ = 3.0 Hz, 1H, H-4eq), 1.13 – 1.03 (m, 1H, H-6), 0.95 (tdd, $J_{1,6} = J_{1,7exo}$ = 9.1 Hz, $J_{1,7endo}$ = 5.2 Hz, $J_{1,2}$ = 2.9 Hz, 1H, H-1), 0.87 (td, $J_{7exo,1} = J_{7exo,6}$ = 9.1 Hz, J_{gem} = 4.7 Hz, 1H, H-7exo), 0.11 (q, $J_{gem} = J_{7endo,1} = J_{7endo,6}$ = 5.2 Hz, 1H, H-7endo).

^{13}C-NMR (101 MHz, MeOH-d_4): δ 65.5 (C-3), 64.5(C-1'), 57.5 (C-5), 43.2 (C-2), 33.4 (C-4), 14.9 (C-6), 12.7 (C-1), 11.0 (C-7).

COSY, **DEPT-135**, and **HSQC** experiments have been recorded.

HRMS (ESI+): calcd. for $[C_8H_{13}N_3O_2+Na]^+$: 206.0905, found: 206.0904.

R_f (CH_2Cl_2-MeOH, 20:1) = 0.32 (vanillin, brown spot).

2.4.4. General procedure for the cooper(I) alkyne-azide cycloaddition (CuAAc) by MW irradiation.

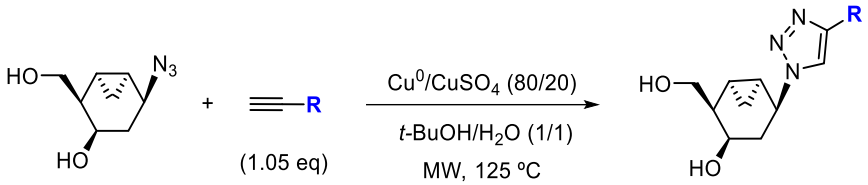

Exp.	R	Triazole	Time	Yield (%)
1	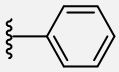	**150**	2 min	**97**
2	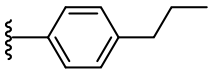	**151**	10 min	**94**
3	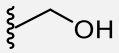	**152**	<1 min	**80**

To a solution of azide **149** in a 1:1 mixture of water and *t*-BuOH (10 mL/mmol) in a glass vial equipped with a magnetic stirring bar, copper powder (80 mol%), a solution 1 M of copper sulfate in water (20 mol%), and finally the alkyne (1.05 eq) was added. The vial was sealed with a Teflon® crimp top and the reaction mixture was then MW irradiated at 125 °C. Upon completion of the reaction, the vial was cooled to 50 °C by air jet cooling before opening. The mixture was filtered over plug of Celite® (dragged with MeOH) and the filtrate was evaporated under reduced pressure.

2.4.4.1 Synthesis of (1*R*,2*R*,3*R*,5*S*,6*S*)-2-(hydroxymethyl)-5-(4^{II}-phenyl-1*H*-1^{II},2^{II},3^{II}-triazol-1-yl)bicyclo[4.1.0]heptan-3-ol, 150.

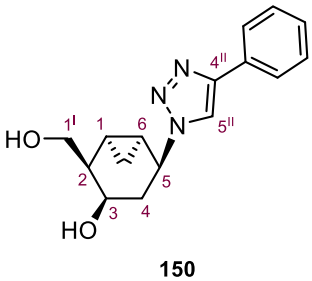

150

The title compound was prepared from azide **149** (19 mg, 0.11 mmol) and phenylacetylene (12 µL, 0.110 mmol) after 2 min of microwave irradiation. The reaction mixture was filtered through Celite® (MeOH), the solvent was evaporated under reduce pressure and the residue was purified by flash column chromatography (SiO_2, EtOAc 100%), to give compound **150** (29 mg, 0.102 mmol, 97% yield) as a white solid.

Spectroscopic and physical data of **150**

^{1}H-NMR (400 MHz, MeOH-d_4): δ 8.52 (s, 1H, H-5^{II}), 7.86 – 7.79 (m, 2H, H-*orto*), 7.46 – 7.41 (m, 2H, H-*meta*), 7.37 – 7.31 (m, 1H, H-*para*), 5.02 (td, $J_{5,4ax} = J_{5,4eq} = 6.6$ Hz, $J_{5,6} = 1.8$ Hz, 1H, H-5), 4.02 – 3.91 (m, 2H, H-3, H-1^{I}a), 3.84 (dd, $J_{gem} = 10.7$ Hz, $J_{1Ib,2} = 6.8$ Hz, 1H, H-1^{I}b), 2.16 (dt, $J_{gem} = 13.9$ Hz, $J_{4ax,3} = J_{4ax,5} = 7.0$ Hz, 1H, H-4ax), 2.00 (ddd, $J_{gem} = 14.2$ Hz, $J_{4eq,5} = 6.7$ Hz, $J_{4eq,3} = 3.3$ Hz, 1H, H-4eq), 1.90 (tt, $J_{2,1I} = 6.8$ Hz, $J_{2,3} = J_{2,1} = 3.6$ Hz, 1H, H-2), 1.39 – 1.31 (m, 1H, H-6), 1.20 (tdd, $J_{1,6} = J_{1,7exo} = 8.7$ Hz, $J_{1,7endo} = 5.4$ Hz, $J_{1,2} = 3.2$ Hz, 1H, H-1), 1.01 (td, $J_{7exo,6} = J_{7exo,1} = 9.2$ Hz, $J_{gem} = 5.4$ Hz, 1H, H-7exo), 0.37 (q, $J_{gem} = J_{7endo,6} = J_{7endo,1} = 5.4$ Hz, 1H, H-7endo).

^{13}C-NMR (101 MHz, MeOH-d_4): δ 148.5 (C-4^{II}), 131.9 (C-*ipso*), 130.0 (C-*meta*), 129.2 (C-*para*), 126.6 (C-*orto*), 121.7 (C-5^{II}), 65.5 (C-3), 64.3 (C-1^{I}), 57.6 (C-5), 43.0 (C-2), 35.6 (C-4), 15.6 (C-6), 13.5 (C-1), 11.4 (C-7).

COSY, **DEPT-135**, **HSQC** and **HMBC** experiments have been recorded.

HRMS (ESI+): calcd. for $[C_{16}H_{19}N_3O_2+H]^+$: 286.1556, found: 286,1555.

R_f (EtOAc, 100%) = 0.21 (vanillin, garnet spot).

2.4.4.2. Synthesis of (1*R*,2*R*,3*R*,5*S*,6*S*)-2-(hydroxymethyl)-5-[4^{II}-(4^{III}-propylphenyl)-1^{II}*H*-1^{II},2^{II},3^{II}-triazol-1^{II}-yl]bicyclo[4.1.0]heptan-3-ol, 151.

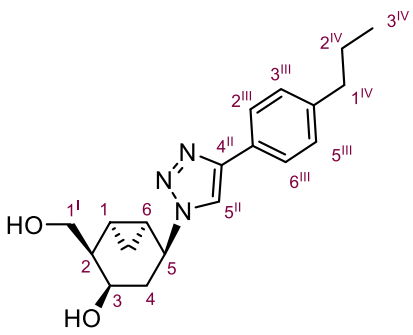

151

The title compound was prepared from azide **149** (20 mg, 0.11 mmol) and 1-ethynyl-4-propylbenzene (18 µL, 0.115 mmol) after 10 min of microwave irradiation. The reaction mixture was filtered through Celite® (MeOH), the solvent was evaporated under reduce pressure and the residue was purified by flash column chromatography (SiO_2, EtOAc 100% → EtOAc-MeOH, 95:5), to give compound **151** (33 mg, 0.10 mmol, 94% yield) as a white solid.

Spectroscopic and physical data of **151**

^{1}H-NMR (400 MHz, MeOH-d_4): δ 8.47 (s, 1H, H-5^{II}), 7.72 (d, $J_{2III/6III,3III/5III} = 8.5$ Hz, 2H, H-2^{III}/6^{III}), 7.25 (d, $J_{3III/5III,2III/6III} = 8.5$ Hz, 2H, H-3^{III}/5^{III}), 5.00 (td, $J_{5,4ax} = J_{5,4eq} = 6.6$ Hz, $J_{5,6} = 1.8$ Hz, 1H, H-5), 4.00 – 3.90 (m, 2H, H-3, H-1^{I}a), 3.84 (dd, $J_{gem} = 10.7$ Hz, $J_{1Ib,2} = 6.8$ Hz, 1H, H-1^{I}b), 2.62 (t, $J_{1IV,2IV} = 7.4$ Hz, 1H, H-1^{IV}), 2.21 – 2.10 (m, 1H, H-4ax), 1.99 (ddd, $J_{gem} = 14.1$ Hz, $J_{4eq,5} = 6.7$ Hz, $J_{4eq,3} = 3.3$ Hz, 1H,

H-4eq), 1.94 – 1.86 (m, 1H, H-2), 1.67 (h, $J_{2^{IV},1^{IV}} = J_{2^{IV},3^{IV}} =$ 7.4 Hz, 1H, H-2^{IV}), 1.32 (tdd, $J_{6,7exo} = J_{6,1} =$ 9.2 Hz, $J_{6,7endo} =$ 5.6 Hz, $J_{6,5} =$ 1.9 Hz, 1H, H-6), 1.20 (tdd, $J_{1,7exo} = J_{1,6} =$ 8.7 Hz, $J_{1,7endo} =$ 5.4 Hz, $J_{1,2} =$ 3.1 Hz, 1H, H-1), 1.01 (td, $J_{7exo,1} = J_{7exo,6} =$ 9.2 Hz, $J_{gem} =$ 5.4 Hz, 1H, H-7exo), 0.96 (t, $J_{3^{IV},2^{IV}} =$ 7.4 Hz, 1H, H-3^{IV}), 0.36 (q, $J_{gem} = J_{7endo,6} = J_{7endo,1} =$ 5.4 Hz, 1H, H-7endo).

^{13}C-NMR (101 MHz, MeOH-d_4): δ 148.6 (C-4^{I}), 144.1 (C-4^{II}), 130.0 (2C, C-2^{II}/C-6^{II}), 129.4 (C-1^{II}), 126.6 (2C, C-3^{II}/C-5^{II}), 121.4 (C-5^{I}), 65.5 (C-3), 64.3 (C-1^{IV}), 57.6 (C-5), 42.9 (C-2), 38.8 (C-1^{III}), 35.6 (C-4), 25.7 (C-2^{III}), 15.6 (C-6), 14.1 (C-3^{III}), 13.5 (C-1), 11.4 (C-7).

COSY, **HSQC**, **HMBC** and **DEPT-135** experiments have been recorded.

HRMS (ESI+): calcd. for $[C_{19}H_{25}N_3O_2+H]^+$: 328.2025, found: 328.2027.

R_f (EtAOc, 100%) = 0.20 (vanillin, garnet spot).

2.4.4.3. Synthesis of (1*R*,2*R*,3*R*,5*S*,6*S*)-2-(hydroxymethyl)-5-[4^{II}-(hydroxymethyl)-1*H*-1^{II},2^{II},3^{II}-triazol-1^{III}-yl]bicyclo[4.1.0]heptan-3-ol, 152.

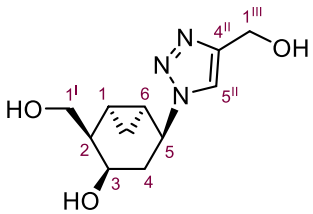

152

The title compound was prepared from azide **149** (49 mg, 0.27 mmol) and propargyl alcohol (16 µL, 0.278 mmol) after 1 min of microwave irradiation. The reaction mixture was filtered through Celite® (MeOH), the solvent was evaporated under reduce pressure and the residue was purified by flash column chromatography (SiO_2, EtOAc-MeOH 95:5 → 90:10), to give compound **152** (51 mg, 0.21 mmol, 80% yield) as a white solid.

Spectroscopic and physical data of **152**

^{1}HNMR (400 MHz, MeOH-d_4): δ 8.14 (s, 1H, H-5^{II}), 4.96 (td, $J_{5,4ax} = J_{5,4eq} =$ 6.8 Hz, $J_{5,6} =$ 1.9 Hz, 1H, H-5), 4.68 (br s, 2H, H-1^{III}), 3.97 – 3.89 (m, 2H, H-3, H-1^{I}a), 3.81 (dd, $J_{gem} =$ 10.7 Hz, $J_{1^{I}b,2} =$ 6.8 Hz, 1H, H-1^{I}b), 2.09 (dt, $J_{gem} =$ 14.1 Hz, $J_{4ax,3} = J_{4ax,5} =$ 6.8 Hz, 1H, H-4ax), 1.96 (ddd, $J_{gem} =$ 14.1 Hz, $J_{4eq,5} =$ 6.8 Hz, $J_{4eq,3} =$ 3.4 Hz, 1H, H-4eq), 1.88 (tt, $J_{2,1^{I}} =$ 6.8 Hz, $J_{2,3} = J_{2,1} =$ 3.7 Hz, 1H, H-2), 1.28 – 1.21 (m, 1H, H-6), 1.17 (tdd, $J_{1,7exo} = J_{1,6} =$ 8.7 Hz, $J_{1,7endo} =$ 5.4, $J_{1,2} =$ 3.7 Hz, 1H, H-1), 0.97 (td, $J_{7exo,1} = J_{7exo,6} =$ 9.2 Hz, $J_{gem} =$ 5.4 Hz, 1H, H-7exo), 0.34 (q, $J_{gem} = J_{7endo,1} = J_{7endo,6} =$ 5.4 Hz, 1H, H-7endo).

^{13}CNMR (101 MHz, MeOH-d_4): δ 148.9 (C4^{II}), 123.6 (C5^{II}), 65.5 (C-3), 64.3 (C-1^{I}), 57.5 (C-5), 56.6 (C-1^{III}), 42.9 (C-4), 35.7 (C-2), 15.6 (C-6), 13.5 (C-1), 11.3 (C-7).

COSY, **HSQC**, **HMBC** and **DEPT-135** experiments have been recorded.

HRMS (ESI+): calcd. for $[C_{11}H_{17}N_3O_3+H]^+$: 240.1348, found: 240.1348.

R_f (CH_2Cl_2-MeOH, 10:1) = 0.1 (vanillin, garnet spot).

2.4.5. Synthesis of 5-amino-1-[(1'*S*,2'*S*,4'*R*,5'*R*,6'*R*)-4'-hydroxy-5'-(hydroxymethyl)bicyclo-[4.1.0]hept-2'-yl]-1*H*-1,2,3-triazole-4-carboxamide, 153.

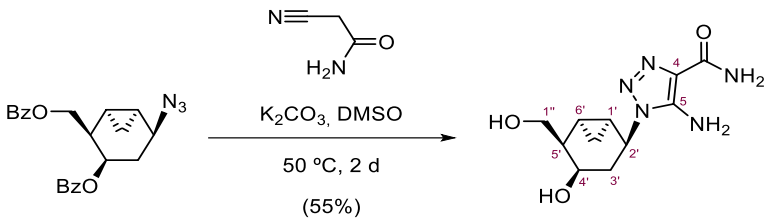

94 **153**

To a solution of 2-cyanoacetamide (35 mg, 0.42 mmol) in dry DMSO (500 µL) at rt was added K_2CO_3 (54 mg, 0.39 mmol) under Ar atmosphere. The mixture was stirred at the same temperature for 1 h. After this time, a DMSO solution (500 µL) of **94** (50 mg, 0.13 mmol) was added and the stirring was continued for 2 d at 50 °C. After evaporation of the solvent, the solid residue was purified by flash column chromatography (SiO_2, CH_2Cl_2-MeOH, 15:1 → 10:1) to give **153** (19 mg, 0.07 mmol, 55% yield) as whitish solid.

Spectroscopic and physical data of **153**

^{1}H-NMR (400 MHz, MeOH-d_4): δ 4.72 (td, $J_{2',3'ax} = J_{2',3'eq}$ = 7.5 Hz, $J_{2',1'}$ = 1.9 Hz, 1H, H-2'), 3.95 (dd, J_{gem} = 10.6 Hz, $J_{1''a,5'}$ = 6.4 Hz, 1H, H-1''a), 3.91 – 3.80 (m, 2H, H-4', H-1''b), 2.12 (dt, J_{gem} = 13.7 Hz, $J_{3'ax,2'} = J_{3'ax,4'}$ = 8.2 Hz, 1H, H-3'ax), 1.97 – 1.87 (m, 2H, H-3'eq, H-5'), 1.29 – 1.17 (m, 2H, H-1', H-6'), 0.95 (td, $J_{7'exo,1'} = J_{7'exo,6'}$ = 9.2, J_{gem} = 5.4 Hz, 1H, H-7'exo), 0.32 (q, $J_{gem} = J_{7'endo,1'} = J_{7'endo,6'}$ = 5.4 Hz, 1H, H-7'endo).

^{13}CNMR (101 MHz, MeOH-d_4): δ 167.1 (*C*=O), 146.0 (C-5), 123.3 (C-4), 65.7 (C-4'), 63.8 (C-1''), 54.2 (C-2'), 42.3 (C-5'), 34.4 (C-3'), 14.4 / 14.2 (C-1'/C-6'), 11.2 (C-7').

COSY, **NOESY**, **HSQC**, **HMBC** and **DEPT-135** experiments have been recorded.

IR (ATR): ν 3308, 3174, 1662, 1633, 1561, 1517, 1226, 1096, 1021, 877, 784 cm^{-1}.

HRMS (ESI+): calcd. for $[C_{11}H_{17}N_5O_3+Na]^+$: 290.1229, found: 290.1229.

m.p.: 210-213 °C (from MeOH-CH_2Cl_2).

R_f (CH_2Cl_2-MeOH, 10:1) = 0.1 (vanillin, garnet spot).

VI. SPECTRA OF SELECTED COMPOUNDS

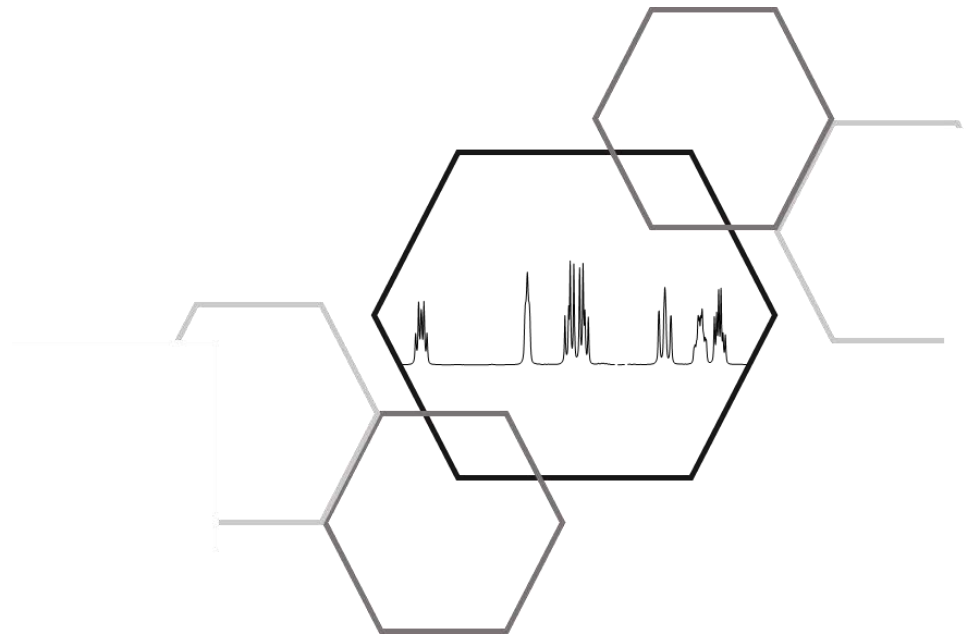

1. CHATER I. Synthesis of key pivotal intermediate 36.

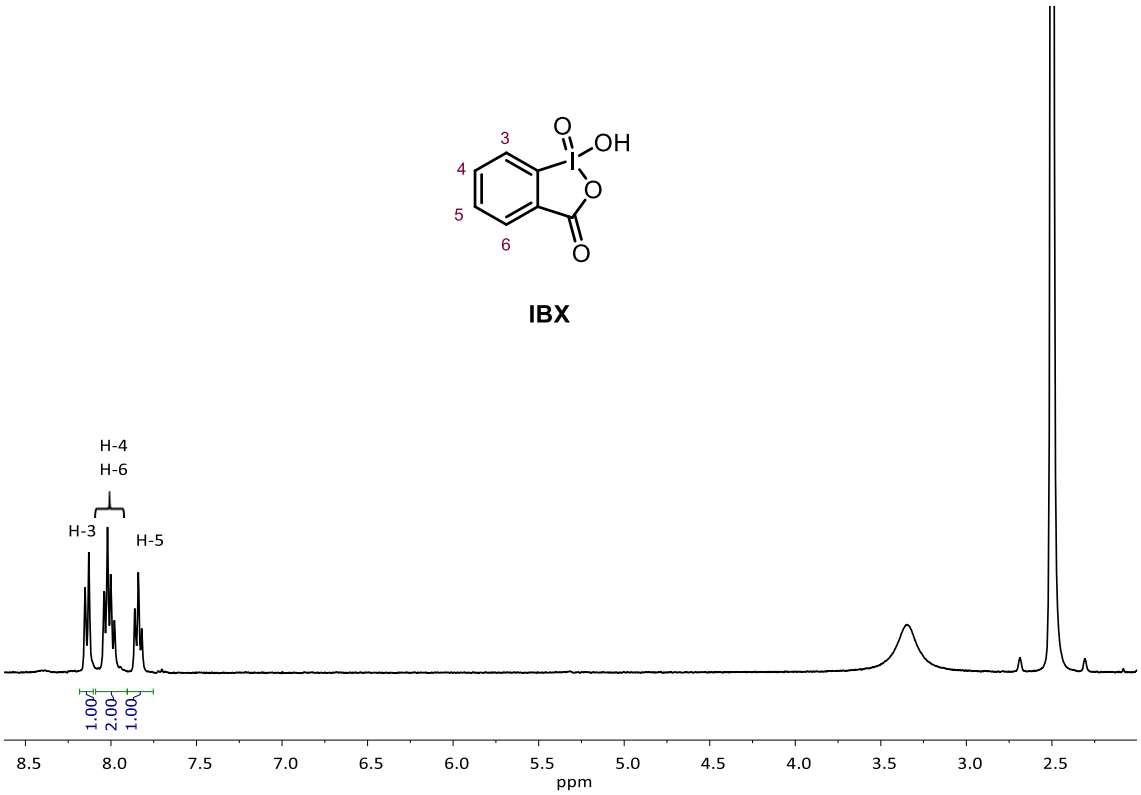

^{1}H-NMR (250 MHz, DMSO-d_6)

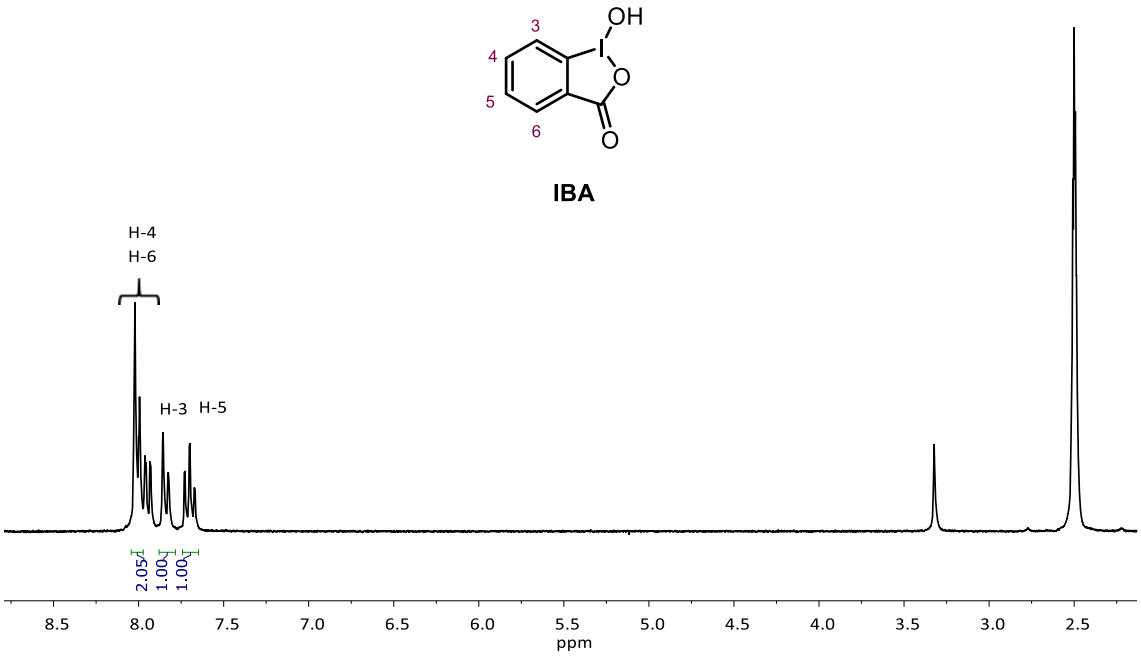

^{1}H-NMR (250 MHz, DMSO-d_6)

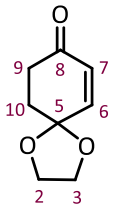

RY12

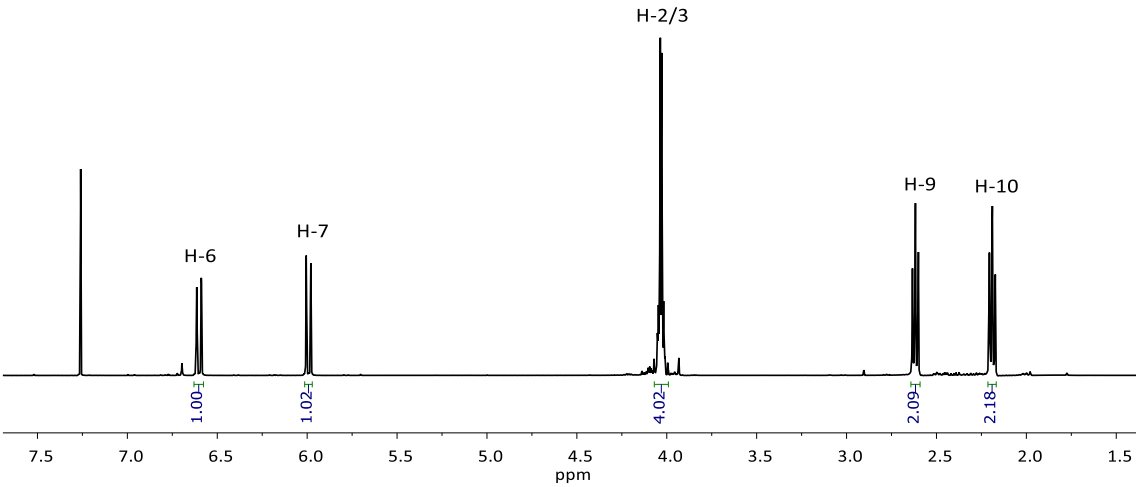

^{1}H-NMR (250 MHz, $CDCl_3$)

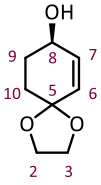

(*R*)-**RY13**

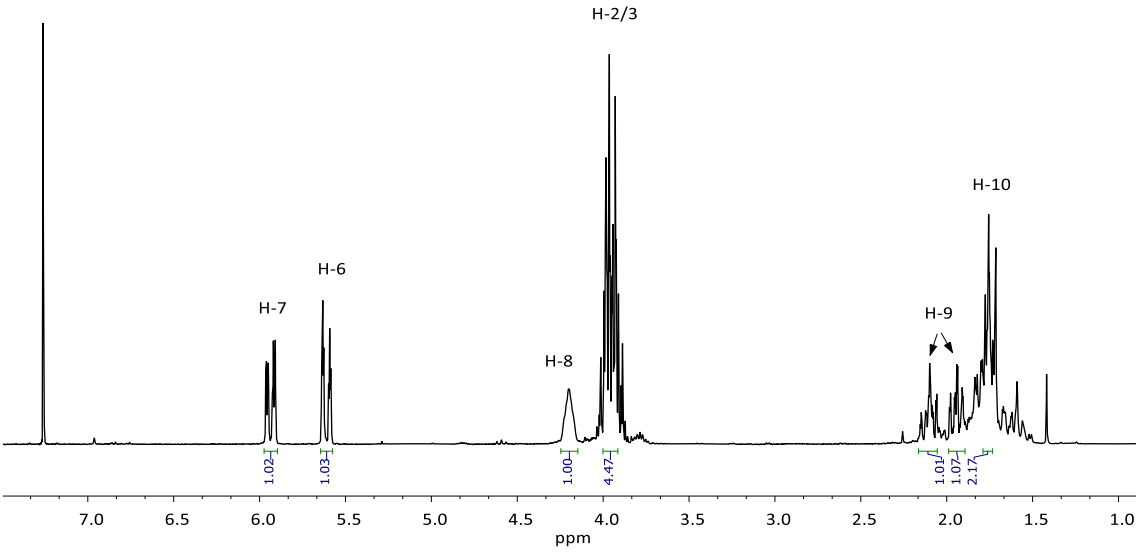

^{1}H-NMR (250 MHz, $CDCl_3$)

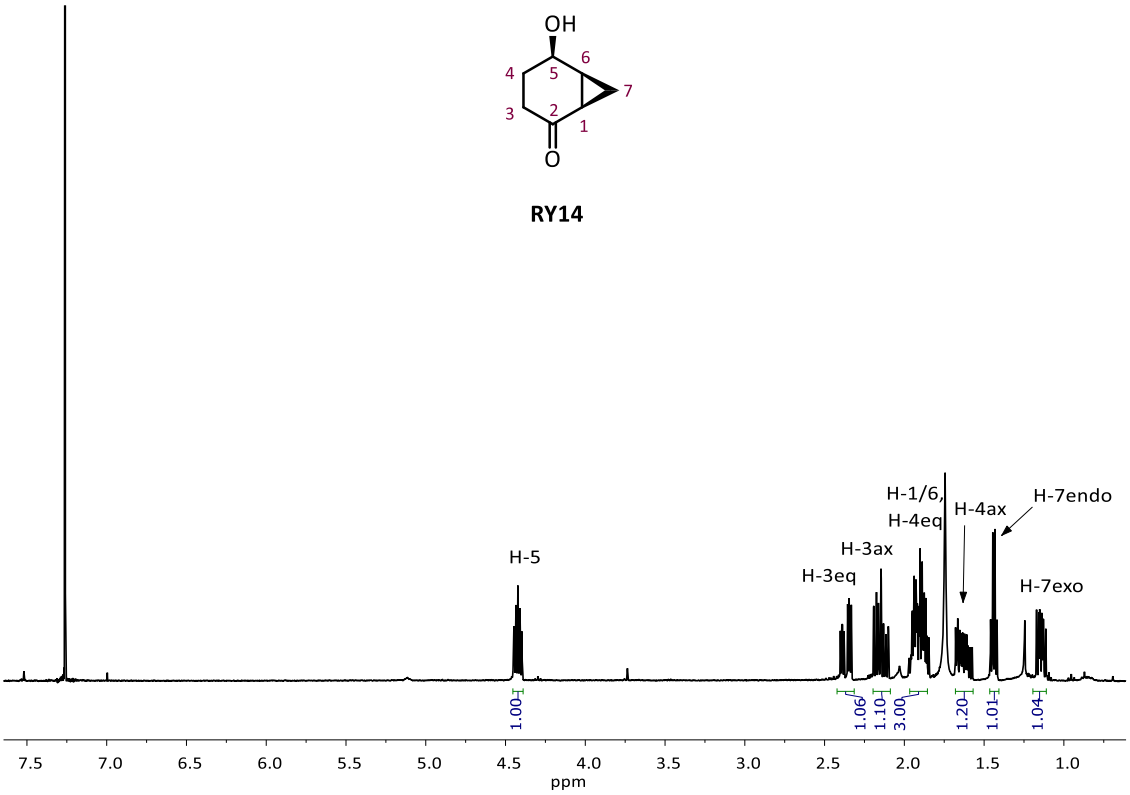

^{1}H-NMR (400 MHz, $CDCl_3$)

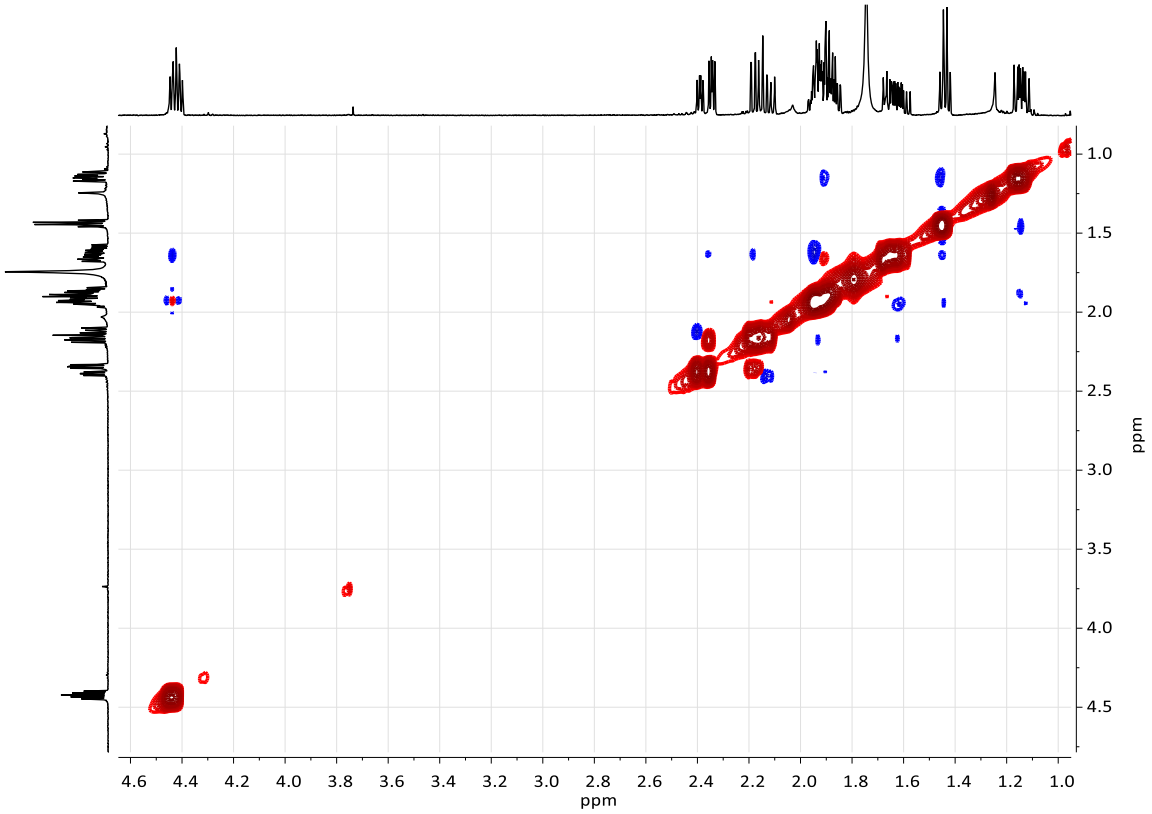

NOESY (400 MHz, $CDCl_3$)

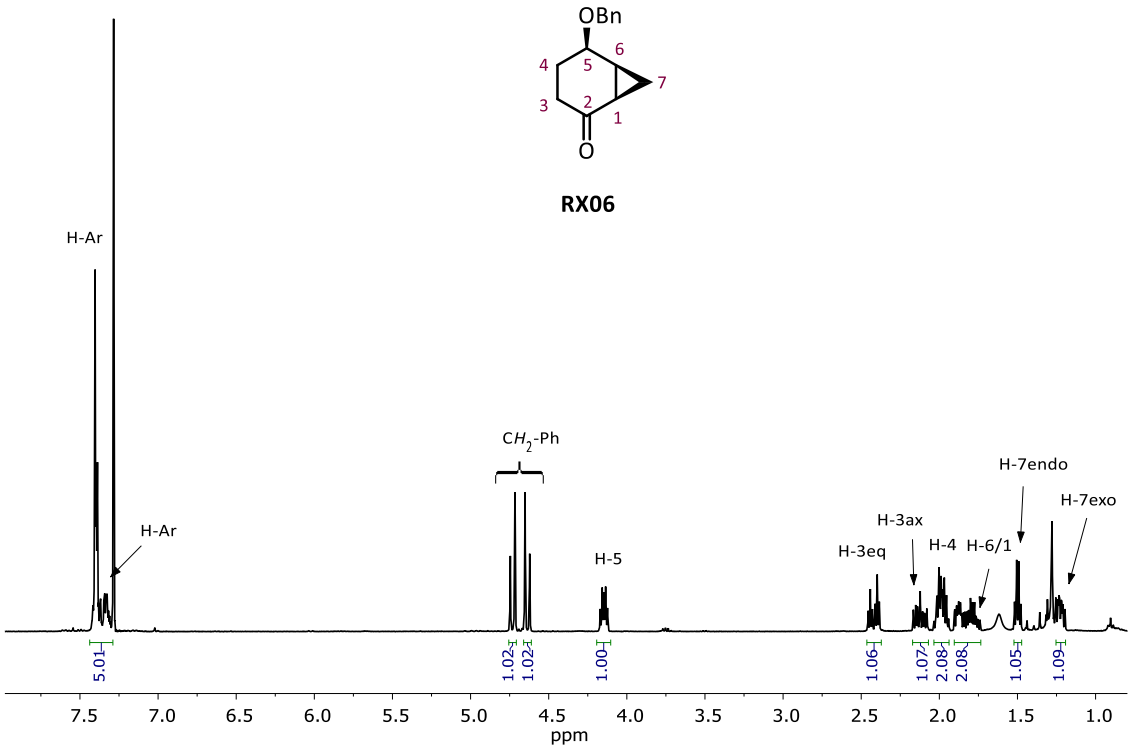

^{1}H-NMR (400 MHz, $CDCl_3$)

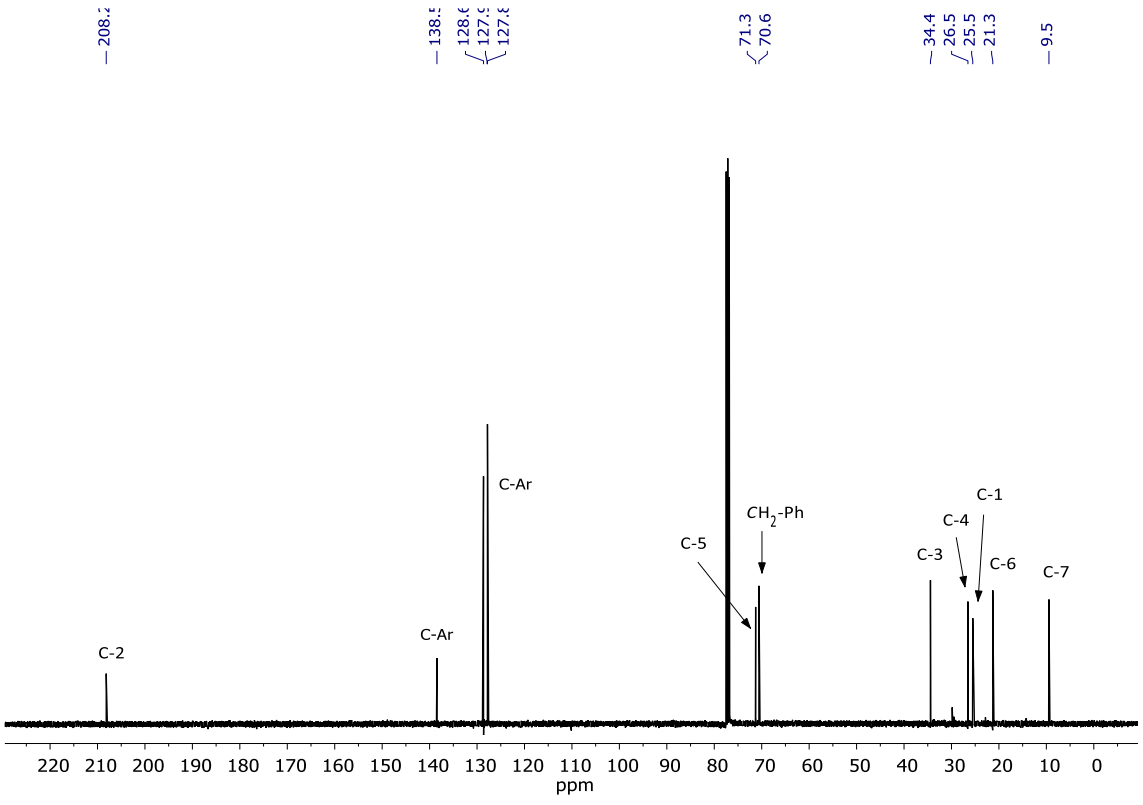

^{13}C-NMR (100 MHz, $CDCl_3$)

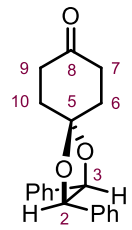

RX01

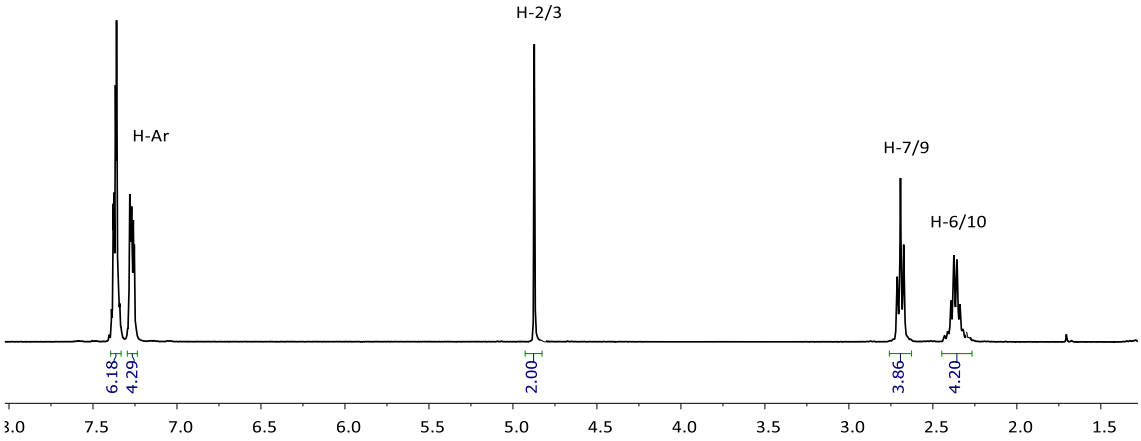

^{1}H-NMR (250 MHz, $CDCl_3$)

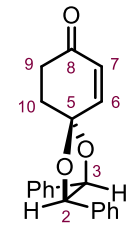

RX02

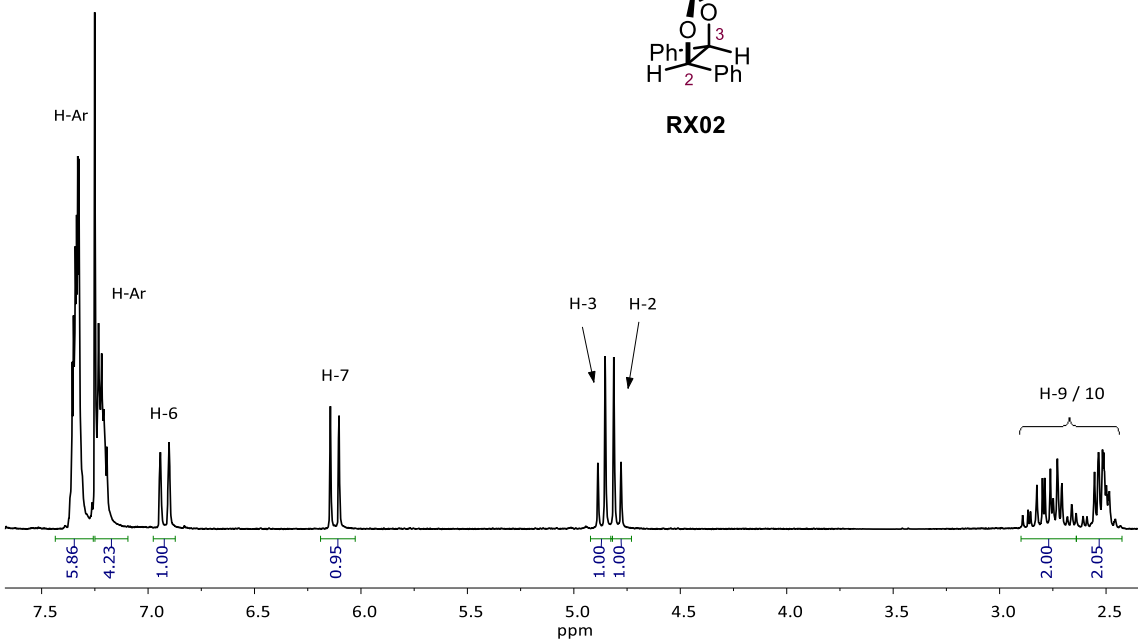

^{1}H-NMR (250 MHz, $CDCl_3$)

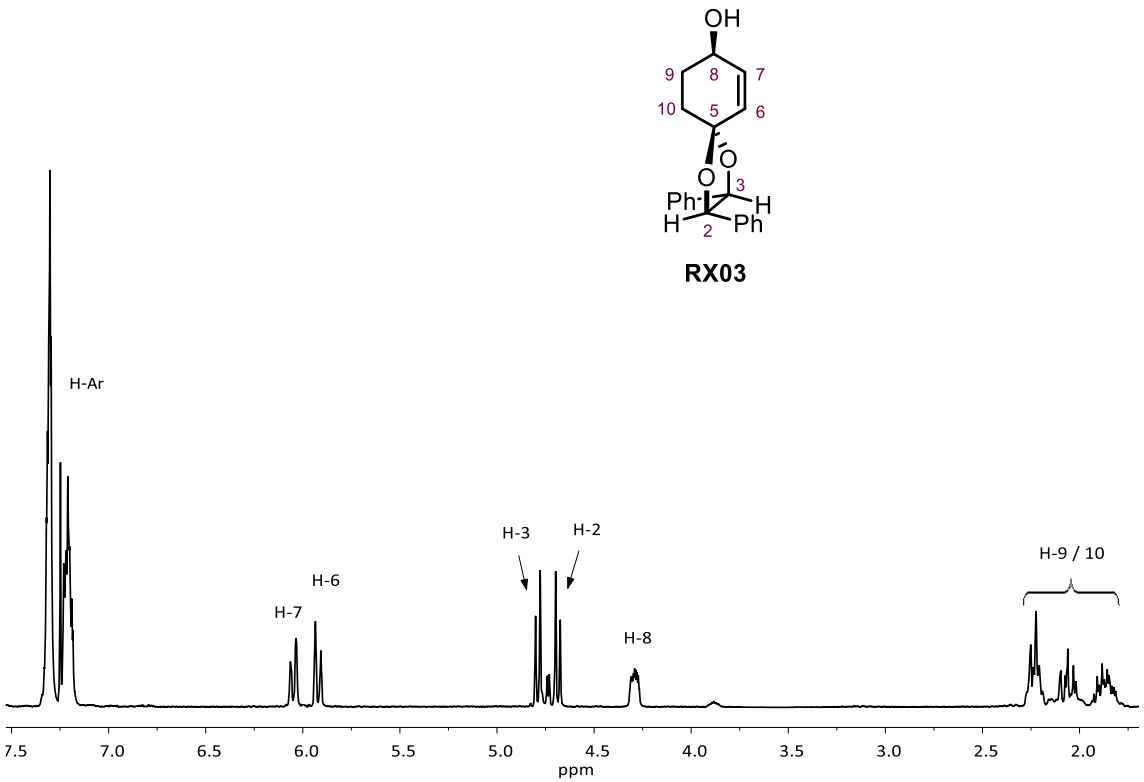

^{1}H-NMR (400 MHz, $CDCl_3$)

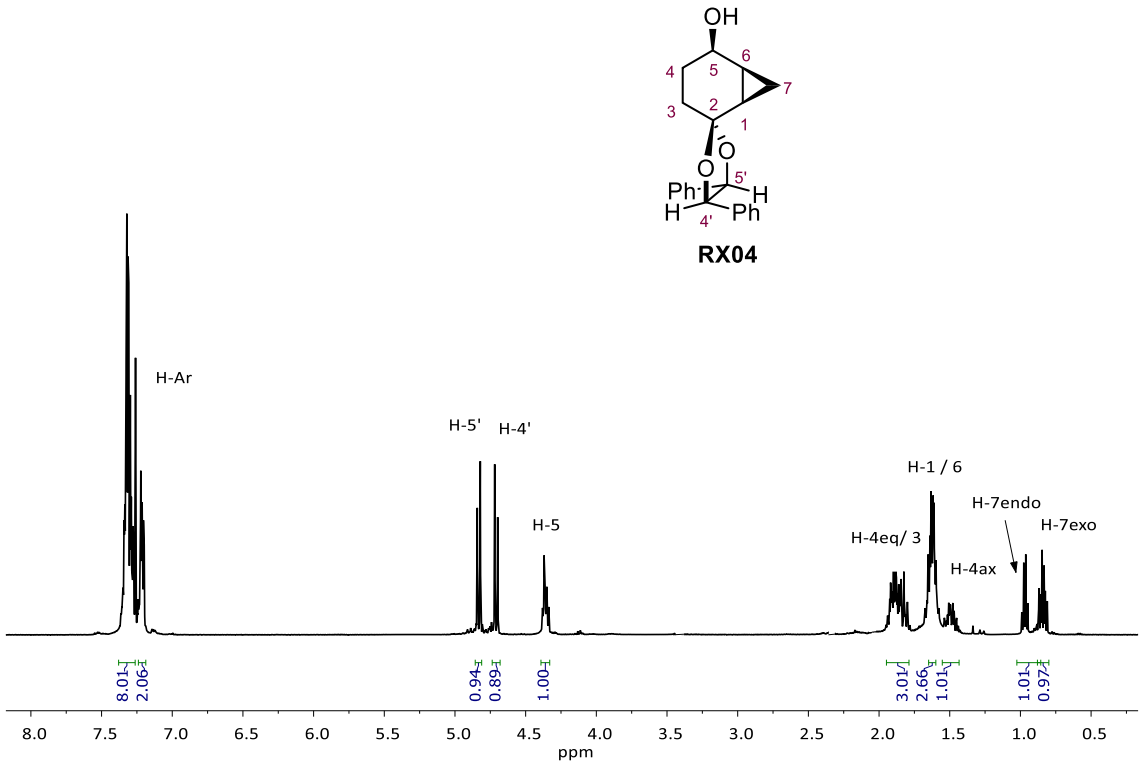

^{1}H-NMR (400 MHz, $CDCl_3$)

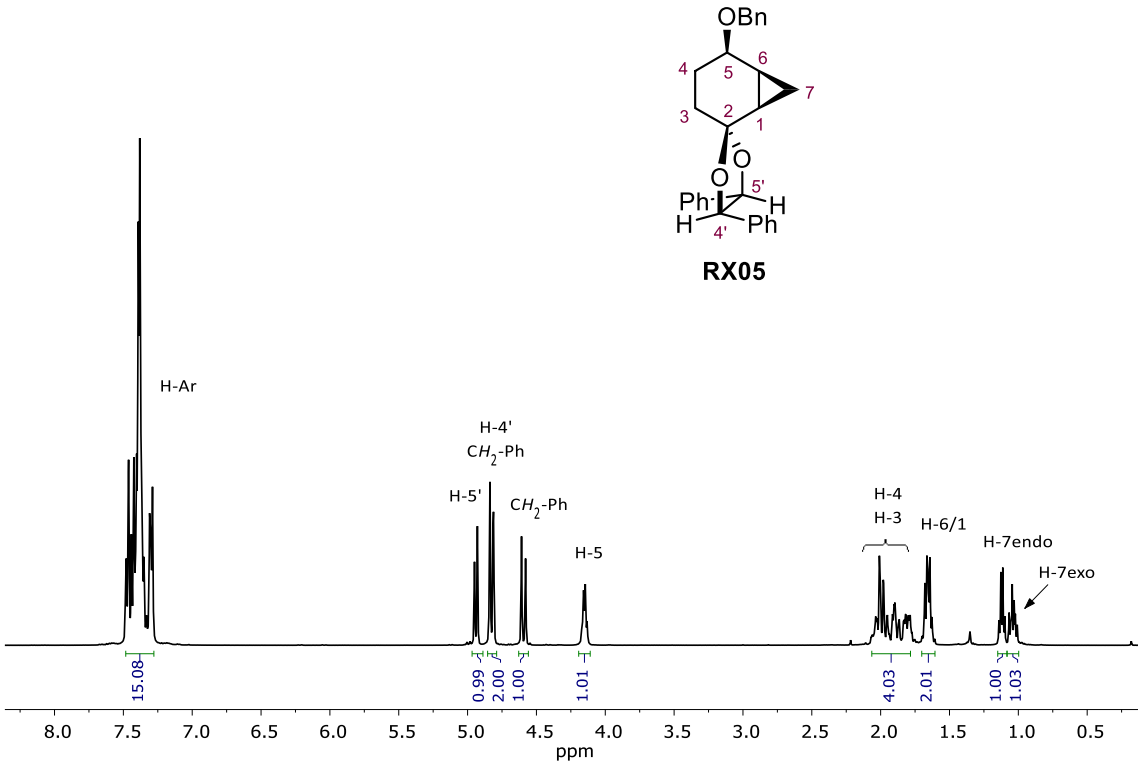

^{1}H-NMR (400 MHz, $CDCl_3$)

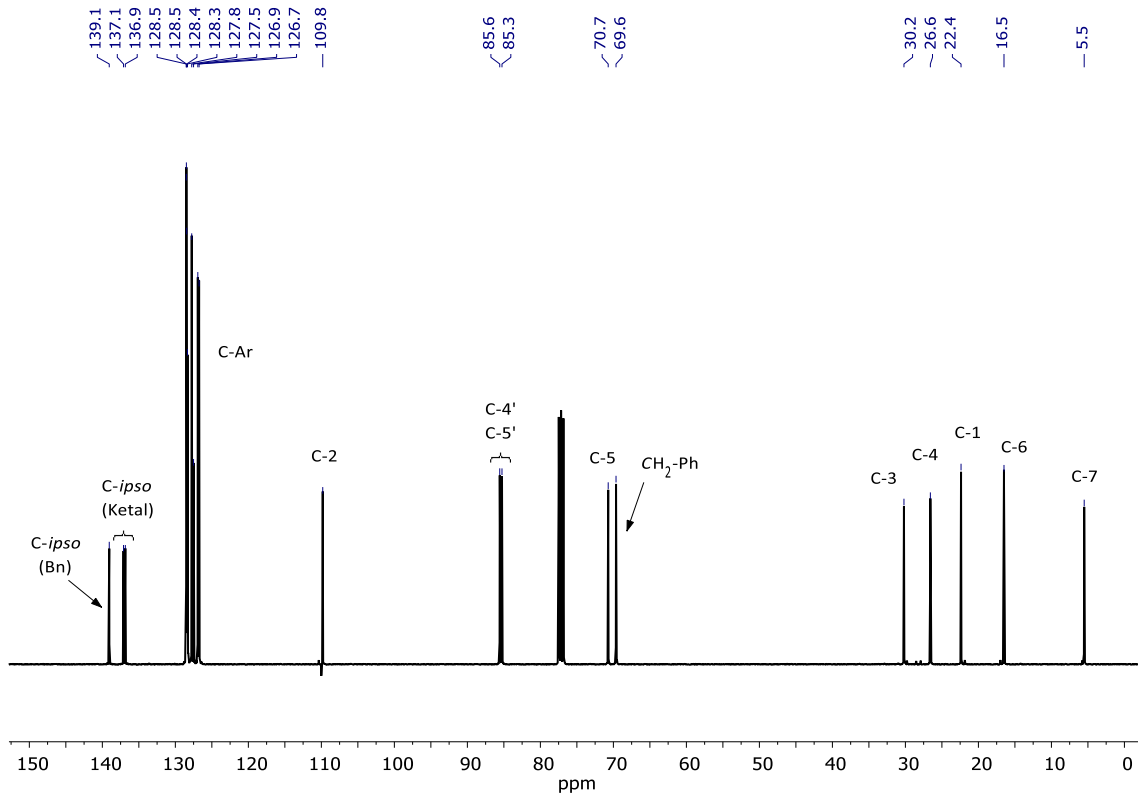

^{13}C-NMR (101 MHz, $CDCl_3$)

2. CHAPTER II. Synthesis of cytosine nucleoside analogue, 28.

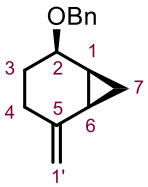

42

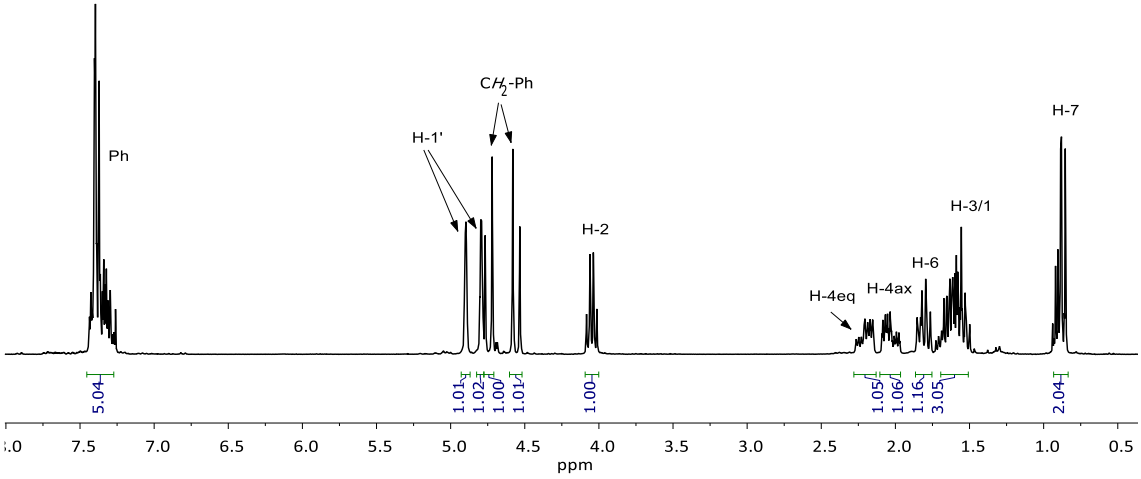

^{1}H-NMR (400 MHz, $CDCl_3$)

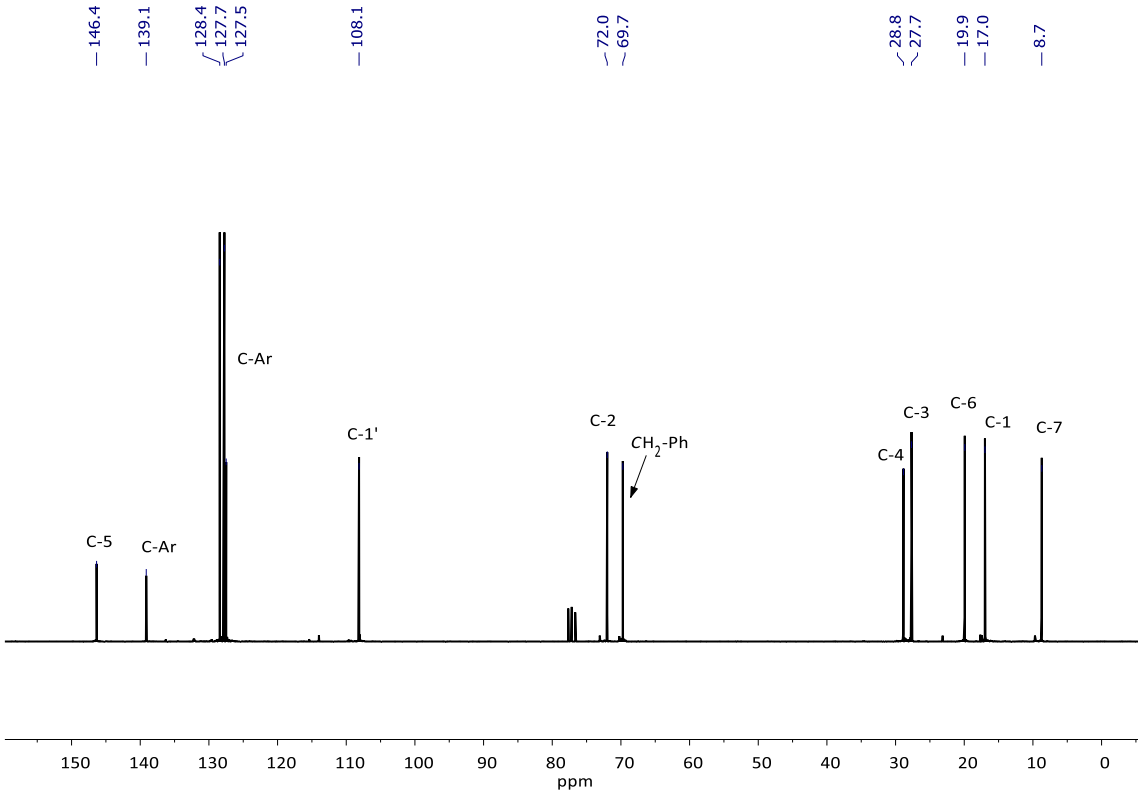

^{13}C-NMR (101 MHz, $CDCl_3$)

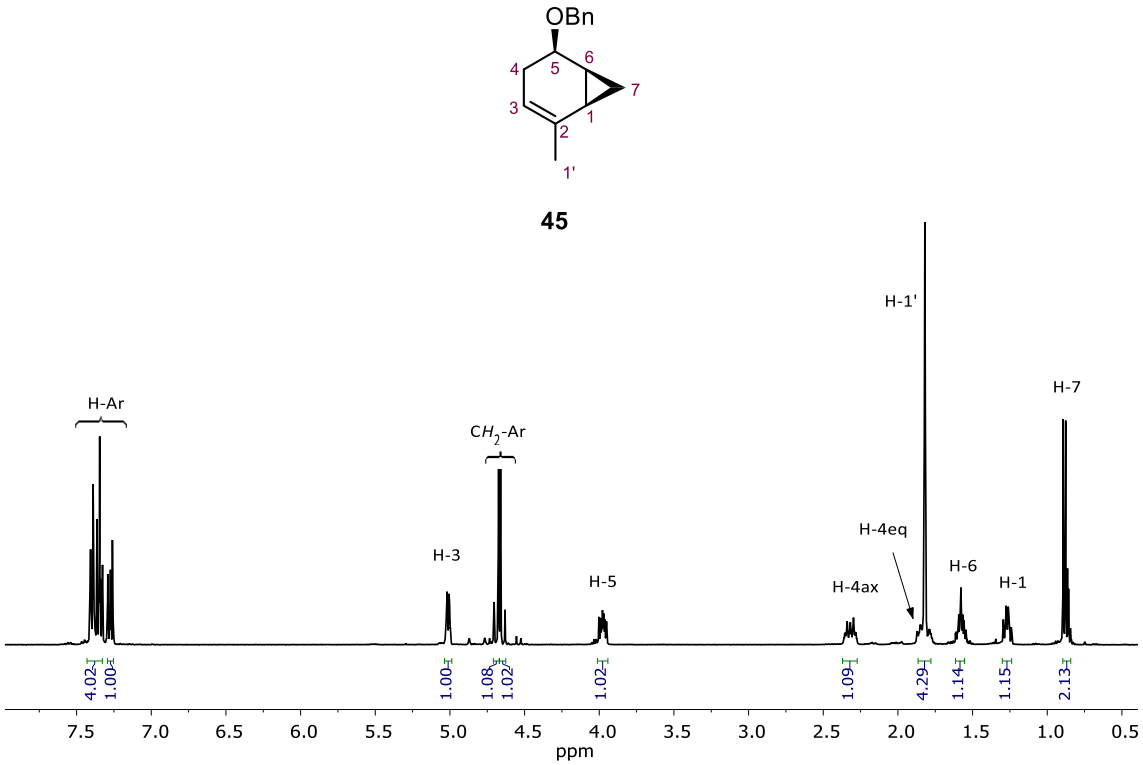

^{1}H-NMR (400 MHz, $CDCl_3$)

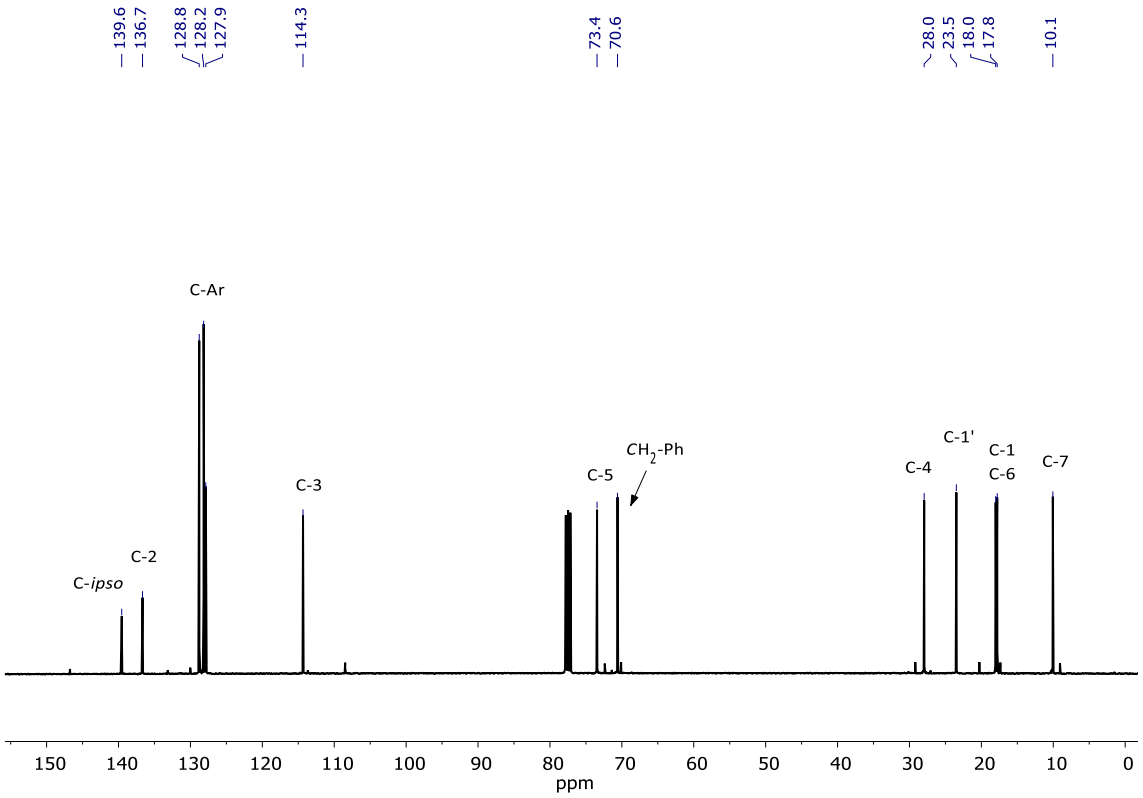

^{13}C-NMR (101 MHz, $CDCl_3$)

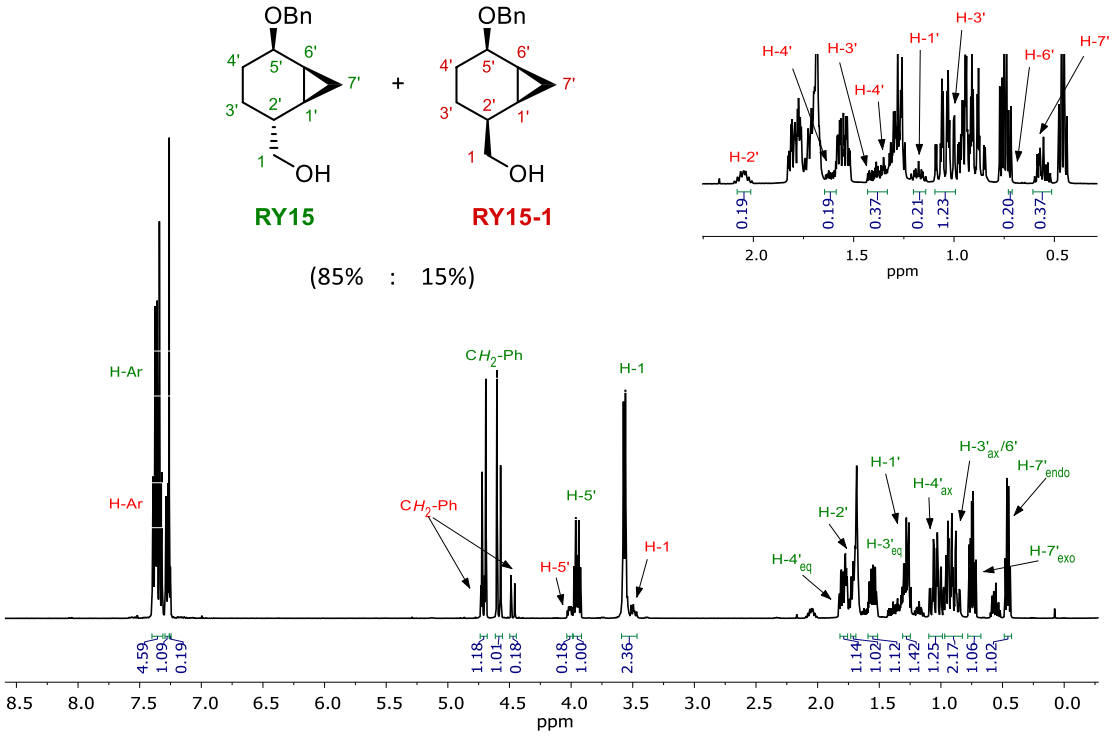

^{1}H-NMR (400 MHz, $CDCl_3$)

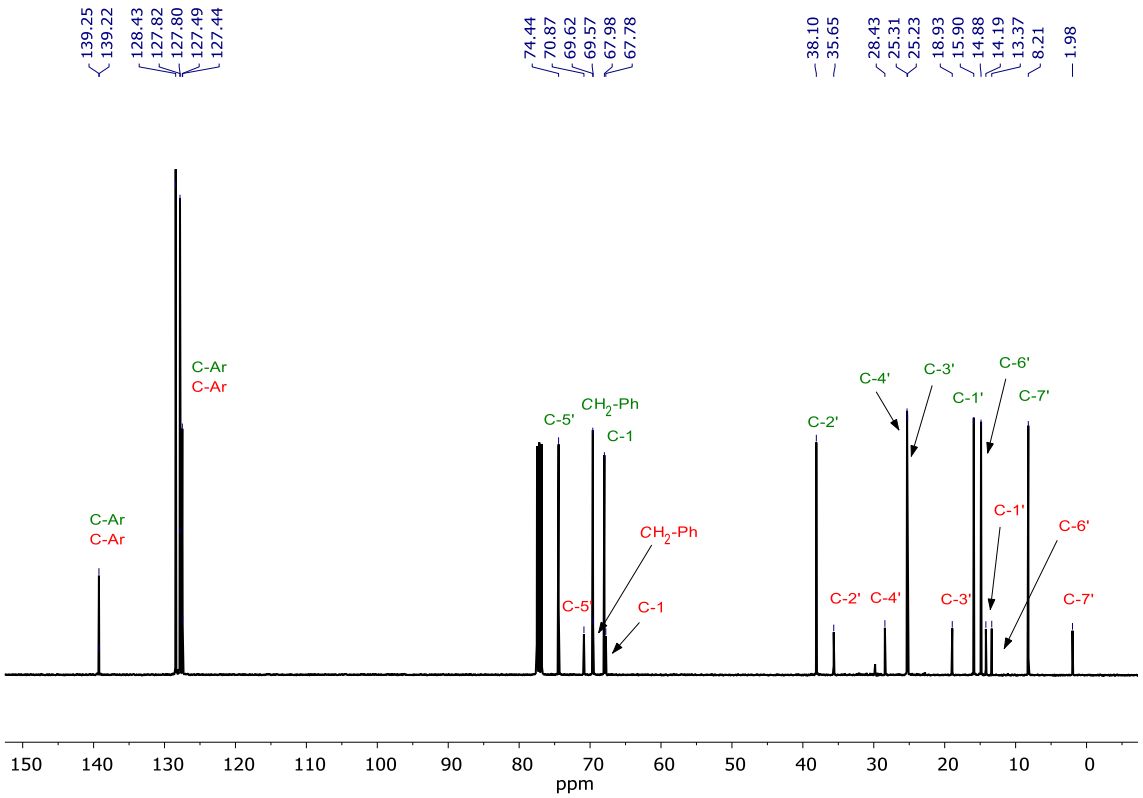

^{13}C-NMR (101 MHz, $CDCl_3$)

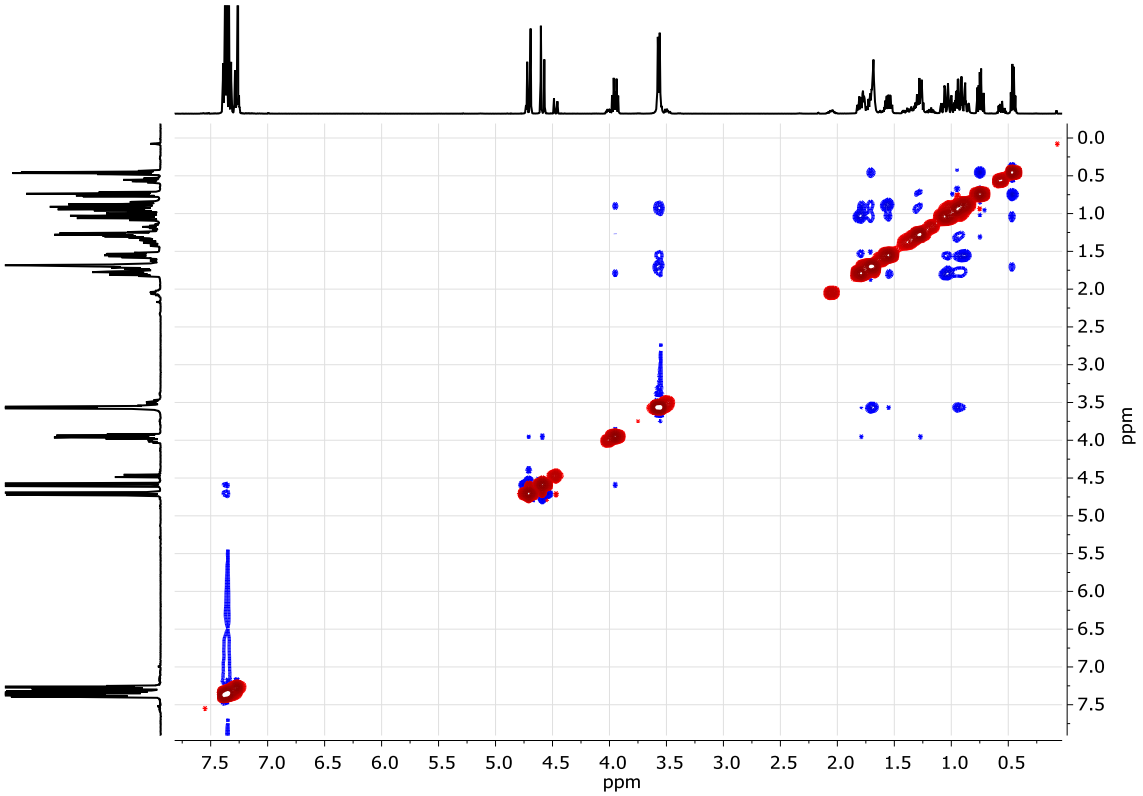

NOESY (400 MHz, $CDCl_3$)

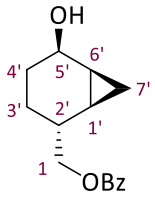

24

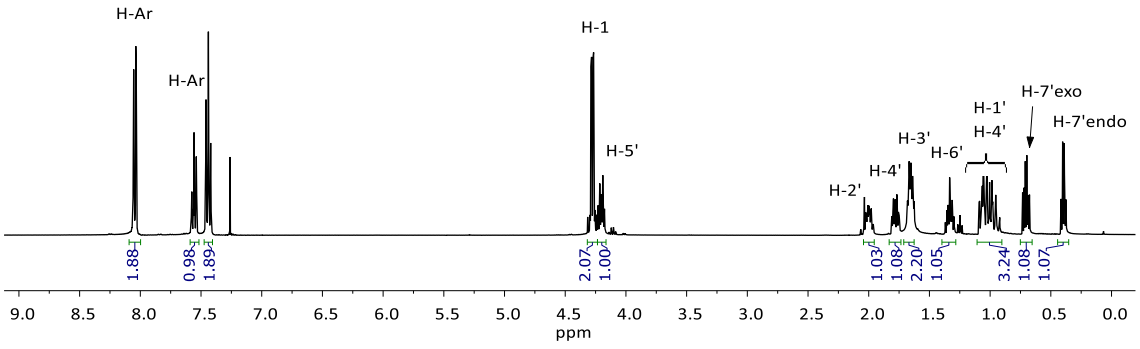

^{1}H-NMR (400 MHz, $CDCl_3$)

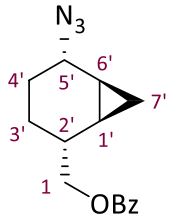

44

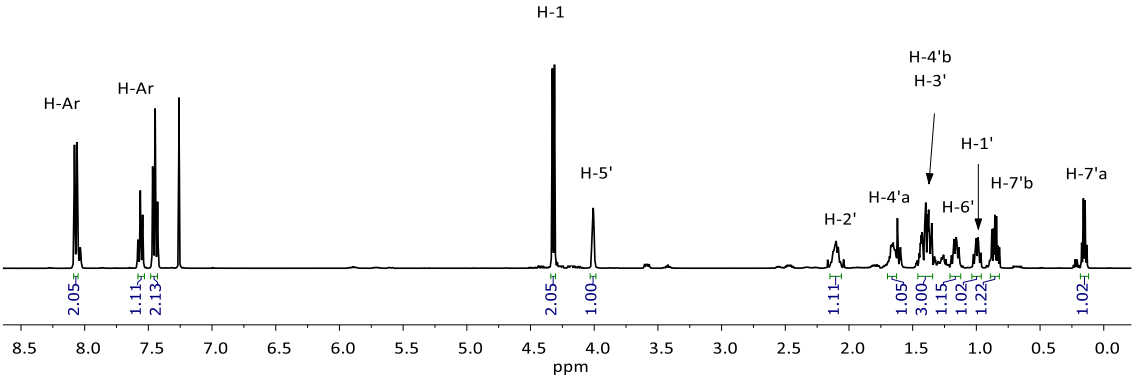

^{1}H-NMR (400 MHz, $CDCl_3$)

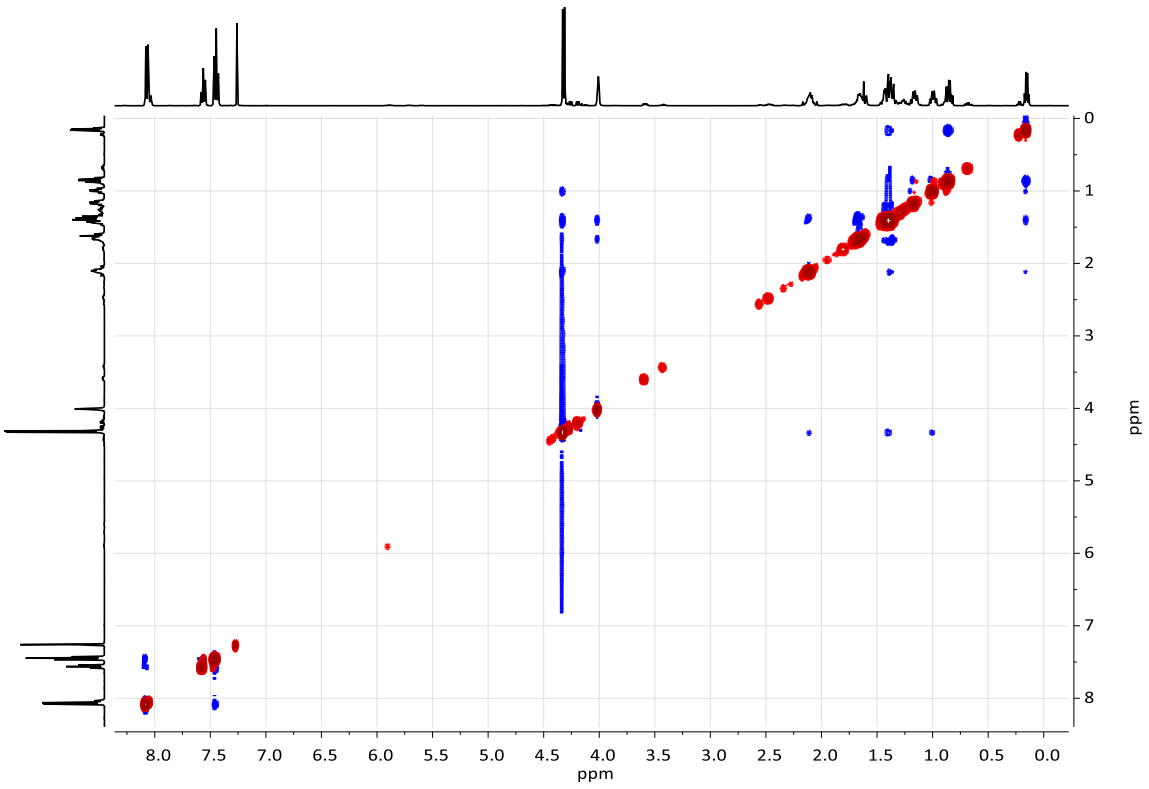

NOESY (400 MHz, $CDCl_3$)

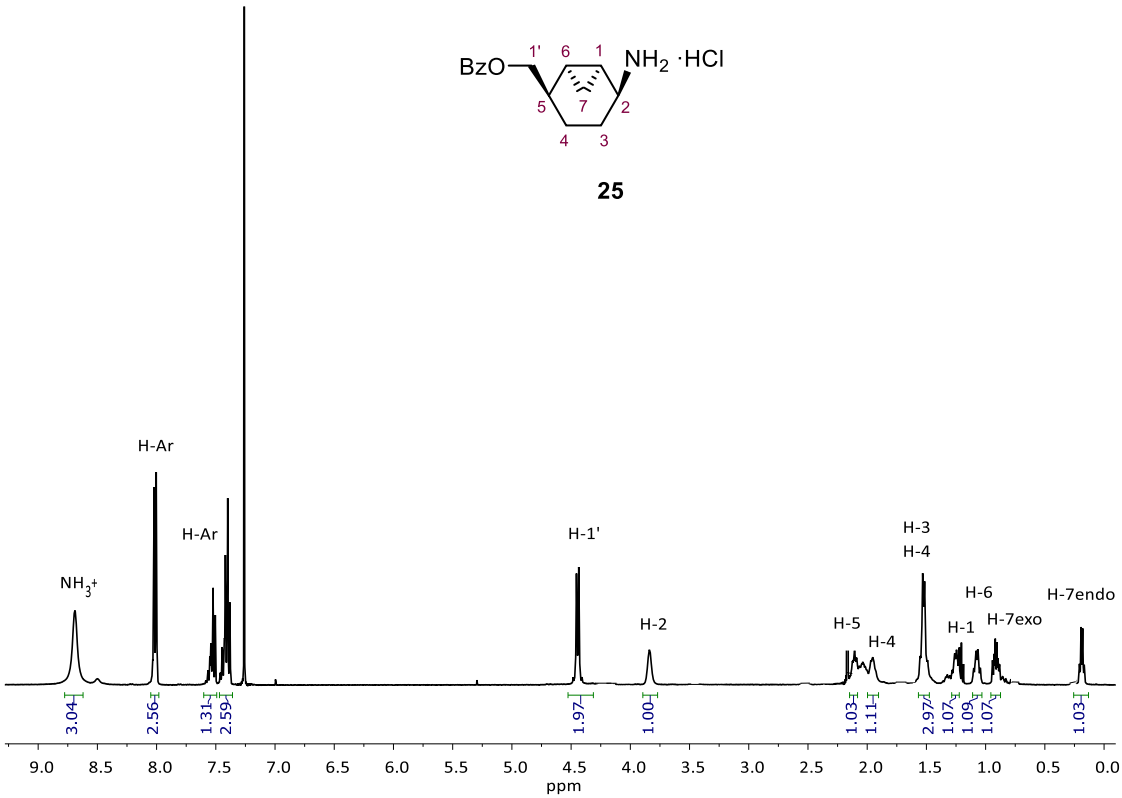

25

^{1}H-NMR (400 MHz, $CDCl_3$)

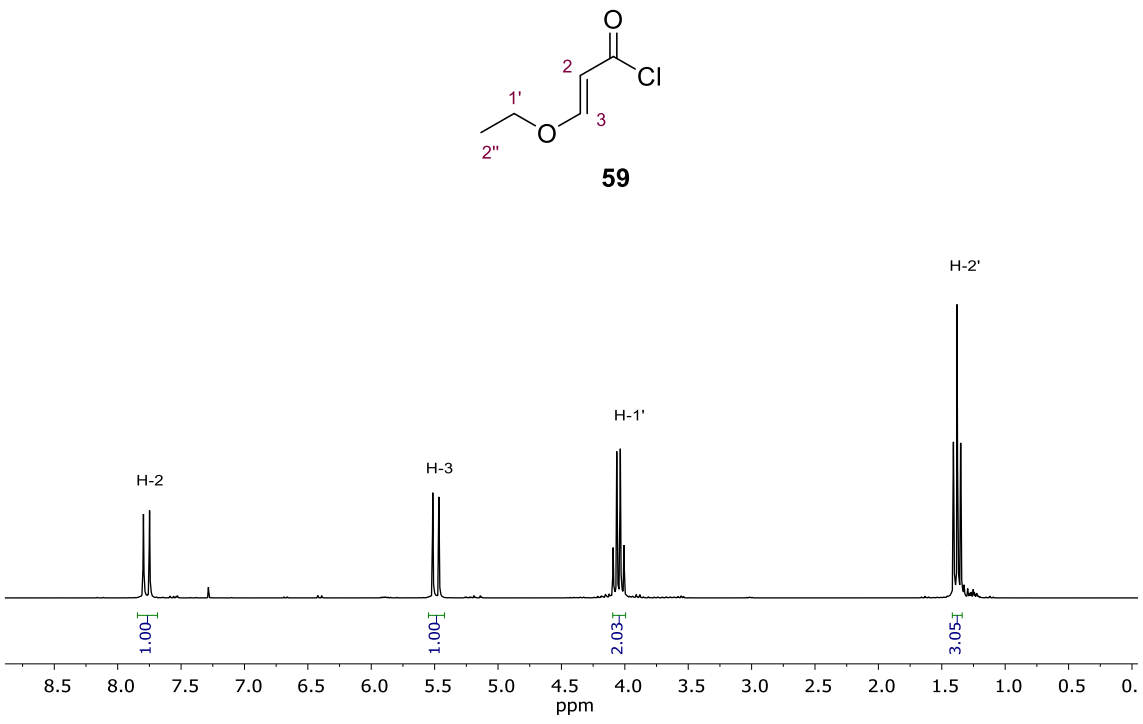

59

^{1}H-NMR (250 MHz, $CDCl_3$)

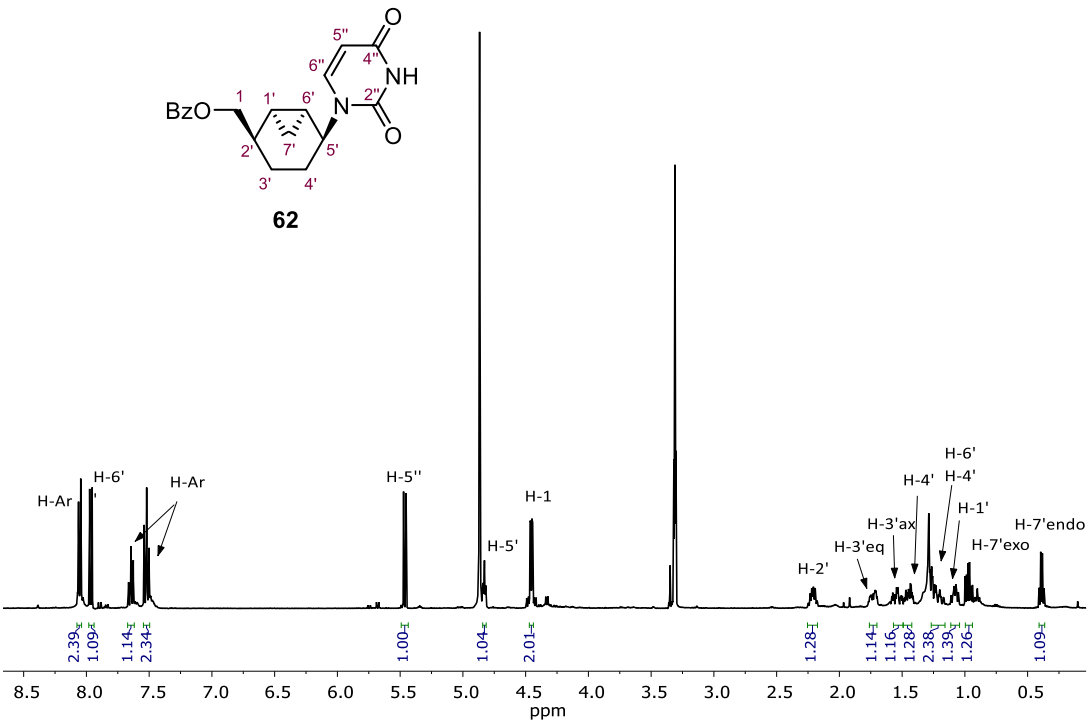

^{1}H-NMR (400 MHz, MeOH-d_4)

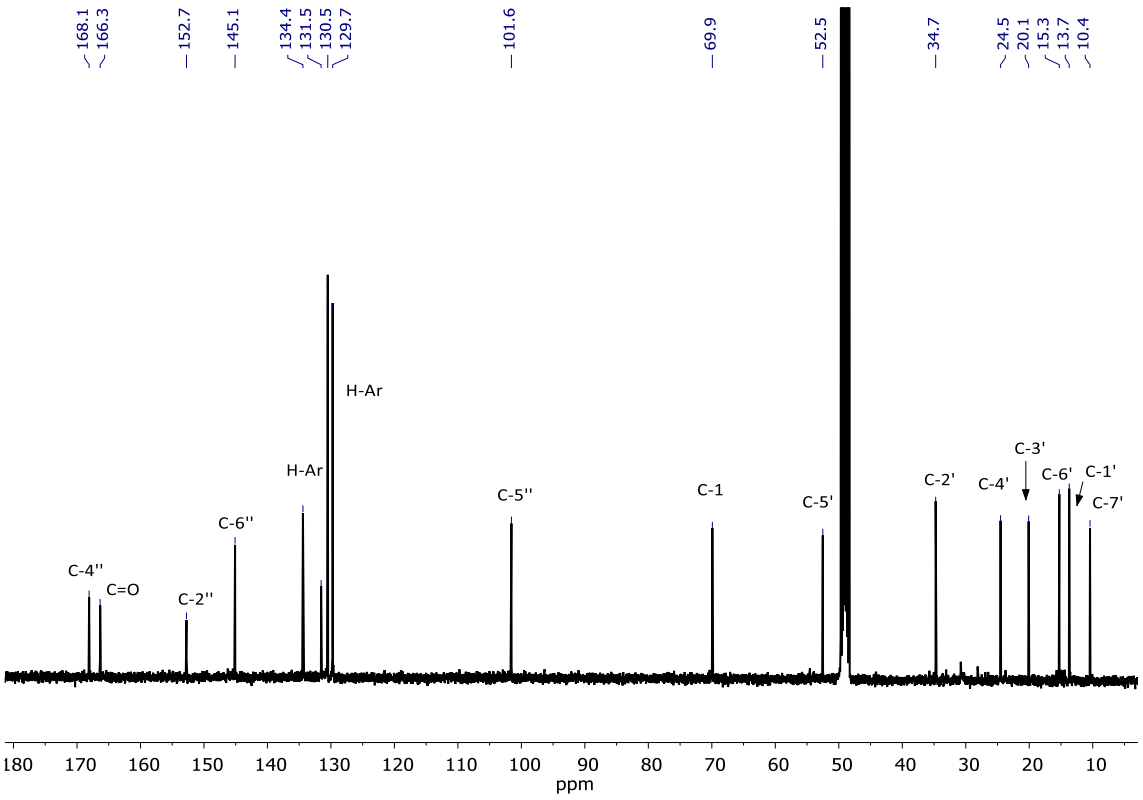

^{13}C-NMR (101 MHz, MeOH-d_4)

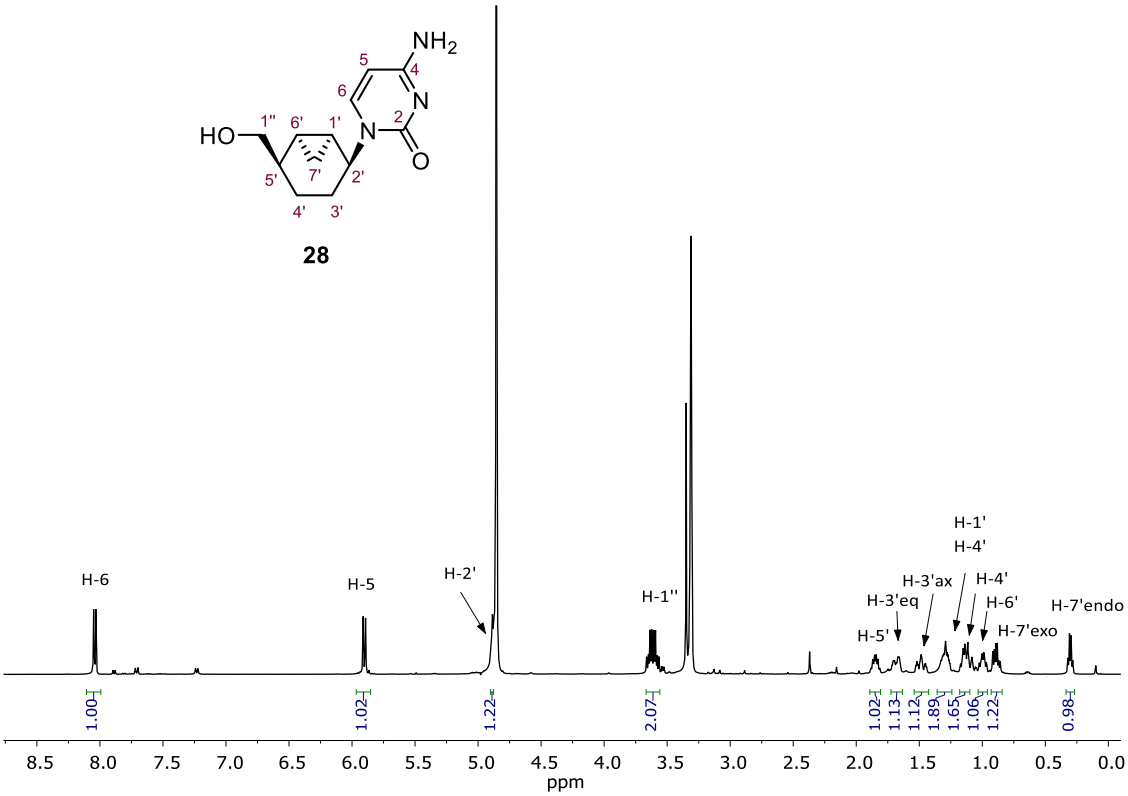

^{1}H-NMR (400 MHz, MeOH-d_4)

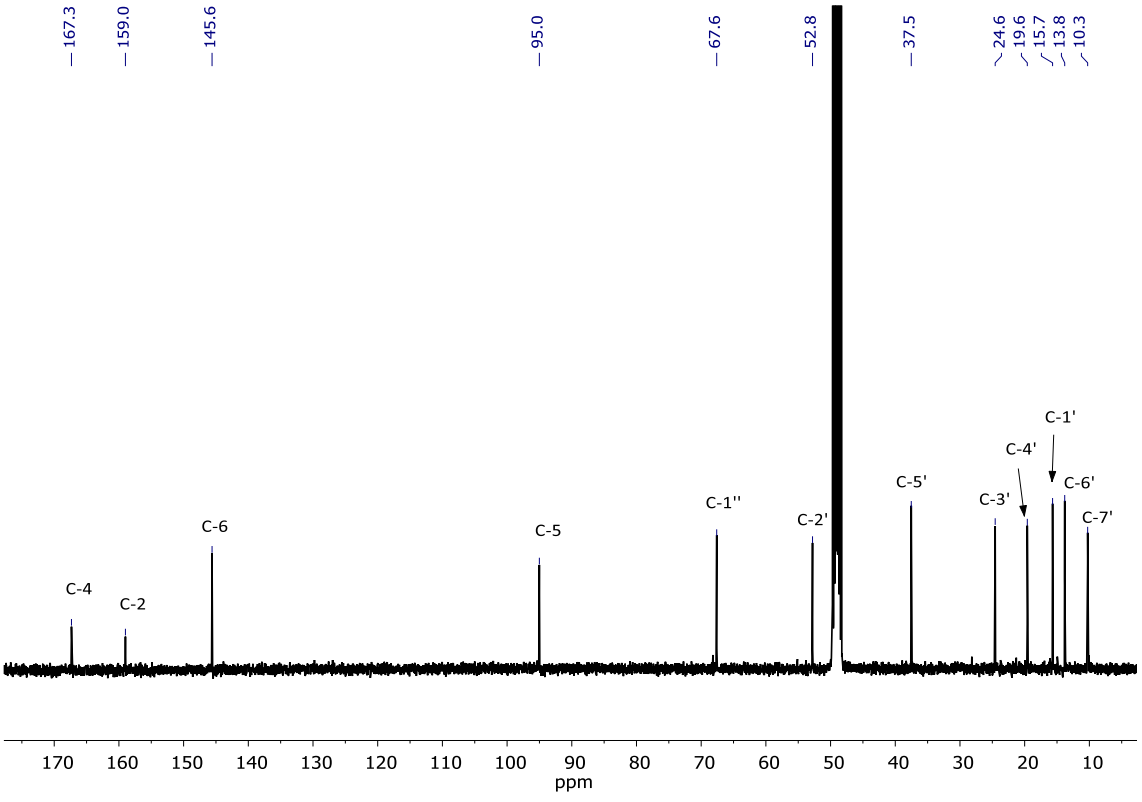

^{13}C-NMR (101 MHz, MeOH-d_4)

3. CHAPTER III. Synthesis of 4'-hydroxymehtyl-3'-hydroxybicyclo[4.1.0]-heptane NAs.

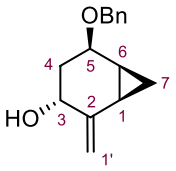

63

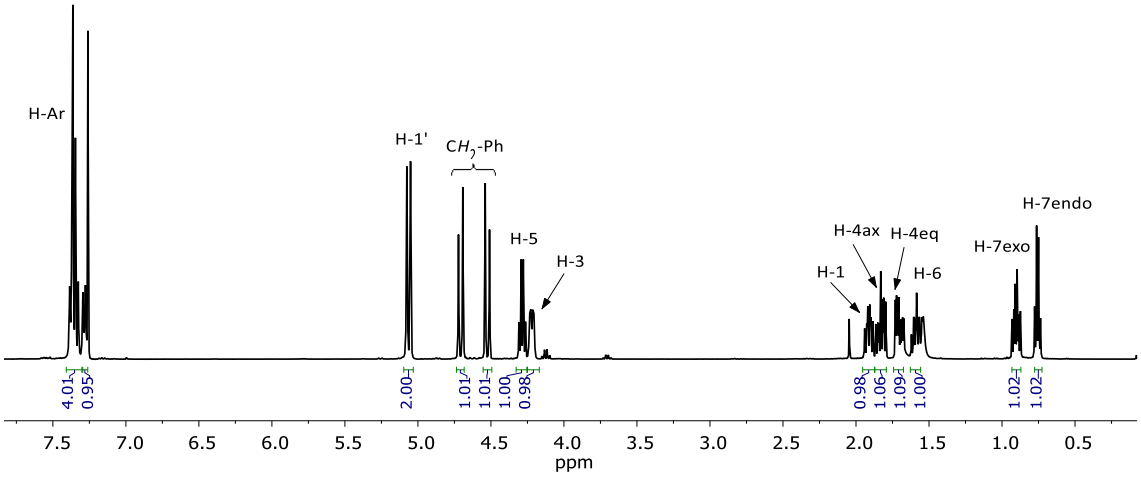

^{1}H-NMR (400 MHz, $CDCl_3$)

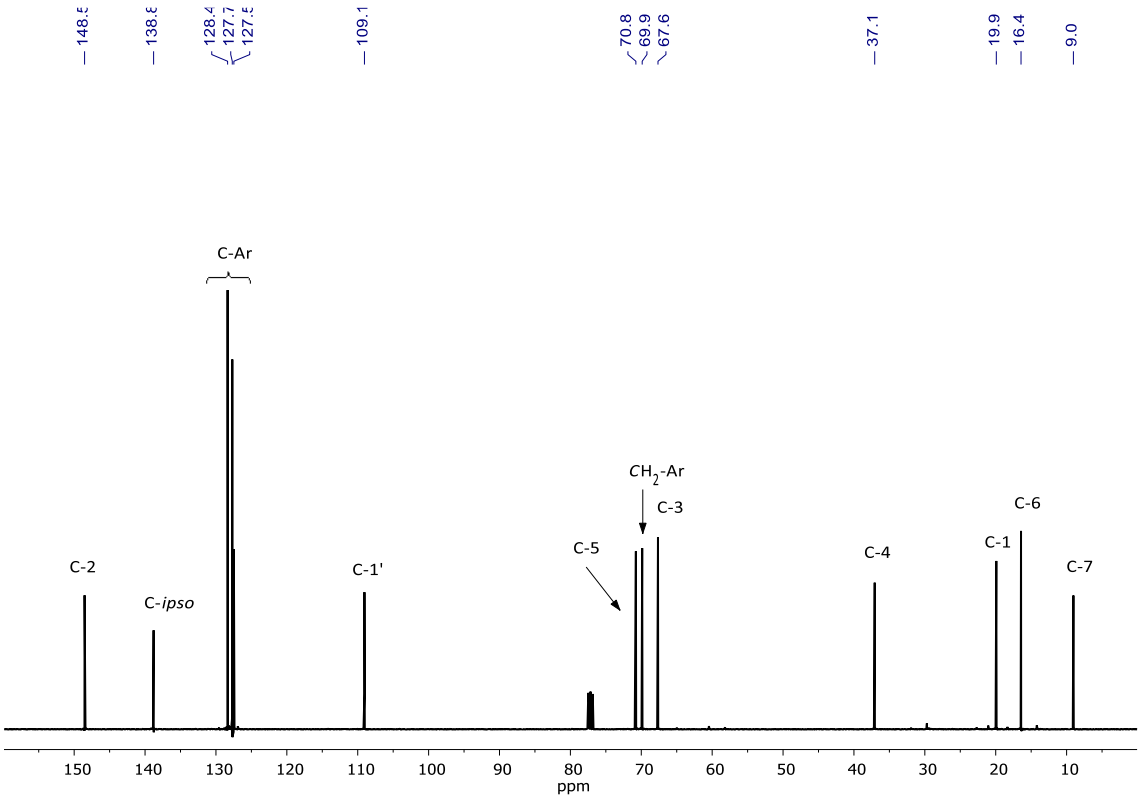

^{13}C-NMR (101 MHz, $CDCl_3$)

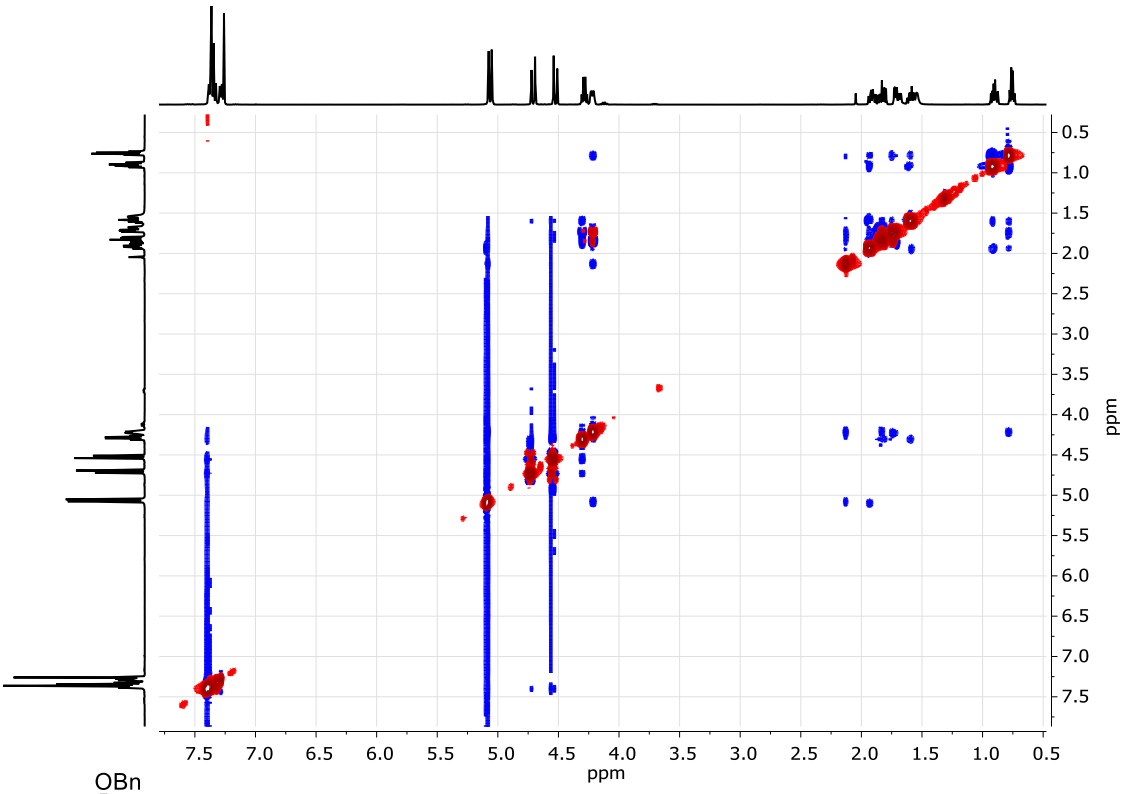

NOESY (400 MHz, $CDCl_3$)

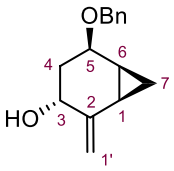

63

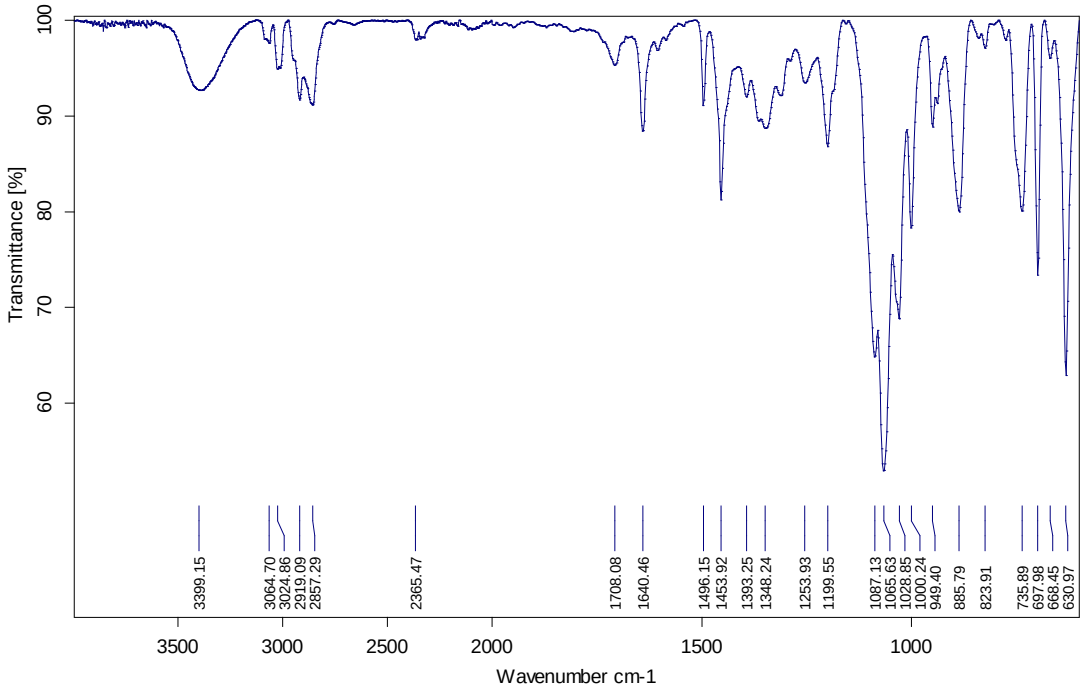

IR (ATR)

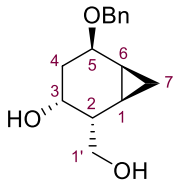

64

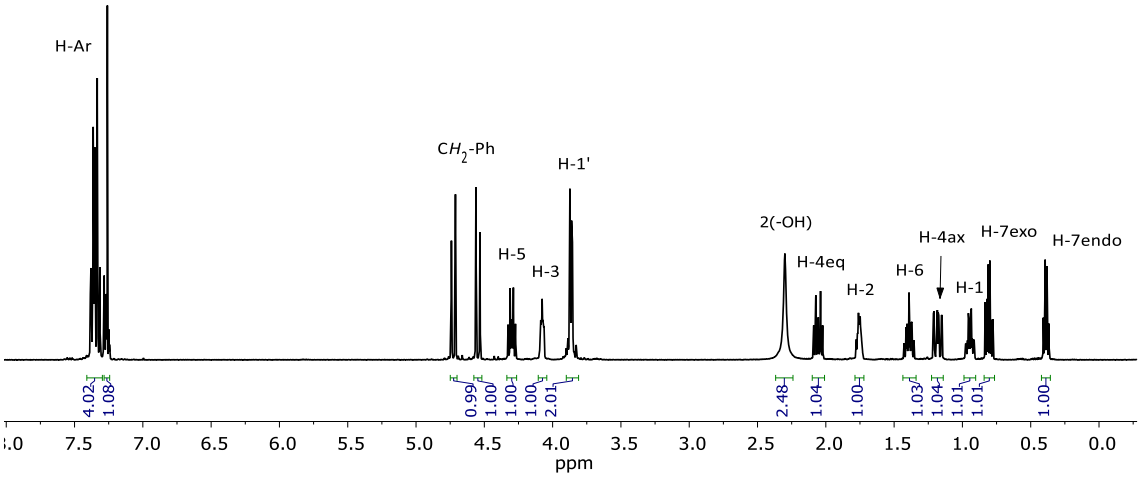

^{1}H-NMR (400 MHz, $CDCl_3$)

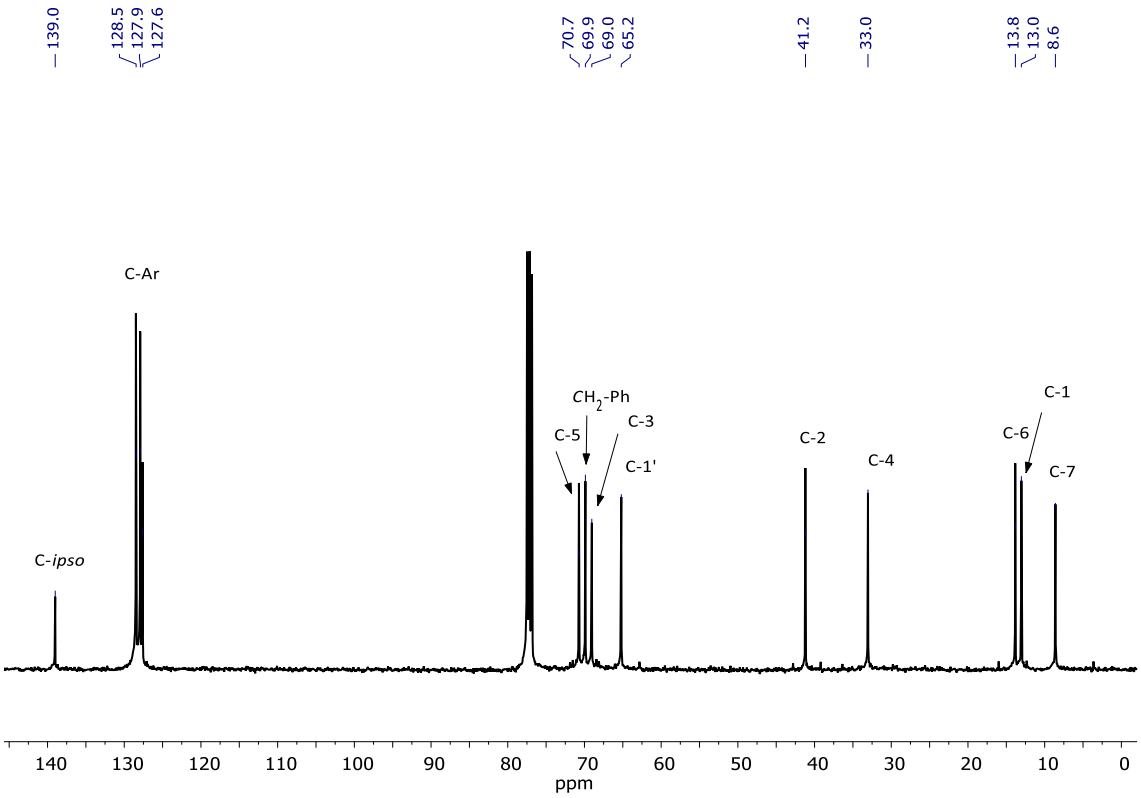

^{13}C-NMR (101 MHz, $CDCl_3$)

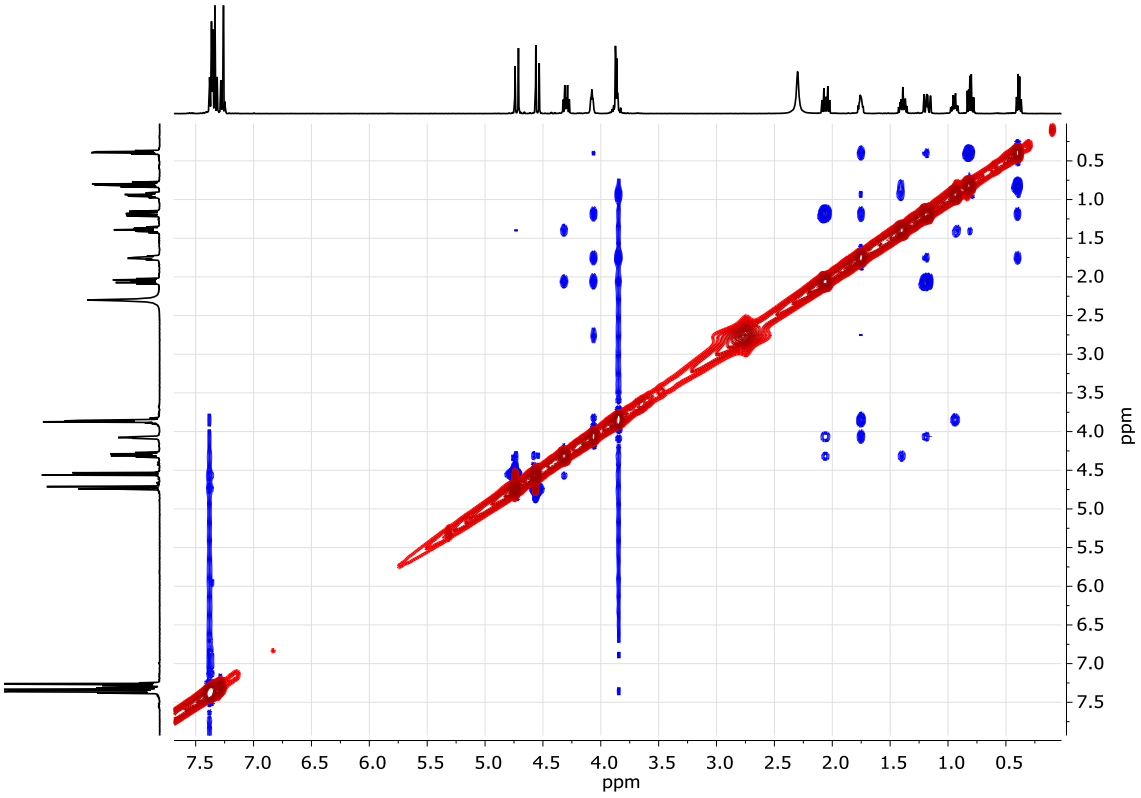

NOESY (400 MHz, $CDCl_3$)

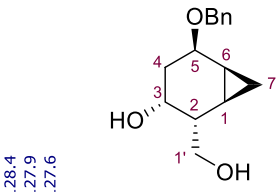

64

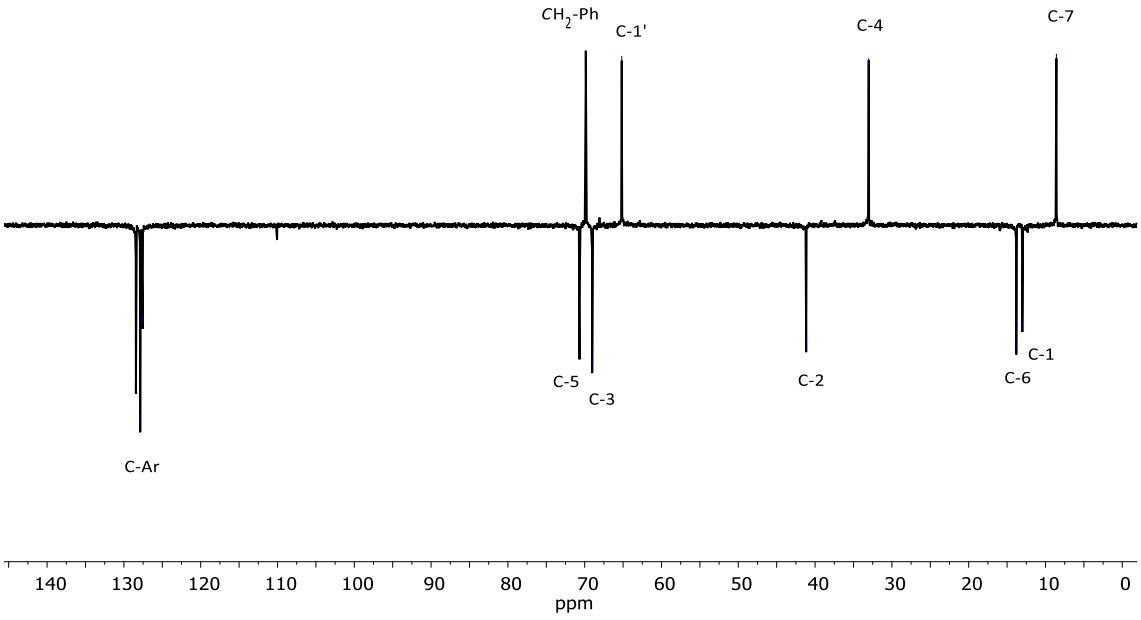

DEPT-135 (101 MHz, $CDCl_3$)

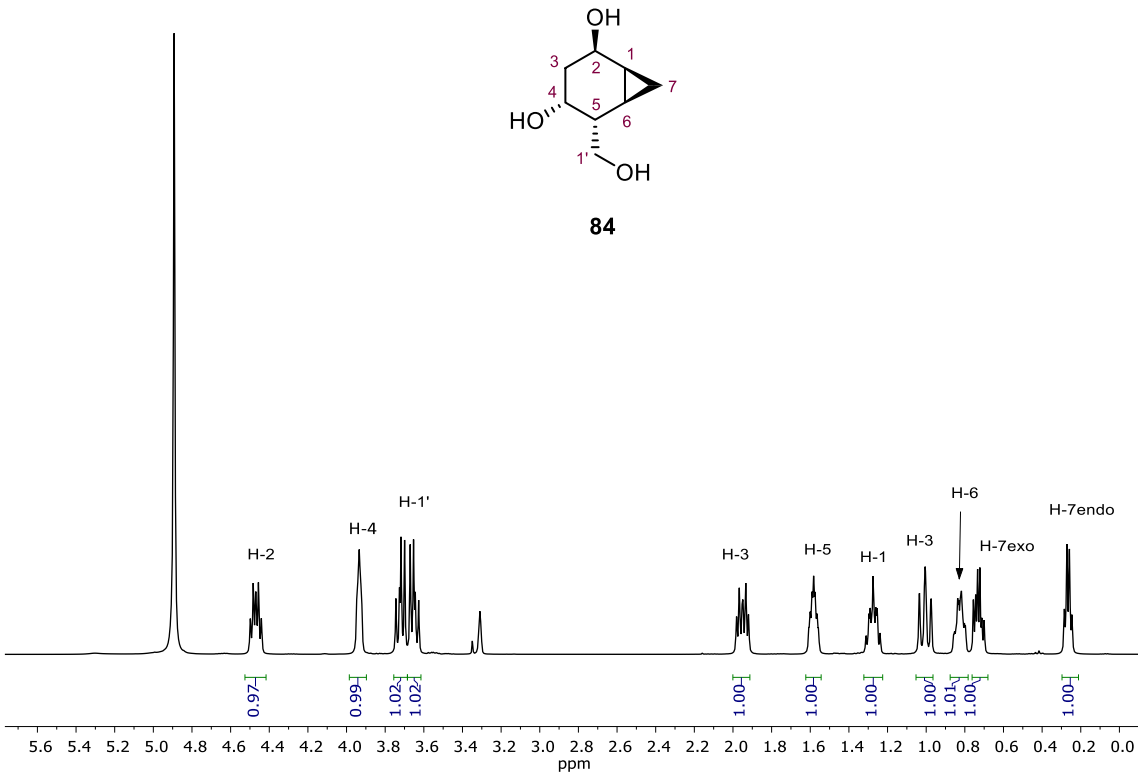

84

^{1}H-NMR (400 MHz, MeOH-d_4)

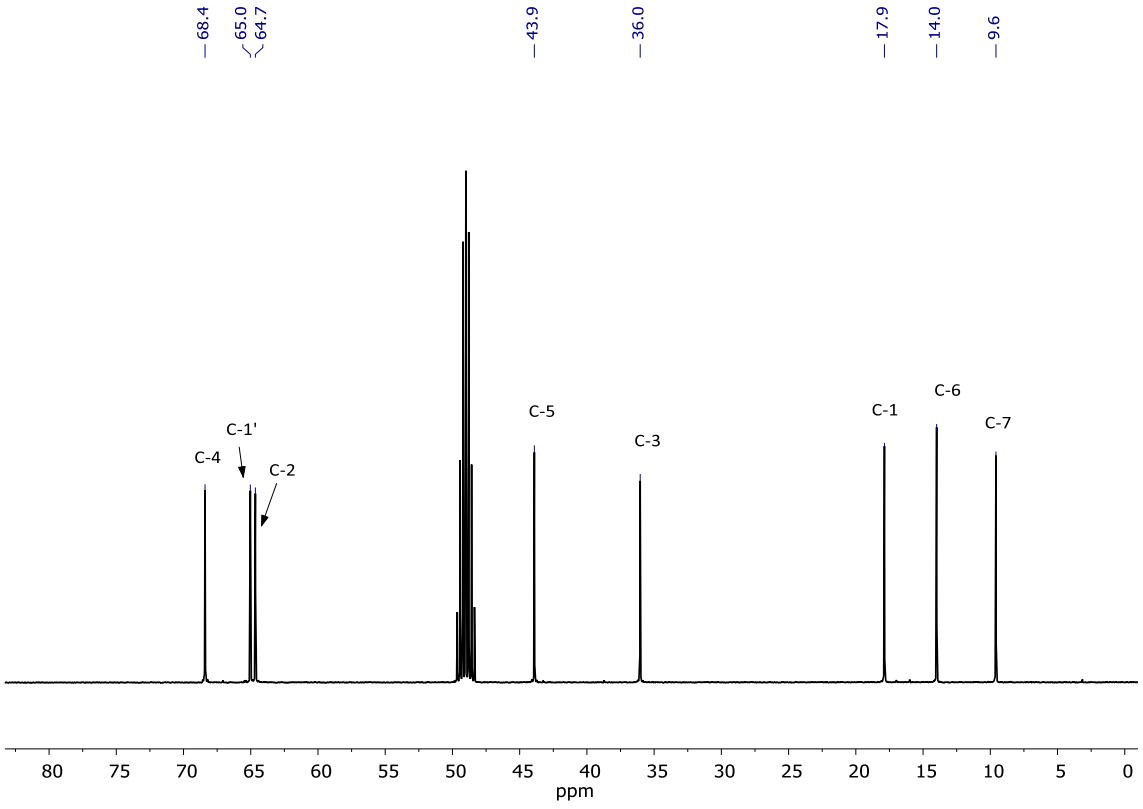

^{13}C-NMR (101 MHz, MeOH-d_4)

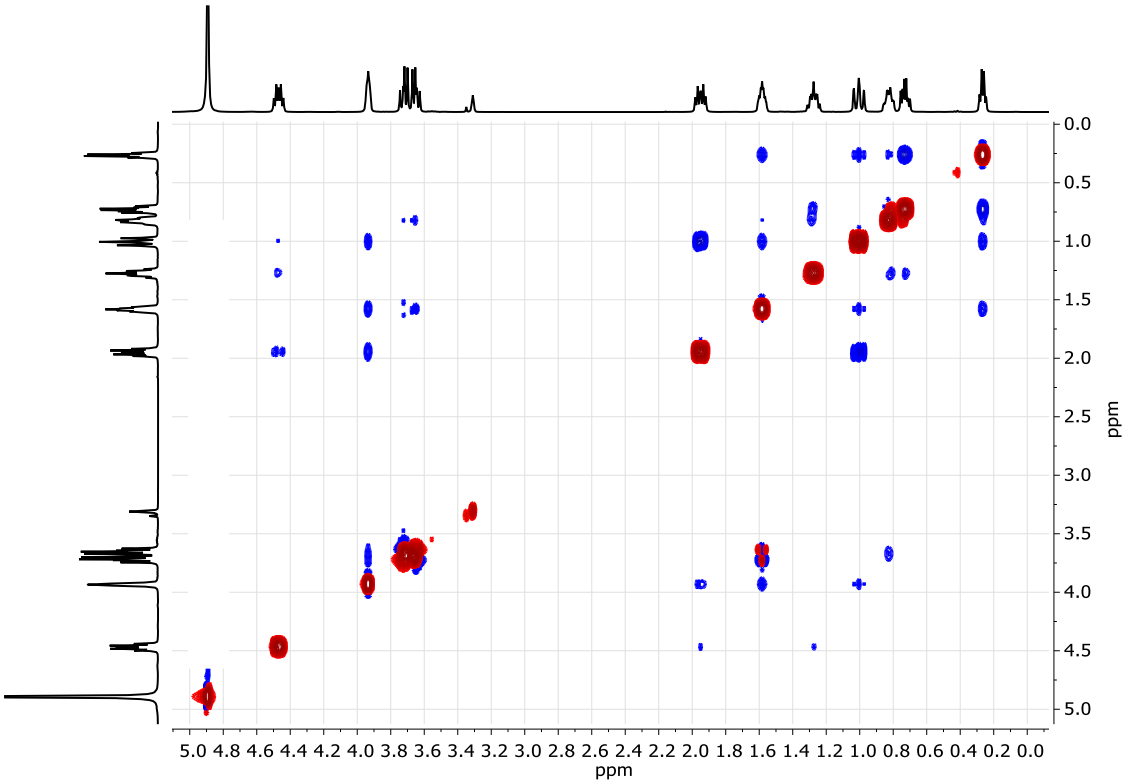

NOESY (400 MHz, MeOH-d_4)

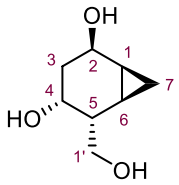

84

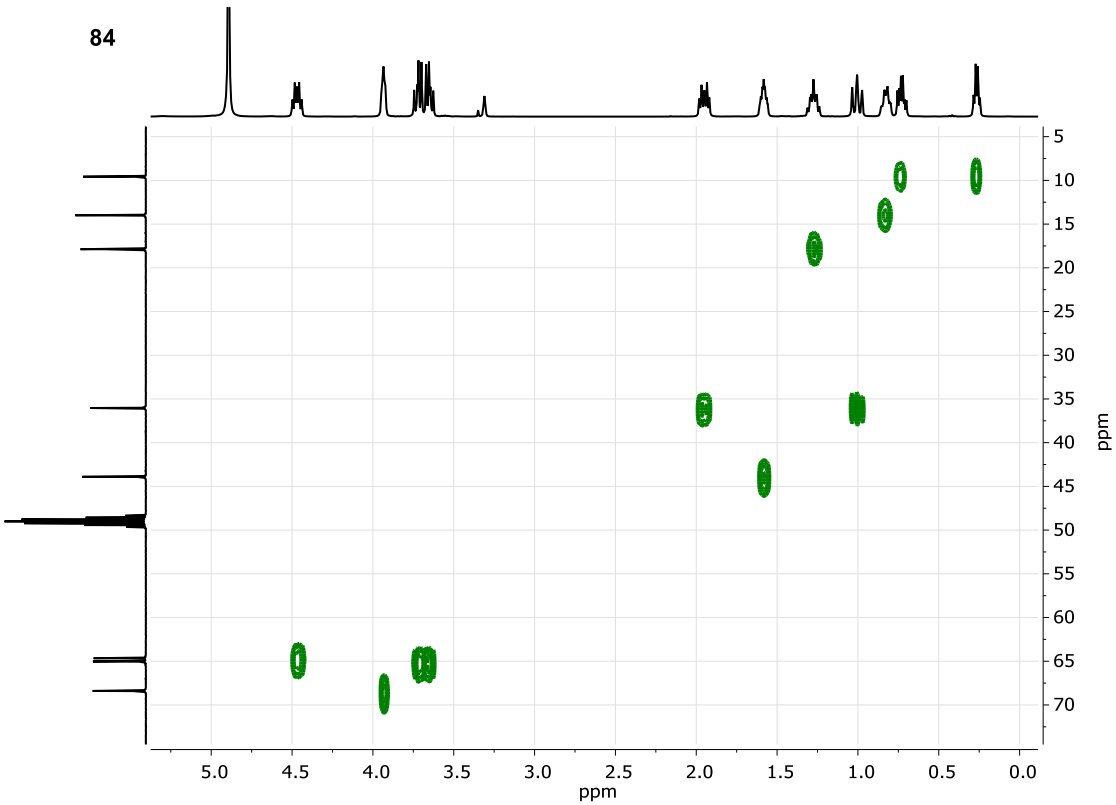

HSQC (400 MHz, MeOH-d_4)

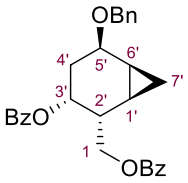

91

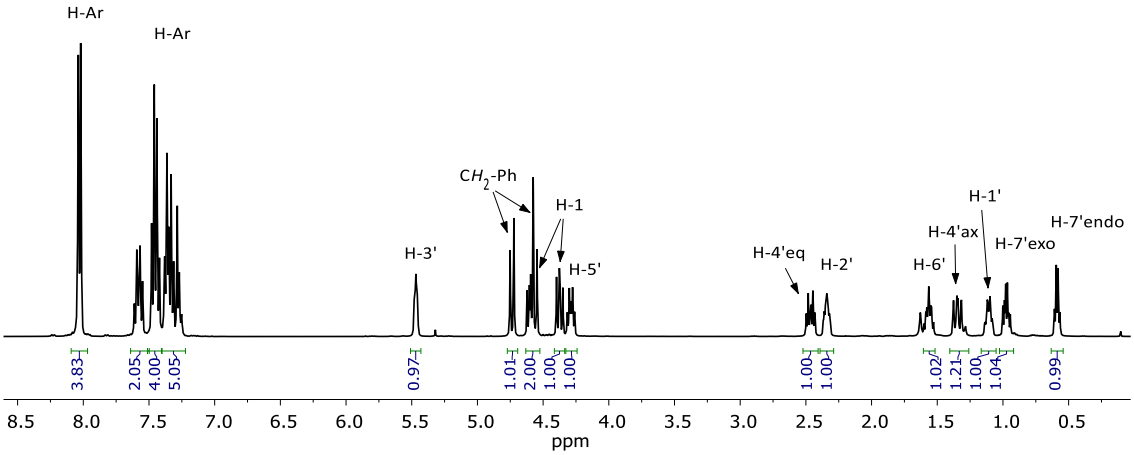

^{1}H-NMR (400 MHz, $CDCl_3$)

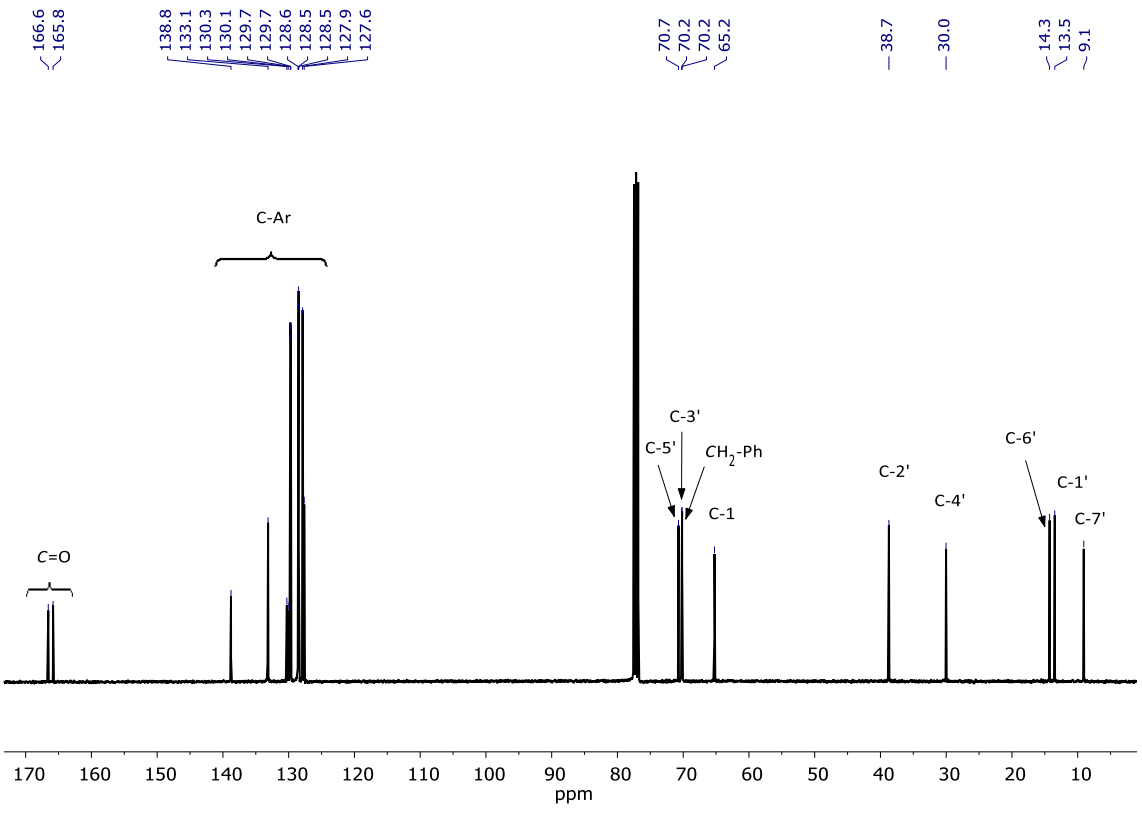

^{13}C-NMR (101 MHz, $CDCl_3$)

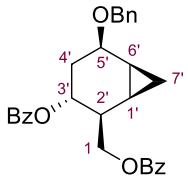

92

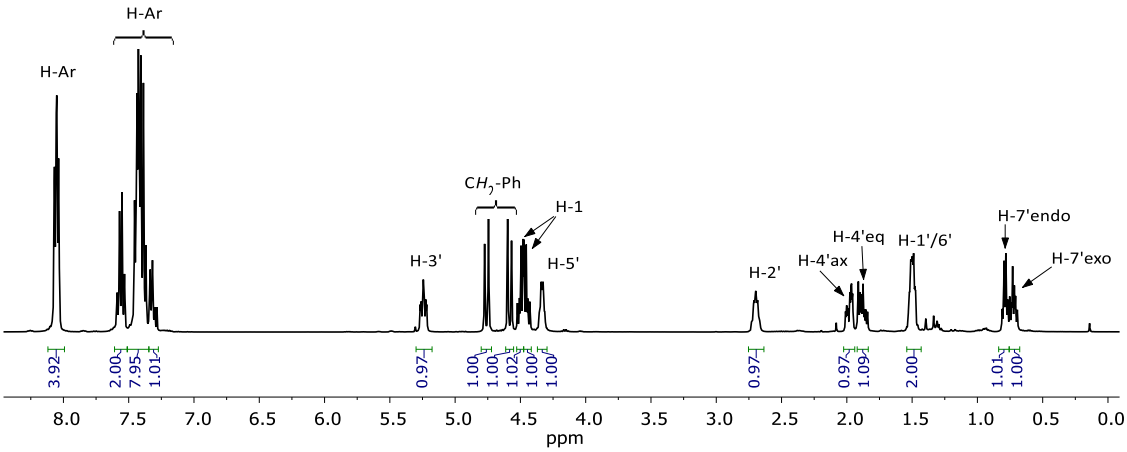

^{1}H-NMR (400 MHz, $CDCl_3$)

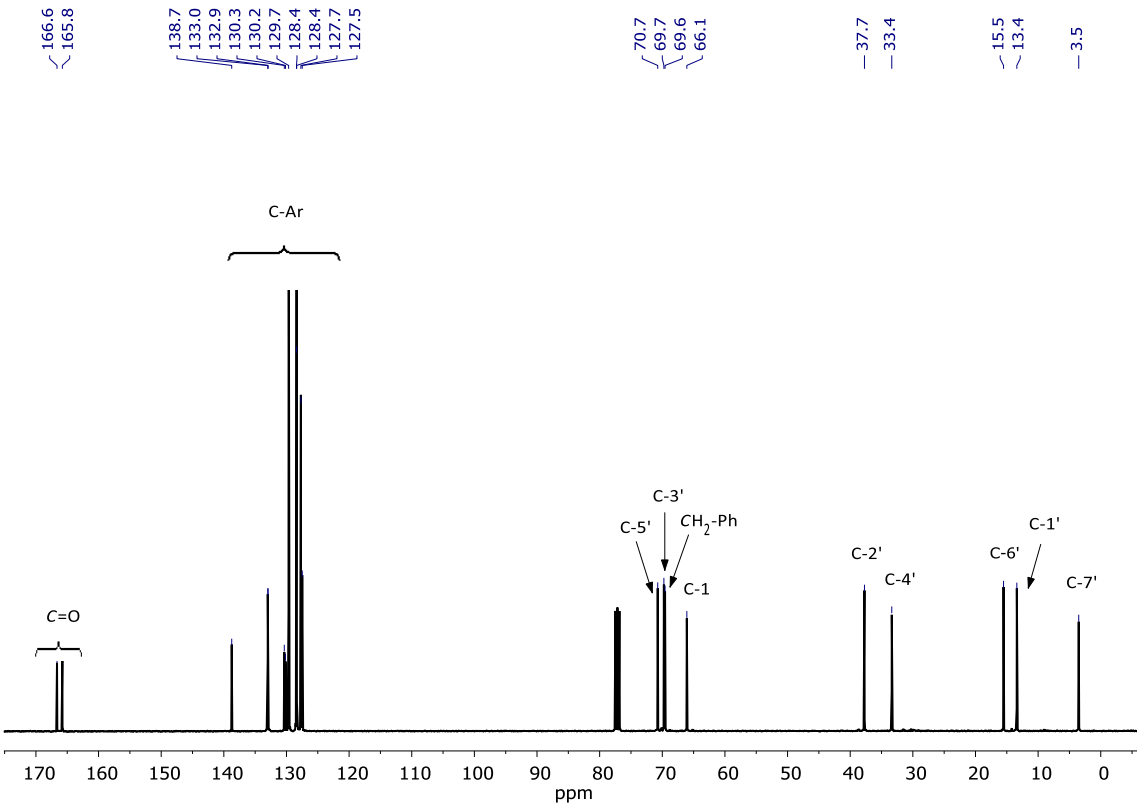

^{13}C-NMR (101 MHz, $CDCl_3$)

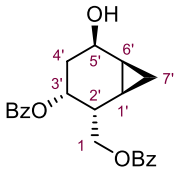

93

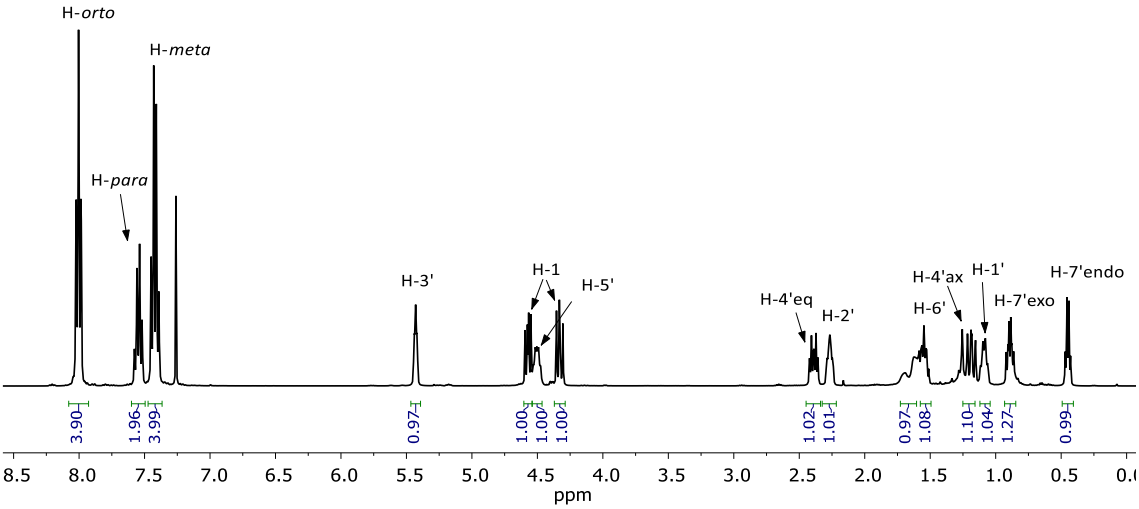

^{1}H-NMR (400 MHz, $CDCl_3$)

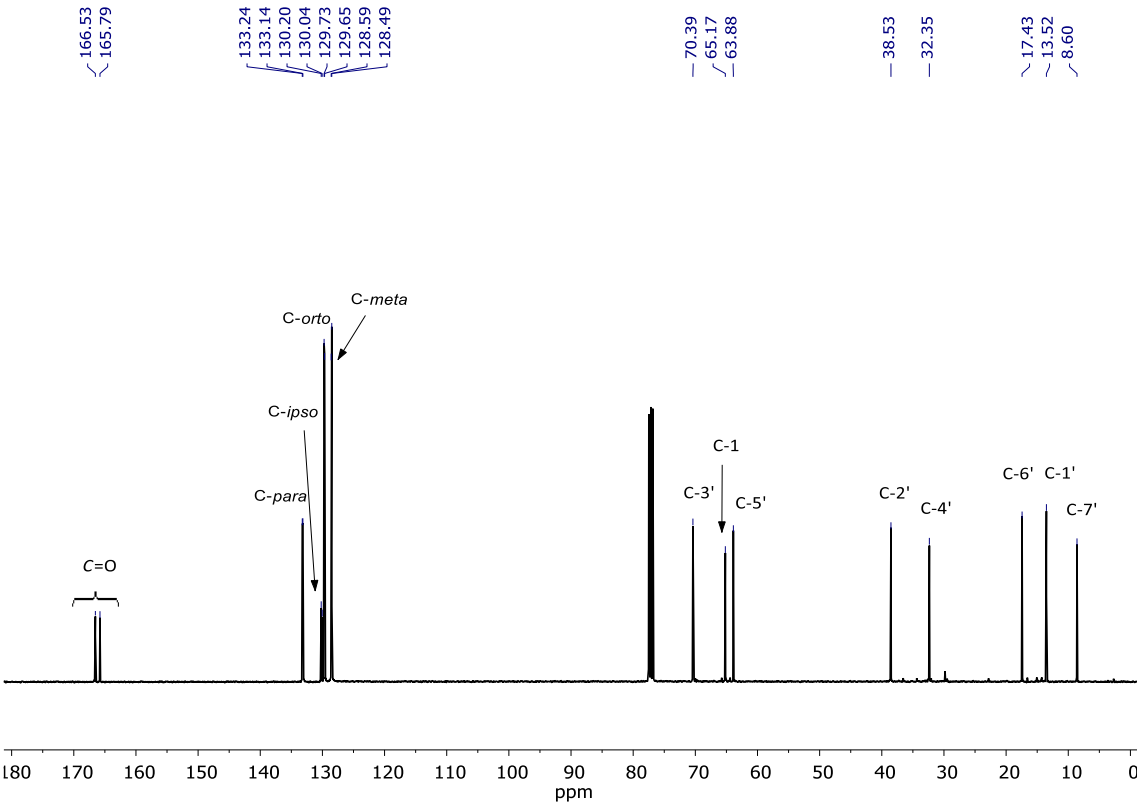

^{13}C-NMR (101 MHz, $CDCl_3$)

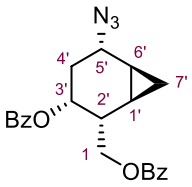

94

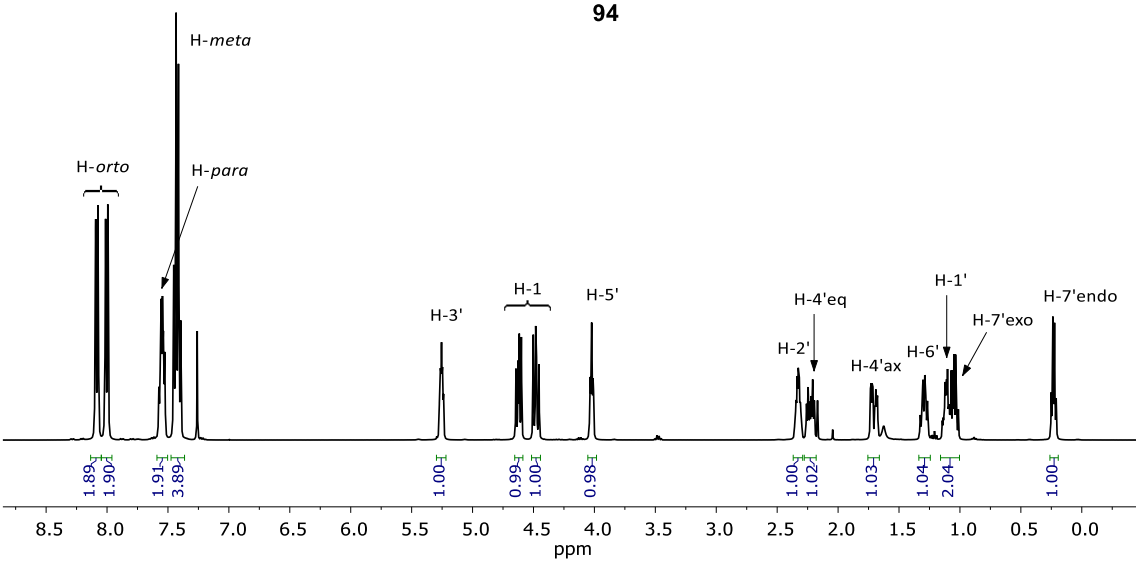

^{1}H-NMR (400 MHz, $CDCl_3$)

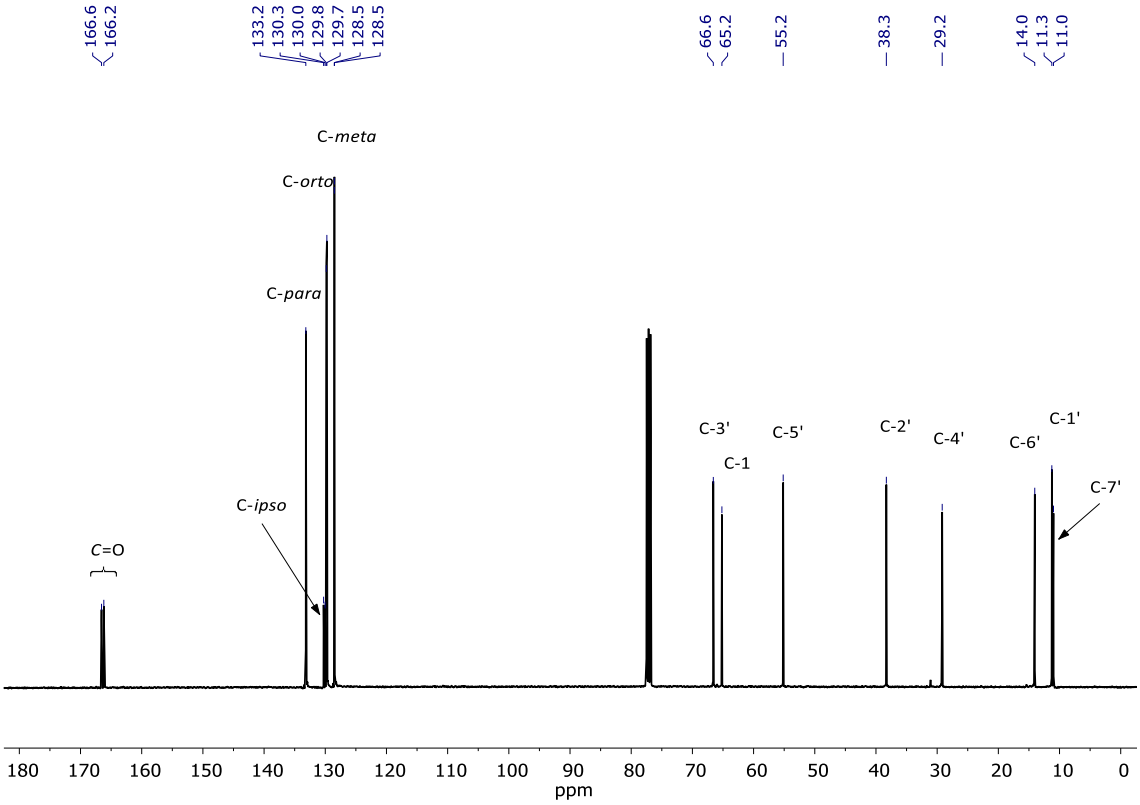

^{13}C-NMR (101 MHz, $CDCl_3$)

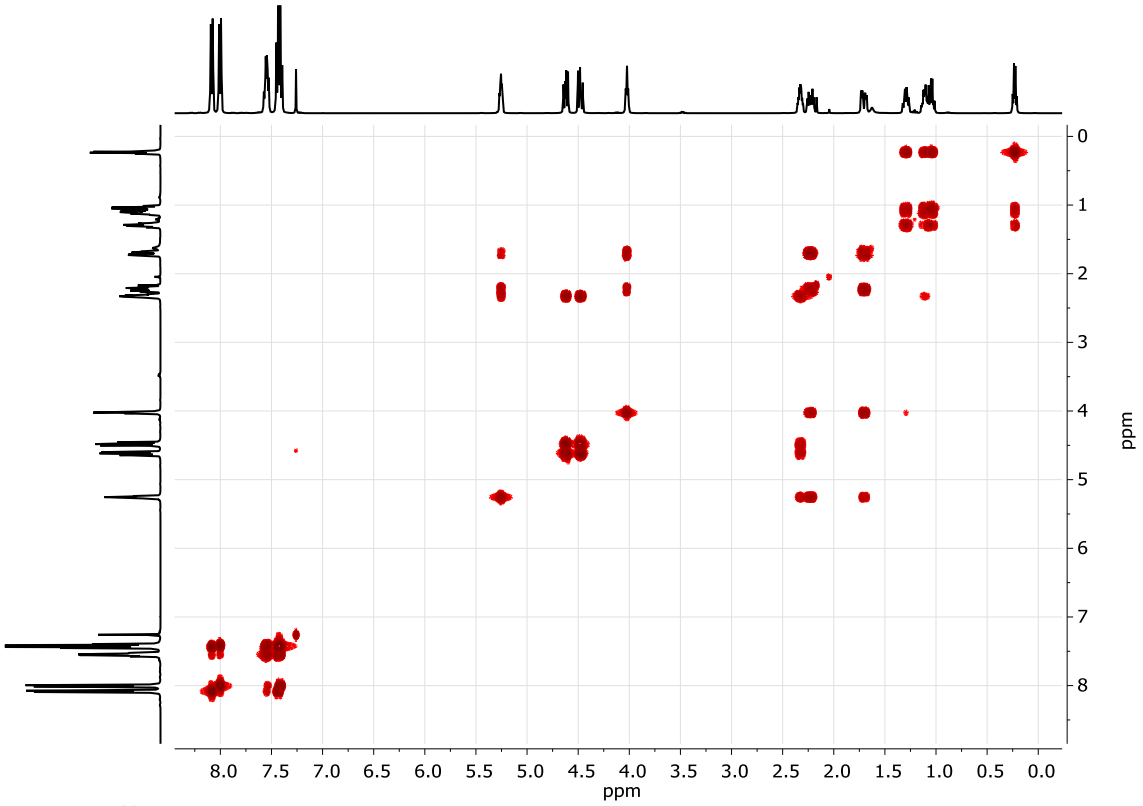

COSY (400 MHz, $CDCl_3$)

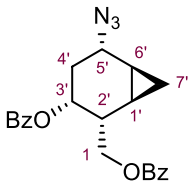

94

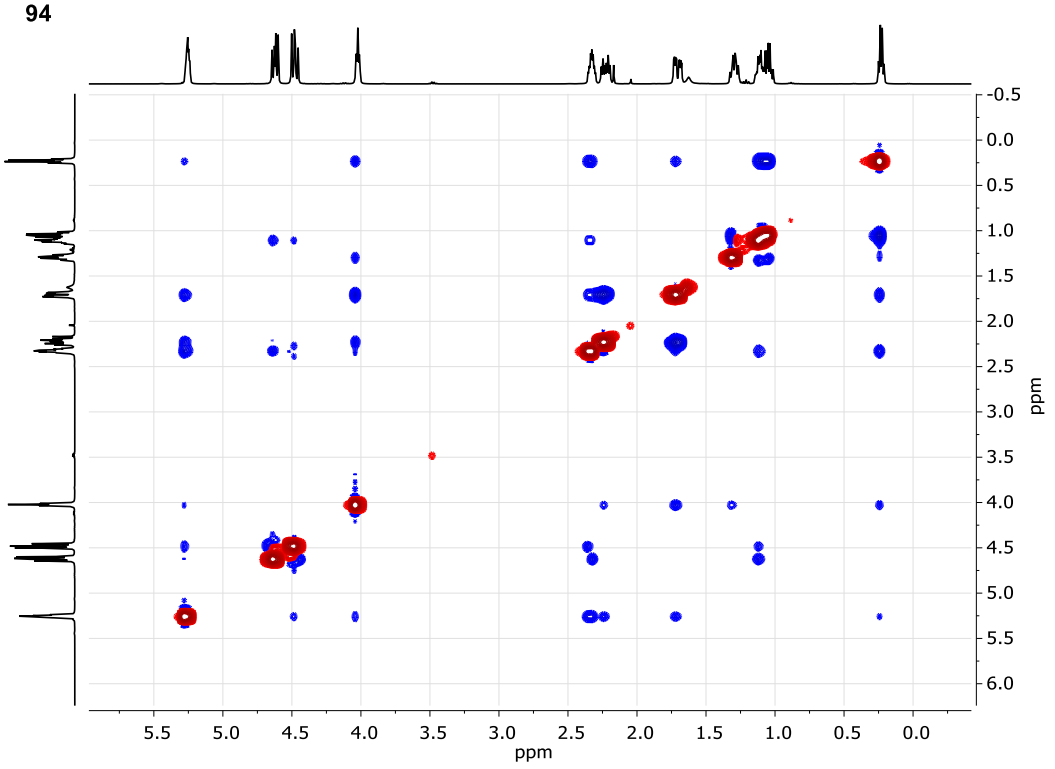

NOESY (400 MHz, $CDCl_3$)

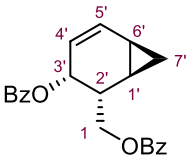

95

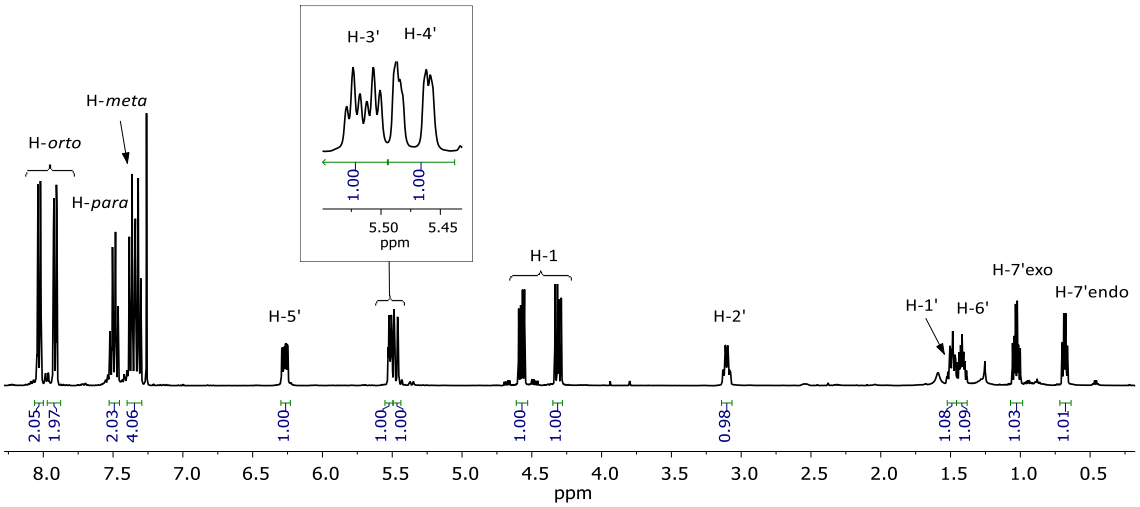

^{1}H-NMR (400 MHz, $CDCl_3$)

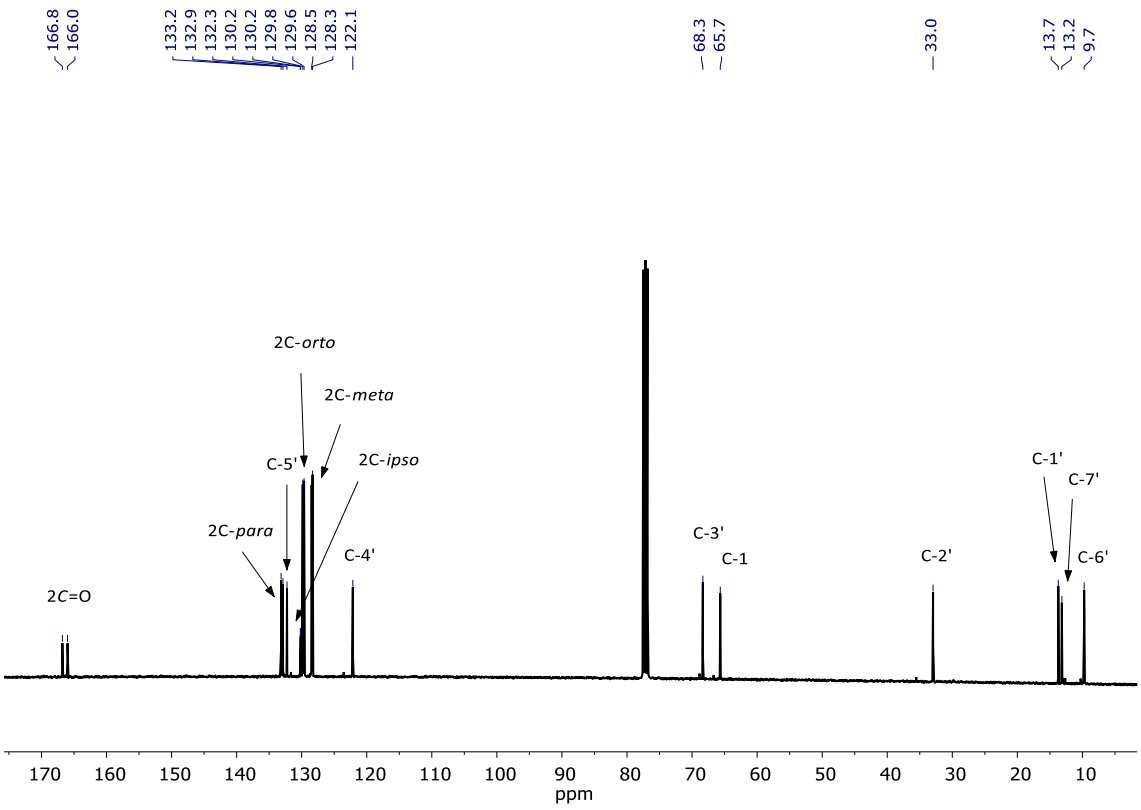

^{13}C-NMR (101 MHz, $CDCl_3$)

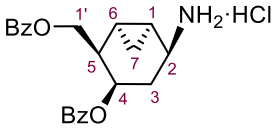

96

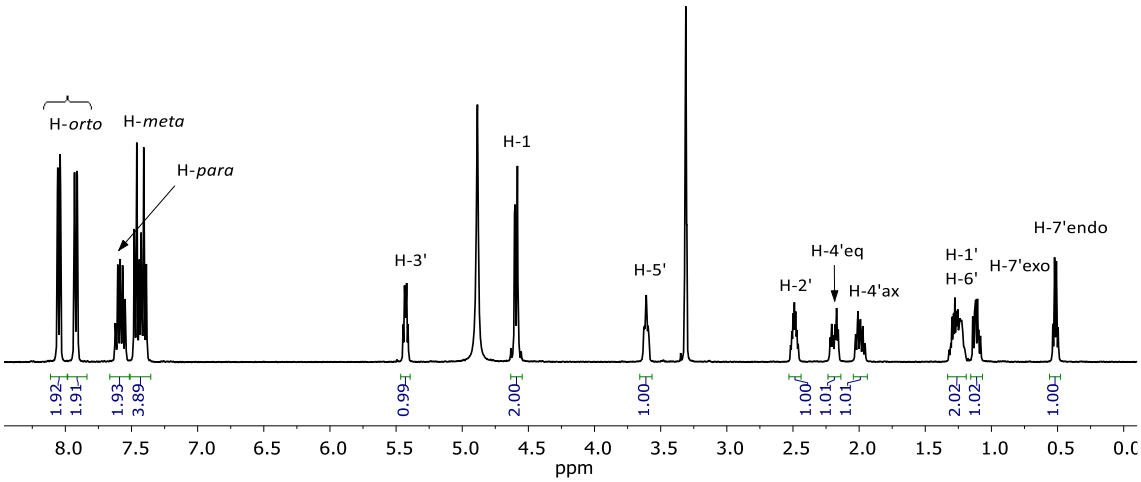

^{1}H-NMR (400 MHz, MeOH-d_4)

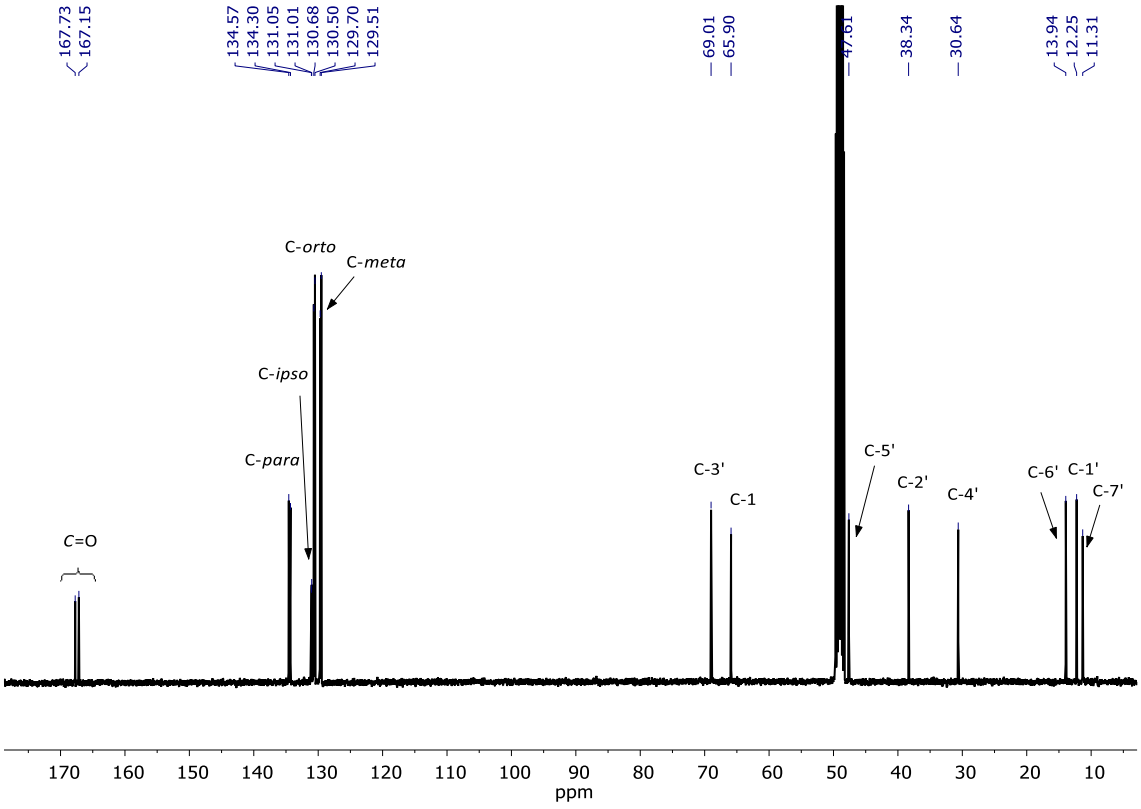

^{13}C-NMR (101 MHz, MeOH-d_4)

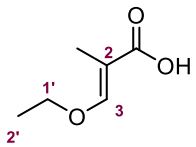

101

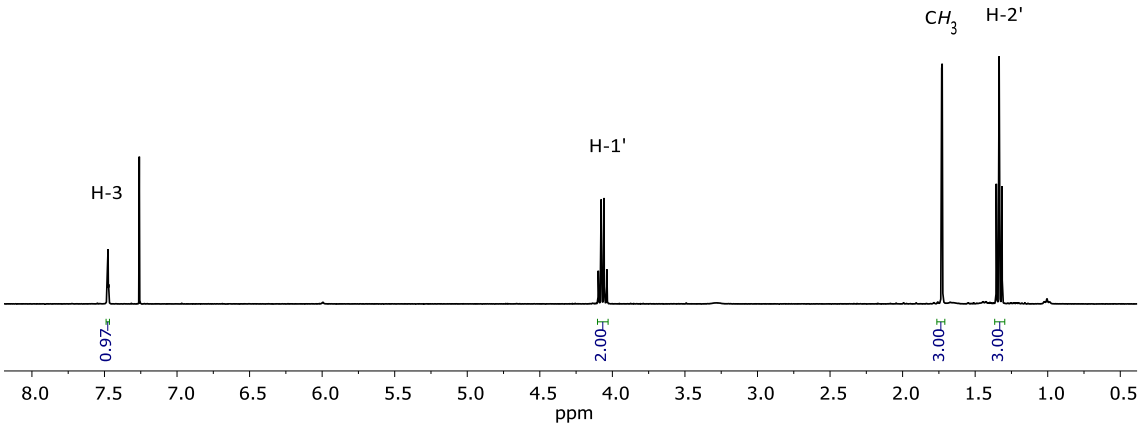

^{1}H-NMR (360 MHz, $CDCl_3$)

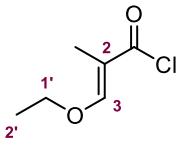

99

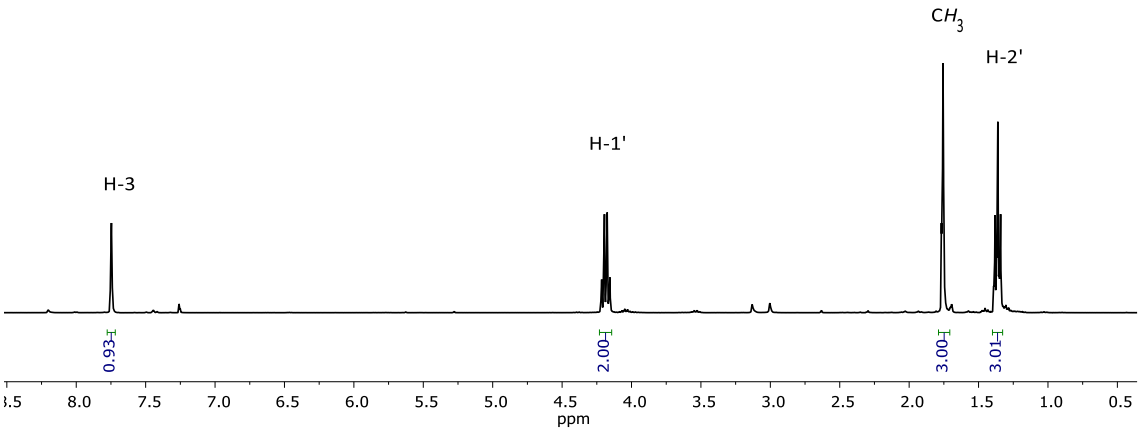

^{1}H-NMR (360 MHz, $CDCl_3$)

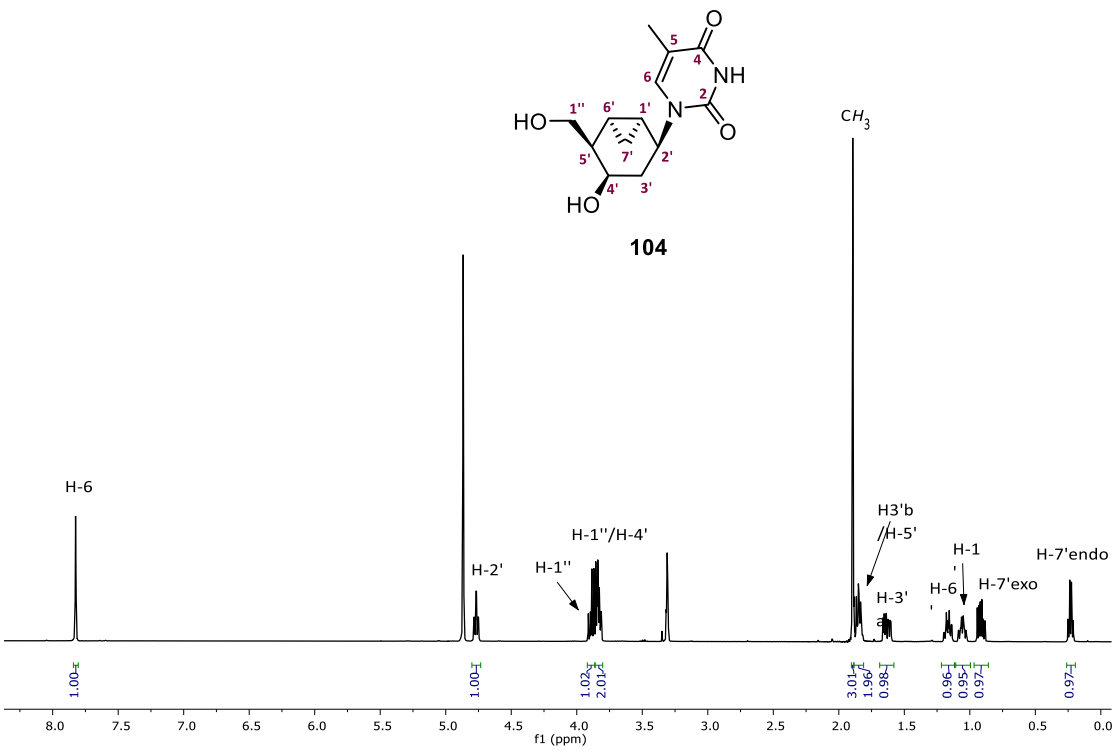

^{1}H-NMR (400 MHz, MeOH-d_4)

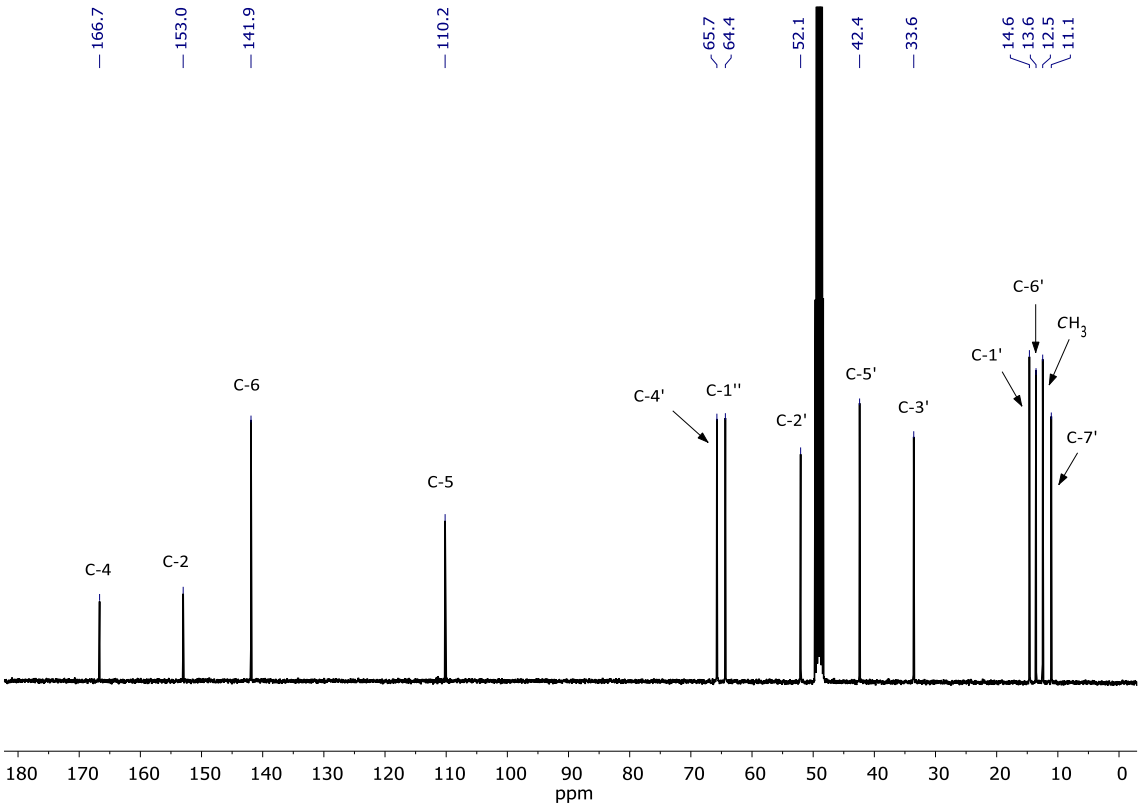

^{13}C-NMR (101 MHz MeOH-d_4)

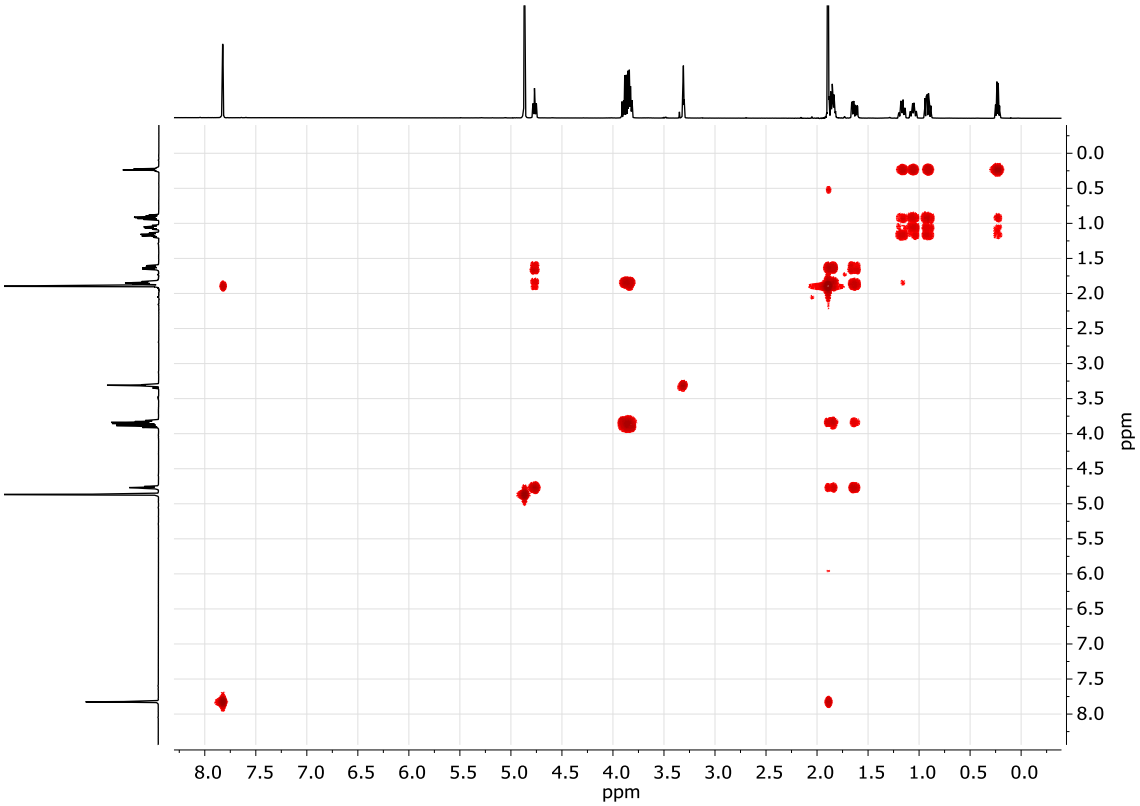

COSY (400 MHz MeOH-d_4)

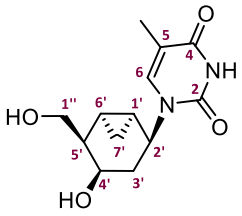

104

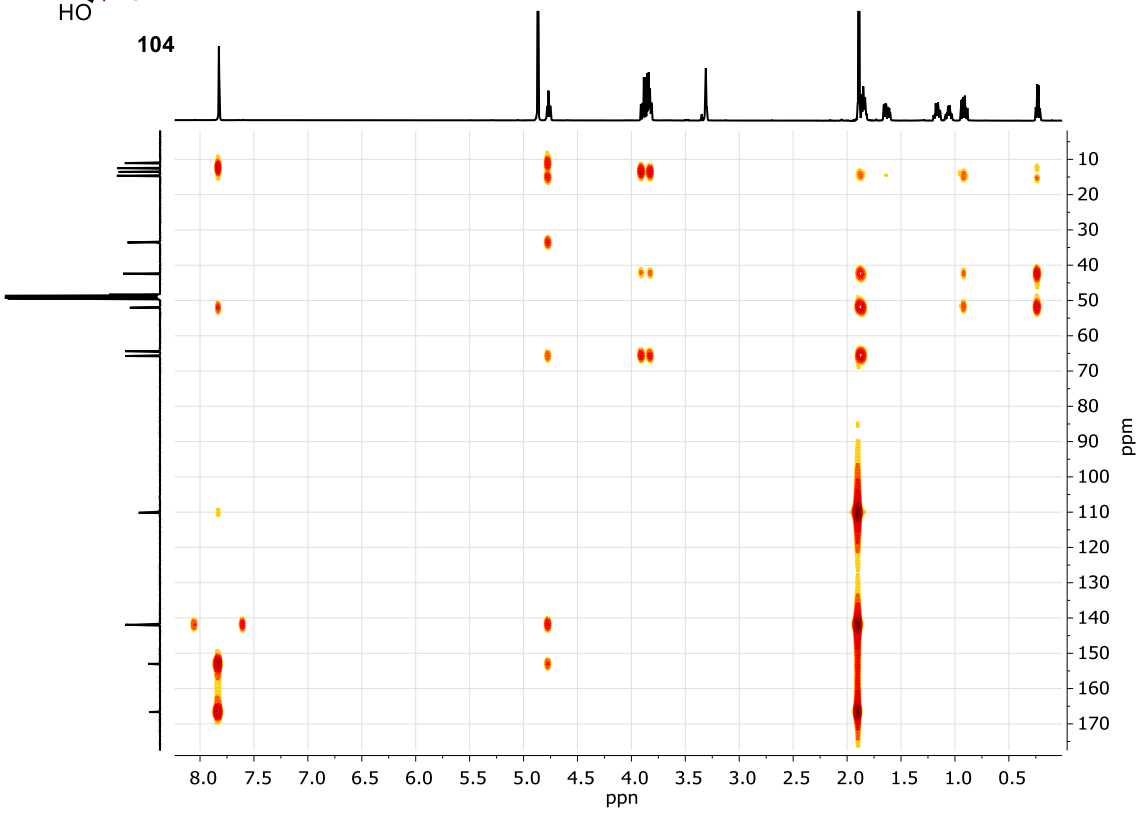

HMBC (400 MHz, MeOH-d_4)

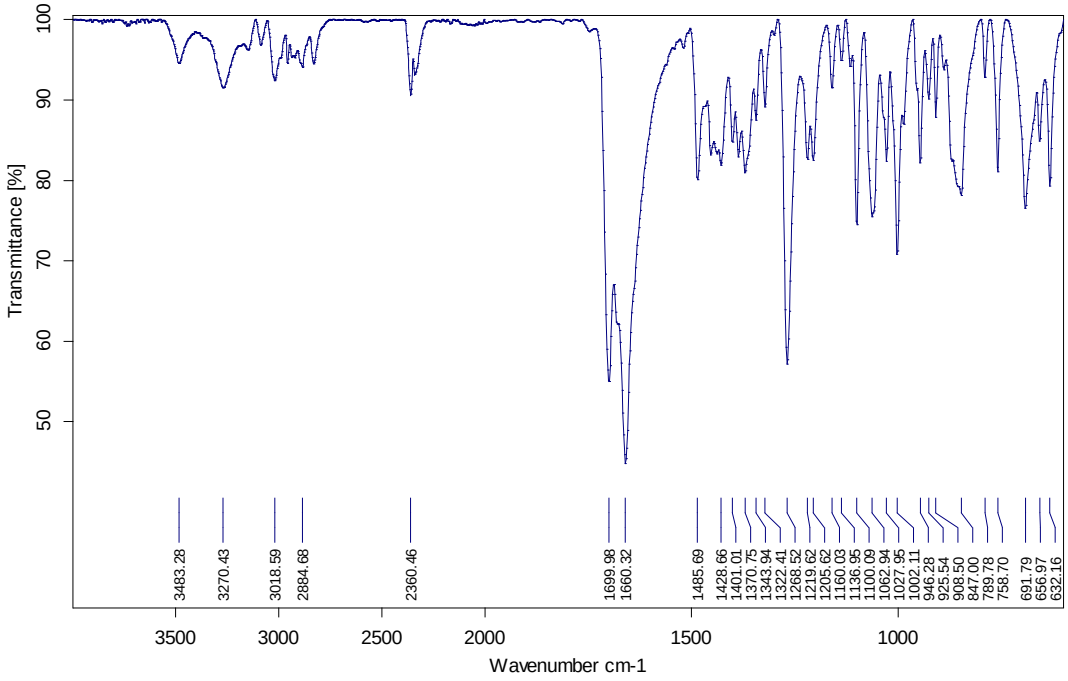

IR (ATR)

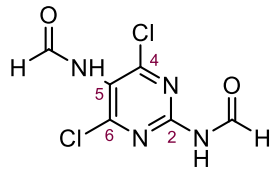

106

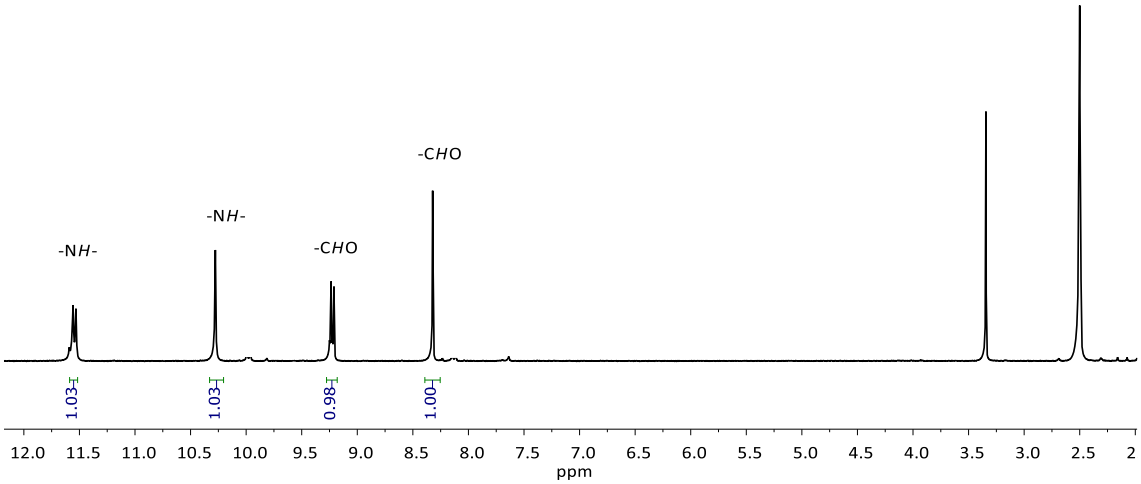

^{1}H-NMR (360 MHz, DMSO-d_6)

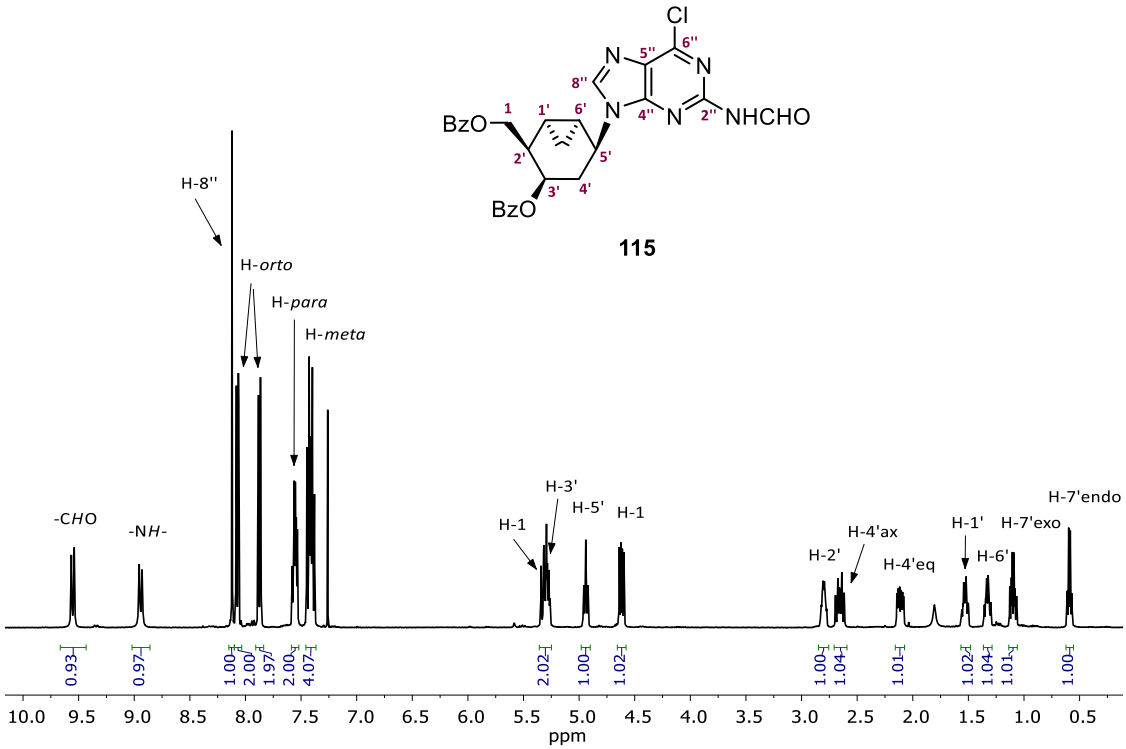

^{1}H-NMR (400 MHz, $CDCl_3$)

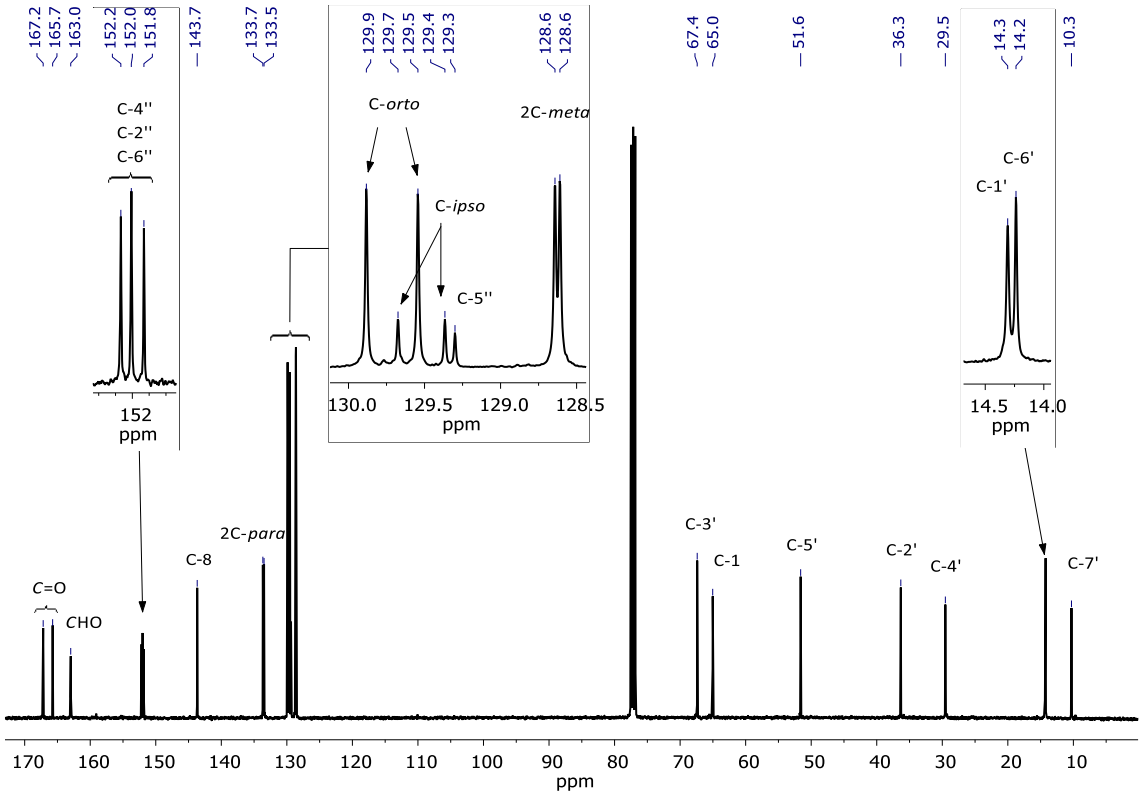

^{13}C-NMR (101 MHz, $CDCl_3$)

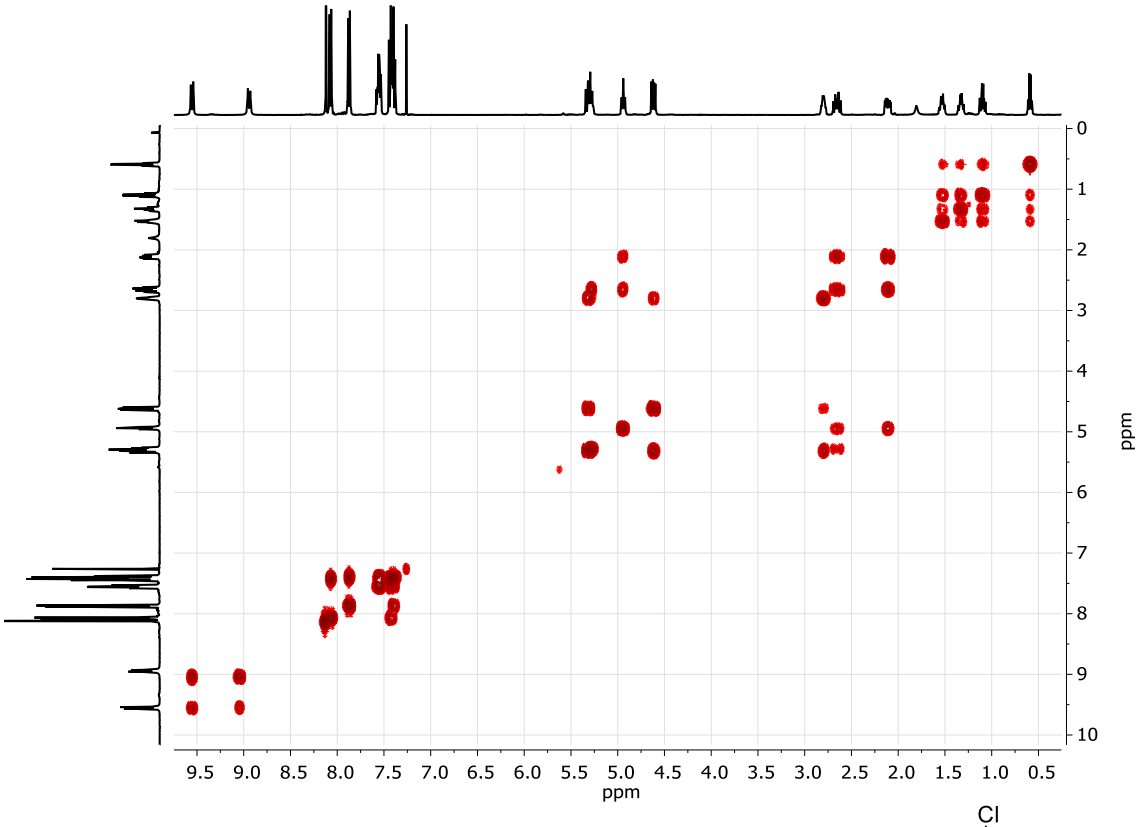

COSY (400 MHz, $CDCl_3$)

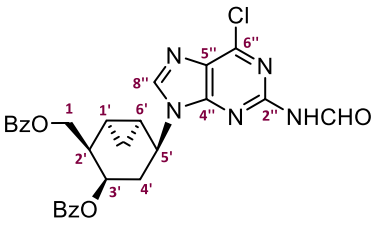

115

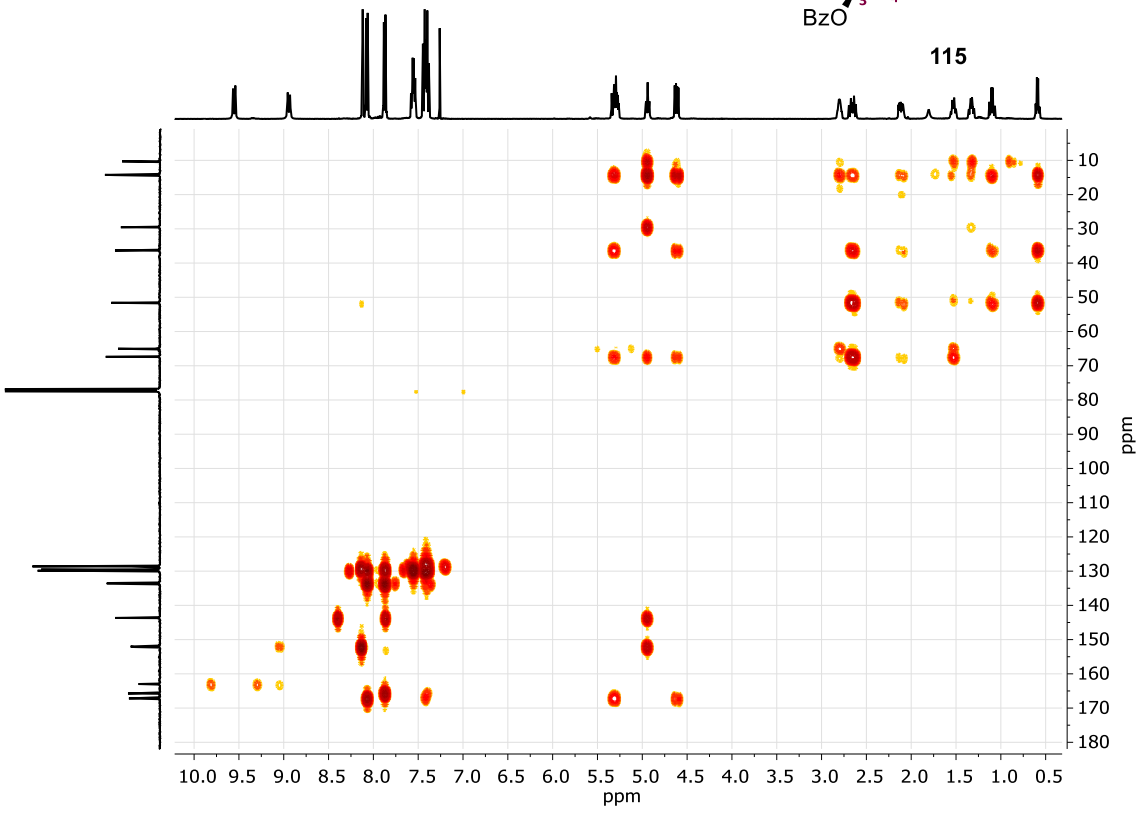

HMBC (400 MHz, $CDCl_3$)

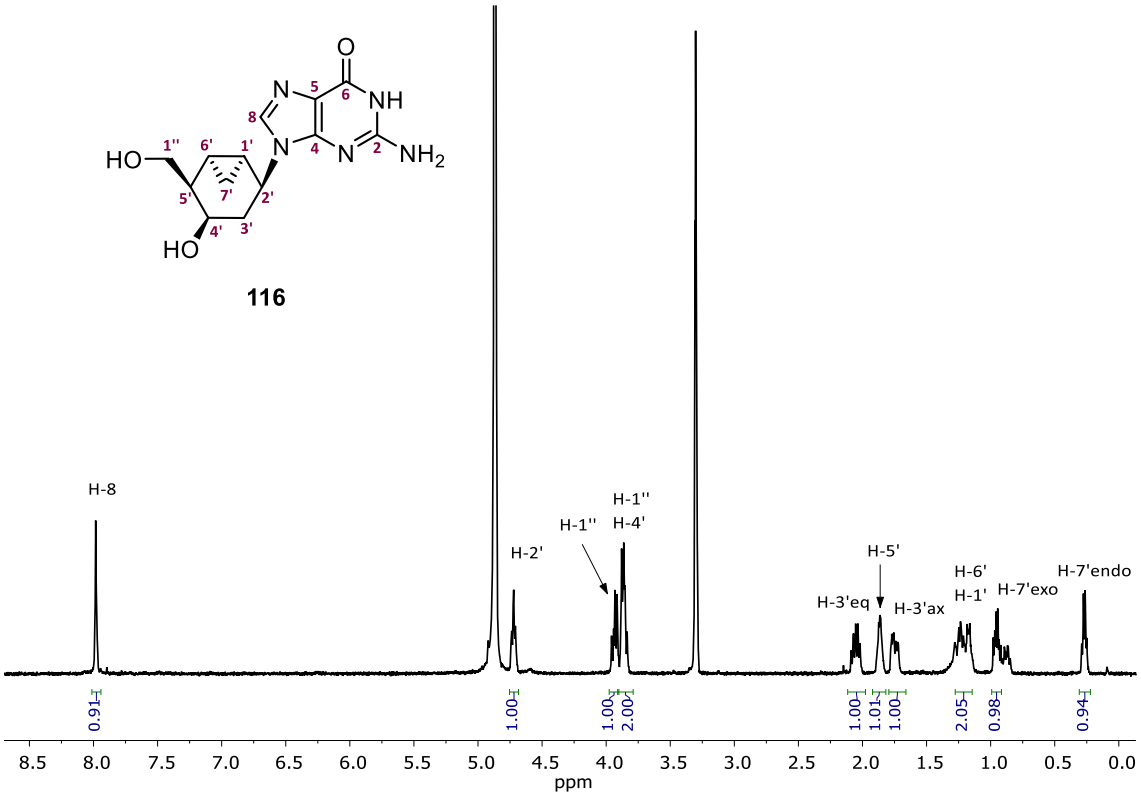

116

^{1}H-NMR (400 MHz, MeOH-d_4)

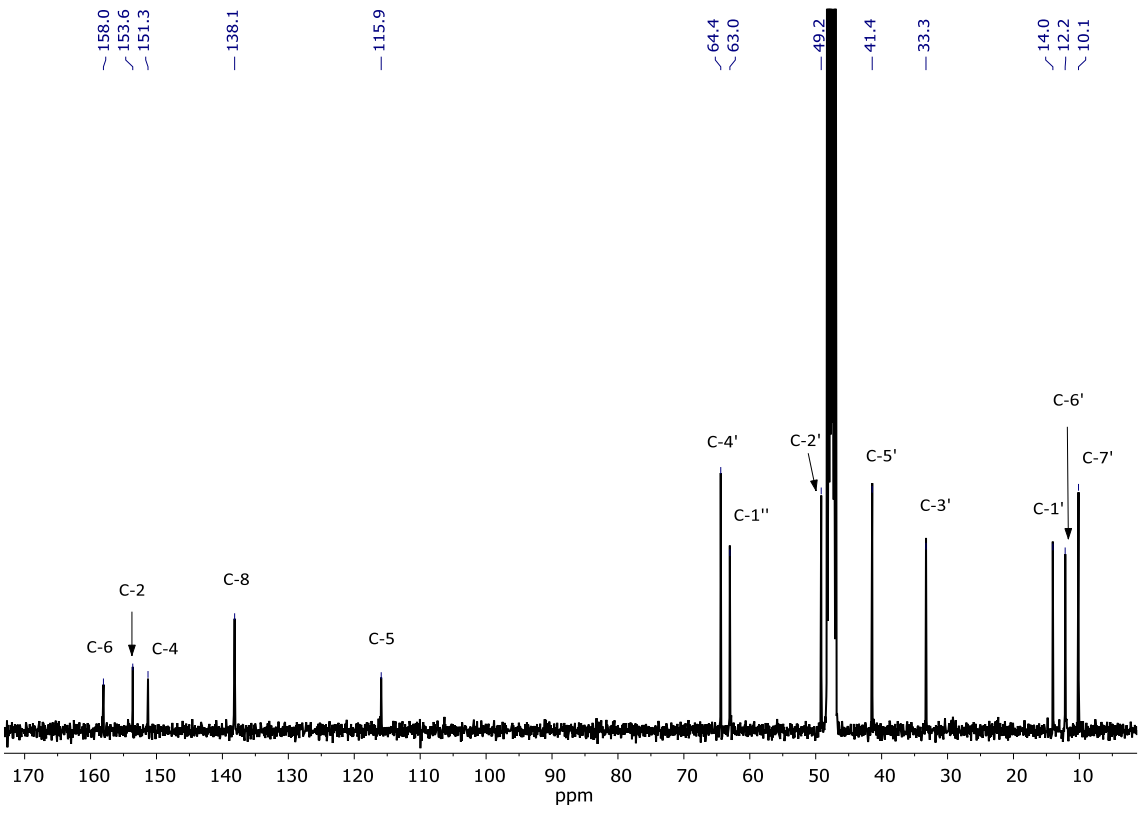

^{13}C-NMR (101 MHz, MeOH-d_4)

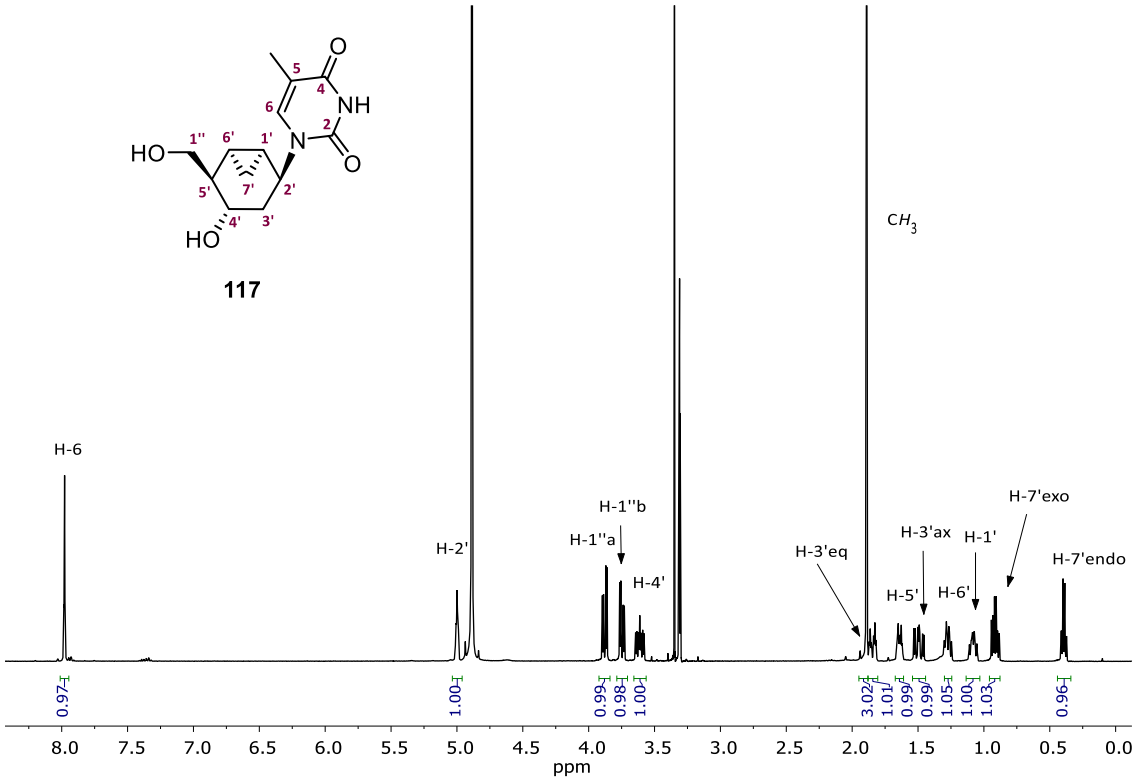

^{1}H-NMR (400 MHz, MeOH-d_4)

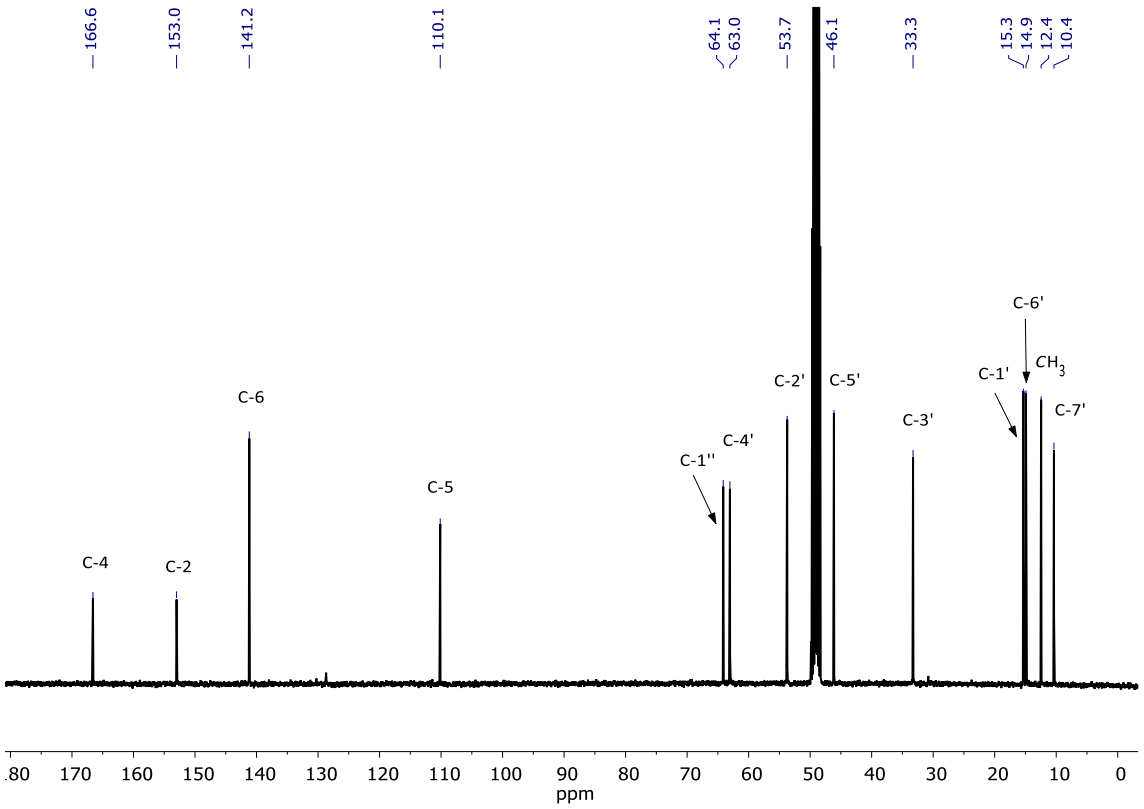

^{13}C-NMR (101 MHz, MeOH-d_4)

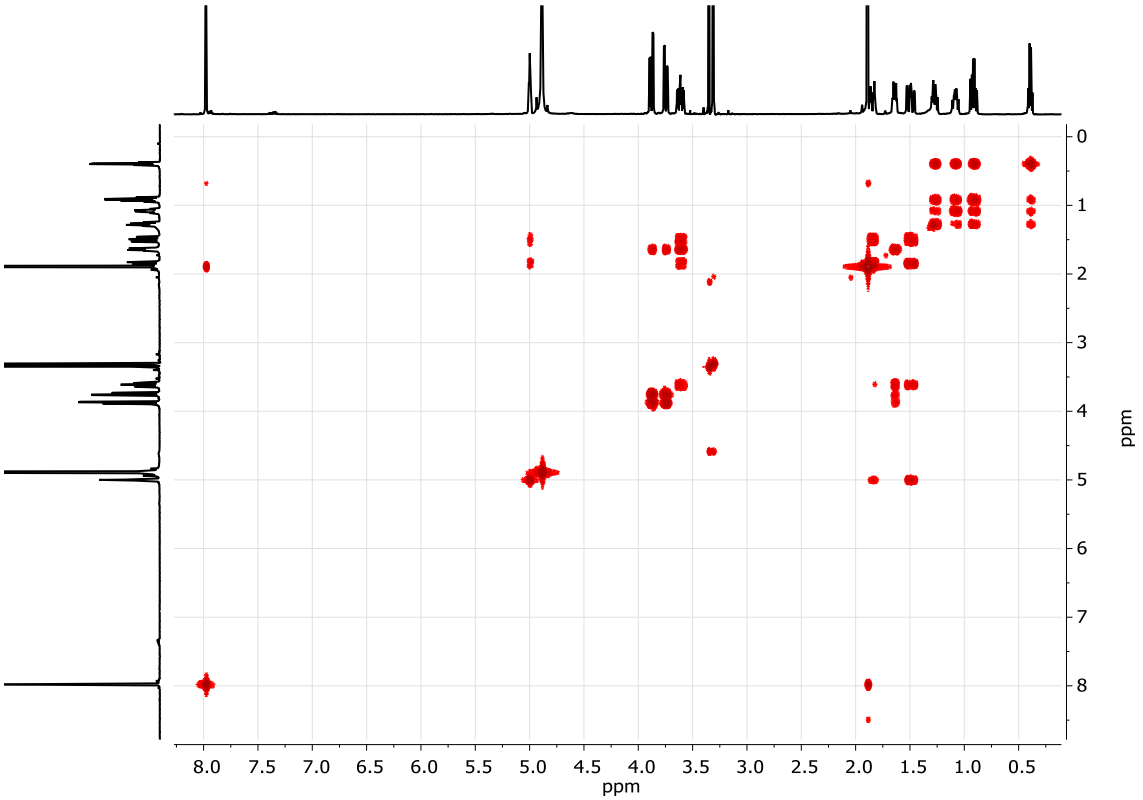

COSY (400 MHz, MeOH-d_4)

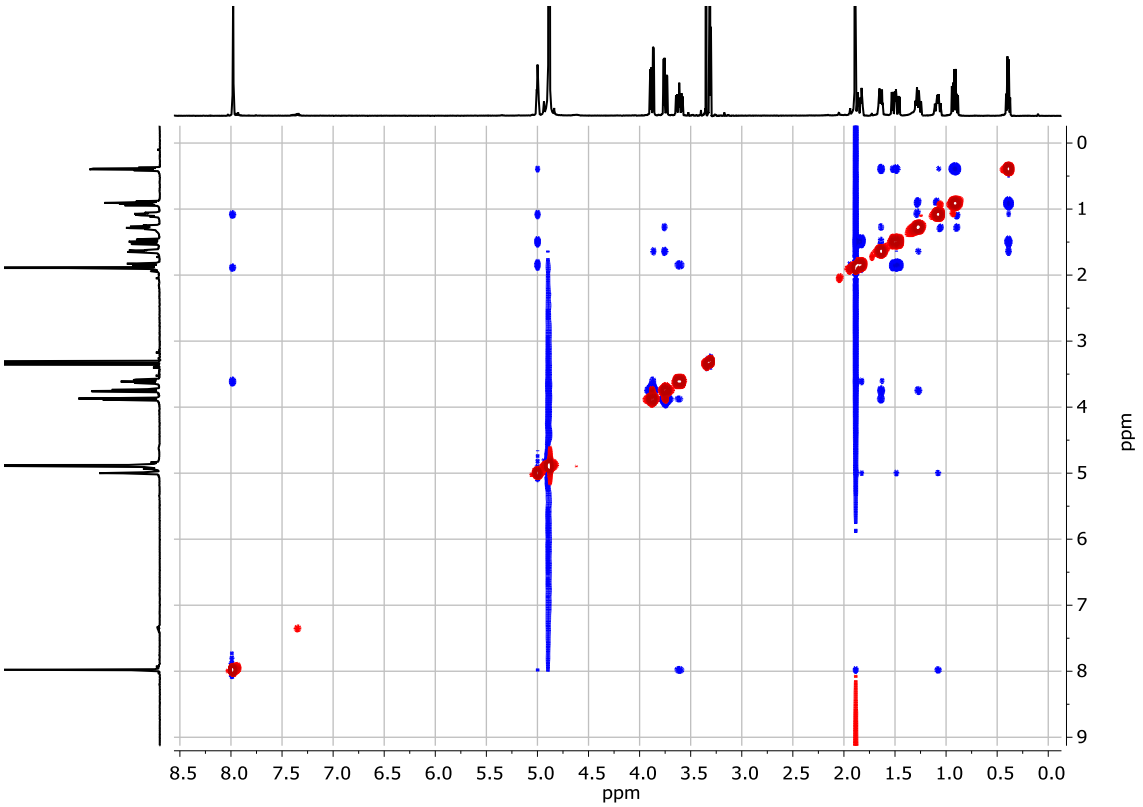

NOESY (400 MHz, MeOH-d_4)

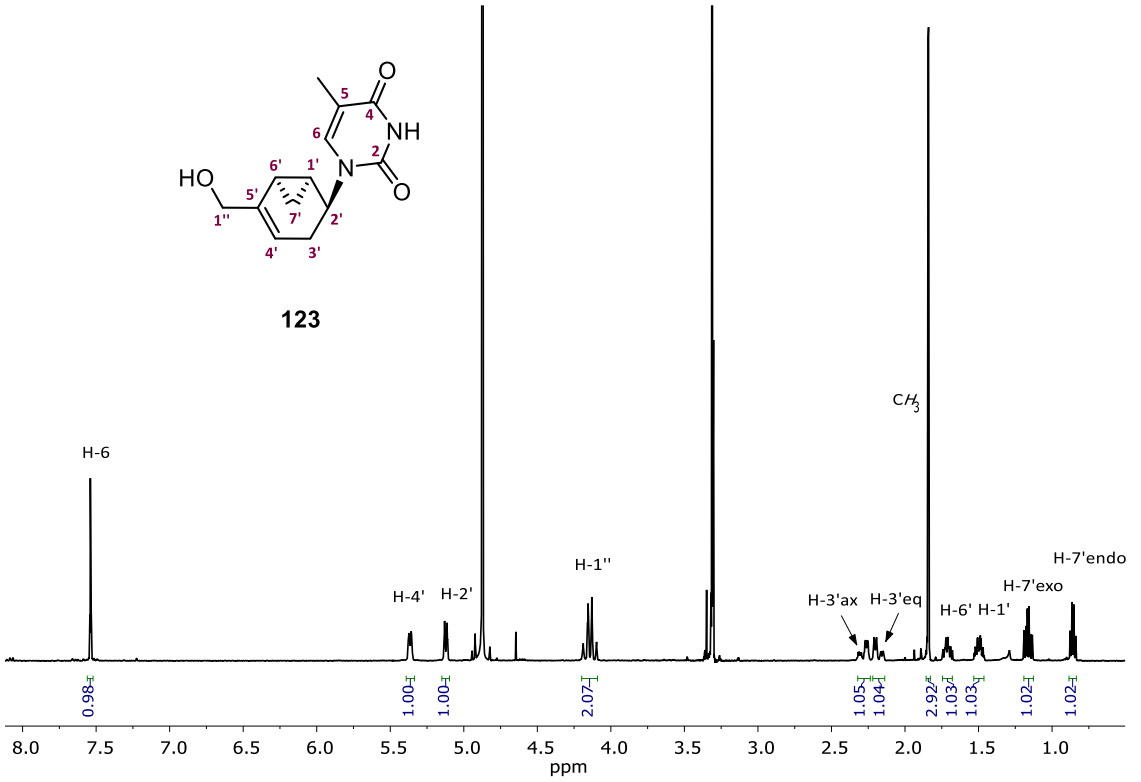

^{1}H-NMR (400 MHz, MeOH-d_4)

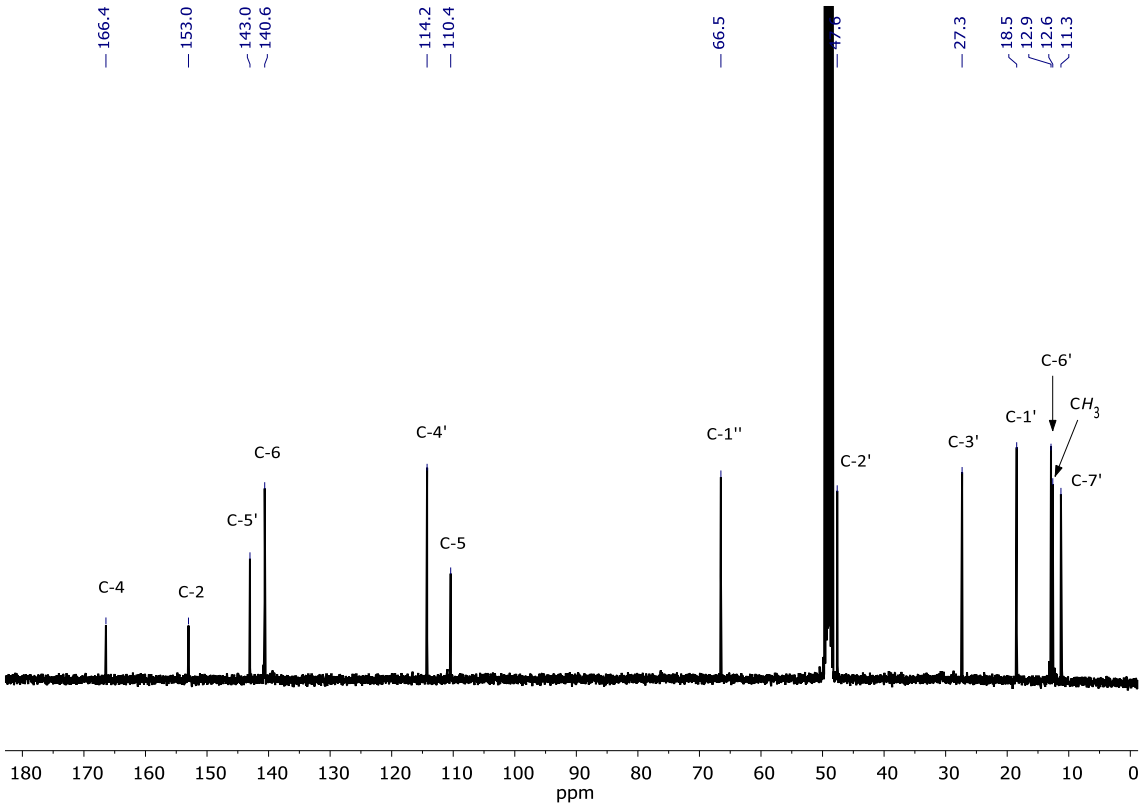

^{13}C-NMR (101 MHz, MeOH-d_4)

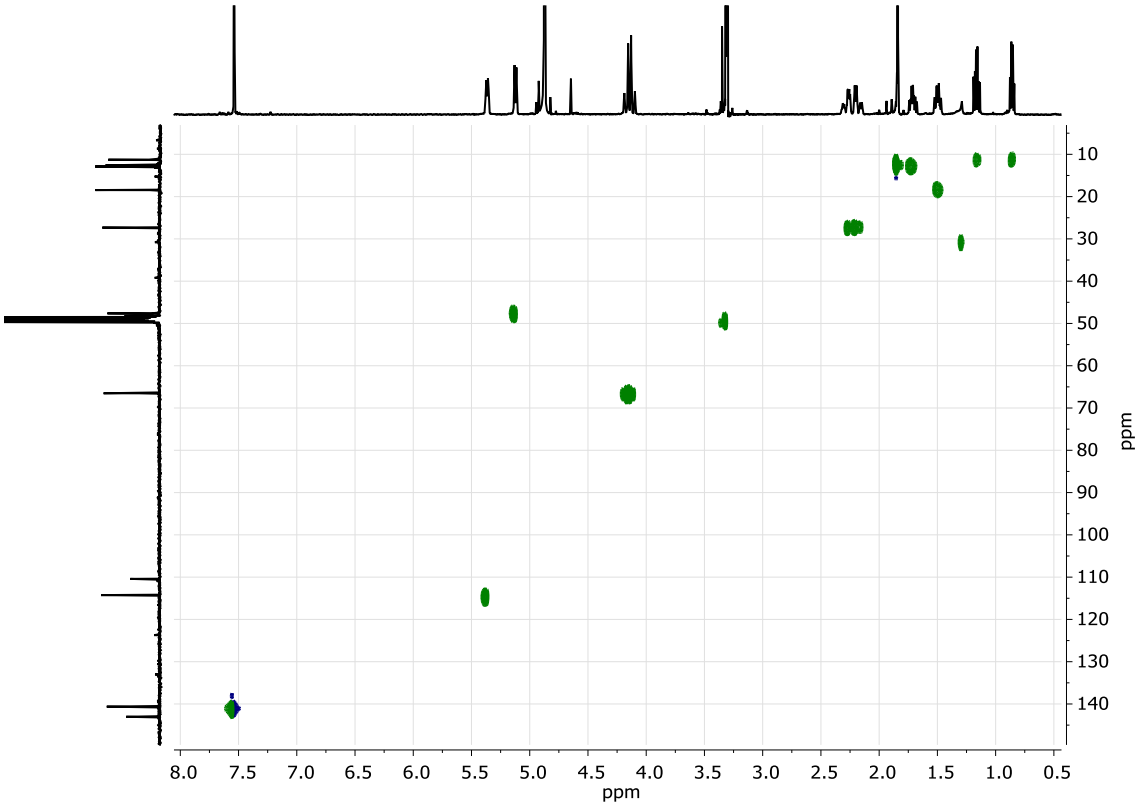

HSQC (400 MHz, MeOH-d_4)

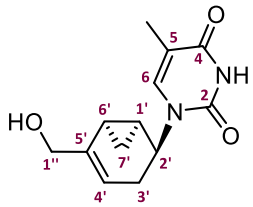

123

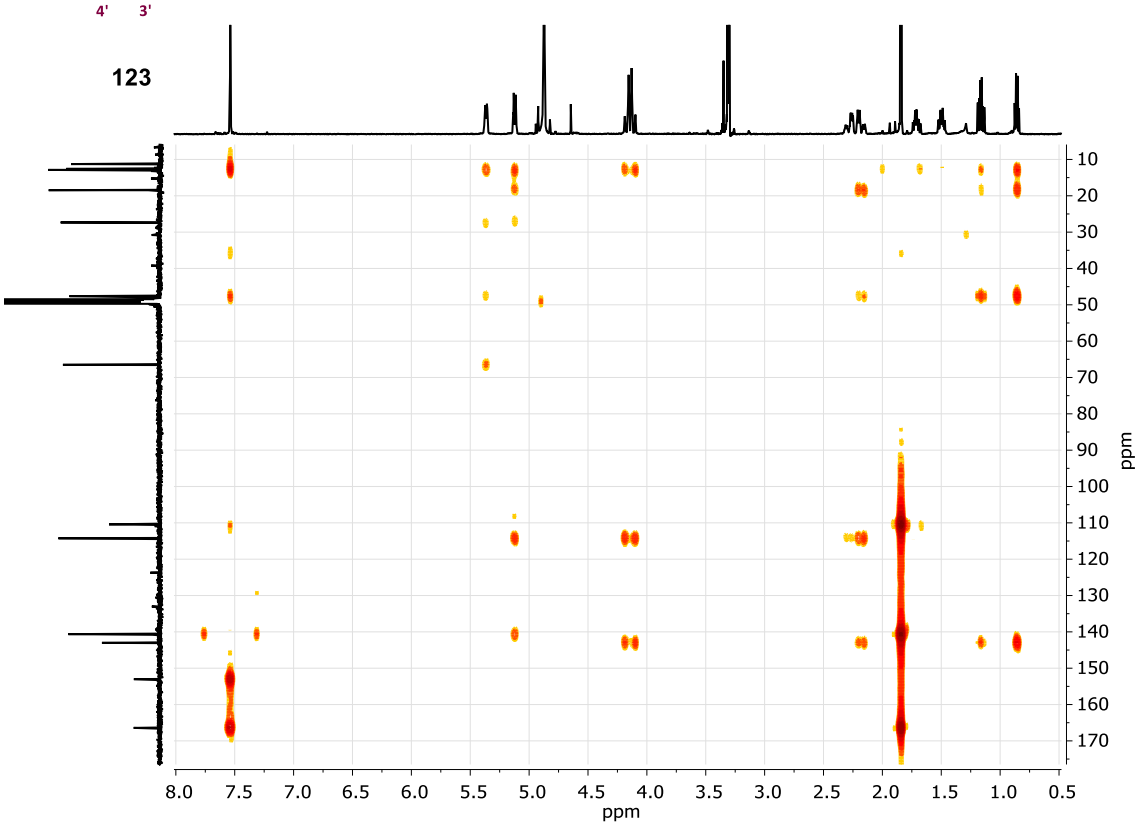

HMBC (400 MHz, MeOH-d_4)

4. CHAPTER IV. Synthesis of new substituted 1,2,3-triazolo-CNAs.

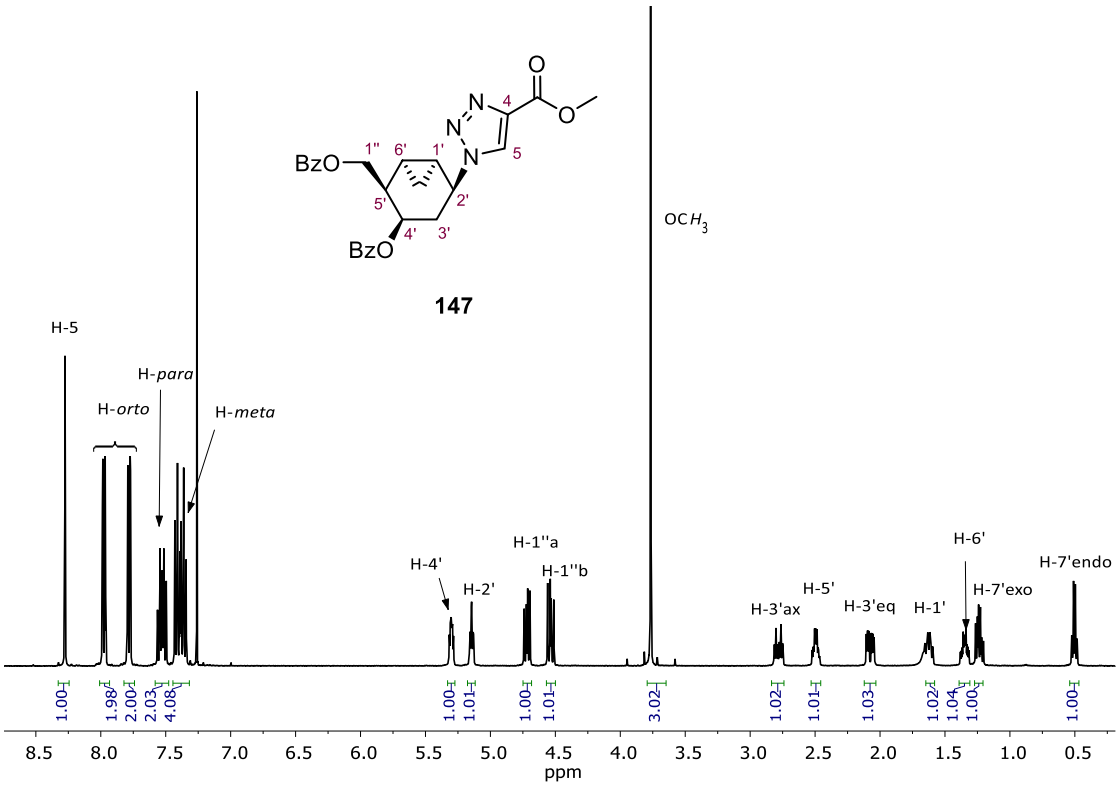

^{1}H-NMR (400 MHz, $CDCl_3$)

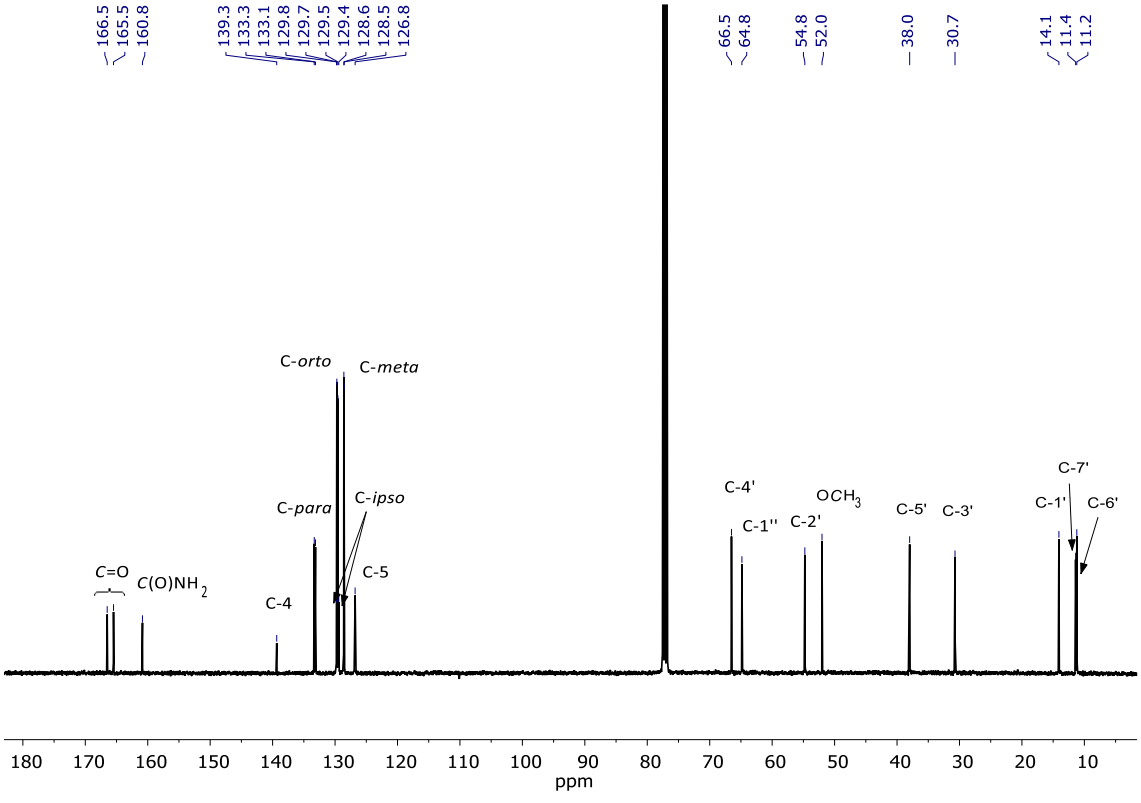

^{13}C-NMR (101 MHz, $CDCl_3$)

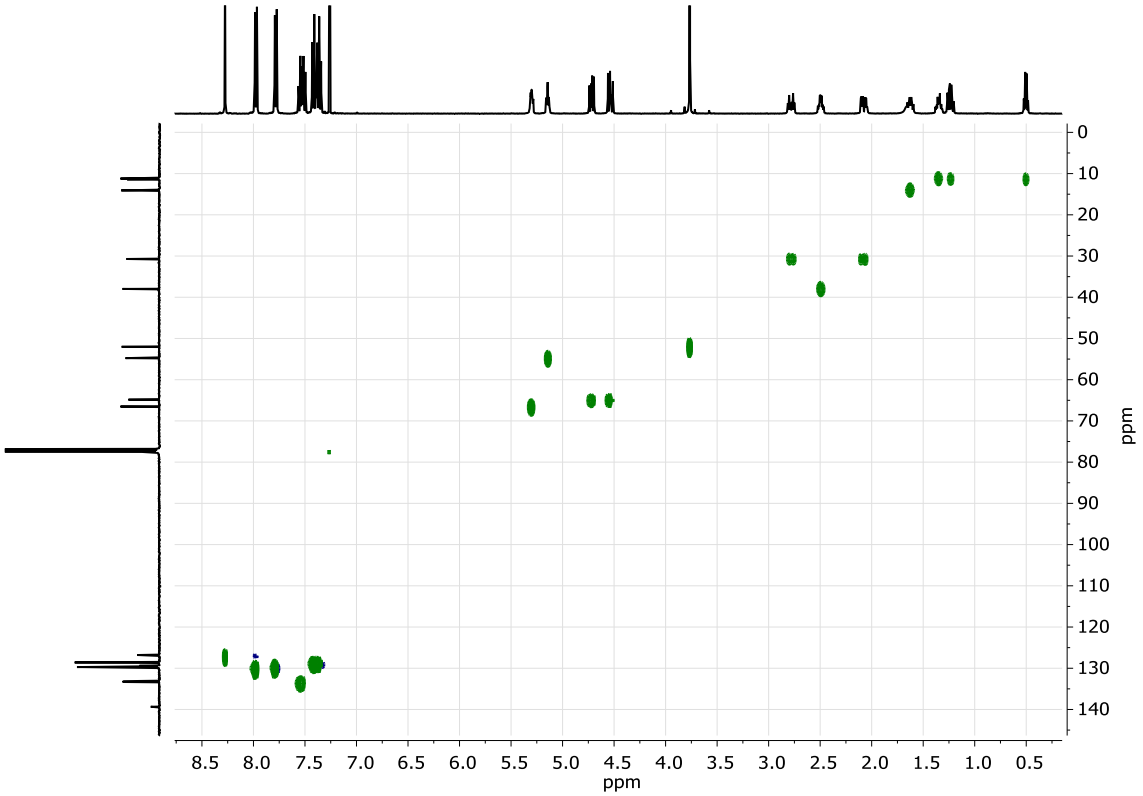

HSQC (400 MHz, $CDCl_3$)

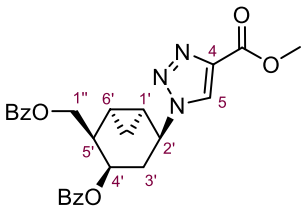

147

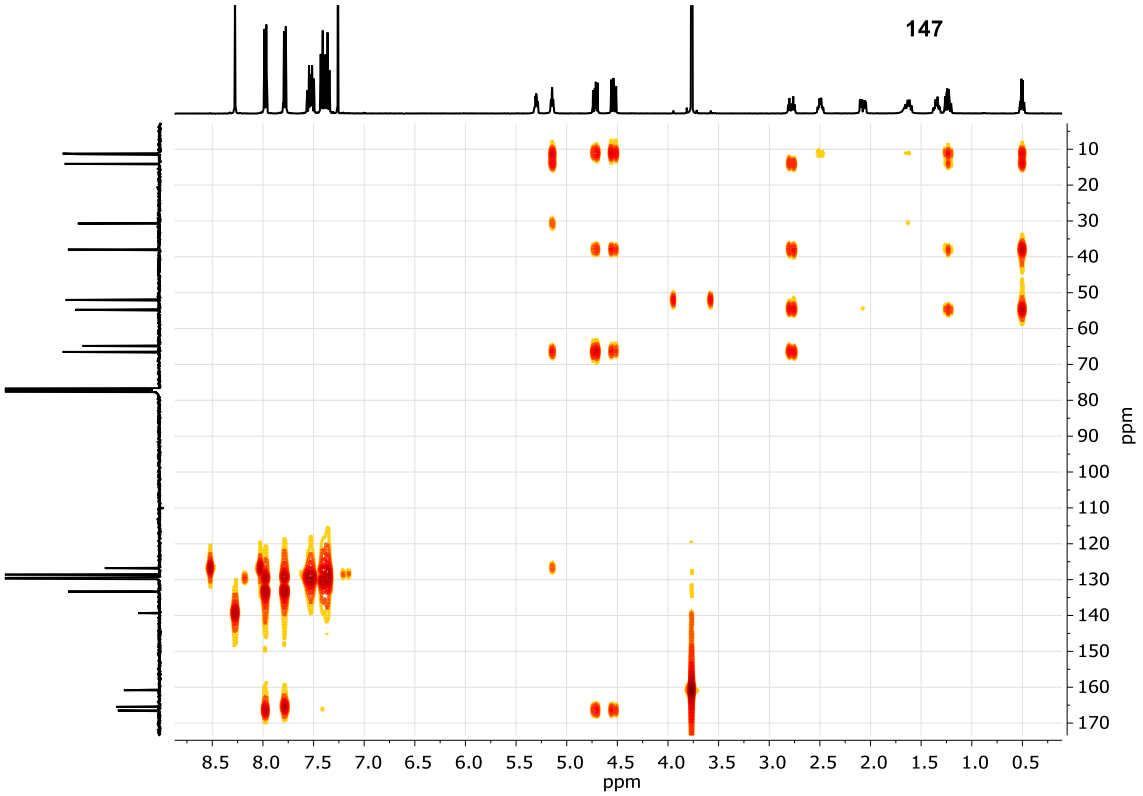

HMBC (400 MHz, $CDCl_3$)

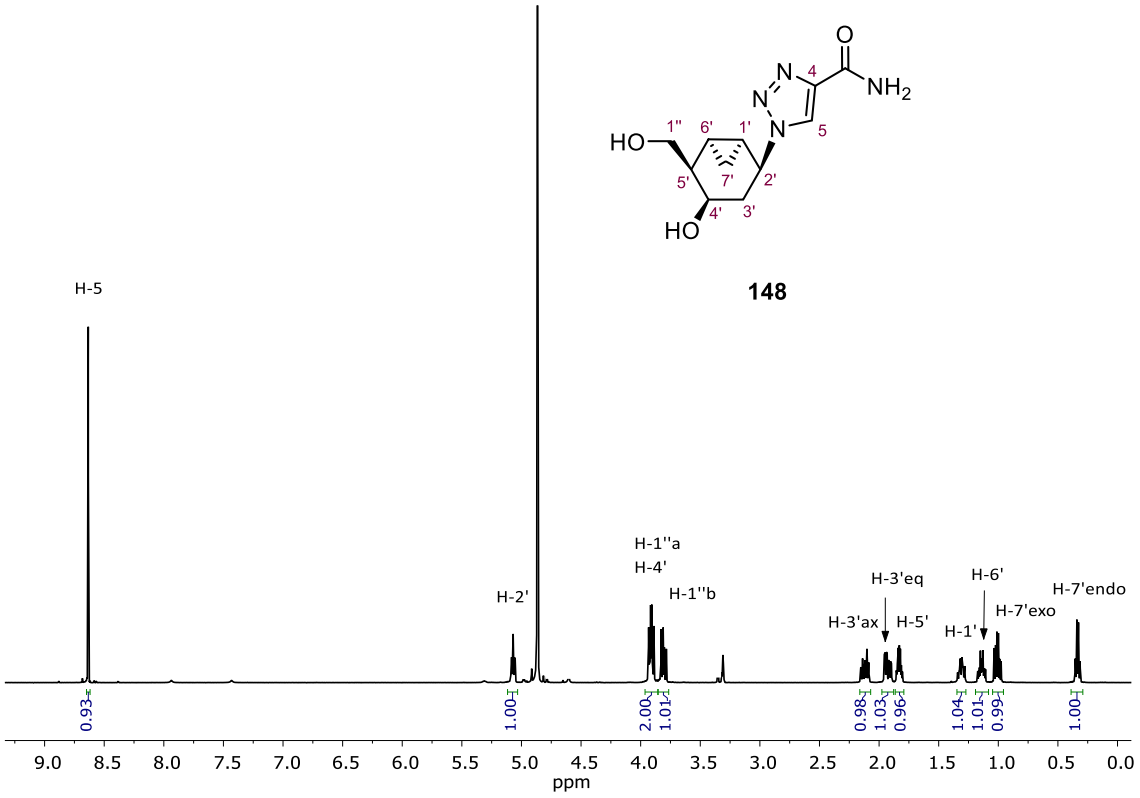

^{1}H-NMR (400 MHz, MeOH-d_4)

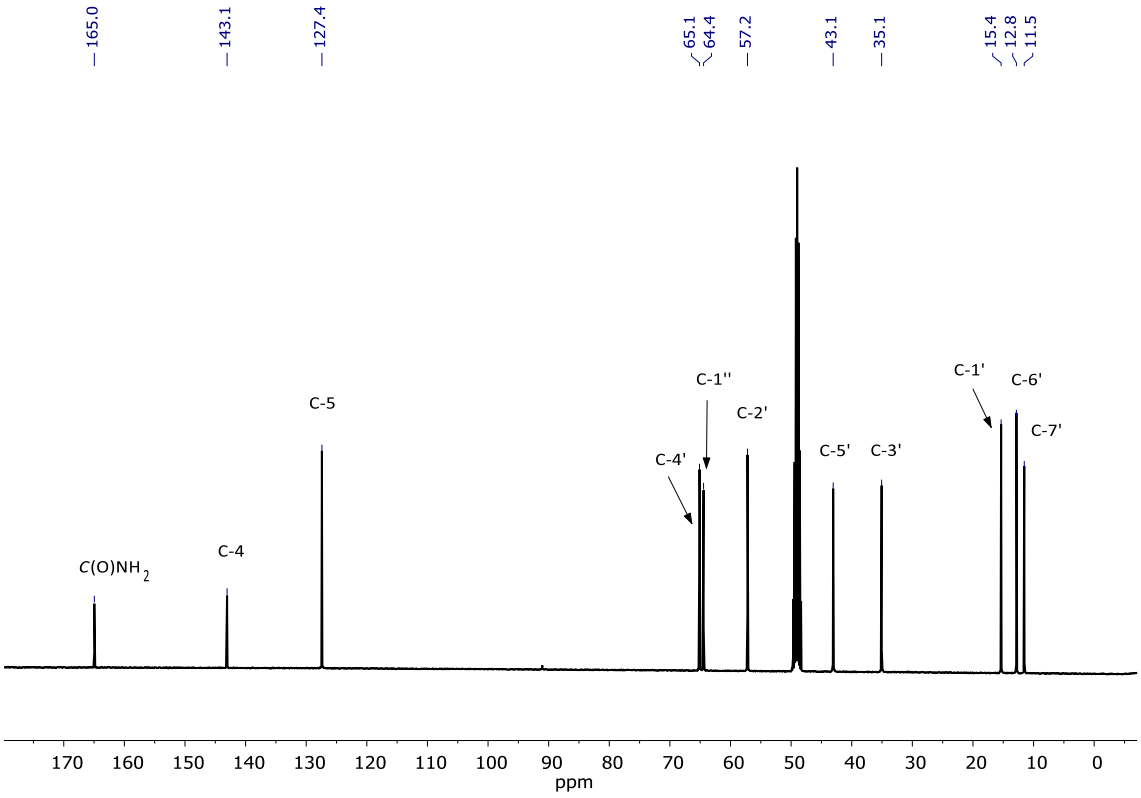

^{13}C-NMR (101 MHz, MeOH-d_4)

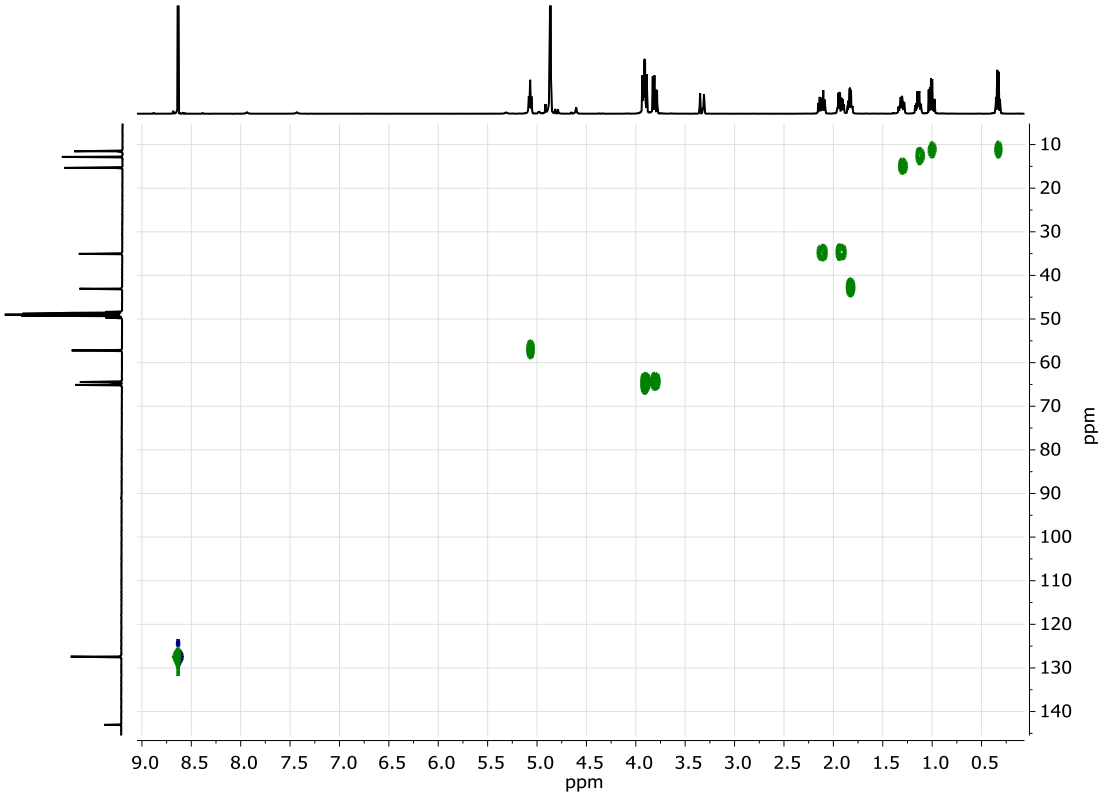

HSQC (400 MHz, MeOH-d_4)

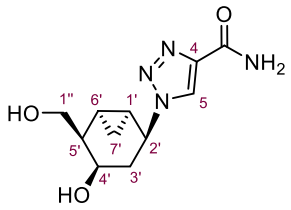

148

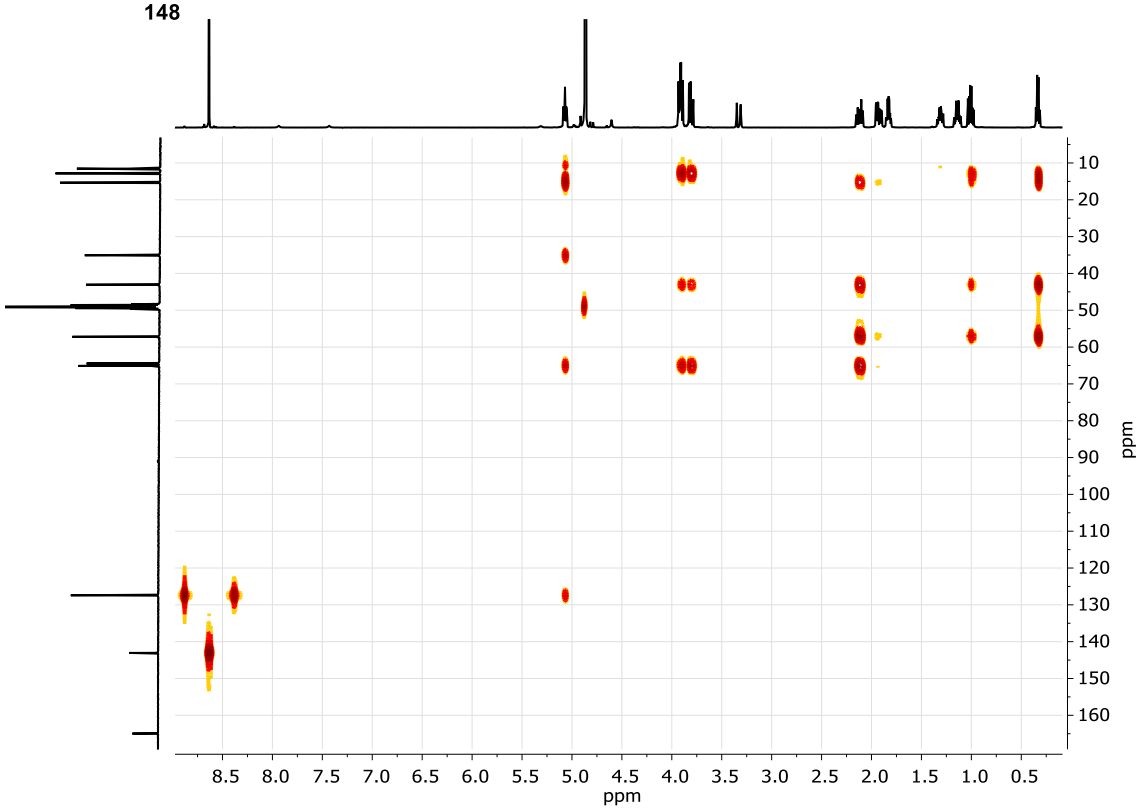

HMBC (400 MHz, MeOH-d_4)

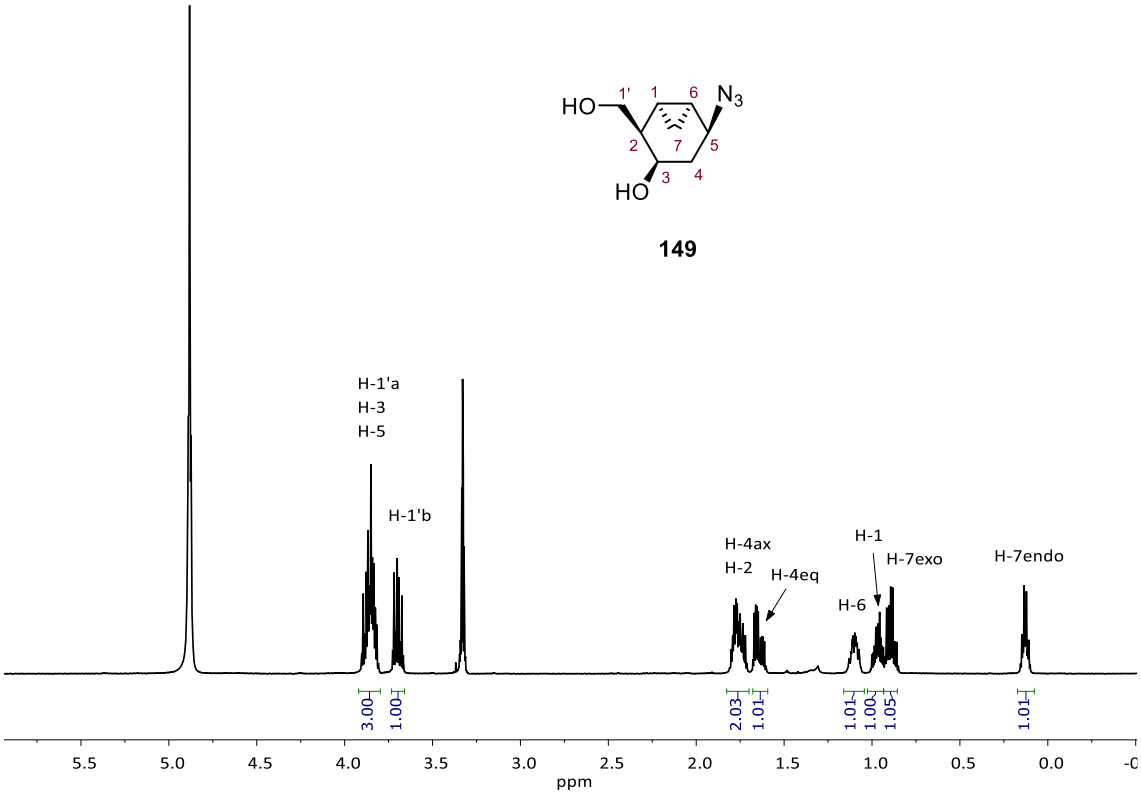

149

^{1}H-NMR (400 MHz, MeOH-d_4)

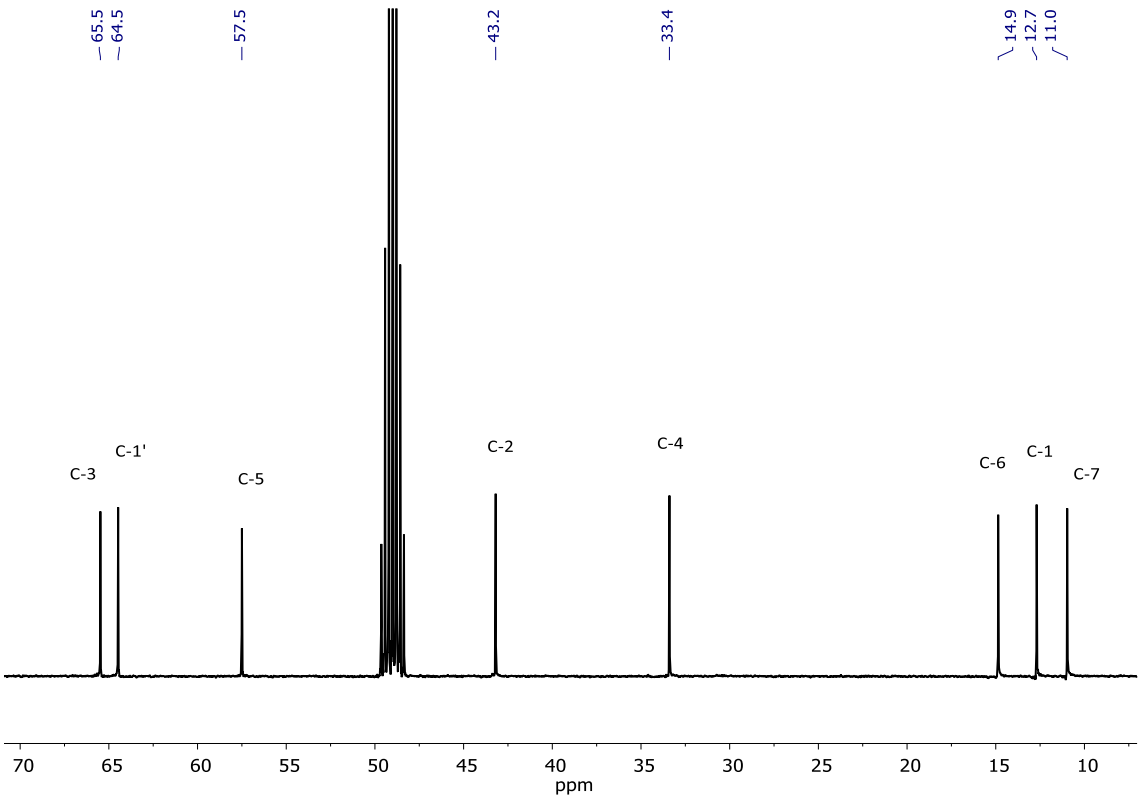

^{13}C-NMR (101 MHz MeOH-d_4)

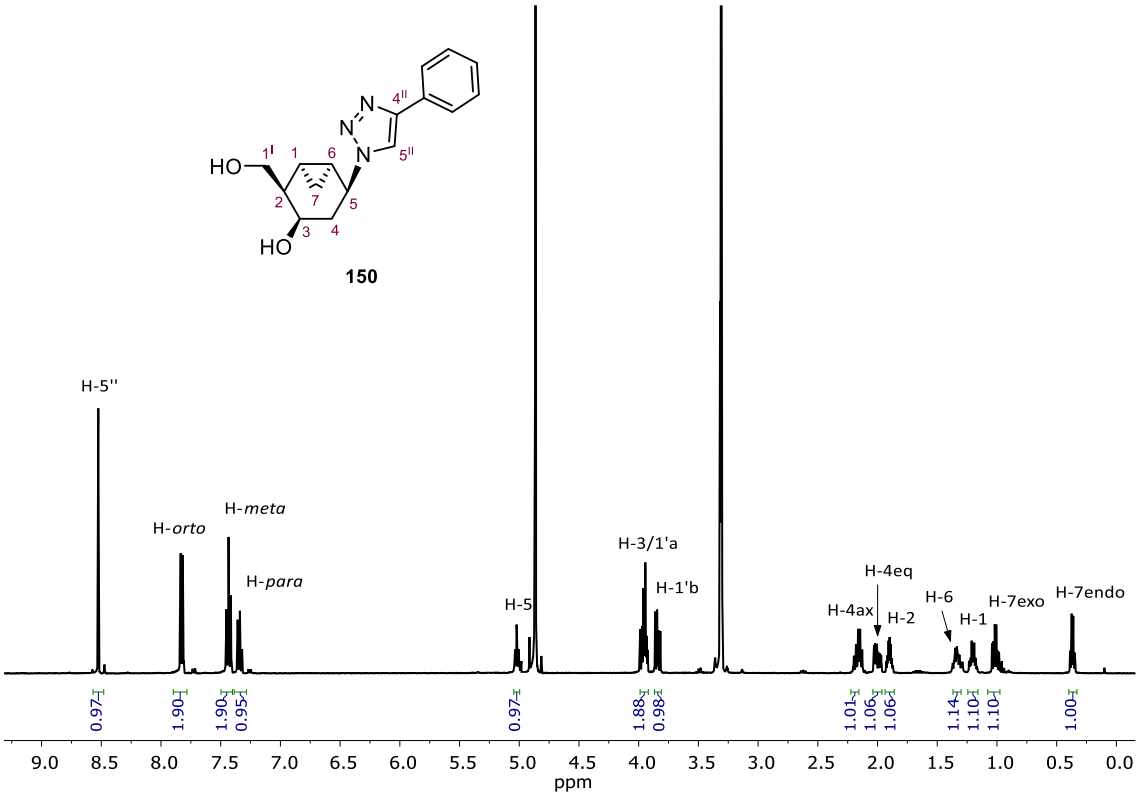

^{1}H-NMR (400 MHz, MeOH-d_4)

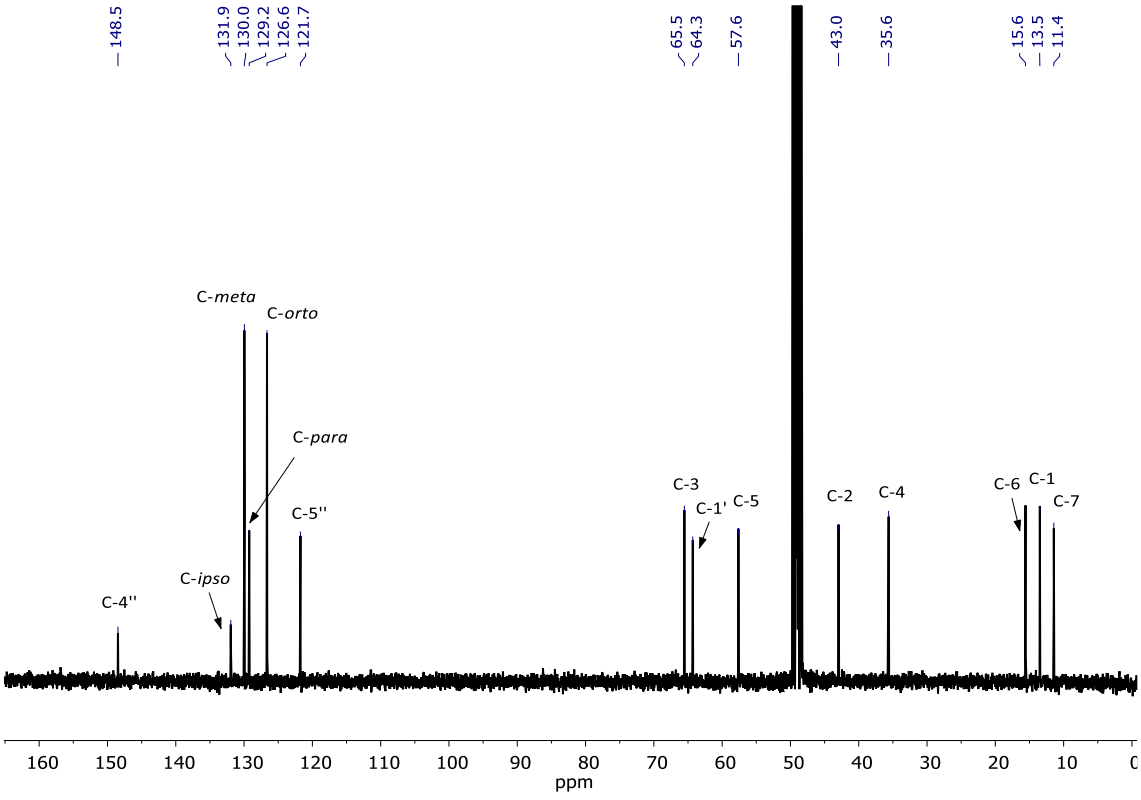

^{13}C-NMR (101 MHz, MeOH-d_4)

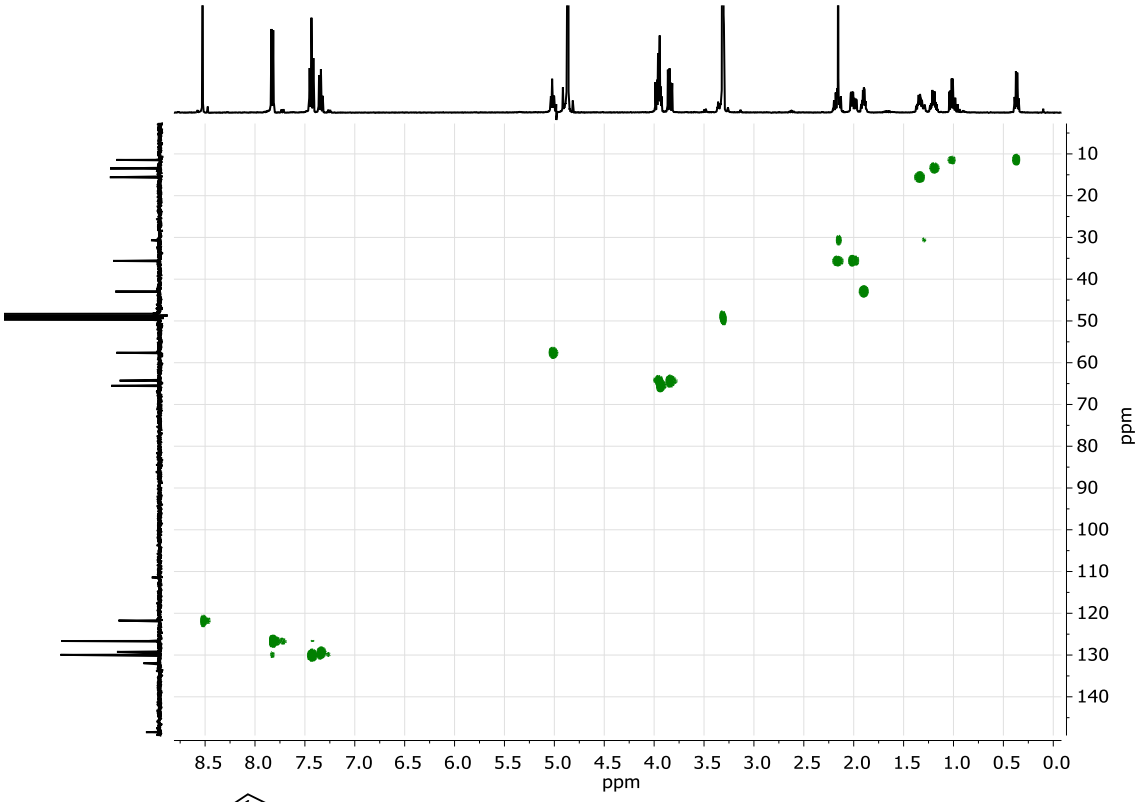

HSQC (400 MHz, MeOH-d_4)

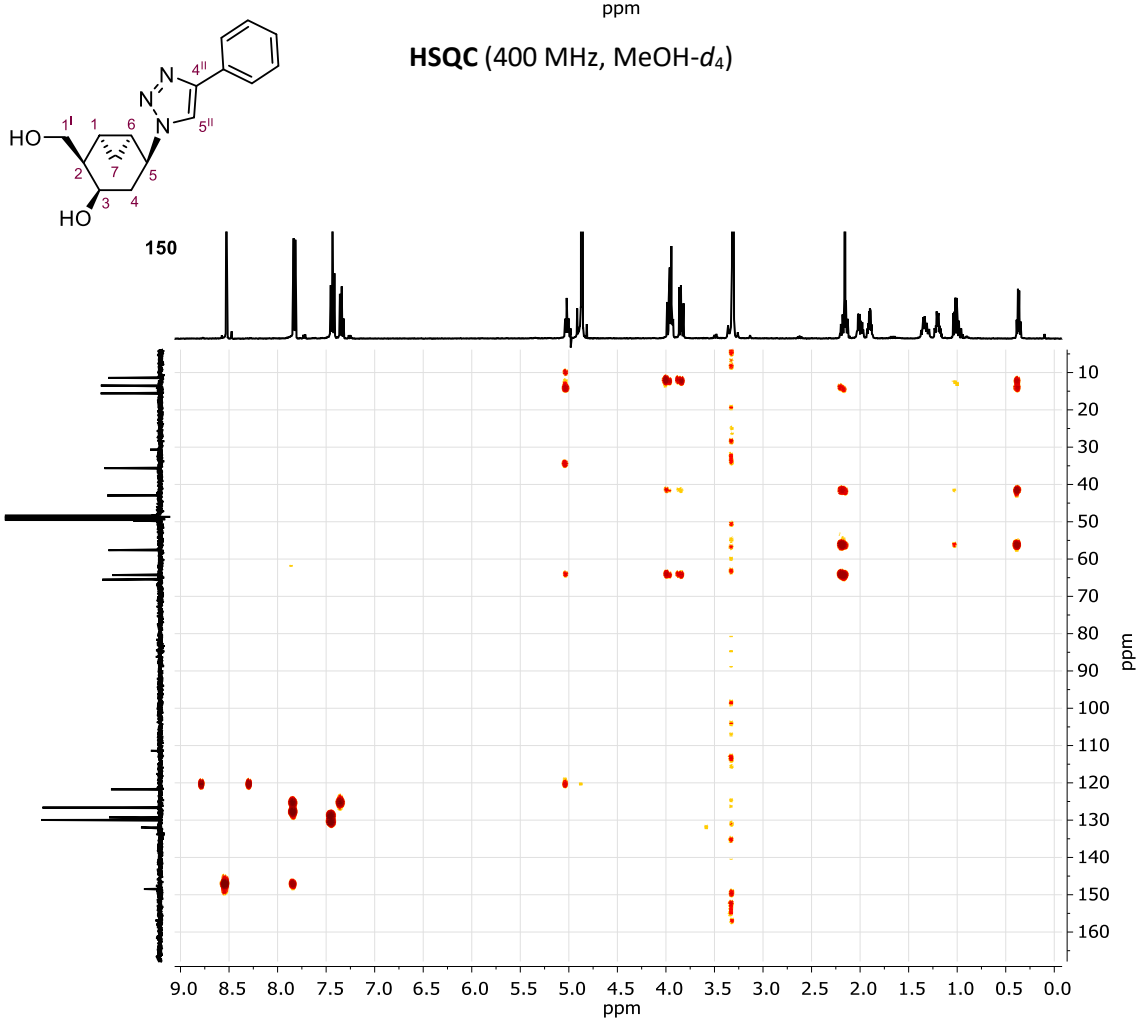

HMBC (400 MHz, MeOH-d_4)

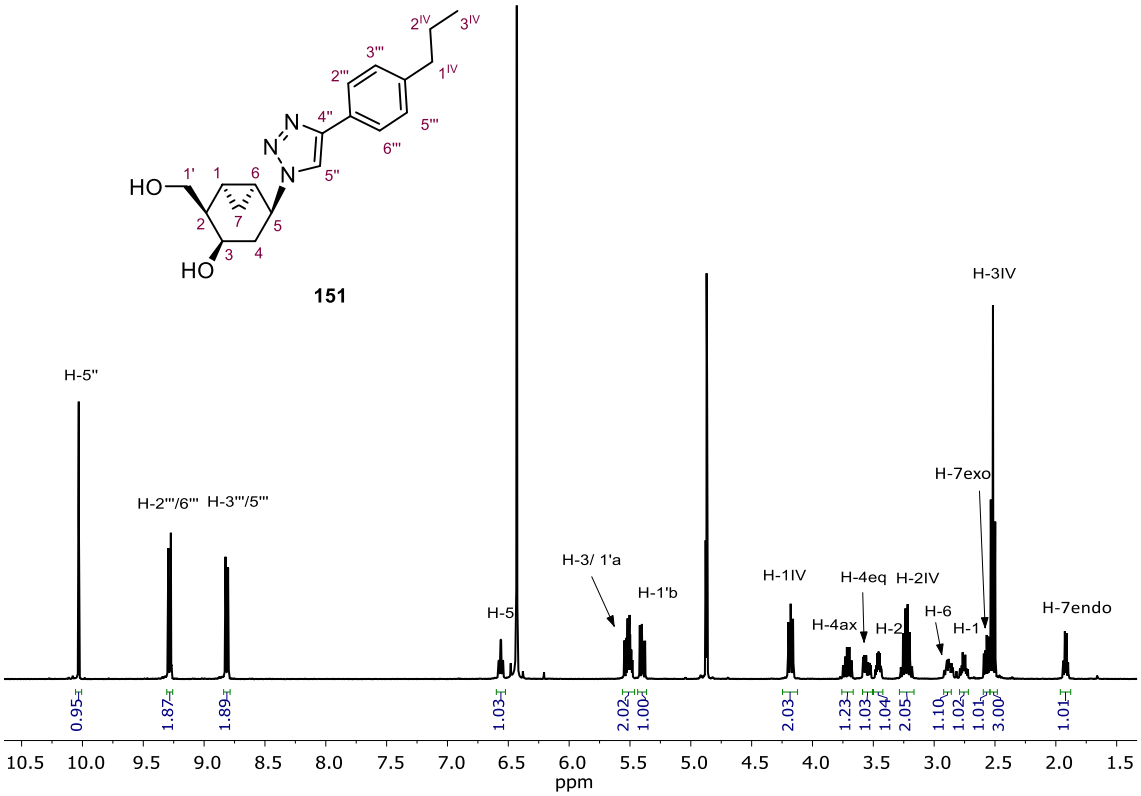

^{1}H-NMR (400 MHz, MeOH-d_4)

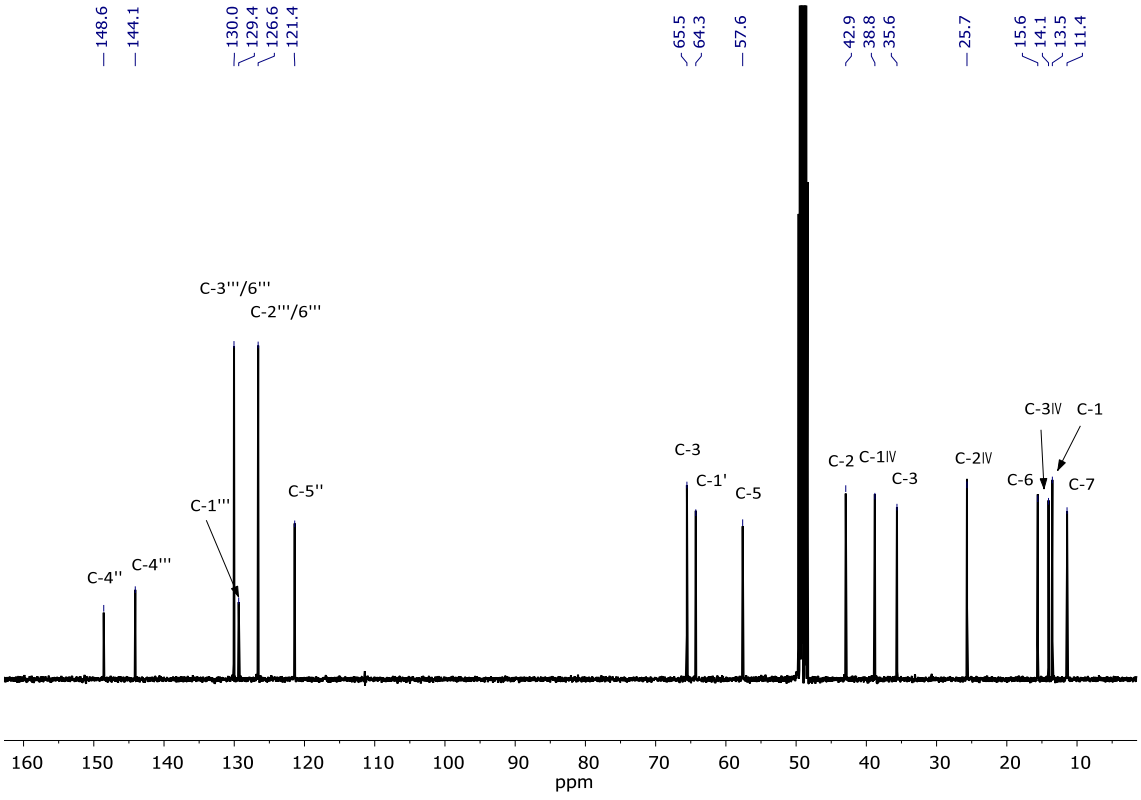

^{13}C-NMR (101 MHz, MeOH-d_4)

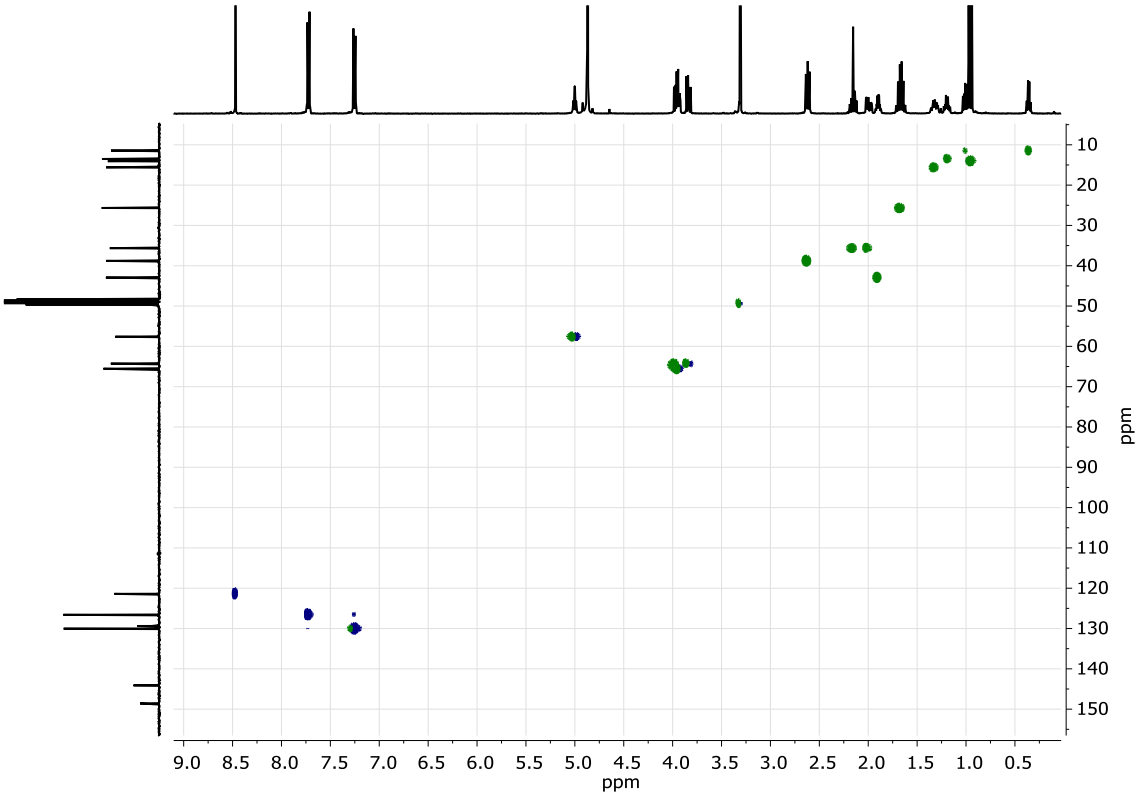

HSQC (400 MHz, MeOH-d_4)

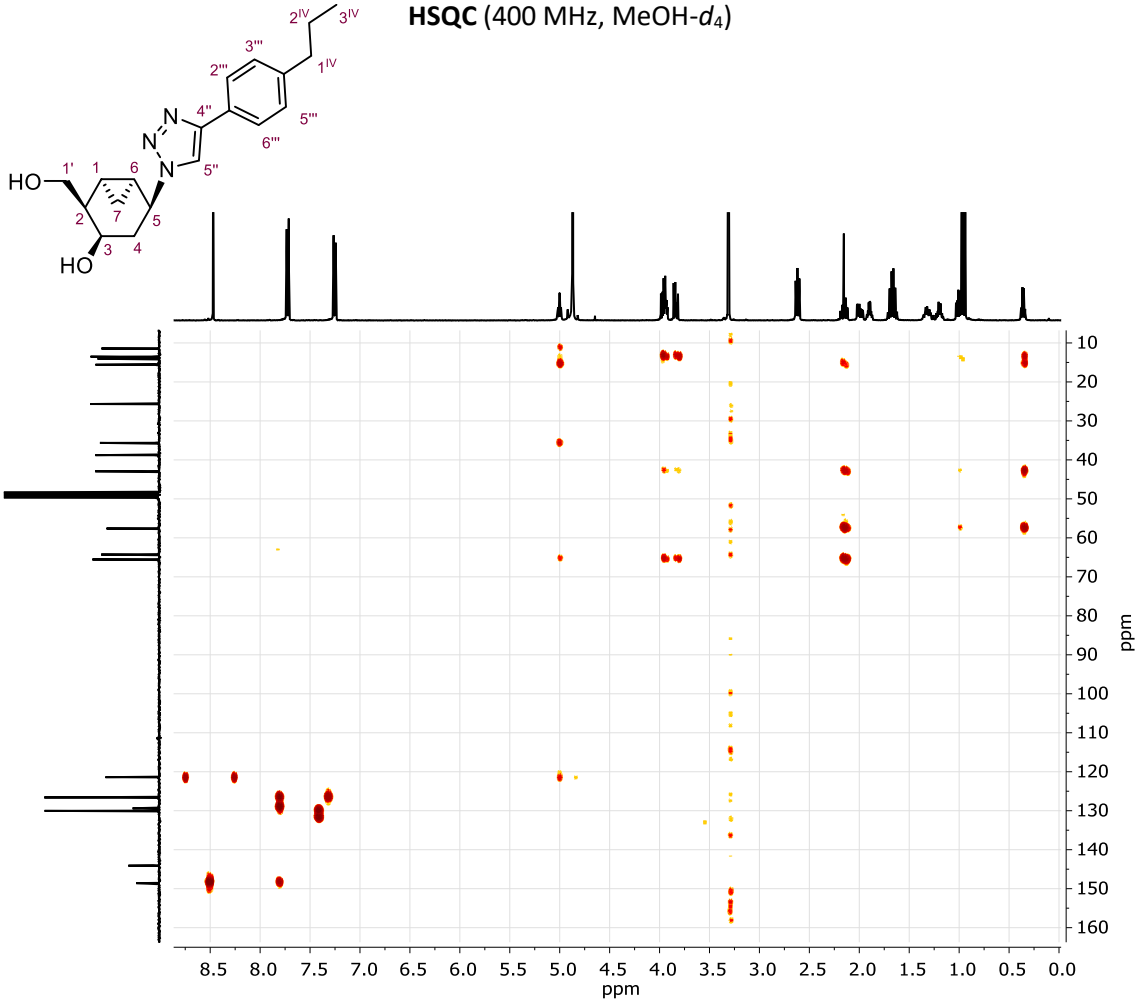

HMBC (400 MHz, MeOH-d_4)

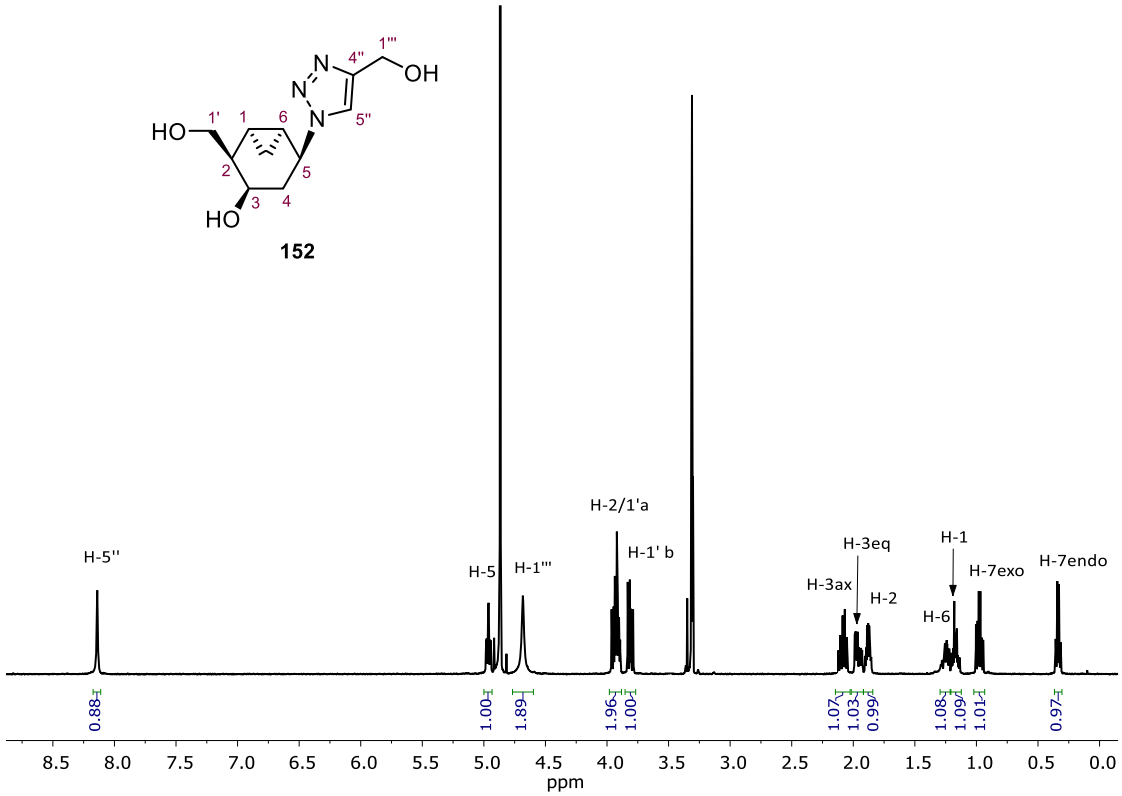

^{1}H-NMR (400 MHz, MeOH-d_4)

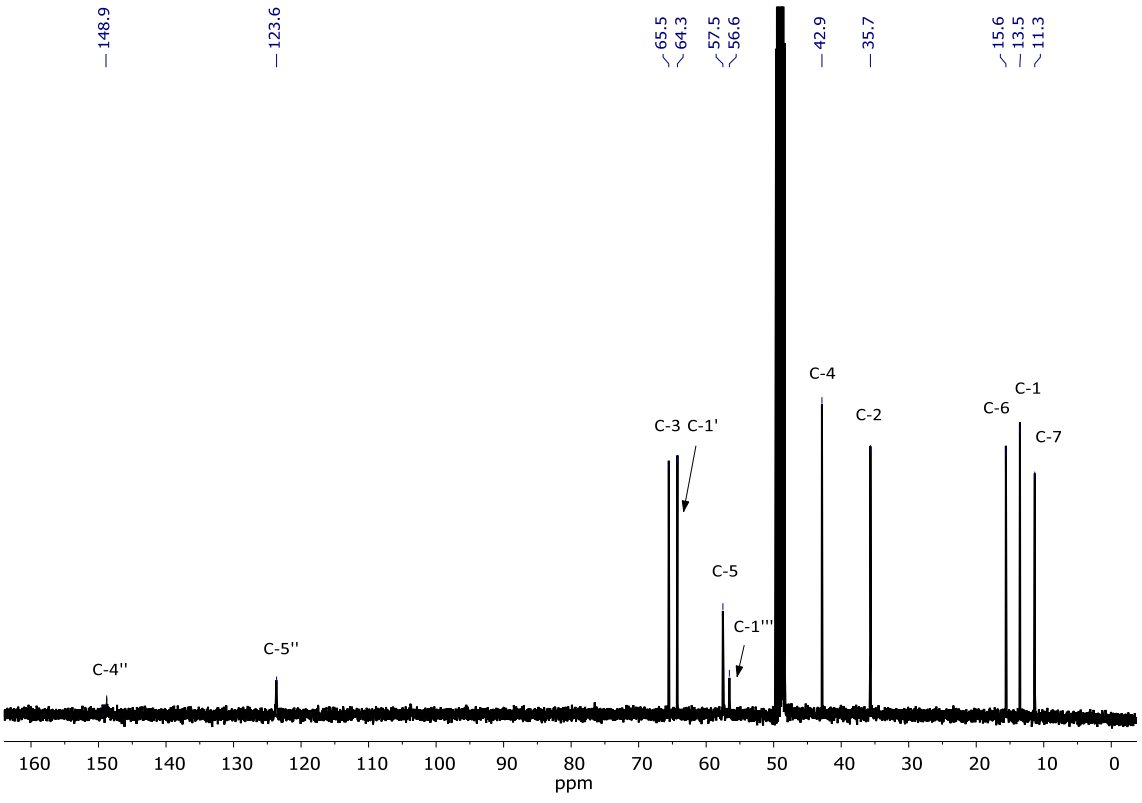

^{13}C-NMR (101 MHz, MeOH-d_4)

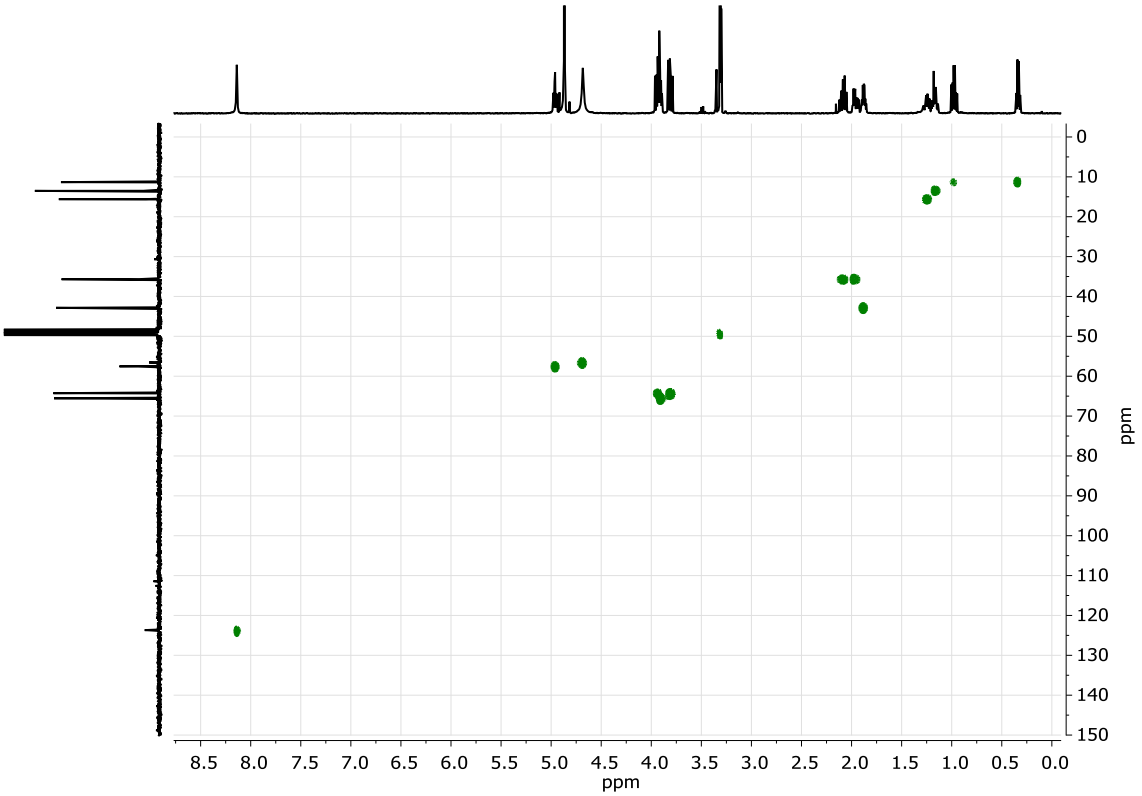

HSQC (400 MHz, MeOH-d_4)

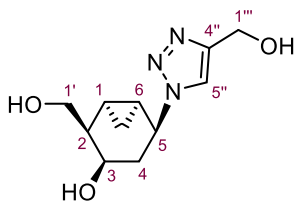

152

HMBC (400 MHz, MeOH-d_4)

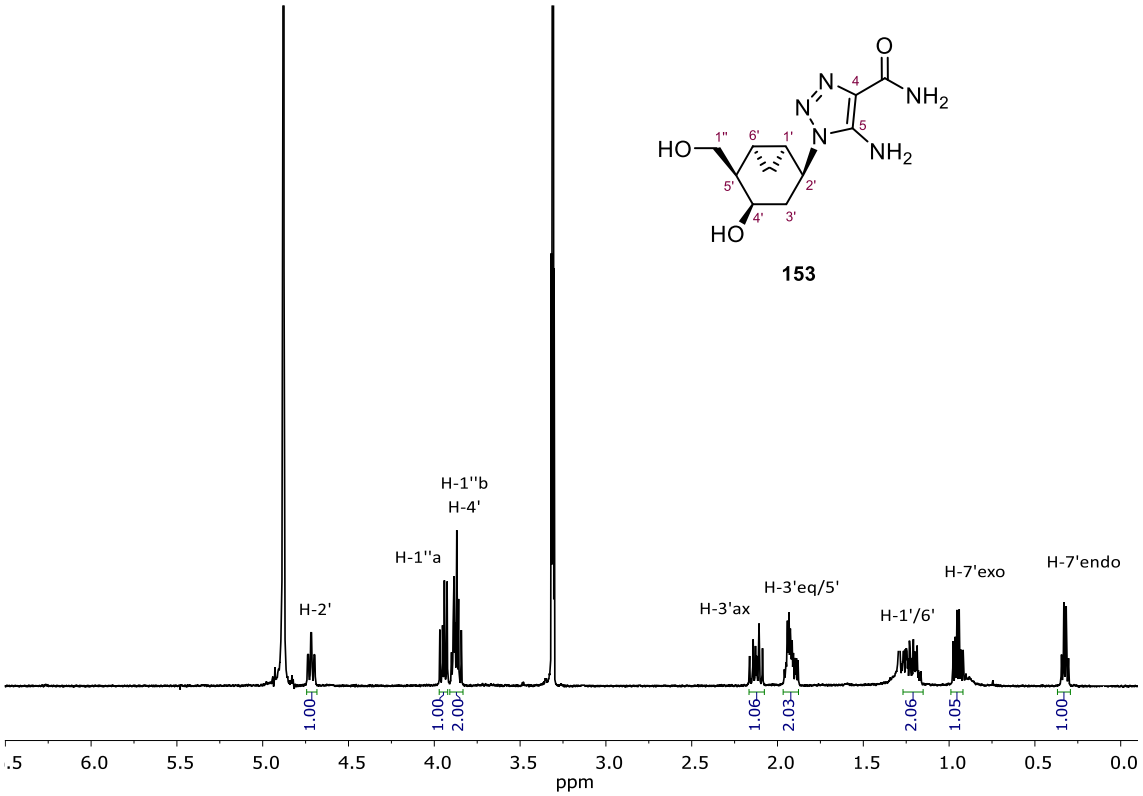

^{1}H-NMR (400 MHz, MeOH-d_4)

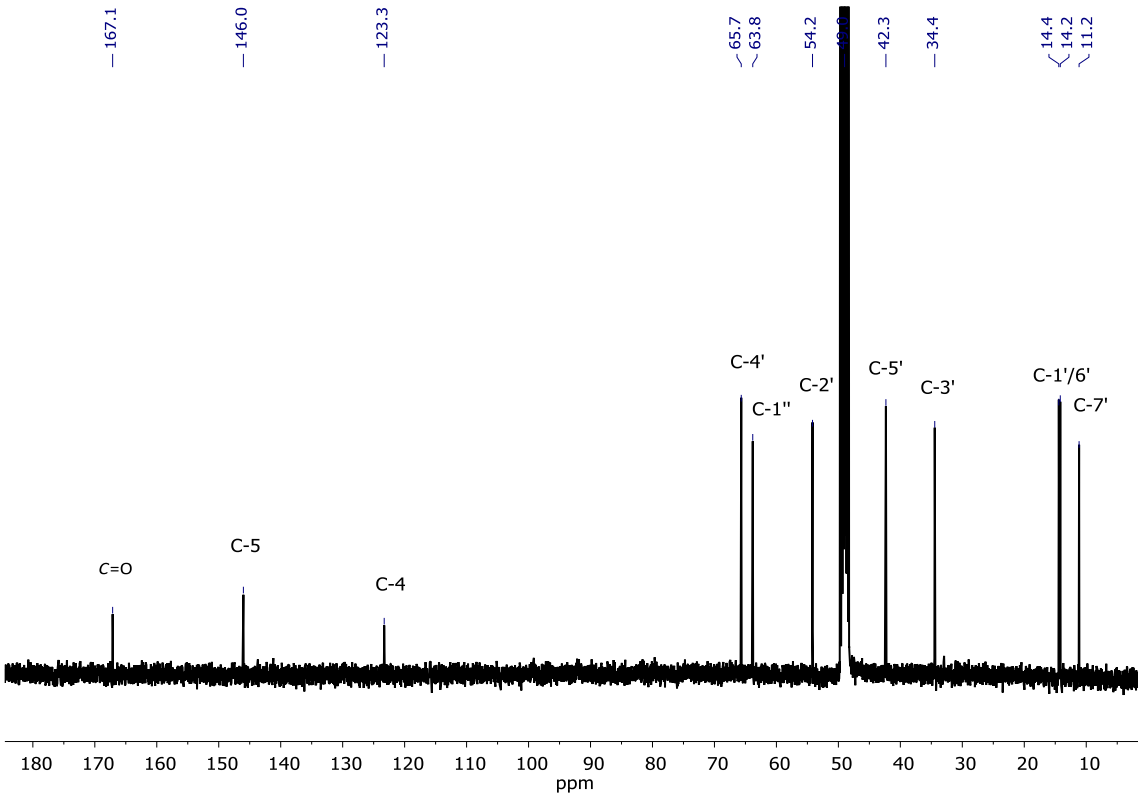

^{13}C-NMR (101 MHz, MeOH-d_4)

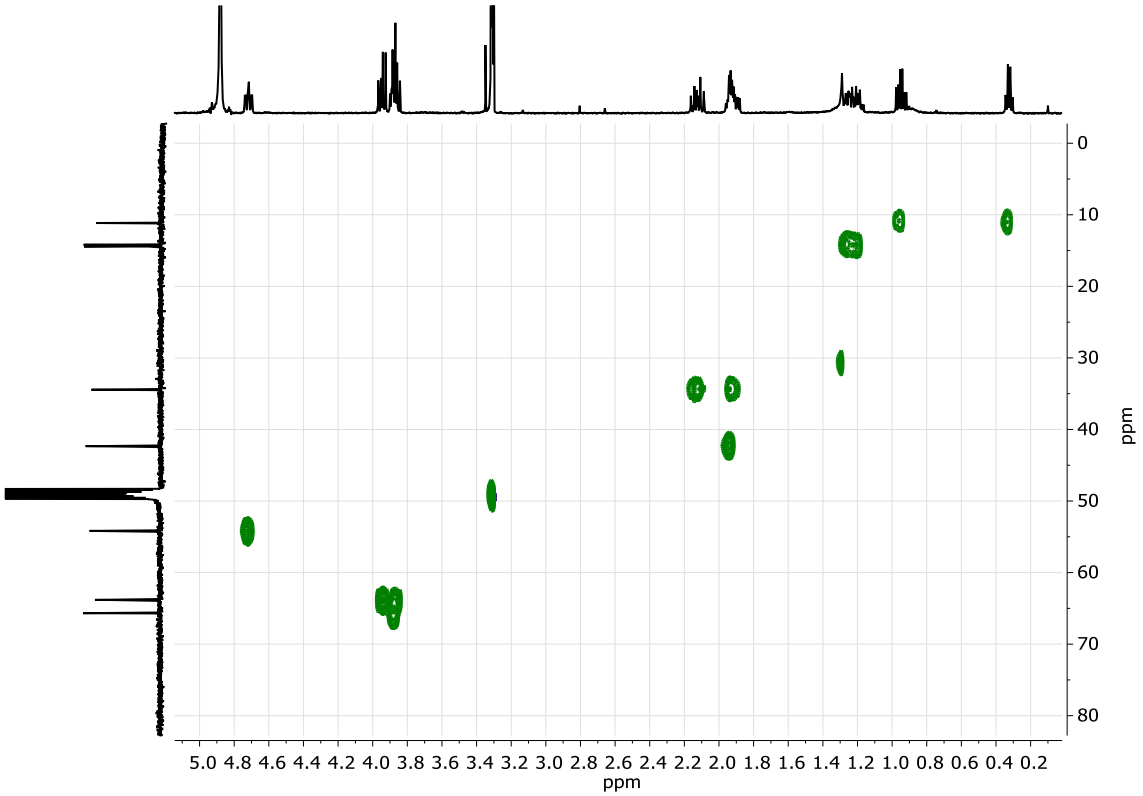

HSQC (400 MHz, MeOH-d_4)

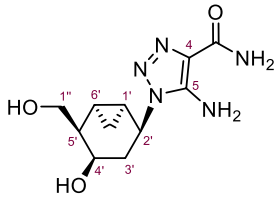

153

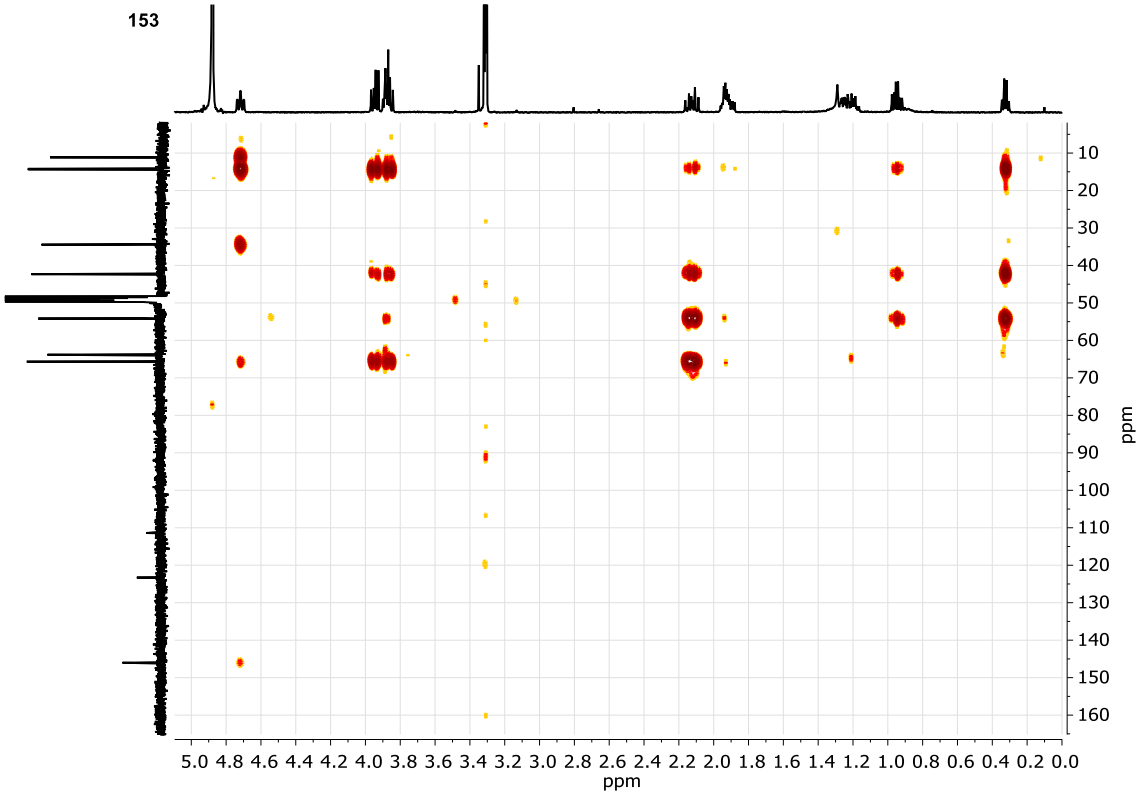

HMBC (400 MHz, MeOH-d_4)

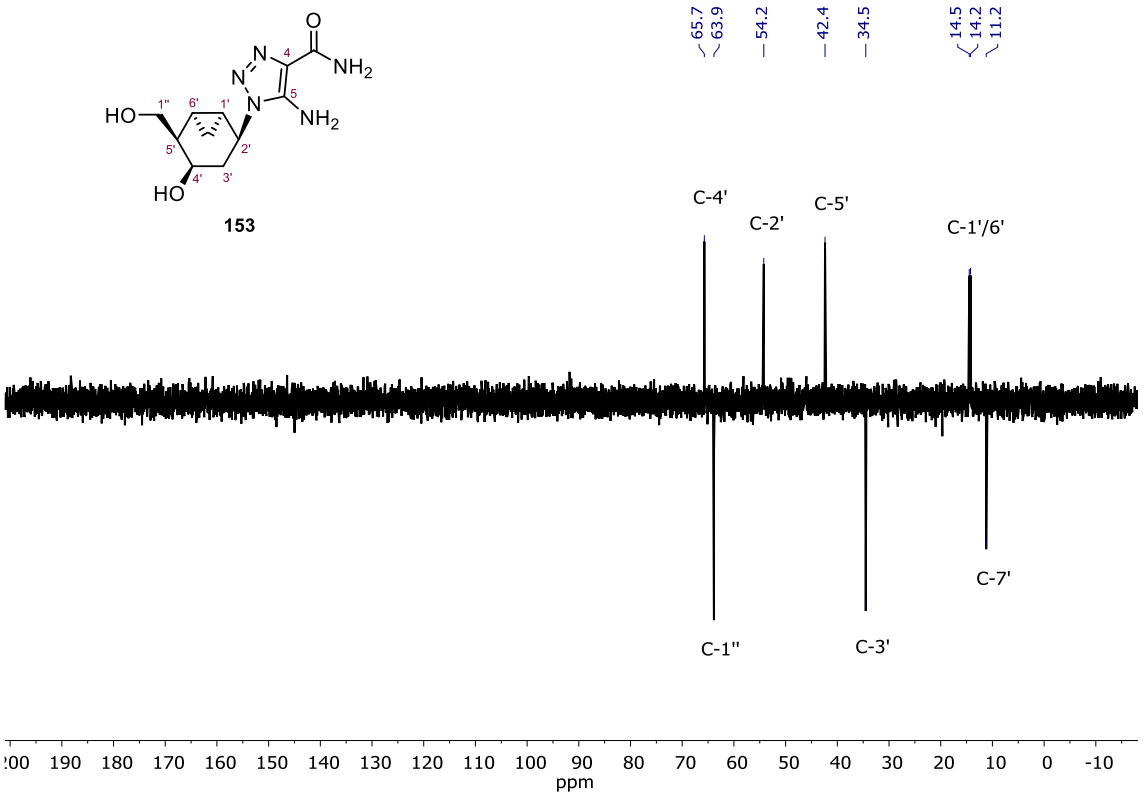

DEPT-135 (400 MHz, MeOH-d_4)

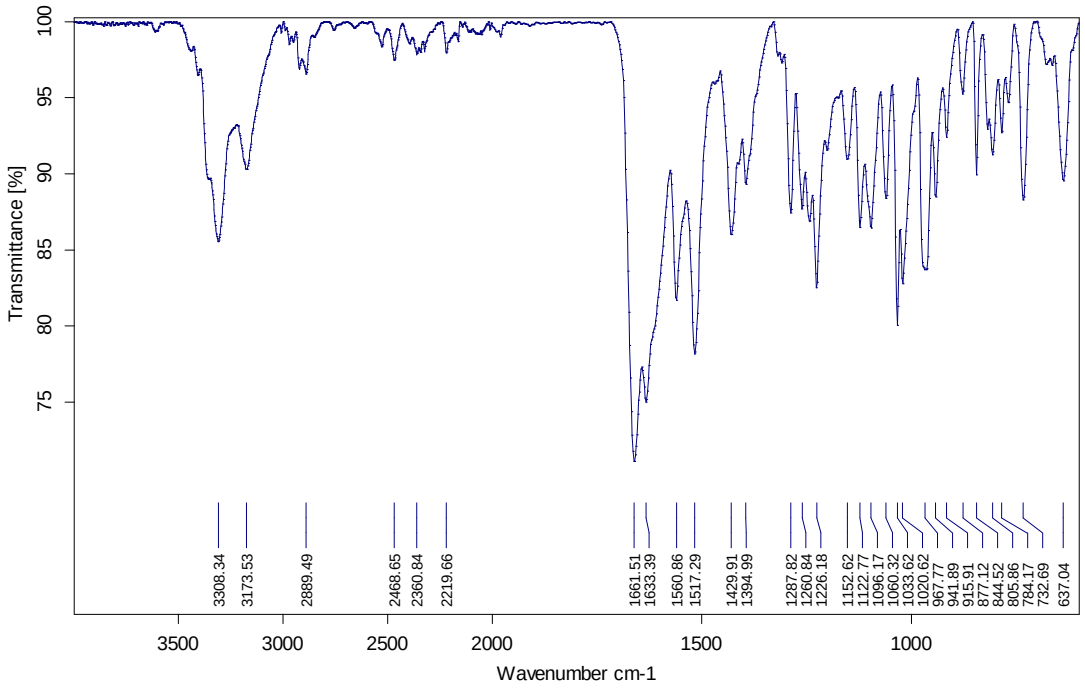

IR (ATR)